

Manfred Harrer · Peter Pfeffer *Editors*

# Steering Handbook

# Steering Handbook

Manfred Harrer · Peter Pfeffer  
Editors

# Steering Handbook



Springer

*Editors*

Manfred Harrer  
Weissach  
Germany

Peter Pfeffer  
Automotive Engineering (FK03)  
Munich University of Applied Science  
Munich  
Germany

ISBN 978-3-319-05448-3  
DOI 10.1007/978-3-319-05449-0

ISBN 978-3-319-05449-0 (eBook)

Library of Congress Control Number: 2015930030

Springer Cham Heidelberg New York Dordrecht London  
© Springer International Publishing Switzerland 2017

This work is subject to copyright. All rights are reserved by the Publisher, whether the whole or part of the material is concerned, specifically the rights of translation, reprinting, reuse of illustrations, recitation, broadcasting, reproduction on microfilms or in any other physical way, and transmission or information storage and retrieval, electronic adaptation, computer software, or by similar or dissimilar methodology now known or hereafter developed.

The use of general descriptive names, registered names, trademarks, service marks, etc. in this publication does not imply, even in the absence of a specific statement, that such names are exempt from the relevant protective laws and regulations and therefore free for general use.

The publisher, the authors and the editors are safe to assume that the advice and information in this book are believed to be true and accurate at the date of publication. Neither the publisher nor the authors or the editors give a warranty, express or implied, with respect to the material contained herein or for any errors or omissions that may have been made.

Printed on acid-free paper

Springer International Publishing AG Switzerland is part of Springer Science+Business Media  
([www.springer.com](http://www.springer.com))

# Preface

In recent years, steering system technologies have undergone rapid development. This was caused by increased regulatory requirements in the areas of environment and safety, through the increased comfort requirements of the customer and not least by the continuing cost pressure. New ways has been taken up for steering components such as steering wheel, steering column, and steering gear. The most substantial change has been the progressive substitution of conventional hydraulic steering systems with electrical steering systems. With this change in technology a variety of new steering functions have been made possible. It is therefore not surprising that the steering system development as such occupies an ever-increasing role in modern chassis development. Due to the lack of a standard English book on the subject of steering systems/steering behavior, which describes the current state of the art, we decided with Springer Verlag to publish the German Steering Handbook also in English. We have taken into account the different interests and requirements of automotive manufacturers, suppliers, and universities in such a standard work by the involvement of proven experts from these areas.

In the first part of this book, the kinematic and vehicle dynamics of steering is explained and discussed, and also the influence of the suspension characteristics for the steering operation is investigated. A chapter is devoted to the interaction between driver and vehicle to analyze the aspects of steering feel. The central chapters of this book are devoted to individual steering modules, their design, and component tests. Described in detail are the components steering wheel, steering column with intermediate steering shaft, and the steering rack in mechanical, hydraulic, and electro-mechanical design. Special steering system technologies such as the superimposed steering system and four-wheel steering are also discussed in detail. Much attention was paid to illustrate the current state of the steering system technology and its interaction with the entire vehicle comprehensibly. Also important secondary aspects such as acoustic performance, energy requirements, and functional safety are treated in detail. Furthermore, the possibilities regarding driver assistance functions enabled by modern steering systems are shown. The profound expertise of nearly 40 experts from industry and academia

was utilized for the creation of the steering handbook. We would like to thank all the authors for their expertise and perseverance. Also we thank Springer for publishing. Only through the dedication of all those involved, this textbook has been possible.

The readers of this book were asked by us to give feedback for improvements. Please send your suggestions to the following email address: [peter.pfeffer@hm.edu](mailto:peter.pfeffer@hm.edu). We will accommodate your suggestions in the next editions.

Stuttgart, Feldafing  
January 2014

Manfred Harrer  
Peter Pfeffer

# Contents

<b>1</b>	<b>Introduction and History . . . . .</b>	1
	Peter Pfeffer and Hartmut Ulrich	
<b>2</b>	<b>Basic Principles of the Steering Process . . . . .</b>	27
	Peter Pfeffer, Jens Holtschulze and Hans-Hermann Braess	
<b>3</b>	<b>Steering Requirements: Overview . . . . .</b>	53
	Sina Brunner and Manfred Harrer	
<b>4</b>	<b>Steering Kinematics . . . . .</b>	63
	Trzesniowski Michael	
<b>5</b>	<b>Basics of Lateral Vehicle Dynamics . . . . .</b>	91
	Peter Pfeffer and Hans-Hermann Braess	
<b>6</b>	<b>Acoustics and Vibrations . . . . .</b>	121
	Stefan Sentpali and Rupert Hintersteiner	
<b>7</b>	<b>Steering-Feel, Interaction Between Driver and Car . . . . .</b>	149
	Manfred Harrer, Peter Pfeffer and Hans-Hermann Braess	
<b>8</b>	<b>Layout of Steering Systems . . . . .</b>	169
	Sina Brunner, Manfred Harrer, Manuel Höll and Daniel Lunkeit	
<b>9</b>	<b>Steering Wheel . . . . .</b>	191
	Markus Walters	
<b>10</b>	<b>Steering Column and Intermediate Steering Shaft . . . . .</b>	215
	Jörg Hauhoff and Ralf Sedlmeier	
<b>11</b>	<b>Mechanical and Hydraulic Gears . . . . .</b>	249
	Johannes Hullmann, David James, Alois Seewald, Eduard Span and Alexander Wiertz	
<b>12</b>	<b>Tie Rods . . . . .</b>	339
	Dirk Adamczyk, Wolfgang Kleiner and Dirk Maehlmann	

<b>13 Hydraulic Power Supply . . . . .</b>	357
Dieter Semmel	
<b>14 Electrically Powered Hydraulic Steering . . . . .</b>	381
Jochen Gessat, Alois Seewald and Dirk Zimmermann	
<b>15 Electric Power Steering Systems . . . . .</b>	403
Alexander Gaedke, Markus Heger, Michael Sprinzl, Stefan Grüner and Alexander Vähning	
<b>16 Superimposed Steering System . . . . .</b>	469
Mirko Reuter and André Saal	
<b>17 All-Wheel Steering . . . . .</b>	493
Peter Herold and Markus Wallbrecher	
<b>18 Steer by Wire . . . . .</b>	513
Pei-Shih Huang and Alfred Pruckner	
<b>19 Overview: Driver Assistance System Functions . . . . .</b>	527
Stefan Brosig and Markus Lienkamp	
<b>20 Outlook: The Future of Steering Systems . . . . .</b>	545
Manfred Harrer and Peter Pfeffer	
<b>Advertisements . . . . .</b>	553
<b>Index . . . . .</b>	559

# Abbreviations and Symbols

## Abbreviations

4WAS	4 Wheel Active Steer (Nissan)
ABS	Anti-Lock Brake System
AC	Alternating Current
AD	Analog-Digital Converter
AFS	Active Front Steering
AHK	Aktive rear axle kinematic
AMR	Anisotropen Magnetoresistiv
APA	Paraxial drive unit
ASIC	Application-Specific Integrated Circuit
ASIL	Automotive Safety Integrity Level
ASM	Asynchronous Motor
ASM	Assembly
ATF	Automatic Transmission Fluid
BCM	Body-Control-Modul
BLDC	Brushless Direct Current Motor
BRIC	Brasil, Russia, India, China
CAE	Computer Aided Engineering
CAN	Controller Area Network
C-EPS	Steering Column Assisted EPS
CFD	Computational Fluid Dynamics
CFK	Fiber-Reinforced Plastic Material
CGR	Constant Gear Ratio
CPU	Central Processor Unit
CR	Chloroprene Rubber
CR-EPS	Rack Concentric EPS
CS	Circular-Spline
CSM	Chlorosulphonated-Polyethylene-Rubber
CV	Concept Verification
DBC	Direkt Bonded Copper

DBV	Pressure Limitation Valve
DC	Direct Current
DCM	Direct Current Motor
DMS	Strain gauge
DP-EPS	Dual Pinion EPS
DV	Design Verification
EC	Electronically Commutated Motor
ECE	Economic Commission for Europe
ECU	Electronic Control Unit
EHPS	Electro Hydraulic Power Steering
EMC	Electro Magnetic Compatibility
EPS	Electric Power Steering
EPsapa	EPS with Paraxial Drive
EPSc	Column EPS
EPSdp	Dual Pinion EPS
EPSp	Pinion EPS
EPSrc	Rack Concentric EPS
ESD	Electrostatic Discharge
ESP	Elektronisches Stability Program
ESV	Experimental-Safety-Vehicle
EU	European Union
EV	Electric Vehicle
EVLS	Elektric adjustable steering column
EWG	European Economic Community (Europäische Wirtschaftsgemeinschaft)
FA	Front Axle
FAD	Front Axle Damper
FB	Flex-Bearing
FCV	Fuel Cell Vehicle
FEA/FEM	Finite-Element-Analysis/Method
FMVSS	Federal Motor Vehicle Safety Standard
FS	Flex-Spline
FS (FDR)	Vehicle Stability (Vehicle Dynamics Control)
FS (VS)	Vehicle Stability (Feedforward)
GAAI	German Association of the Automotive Industry
GFK	Glass fiber reinforced plastic
GIS	German Institute for Standardization
GND	Ground
HA	Rear Axle
HAD	Rear Axle Damper
HEV	Hybrid Electric Vehicle
HICAS	High Capacity Actively Controlled Suspension
HNBR	Hydrierter Acrylnitrilbutadien-Kautschuk
HPS	Hydraulic Power Steering
IAS	Integral Aktiv Steering

IC	Electrical Circuit
IEC	International Electrotechnical Commission
IGBT	Insulated-Gate Bipolar Transistor
IMS	Insulated Metal Substrate
ISO	International Standards Organization
KGT	Recirculating ball
KTL	Cathodic dip painting
LCV	Light Commercial Vehicle
LDM	Free steering torque
LDS	Steering nibble (steering torsional vibrations)
LDW	Lane Departure Prevention
LED	Light Emitting Diode
LIN	Local Interconnected Network
LKS	Lane Keeping Support
MAC	Manual Adjustable column
MFS	Magnetic Field Sensor
MFS	Multi-Function Switch
ML	Engine Mount
MOST	Media Oriented Systems Transport
MPA	Motor-Pump-Unit
MR	Magnetoresistiv
MS	Manual Steering
NBR	Nitrile Butadiene Rubber
NEDC	New European Driving Cycle
Nfz CV	Commercial Vehicle
NHTSA	National Highway Safety Traffic Administration
NVH	Noise Vibration Harshness
OA-EPS	Offset Axis-EPS
OEM	Original Equipment Manufacturer
OOP	Out Of Position
OSEK/VDX	Offene Systeme und deren Schnittstellen für die Elektronik in Kraftfahrzeugen/Vehicle Distributed eXecutive
PA	Polyamide
PC	Passenger Car
PCB	Printed Circuit Board
PDC	Park Distance Control
PEEK	Polyetherketone
P-EPS	Pinion EPS
P-EPS	Paraxial EPS
PMSM	Permanent Magnet Synchronous Motor
POM	Polyoxymethylene
ppm	parts per million
PTFE	Polytetrafluoroethylene
PUR	Polyurethane
PV	Product Validation

PVD	Physical Vapour Deposition
PWM	Pulse Width Modulation
QM	Quality Management
RAM	Random Access Memory
ROM	Read Only Memory
ROW	Rest of the World
RTLG	Road Traffic Licensing regulations
SA	Steering Arm
SAE	Society of Automotive Engineers
SAW	Surface Acoustic Wave
SCU	Steering Control Unit
SH	Sensor Host
SIL	Safety Integrity Level
SISO	Single Input Single Output
SMD	Surface Mounted Device
SR	Switched Reluctance
SUV	Sport Utility Vehicle
TCR	Turning Circle Reduction
TFC	Thick Film Copper
THC	Through Hole Component
UV	Ultra Violette
VCC	Common-Collector Voltage
VGR, VGS	Variable Gear Ratio
WG	Wave Generator
ZFLS	ZF Lenksysteme GmbH (now Robert Bosch Automotive Steering GmbH)

## Formula Index

$\alpha$	Tire side slip angle (rad)
$\alpha$	Working angle of joint steering countershaft (rad)
$\beta$	Slip angle (rad)
$\beta$	Angle between joint planes (rad)
$\beta_{T/\beta_U}$	Transmission angle
$\beta_x$	Separation ratio
$\beta_z$	Helix angle (rad)
$\gamma$	Shearing angle (rad)
$\gamma$	Offset angle steering countershaft (rad)
$\gamma$	Installation angle bevel axle (rad)
$\delta^*$	Steering arm rotation angle (rad)
$\delta, \delta$	Steering angle, velocity (rad, rad/s)
$\delta_A$	Ackermann angle (rad)
$\delta_D$	Dynamic reference steering angle (rad)
$\delta_G$	Rotation angle of steering arm lever (rad)

$\delta h$	Rear steering angle (rad)
$\delta H$	Steering wheel angle (rad)
$\delta H^*$	Bevel rotation axle (rad)
$\delta LS$	Steering column angle (rad)
$\delta M$	Superposing angle (rad)
$\delta o, \text{max}$	Maximum steering angle of front outer wheel (rad)
$\delta v$	Front steering angle (rad)
$\Delta\delta$	Required difference steering angle (rad)
$\Delta\delta A$	Track difference angle, difference steering angle according to Ackermann (rad)
$\Delta\delta F$	Difference steering angle (rad)
$\Delta\delta H$	Steering wheel angle (rad)
$\Delta\delta H,e$	Steering system compliance at steering wheel (rad)
$\Delta\delta H,Re$	Steering wheel rest angle (rad)
$\varepsilon$	Wheel camber angle (rad)
$\varepsilon V,\phi,F$	Roll induced steering factor (rad)
$\varepsilon \alpha$	Gearing transverse contact ratio
$\varepsilon \beta$	Gearing overlap ratio
$\varepsilon \gamma$	Gearing overall overlap
$\Delta\varepsilon V,\phi,F$	Camber part due to rolling (rad)
$\zeta$	Attenuation ratio
$\eta$	Efficiency
$\eta$	Frequency rate
$k$	Is Curvature (1/m)
$\lambda$	Direction of steering arm (rad)
$\rho$	Path curve radius (m)
$\sigma$	Spread (rad)
$\tau$	Castor angle (rad)
$\phi$	Rotation angle (rad)
$\chi$	Roll angle (1/m)
$\psi, \dot{\psi}$	Yaw angle, yaw angle velocity (rad), (rad/s)
$\omega$	Angle velocity (rad/s)
$\omega E$	Cutt-off frequency (rad/s)
$\omega n$	Steering system natural frequency (1/s)

## Symbol Description

a	Air
dyn	Dynamic
$o$ (curve)	Outside
$i$ (curve)	Inside
F	Front
R	Rear

# Advertisements



The advertisement features a red sports car driving on a road at sunset, with a blurred background suggesting speed. The IPG Automotive logo is at the top left, and the tagline "Taking you to the next level" is to its right. Below the car, the slogan "Create driving experience customers will love" is displayed. At the bottom, there are three smaller images: one showing people working on a computer, another showing a steering system being tested, and a third showing a driver in a car.

**Create driving experience customers will love**

CarMaker® is optimally suited for on-center steering feel, stability, agility and comfort applications

The open integration and test platform CarMaker® created by IPG Automotive is optimally suited for on-center steering feel, stability, agility and comfort applications through the use of "Virtual Test Driving". CarMaker® empowers the development and evaluation of steering systems across the entire process chain in combination with X-in-the-Loop applications at various integration levels. Advanced Driver Assistance Systems like lane keeping assistants or autonomous parking systems as well as Control Systems like AFS or EPS can be realized in the CarMaker® environment with ease.

In these use cases, the integration of the Pfeffer steering model with the focus on specifying individual steering components and the modeling of mechanical friction mechanisms plays the key role. Concerning the method of "Virtual Test Driving", it opens up a new dimension of steering accuracy and handling feel. Furthermore, it allows a good and authentic reflection of steering torque to be achieved.

[www.ipg.de](http://www.ipg.de)

**tedrive**  
Steering  
Systems GmbH



intelligent. modular. safe.

## TEDRIVE iHSA® ACTIVATES STEERING SYSTEMS

In the commercial vehicle sector, tedrive premieres its patented iHSA® module, the intelligent Hydraulic Steering Assist. The iHSA® module can be integrated into tedrive rack & pinion and tedrive recirculating ball steering systems, offering commercial vehicle manufacturers a high degree of design and functional flexibility for all hydraulic steering systems. The result is a compelling combination of optimized ride and handling performance, comfort and safety, with the optional iHSA® module facilitating functions such as active lane-keeping aimed at reducing serious accidents. With the iHSA® torque overlay, heavy trucks and buses can now be steered without driver input for active lane-keeping, and equipped with a range of additional functions such as CV park assist and crosswind stabilisation.



## TEDRIVE STEERING – SUPERIOR STEERING FOR STRONG VEHICLES

tedrive Steering Systems GmbH, Henry-Ford II-Strasse 15, 42489 Wülfrath, Germany  
Phone: +49 (0) 2058 905-0, sales@td-steering.com, [www.td-steering.com](http://www.td-steering.com)





**M dynamix**

## Innovation simplified

The MdynamiX AG is an affiliated institute of the Munich University of Applied Sciences. As such, we are a scientific innovation partner for solving complex tasks in the automotive industry with customers benefiting from our access to entire know-how and to the facilities at one of Germany's leading institution.

Our fields of expertise cover vehicle dynamics & ride quality, acoustics & vibration technology, and advanced driver assistance systems (ADAS). Our comprehensive services range from methodology development, trials & testing, training to products & tools as:

**MXmount**                    **MXmountdesigner**  
**MXsteering**                **MXsteeringdesigner**  
**MXsteeringfeel**

We provide our customers with perfect prerequisites to successfully convert their ideas and inventions into marketable innovations and forward-thinking solutions.

Please keep informed on our website [www.mdynamix.de](http://www.mdynamix.de)

MdynamiX AG, Heßstrasse 89, 80797 München, GERMANY  
[www.mdynamix.de](http://www.mdynamix.de), [info@mdynamix.de](mailto:info@mdynamix.de)

# Chapter 1

## Introduction and History

Peter Pfeffer and Hartmut Ulrich

The main advantage of automobiles over the railway is that the driver determines the trajectory of the vehicle. In other words, motor vehicles can be steered and are not tied to any defined track. The steering assembly is part of the chassis. With the exception of aerodynamic forces, all the forces acting between the vehicle body and the road are transmitted via the chassis. The tasks of the chassis are typically divided into vertical, longitudinal and lateral dynamics. The lateral momentum is largely a function of the steering system in conjunction with the suspension and the tires.

The components of the steering system are the steering wheel, steering column, steering gear and tie rod (steering linkage) (Fig. 1.1). The driver gives his steering commands through the steering wheel. These are transferred via the steering column to the steering gear. Nowadays, the steering gear is usually implemented as a rack-and-pinion drive. It translates the rotary motion into a linear motion. The linear motion is transmitted to the wheel carrier via the tie rod with its ball joints. As the wheel carrier is not directly linked to the steering axle, the wheel is forced to perform a rotary motion around the steering axle. The lateral forces caused by the inclination of the wheel cause the desired yawing moment of the vehicle and thus the movement around the curve. To reduce the forces the driver has to apply when turning, the steering gear usually provides a support for the force of the driver. Steering systems with such a support are called power- or servo-assisted steering systems. The steering system has to allow for predictable and comfortable

---

P. Pfeffer (✉)

Munich University of Applied Science, Munich, Germany  
e-mail: peter.pfeffer@steeringhandbook.org

H. Ulrich

Hochschule Ruhr West—University of Applied Science, Mülheim an der Ruhr, Germany  
e-mail: hartmut.ulrich@steeringhandbook.org

**Fig. 1.1** Components of a steering assembly (*Porsche 997*)



driving without suppressing useful feedback to the driver. At the same time disruptive interferences coming from the road surface and the wheels should be kept away from the driver.

This steering handbook is aimed at experts working on the design and construction of vehicle chassis professionally, as well as students and lecturers at universities. It covers the scientific fundamentals of steering systems in motor vehicles. In addition, it documents the present state of the art and identifies current trends. Here, we make use of the expertise of many renowned experts from industry and academia.

The first few chapters deal with the history, the basic principles, and the different types of steering systems as well as the requirements they have to meet. We shall focus on steering kinematics, the requirements of driving dynamics, occurring vibrations, the steering experience of the driver, and the basic functional design (Chaps. 1–8). Chapters 9–15 deal with the different components of the steering system, from the steering wheel to the tie rod. We shall discuss the different types of steering gears such as hydraulic power steering (HPS) or electric power steering (EPS). Special types of steering systems such as the superimposed steering system (Chap. 16), four-wheel steering (Chap. 17) and steer by wire steering (Chap. 18) provide a significant number of additional functions. Chapters 19 and 20 deal with electronic stability control, driver assistance in steering systems and test systems for steering systems and offer an outlook on future trends.

## 1.1 Definition and Delimitation

The purpose of the steering system is to provide the driver with the possibility of lateral vehicle guidance, i.e. to influence the lateral dynamics of the vehicle. It is a system that connects the driver with the steered wheels of the vehicle. In most cases, turning the steering wheel causes a rotational movement of the steered wheels around the steering axles. This pitching of the (steered) wheels creates lateral forces which turn the vehicle around the vertical axis while driving. This manual covers the dynamics of this steering process in connection with the vehicle and the necessary components. These are the steering wheel, the steering column, the steering gear, the tie rods, the steering assistance and the components necessary for their control and power supply. As for the components of the axle we refer to the specialist literature (cf. Heißing and Ersøy 2007 or Reimpell and Betzler 2005). In addition we shall discuss special designs such as superimposed steering, rear-wheel steering, steer by wire, and active suspension, as well as driver assistance systems, which are closely related to the steering system. This book is limited to the steering systems of passenger cars (also referred to as vehicles in this book). The steering systems of racing cars, commercial vehicles, motorcycles, airplanes and trains will not be discussed in detail.

## 1.2 Task and Significance of the Steering System

Road vehicles are controlled by the driver almost entirely via the steering system. For traffic safety, it is crucial that the vehicle precisely follows the course set by the driver on the basis of the course of the road and the traffic situation and largely retains it (Braess and Seiffert 2007, p 580). The driver must always have the reassuring feeling that the vehicle responds predictably and reliably to his steering input. To ensure a high quality directional stability, it is crucial that the steering input is promptly translated by the steering system and the vehicle in the expected way, so that the driver can recognise changes of the course and, in turn react to them.

Developers of steering systems therefore have to consider numerous demands and tasks to achieve a customer-friendly design:

- Sufficiently low steering wheel torques and a narrow steering wheel angle required for parking
- Ease of movement, sensitivity, accuracy, a high degree of directional stability, sufficient immediacy and spontaneous responsiveness
- Pronounced road contact, responsiveness of tire-road adhesion
- Automatic return to the central position, good centering, stabilising behaviour in any driving situation
- Compensation of disturbance variables stemming from road surface irregularities, drive, braking, and irregularities of the tires

- Adequate absorption to suppress self-induced vibrations of the vehicle
- Compliance with the crash safety requirements and passenger safety regulations
- Low energy consumption
- Sufficiently low noise level
- Vibrational stability (no self-induced vibrations)
- Low wear and low maintenance over the entire vehicle life cycle.

### 1.2.1 Basic Types

The steering of two- or multi-axle road vehicles is generally affected by changing the angle between the vehicle's longitudinal axis and the centre planes of some, or all, of the vehicle wheels (Matschinsky 2007). The oldest type is the turntable steering, a design in which a rigid axle is turned around its centre (Fig. 1.2a). This turntable steering is commonly used in coaches and trailers. The same effect can be achieved by turning the front section of the vehicle towards the rear. This type of steering system is called articulated steering (Fig. 1.2b) and is primarily employed in machines and special purpose vehicles. A disadvantage for the turntable and articulated steerings may arise when disturbing forces occur, stemming from their reduced footprint and their long lever arm. This so-called kingpin offset at hub equals half the track width.

Modern road vehicles are almost exclusively steered at the front wheels with a so-called Ackermann steering. In the case of rigid axles this is designed with a continuous tie rod (Fig. 1.2c), in the case of independent suspension a split design of the tie rod is used, as shown in Fig. 1.2d in diagram form (cf. Chap. 4).

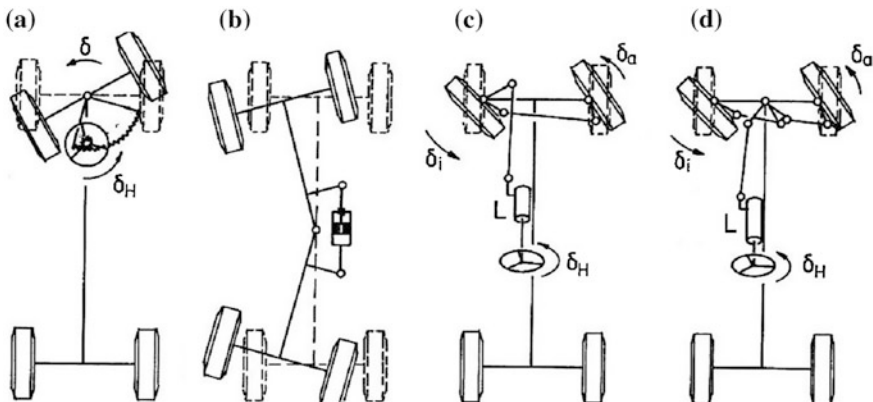


**Fig. 1.2** Basic types of vehicle steering systems (Matschinsky 2007)

### 1.2.2 Designs

The two standard designs of mechanical steering systems, as shown in Fig. 1.3, are recirculating ball steering and rack-and-pinion steering. Because of its reduced steering force recirculating ball steering is used mainly in the commercial vehicle sector and to some extent in SUVs, while rack-and-pinion steering is the most common approach in the passenger car segment. With the increase in car weight, purely mechanical steering has been gradually replaced by hydraulically assisted steering systems. Rack-and-pinion hydraulic power steering (HPS) has prevailed over recirculating ball hydraulic power steering, as it has proved to be a cheaper option.

The supporting power of HPS is provided by a volume flow, which is usually generated by a vane pump. This pump is driven by the internal combustion engine. A pump operating independently of the internal combustion engine is used for electro hydraulic power steering (EHPS). The flow rate can be controlled in some HPS systems and in all EHPS systems. This leads to very smooth and easy steering when parking. With increasing travel speed this flow rate is lowered to achieve a higher steering wheel torque to increase the stability of the vehicle. In addition to the hydraulically assisted steering systems, electrically assisted steering systems (electric power steering—EPS) are becoming more common. In these systems, the supporting power is generated by an electric motor, which is powered by the electrical system on board. Depending on the location of the electric motor in the steering system, the EPS can be subdivided into different designs (cf. Chap. 15).

In the superimposed steering system a synthetically generated steering angle is added to or subtracted from the steering angle given by the driver. Here, an ordinary hydraulic or electric steering system is amplified by a steering angle actuator.

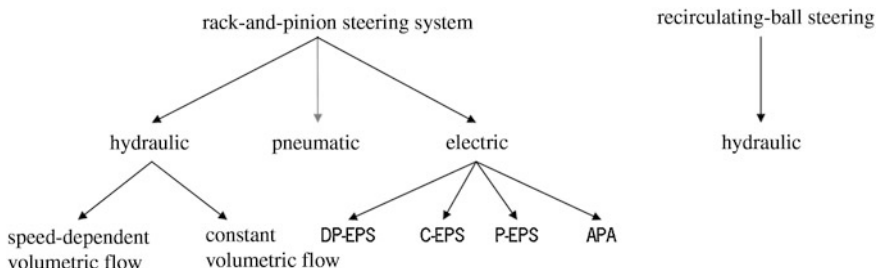


**Fig. 1.3** Breakdown of the standard designs of mechanical steering systems

### 1.3 History of Lateral Dynamics

In the early days of mankind single-axle carts were often drawn by animals or humans. Behind a long drawbar the cart followed. It was only when the driver himself was sitting on the cart that he could feel the forces acting on the steering axle. These are caused by different rolling resistance and irregularities on the road surface. For that reason the first and often very heavy steam vehicles were designed as tricycles with only one steered wheel (Fiala 2006). The single steered front wheel causes much smaller interference torques that need to be compensated by the driver. This explains why the first steering systems were partially self-locking.

The early motor vehicles in their present form were shaped by Gottlieb Daimler and Carl Benz. While Gottlieb Daimler devoted himself to the motorisation of existing vehicles such as carriages or velocipedes, Carl focused his attention on the problem of steering right from the beginning. In his Patent-Motorwagen of 1886 (Fig. 1.9) he eliminated the disturbances by means of fork steering with a zero offset radius, i.e. axial force fluctuations generated by irregularities of the road surface could not impact the actuating force. In contrast, axle pivot steering with its offset radius of half a track width is impeded very strongly. For this reason, this steering technique is nowadays only used for trailers, carriages, and special purpose vehicles. The steering systems of modern motor vehicles are derived from the axle pivot steering of Carl Benz's Patent of 1893 (cf. Sect. 1.3).

The influence of the steering system on vehicle behaviour was recognized quite early. In the annual issues of the periodical “Der Motorwagen” VII–X (from 1904 onwards) various theories of the sideway skid were published (Zomotor 1991). The engineers were particularly concerned with the question of how many and which of the wheels of the vehicle should be driven or steered. In 1907, in a lecture to the Berlin Automotive Engineering Society, Dr. Fritz Huth aptly summed up the following guiding principles:

1. “Any means to increase the friction on the ground is advantageous not only for the drive, but also improves steering and reduces skidding.”
2. It is advisable to steer *all four wheels of the car*.
3. It is always advisable and sometimes even necessary to drive each of the four wheels.
4. In cars with a two-wheel drive, the superiority of a front-wheel drive compared to a the rear-wheel drive is so marginal, that the additional complications resulting from combining steering and locomotion are not worth the effort.
5. The centre of gravity of the vehicle should be as close as possible to the middle of the car.
6. It is desirable that the relationship between friction and load is further investigated for different tires and road conditions.”

Thus the potential of four-wheel steering to improve driving behaviour was recognised even in the early phase of the automobile. Interestingly, in the same

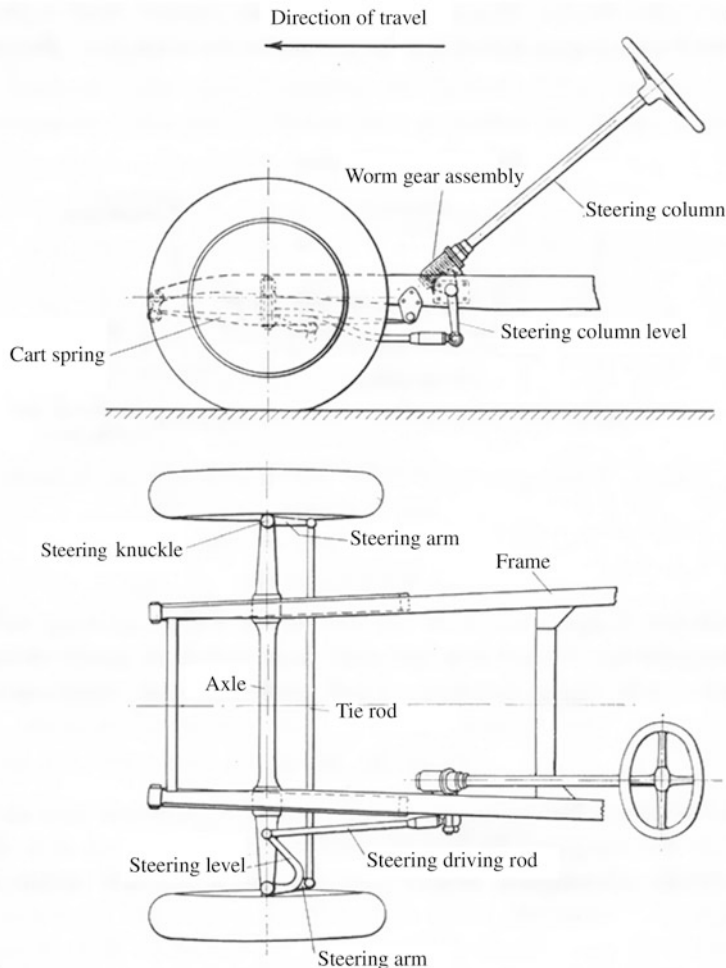


**Fig. 1.4** Schematic view of the standard steering system from 1930 (from Becker et al. 1931)

year a study was published by Lanchester of the “Institution of Automobile Engineers” (IAE), in which for the first time the term ‘oversteering’ was mentioned in connection with the phenomenon of sideways skidding (Fig. 1.4).

A further important step towards understanding the fast turning was the realisation that a tire needs a slip angle to transfer the lateral forces. This insight is attributed to Georges Broulhiet. In 1925 he published a report to the French Institution of Civil Engineers entitled ‘The Suspension and the Automobile Steering Mechanism’. These studies were certainly furthered by the first introduction of low-pressure tires by the Michelin Company for Citroën. But these tires produced the new safety-affecting phenomenon of shimmy to the steered wheels. Shortly afterwards Becker et al. (1931) published an in-depth analysis with

proposals to solve the ‘shimmy in automobile steering systems’ which became the most common steering design of the time (Fig. 1.11). In the context of these studies the first tire measurements were performed on a roller drum test rig. At around the same time, Sensaud de Lavaud worked on the mathematical theory of the relation between shimmy and rolling motion in Paris. He showed that the wheels must be uncoupled at the axles to prevent the vehicle from rolling. It was he who patented the swing axle in 1928. This design for driven rear axles dominated our streets until the sixties of the last century. Well-known examples of this design were the VW Beetle or the Tatra 87. De Lavaud was also the creator of the principle of the descending roll axle, i.e. the roll center is very low at the front of the vehicle, while it is located at the level of the suspension at the rear axle. One disadvantage was the resulting self-steering behaviour characterized by oversteering, which was, however, considered to be desirable at the time. In the Mercedes Benz Type 380 of 1933 a combination of decoupled front wheels and a descending roll axle was implemented. For the first time front wheels were linked to elastically mounted wishbones and mounted on unguided coil springs. This compliance enabled the wheel to move to the back when encountering obstacles, thus marking the beginning of elastokinematics.

Vehicle dynamics and self-steering behaviour were first systematically studied in the nineteen-thirties. The term *understeering*, which had been introduced by Lanchester, was complemented with the terms *oversteering* and *neutral behaviour*. These terms were first published by Maurice Olley in 1938 (Fig. 1.5), although he had already investigated vehicle dynamics at General Motors for many years before. As early as 1931 he had studied the importance of roll steer and the influence of tire pressure on vehicle stability. Later he established the definition of under- and oversteering, depending on the slip angles occurring at the front and rear axles. If these slip angles were greater at the front axle than at the rear axle, this was described as understeering, while the opposite was defined as oversteering. When these angles were similar at both axles, the vehicle behaviour was described as neutral. Nowadays, this definition is no longer used and has been replaced by a definition based on the occurring steering wheel angle gradient in relation to the lateral acceleration (see Chap. 5).

The above terms over- and under-steering are related to the stationary circular movement of a vehicle. At the same time the first transient driving tests were conducted (Stonex 1941). Stonex introduced the so-called checkerboard test, a drivability test similar to the step steering input.

By the end of the nineteen-thirties the theoretical treatment of stationary driving conditions had already been established. Our understanding of the transient vehicle behaviour was significantly enhanced by Riekert and Schunck (1940) in their ground-breaking study on the driving mechanics of rubber-tired motor vehicles. For the first time, they analytically solved the motion equations of a simplified vehicle model, which today is referred to as the single-track model. The two degrees of freedom used for the equation were the yaw and the sideslip angle, and even the aerodynamics were taken into account. Interestingly, their analysis concluded that all the vehicles of that time were unstable, even at low speeds.

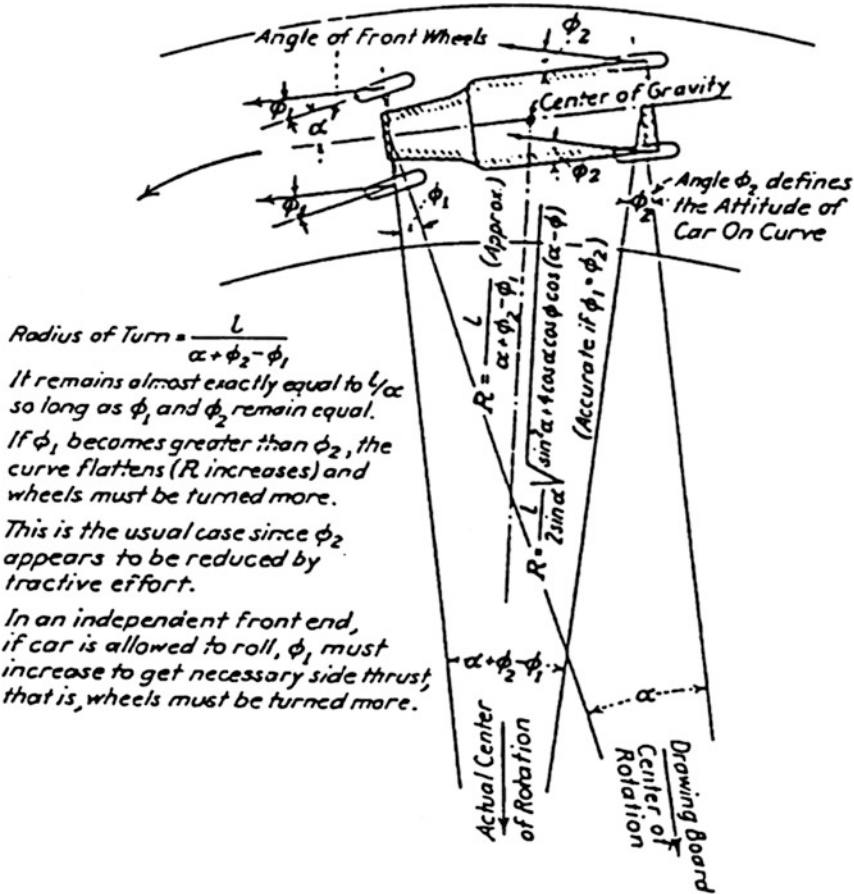


Fig. 1.5 First studies on vehicle dynamics by Olley (1934) (from Dixon 1996)

But these instabilities occurred only at high lateral acceleration and were produced by the saturation of the lateral traction of the tires. This paradox was only solved with the introduction of steering elasticity into the theoretical examination of vehicle behaviour by Fiala (1960). The reduction of lateral tire stiffness by the steering elasticity had already been recognised by Fujii (1956). Based on the findings of Riekert and Schunck, many other practical and theoretical studies followed in the nineteen-forties. The first basic theory of the pneumatic tire was formulated by Von Schlippe and Dietrich (1942). This theory describes the relationship between cornering stiffness, lateral tire stiffness, and the chronological sequence of the lateral forces subject to the slip angle.

Inspired by aircraft stability analysis, Milliken, Whitcombe, and Segel published a series of fundamental studies on vehicle behaviour at the IMechE in 1956 (Segel 1956). They extended Riekert's and Schunck's vehicle model to include the

additional degree of freedom of rolling and conducted thorough stability tests. Böhm (1961), Schmid (1964), and Mitschke (1968) pointed out that driving stability is not the same as directional stability. From then the studies on the steering feel of vehicles began. At the time the vehicles differed a lot in the steering characteristics and the required steering wheel torque. The driver, as a ‘controller’, was also taken into account. Segel (1964) presented the first reference values for optimally perceived steering wheel torque gradients as well as damping and friction in the steering system. Reference should be made here to the very comprehensive summary of the historical development of vehicle dynamics by Milliken and Whitcomb (1956) with an extensive bibliography. Other historical contributions can be found in Dixon (1996) or in Zomotor (1991). The theoretical foundations of vehicle dynamics were first summarised by Mitschke in his “Dynamik der Kraftfahrzeuge” (Dynamics of Motor Vehicles) first published in 1972. The current fourth edition remains the most comprehensive work on this subject.

In 1966 Ralph Nader (1996) published his “Unsafe at any Speed”. In this book he highlighted how critically unsafe the cars marketed at the time were. Among other things, he denounced the extreme oversteering driving behaviour of the Chevrolet Corvair, which led to many fatal accidents. Because of the strong political pressure afterward, the automotive industry started to improve the safety of their products and push the research into vehicle dynamics. Another consequence of the criticism was the launching of the Experimental Safety Vehicle (ESV) program by the NHTSA (National Highway Traffic Safety Administration), a sub-agency of the U.S. Department of Transportation. Its aim was to identify objective parameters for a safe vehicle. These efforts resulted in a series of standardized drivability tests and test methods, though they did not succeed in finding any comprehensive limits for the safety of the vehicle or the design of the steering system.

Due to unsatisfactory driving behaviour of the vehicles, better axle suspensions und safer vehicle designs were developed. Cars with swing axles disappeared from the market and were replaced by inherently understeering vehicles. This was realized by equipping front-heavy vehicles with a front-wheel drive. The most well-known example of this design is the Volkswagen Golf which was launched in 1974. Regarding the axle suspensions, the trend was towards independent suspensions, as they allowed an easier resolution of the conflicting goals. To improve steering and braking behaviour a negative offset radius and the Weissach axle were introduced in the nineteen-seventies. Increased attention was paid to the kinematic effects such as the roll steer and elastokinematics.

Other milestones included the introduction of the anti-lock braking system (ABS) in the nineteen-seventies and the large-scale production of four-wheel steering systems in the nineteen-eighties (see Chap. 17). With the introduction of a yaw-moment control (electronic stability program—ESP) an even greater improvement of the stability of the vehicle was obtained compared to four-wheel steering, so that the latter system was forced out of the market again. But in recent years, four-wheel steering is once more in the ascendant. The superimposed steering system (Chap. 16) has been reserved to the optional equipment of

premium vehicles up to now. The same applies to systems which influence the yawing moment via drive torques, the so-called torque vectoring. In recent years, the introduction of driver assistance systems has come to the fore. Many of those systems are based on the steering or use the steering as an actuator ([Chap. 19](#)). Here we shall only mention steering torque overlay systems and the parking assistant. Chapter [20](#) presents an outlook on future systems.

## 1.4 The History of Vehicle Steering Systems

With the development from towed vehicles to powered vehicles, from a chassis with rigid axles to a single-wheel chassis and the constant increase of vehicle speeds and traffic requirements, demands on the steering equipment of vehicles have become more and more complex.

For motorised vehicles, the hitherto proven turntable steering for carriages was replaced by the Ackermann steering. To reduce the steering forces various types of mechanical steering gears were developed over the decades, until finally in the nineteen-fifties hydraulic power steering systems were introduced for commercially available cars. These were complemented by electric power steering systems in the nineteen-nineties. Advances in mechatronics finally enabled the serial production of active steering systems.

### 1.4.1 Turntable Steering

Transom and turntable steering were invented in the Celtic and Roman era. In the Roman chariot ([Fig. 1.6](#)) the front axle could swing around the lynchpin through which it was connected to the drawbar and its shafts. The front of the chariot was supported by the transom under the perch and thus maintained in a horizontal position.

Turntable steering allowed wide steering angles and hence a good steerability of the vehicle. There was however the danger of tilting the chariot, when the axle was turned strongly in curves. For towed vehicles, the turntable steering proved to be satisfactory. The steering was affected only slightly by bumps in the track, since the tensile forces acting in the steering direction counteracted the resistances of the track surface.

Because of the limitations of available materials and the slow speeds which could be attained by horse-drawn vehicles, the steering systems made only slow progress in the following centuries. The basic principle of turntable steering was retained, although the transom and the lynchpin were gradually replaced by ball rows and ball joints.

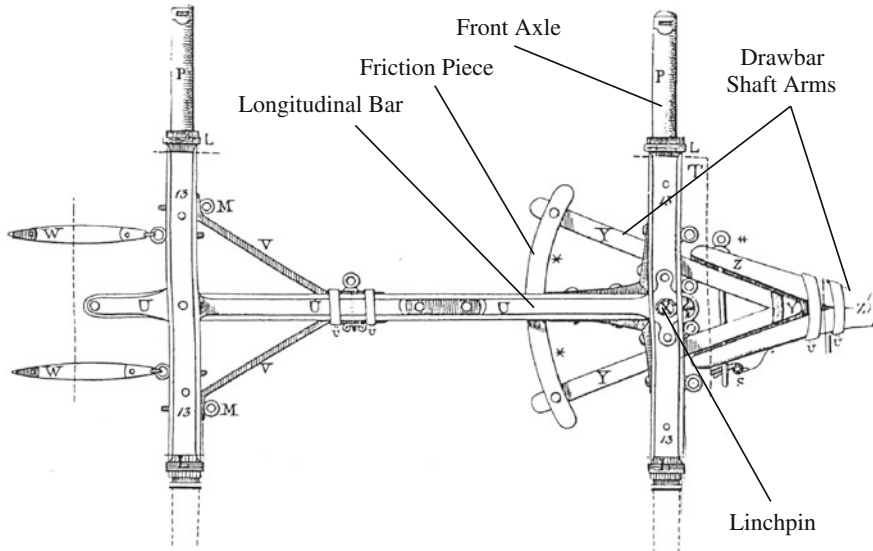


**Fig. 1.6** Roman chariot with turntable steering, Eckermann (1984)

### 1.4.2 *The Ackermann Steering*

Increasing passenger transport and higher demands on the comfort and speed of the vehicles promoted the evolution of the coach chassis, until, in 1816, the carriage builder Georg Lankensperger received the royal privilege from the Bavarian Court of producing a type of axle pivot steering which made use of steering arms and tie rods.

The characteristic feature of this steering architecture is that the wheels of an axle are mounted on steering knuckles, which are pivotable about almost vertical steering axles. In a curve the inside wheel has to be turned to a narrower angle than the outside wheel. In addition, the extensions of the axles of the left and right front wheels have to intersect at a point which is on the extension of the rear axle (Fig. 1.7).

In 1818 Georg Lankensperger had his invention patented by his friend Rudolf Ackermann under the number 3212 in England, which is the reason for its designation as Ackermann steering.

### 1.4.3 *The Steering of the First Motor Vehicles*

The matter of steering gained additional relevance with the development of lightweight, high-speed petrol engines and the first motor vehicles by Gottlieb Daimler and Karl Benz.

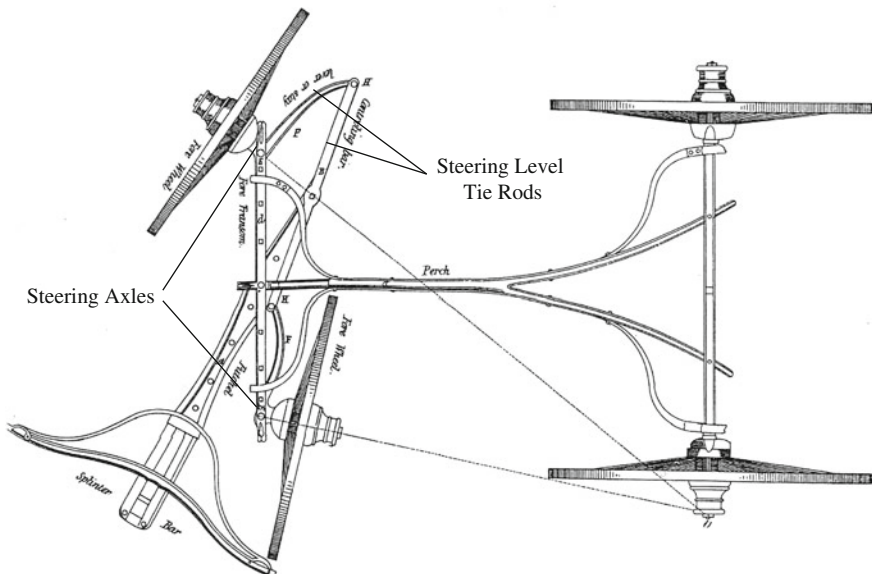


**Fig. 1.7** Lankensperger's axle pivot steering with a continuous tie rod, Eckermann (1998)

Daimler's first automobile in 1886 emerged from a carriage (Fig. 1.8), the rear wheels of which were driven via a belt drive. The steering system was a turntable steering, which was operated by the driver via a steering tiller. The tiller was used to rotate the steering column, which—via a pinion and a turntable—turned the front axle around a central stud. In spite of the low travel speed of the carriage car—about 10 km/h—the steering system was suitable to only a limited extent. Due to the large lever arm between the wheel and the swiveling axis, obstacles which were passed by one of the wheels produced steering forces which were difficult to master by the driver at the tiller.

Benz solved this problem when he developed his Patent-Motorwagen in 1886 (Fig. 1.9) by using only one front wheel which, like a bicycle, was steered by fork steering.

The rotation of the steering column, which was effected by turning the tiller, produced, via the pinion and the rack, a displacement of the steering rod. This in turn rotated, via the steering arm as the lever arm, the steering fork with the front wheel.

A disadvantage of the vehicle was its low tipping stability, which led Wilhelm Maybach in 1889 to develop his “Stahlradwagen” (Fig. 1.10), a chassis which was entirely independent of the principles of carriage construction. Like Benz, he was inspired by the principles of bicycle construction.

Maybach transferred the movement of the steering tiller via a V-shaped pitman arm and two tie rods to the front wheel forks. As Maybach had no knowledge of

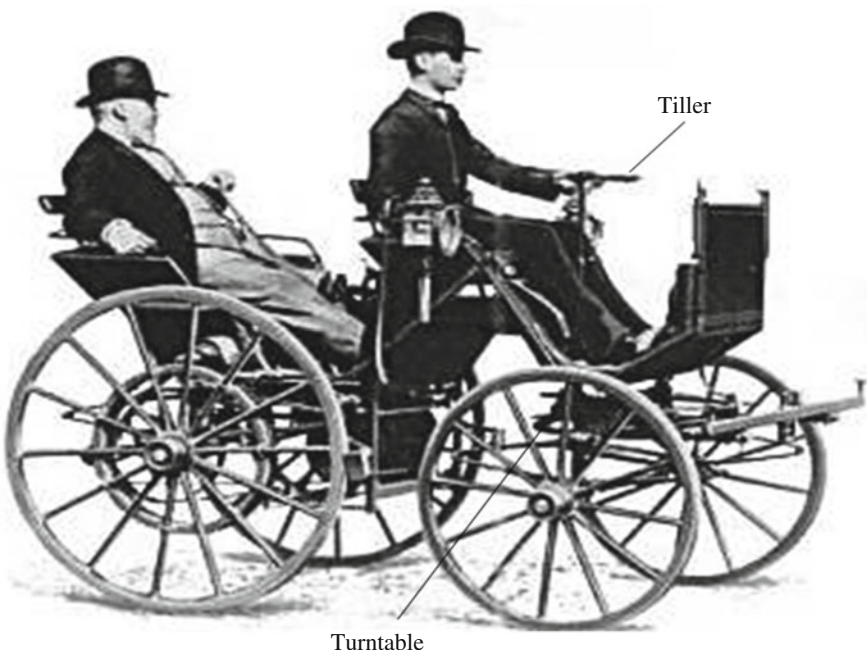


**Fig. 1.8** Daimler motor carriage with turntable steering, Walz (1983)

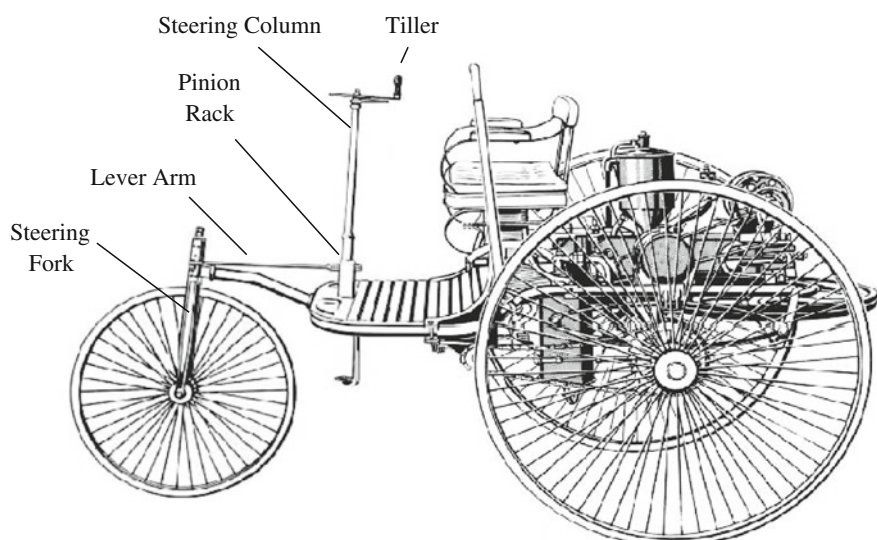


**Fig. 1.9** Benz Patent-Motorwagen with fork steering

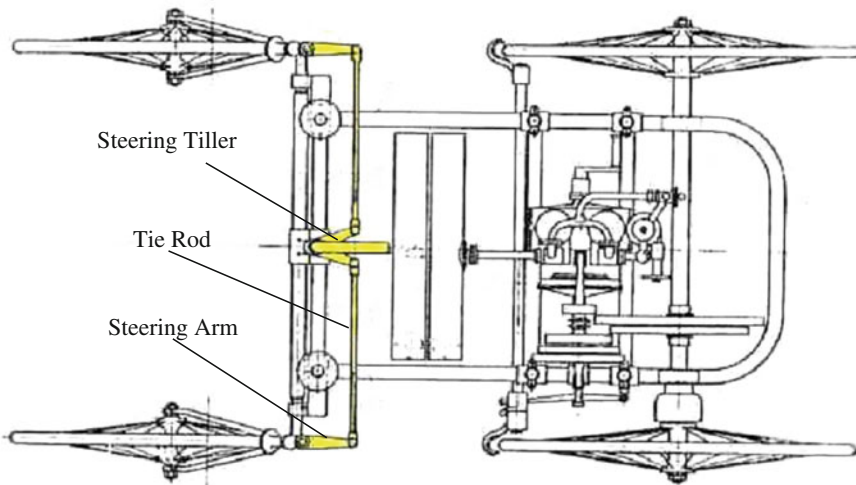
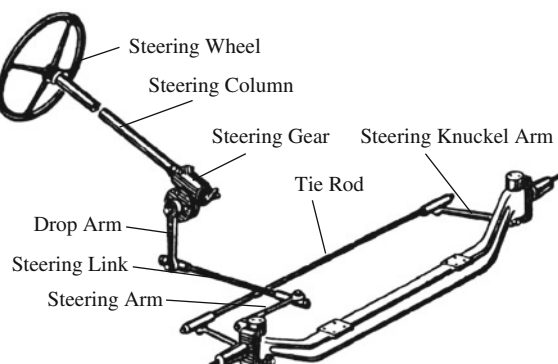


**Fig. 1.10** Maybach Stahlradwagen with fork steering, Walz (1983)

the Ackermann steering architecture, which had already been patented in England in 1818, the steel-spoked wheels with solid rubber tyres of the Stahlradwagen remained parallel to each other even in curves.

After Ackermann, Bollée received a second patent for axle pivot steering in France, and Benz received the third patent for the same solution in 1893. He employed it for the first time on his Victoria automobile. Despite its significantly improved steerability the steering forces affecting the vehicle were still very strong. In the following years better steering gears were developed, with which virtually every new automobile was equipped by around 1900 (Fig. 1.11).

**Fig. 1.11** Steering system in a vehicle with a rigid axle



#### 1.4.4 Mechanical Steering Gears

Steering gears transmit the movement of the steering wheel to the steering linkage and thus to the front wheels. In addition, the forces acting on the wheels are transmitted via the steering gear to the steering wheel as manual force and steering torque. The steering gear essentially determines the steerability and manoeuvrability of the vehicle. The transmission ratio of the steering gear has to be designed in such a way that, on the one hand, the driver can apply the required steering torques in any situation, while on the other hand the number of turns of the steering wheel should not get too high when cornering.

Mechanical steering gears have gone through various stages of development. Development was mainly pushed in the United States, where first the Electric Motive Power Co. and then the development departments of the automotive manufacturers expanded their efforts into the evolution of the steering gear. After spur gears and screw-and-nut type steering gears, worm gears with wheel sectors, fingers, rollers, and recirculating balls (Fig. 1.12) were introduced onto the market.

P. W. Northey invented the worm-and-wheel steering gear. If the worm is set in motion by a turn of the steering wheel, the wheel sector which touches the worm is turned and drives the pitman arm.

This system was revised by Henry Marles, who introduced his design of a “drive shaft steering” in 1913. A steering finger which is stationary or mounted on roller bearings engages into the thread of the steering worm and transmits the rotational movement of the worm into a pivoting movement of the pitman arm.

Ten years later Robert Bishop received a patent for his simpler cam-and-roller steering gear with a conical roller.

Finally, the recirculating ball gear was developed. The worm has a round thread with recirculating balls, which drive the steering nut. The teeth on the nut then transmit the movement onto the steering linkage.

Together with the issues of wear and adjustability, the aspects of friction and efficiency have been a main driving force for the evolution of steering gears.

The one-finger steering system is commonly known as Ross steering (Fig. 1.13). Since the nineteen-thirties this type of steering system has been

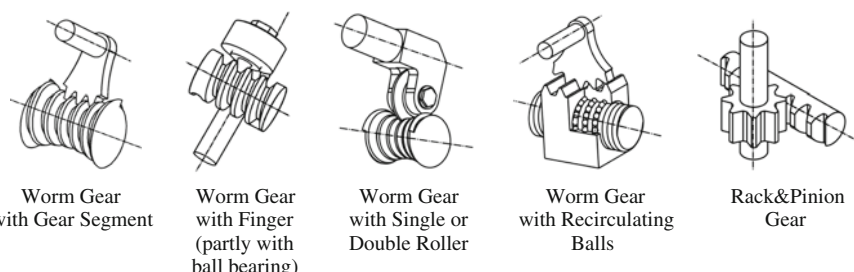
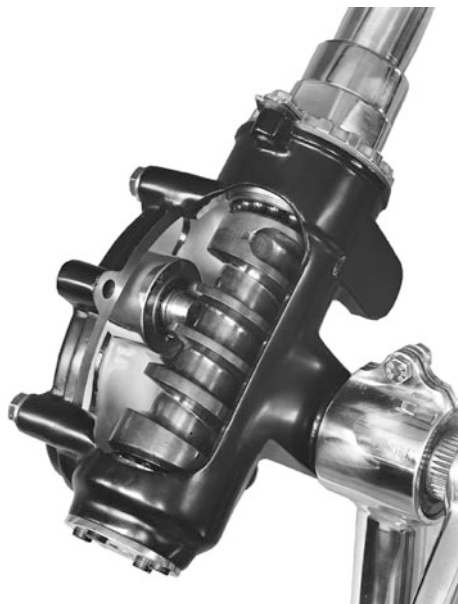


Fig. 1.12 Basic designs of steering gears

**Fig. 1.13** ZF Ross steering

produced by the company ZF Zahnradfabrik Friedrichshafen for passenger cars and commercial vehicles.

Rack-and-pinion steering gears (Fig. 1.12) represent another step in the evolution of steering drives. Rack-and-pinion steering systems proved to be inexpensive and—due to the direct transmission of the steering forces to the tie rods—to have a high degree of rigidity, which is advantageous in particular for the steering precision, though it increases the bumpiness of the steering. By bearing the steering housing in rubber and using elastic clutches in the steering column the bumpiness and transmission of vibrations to the driver could be reduced, though this negatively affected the steering precision.

With the reduction of friction in the steering gears an additional damper had to be introduced to reduce the steering vibrations and the bumpiness. In rotary steering gears it was often attached to the idler arm or the drag link. In rack-and-pinion steering systems, with tie rods at the end of the rack, the vibration damper could be arranged parallel to the rack or integrated into the steering unit.

#### **1.4.5 Power Steering Drives**

Despite all the advances of the mechanical steering gears a need for an auxiliary power arose, which would improve the steerability of the vehicles without compromising their manoeuvrability. Vehicles were getting heavier and heavier and with the introduction of pneumatic tires with low pressure, the steering forces

steadily increased. By the mid-nineteen-forties the steering torques for heavy passenger cars in the USA reached values of up to 80 Nm on dry concrete, although very indirect total steering ratios of 24:1 were applied, Davis (1945).

Chrysler was the first automotive manufacturer to introduce a power-assisted steering system for their models New Yorker and Imperial in 1951. This steering system was based on the patents of Francis W. Davis. Davis, however, had developed his power steering almost 30 years earlier. He can be regarded as the inventor of power steering.

Davis studied engineering at Harvard University from 1906 to 1910 and began his professional career at Pierce-Arrow in Buffalo, where he worked in manufacturing at first, then in test drives for trucks and finally in the sales department. His first invention in the field of steering systems was a rubber block for the steering column which could absorb the shocks coming from the road into the steering wheel. But he believed that the real solution to all the steering problems was the development of a power-assisted steering system. Although the first patents had already been granted for power steering systems for ships and vacuum-powered steering systems for wheeled vehicles, there was no principle which had prevailed for the application in motor vehicles.

Davis left Pierce-Arrow in 1922 and started to freelance as an engineer. Due to his experience with hydraulic presses acquired during his time at Pierce-Arrow he opted for hydraulics as the assisting power when he developed power steering. He tried to apply the classic principle of the hydraulic drive to the motor vehicle. This consisted of a pressure supply with a pump, a reservoir, and valves which would be opened only when hydraulic pressure was required in the drive. But in this he failed because of the many sealing and leakage problems which occurred under high pressure.

Davis asked himself whether he could not reverse the steering system and let the oil flow without pressure as long as power assistance was not required, so that the valves would only close to build up pressure when steering was used.

He then developed the principle of the open-center valve. Based on a steering gear with a shaft and a nut he designed and built the first power steering gear, together with his mechanic and toolmaker George W. Jessup. The first power steering gear. As there were no suitable hydraulic pumps available on the market, he developed an additional 3-piston pump which was driven by the combustion engine.

In 1925 he equipped his own 1921 Pierce-Arrows Roadster with power steering and optimized the system. In 1926 he applied for the patent on the principle of power-assisted steering in the U.S. (Fig. 1.14).

The rotation of the steering shaft is converted via a pinion-and-nut connection into a linear movement of the inner valve sleeve of the open-center valve (29). Due to the variation of the opening cross sections (control edges) of the open-center valve, a pressure difference builds up in the cylinder chambers (27, 28) and the piston and the outer part of the valve (26) move until the initially introduced shift is compensated.

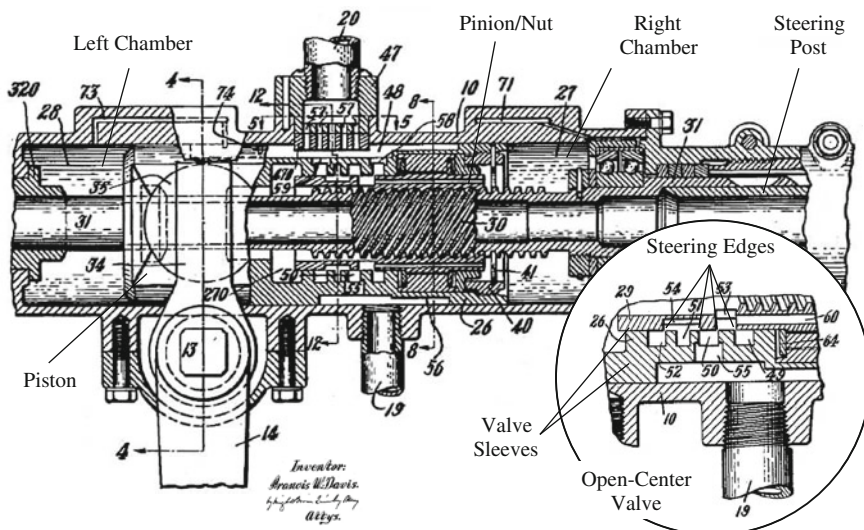


**Fig. 1.14** Patent drawing (US 1,790,620) for the hydraulic steering gear of F. W. Davis

Davis's steering gear, strictly speaking, is a hydro-mechanical position feedback control. With this principle, however, the driver needs to apply barely any force. This means that in a power steering system, the driver receives hardly any feedback concerning the forces acting on the wheels as steering torque.

Davis recognised this disadvantage. The steering could be easily operated by the touch of a finger on the steering wheel and was therefore hard to sense. He therefore developed a preloaded spring mechanism that was integrated into the steering valve. To actuate the valve a force had to build up against the spring assembly. In connection with the design of the control edges of the valve and the stiffness and preload of the spring assembly, Davis had invented a mechanism with which the steering feeling could be accurately set.

With this kind of power steering Davis wanted to conquer the American automotive market. In October 1926, he presented his vehicle with power steering to the professional world, to the automobile manufacturers General Motors, Packard, and Chrysler, as well as the suppliers Gemmer, Saginaw and Timken. Everybody was excited about the car with its very direct steering ratio of 8:1, which could be steered easily without showing any steering wobble or shimmy.

General Motors made sure to get the cooperation of Davis, and within the following four years the power steering system was optimised for use in commercial vehicles and large cars. The number and quality of the ideas Davis had developed and patented for his hydraulic power steering, such as the rotary valve with C spring (Fig. 1.15), is truly remarkable. In this example the control or spline valve is rotated together with the steering post. The differential angle between the two rotary valve sleeves causes the control edges to open and close. At the same time the differential angle is fed back to the driver as a steering torque via the

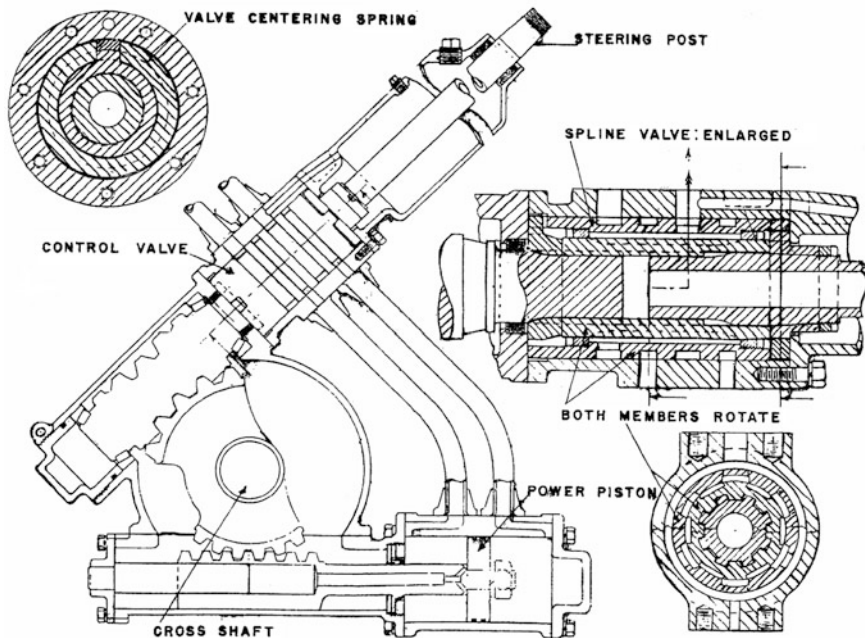


**Fig. 1.15** Steering gear with rotary valve and C spring, Davis (1945)

preloaded rotating C spring (valve centering spring). The principle of the rotary valve is still to be found in modern hydraulic steering gears (see [Chap. 11](#)).

In 1933 power steering was sufficiently advanced to be ready for serial production. It had been planned to install it into Cadillac vehicles, but due to the Great Depression Cadillac had to reduce its production to a mere 15,000 vehicles a year. As the additional costs of tools and the manufacturing of power steering would have been too high for such a small number of vehicles, General Motors halted the project. This delayed the introduction of power steering for almost two decades.

Davis terminated his cooperation with General Motors and searched for new clients. In 1936 he entered into cooperation with Bendix. Bendix equipped a number of different test vehicles with hydraulic power steering and, interestingly, Buick, a division of General Motors, wanted to introduce the system. But the Second World War abruptly stopped all activities in the field of civilian automobile production.

On the other hand, a different door was opened for Davis's power steering. The American and British armies equipped their military vehicles with the Bendix-Davis steering system. More than 10,000 steering systems had to prove themselves under the conditions of an army at war. After the war this experience opened the market for earth-moving equipment, tractors, busses and trucks.

Davis was still trying to win over the passenger car industry for his steering system, but to no avail. The time for that had not yet come.

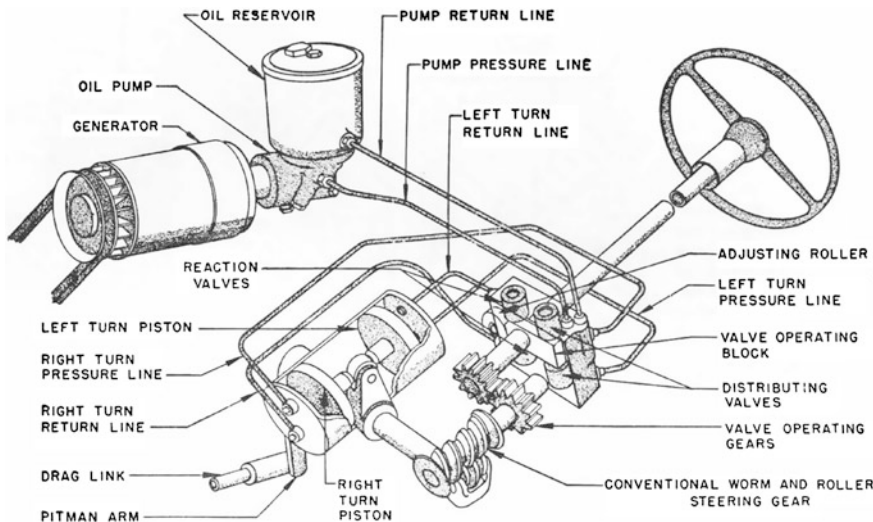


**Fig. 1.16** Principle of the Hydraguide power steering by Gemmer

In 1951 Chrysler was the first automotive manufacturer to introduce power steering onto the market. The steering system was produced by Gemmer and was based on an expired patent of Davis's (Fig. 1.16).

In this steering system, the steering column consists of two parts, which are connected to each other by a flexible clutch. The lower part is mounted in a self-aligning ball bearing and in a bearing of the valve housing in such a way that a small angular deflection around the self-aligning bearing is possible. At the lower end of the steering column a drive pinion is mounted, it engages with a toothed wheel at the upper end of the worm shaft.

When a steering torque is applied, the lower part of the steering column is deflected and actuates the four seat valves in the valve block by a few tenths of a millimeter. The change in the flow passages produces a supporting pressure difference at the pistons.

Although Davis did not draw any financial benefit from the introduction of the steering system by Chrysler, he was neither angered nor worried. As he had expected, he soon got a call from General Motors asking for his support with the immediate introduction of power steering systems. From now on the only question that mattered was how fast and how many power steering systems could be built.

This was the breakthrough of power steering. Within two years, the production soared to a million steering systems per year. In 1956 one in four new vehicles delivered in the United States was equipped with hydraulic power steering. For the German market, the Gemmer steering system had been produced under license by the ZF Zahnradfabrik Friedrichshafen since 1953, Fig. 1.17.

From the beginning, hydraulic power steering gears were supplied almost exclusively by pumps which were driven by the combustion engine via a belt.

**Fig. 1.17** ZF-Gemmer hydro steering



For reasons of space there were a few applications in which the pump was driven by an electric motor. To save energy, such electric pump units were serially introduced in passenger cars by the end of the nineteen-nineties. The development of electric motors and pumps with high individual efficiency and a demand-dependent control of the pump speed led to significant energy saving of these electro-hydraulic steering systems in comparison with conventional systems using a belt-driven pump (cf. [Chap. 14](#)).

In the course of the history of the steering system there had been numerous ideas and patents for purely electrically supported power steering systems and even for electric steer by wire systems, long before the hydraulic and electro-hydraulic systems were launched onto the market. But it was only much later that developments such as the patent of the Gemmer company from 1972 ([Fig. 1.18](#)) were proposed, and they could be implemented and marketed.

The manual torque of the driver is detected by the torque sensor. The calculation unit then calculates the required power assistance and actuates the electric motor, which transmits the torque either directly or via another drive to the mechanical steering gear. A remarkable feature of the patent is that the vehicle speed is already taken into account as an input variable of the calculation unit, so that it is possible to adapt the steering feel to the driving situation.

A first application of such an electro-mechanical steering system can be found in the Japanese compact car Suzuki Servo of 1988 ([Stoll 1992](#)), [Fig. 1.19](#). Due to the low front axle load of the vehicle, it was possible to design the power steering on a purely electrical basis, although the electric motor had a capacity of only 240 W.

The basic structure of modern electro-mechanical steering systems with a torque sensor, a geared electric motor, a controller and a mechanical steering gear

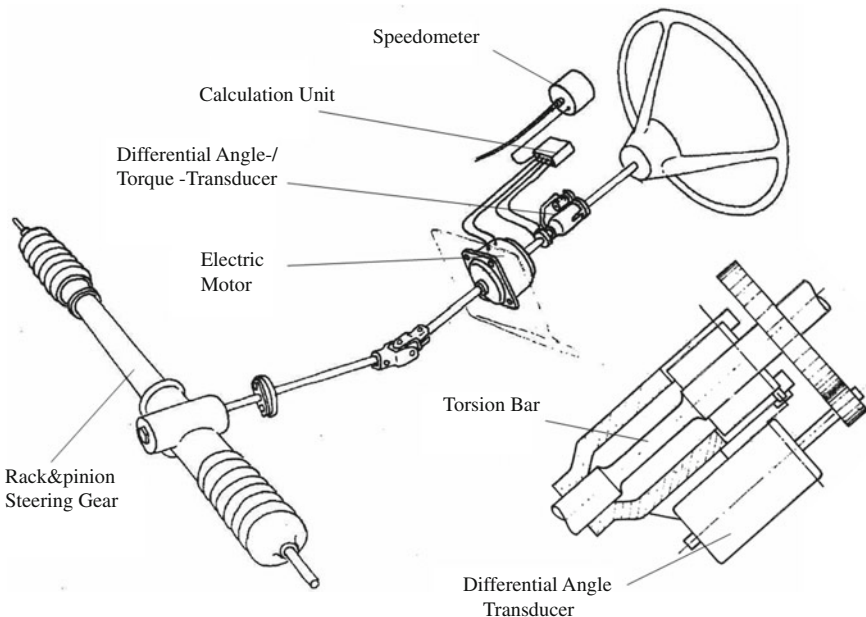


**Fig. 1.18** Patent drawing (DE 2 237 166) of an electro-mechanical power steering system, Gemmer 1972

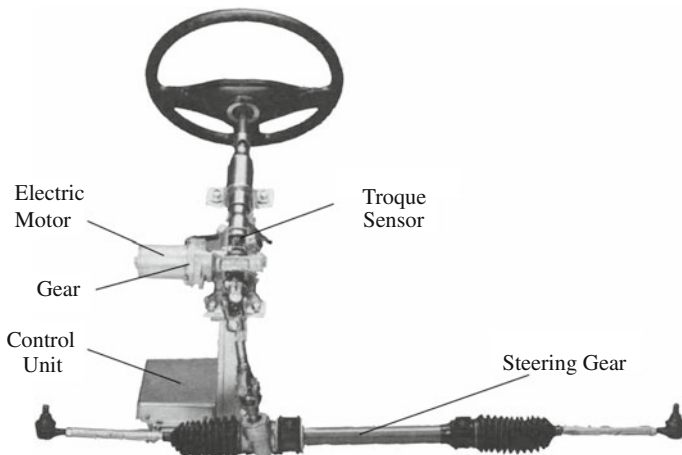


**Fig. 1.19** Electro-mechanical steering column unit (from Stoll 1992)

has remained unchanged to this day (cf. [Chap. 15](#)). The spatial arrangement varies, depending on application. The engine performance and, of course, the computational ability of the control units have increased dramatically, so that nowadays,

electro-mechanical steering can be considered to be the standard steering system for passenger cars, both for energetic and functional reasons.

Lankensperger's invention of the axle pivot steering only gained acceptance with the development of the motor vehicle. Hydraulic power steering was marketed for passenger cars only after the Great Depression and World War II. The triumph of electrically assisted and electromechanical steering systems was driven by the increasing demand for energy efficiency and emission reduction. Inventions take time. Technical, economic and political conditions must be met before even brilliant ideas can be implemented in the serial production of the automotive industry.

## References

- Becker G, Fromm H, Maruhn H (1931) Schwingungen in Automobillenkungen ("Shimmy"). Bericht der Versuchsanstalt für Kraftfahrzeuge der Technischen Hochschule zu Berlin, Krayn Verlag: Berlin 1931
- Böhm F (1961) Fahrtrichtungsstabilität des Kraftwagens, ATZ Vol. 1963, No. 5, May 1961
- Braess H-H, Seiffert U (2007) Vieweg Handbuch für Kraftfahrzeugtechnik, 5th edn. Vieweg +Teubner Verlag, Wiesbaden
- Davis FW (1945) Power steering for automotive vehicles. SAE Paper 450181
- Dixon JC (1996) Tires, suspension and handling, 2nd edn. Society of Automotive Engineers, Warrendale, Pa. 1996
- Eckermann E (1984) Vom Dampfwagen zum Auto, Motorisierung des Verkehrs. Rowohlt Taschenbuch Verlag GmbH, Hamburg
- Eckermann E (1998) Die Achsschenkellenkung und andere Fahrzeug-Lenksysteme. Deutsches Museum, München
- Fiala E (1960) Zur Fahrdynamik des Straßenfahrzeugs unter Berücksichtigung der Lenkelastizität. ATZ Automobiltechnische Zeitschrift 62 (1960) 3, pp 71–79
- Fiala E (2006) Mensch und Fahrzeug: Fahrzeugführung und sanfte Technik. Vieweg+Teubner Verlag, Wiesbaden
- Fujii S (1956) The influence of elasticity of the steering mechanism on the motion of the vehicle. Trans Jpn Soc Mech Eng 22(119):492–496
- Heißing B, Ersoy M (2007) Fahrwerkhandbuch, 1st edn. Vieweg+Teubner Verlag, Wiesbaden
- Milliken WF, Whitcomb DW (1956) General introduction to a programme of dynamic research. Proc Auto Div Instn Mech Eng 1956(7):287–309
- Mitschke M (1968) Fahrtrichtungshaltung—Analyse der Theorien. ATZ 70, 1968, No. 5
- Matschinsky W (2007) Radführungen der Straßenfahrzeuge, 3rd edn. Springer, Berlin, Heidelberg
- Nader R (1966) Unsafe at Any Speed—Designed-In Dangers of the American Automobile. PB Special, New York
- Reimpell J, Betzler JW (2005) Fahrwerktechnik: Grundlagen: Fahrwerk und Gesamtfahrzeug. Radaufhängungen und Antriebsarten. 5th ed. Vogel Buchverlag: Würzburg
- Riekert P, Schunck TE (1940) Zur Fahrmechanik des gummibereiften Kraftfahrzeugs. Ingenieur Archiv 11(3):6, pp 210–224
- Schmid C (1964) Fahrsicherheit durch Konstruktion. Fisita
- Segel L (1956) Theoretical prediction and experimental substantiation of the response of the automobile to steering control. IMechE. Proceedings of automobile division, research in automobile stability and control and in tyre performance, 1956–1957, pp 310–330

- Segel L (1964) An investigation of automobile handling as implemented by a variable-steering automobile. *Hum Factors* 6(4):333–341
- Stoll H (1992) *Fahrwerktechnik: Lenkanlagen und Hilfskraftlenkungen*. Würzburg, Vogel Buchverlag
- Stonex KA (1941) Car control factors and their measurements. SAE Paper 410092, Society of Automotive Engineers: Warrendale, Pa
- Von Schlippe B, Dietrich R (1942) Zur Mechanik des Luftreifens. Zentrale für wissenschaftliches Berichtswesen, Berlin Adlershof
- Walz W (1983) Daimler-Benz, Wo das Auto anfing. Verlag Friedr. Stadler: Konstanz
- Zomotor A (1991) *Fahrwerktechnik: Fahrverhalten*. ed.: Reimpell J., 2nd ed., Vogel Buchverlag: Würzburg

# **Chapter 2**

## **Basic Principles of the Steering Process**

**Peter Pfeffer, Jens Holtschulze and Hans-Hermann Braess**

When we drive a car we do not really think about the steering process and the lateral control of the vehicle. Driving has become a natural and familiar action. In our childhood we learn and internalize this complex process on a tricycle or in a bobby-car. Without any conscious thought, our reflexes control all the actions we perform to drive the vehicle. But modern axle kinematics and power steering systems are the result of over a century of continuous optimization. And yet, the automotive press frequently criticizes the steering characteristics of motor vehicles.

### **2.1 Steering: Lateral Control of Vehicles**

The process of driving a car can be split into two sub-tasks. With the accelerator and the brake pedals, the driver controls the speed and thus the longitudinal movement of the vehicle. The steering wheel is the lateral actuator that influences the vehicle's lateral movement. This corresponds to two degrees of freedom of movement, yaw (rotation around the vertical axis) and thrust (translation into the lateral direction) (For a detailed definition cf. DIN 70000 or ISO 8855). The occurring lateral forces also affect other degrees of freedom, in particular swaying

---

P. Pfeffer (✉)

Munich University of Applied Science, Munich, Germany  
e-mail: peter.pfeffer@steeringhandbook.org

J. Holtschulze

BMW Group, Munich, Germany  
e-mail: jens.holtschulze@steeringhandbook.org

Hans-HermannBraess

Ehemals BMW AG, Munich, Germany

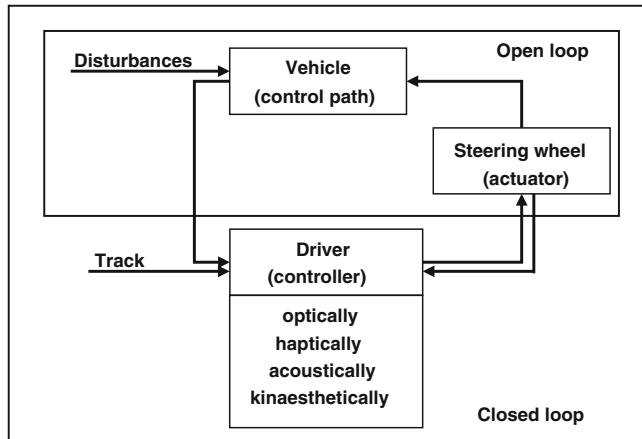


**Fig. 2.1** Closed loop driver—vehicle

(rotation around the longitudinal axis of the vehicle). These lateral forces are transmitted by the steering system from the steered axle to the driver.

Driving can be considered a control task. The driver is the controller and the vehicle is the control path. Figure 2.1 illustrates the lateral guidance of a vehicle. In a closed loop, the driver visually and kinesthetically takes in the course of the vehicle and uses the steering wheel as an actuator to follow the course of the road. The resulting actuating force provides him with an immediate feedback on the condition of the road and possible sudden changes of the friction coefficient. Through the input of the steering wheel angle the direction of the course is changed, this change is perceived by the driver, and thus the loop closes. There are additional interferences acting on the closed loop, such as side winds, uneven road surfaces and influences of the drive train. These have to be compensated by the driver, too.

For the vehicle developer, the control path, i.e. the vehicle and the steering system, are at the center of his interest. Therefore, a lot of vehicle dynamics tests that take no account of the driver have been developed (Chap. 7). In these, a predefined steering angle or steering wheel torque input is applied to measure or simulate the response of the vehicle as lateral acceleration, roll frequency, yaw frequency, and steering wheel torque. According to DIN 70000 the following control modes are to be distinguished:

- Position control: A predefined motion is applied to any point of the steering system (steering wheel, steering column, rack, ...)
- Fixed control: An arbitrary point in the steering system is locked. Usually it is the steering wheel which is fixated.
- Force control: An actuating force is applied to an arbitrary point and continues to act on this point independently of its displacement.
- Free control: In this special case of power-dependent steering no actuating forces are applied to the steering system.

With the help of powerful GPS-based gyroscopic platforms and automated steering machines, which have become available in the last few years, it is now possible to follow road courses with a high degree of precision. Strictly speaking though, these tests are closed-loop tests, in which the driver is simply replaced by a physical control unit.

## 2.2 Cornering

When cornering, the vehicle itself, and thus the control path, is analyzed. In general, a distinction is made between slow and fast cornering. In the process of slow cornering the vehicle is moved slowly, so that no considerable lateral acceleration occurs. The tire rolls towards its center plane. During the process of fast cornering, in contrast, lateral acceleration takes place, which causes a centrifugal force towards the outside of the curve. This centrifugal force has to be absorbed by the tires.

### 2.2.1 Slow Cornering

When a curve is negotiated slowly, the wheels try to roll towards their center planes without any occurrence of a slip angle. For this to happen, the normals to the center planes of the wheels have to intersect at a point, the so-called instant center (Fig. 2.2). These conditions are met by the so-called Ackermann steering angles at the front wheels (cf. [Chap. 4](#)). The Ackermann law states, that the front wheel on the inside of the curve has to be steered to a steeper angle than the wheel on the outside. This condition has to be met at least approximately by steering kinematics (cf. [Chap. 4](#)).

### 2.2.2 Fast Cornering

During the fast cornering process the vehicle turns around its instant center, too (see Fig. 2.3). Now a significant rotational or lateral acceleration of the vehicle takes place, this produces tire forces, and these tire forces in turn produce acceleration. For the cornering process, mainly the lateral forces are important. These forces occur, when the direction of movement of the wheel center is not in the center plane of the wheel. The angle contained between the movement direction and the center plane of the wheel is referred to as the slip angle  $\alpha$ . The lateral forces have to occur at the rear wheels as well. In vehicles with a steered front axle this leads to a shift of the instant center to the front (see Fig. 2.3).

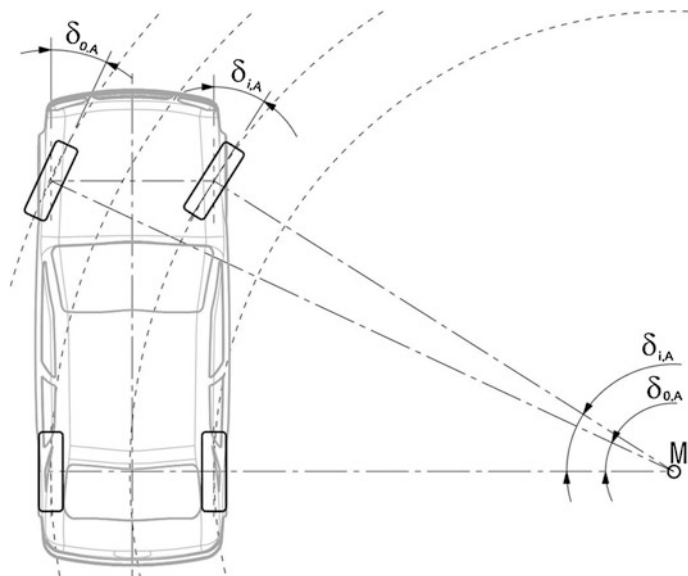


**Fig. 2.2** Slow cornering

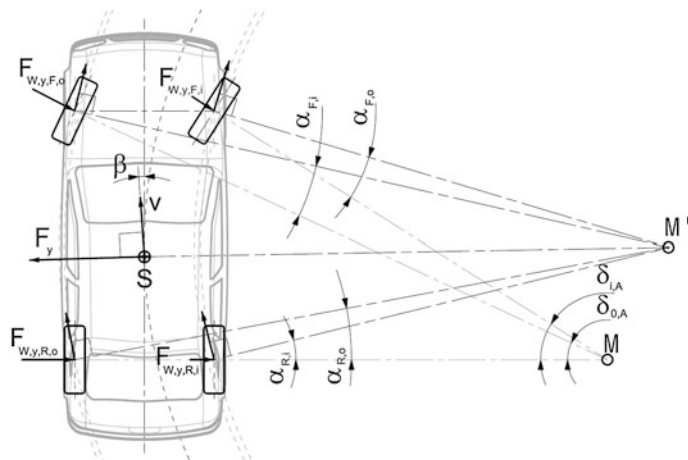


**Fig. 2.3** Fast cornering of a vehicle

At the outset of the steering process the slip angle, and thus the lateral force, first occurs at the front wheels. This initiates the yaw motion (rotation) of the vehicle. Only after that, the lateral acceleration of the vehicle is built up, as the slip angles build up at the rear axle through the shift of the instant center to the front. If the angle of the steering wheel remains unchanged, the movement of the vehicle turns into a stationary circular movement. The resultant constant lateral

acceleration is the product of the yaw ratio and the radius of the circle. The radius of curvature coincides with the instant center of the vehicle.

As the centrifugal forces do not—in contrast to the tire forces—act on the road plane, but at the center of gravity, they produce a rolling moment that tilts the vehicle towards the outside of the curve. This compression movement on the outside of the curve or rebound movement on the inside is used for the so-called roll steer, a kinematic effect in which the wheel suspensions produce a steering angle, too. As the front axle steers towards the outside of the curve and the rear axle towards the inside, the understeering self-steering behaviour is supported. The change of the wheel camber (inclination of the wheel in relation to the vertical angle) provides an additional increase of the lateral force. But the wheel alignment is also changed by so-called elastokinematic effects. The wheel suspensions are deliberately designed with a certain resilience which enables the acting forces to positively influence the wheel alignment. For example, to compensate for the naturally occurring inward turn when the brakes are applied in a curve, the dominant outer front wheel is supposed to steer outwards (Matschinsky 2007). The driving behaviour of modern vehicles can only be achieved by a differentiated harmonisation of tire, suspension and steering system.

## 2.3 Lateral Properties of the Tire

Most relevant for the steering behaviour of the vehicle are the properties of the build-up of the forces acting laterally on the tire. But the forces acting longitudinally and vertically on the tire, caused by irregularities of the tire, the wheel or the brake system, as well as uneven road surfaces, can create disturbing forces. This can impact the steering process by producing significant steering wheel torque fluctuations and vibrations at the steering wheel. These phenomena are caused by the interaction of the wheels, the axle suspension and the steering system, and will be discussed in Chap. 6.

### 2.3.1 Vertical Force Transmission: Influence on the Length of the Contact Patch

The mechanism of force transfer in the vertical direction has a significant influence on the lateral properties of the tire. Broadly speaking, modern radial tires for passenger cars consist of six key items which provide a transfer of forces:

- two bead cores which are circumferentially positioned on the two flanges,
- the carcass which connects and contains the two bead cores with its cords made of textile fabrics or sometimes steel which run radially across the tire,
- the ply with its steel wire cords running circumferentially in the area of the tread over the carcass cords,

- the rubber tread above the belt, which makes contact with the road surface,
- and the pressurized gas in the tire.

The other tire components, like the inner liner for sealing, the apex, the side bandages for optimized properties, the sidewalls protecting the carcass and the flange, as well as additional cushion gums above the ply for an improvement of the strength and the shape of the tire, and, in the case of run-flat tires a self-sealing lining, can be considered as “simply complementary” features to warrant the general functionality of the tire.

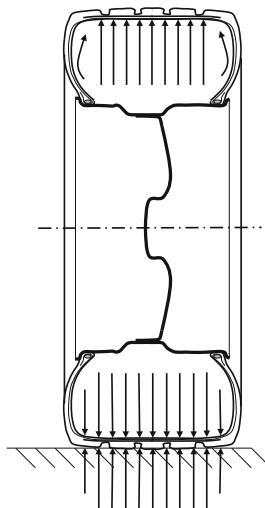
Internal pressure acts from the inside of the tire over its entire circumference. Any wheel load that acts on the tire from the outside produces a compression at the contact patch (latch). The carcass cords connected to the ply cannot absorb any pressure forces, and the rubber surrounding them can do so only to a small extent. The wheel load is thus transferred via the filling pressure, which pulls the tire upwards at the carcass cords in the area opposite the contact patch. These carcass cords, in turn, transfer the tensile forces to the bead cores at the flanges. If the tire load is increased, the size of the contact patch must increase, too (Fig. 2.4).

The filling pressure of the tire is therefore crucial for the size of the contact patch. If the effects of the stiffness of the tire components are disregarded, the size of the contact patch is dependent on the wheel load and the filling pressure only.

We can therefore state the following about the length of the latch, which—as described below—has a considerable influence on the lateral dynamic properties of the tire:

- The length of the contact patch increases with an increased wheel load.
- The length of the contact patch increases with a reduced filling pressure.
- The length of the contact patch decreases with an increased tire width.

**Fig. 2.4** The tire carries the wheel load via the filling pressure, schematic



The filling pressure in the area opposite to the contact patch acts upwards and pulls via the carcass cords at the bead cores, thus transferring the load to the rim.

Filling pressure and ground pressure offset each other at the contact patch.

The dependence of the length of the contact patch on these parameters is, to a limited extent, influenced by the stiffness of the tire components. This is one of the parameters which can be functionally adjusted by the tire producers.

### **2.3.2 Lateral Force of the Tire, Pneumatic Trail and Self-Aligning Torque**

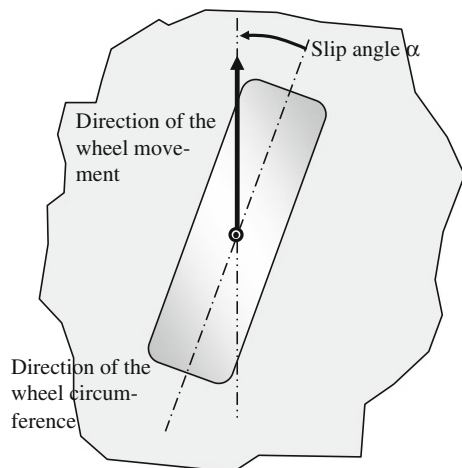
#### **2.3.2.1 Range of Minor Lateral Accelerations (Linear Tire Properties)**

The lateral forces of the tire are produced by a lateral deformation of the rubber enclosed in the tread between the road surface and the ply. These lateral deformations depend on the relative movement between the ply and the road surface. It is caused by the slip angle, which is defined as the angle between the direction of the wheel circumference and the direction of the movement of the wheel (Fig. 2.5).

The tread bars (*tread bar* here indicates a rubber block in the tread, which may indeed be a single tread block, but which may also be part of a circumferential tread rib) are increasingly deformed from the entry point of the contact patch to its exit point by the constant relative lateral movement between the road surface and the ply, as long as the traction between tread bars and road surface remains sufficient. On a dry surface the traction is largely upheld up to an acceleration of about  $3\text{--}4 \text{ m/s}^2$ . Looking at the deformations, a triangular deflection profile can be observed if the ply has been initially regarded as rigid (cf. Fig. 2.6). The deflection of the tread bars between the road surface and the ply is transformed by the shear modulus of the rubber, the height of the rubber, and the surface of the tread bar to a force acting on the tread bar.

The total force at the contact latch is the sum of the individual forces of the tread bars in the longitudinal and lateral directions of the contact patch. When this

**Fig. 2.5** Slip angle defined by the directions of the wheel circumference and the wheel movement



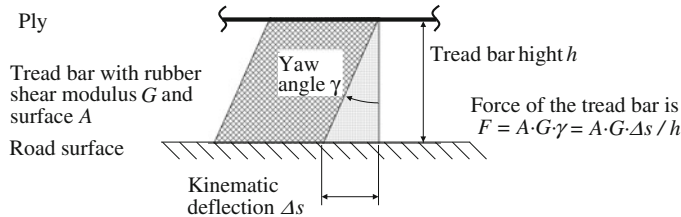


**Fig. 2.6** The deflection of the tread bars at the contact patch produces forces, schematic

force is related to the slip angle, the cornering stiffness  $C_a$  of the tire can be calculated. The cornering stiffness is an important parameter for the characterization of a tire regarding the driving and steering properties of the vehicle. In the so-called linear operating range of the tire, which—as mentioned above—corresponds to the range of pure traction on a dry surface at accelerations up to  $3\text{--}4 \text{ m/s}^2$ , the side force of the tire  $F_Y$  under a constant wheel load can be calculated by multiplying the cornering stiffness  $C_a$  with the slip angle  $\alpha$ :

$$F_Y = C_a \cdot \alpha$$

This simplified approach draws our attention to three parameters of the tire, which significantly affect its cornering stiffness:

- the rubber shear modulus of the tread, which is highly temperature-dependent,
- the rubber height/tread depth, which is dependent on the wear conditions of the tire,
- the tread bar surface/tread pattern percentage, which is dependent on the design of the tread and also affected by wear.

Both the temperature dependency of the rubber shear modulus and the dependency of the stiffness on the height of the tread can cause variations of the cornering stiffness of 20 % and more between different operating conditions. This shows how important it is that the operating condition of the tire regarding temperature and wear is taken into account during the dynamic adjustment of the vehicle (Fig. 2.7).

As mentioned above, the deflection of the tread bars over the length of the entire contact patch ideally has a triangular shape. The point of action of the total force—which is the sum of the individual forces of the tread bars—is not in the center of the contact patch, but somewhat to the rear of it in the centre of mass of the idealized triangle (cf. Fig. 2.8). This offset between the centre of the contact patch and the effective acting point of the lateral forces is called *pneumatic trail*. The self-aligning torque is the product of lateral force and pneumatic trail. During the cornering process this torque makes up a significant share of the total torque which has to be transferred and supported by the steering system.

It has been mentioned above that the length of the contact patch increases with an increase in the wheel load or a reduction of the filling pressure. For the triangle

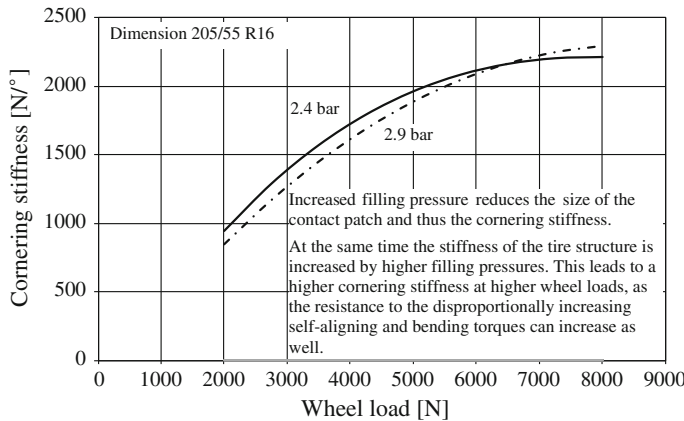


**Fig. 2.7** Cornering stiffness as a function of the wheel load for two different filling pressures

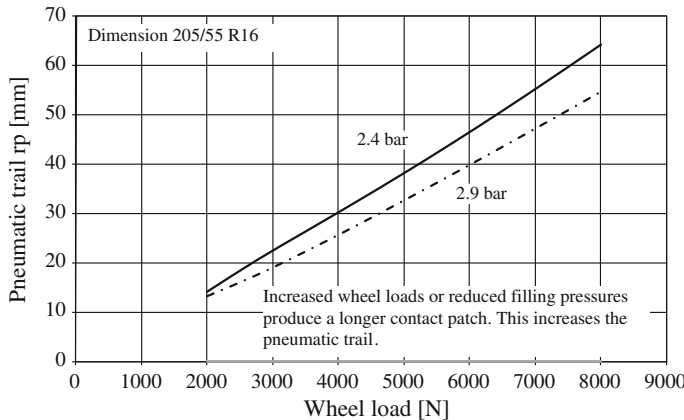


**Fig. 2.8** The pneumatic trail as a function of the wheel load in the case of two different filling pressures

described in Fig. 2.9 this means that its surface increases to the same degree, and that the lateral force, and thus the cornering stiffness, also increases. The pneumatic trail gets longer since the centre of mass of the approximate triangle moves away from the centre of the contact patch (Fig. 2.8). The self-aligning torque as the product of lateral force and pneumatic trail increases therefore disproportionately with an increase of the wheel load or a reduction of the filling pressure. This relationship, which is based on idealized assumptions, generally applies to modern high-performance tires with filling pressures within the normal range, as they are used in today's sports vehicles. Only for narrower tires with higher aspect ratios is this rule affected by other effects in a significant way.

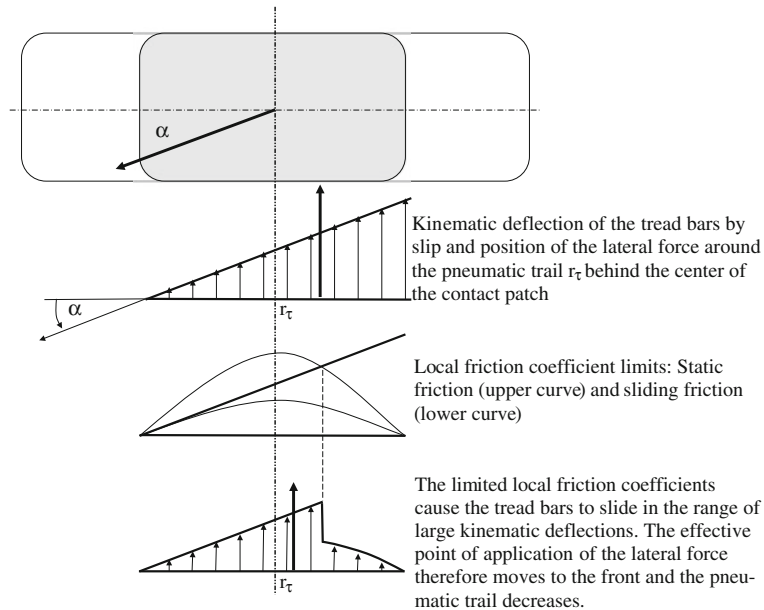


**Fig. 2.9** Kinematic deflection of the tread bars at the contact patch and limitation by local friction coefficient, without consideration of ply deflection, schematic

The above assumption of a ply with ideal stiffness obviously does not fully apply. The ply is bent at the contact patch by the forces of the tread bars acting on it. The self-aligning torque provides for an additional twist of the ply in relation to the rim. These two factors lead to a reduction of the effective deformation of the tread bars and thus to a reduction of the effective lateral force. As the self-aligning torque at the contact patch increases disproportionately with an increased length of the patch, the twist of the ply in relation to the rim increases, too. The restoring effects thus increase with a heavier load or a reduction of the filling pressure. The cornering stiffness regarded as a function of the wheel load therefore is not linear, but characterized by a degressive curve which reaches its maximum at increased wheel load. The position of this maximum depends on the type of tire. It particularly depends on the bending stiffness of the ply in relation to the vertical axis. By changing the design of the ply the degressive properties can be influenced, but the decisive factor to determine the position of the maximum is the width of the ply (area moment of inertia), and thus the width of the tire.

Two different factors are thus effective in wider tires. First, the length of the contact patch,—and with it the effective lever arms and the self-aligning torque— are reduced, and second the stiffness of the ply increases. The two factors both provide for reduced bending and twisting of the ply. Therefore the cornering stiffness of a wide tire is usually higher and characterised by a reduced degressivity as a function of the wheel load than that of a narrower tire of the same design and with the same filling pressure.

As the ply with an increasing width approaches the idealised ply described above, the increase of the cornering stiffness with wider plies is limited. The standard cornering stiffnesses for passenger car tires at a static axle load and the usual filling pressures are in the range of 1,250–2,500 N/ $^\circ$ , depending on the type of vehicle and the tire. The pneumatic trail usually is in the range of 20–40 mm.

### 2.3.2.2 Range of Higher Lateral Acceleration (Non-linear Tire Characteristics)

The *triangle model* applied above is commonly referred to as brush-type model, in which the tread bars are depicted by bristles; it can be applied to the range of higher lateral accelerations too, in which the tread bars start to slip in the contact patch.

The forces that are caused by the lateral deformation of each of the tread bars have to be transmitted by the frictional forces between the road surface and those tread bars. When the slip angle increases and the deformation increases accordingly, the tread bars are torn off in the rear area of the contact patch at first and start to slip on the road surface. As the level of sliding friction of the rubber on the road surface usually is lower than the maximum of the previously present static friction, the deformation of the tread bars is slightly reversed. While the lateral force continues to increase in line with the slip angle in the linear operating range of the tire, it decreases degressively at an additional increase of the slip angle until a more or less pronounced maximum of force is built up. If the slip angle is very large, the tire starts to slide very close to the entry point of the contact patch. In that case any additional increase of the slip angle does not lead to an increase of the lateral force. What happens is rather the reverse, as the increased slip angle leads to an increase of the sliding speed of the tread on the road surface and an increase of the local temperature of the rubber, which further reduces the coefficient of sliding friction.

The pneumatic trail is almost constant in the linear trail of the tire. When the first sections of the tire at the rear of the contact patch start to slide, the center of the tread bar forces moves towards the front. The pneumatic trail is thus reduced with increased slip angles (cf. Fig. 2.10). As the lateral force ceases to increase as strongly as before, the self-aligning torque on top of the slip angle decreases degressively. An additional increase of the slip angle moves the point of application of the force towards the center of the contact patch so that somewhere in the range in which the lateral force reaches its maximum, the self-aligning torque of the tire decreases suddenly (cf. Fig. 2.10). If the steering assistance is designed appropriately, the driver will clearly feel when he approaches the range of the limits of the vehicle through the feedback of the steering wheel torque. At even larger slip angles the effective point of application of the lateral force can even move to a point in front of the centre of the contact patch, so that the pneumatic trail turns negative. If the slip angle increases even more, the forces acting on the front and the rear of the contact patch neutralize each other and the pneumatic trail

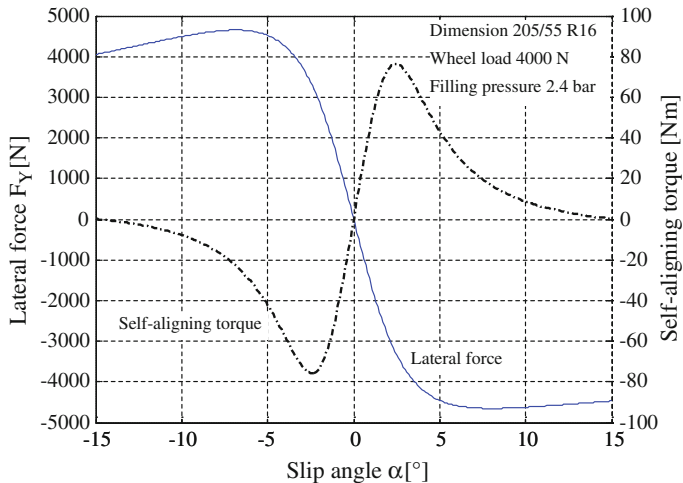


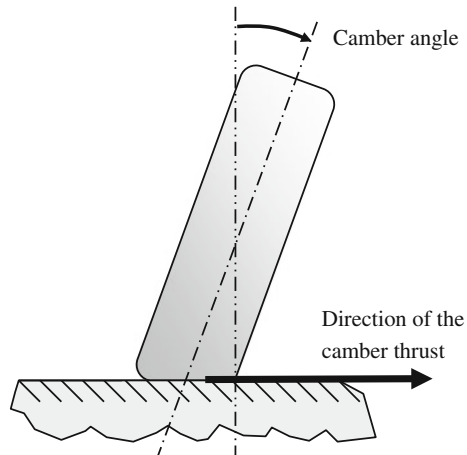
**Fig. 2.10** Lateral force and self-aligning torque as functions of the slip angle

approaches zero. This behaviour of the contact patch is especially relevant for the kinematic adjustment of the steering behaviour when parking, when the front wheels have to turn approximately in parallel to each other to reduce the turning circle, thus producing increased slip angles by straining the axle, which, in conjunction with the changing kinematic trail, can cause a self-reinforcing steering behaviour in the worst case scenario.

The upper limits of the transferable lateral forces on solid surfaces strongly depend on the properties of the frictional factors, road surface and tread rubber. On dry asphalt roads the local static friction coefficients at the tread bar can exceed two (transferred horizontal force in relation to the vertical force). But as explained above, there is always a mixture of traction and sliding sectors at the contact patch, so that the adhesion potential of the complete tire always stays significantly below this value. On a good asphalt surface currently produced high-performance tires can attain friction coefficients of about 1.3, while those of ordinary tires are in the range of 1.1 and can drop just below one, under certain circumstances.

The maximum traction of the tire is determined by its structural stiffness, too. If the wheel loads and the lateral forces are high, the contact patch is strongly deflected in relation to the rim. In extreme cases it can even lift off the road surface on one of the sides. This leads to an increase of the local contact pressure of those tread bars at the contact patch, which remain on the road surface. But an increased local pressure does not produce a corresponding increase of the friction coefficient. This reduces the adhesion potential of the tire. As this “buckling” of the tire structure increases under higher loads, the deposable adhesion potential decreases when the wheel load is increased. Thus the maximum transferable horizontal force decreases degressively with any increase of the wheel load. This applies to the lateral force in particular. In the direction of the wheel circumference the structure

**Fig. 2.11** Camber angle and direction of the resulting camber thrust (road surface on wheel)



of the tire is much stiffer, so that it shows less of a deformation under longitudinal forces.

The structural stiffness is increased either by choosing a stiffer or wider design, reinforcing the sidewalls, reducing the aspect ratio of the tire, extending the rim width or increasing the filling pressure. As these methods to increase the stiffness reduce the size of the contact patch, they can also result in an uneven distribution of the pressure or an increase of the average pressure at the contact patch. For an optimal solution the tire thus has to be adapted to the individual vehicle.

### 2.3.2.3 Influence of the Camber Angle

If the tire runs straight or if its slip angle in the linear operating range is small, the camber angle produces deformations of the tread bars, which in turn generate lateral forces. These lateral forces amount to only 1/10 of the cornering stiffness in relation to the slip angle (camber thrust stiffness) and are not directly related to the cornering stiffness. They act in the direction of the wheel camber (Fig. 2.11).

Camber angles generate a torque around the vertical axis of the tire, too. It results from the torsion of the tread bars at the contact patch and the asymmetric shape of the contact patch in the lateral direction under camber. While the self-aligning torque acts in the opposite direction of the camber thrust, and thus reduces the slip angle; the camber torque turns the tire in the direction of the lateral force that acts from the road surface on the wheel.

When driving at high lateral accelerations in the non-linear range of the tire, the position of the tire in relation to the road surface can be partly optimized by compensating the deflection of the contact patch in relation to the rim under the influence of high lateral forces by a “countertilt” of the wheel, thus enabling the achievement of higher lateral force potentials.

Camber angles are caused not only by tilting the wheels, but also by driving on a transversely inclined road surface. Even when driving in a straight line, road surface irregularities can thus produce lateral forces and torques around the vertical axis, which are independent of toe-in effects and which have to be compensated by the steering wheel.

### 2.3.3 Transient Behaviour of Tire Lateral Forces

The tire generates lateral and longitudinal forces due to local deformation of the rubber in the tread, which is supported by the ply.

The deformations of the tread are generated very quickly (if the ply is rigid), that is after an individual tread bar has passed the contact patch one and a half times after a change of the slip angle. At a driving speed of 20 m/s and a length of the contact patch of 15 cm this takes only a little more than 1/100 s, a time span which is irrelevant from the perspective of vehicle dynamics. Only at very low speeds, such as while parking, when portions of drilling torques have to be considered, the chronological mechanisms at the contact patch acquire a relevance for the calculation of the steering torque.

The ply has to transfer the forces generated at the contact patch via the carcass to the rim. To do so, the ply has to be deflected in relation to the rim in the range of the contact patch. The value of the deflection is dependent on the stiffness of the bearing of the contact patch in relation to the rim. In the presence of lateral forces the deflection of the contact patch in relation to the rim can occur at the maximum relative speed of  $v_{yL} = \alpha \cdot v_x$ . For a tire with a lateral spring stiffness of  $c_{Ly} = 200 \text{ N/mm}$  and a cornering stiffness of  $C_\alpha = 2,000 \text{ N/}^\circ$  and a driving speed of  $v_x = 20 \text{ m/s}$  the delay approach of the first order of Böhm (1966) results in a cutoff frequency of about  $f_c = 5 \text{ Hz}$ . This is a frequency which can be relevant for vehicle dynamics. But due to speed proportionality this effect loses its relevance with increasing speed.

$$\frac{1}{2\pi \cdot f_e} = T_e = \frac{C_\alpha}{c_{yL} \cdot v_x} \quad (2.1)$$

The lateral tire stiffness relevant in this context is mainly influenced by the tire width/rim width, tire sidewall height, filling pressure and sidewall stiffness. In this context the nature of the filling gas supplied to the tire is of major importance.

### 2.3.4 Summary of Tire Properties

The decisive properties of a tire for its steering behaviour are cornering stiffness and pneumatic trail. In the range of low lateral accelerations of up to  $3\text{--}4 \text{ m/s}^2$ , the cornering stiffness can be used to calculate the lateral force as a function of the slip

angle, if the wheel load is considered as constant. As a function of the wheel load, the cornering stiffness behaves degressively, while the pneumatic trail, which also remains almost constant in the range of low lateral accelerations, is approximately proportional to the wheel load.

At higher lateral accelerations, the lateral force as a function of the slip angle reaches a maximum and then generally decreases slightly. In this range, the pneumatic trail strongly decreases and in some cases can even turn negative, i.e. at a large slip angle the self-aligning torque of the tire can change its direction.

The behaviour of any given tire can be altered by a change of the filling pressure. In general an increase of the filling pressure has the following effects:

- Lower cornering stiffness at a static wheel load (if the tires are very narrow or the initial filling pressures are very low an increase of the filling pressure can also result in an increase of the cornering stiffness).
- Lower degressivity of the cornering stiffness as a function of the wheel load (this leads to an increase of the cornering stiffness at very high wheel loads in comparison to the lower filling pressure).
- Lower degressivity of the adhesion maximum in the lateral direction as a function of the wheel load.
- Shorter pneumatic trail and thus a reduced self-aligning torque.
- Faster transient build-up of the lateral force of the tire.

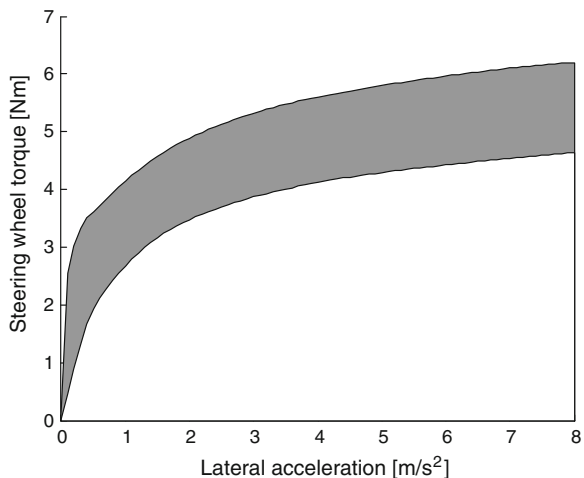
Other factors, which have a significant impact on the properties of the tire in its linear operating range in particular, are tire temperature and wear.

## 2.4 Steering Wheel Torque

Apart from the vehicle reaction, the steering wheel torque is the most important variable affecting the steering feel of a vehicle (cf. [Chap. 7](#)). It is perceived via the sense of touch and can thus be processed very quickly. In the development praxis the flow of the steering wheel torque is iteratively optimized in many test drives. To obtain the desired steering feel, different power steering settings, axle kinematics, tire properties, etc. are applied and tested. This approach requires very experienced test engineers and relatively long development times. To reduce these expenditures, many efforts have been undertaken to develop reference values for the steering wheel torque, which could ensure a harmonious steering feel. [Mitschke \(2003\)](#) provides a summary of the theoretical background as well as aspects of the steering wheel torque curve in relation to the lateral acceleration of the vehicle. The steering wheel torque ranges of present-day vehicles continue to differ significantly ([Bartenheier 2004](#)).

These studies resulted in a reduced steering torque gradient with rising lateral acceleration for vehicles with power steering. To obtain a pronounced mid feeling the power assistance from the center position is set very low. With increasing lateral acceleration and thus rising lateral force at the tires the power assistance

**Fig. 2.12** Range of measured steering wheel torques of sports cars (Pfeffer and Harrer 2007)



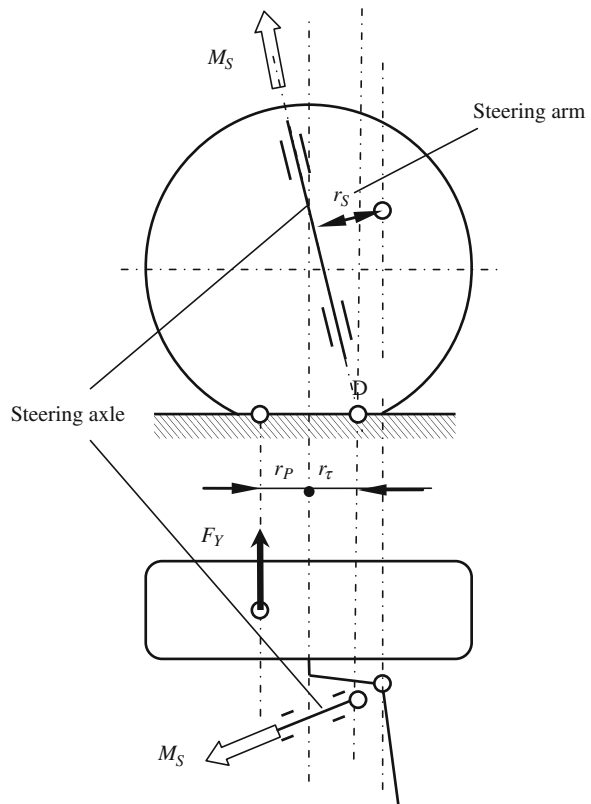
increases disproportionately, thus causing the steering wheel torque to decrease degressively. Figure 2.12 shows the range of measured steering wheel torques for various sports cars. It can be seen that the steering wheel torque curves are widely spread even for this specific sector of the vehicle market. Vehicle developers are therefore posing themselves the question of what the best possible curve should be for attaining a harmonious steering wheel torque curve (Heißing and Brandl 2002). Therefore, this chapter discusses the calculation of the vehicle torque for stationary cornering. In addition we will present a method to analytically factor in the power assistance to achieve a harmonious steering support. These observations exclusively consider quasi-stationary cornering without any input of friction or dynamics. The frictional and dynamic behaviour of the steering wheel torque is of course very important for vehicle development, but the quasi-stationary behaviour establishes the basis for any additional fine tuning of the power steering system (Braess 2001).

#### 2.4.1 Calculation of Steering Wheel Torques

The steering feel is particularly important for speeds above 60 km/h, as the steering wheel angles decrease in this speed range. For this reason the kinematic steering ratio will be considered as constant in the following discussion. We can also neglect the self-aligning torque caused by axle kinematics at smaller steering wheel angles. By restricting ourselves to moderate lateral accelerations, the pneumatic trail can be regarded as constant, too. In addition, we shall also disregard the friction within the steering system.

The steering torque around the steering axle  $M_S$  can be calculated as the product of the lateral forces  $F_Y$  of the left and right front wheel and the sum of the

**Fig. 2.13** Steering torque at the left front wheel



constructive trail  $r_\tau$  and the pneumatic trail  $r_P$  (Fig. 2.13). Formula 2.2 is valid for smaller steering angles, which are typical for higher driving speeds.

$$M_S = F_Y \cdot (r_\tau + r_P) \quad (2.2)$$

The driver has to apply a steering wheel torque  $M_H$  reduced by the kinematic steering ratio  $i_S$  and the steering assistance ratio  $A_S$  (Mitschke 2003).

$$M_H = \frac{M_S}{i_S \cdot A_S} \quad (2.3)$$

This equation is also valid as definition of the steering assistance ratio.

The lateral force, which has to be supported at stationary circular travel, and has to be equal to the lateral force at the front axle, is the product of the proportional mass of the vehicle at the front axle  $m_F$  and the lateral acceleration  $a_y$ .

$$F_Y = m_F \cdot a_y \quad (2.4)$$

The equation for the steering wheel torque, which has to be applied by the driver, is found by combining the Eqs. (2.2)–(2.4).

$$M_H = \frac{m_F \cdot (r_\tau + r_P)}{i_S \cdot A_S} \cdot a_Y = \frac{m_F \cdot r}{i_S \cdot A_S} \cdot a_Y = \frac{M_S}{i_S \cdot A_S} \quad (2.5)$$

In this equation  $r$  is the total trail.

Assuming a constant total trail  $r$  and a constant steering ratio, the lateral acceleration gradient of the steering wheel torque is derived from the lateral acceleration as follows:

$$\frac{dM_H}{da_Y} = \frac{m_F \cdot r}{i_S} \frac{\left(A_S - a_Y \frac{dA_S^2}{da_Y}\right)}{A_S^2} \quad (2.6)$$

For vehicles without power steering the increase of the steering reinforcement is  $A_S = 1$ . This results in a constant lateral acceleration gradient of the steering wheel torque independently of the lateral acceleration. The target ranges for this gradient are presented in [Chap. 7](#).

$$\frac{dM_S}{da_Y} = \frac{m_F \cdot r}{i_S} \quad (2.7)$$

## 2.4.2 Steering Reinforcement

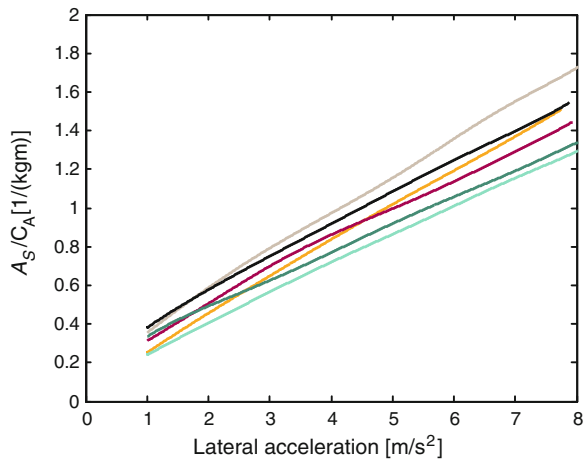
By introducing the self-aligning factor  $C_A$  in Eq. (2.5) the steering assistance can be calculated as follows:

$$A_S = \frac{m_F \cdot r}{i_S \cdot M_S} \cdot a_Y = C_A \cdot \frac{a_Y}{M_S} \quad (2.8)$$

The self-aligning factor is calculated by multiplying the proportional vehicle mass at the front axle by the total trail divided by the kinematic steering ratio. It represents a vehicle-specific measure for the self-aligning or centering potential of the vehicle. The numerical value of the self-aligning factor is equal to  $1 \text{ m/s}^2$  lateral acceleration without steering assistance. The unit to express the self-aligning factor can be  $\text{kg m}$  or  $\text{Nm}/(\text{m/s}^2)$ . As the self-aligning factor is vehicle-specific and thus independent of the lateral acceleration, the shape of the steering reinforcement can be determined via the lateral acceleration ([Fig. 2.14](#)).

Evaluation of various vehicles showed that the steering reinforcement  $A_S$  of the vehicles increased almost linearly with the lateral acceleration ([Fig. 2.14](#)). Vehicles, which were subjectively considered to display a very harmonious steering wheel torque range, were characterized by a particularly pronounced linear behaviour. We will therefore proceed with the assumption that the optimum steering reinforcement increases linearly to the lateral acceleration (Pfeffer and Harrer 2007).

**Fig. 2.14** Steering reinforcement function  $A_S$  related to the self-aligning factor in dependence on the lateral acceleration for different vehicles



This allows us to represent the steering reinforcement  $A_S$  as a linear function of the lateral acceleration. This results in the following equation:

$$A_S = C_A \cdot (D_A + K_A \cdot a_Y) = \frac{m_F \cdot r}{i_S} \cdot (D_A + K_A \cdot a_Y) \quad (2.9)$$

The parameter  $D_A$  describes the basic support and is therefore denoted as gradient factor. The degressivity factor  $K_A$  defines the measure of leveling of the increase of the steering wheel torque with an increase of lateral acceleration. This steering reinforcement function is applicable for purely manual steering systems (without support, i.e.  $D_A = i_S/(m_F \cdot r) = 1/C_A$  and  $K_A = 0$ ) and for various parameters  $K_A$  shown in Fig. 2.15.

Combining the Eqs. (2.4) and (2.8) results in the following equation for the steering wheel torque curve in relation to lateral acceleration:

**Fig. 2.15** Steering acceleration as a function of lateral acceleration

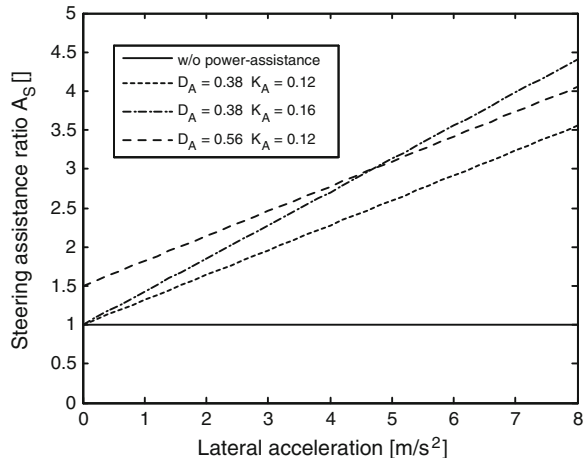
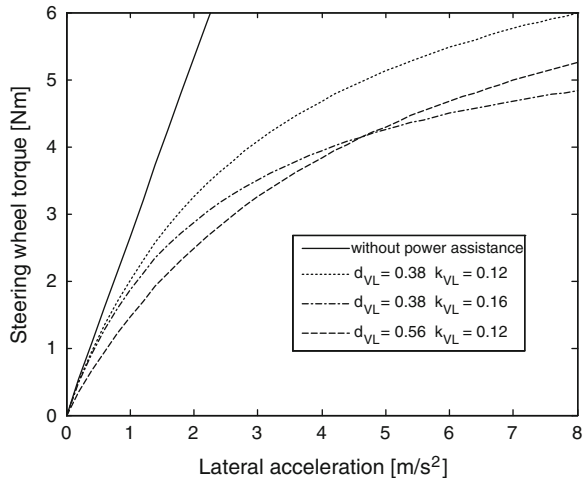


**Fig. 2.16** Steering wheel torque as a function of lateral acceleration with linear steering assistance ratio  $A_S$



$$M_H = \frac{m_F \cdot r}{i_S \cdot A_S} \cdot a_Y = \frac{m_F \cdot r}{i_S \cdot \frac{m_F \cdot r}{i_S} \cdot (D_A + K_A \cdot a_Y)} \cdot a_Y = \frac{1}{\frac{D_A}{a_Y} + K_A} \quad (2.10)$$

The steering wheel torque curve of Eq. (2.10) is shown in Fig. 2.16. Without steering assistance the steering wheel torque increases linearly with the lateral acceleration. In contrast, in the presence of steering assistance the curve rises degressively. This characteristic is naturally detectable in the measurements, too (Fig. 2.12).

The larger the chosen degressivity factor  $K_A$ , the sooner the steering wheel torque curve levels off. A linear steering reinforcement function provides for a harmonious increase of the steering wheel torque. The only requirement is to determine the gradient factor  $D_A$  and the degressivity factor  $K_A$ . In practice this can be done by determining the target values for the steering wheel torque in relation to the lateral acceleration for two or more points. A time-consuming, selective optimization of steering assistance diagrams becomes obsolete.

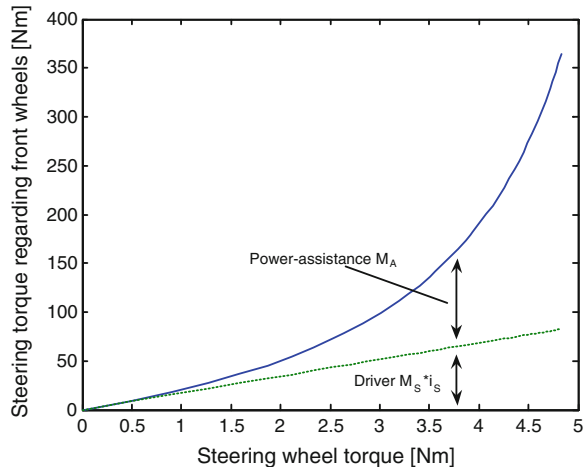
### 2.4.3 Steering Assistance Torque

The total steering torque around the steering axle of the front wheels now results from the steering assistance torque and the torque applied by the driver (Fig. 2.17).

In practice the dependence of the power-assistance curve on the steering wheel torque is used to tune steering systems. The required steering assistance torque  $M_A$  is calculated as the difference between the steering torque at the wheels and the torque applied by the driver:

$$M_A = M_S - M_H \cdot i_S \quad (2.11)$$

**Fig. 2.17** Steering torque and steering assistance torque in relation to the steering wheel torque



By inserting the Eqs. (2.2), (2.7) and (2.9) the steering assistance torque can be expressed as a function of lateral acceleration or as a function of the steering wheel torque.

$$M_A = \frac{a_Y(m_F \cdot r \cdot D_A + m_F \cdot r \cdot K_A \cdot a_Y + i_S)}{D_A + K_A \cdot a_Y} = \frac{M_H(m_F \cdot r \cdot D_A + i_S \cdot M_H \cdot K_A - i_S)}{1 - K_A \cdot M_H} \quad (2.12)$$

With the help of this formula, the required steering assistance torque can be expressed analytically. This allows the parameterization of the assistance range using only the gradient factor  $D_A$  and the degressivity factor  $K_A$  in relation to the steering wheel torque or the lateral acceleration.

In hydraulic steering systems the power steering assistance results from the pressure differential between the right and the left chamber of the cylinder, while in electromechanical steering systems it results from the applied motor current. The differential pressure is calculated as follows:

$$\Delta p = \frac{M_A}{r_S \cdot A_p} \quad (2.13)$$

For electromechanical steering systems the required motor current  $I_E$  is calculated with the help of the motor constant  $K_T$  and the transmission ratio  $i_E$  between motor shaft and steering angle at the front wheel:

$$I_E = \frac{M_A}{i_E \cdot K_T} \quad (2.14)$$

With this approach of a linear steering reinforcement via the lateral acceleration, a harmonious, quasi-stationary steering wheel torque curve can be derived. By applying this compact, analytical determination of the steering reinforcement, it is possible to determine the necessary steering assistance with the help of only

two parameters. To map the acceleration dependence a data pair of gradient factor and degressivity factor has to be assigned to each acceleration. The gradient factor  $D_A$  indicates the degree of the increase of the steering wheel torque from the center position and the degressivity factor  $K_A$  influences the leveling of the steering wheel torque at increasing steering angles. This analytical approach is an elegant and efficient way to determine the shape of the steering assistance, with which a point-by-point determination of the steering assistance becomes obsolete. In order to attain a harmonious curve of the steering wheel torque, the required curve of the supporting pressure in hydraulic steering systems or the motor current required for electromechanical systems can be derived directly from the level of the desired steering assistance.

## 2.5 Four-Wheel Steering

Known for special purpose vehicles for a long time, this was introduced to the passenger car industry by Japanese manufacturers in 1985 (Sano et al. 1985, 1987). To improve driving dynamics a rear-wheel steering was mechanically coupled to the front axle.

As shown in Fig. 2.18, the system was designed to ensure an increased agility at large steering angles (low driving speeds), while the sideslip angle and the phase shift between lateral acceleration and yaw rate are reduced and the stability of the vehicle behaviour is improved.

The next important step was the introduction of the electrically controlled rear-wheel steering by BMW. The steering was controlled by a characteristic map dependent on the speed and the steering angle of the vehicle. In difficult driving

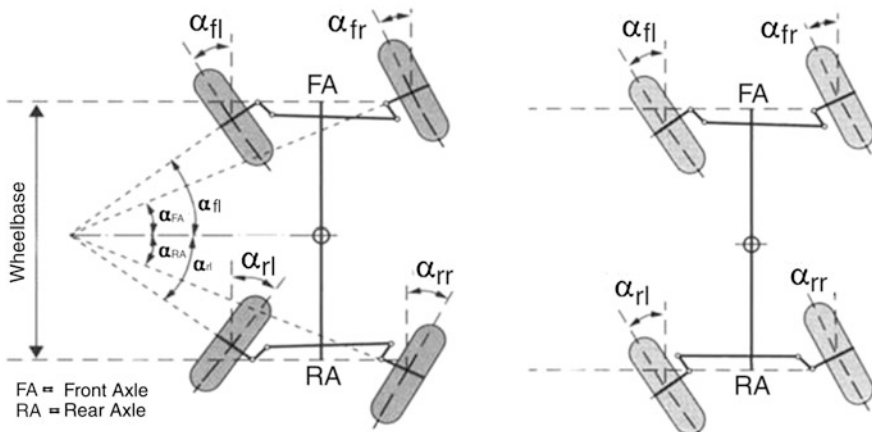


**Fig. 2.18** Steering strategy for four-wheel steering: At low speeds the wheels turn in opposing directions (left) while they turn in the same direction at high speeds

situations such as in a double lane change this system displayed significant improvements with respect to the steering effort, the sideslip angle, and the yaw rate curve. This system was followed by others which will be described in detail in [Chap. 17](#).

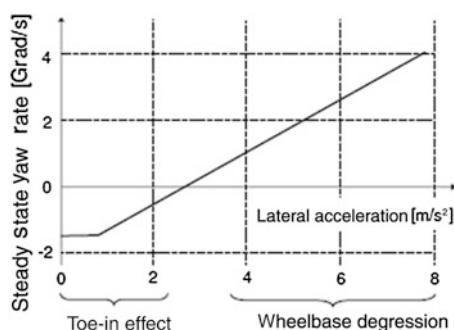
## 2.6 Active Suspension Steering

Any action, which produces lateral forces acting on the vehicle, can be utilized to steer. The term ‘roll steer’ denotes any steering movement characterized by a change of track or camber, which results from a rolling motion of the body of the vehicle and its (elasto-) kinematics ([Matschinsky 2007](#)). This roll steering behaviour is utilized only when cornering to influence the self-steering behaviour of the vehicle. An active generation of a rolling movement to steer the car would hardly be accepted by the driver and has therefore never been applied, although roll steering can generate considerable yaw rates.

Another effect is wheel load control as utilized for active suspension steering. The vehicle with its four wheels is hyperstatic. For that reason, an active suspension system enables a change of the individual wheel loads. The wheel suspension design provides for a camber or a toe angle. Under normal driving conditions the lateral forces at the two sides of the vehicle compensate each other, as the vertical wheel loads are approximately equal, too. By actively generating unequal wheel loads the lateral forces become unequal too and can be utilized to steer the vehicle without any activation of the actual steering system (cf. [Fig. 2.19](#)). This effect is produced by a diagonal change of the vertical wheel loads and does not generate any movement of the vehicle body.

This toe-in and camber effect decreases at higher lateral acceleration rates and changes of the yaw ratio caused by wheel load depression become dominant. During wheel load depression the following effect comes into play. The lateral traction increases depressively with the wheel load, i.e. the bigger the difference between the wheel loads on the inner and outer side of the bend gets, the lower the resulting lateral force and the lateral force potential (cf. also [Chap. 2](#)). Active

**Fig. 2.19** Active suspension steering in relation to lateral acceleration ([Rau 2007](#))



suspension can thus influence the self-steering behaviour of the vehicle, too (over- and understeering). An increase of the roll stabilization at the front axle can promote the understeering behaviour of the vehicle, while an increase of roll stabilization at the rear axle promotes its oversteering tendency.

This effect is utilized by active stabilizers, which are primarily used for roll stability, to influence the self-steering behaviour (over- and understeering). It can also be generated and utilized by active power generating elements such as the ABC system. The steering effect of active suspension is dependent on the speed and on the toe-in and camber design of the wheel suspension. This steering effect is in any case considerable (cf. Fig. 2.20). Rau (2007) quantifies this effect with 10° per wheel for a speed of 80 km/h and a tension of 2,500 N.

Active suspension steering can be used to improve the driving comfort on the one hand and to increase driving security and agility on the other. It serves to fulfill the following functions:

- crosswind compensation
- compensation of transversely sloped road surfaces
- track-keeping assistance
- variation of yaw amplification and enhancement of stability and agility of the vehicle
- support for  $\mu$ -split brake maneuvers
- stabilization in the limit ranges.

As the effect of active suspension steering is reduced at lower driving speeds, it can only be employed as an additional feature for vehicles with regular steering

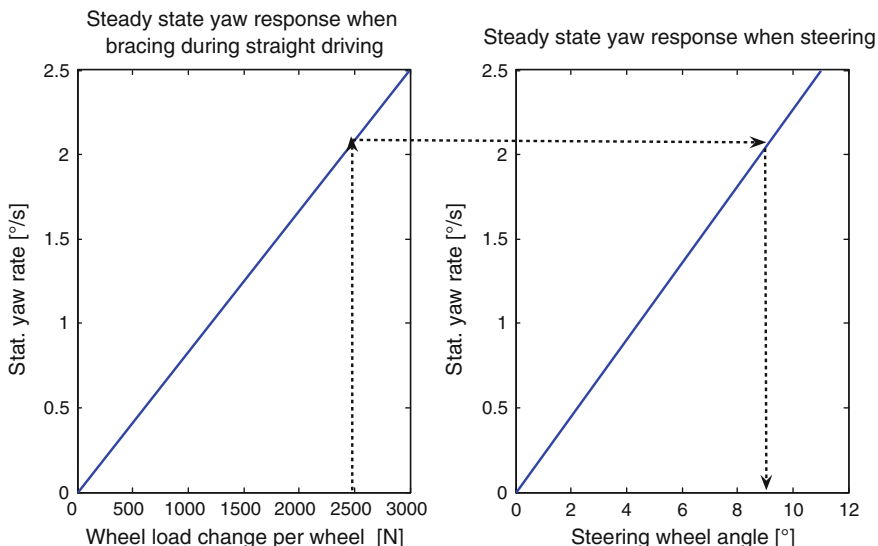


**Fig. 2.20** Comparison between steering effect by active suspension and regular steering according to Rau (2007); 80 km/h and 0.5° toe-in

systems, which it will therefore never replace. However, the increased use of active elements in the chassis will broaden the application of active suspension for all of its different possible functions.

## References

- Bartenheier T (2004) Potenzial einer fahrertyp- und fahrsituationsabhängigen Lenkradmomentgestaltung. VDI Fortschritt-Berichte, Reihe 12, Nr. 584, VDI, Düsseldorf
- Böhm F (1966) Zur Mechanik des Luftreifens. Postdoctoral dissertation, Technische Hochschule Stuttgart
- Braess H-H (2001) Lenkung und Lenkverhalten von Personenkarfawagen—Was haben die letzten 50 Jahre gebracht, was kann und muss noch getan werden? VDI-Berichte Nr. 1632, VDI, Düsseldorf
- Heißing B, Brandl HJ (2002) Subjektive Beurteilung des Fahrverhaltens, 1st edn. Vogel Buchverlag, Würzburg
- Matschinsky W (2007) Radführungen der Straßenfahrzeuge, 3rd edn. Springer, Berlin
- Milliken WF, Whitcomb DW (1956) General introduction to a programme of dynamic research. Proc I Mech E (A.D.), pp 287–309
- Mitschke M, Wallentowitz H (2003) Dynamik der Kraftfahrzeuge, 4th edn. Springer, Berlin
- Pfeffer PE, Harrer M (2007) Optimaler Lenkradmomentenverlauf bei stationärer Kurvenfahrt. VDI-Tagung Reifen-Fahrwerk-Fahrbahn, Hannover, 23–24 Okt 2007
- Rau M (2007) Koordination aktiver Fahrwerk-Regelsysteme zur Beeinflussung der Querdynamik mittels Verspannungslenkung. Postdoctoral dissertation, Institut für Flugmechanik und Flugregelung der Universität Stuttgart
- Sano S et al (1985) Modification of vehicle handling performance by four-wheel-steering systems. In: 10th ESV conference, Oxford, UK, pp 248–261
- Sano S et al (1987) Operational and design features of the steer angle dependent four-wheel-steering system. In: 11th ESV conference, Washington DC, 12–15 May 1987

# **Chapter 3**

## **Steering Requirements: Overview**

**Sina Brunner and Manfred Harrer**

The decision to buy a new car is significantly influenced by the customer's subjective impression when driving. Here, the chassis exerts a critical influence on driveability. In chassis development, particular attention is paid to vehicle dynamics, driving comfort and driving safety. A major part of vehicle dynamics is determined by the steering response, essentially dependent on the steering. The prime task of the steering is to transform the angle of the steering wheel, as given by the driver, into a corresponding change of direction. The wheels turn as the driver initiates a change of the steering angle, resulting in a change of orientation. The driver must be enabled to clearly predict the response of the vehicle.

This chapter gives a short overview of the various requirements for a steering system, outlining the subjects Function and steering feel, Package, Weight, Costs, Quality, Energy and environment, Acoustics and vibrations, System safety and Legal requirements.

### **3.1 Function and Steering Feel**

Steering feel is the subjective perception of the dynamic response by the vehicle on the driver's control of the steering wheel. Steering feel may be defined in two ways: steering behaviour and response behaviour.

Steering behaviour is the ability of the vehicle to transform any change of course that the driver initiates with the steering into a response that the driver may

---

S. Brunner (✉) · M. Harrer  
Dr. Ing. h.c. F. Porsche AG, Porscheplatz 1 70435 Stuttgart, Germany  
e-mail: [sina.brunner@steeringhandbook.org](mailto:sina.brunner@steeringhandbook.org)

M. Harrer  
e-mail: [manfred.harrer@steeringhandbook.org](mailto:manfred.harrer@steeringhandbook.org)

predict. The steer-angle, set at the steering wheel, has to correlate to the angle of the wheels by a continuous function, i.e. the installed steering transmission may not produce any jumps.

Response behaviour is the ability to transmit information on changes of wheel load, rolling resistance and side force by a change of the applying steering wheel momentum. Information transmitted by the steering may be distinguished into useful and disturbing information. Useful information is any information supporting the vehicle control, including, for example, feedback on the limit of adhesion of the wheels. Disturbing information is, for example, periodic agitation, such as fluctuations of the braking power. Disturbing information should therefore be suppressed within the steering system.

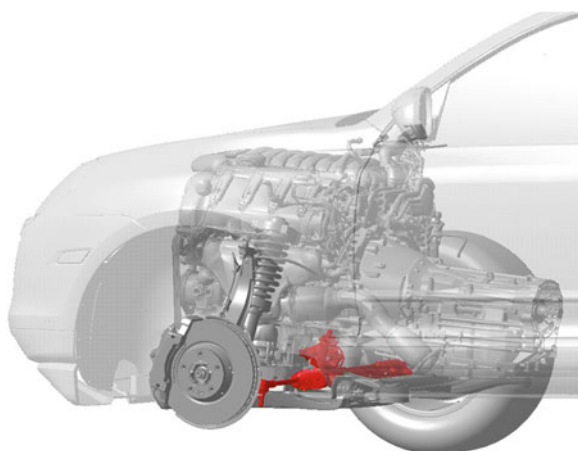
Besides the tyres and axle kinematics, the steering feel depends significantly on the design of the steering system. Each steering has its specific advantages and disadvantages, depending on the construction. For example, hydraulic steering is superior to electro-mechanical steering with regard to the response behaviour, while electro-mechanical steering is better adapted to suppressing disturbing information. Concerning the manipulation of the steering behaviour, electro-mechanical steering provides substantially more parameters than hydraulic systems. This includes speed-dependent power assistance, active return and the dampening depending on the steer-angle speed.

### 3.2 Package

The package is any geometrically and technically suitable arrangement of all the components in a vehicle, basically eliminating targeting conflicts concerning the space required by the individual components and their functional dependence on each other.

In passenger cars, rack-and-pinion steering has been used almost exclusively for quite some time now. Different arrangements of the steering arise from the way the engine is installed. In the case of transversely installed engines, that nowadays drive the major part of front-wheel drive vehicles, the steering gear is almost always arranged in the direction of the traffic behind the engine-gear unit, because otherwise no suitable connection with the intermediate steering shaft can be achieved. Thus, the tie rod has to be connected behind the centre of the wheel as well, hence the steering gear is usually connected elastically with the front-axle support. Rubber bushings are used, so that the elastokinematically desired toe-in change is maintained when a side force applies. If the engine is installed in parallel (which is common in rear-wheel drive vehicles of the superclass), the steering gear is preferably arranged in front of the axis, because connecting the tie rod in front of the wheel centre results in a higher tuning potential with regard to elastokinematics. Here the steering gear is rigidly screwed on the axle support, merging very agile and immediate steering with the desired elastic toe-in change via the front-axis wishbone. If space considerations force the connection of the tie rod behind the wheel

**Fig. 3.1** Location of the steering gear of a Porsche Cayenne



centre, the steering gear has to be connected elastically with the front-axle support, as in the case of the transversely installed engine. Then it is usually located between the engine and the gearbox under the clutch housing (Fig. 3.1).

By comparison, vehicles with steering that is integrated above the engine-gear unit are only rarely found. The unavoidable connection of the steering gear to the cowl resulted on the one hand in problems with the rigidity and, hence, in unintentional steering elasticity. On the other hand, the fluid noise in the steering gear was amplified by the cowl metal acting as a resonator.

In addition to the arrangement of engine and gear, the axle kinematics critically affect the location of the steering. The maximum wheel turning angle, the effective lever length of the tie rod and its stretched position are crucial for the arrangement of the steering gear. One needs to consider as well that tie rods do not stay in their original place in traction mode but will describe ‘envelopes’, as the gear rack and the wheel support are moving. A defined minimum distance of approx. 15 mm from any adjacent component has to be generally maintained during these motion sequences, and the admissible joint bending angles may not be surpassed.

Other than the typical problems of packages, as, for example, conflicts of space between the upper steering column and the arrangement of the pedals or the separation of the intermediate steering shaft from the cowl, other specific problems of the front-end package have to be solved with regard to the various implementations of the steering assistance. With any power-assisted steering, the arrangement of the power steering pump and of the required tubes or pipes is a major challenge. Often, several dozen tube variations may arise, especially when different engine units are used on one vehicle platform. The electro-mechanically supported steering requires the electric motor, the control device and the output reduction gear to be fitted into the available space while observing that the distance to the vehicle battery has to be kept short in order to minimise conduction loss. Heterodyne steering requires, in addition, that the superposition angle actuator will be integrated into the present package. It is evident that the superposition angle

actuator is ever more often relocated into the upper area of the steering column, to minimise space conflicts in the front-end.

The arrangement of the steering gear and the steering column in the engine compartment will often result in considerable thermal charges as well. This problem is further aggravated by the desire to improve vehicle aerodynamics, reducing the flow through the front-end. At some steering components, continuous temperatures of 100 °C are increasingly common. Plastics, elastomers, surface coatings and lubricants in the steering gear and the steering column and the electrical system components are pushed to their limits as complex temperature shieldings must often be fitted into the available space. Thermally favourable variations are combinations of a transverse engine (exhaust duct and catalytic converter in front) with a rear steering gear or, in case of the parallel engine, a steering gear that is implemented in front, close to the cooling air duct. On the other hand, a rear steering that must be placed between the parallel engine and the gearbox will face the highest thermal charges.

### 3.3 Weight

Increased demand for efficient vehicles and low CO<sub>2</sub> emissions puts pressure on the car development to reduce weights. Therefore the weight of the steering matters as well.

The weight of a steering increases with complexity. Its specific power is an important characteristic of the weight of the steering. The specific power is defined as power per mass; its dimension is [W/kg]. Among the steering types described here, the electro-hydraulic power steering has the highest specific power and the lowest weight in comparison to other steering variations. The overall weight of the hydraulic steering is, according to the vehicle class, something between 12 and 16 kg, comprising of the components steering gear, power steering pump, pipes and hydraulic oil. Electro-mechanical power steering (EPS) has a higher overall weight than hydraulic power steering (HPS). The weight of the EPS is essentially dependent on the mechanical power demand and, thus, mainly on the front-axle load of the vehicle. If little power is demanded from the electro-mechanical power steering—for example, by vehicles in the compact car segment—the weight of the EPS is almost equal to that of the hydraulic power steering. In general, the higher the required mechanical power, the heavier is the electric power steering (Fig. 3.2).

The excess weight of an electro-mechanical power steering unit may be justified only by the fuel saving attainable and its extended functionality, compared with conventional steering. There is a clear trend for steering manufacturers to make a significant effort to try to reduce the unfavourable weight of the electro-mechanical power steering for larger vehicle classes as well.

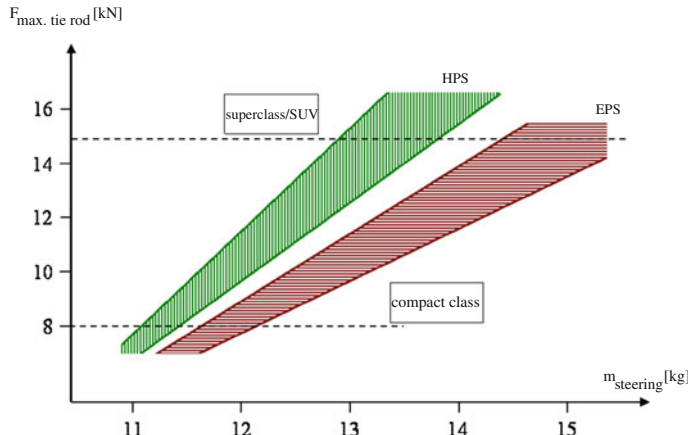


**Fig. 3.2** Weight comparison HPS versus EPSEPS

### 3.4 Costs

Hydraulic steering assistance of the kind built and integrated today has been used to support the steering power since the 1950s. It is a highly standardised technology developed during this time which is still found in most modern vehicles. The commonly used vane-type pumps and hydraulic steering gears are produced by millions and, due to their high level of maturity, provide little further possibilities for cost reduction.

The challenge that all the OEMs (Original Equipment Manufacturers) are facing now is the switch to new steering technologies, following the electrification of the steering line. This switch produces a rise of costs especially for high-power electro-mechanical steering units. Here, the main cost factors are the brushless DC motor, the control device, the sensors and the necessary output reduction gear that converts the rotation of the engine into a translational movement of the gear rack.

It is therefore sensible to define, develop and use components that are standardised for all the OEMs. This entails the realisation of larger scale effects and, thus, cost savings. Various modular designs for the above-mentioned purposes are currently emerging in the automotive industry.

### 3.5 Quality

Steering units of modern vehicles are subject to highest quality standards, e.g., the effectiveness of the steering has to be maintained for the whole life span, without servicing. This corresponds to a driving distance of approx. 300,000 km or an active period of 10 years, the typical desired complaint rate being as low as 500 ppm (parts per million).

In spite of the mature technology of hydraulic power steering, there are still appreciable complaint rates. Foremost among these are leakages due to the high number of tube connections between the system components, internal pollution increasing wear and leakage, and fluid noise of the circulating oil per se (see Sect. 3.7).

With electro-mechanical steering, the number of warranty cases is significantly lower. Here the challenge is rather to improve the quality in terms of noise and wiring load. One disadvantage of electro-mechanical steering is the higher warranty cost. Unlike with HPS systems, individual subunits cannot be exchanged any more if warranty cases arise; the higher complexity of EPS systems, due to integrated control devices and permanently connected electric motors, requires in most cases the exchange of the complete steering gear including its electrical components, causing substantial add-on costs for the after-sales.

### 3.6 Energy and Environment

Due to increasing discussions about climate protection, the automotive industry has lately been criticised quite frequently. Consequently, the European car manufacturers, in compliance with the EU, undertook major efforts to decrease the CO<sub>2</sub> output of their vehicles. It was reduced by intelligent lightweight construction, reduction of the road resistance, hybridisation of the powertrain and the associated electrification of the auxiliary units.

Two ways of development are emerging in the area of steering. One of them is the spreading application of power steering pumps with variable flow volume in electro-hydraulic power steering, reducing the pump loss. The other is the advancing substitution of hydraulically assisted steering by electro-hydraulic or electro-mechanical steering in the compact and middle class.

This switch of technology will soon also affect superclass and SUV vehicles. Those power steering technologies allow the realisation of the highest savings in consumption, meaning that the required electric power is drawn from the wiring only when the driver is actively steering. Furthermore, this steering equipment is able to maintain the steering assistance of hybrid vehicles in the electric traction mode.

### 3.7 Acoustics and Vibrations

Increasing demand for comfort in all areas of life extends inevitably into the automotive industry as well. Overall vehicle acoustics are gaining importance. The noise level of new vehicles is continuously reduced, so that the noise of the auxiliary units will appear more and more prominent. The development of steering is facing various problems of an acoustic nature.

Borne noise is the main problem of electro-mechanical steering, being induced by vibrations of the electric motor and the output reduction gear. As for electro-hydraulic power steering, fluid noises like hissing valves, the noise of the power steering pump and vibrations by system instabilities, for example the rattle of the steering, should be mentioned.

### 3.8 System Safety

DIN EN 61508 stipulates that safety is the absence of unacceptable risks and that damage to the health of people, either directly or indirectly, is a result of damages to objects or the environment. Referring to steering equipment, safety requirements can be distinguished into legal, mechanic, actuator-based and functional safety (Fig. 3.3).

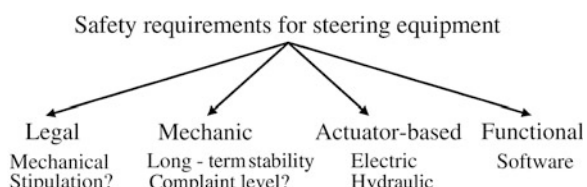
Different requirements for system safety emerge from the individual systems. The steering is a component that is relevant to safety, therefore special legal requirements apply (see Sect. 3.9).

Mechanical requirements essentially concern static and dynamic solidity, e.g., in the most critical cases of load, as in parking or kerb impact collision, the tie rod may be exposed to static forces of 15 kN and higher. Yet it may not be extremely rigidly designed, because in the case of abuse, the wheel supports, screw connections and especially the steering gear have to be protected against damage by purposeful distortion of the tie rod. Results of abuse even have to be obvious to the driver due to the skewed position of the steering or the wheel, and because the necessary visit to the garage will spare the components and especially the vehicle passengers from more considerable secondary damage.

Safety requirements are distinguished by electro-mechanical and hydraulic power steering equipment, depending on the kind of actuator. The hydraulic steering provides one critical case, which is the sudden loss of power support, e.g., by a failure of the power steering pump. If that happens, the steering forces rise dramatically, however, the vehicle will remain under control because the steering wheel is mechanically coupled to the steering gear. The necessary steering forces, however, must not exceed a level that the driver can reasonably apply.

Safety requirements for active steering systems like electro-mechanical or heterodyne steering are much more complicated and complex. Simply put, the serious fault case, unintentional actuator activity, must be avoided. Therefore, not

**Fig. 3.3** Safety requirements for steering equipment



only the control functions of the actuator must be developed and approved according to criteria relevant for safety but any potential external impacts, such as faulty sensor signals, electromagnetic incompatibility, insufficient energy supply etc., have to be considered in system safety as well.

### 3.9 Legal Requirements

The steering is a component that is relevant for safety and therefore subject to strict legal requirements. These requirements are intended to ensure that the vehicle will remain steerable in any active condition. The statutory requirements can be found in the corresponding directives, including §38 StVZO (German traffic law) and the European directive 70/311 EEC that will be replaced by ECE-R 79 in 2014.

§38 StVZO stipulates that the steering equipment must ensure easy and safe handling of the vehicle; if necessary, the vehicle must be equipped with assisted steering. If assisted steering fails, the vehicle must remain manageable.

The steering equipment shall ensure easy and safe handling of the vehicle up to its maximum design speed... There must be a tendency to self-centre... If a vehicle is fitted with ASE [auxiliary steering equipment], it shall also meet the [additional] requirements...

Section 70/311 EEC, as of 2008.<sup>1</sup>

In addition, the directive 70/311 EEC stipulates the permissible control effort. In a vehicle that is steered by muscular power (without steering assistance) and maximum permissible load of the steered axis, the power applied to the steering wheel must not be more than 250 N (ECE-R 79: 150 N) when steering a vehicle at 10 km/h out of a straight course into a circle of 12 m radius. In vehicles with auxiliary steering, the power required on failure of the auxiliary steering must not exceed 600 N (ECE-R: 300 N at 20 m of radius), this is safely realised in modern steering equipment. Moreover, this directive stipulates that the back wheels may not be the only steered wheels of a vehicle. Vehicles with all-wheel steering shall be able to cross a straight level distance at 80 km/h without unusual steering correction by the driver.

Legal requirements for the steering column are found, e.g., in ECE-R 116. This is a law that stipulates the test of an anti-theft device which is mounted at the steering column. When abused (by turning the steering wheel while the locking mechanism is closed), the locking system has to resist either a torque of 300 Nm under static conditions or a torque of at least 100 Nm shall cause slippage of the lock without damaging parts of the steering equipment.

---

<sup>1</sup> English quotation acc. to <http://eur-lex.europa.eu/LexUriServ/LexUriServ.do?uri=CONSLEG:1970L0311:19990216:EN:PDF> Sect. 4.1.1 [Translator's note].

Other directives of the *FMVSS (Federal Motor Vehicle Safety Standard)* and the *ECE (Economic Commission for Europe)* include provisions on the protection of passengers during a traffic accident. They will be only cursorily listed here, however:

- FMVSS 208: Occupant Crash Protection [in connection with the steering column]
- FMVSS 204: Steering Control Rearward Displacement
- FMVSS 203/ECE 12: Impact Protection for the Driver from the Steering Control System
- FMVSS 302: Flammability of Interior Materials
- FMVSS 107: Limitation of Surface Reflexions.

## References

- Braess HH, Seiffert U (2007) Handbuch Kraftfahrzeugtechnik. Vieweg Verlag, Wiesbaden  
Harrer M, Schmitt T, Fleck R (2006) Elektromechanische Lenksysteme—Herausforderungen und Entwicklungstrends, 15. Aachener Kolloquium Fahrzeug und Motorenmechanik, Aachen  
Heißing B, Ersoy M (2007) Fahrwerkhandbuch. Vieweg Verlag, Wiesbaden  
Mäder W (2002) Nationale und internationale Vorschriften für Lenkanlagen  
Walentowitz H, Freialdenhoven A, Olszewski I (2009) Strategien in der Automobilindustrie. Vieweg+Teubner, Wiesbaden

# Chapter 4

## Steering Kinematics

Michael Trzesniowski

### 4.1 Introduction

There are different basic methods how to control the direction of a car purposefully. Wheeled cars with pneumatic tyres may have integrated either single-pivot, buckling or axle-pivot steering. The first two types suffer the disadvantage that their footprint shrinks when steering and interfering forces will act on a lever arm that corresponds to half a tyre track. Moreover, either the front or rear tyres or all the tyres together may be steered. For high-speed cars, however, a third design is favoured: axle-pivot steering on the front axle. Therefore, only this type will be considered here. The rotational axis of the tyre trunk, or “steering knuckle”, on the tyre suspension (e.g., a “kingpin”) is usually steady when the car is steered (pure rotation of the tyre trunk); however, there are now many cars whose suspensions feature a variable (“virtual”) axis of rotation.

### 4.2 Characteristics of the Steering Geometry

When a car is turning very slowly, strictly speaking, without any lateral force, then all the tyres have to be oriented tangentially to concentric arcs. Their centre is called the instantaneous centre of the car.

This suggests Ackermann’s or the A-condition. According to Ackermann, these ideal steering wheel angles at the inner and outer tyre result from the relationship depicted in Fig. 4.1 (ignoring the changing longitudinal position of the tyres):

---

M. Trzesniowski (✉)  
FH Joanneum, Graz, Austria  
e-mail: michael.trzesniowski@steeringhandbook.org

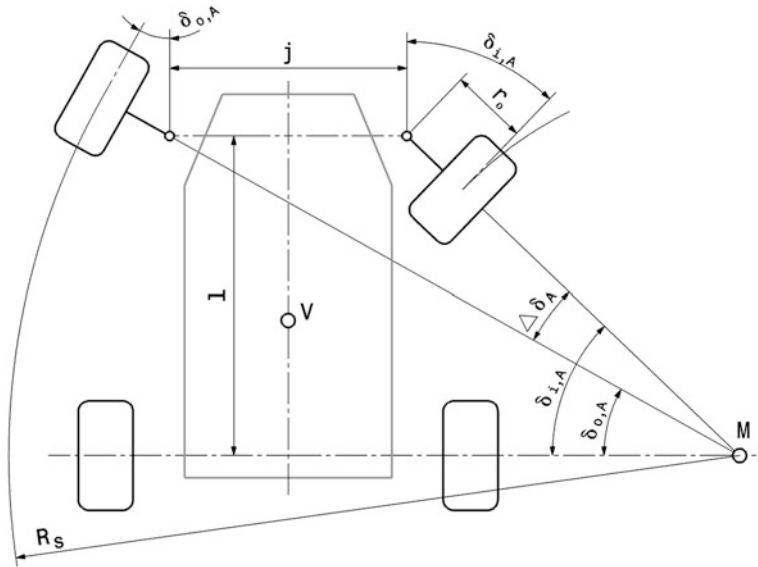
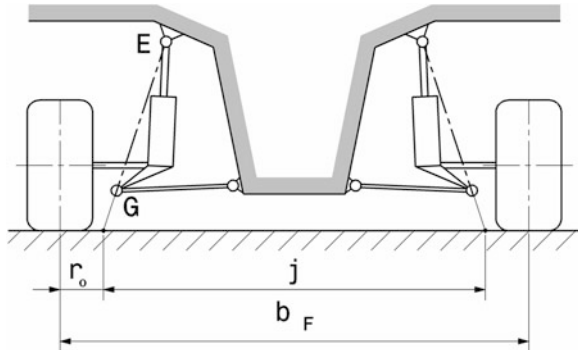


**Fig. 4.1** Kinematic relationships when cornering (Ackermann), car behaviour when rolling around the centre  $M$ ,  $j$  distance of the steering axes on the road, see Fig. 4.22;  $\delta_{o,A}$  steering wheel angle at the outer tyre;  $\delta_{i,A}$  steering wheel angle at the inner tyre;  $\Delta\delta_A$  Ackermann angle;  $R_s$  track arc radius;  $L$  wheelbase;  $V$  centre of mass of car

**Fig. 4.2** Distance descriptions to Fig. 4.1  $EG$  steering axis (kingpin axis);  $j$  distance of the steering axes on the road;  $b_F$  front track;  $r_o$  scrub radius (positive)



$$\cot \delta_{o,A} = \cot \delta_{i,A} + \frac{j}{l} \quad (4.1)$$

$\delta_{i,A}, \delta_{o,A}$  steering wheel angle according to Ackermann, ° see Fig. 4.1  
 $l$  wheelbase, mm  
 $j = b_F - 2r_o$  distance of the steering axes, in mm, see Fig. 4.2

If the scrub radius is negative, this is a positive number.

The difference of the steering wheel angles inside ( $i$ ) and outside ( $o$ ) is called the Ackermann angle (relative steering angle):  $\delta_A = \delta_{i,A} - \delta_{o,A}$ .

The track diameter  $D_S$ , i.e. the diameter of the smallest arc that the outer steered tyre may describe, results from:

$$D_S = 2R_S = 2 \left( \frac{l}{\sin \delta_{o,\max}} + r_o \right) \quad (4.2)$$

$D_S$  track diameter, in mm

$\delta_{o,\max}$  largest steering wheel angle of the outer tyre, in °.

It is obvious that speedy cars require a small wheelbase and a wide steering wheel angle. The steering wheel angles are limited by the design of the suspension, the space for bumping, compression/rebounding of closed wheels and the working angle of the drive shafts of powered axles. A short wheelbase has less favourable driving dynamics and is not a solution for lengthy cars anyway.

For a given track arc diameter, the main chassis dimensions, wheelbase and wheel track, directly affect the required steering wheel angle. This relationship has to be properly discussed during the early development stages of a car.

A kinematic discussion of these variables is shown in Fig. 4.3 (static steering design).

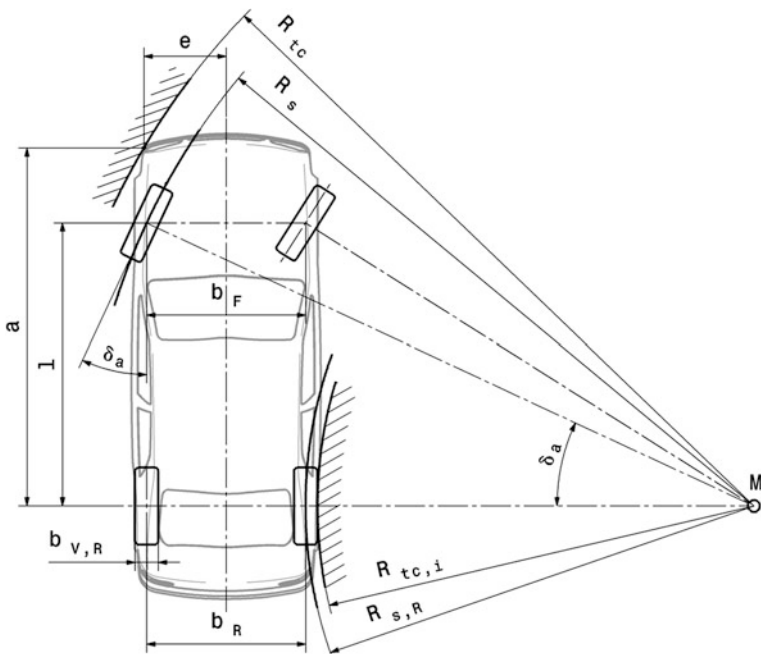


Fig. 4.3 Kinematic relationship between wheelbase, wheel track and track arc

Pure rolling (without the effects of tyre slip and suspension elasticities) implies a geometric relationship between wheelbase, wheel track, steering wheel angle and track arc diameter. In the conceptual phase of car development a comprehensive consideration of these parameters may be attained either from legal stipulations (least radii of roads) or from specification demands. If the speed and, hence, the slip angles are low, the instantaneous centre of the car M will be located on the rear axle (see Fig. 4.3). The cornering forces increase with increasing speed, the tyres respond with higher slip angles so that the instantaneous centre moves towards the front axle, cf. also Fig. 4.4.

The track radii result from the dimensions as follows:

$$\delta_o = \arcsin \frac{l}{R_S} \quad (4.3)$$

$R_S$  track arc radius, mm

$R_{S,R}$  rear track arc radius, mm

$\delta_o$  steering wheel angle of the outer tyre, °

$$R_{tc,i} = \sqrt{R_S^2 - l^2} - 0,5(b_F + b_R + b_{V,R})$$

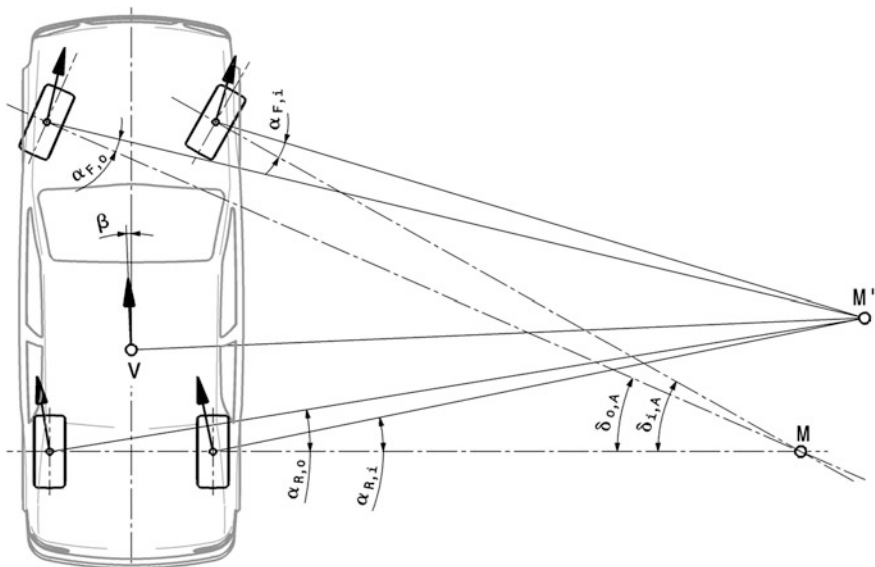


**Fig. 4.4** Cornering with lateral acceleration.  $\alpha_{F,i}$ ,  $\alpha_{R,i}$ ,  $\alpha_{F,o}$ ,  $\alpha_{R,o}$  slip angles in front or behind, inside or outside;  $\beta$  sideslip angle;  $M$  instantaneous centre acc. to Ackermann;  $M'$  actual instantaneous centre

$R_{tc,i}$  turning circle radius of the rear tyre, mm

$b_{V,R}$  rear tyre width, mm

$$R_{tc} = \sqrt{a^2 + (R_S \cos \delta_o + e - \frac{b_F}{2})^2}$$

$b_F, b_R$  wheel track in front or rear, mm

$R_{tc}$  track arc radius, mm

$a, e$  distances, mm.

A wheelbase  $l$  of 3,000 mm, front and rear track widths of 1,490 and 1,540 mm and a track arc radius of 7,500 mm will result in a required steering wheel angle at the outside tyre of 23.6°. The smallest radius  $R_{tc,i}$ , circled by an inner rear tyre that is 346 mm wide, is 5,186 mm.

The track arc radius is rather a theoretical value. The turning circle radius (between kerbstones) or, more accurately, the turning circle diameter is more obvious to the driver, that is why this value is found in the specifications, such as model sheets and measuring reports. Common values of passenger cars are about 11 m.

When a car turns, there is a lateral acceleration and the tyres have to build up a slip angle to transfer the lateral forces. The centre on which the car is cornering results from the intersection of the perpendicular line to the actual path of the moving wheels, see Fig. 4.4. In contrast to the ideal A-centre, this centre is moving forwards. The picture also demonstrates that in the case of an A-steering, the slip angles of the outer tyres are smaller than those of the inner tyres.

Other observations on the maximum steering wheel angle arise from the actual behaviour of the cornering tyres. When cornering fast, an A-design prevents the lateral force potential of the tyres from being fully exploited. Especially higher wheel loads on the outside would permit higher lateral forces. Yet the slip angles are behaving exactly the opposite way. If the outer wheel is turned more than the inner one (Fig. 4.5), the available space in the wheel arch is better used (this matters only in slow corners), the steering will respond faster and forces the higher loaded outer wheel to assume a higher slip angle (dynamic steering design). The cornering stability of the front axle can be increased in this manner. This advantage, however, is only effective when cornering fast; tight cornering will hardly exploit the lateral force of the tyres. This effect will therefore occur only at turning radii of  $\rho = 20$  m (Reimpel and Betzler 2000), corresponding, according to the car, to a steering wheel angle of 5–10°. Higher steering wheel angles should cause the actual curve of the Ackermann angle to approach the nominal curve again, so that tension, wear of the tyres and road resistance in narrow corners are reduced. Figure 4.6 shows such a course of the A-angle.

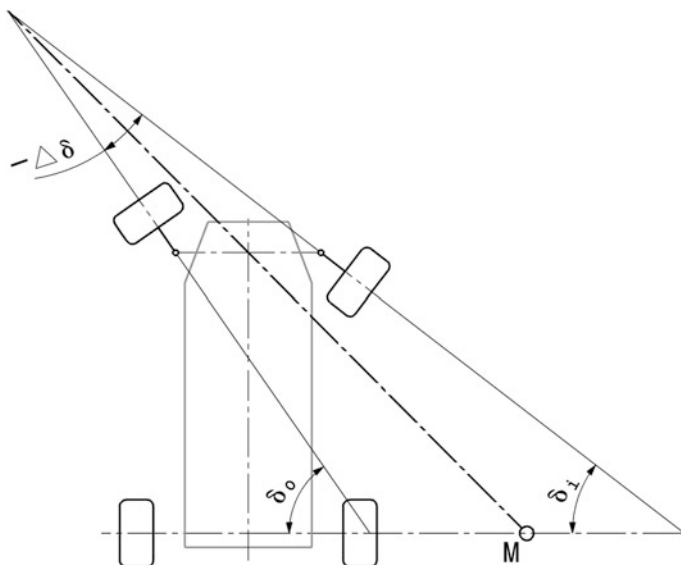


**Fig. 4.5** Increase of the cornering force in *front* when cornering wide, i.e. for small steering wheel angles. The *outer tyre* is turned more than the *inner tyre*. The A-angle  $\Delta\delta$  is therefore negative

If the steering wheel angle is small, the steer angles of the inner and outer wheels may therefore be equal (a parallel steer, then the A-angle is zero).

The difference from the ideal A-angle is called steering error:

$$\Delta\delta_F = \delta_o - \delta_{o,A} = \Delta\delta_A - \Delta\delta \quad (4.4)$$

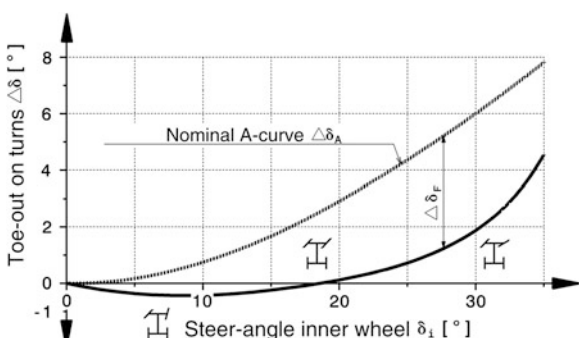
$\Delta\delta_F$  steering error, better: artificial steering divergence, °

$\delta_i, \delta_o$  steering wheel angle inside or outside, °

$\Delta\delta_A$  toe-out on turns according to Ackermann, °.  $\Delta\delta_A = \delta_{i,A} - \delta_{o,A}$

$\Delta\delta$  artificial toe-out on turns, °.  $\Delta\delta = \delta_i - \delta_o$ .

**Fig. 4.6** Curve of an ideal, A-angle  $\Delta\delta$ . In addition, the position of the *front* wheels is schematically shown for this ideal curve



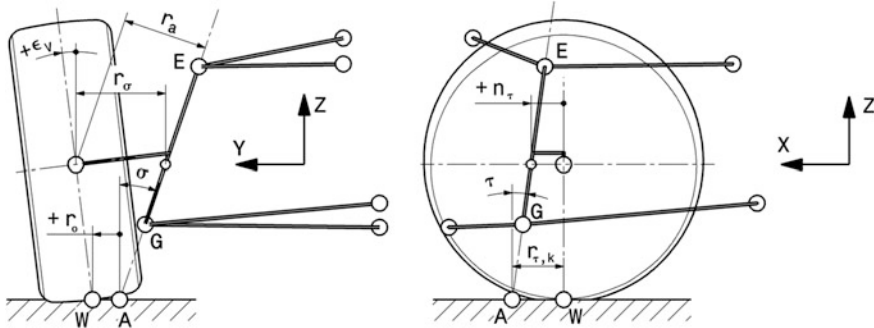


**Fig. 4.7** Steering geometry parameters acc. to Matschinsky (2007). Rear view (left, cross-plane YZ) and side view (right, parallel plane XZ)  $\sigma$  kingpin inclination angle. Typical values design attitude: 5 to 16°;  $\tau$  castor angle. Typical values design attitude: 1–5°;  $r_o$  scrub radius. Counted positively outward from the penetration point A. Typical values when mounted: -20 to +80 mm;  $r_\sigma$  lateral offset;  $r_a$  interfering force arm;  $r_{\tau,k}$  castor offset. Typical values when mounted: 15–45 mm;  $n_t$  trail: Positive if the wheel centre is behind the steering axis EG. Typical values when mounted: -5 to 18 mm;  $\varepsilon_V$  Camber angle. Positive if the wheel is outwardly tilted (slanted). Typical values when mounted: -2 to 0°

The steering should therefore generate a toe-out curve similar to the one shown in Fig. 4.6. This diagram displays the curve of the A-angle as a function of the steering wheel angle at the inner wheel  $\delta_i$ . In addition, the curve of the toe-out  $\Delta\delta_A$  is shown. The resultant steering divergence  $\Delta\delta_F$  is depicted for a steering wheel angle.

If the steering wheel angle is low, the outer tyre is turned more than the inner tyre. There is a transitional zone in which the tyres are parallel, and for stronger turns, the curve approaches the A-curve by about 50 % of its value (Remark: For tighter turns the curve reaches 4° and the A-curve 8°).

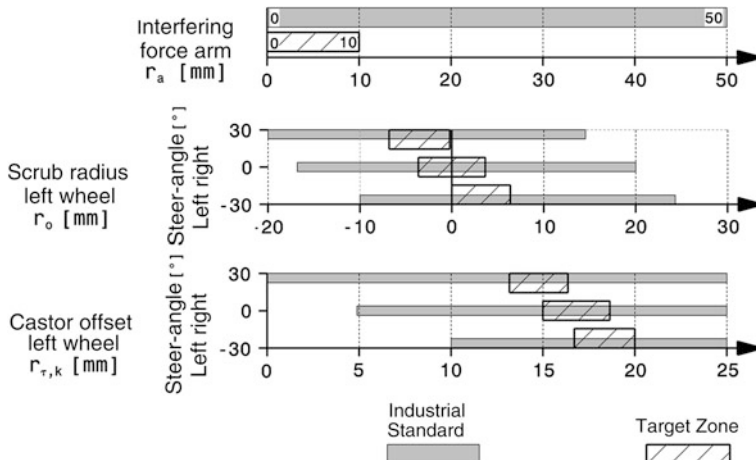


**Fig. 4.8** Target areas of parameters of passenger car front axles, acc. to Heissing (2004)

The divergence from the Ackermann design is sometimes given in percent:

$$\text{Percent Ackermann} = \frac{\Delta\delta}{\Delta\delta_A} \cdot 100\% \quad (4.5)$$

- 0 % Ackermann: Parallel turn
- 100 % Ackermann: The artificial toe-out on turns corresponds neatly to the Ackermann angle.

A divergence from the Ackermann design has the favourable side effect that the track diameter will be smaller while the car geometry remains the same. A measurement series has shown that the track diameter can be reduced by approx. 0.1 m for each 1° of steering divergence (Reimpel and Betzler 2000). The following numerical equation illustrates this:

$$D_S = 2 \left( \frac{l}{\sin \delta_{o,A,\max}} + r_o \right) - 0,1 \cdot \Delta\delta_F \quad (4.6)$$

$\Delta\delta_F$  artificial steering divergence, °

$D_S$  track diameter, m

$r_o$  scrub radius, m

$l$  wheelbase, m.

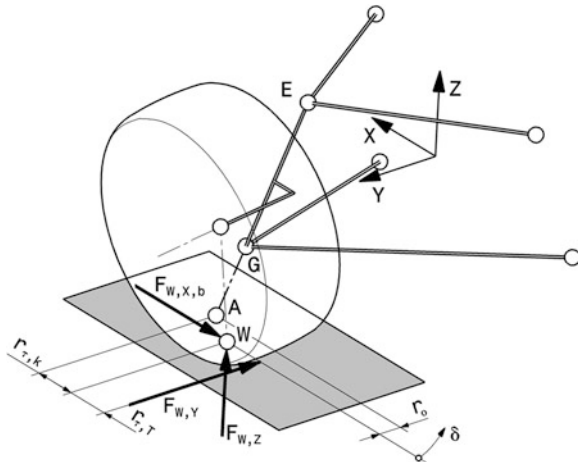
The maximum steering wheel angles of passenger car wheels are 45–50°. This permits for middle class cars typical track diameters of about 8 m.

### 4.3 Characteristics of the Wheel Position

The position of the front wheels is described by different parameters, some of them are discussed in Chap. 5. There are further variables that cannot be represented by visible design parameters but result from computing several geometrical variables. They are helpful for the assessment and layout of the steering geometry (Fig. 4.7).

The kingpin inclination angle  $\sigma$  and the castor angle  $\tau$  substantially affect the change of the camber  $\varepsilon_V$  when the wheel is turned. The steering axis EG intersects the road in point A. The horizontal distance between the CTC W and A, as seen in the rear view, is the scrub radius  $r_o$ , although the CTC W usually does not move at this radius, because the actual distance of the two points is wider when steering (cf. also Fig. 4.9). The steering axis is tilted with the castor angle  $\tau$ . The wheel centre does not need to be located on the projection of the steering axis but can be shifted either forwards (positive along X) or backwards (negative along X) by a trail  $n_\tau$ . The distance of the points W and A, as seen in the side view, is the castor offset  $r_{\tau,k}$ . If a negative trail  $n_\tau$  is provided (negative along X), the trail  $r_{\tau,k}$  is reduced by the same amount and the camber will change more favourably upon steering.

**Fig. 4.9** Forces at the front tyre: a *left front* wheel is shown. W CTC; A intersection of steering axis and road; EG steering axis;  $\delta$  steering wheel angle;  $F_{W,X,b}$  braking force;  $F_{W,Y}$  lateral force;  $F_{W,Z}$  wheel load;  $r_{t,k}$  castor offset;  $r_{t,T}$  trail



Corresponding to the trail there is a lateral offset  $r_\sigma$ . The lateral offset is the horizontal distance between wheel centre and steering axis, as seen in the rear view. The vertical distance  $ra$  of the wheel centre from the steering axis is important for the response to longitudinal forces (from drive torques) acting on the steering. This distance is also called longitudinal or interfering force arm, because all the forces issued by the tyre of the passively rolling wheel upon the bearings in the wheel centre, are transferred to the hub carrier and on to the steering.

Figure 4.8 shows target values of some parameters from the passenger car development.

The above geometrical values describing the wheel position allow to the computation of the effects of forces on the tyre, Fig. 4.9.

If a braking force  $F_{W,X,b}$  applies at the tyre in X direction, it combines with the scrub radius to generate a spatial moment around the Z axis (Matschinsky 2007):

$$M_{A,Z,b} = F_{W,X,b} \cdot r_o \quad (4.7)$$

$M_{A,Z,b}$  moment of the braking power around the intersection A of the steering axis, in Nm. This moment turns around the Z axis and not around the steering axis

$F_{W,X,b}$  braking power of the tyre, N

$r_o$  scrub radius, m.

The moment around the steering axis results from the projection of its vector on the axis:

$$M_{A,b} = F_{W,X,b} \cdot r_o \cdot \cos \sigma \cdot \cos \tau \quad (4.8)$$

$M_{A,b}$  moment of the braking power around the steering axis, Nm.

It is obvious that a larger scrub radius  $r_o$  causes a larger moment of the braking power around the steering axis. The scrub radius should therefore be very small, so that differing friction conditions on braking will affect the steering less. Negative scrub radii (i.e.  $r_o$  is turned from the CTC W outwards) are also used in passenger cars to generate a stabilising righting effect if the brakes should respond unequally. The geometry of a negative steering offset may be described like this: the joint points E and G of the hub carrier have to shift towards the wheel centre so that the brake disk will have to be relocated farther out. This can entail that the brake disk of narrow drop-centre rims loses about 25 mm of diameter while the rim diameter remains the same. This target conflict can be resolved by separating the triangular wishbone into two support rods that engage at two separate joints of the hub carrier, creating a quadrangle. At the intersection of two support rods, the usually solid joints E or G turn into virtual joints and the solid steering axis becomes an ideal axis. These virtual joints may be arranged in or beyond the brake disk without any problems.

Corresponding to the braking power, a lateral force  $F_{W,Y}$  is effective over the longitudinal distance between the force and the penetration point A of the steering axis on the road. The overall distance results from the addition of kinematic castor (castor offset  $r_{\tau,k}$ ) and pneumatic trail  $r_{\tau,T}$ .

The steering axis is not perpendicular to the road, therefore the distance of the wheel centre to the road changes when steering. The front end rises or lowers. This means that the wheel load effects the steering moment, a part of which has to be contributed by the driver. This phenomenon can be computed using the wheel load arm  $q$ , unfortunately, it cannot be visualized that easily. The wheel load arm referring to the Z axis is:

$$q = r_o \cdot \tan \tau + r_{\tau,k} \cdot \tan \sigma \quad (4.9)$$

$q$     wheel load arm, mm.

Angles and lengths: see Figs. 4.7 and 4.9.

A wheel load does not issue a moment around the steering axis if the axis is either vertical or the vertical force intersects the steering axis.

The wheel load arm  $q$  is defined to be positive if the moment generated by the wheel load produces a self-centring action, i.e. acts to reduce the steering wheel angle  $\delta$ . This is also called a weight righting of the steering because the wheels are returned by the wheel load into the straight position. This definition of a positive wheel load arm means that the wheel load is righting as soon as  $q$  and  $\delta$  have the same sign.

The wheel load arm can also be considered an alteration of the front end's level above the steering wheel angle:

$$q = -\frac{dz}{d\delta} \quad (4.10)$$

If the wheel load arm  $q$  is positive, steering with a positive steering wheel angle  $\delta$  (turning the inner wheel) will lift the body.

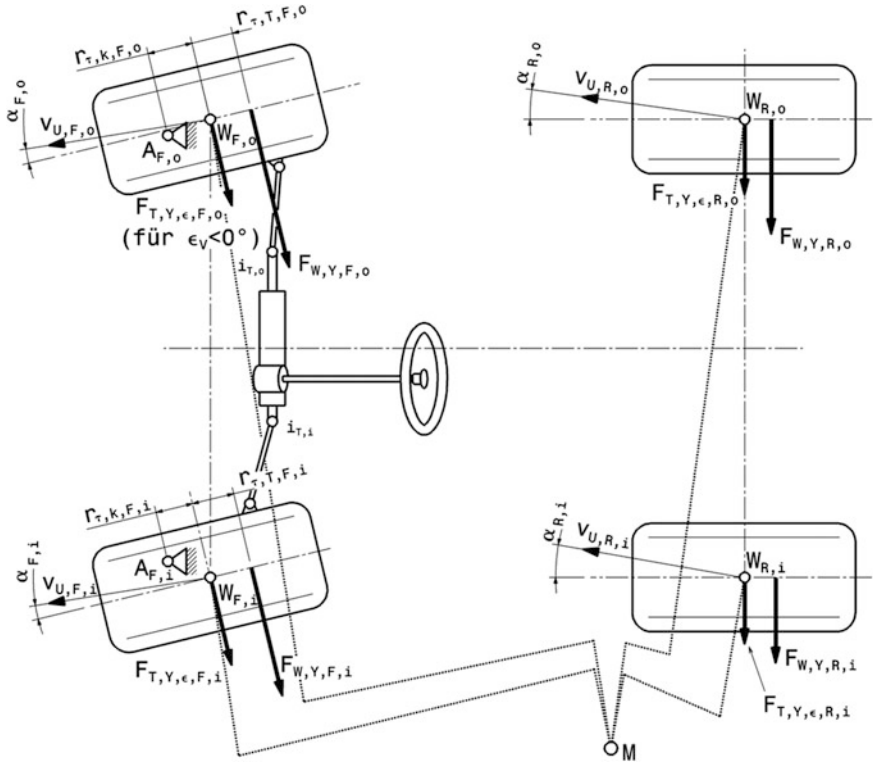


**Fig. 4.10** Righting of the steering by lateral acceleration, acc. to Matschinsky (2007). A Penetration point of the steering axis with the road; W CTC;  $\alpha$  slip angle; M centre of corner Index values: i or o inside or outside; F or R front or rear

The wheel load arm should be very small, so that fluctuations of the wheel load will not impact the steering.

However, weight righting matters almost exclusively at very low speed or when parking. At high speed, the aligning moments of the side forces are much bigger, Fig. 4.10.

The steering wheel angles are generally smaller at high speed than they are in slow corners. The nature of the Ackermann angle at the front wheels is therefore negligible, e.g., whether it is an Ackermann design or a parallel turn. The slip of all the wheels makes the centre M shift forwards. The side forces  $F_{W,Y,F}$  resulting from the slip are chiefly responsible for generating the perceptible torque at the steering wheel. The righting effect of the wheel loads is low in comparison. In contrast to the camber side forces  $F_{T,Y,\epsilon}$ , the slip side forces engage around the castor offset  $r_{\tau,T}$  behind the CTC W; they are larger at the outside because the wheel load shifts towards the outer wheels. If the front axle is driven, the driving forces, effecting a torque around the steering axis by way of the interfering force arm  $ra$ , add to the forces shown in Fig. 4.10.

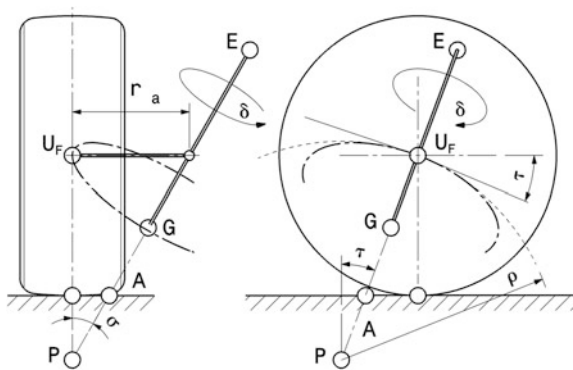
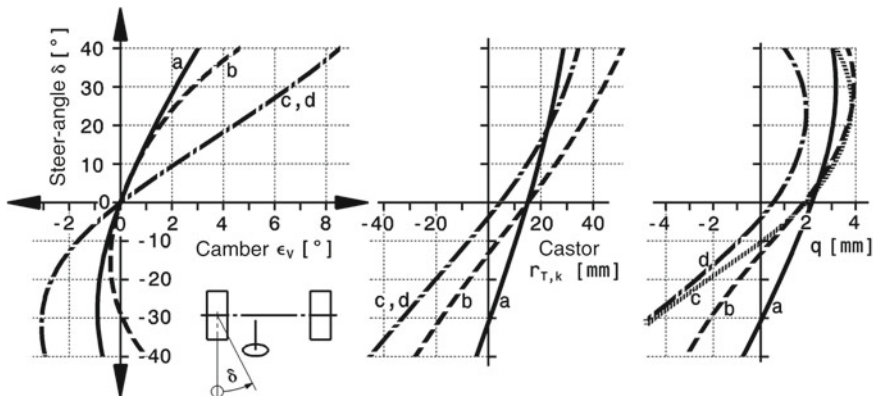


**Fig. 4.11** Influence of castor and steering axis inclination on the change of camber.  $U_F$  front wheel centre;  $\delta$  steering wheel angle;  $P$  instantaneous centre of the wheel centre  $U_F$ ;  $\rho$  curvature radius of the trajectory of  $U_F$



	$\sigma$	$\tau$	$r_o$	$r_{\tau,k}$
a	5°	3°	50	16
b	12°	3°	0	16
c	12°	9°	15	5
d	12°	9°	0	5

$$\epsilon_v(\delta = 0^\circ) = 0^\circ$$

tyre radius 300 mm

**Fig. 4.12** Curves of camber, castor and wheel load arm  $q$  upon steering, acc. to Matschinsky (2007). Positive steering wheel angles  $\delta$  at the inner wheel, negative angles at the outer

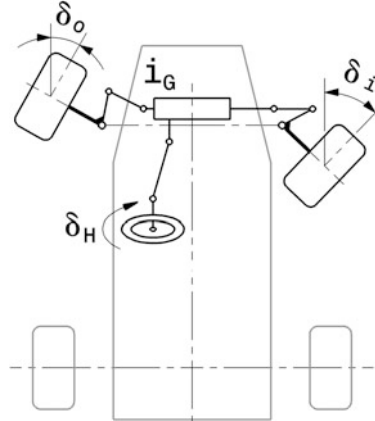


**Fig. 4.13** System overview, axle-pivot steering. The steering wheel angle  $\delta_H$  at the wheel is transformed into the steering angles  $\delta_o$  and  $\delta_i$  of the outside and inside wheels by the gear, with the internal gear ratio  $i_G$ , and by the linkage

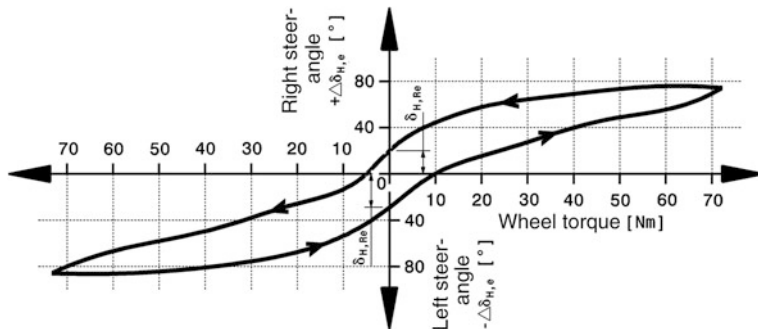


**Fig. 4.14** Compliance measurement of the steering of an immobile passenger car, acc. to Reimpel and Betzler (2000). The wheels were fixed during the measurement and a torque was applied to the steering wheel. As expected, the yielding  $\Delta\delta_{H,e}$  at the wheel increases with the torque. The resistance, that is the stiffness of the steering, increases as well. Thus the curve becomes less steep. The wheel is turned to the *right* and *left*. A hysteresis occurs and a residual angle  $\Delta\delta_H$ ,  $Re$  remains at the unloaded wheel

The righting moment at the steering gear, including all the forces, according to Matschinsky (2007), derives from:

$$\begin{aligned}
 M_G &= [F_{W,Y,F,o} \cdot (r_{\tau,k,F,o} + r_{\tau,T,F,o}) - F_{T,Y,e,F,o} \cdot r_{\tau,k,F,o} - F_{W,Z,F,o} \cdot q_{F,o} - F_{W,X,a,F,o} \cdot r_{a,F,o}] / i_{T,o} \\
 &\quad + [F_{W,Y,F,i} \cdot (r_{\tau,k,F,i} + r_{\tau,T,F,i}) + F_{T,Y,e,F,i} \cdot r_{\tau,k,F,i} + F_{W,Z,F,i} \cdot q_{v,i} + F_{W,X,a,F,i} \cdot r_{a,F,i}] / i_{T,i} \\
 M_H &= \frac{M_G / i_G}{A_s}
 \end{aligned} \tag{4.11}$$

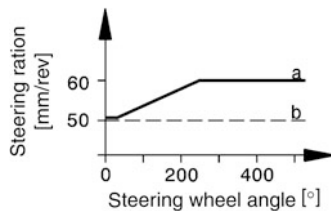


**Fig. 4.15** Variable steering ratio of a hydraulically assisted rack-and-pinion steering in a sports car (Porsche 911 Carrera), acc. to Achleitner (2005). **a** Model year 2005. While the steering wheel angle is small, the gear ratio is similar to that of the predecessor model, 17.1:1. If the steering wheel angle is more than 30°, the steering ratio drops down to 13.8:1. **b** Predecessor model with steady gear ratio

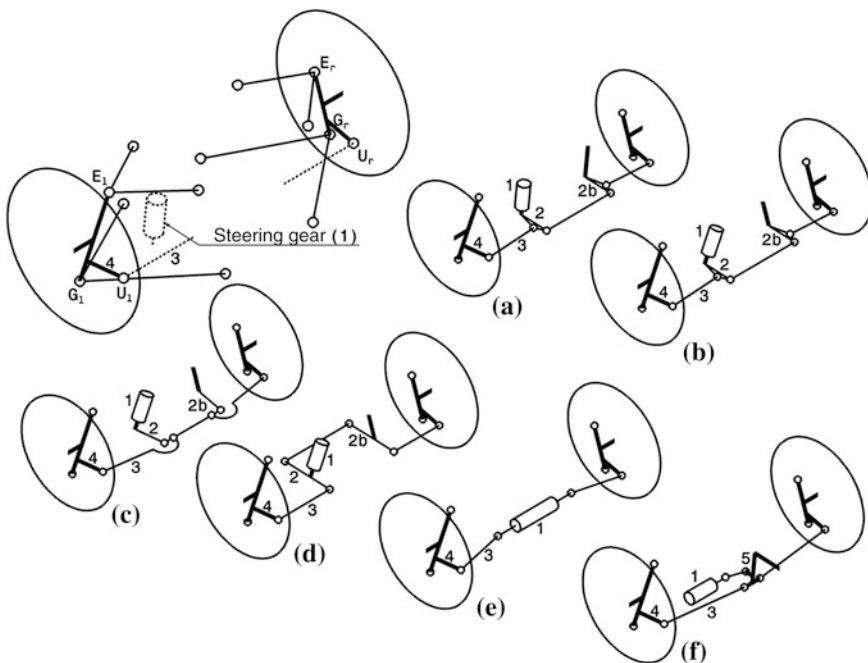


**Fig. 4.16** Steering linkage for independent suspension. Initial situation top left: The two joints  $U_l$  and  $U_r$  of the steering arms (4) on the left and on the right must be conveniently connected to the steering gear (1). **a** Vertical steering gear; **b** steering gear parallel to the steering axis EG; **c** central tie rod and ball joints; **d** rocker arm as intermediate lever; **e** gear rack as tie rod; **f** gear rack and intermediate lever

$M_G$	Moment at the steering gear when rotating, Nmm
$r_{\tau,k}$	kinematic castor, mm
$r_{\tau,T}$	pneumatic trail, mm
$F_{W,Y}$	side forces by tyre slip, N

$F_{T,Y,\varepsilon}$	side forces by tyre camber, N
$F_{W,Z}$	wheel loads, N
$F_{W,X,a}$	drive at a wheel, N
$r_a$	drive rocker arm, mm. See Fig. 4.7
$i_T$	steering linkage gear ratio,—See Fig. 4.17
$M_H$	moment at the steering wheel (steering wheel torque), Nm
$i_G$	steering gear ratio, with $i_G = \delta_H/\delta_G$ . $\delta_H$ angle at the steering wheel,
$\delta_G$	angle at the drop arm,
$A_S$	Steering amplification.

For most kinds of wheel suspensions, the kinematic castor  $r_{\tau,k}$  increases at the inner steering wheel angle  $\delta$  and drops at the outer steering wheel angle. The castor offset  $r_{\tau,T}$  decreases with increasing lateral acceleration. This reduces the influence of the outer side force  $F_{W,Y,F,o}$  until it may even reverse, i.e. the side force will then act to increase the steering wheel angle. This effect is usually not very pronounced, however, because the steering linkage gear ratio grows at the outer turn more than at the inner turn. Thus the contribution of the outer tyre to the steering moment drops relative to the inner tyre.

The spatial slip of the steering axis to the road (castor and steering axis inclination angle) causes the camber angle of the wheel to alter when steering. The tendency is obvious from the following. If the steering axis does not have a castor angle ( $\tau = 0^\circ$ ) and if the camber is  $0^\circ$  in the straight position, then a cornering steering angle  $\delta$  of  $90^\circ$  will add an amount to the camber angle that is exactly equal to the steering axis inclination. More detailed analysis results in Fig. 4.11. When

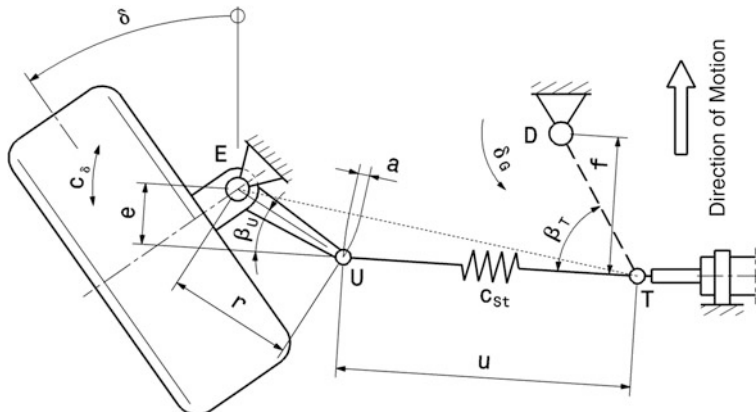


**Fig. 4.17** Transmission angles of steering linkages, acc. to Matschinsky (2007). The linkage with rack gear and, alternatively, with a drop arm (dashed) in point D are depicted for a *left* front wheel.  $\beta_U, \beta_T$  Transmission angles;  $u$  Length of the tie rod;  $a$  Longitudinal overlap of steering arm and tie rod;  $r$  length of the steering arm;  $c_{st}$  Stiffness of the tie rod;  $c_\delta$  torsional stiffness of a wheel around the steering axis;  $e$  effective lever arm of the tie rod;  $f$  effective lever arm of the drop arm

steering, the wheel centre  $U_F$  circles around the steering axis EG. In the side view, this trajectory looks like an ellipse. In the straight position ( $\delta = 0$ ), the tangent to this trajectory is inclined by the castor angle  $\tau$  (with  $n_\tau = 0$ ). The associated radius of curvature  $\rho$  is determined by the centre P. The centre itself is the intersection of the steering axis with the vertical level at  $U_F$ . The geometry gives:

$$\rho = r_o / (\tan \sigma \cdot \cos \tau) \quad (4.12)$$

The curvature  $\varepsilon_V(\delta)$  is therefore proportional to the steering axis inclination angle  $\sigma$ . When a steering wheel angle is applied, a positive steering axis inclination bends the curve towards positive camber angles.

The change rate of the camber over the steering wheel angle depends on the castor angle and the steering axis inclination angle, cf. Matschinsky (2007):

$$\frac{d\varepsilon_V}{d\delta} = \frac{\tan \tau \cdot \cos \delta + \tan \sigma \cdot \sin \delta}{\tan \varepsilon_V \cdot (\tan \tau \cdot \sin \delta - \tan \sigma \cdot \cos \delta) + 1} \quad (4.13)$$

$\varepsilon_V$  camber angle,  $\delta$  steering wheel angle.

Figure 4.12 compares the effects of some different designs of steering geometry.

Version a has a low steering axis inclination and a low castor, hence, wider distances to the CTC, i.e. scrub radius  $r_o$  and kinematic castor  $r_{\tau,k}$ . Versions c and d have the widest angles of steering axis inclination and castor; they differ only in the scrub radius.

The tangent of the camber curve at a steering wheel angle = 0° in the versions c and d is substantially more level than those of the other curves. The inclination of the tangent at the curves a and b is about three times larger, corresponding to the relation of the castor angles  $\tau$ . The wider steering axis inclination of version b bends the curve much stronger than that of version a. Hence, beyond a steering wheel angle of -30° (outside) the camber will turn positive. In general, the camber of the (deflecting) outer wheel should drop into the negative zone while the inner wheel should have a positive camber or at least not an increasingly negative one. Versions c and d are therefore more favourable with regard to the camber while b has an undesirable positive outer camber.

The castor increases at the inner wheel in all the versions and decreases at the outer wheel down to negative values.

All versions suffer the effect of weight centering in the straight position, because the wheel load arm  $q$  is positive when the steering wheel angle is  $\delta = 0^\circ$ . At the inner wheel (positive steering wheel angles) this is also true when other steering wheel angles apply ( $q$  and  $\delta$  having the same sign), for the outer wheels it is only true beyond a specific steering wheel angle. Version d gives the best result in that respect. Version a, as expected, requires the largest steering wheel angle:  $\delta = -30^\circ$ .

If the castor offset  $r_{\tau,k}$  is non-zero, the CTC moves laterally to the steered car. If the castor offsets of both front axle wheels are equal, the front end is laterally shifted. In any case, all versions display this behaviour in the straight position.

Different castor offsets cause a relative transverse movement of the two wheels. This increases the deformation of the tyres and therefore the steering forces when parking. Version a is closest to the ideal of inner and outer castor being equal. Versions c and d may expect the largest parking forces.

Versions b and d have a scrub radius of 0 mm, however, their CTCs still move when cornering because the castor is non-zero. If the steered wheel should really turn on the spot, then the steering axis would have to cut the road in the CTC W. Then scrub radius and castor alike would be zero.

### 4.3.1 Steering Ratio

Once the greatest necessary steering wheel angle is known, the required gear ratio between steering wheel and front tyres must be defined. Regulations for road vehicles stipulate (so far) a permanent mechanical connection between steering wheel and steered tyres. The steering movement is transferred from the wheel to the tyres by the steering linkage (tie rods, drag links etc.), operated by a steering gear (Fig. 4.13). The gear has an internal gear ratio  $i_G$  to reduce the steering wheel forces. The linkage usually has a gear ratio between gear and tyres that is changing with the steering wheel angle.

The kinematic steering ratio  $i_S$  from wheel to tyres results from the wheel angle  $\delta_H$  and the steering wheel angles:

$$i_S = \delta_H / \delta_m \quad (4.14)$$

$i_S$  kinematic steering ratio, -

$\delta_H$  steering wheel angle, °

$\delta_m$  mean steering wheel angle of the tyres, °.  $\delta_m = (\delta_o + \delta_i)/2$ .

The gear ratio will usually not be the same all over the steering range. The above equation therefore applies only to individual ranges of wheel angle and steering wheel angle.

The overall gear ratio has a lower limit because at high speed the steering response should be indirect; values of less than 14 are rarely found in passenger cars. The upper limit results from what steering force is sensible when parking, this depends on whether power-assistance is given and rarely surpasses a gear ratio of 20 (i.e. 4–5 wheel turns, end-stop to end-stop; 3–4 are more common). The overall gear ratio is realised by the product of linkage ratio and gear ratio. The average of outer and inner steering angle has to be considered for the linkage ratio. If the effective trace levers are known (projection of the levers onto a plane that is normal to the kingpin axis), the linkage ratio may be computed from the relation of steering arm to drop arm. The quotient of effective steering arm and pinion radius is used for rack-and-pinion steering (cf. Sect. 5.2.2).

The kinematic steering ratio differs from the real conditions by the fact that all transmission elements will display elasticities and free travel. The steering wheel can therefore be turned without moving the tyres. A measurement at a passenger car with rack-and-pinion steering may illustrate how significant these divergences can be for car, Fig. 4.14.

Typically, the effective steering ratio which the driver will perceive upon driving is the dynamic steering ratio, resulting from the kinematic gear ratio by overlapping the yielding of the transmission elements:

$$i_{dyn} = i_S + \frac{\Delta\delta_{H,e}}{\Delta\delta_H} \quad (4.15)$$

$i_{dyn}$  dynamic steering ratio,

$\Delta\delta_{H,e}$  elastic yielding at the wheel,

$\Delta\delta_H$  steering wheel angle range at the wheel when  $\Delta\delta_{H,e}$  occurs.

In other words, the driver perceives that elasticities in the steering system will amplify the steering ratio. The steering wheel must in fact be turned more than what is necessary in theory to apply a specific steering wheel angle of the tyres. If the steering torque is increased—e.g., by a power-assistance, aerodynamic downforce or off-road driving—the proportion of the yielding will also increase (see Sect. 5.2.2).

If several articulated chains are active, they may cause car steering with gear racks to suffer unintentional changes of the kinematic steering ratio across the steering wheel angle range. Of course, front-wheel drives are inferior to standard drives here, because of the cramped space between engine and gearbox. The gear ratio of front-wheel drives will therefore drop to 17 or 30 % from the straight position to the full steering wheel angle while rear-wheel drives face only a drop of 5–15 % (Reimpel and Betzler 2000).

One way to overcome the required compromise of any specific steering ratio is to use gears with variable gear ratios.

The steering ratio  $i_S$  or  $\delta_H/\delta_m$  may then be high around the middle position (straight driving and minor steering wheel angles) but large steering wheel angles of the tyres will lower the ratio, cf. Fig. 4.15 (see also Chap. 11).

## 4.4 Steering Linkage

No matter whether a rack-and-pinion steering or any other steering gear is used, the movement of this gear, fixed to the frame, must be transferred to the steering arms at the hub carrier. The best solution for an independent suspension is to apply (flexibly coupled) linkages that have to transmit not only the steering movement but also the motion of the lifting wheel when giving. Figure 4.16 shows some possible arrangements of linkages.

Version a has parallel rotational axes of the steering gear (1) and the opposite guide lever (2b). The drop arm (2), the guide lever and the middle section of the

three-piece tie rod (3) are arranged in a planar four-bar linkage (more precisely, in a parallelogram). The two levers move the outer parts of the tie rod. This version has an unfavourable friction. All six joints of the leverage will trace almost the full steering wheel angle. Additionally, there is the undesirable impact of free travel of the joints. Version b is very similar to version a, but the axes of the steering gear (1) and the guide lever (2b) are adapted to the inclination of the steering axis EG. This is required for wide steering axis inclination angles, as otherwise, the righting effect caused by the giving of the wheels would be too large. Version c has a middle section of the tie rod (3) that is supported in ball joints. This rod has one more degree of freedom: a rotation around its axis. Therefore, the centres of the joints of the two outer tie rods have to be positioned on this axis of the central tie rod, so that they cannot perform any undesirable rotation. Version d transmits the movement of the steering gear (1) via two relay arms (2, 2b) to the tie rods (3). A clearance develops in the middle of the car (possibly for the engine), but unfavourably high reaction forces occur, resulting in big elastic distortions. Version e is a rack-and-pinion steering. Its simplicity and its low number of parts are evident. Version f has a gear rack that does not move the steering arms (4) directly but via an inserted lever (5). The disadvantages are obvious from a comparison with the above considerations. There are more parts integrated than in a simple gear rack, increasing mass, free travels and elasticities.

Consider the transmission angles occurring at the basic arrangement of levers and push rods (here called tie rods). They are critical for the safety of the steering, Fig. 4.17.

If the transmission angle  $\beta_U$  or  $\beta_T$  is equal to zero, then the linkage is unstable. Though rack-and-pinion steerings are lacking the drop arm and the centre of rotation D is a distant point, there is still the steering arm. The angle  $\beta_U$  of the driven steering arm in particular may not drop below a least value, so that the steering linkage will not be strained. A least angle is necessary to accommodate for free travels and elasticities. The transmission angle should not fall short of  $25^\circ$ . The linkage gear ratio results from:

$$i_T = \frac{d\delta_G}{d\delta} = \frac{e}{f} \quad (4.16)$$

- $i_T$  linkage gear ratio, -
- $\delta_G$  rotary angle of the drop arm,
- $\delta$  steering wheel angle of the tyre,
- $e, f$  effective lever arms, mm. See Fig. 4.17.

The length of the steering arm  $r$  is a factor for assessing the safety reserves of the steering. Figure 4.18 shows the curve of important variables over the transmission angle  $\beta_U$  for a numerical example of a tie rod of  $u = 300$  mm in length. Diagram c, representing the critical energy consumption until the leverage is strained, reveals that short steering arms require wider transmission angles so that the least energy consumption will not be undercut. In fact, the minimum

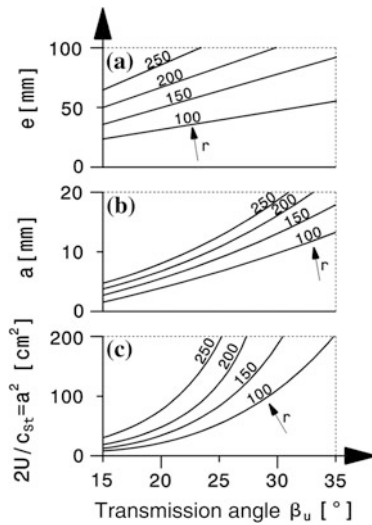


**Fig. 4.18** Effect of the transmission angle on the safety of the steering, acc. to Matschinsky (2007). See also Fig. 4.17.  $u = 300$  mm. **a** The effective rocker arm  $e$  of the steering arm around the steering axis E increases with the transmission angle and the length of the steering arm  $r$ . **b** The longitudinal overlap  $a$  of steering arm and tie rod is a measure of the distance from the straining point. Small values of  $a$  increase the risk of straining. Long steering arms and large transmission angles are desirable with regard to this aspect as well. **c** The tie rod is the only elastic link in the transmission chain with the stiffness  $c_{st}$ . The effective torsional stiffness of a wheel around the steering axis is then  $c_\delta = c_{st}e^2$ . Therefore the energy consumption before buckling of the linkage is  $U = c_{st}a^2/2$

transmission angles of passenger cars are  $20^\circ$  for long steering arms and  $30^\circ$  for short steering arms (Matschinsky 2007).

Now the transmission of rack-and-pinion steerings shall be examined in detail. The position of the steering gear (in front of or behind the axis) is decisive for how to arrange the pinion in respect to the gear rack and how to adjust the steering arms. The steering by the driver is transferred from the steering shaft to the pinion and further to the gear rack. The transmission chain has to be set up in such a way that the tyres will turn right when the wheel is turned right, Fig. 4.19.

The steering arms may point forwards or backwards, whatever the position of the steering gear. The levers, however, must be tilted along the longitudinal plane of the car to achieve a proper A-steering, see Fig. 4.20.

When seen from above, the transmission links (tie rods and levers) and the front axle describe in any case a trapezoid and not a parallelogram. Therefore this arrangement is called a steering trapezoid. If the tie rods are pointing outward, then the steering arms are longer, though it is the same gear. The vertical movement of the wheels will then provoke less relative movement of the tie rods and a smaller righting effect.

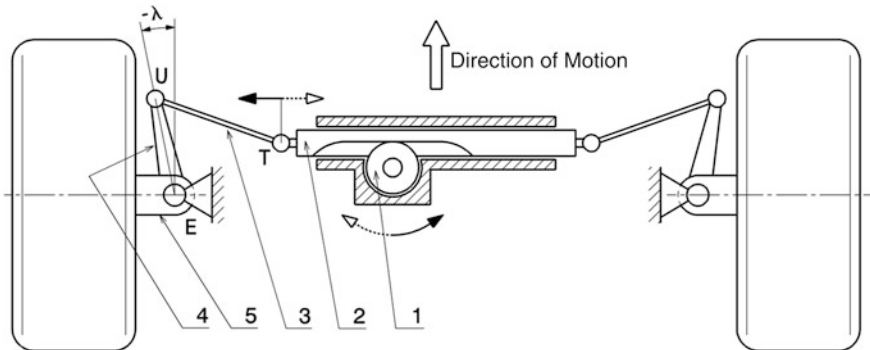


**Fig. 4.19** Steering gear in front of the axis. The motion of the wheel is transferred from the pinion or gear (1) on the steering shaft to the gear rack (2). Its ends are jointly connected by the tie rods (3) to the steering arms (4). When the gear rack is shifted, the hub carrier (5) turns around point E. The pinion (1) must be arranged below the gear rack so that the motion of the steering wheel is transferred in the same direction. The steering arms point outward to fulfil Ackermann's condition (angle  $\lambda$  is negative)

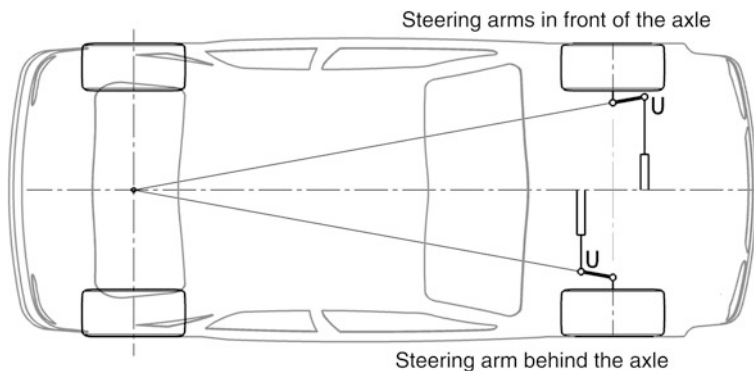


**Fig. 4.20** Arrangement of the steering arms for an A-steering. If the connection of the tie rod U is located in front of the axle, then the steering arm has to point outward. If, on the other hand, the joint U is behind the axle, the lever will point towards the car. The backward extension of the lever meets the intersection of the rear axle and the middle of the car to create ideal A-angles

However, the basic adjustment of the steering arms does not ensure, that the desired curve of the A-angle (see Fig. 4.6) will really be achieved. The joint points T and U at the tie rod move in a very different manner when the car is steered, Fig. 4.21. The gear rack joint T moves in a straight line, crosswise to the direction of the traffic, but the connection U at the steering arm rotates around the steering axis EG, describing a circle in space.

When the steering is designed, the joint points defined by the following methods must be precisely adjusted, so that the actual curve of the steering wheel approaches the desired curve (nominal curve) in the best way possible.

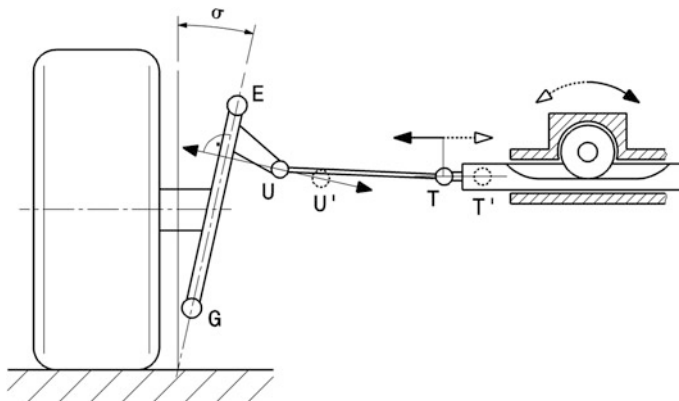


**Fig. 4.21** Motion of the tie rod upon steering. Steering causes the point T to move with the gear rack, parallel to the road, towards, T'. The second tie rod link U turns on the steering axis EG, becoming U'. This example does not include any castor angle, hence, in the rear view, the circular path is perpendicular to the steering axis

There are several basic ways to arrange gear and linkage around the front axle. The gear may be either in front of or behind the axle and, independent from this, the steering arms may point either forward or backward. The pinion may be above or below the gear rack. Figures 4.22, 4.23 and 4.24 show basic arrangements of approximately equal steering geometry. The tie rods represent the mobile link between the gear rack and the steering arms, transferring push-and-pull forces.

Compression and rebound of the wheels should not produce a toe-in change of the wheels, i.e. no steering movement. The decisive factor in this context is the relative position of the joint points T and U at the tie rod with regard to frame and

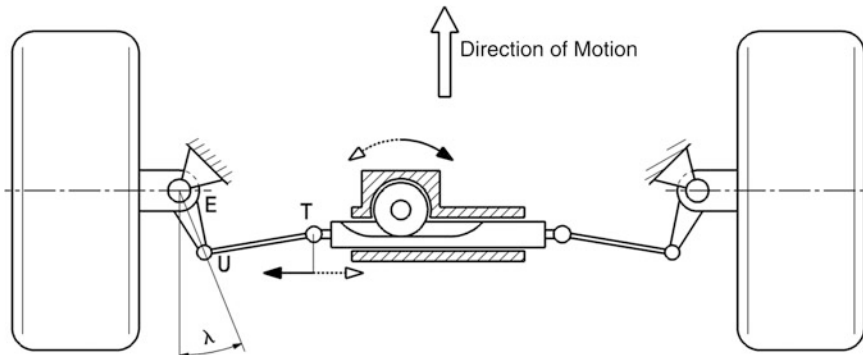


**Fig. 4.22** Steering behind the axle. If the gear is located behind the front axle, then the steering arms are pointing inward. The gear is asymmetrical, which is common for two-seaters (driver at left). The pinion is located above the gear rack. The tie rods are mounted at the ends of the gear rack

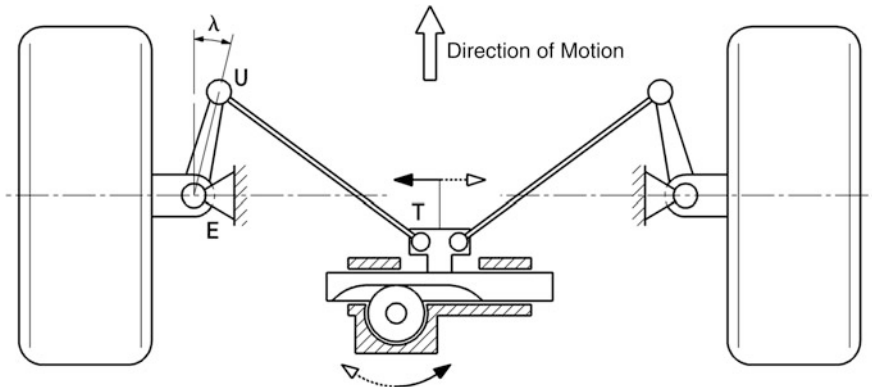


**Fig. 4.23** Steering behind the axle. The gear is behind and above the central line of the front axle. The steering arms are facing forward. Kinematic arguments demand extended tie rods, therefore the connection to the gear rack is established in the middle ('centre tap'). If the tie rods are too short, an undesirable righting effect upon compression and rebound will be the result. The pinion is located under the gear rack. Note that in this case the steering arms are not oriented like in Fig. 4.20 but the other way, inward. Nevertheless, the whole arrangement of the steering produces a *curve* of the A-angle according to Ackermann

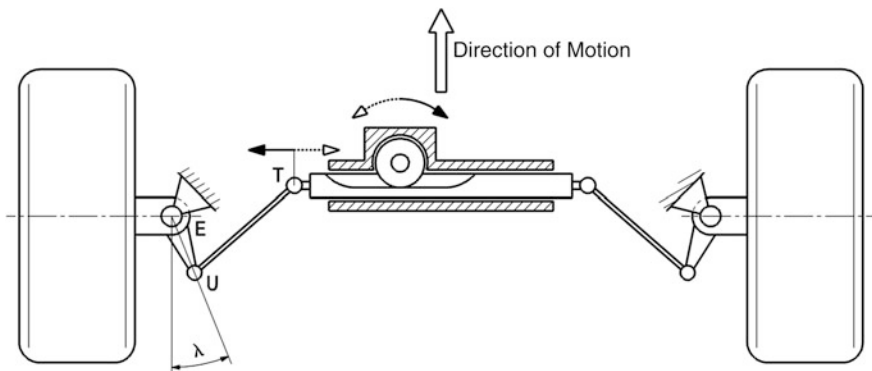


**Fig. 4.24** Steering in front of the axle. This arrangement has the gear located in front of the axle and the steering arms pointing to the back and inwards. The pinion is seated *above* the gear rack

chassis. If there is a relative movement between the giving of the joint points, a steering movement of the wheels is the unavoidable result (*bump steering*).

The steering arm needs to be defined before carrying out any kinematic studies. Figure 4.25. The length of the steering arm  $r$  is commonly in the range of about 100 mm.

Another argument for the position of steering arm and tie rod—if the steering arms are in front—is the space available in the rim. Even the largest steering wheel angle of the wheels should not cause a collision of tie rod and rim. On the contrary—a safety distance will be left so that, in spite of elasticities of the steering, there

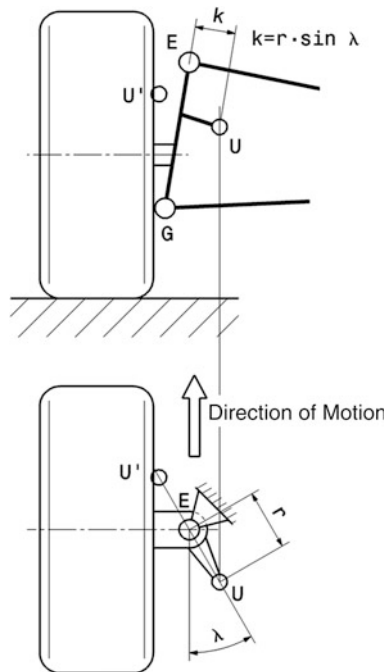


**Fig. 4.25** Defining the steering arm joint point. U the link to the steering arm is required for determining the position of gear and tie rod. The steering arm is pointing either outwards ( $U'$ ) or inwards ( $U$ ), cf. Fig. 4.20, in the rear view it is found either *left* or *right* of the steering axis EG. Compute the distance  $k$  from the defined values of the angle  $\lambda$  and the length of the steering arm  $r$

will always be sufficient space left between the parts, Fig. 4.26. If a large steering wheel angle is needed, it may be necessary to shift the steering arm vertically towards the wheel centre, where the rim offers the widest space in longitudinal direction.

Once the steering arm point  $U$  is defined, the second link to the tie rod  $T$  has to be determined. Instantaneous centres may help, see Figs. 4.27, 4.28, 4.29, 4.30 and 4.31. Once the linking point  $T$  is defined, the position of the steering gear is given, because the corresponding points of the other side of the car result from mirroring along the central plane of the car.

If the steering gear requires a high position, the tie rod may be positioned above the upper wishbone as well, Fig. 4.28.

If the wishbones are initially parallel, the tie rod will also be parallel to them, Fig. 4.29.

The position of the tie rod may be projected for other wheel suspensions as well by computing the instantaneous centres. Figures 4.30 and 4.31 show the realisation for a strut suspension (MacPherson). It is obvious that, the higher the linking point  $U$  of the tie rod is located at the steering arm, the further will the mounting point  $T$  shift along the gear rack to the middle of the car. This may cause problems if the

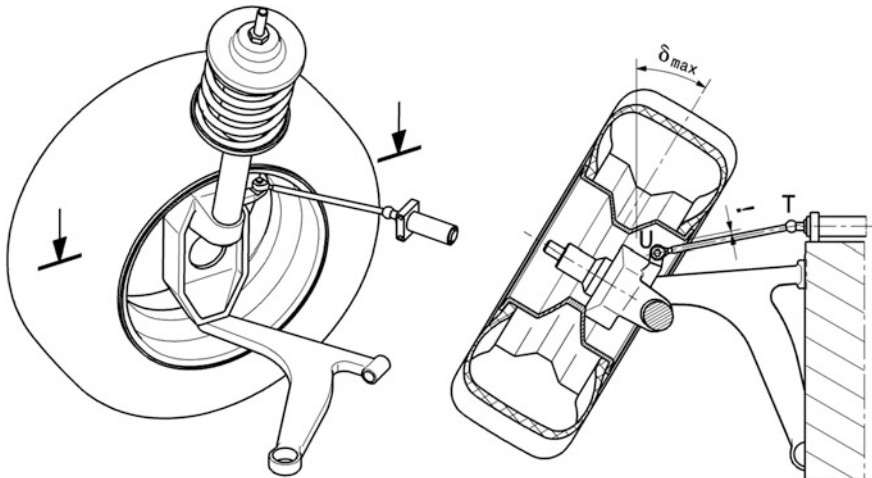


**Fig. 4.26** Necessary clearance of the linkage. The *left* front wheel is shown. Even at the largest steering wheel angle  $\delta_{\max}$ , the tie rod UT has to stay some distance away from the rim. This limits the available space. It is also obvious that the steering arm has less available space the higher it is located in the rim

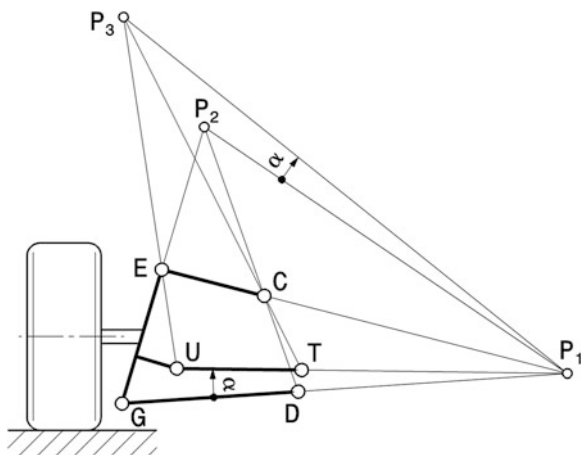
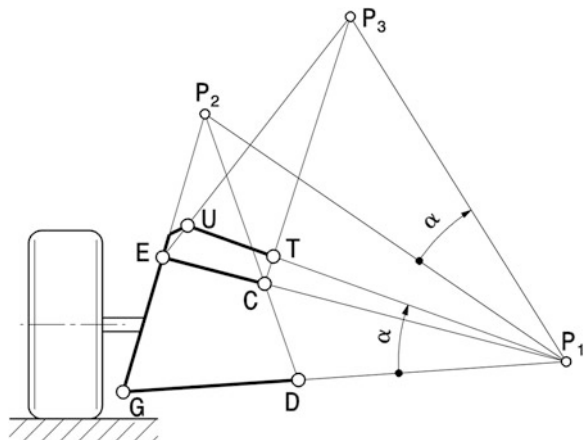


**Fig. 4.27** Determining the position of the tie rod. The joint points of the wishbones, E and C as well as G and D, are known, as is the steering arm connection U. This helps to compute the centre  $P_1$ . The centre  $P_2$  results from the intersection of the straight lines GE and DC. Next, determine the angle  $\alpha$  of the straight line  $UP_1$  and the lower wishbone GD. It is important which way the angle is turned, starting at the wishbone, because the angle from the connection of the centres  $P_1P_2$  has to be applied in the same direction. In other words, if U was beneath the wishbone, then  $\alpha$  had to be applied the opposite way, beginning at the line  $P_1P_2$ . The instantaneous centre of the tie rod  $P_3$  results from the intersection of the straight line  $UE$  with the leg that was drawn last. Now the articulation point T of the tie rod can be determined, since it results from the intersection of  $P_3C$  and  $P_1U$

**Fig. 4.28** Determining the position of the tie rod. The approach for this figure is the same as for Fig. 4.27. The only difference is the arrangement of the steering arm UE. It is above the *upper* wishbone EC, pointing backwards and inside. As a result, the articulation point T is attached to the gear rack above the wishbone



track is small and the steering gear is long. An extreme case may require to mount the tie rods not at the ends of the gear rack but in its middle.

Double wishbone axles suggest to arrange the steering gear in such a way that the tie rods will be located in the planes of the upper or lower triangular wishbones. If the articulation points T of the gear rack are on the axes of rotation, then there will be no steering movement upon compression and rebound, at least when driving straight, see Fig. 4.32.

The methods described above assume a planar model, rarely found in actual cars. The points of the linkage computed that way can therefore only serve as

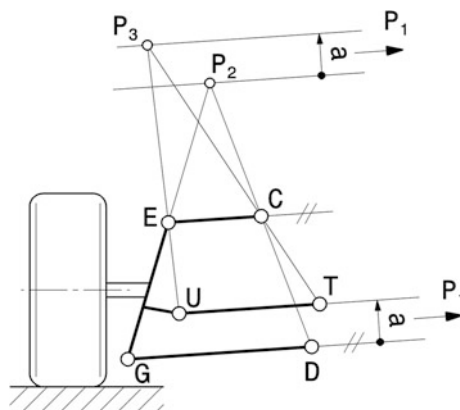


**Fig. 4.29** Determining the position of the tie rod. The approach for this figure is for the major part the same as for Fig. 4.27. The joint points E, C and G, D are known, as is the steering arm link U. The centre P<sub>1</sub> is here an infinitely distant point, though, and the wishbones are parallel. P<sub>3</sub>, may be determined by the help of a parallel of P<sub>2</sub>, removed by a distance a, that intersects the line UE (observe the orientation, whether up or down, as in Fig. 4.27). Include the tie rod centre P<sub>3</sub> to compute the rack articulation point T just from the intersection of the line P<sub>3</sub>C and the tie rod

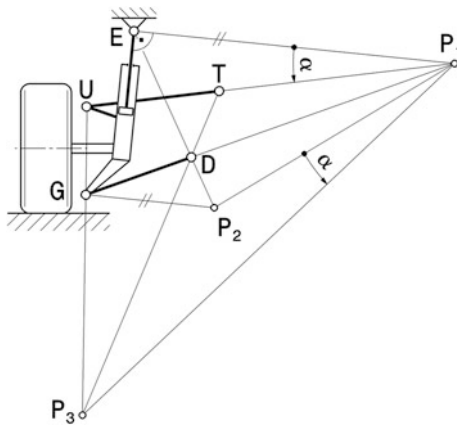


**Fig. 4.30** Determining the tie rod position at a MacPherson axle. The steering arm of this MacPherson axle and its connection U are located above and in front of the front axle. The wheel support and its joints E and G are known, as is the wishbone GD. The support E, mounted to the chassis, and the wishbone help to construct the lateral centre  $P_1$ , intersecting the normal on the direction into which the shock strut moves with the extension of the wishbone. Now the centre  $P_2$  results from the intersection of a parallel of the centre line  $P_1E$ , crossing G and the line ED. The angle  $\alpha$  is applied, beginning at the line  $P_1P_2$ , in the same direction as the angle measured between  $P_1E$  and  $P_1U$ . Based on the line  $UG$ , the centre  $P_3$  can be designed. The tie rod centre  $P_3$  immediately yields the second tie rod articulation point T, located on the line  $P_3D$

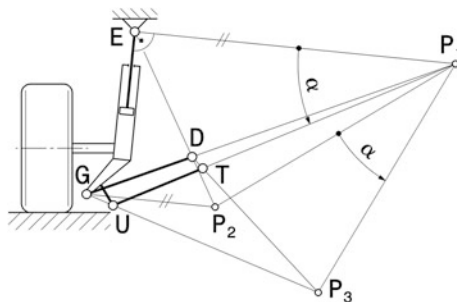


**Fig. 4.31** Determining the position of the tie rod at a MacPherson axle. The approach to determine the second tie rod articulation point T is as for the preceding picture, only the arrangement of the steering arm is different. Here it is turned inwards and its articulation point U at the tie rod may also be located beneath the wishbone connection G

clues. The designer will ‘approach’ the exact definition of the linkage by drawings or, more up-to-date, at the computer. This will be successful faster than extensive auxiliary designs considering the 3D nature of steering and chassis (Matschinsky 2007).

**Fig. 4.32** Position of the tie rods without self-steering effect. Plan view (*below*) and rear view (*top*). When driving straight, the tie rod with the joints T and U is located in the plane of the upper triangular wishbone with the articulation points E, C and F. The gear rack joint T is on the axis of rotation CF of the wishbone. The connection U between tie rod and steering arm is also arranged in the plane of the wishbone

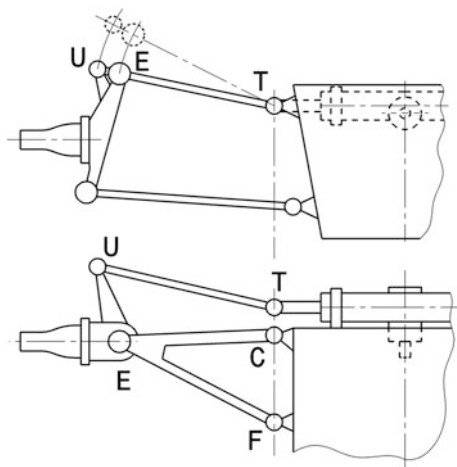


**Table 4.1** Remedial actions against self-steering effect, acc. to Staniforth (1999)

Steering movement upon		Remedial action	
Compression	Rebound	Shifting the gear	Tie rod length
Toe-in	Toe-out	In front of the axle: raise Behind the axle: lower	–
Toe-out	Toe-in	In front of the axle: lower Behind the axle: raise	–
Toe-out	Toe-out	–	In front of the axle: extend Behind the axle: shorten
Toe-in	Toe-in	–	In front of the axle: shorten

If steering movements occur in the car prototype built when giving, this behaviour can be improved by shifting the steering gear or by adapting the length of the tie rods, see Table 4.1.

## References

- Achleitner A (2005) Der neue Porsche 911 Carrera. Lecture of the ÖVK (Österr. Verein für Kraftfahrzeugtechnik) lecture programme, Vienna
- Heissing B (2004) Moderne Fahrwerksauslegung. Lecture of the ÖVK (Österr. Verein für Kraftfahrzeugtechnik) lecture programme. Graz 2004
- Matschinsky W (2007) Radführungen der Straßenfahrzeuge, 3rd edn. Springer, Berlin
- Reimpel J, Betzler J (eds) (2000) Fahrwerktechnik Grundlagen, 4th edn. Vogel Buchverlag, Würzburg
- Staniforth A (1999) Competition car suspension, 3rd edn. Haynes, Sparkford

# Chapter 5

## Basics of Lateral Vehicle Dynamics

Peter Pfeffer and Hans-Hermann Braess

This chapter is an introduction to lateral vehicle dynamics and steady and dynamic cornering. Basic discussions will serve to analyse the essential factors influencing the lateral vehicle dynamics of a car and the steering wheel angle and torque indicated by the driver. Models are required for a more detailed analysis, they expand upon the fundamental relationships for slow and fast cornering (see [Chap. 2](#)). Steady-state circular driving will be discussed based on the linear single track model. This leads to dynamic cornering. We do this the classic way by applying analytic equations. Their big advantage is that the relationships may be easily understood. When the effects of shifting the dynamic wheel load will be included, the single track model has to be extended into a Dual-track model. This is usually done using numerical simulations, because closed equations serve little to illustrate these relationships.

### 5.1 Vehicle Modelling: Linear Single Track Model

The most important aspects of driving dynamics are probably these: why can a car be steered in a defined manner, why does it go consistently and why is it not substantially deflected from its course by outside influences? Especially at higher speed and cornering this was a marked problem until the 1960s. As was shown in [Sect. 1.2](#), the theoretical examinations trace back to Riekert and Schunck ([1940](#)). They developed the single track model which gets by with very few degrees of

---

P. Pfeffer (✉)

Munich University of Applied Science, Munich, Germany  
e-mail: peter.pfeffer@steeringhandbook.org

H.-H. Braess  
ehemals BMW AG, Munich, Germany

freedom. Yet these help to analyse and discuss the most important aspects of driving dynamics. The following two essential simplifications were assumed:

- All the forces act on a plane flat road. The height of the centre of gravity must be ignored, because the centrifugal force is acting there, hence, it does not apply any additional load to the outer tyre or discharge to the inner tyre, i.e. the left and right tyre of each axle is exposed to the same load. They may therefore be added up to ‘one tyre’. This assumption excluded rolling of the car, eliminating this degree of freedom.
- The equations of the system are linearised. The tyre force is assumed proportional to the slip angle, without any lead-in area. The trail is negligibly small in comparison to the wheelbase. Assuming small angles (slip, sideslip angle, ...) the trigonometric functions are linearised.

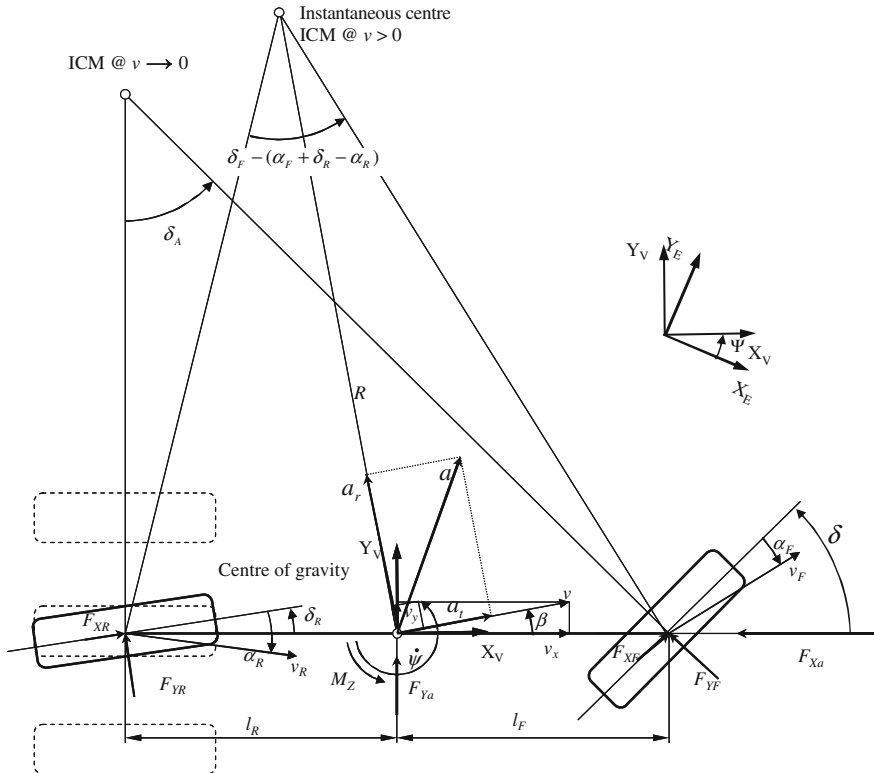
With these assumptions the model is suitable for the on-centre area and normal driving up to approx.  $4 \text{ m/s}^2$ . The dynamic range near the force closure limit cannot be computed, because the dynamic wheel load distribution and the tyre force limit will dominate then. However, a normal driver drives mostly within this very range, therefore it is crucial for the perceived driveability.

Figure 5.1 shows the axis systems used.  $X_E$  and  $Y_E$  refer to the earth-fixed level axis system. The car is moving with an on-board axis system  $X_V$  and  $Y_V$  at its centre of gravity (ISO 8855). The angle that the car’s central plane assumes against the earth-fixed  $X_E$  axis is the yaw angle  $\psi$ . The centre of gravity moves at the speed  $v$ . The speed vector  $v$  will usually not point towards the central plane of the car but be tilted against it by a sideslip angle  $\beta$ . The course angle results from the sum of yaw and sideslip angle. The car turns around the instantaneous centre ICM that results from the polar radii perpendicular to the speed vectors. On steady circling, the centre ICM is removed from the centre of gravity by the radius of curvature  $R$ . At very low speed, without a steering angle applied to the rear axle and with negligible side forces, the speed vectors are located in the respective central planes of the tyres. In that case the instantaneous centre is on the level of the rear axle. The steering angle  $\delta_A$ , also called Ackermann’s steering angle or A-angle (see Sect. 4.2) is required at the front axle. The orientations marked in the picture are defined as positive. They develop when driving a left turn.

### 5.1.1 Dynamic Equations

For the acting tyre and air forces, see Fig. 5.1. The principle of linear momentum in the on-board coordinate system is along the car:

$$m_V \cdot a_t \cdot \cos \beta - m_V \cdot a_r \cdot \sin \beta = F_{YF} \sin \delta + F_{XF} \cos \delta + F_{YR} \sin \delta_R + F_{XR} \cos \delta_R + F_{xa} \quad (5.1)$$



**Fig. 5.1** Forces and kinematic variables in the single track model

and laterally:

$$m_V \cdot a_t \cdot \sin \beta + m_V \cdot a_r \cdot \cos \beta = F_{YF} \cos \delta + F_{XF} \sin \delta + F_{YR} \cos \delta_R + F_{XR} \sin \delta_R + F_{Ya} \quad (5.2)$$

$\delta$  is the steering angle at the front axle and  $\delta_R$  is the steering angle at the rear axle. The lateral front and rear tyre forces are  $F_{YF}$  and  $F_{YR}$ ,  $F_{Ya}$  is the lateral aerodynamic force. As was seen in Chap. 2, the acting point of the lateral force is shifted by the trail. This trail is very small in comparison to the wheelbase, it may therefore be disregarded for this purpose.

The principle of conservation of angular momentum around the car axis  $Z_V$  in the centre of gravity yields:

$$I_Z \cdot \ddot{\psi} = (F_{YF} \cos \delta + F_{XF} \sin \delta_F) \cdot l_F - (F_{YR} \cos \delta_R + F_{XR} \sin \delta_R) \cdot l_R + M_{Za} \quad (5.3)$$

applying  $M_{Za}$  as the aerodynamic yaw torque.

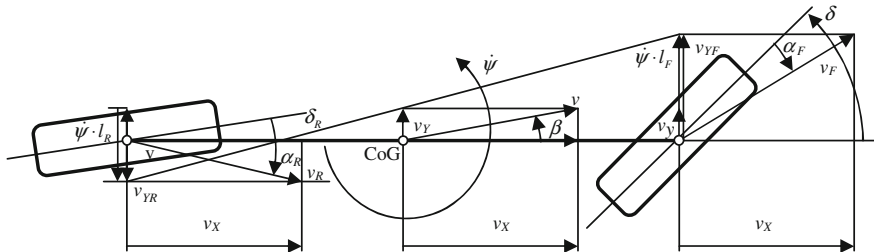


**Fig. 5.2** Relationship of speeds in the single track model

Assuming small side forces and disregarding the transient tyre behaviour, there is a linear relationship between the front and rear slip angles,  $\alpha_F$  and  $\alpha_R$ , and the corresponding (axial) lateral tyre force:

$$F_{YF} = C_{\alpha F} \cdot \alpha_F \text{ and } F_{YR} = C_{\alpha R} \cdot \alpha_R \quad (5.4)$$

The proportionality  $C_\alpha$  is called cornering stiffness.

The relationship between the slip angles, the front and rear steer-angles  $\delta$  and  $\delta_R$  and the sideslip angle  $\beta$  is deduced from Fig. 5.2. Since the car is rigid, the longitudinal component of the speed has to be equal for every point of the car. Applying this to the centre of gravity and the front and rear axles gives:

$$\begin{aligned} v_X &= v \cos \beta = v_R \cos(\delta_R - \alpha_R) \quad \text{and} \\ v_X &= v \cos \beta = v_F \cos(\delta_F - \alpha_F) \end{aligned} \quad (5.5)$$

Along the car, the lateral speed changes by the rotating part of the yaw velocity, multiplied by the distance:

$$\begin{aligned} v_{YR} &= v_R \sin(\delta_R - \alpha_R) = v \sin \beta - \dot{\psi} \cdot l_R \\ v_{YF} &= v_F \sin(\delta_F - \alpha_F) = v \sin \beta + \dot{\psi} \cdot l_F \end{aligned} \quad (5.6)$$

Combining Eqs. 5.5 and 5.6 gives:

$$\tan(\delta_R - \alpha_R) = \frac{v \sin \beta - \dot{\psi} \cdot l_R}{v \cos \beta} \text{ and } \tan(\delta_F - \alpha_F) = \frac{v \sin \beta + \dot{\psi} \cdot l_F}{v \cos \beta} \quad (5.7)$$

If the angles are assumed to be small, the above equation for the front axle simplifies to:

$$\alpha_F = -\beta + \delta_F - \frac{\dot{\psi} \cdot l_F}{v} \quad (5.8)$$

and for the rear axle:

$$\alpha_R = -\beta + \delta_R + \frac{\dot{\psi} \cdot l_R}{v} \quad (5.9)$$

For small angles, the sideslip angle is computed as the quotient of lateral and longitudinal speed.

$$\beta = \frac{v_y}{v_x} \quad (5.10)$$

After linearising the small angles and replacing the radial tyre forces in Eqs. 5.1 and 5.3 by 5.4 and the slip angles by 5.8 and 5.9, this results in the following linearised dynamic equations of the car:

$$m_V \cdot a_t = F_{XF} + F_{XR} + F_{Xa} \quad (5.11)$$

$$m_V \cdot a_t \cdot \beta + m_V \cdot a_r = C_{zF} \cdot \left( -\beta + \delta_F - l_F \frac{\dot{\psi}}{v} \right) + C_{zR} \cdot \left( -\beta + \delta_R + l_R \frac{\dot{\psi}}{v} \right) + F_{Ya} \quad (5.12)$$

$$I_Z \cdot \ddot{\psi} = C_{zF} \cdot \left( -\beta + \delta_F - l_F \frac{\dot{\psi}}{v} \right) \cdot l_F - C_{zR} \cdot \left( -\beta + \delta_R + l_R \frac{\dot{\psi}}{v} \right) \cdot l_R + M_{Za} \quad (5.13)$$

The dynamic equations describe the behaviour of the car in its degrees of freedom. Even if steer-angle, driving and aerodynamics forces are known, speed, yaw angle, sideslip angle and centripetal acceleration remain unknown. The required additional equation was derived by Mitschke and Wallentowitz (2003) from a geometrical discussion of the trajectory. The radius of curvature  $R$  is computed as a function of the course angle  $\beta + \psi$  and the trajectory  $u$ :

$$\frac{1}{R} = \frac{d(\beta + \psi)}{du} \quad (5.14)$$

The speed results from the derivation of the trajectory:

$$v = \frac{du}{dt} \text{ and hence } \frac{1}{R} = \frac{d(\beta + \psi)}{v \cdot dt} = \frac{\dot{\beta} + \dot{\psi}}{v} \quad (5.15)$$

The centripetal acceleration is:

$$a_r = \frac{v^2}{R} = v^2 \frac{\dot{\beta} + \dot{\psi}}{v} = v \cdot (\dot{\beta} + \dot{\psi}) \quad (5.16)$$

This is the previously lacking relationship. Equations 5.11–5.13 and 5.16 help to simulate the motion of the car if the driving forces in front  $F_{XF}$  and rear  $F_{XR}$ , the aerodynamic forces  $F_{Xa}$  and  $F_{Ya}$ , the torque  $M_{Za}$  and the steer-angles at the front axle  $\delta$  and the rear axle  $\delta_R$  are known.

### 5.1.2 Steering Angle: Steering Wheel Angle—Power-Assisted Steering

The driver does not set the steering angle at the tyre but the steering wheel angle, at the steering wheel. The relationships between steer-angle, steering wheel angle, wheel torque and power-assisted steering will therefore be discussed in this section. We suppose for the sake of simplicity that the same steering angle applies at the left and the right tyre, because the single track model does not permit any differentiation; small angles are assumed as well, then the trigonometric functions can be linearised. Any friction, damping and free travel is ignored.

Figure 5.3 shows a simple rack-and-pinion steering system. A steering wheel angle  $\delta_H$  or a torque  $M_H$  is applied to the wheel. This input variable is transmitted by the steering column to the torsion bar with the torsional stiffness  $C_T$ . The pinion, with the degree of freedom  $\delta_H^*$ , transforms this rotation into a translation of the gear rack  $s_R$ . The steering arm with length  $r_L$ , helps to reconvert the translation into a rotation  $\delta^*$ . The elasticity of the tie rod and the axle mounting are included in the steering stiffness  $C_R$  which transfers the steering torque to the wheel, generating a steering angle  $\delta$ . The kinematic relationships describe a steering without distortion of the torsion springs, i.e. without any forces or torques acting. The kinematic steering ratio  $i_S$  produces a steering angle of:

$$\delta = \frac{\delta_H}{i_S} \quad (5.17)$$

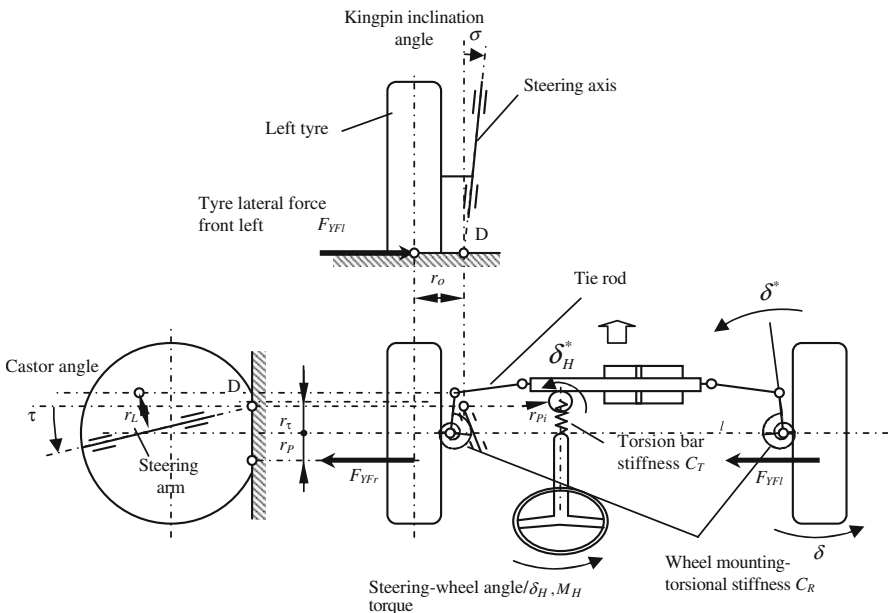


**Fig. 5.3** Integration of the steering into the single track model

The rack shift  $s_r$ , based on the pinion radius  $r_{Pi}$ , is:

$$s_r = \delta_H \cdot r_{Pi} \quad (5.18)$$

If no forces are included, the steering angle is equal to the steering arm angle  $\delta^*$  which can be computed as a function either of the rack shift, the pinion torsion or the steering wheel angle:

$$\delta = \delta^* = \frac{s_r}{r_L} = \delta_H \cdot \frac{r_{Pi}}{r_L} \quad (5.19)$$

So the kinematic steering ratio results as well from the ratio of steering arm length and pinion radius:

$$i_S = \frac{r_L}{r_{Pi}} \quad (5.20)$$

As forces and a torques are applied, these need to be considered. The single track model allows to disregard longitudinal forces when a constant driving speed is assumed, therefore the scrub radius  $r_o$  does not cause a torque around the steering axis. The side forces are observed at the left and right tyres,  $F_{YFl}$  and  $F_{YFr}$ , because they generate a torque around the steering axis. The steering torque  $M_S$  can be computed by adding the side forces times the full castor  $r$  resulting from the sum of constructive castor  $r_\tau$  and trail  $r_P$  (see Sect. 2.4.1).

$$M_S = (F_{YFl} + F_{YFr}) \cdot (r_\tau + r_P) = F_{YF} \cdot r \quad (5.21)$$

This steering torque acts to realign the tyres, therefore it is also called the self-aligning torque of the axle. The torque  $M_H$  that the driver has to apply is reduced by the kinematic steering ratio and the steering assistance ratio  $A_S$ :

$$M_H = \frac{M_S}{i_S \cdot A_S} \quad (5.22)$$

A smaller wheel torque corresponds to a higher kinematic steering ratio and a stronger power-assist. The difference of the steering wheel angle and the pinion angle can also be used to compute the wheel torque:

$$M_H = C_T(\delta_H - \delta^*) \quad (5.23)$$

The torque at the front axle alters the torsional stiffness of the axle support:

$$M_S = C_R(\delta^* - \delta) \quad (5.24)$$

With no elasticity applied between the torsional angles of pinion and steering arm, the following is also valid:

$$\delta_H^* = \delta^* \cdot i_S \quad (5.25)$$

Now the relationship between steering wheel angle and steering angle using the Eqs. 5.22–5.25 yields:

$$\delta_H = \delta \cdot i_S + \frac{M_S \cdot i_S}{C_S} = \delta \cdot i_S + \frac{F_{YF} \cdot r \cdot i_S}{C_S} \quad (5.26)$$

with the total steering stiffness of the steering axes  $C_S$ :

$$\frac{1}{C_S} = \frac{1}{C_R} + \frac{1}{C_T \cdot i_S^2 \cdot A_S} \quad (5.27)$$

If the total steering stiffness is infinite or if there is no steering torque, the steering wheel angle is equal to the steering angle times the kinematic steering ratio. The steering stiffness is the result of the torsion bar stiffness and the torsional stiffness of the axle mounting aligned in series, hence, the less stiff component sets an upper limit to the steering stiffness. A high steering ratio or a strong power-assist stiffens the steering system.

The relationship between steering wheel angle and steering angle is described by Eq. 5.26, disregarding mass and inertia of the steering driveline. This inertia is relevant in particular for very fast steering movements or for free control (see Sect. 5.2.6). Characteristics and target values of real systems are described in Sect. 5.2.

The steering stiffness acts like a reduced cornering stiffness, called the effective cornering stiffness  $C_{\alpha F,eff}$ . According to Mitschke and Wallentowitz (2003), for the front axle, it may be computed as follows:

$$\frac{1}{C_{\alpha F,eff}} = \frac{1}{C_{\alpha F}} + \frac{1}{C_S/r} \quad (5.28)$$

This equation shows that the effective cornering stiffness derives from the cornering stiffness and the steering stiffness relative to the trail. One uses the dynamic Eqs. 5.11–5.13 and 5.16 and replaces the cornering stiffnesses by these effective cornering stiffnesses at the front and rear axles to include the influence of the steering on the driveability. This influence is often disregarded for the rear axle and only the cornering stiffness at the front axle is reduced.

For a more detailed discussion of the steering behaviour, the steering model shown in Fig. 5.3 can be extended as needed (see Sect. 5.1.7).

### 5.1.3 Steady-State Circular Driving

The driveability is evaluated through circular driving at constant speed, also called steady-state circular driving. Many dynamic parameters of a car that are important for lateral dynamics, for example the self-steering gradient, can be determined by this driving manoeuvre. Realisation and evaluation are defined in

ISO 4138 (2004). The single track model serves to compute the relevant variables with simple analytic equations. A detailed derivation of the equations to compute the related variables is found in Mitschke and Wallentowitz (2003). The circular driving test overlaps the centre of curvature with the instantaneous centre of the car; i.e. the car turns around the centre of the very circle it is driving on. The longitudinal acceleration is zero and there is only lateral acceleration. The sideslip angle does not change and the yaw speed is constant, therefore, Eq. 5.16, which serves to compute the lateral acceleration, is reduced to the following:

$$a_Y \approx a_r = \frac{v^2}{R} = v \cdot \dot{\psi} \quad (5.29)$$

The steering wheel angle is proportional to the lateral acceleration. For a car without all-wheel steering, it is:

$$\delta_H = \frac{i_s l}{R} + m \cdot i_s \frac{C_{\alpha R,eff} l_R - C_{\alpha F,eff} l_F}{C_{\alpha F,eff} \cdot C_{\alpha R,eff} l} a_Y = \delta_{H0} + \frac{i_s l}{v_{ch}^2} a_Y \quad (5.30)$$

This provides the characteristic speed as:

$$v_{ch}^2 = \frac{C_{\alpha F,eff} \cdot C_{\alpha R,eff} l^2}{m(C_{\alpha R,eff} l_R - C_{\alpha F,eff} l_F)} \quad (5.31)$$

The characteristic speed is the speed that requires twice the steady steering wheel angle and the highest yaw response in a single track model with linear behaviour. One needs to check in reality whether the linear single track model is still valid at these operating points. Generally it will not be.

At very low speed, the lateral acceleration is about zero and the steering steering wheel angle is equal to the so-called Ackermann steer angle:

$$\delta_H(a_Y = 0) = \delta_{H0} = \frac{i_s l}{R} \quad (5.32)$$

The following steering angle is then required at the front tyre:

$$\delta_D(a_Y = 0) = \frac{l}{R} \quad (5.33)$$

This angle is the Ackermann steer angle or the dynamic reference steer angle.

The steady-state circular driving allows to measure different gradients of car response or to deduce them from models. Table 5.1 lists the variables defined in ISO 8855/DIN 70000 and the way they may be computed in the single track model. The ratio of a parameter change relative to another parameter, beginning at a steady equilibrium, is called the gradient. This equilibrium is given in the steady-state circular driving.

**Table 5.1** Important values of the steady-state circular driving according to DIN 70000/ISO 8855 and their computation in the single track model

Variable	Definition	Single track model <sup>a</sup>
Steering sensitivity	$\frac{\partial \alpha}{\partial \delta_H}$	$= \frac{v_{ch}^2}{i_s l}$
steering angle gradient	$\frac{\partial \delta}{\partial \alpha}$	$= \frac{l}{v_{ch}^2}$
Dynamic reference steering angle gradient (neutral self-steering)	$\frac{\partial \delta_D}{\partial \alpha}$	$= 0$
Steering wheel angle gradient (inverse steering response)	$\frac{\partial \delta_H}{\partial \alpha}$	$= \frac{i_s l}{v_{ch}^2}$
Steering-wheel torque gradient	$\frac{\partial M_H}{\partial \alpha}$	$= \frac{m_F \cdot r}{i_s} = \frac{m \cdot l_R \cdot r}{l \cdot i_s}$
Steering-wheel torque/angle gradient	$\frac{\partial M_H}{\partial \delta_H}$	$= \frac{m \cdot l_R \cdot r}{l^2 \cdot i_s^2 \cdot A_S} \frac{v^2}{1 + \left( \frac{v}{v_{ch}} \right)^2}$
Roll angle gradient	$\frac{\partial \phi_Y}{\partial \alpha}$	n/a
Sideslip angle gradient	$\frac{\partial \beta}{\partial \alpha}$	$= \frac{m l_F}{l \cdot C_{zR,eff}}$
Steering-wheel/sideslip angle gradient	$\frac{\partial \delta_H}{\partial \beta}$	$= - \frac{i_s l}{v_{ch}} \frac{C_{zR,eff} l_R}{m \cdot l_F}$
Self-steering gradient EG	$\frac{\partial \delta_H}{\partial \alpha} \frac{1}{i_s} - \frac{\partial \delta_D}{\partial \alpha} = \frac{1}{i_s} \frac{\partial \delta_H - \partial \delta_D}{\partial \alpha}$	$= \frac{l}{v_{ch}^2}$
Stability factor	Self-steering gradient/wheelbase	$= \frac{1}{v_{ch}^2}$
Directional coefficient	Stability factor/sideslip angle	

<sup>a</sup> Without power-assist (power-assist = 1), with constant overall steering ratio and without four-wheel steering

### 5.1.4 Understeer and Oversteer

The terms understeer and oversteer are very often used to describe car handling. A car is commonly called understeering when its front tyres ‘drift’ during cornering so that the trajectory radius becomes larger. By contrast, oversteer means that the rear of a car is drifting outwards. These terms are often used for unsteady driving manoeuvres, too. However, DIN 70000/ISO 8855 defines these terms only for the steady-state circular driving.

The mode of steering is called understeer if the self-steering gradient is positive, i.e. the lateral acceleration increments and the steering wheel angle, as a function of the kinematic steering ratio, increases faster than the dynamic reference steering angle (see Fig. 5.4):

$$\frac{\partial \delta_H}{\partial \alpha} \frac{1}{i_s} - \frac{\partial \delta_D}{\partial \alpha} > 0 \quad (5.34)$$

The steady state that has a self-steering gradient of zero, i.e. the lateral acceleration increments and the steering wheel angle, as a function of the kinematic steering ratio, is exactly the same as the increase of the dynamic reference steer-angle, is called neutral steer.

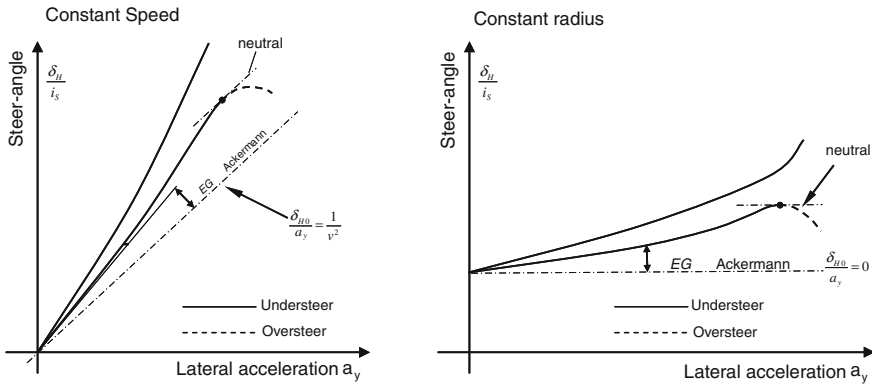


**Fig. 5.4** Definition of understeer and oversteer at constant speed and circle radius at a constant overall steering ratio

$$\frac{\partial \delta_H}{\partial a_Y} \frac{1}{i_s} - \frac{\partial \delta_D}{\partial a_Y} = 0 \quad (5.35)$$

The steady state is called oversteer if the self-steering gradient is less than zero, i.e. lateral acceleration increases and the steering wheel angle as a function of the kinematic steering ratio increases slower than the dynamic reference steer-angle.

$$\frac{\partial \delta_H}{\partial a_Y} \frac{1}{i_s} - \frac{\partial \delta_D}{\partial a_Y} < 0 \quad (5.36)$$

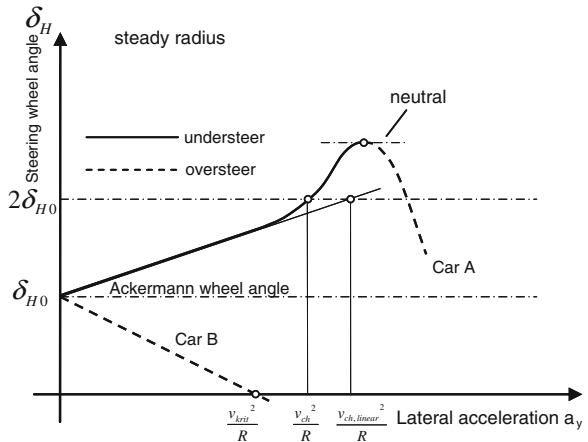
If the car is oversteering, the radius of its circle lessens as the lateral acceleration rises, though the steering wheel is steady. The circular driving with constant radius has a simpler relationship because the dynamic reference steering wheel angle does not change. This circular driving is shown in Fig. 5.4 on the right side.

Both definitions of the self-steering effect given by ISO 8855 assume the steering angle to be a quotient of the steering wheel angle and the kinematic steering ratio (Fig. 5.4). Elasticities of steering driveline and suspension and the variable steering ratio will usually make the actual steering angle deviate from this quotient. Therefore, the self-steering effect of cars with variable steering ratio should be acquired for different speeds or radii (Kraaijeveld et al. 2009).

The steering wheel angle in Fig. 5.5 is illustrated by two cars in steady-state circular driving with a steady radius. Car A is linear and understeering at a low lateral acceleration. Increasing lateral acceleration reveals a rising tendency to oversteer. Then this tendency reverses, and at the transitional point the behaviour is neutral, followed by oversteer. The speed at which twice the A-angle is required is the characteristic speed.

The self-steering gradient is usually unsteady, hence the real non-linear characteristic speed will deviate from the characteristic speed of linear theory. Modern cars are designed to understeer, to ensure stability. A reversal to oversteer is

**Fig. 5.5** Definition of understeer and oversteer for constant speed and radius at a constant overall steering ratio



avoided. Car B, on the other hand, is a purely oversteering car. With increasing speed and lateral acceleration, the steering wheel angle has to be reduced. If the steering wheel angle is zero, the critical speed and therefore the limit of stability is achieved.

### 5.1.5 Transient Response: Response Time of a Steering Wheel Step Input

ISO 7401 stipulates that different steering inputs can be used to assess the transient behaviour. The step steering input is very common. A step is theoretically applied and the steady steering wheel angle is achieved during measurement by a fast steering wheel angle ramp (see Fig. 5.6).

The response time to a quick steering input matters in addition to the stationary yaw gain. The car should not respond either too fast or too slowly. Several response times are available. The response time  $T_A$  is often used; describing for a step steering input, it describes the time difference between the rise of the steering wheel angle and that of the yaw speed to 63.2 % of the steady value.

The time is calculated as follows, acc. to Mitschke and Wallentowitz (2003):

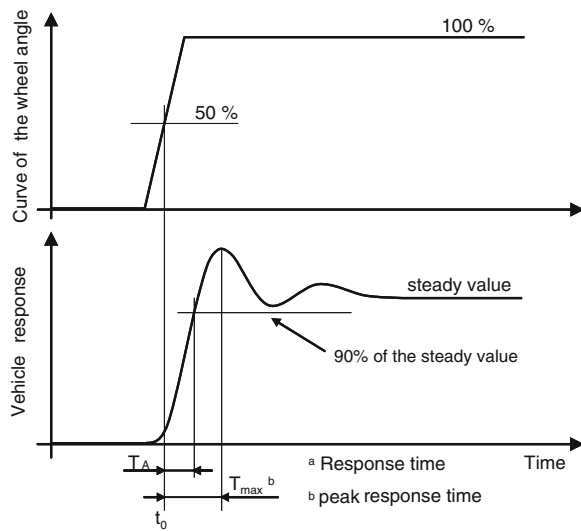
$$T_A = \frac{2 \cdot mv}{C_{zF,eff} + C_{zR,eff}} \cdot \frac{\frac{K_I^2}{l_F \cdot l_R}}{1 + \frac{K_I^2}{l_F \cdot l_R}} \quad (5.37)$$

$T_A$  Response time, 63.2 % of the steady value

$K_I$  Inertia radius around vertical axis.

The response time  $T_A$  corresponds approximately to the equivalent response time (delay time) in the Weir & DiMarco diagram (see Fig. 7.12). Ideal values of

**Fig. 5.6** steering wheel angle and response to step steering input (ISO 7401)



modern cars are less than 0.1 to 0.15 s at 80 km/h. At other times, the 90 % response time (Pacejka 2006) or the time till the first yaw speed maximum (Decker 2009) is used.

### 5.1.6 Yaw Gain

The dynamic response should deviate only slightly from the stationary yaw gain in the range of the steering frequency that the driver has to enter. The natural yaw frequency of cars as a function of speed is the result (see Fig. 5.7).

The yaw gain is characterised by the undamped natural yaw velocity frequency (Mitschke and Wallentowitz 2003).

$$\omega_\psi^2 = \frac{C_{zF,eff} \cdot C_{zR,eff} \cdot l^2 + mv^2 (C_{zR,eff} \cdot l_R - C_{zF,eff} \cdot l_F)}{I_z \cdot m \cdot v^2} \quad (5.38)$$

Yaw damping:

$$D_\psi = \frac{C_{zF,eff} \cdot l_F^2 + C_{zR,eff} \cdot l_R^2}{2I_z \cdot v^2 \cdot \omega_\psi} + \frac{C_{zF,eff} + C_{zR,eff}}{2mv\omega_\psi} \quad (5.39)$$

The following is aimed for: Amplitude response without significant resonance magnification, limited angles of phase difference, natural yaw frequency not too low natural yaw frequency, neither too low or too high yaw damping (Fig. 5.8).

**Fig. 5.7** Natural yaw frequency of different car designs (analytic steering model)

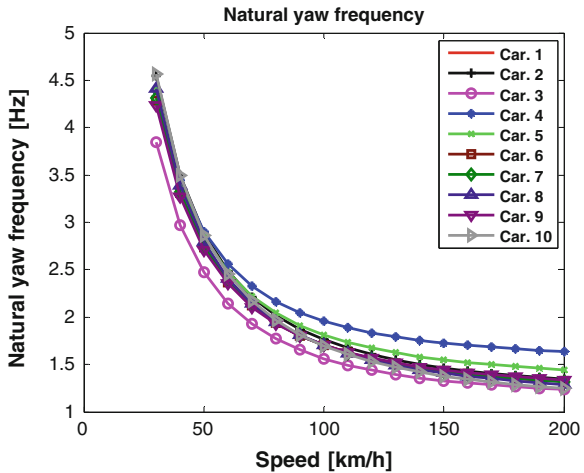
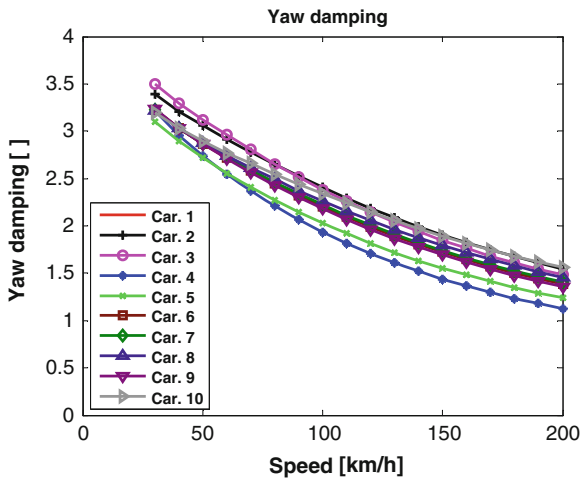


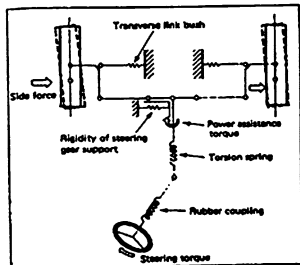
**Fig. 5.8** Yaw damping of different car tunings (analytic steering model)



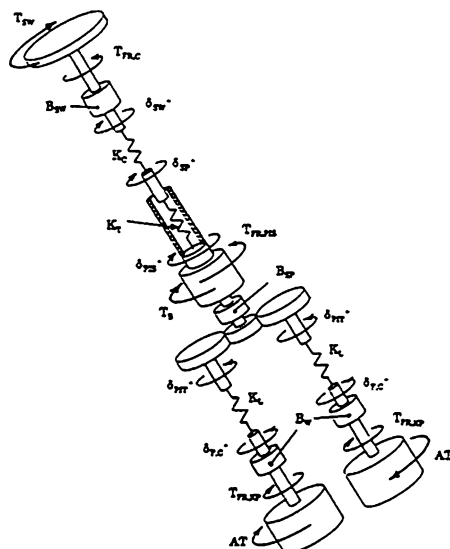
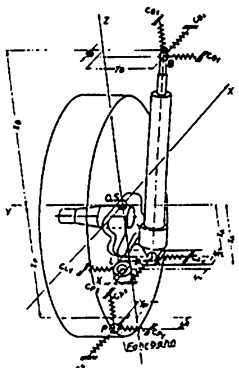
### 5.1.7 Steering Models

The steering influences the driving and steering behaviour of a car decisively. The steering model described in Sect. 5.1.2 already covers the essential elasticities in the steering driveline or in the wheel suspension. Extended steering models are required for detailed examinations and in particular to calculate the steering wheel torque and the transmission behaviour of the steering. Figure 5.9 shows a selection of steering models. An extensive overview of steering models may be found, for example, in Braess (2001) and in Zschocke (2009).

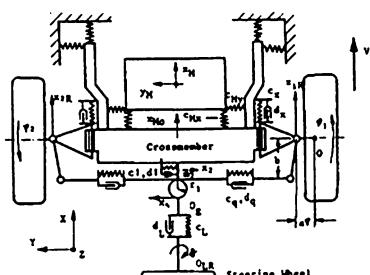
The steering models are extended according to the task, for example, very detailed mechanical, hydraulic and electric steering models have been developed.



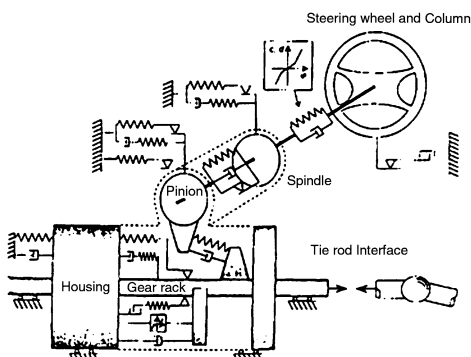
Simple Car Dynamic Model

Extensive Steering Dynamics Model  
(Post)

Strut/Shudder Model



Wheel Shudder Model (including Subframe)



Wheel Shudder/Driveline model

Fig. 5.9 Steering models for different applications, acc. to Braess (2001)

Models with three or more degrees of freedom are used (Pfeffer 2006) to examine wheel shudder and, the transmission behaviour of steerings. Models with two degrees of freedom are mostly used for examinations of driving dynamics. Additional considerations are:

- separate degrees of freedom for both front wheels in connection with the two track model for different wheel loads
- misalignment of the tyre forces and influences of the footprint

- friction, inertia and damping
- axle drive shaft torques of front-wheel drives, possibly complemented by effects of the limited-slip differentials and the electronic chassis system, as, for example, ABS
- steering support

Very detailed modelling of hydraulic and electric components for dynamic purposes is mostly renounced, because the influence of dynamics is low but would considerably prolong the processing times.

### ***5.1.8 Steering Model with Power-Assist and Friction Effects***

Analytic observations of the single track model including steering are based on the disregard of power-assist and friction, as well as the assumption of a constant steering ratio. These simplifications have to be made to derive the closed equations in a manageable way. This analytic car model will in the following be compared to a model with power-assist and friction effects. The car parameters used are listed in Table 5.2.

The difference between the analytic and the simple steering model is the inertia required for the simulation over time. Quasi-steady manoeuvres as, for example, circular driving produce the same behaviour. The complex model applies an ESF friction element according to Pfeffer et al. (2008) to the gear rack and steering column frictions. The complex steering model with power-assist includes an additional two-fold power gain. No steady power-assist is used in reality, because it would rise with increasing wheel torque and lateral acceleration (see Chap. 2).

Figure 5.10 shows the influence of the different modelling methods and the power-assist.

### ***5.1.9 Discussion of the Influence of the Vehicle and Steering Parameters on the Driving and Steering Performance***

The driving and steering performance of a car is marked by the car and steering parameters. The following table describes variations of a middle class car whose order of magnitude is found in the normal tuning area of car design development. The selected diverse car and steering parameters have the greatest influence on driveability, according to experience.

The simulation of the following diagrams applies a single track model, together with the complex steering model and the parameters listed in Table 5.3. The diagrams show to what extent the car and steering parameters influence driveability (Figs. 5.11, 5.12, 5.13, 5.14).

**Table 5.2** Parameters of different steering models

Parameter	Symbols	Units	Analytic model	Simple model	Complex model	Complex including power assist
Car mass	m	kg	1700	2.8	1700	1700
Wheelbase	l_F	m	2.8	1.4	2.8	2.8
Track FA	l_R	m	1.4	1.4	1.4	1.4
Track RA	J_z	kg m <sup>2</sup>	2600	2600	2600	2600
Yaw moment of inertia of the car	C_dF	N/rad	220000	220000	220000	220000
Cornering stiffness front	C_dH	N/rad	220000	220000	220000	220000
Cornering stiffness rear	C_dF,eff	N/rad	119438	119438	119438	138715
Actual cornering stiffness* front	C_dR,eff	N/rad	220000	220000	220000	220000
Actual cornering stiffness* rear	r_t	m	0.02	0.02	0.02	0.02
Mechanical trail	r_p	m	0.04	0.04	0.04	0.04
Pneumatic Trail	r	m	0.06	0.06	0.06	0.06
Full castor	i_S		15	15	15	15
Kinematic steering ratio	I_G	mm/U	50	50	50	50
Steering gear ratio	r_pi	m	0.007958	0.007958	0.007958	0.007958
Pinion radius	r_L	m	0.1194	0.1194	0.1194	0.1194
Steering arm length	C_T	Nm/degree	2	2	2	2
Torsional stiffness torsion bar	C_R	Nm/rad	40000	40000	40000	40000
Torsional stiffness axle mounting	C_S	Nm/rad	15678	15678	15678	22556
Steering stiffness	A_S	1	1	1	1	2
Power assistance ratio	J_C	kg m <sup>2</sup>	0.04	0.04	0.04	0.04
Steering-wheel and column inertia	d_T	Nm s/rad	0.1146	0.1146	0.1146	0.1146
Damping torsion bar	m_ur	kg	45.7	45.7	45.7	45.7
Unsprung mass front wheel + suspension						(continued)

**Table 5.2** (continued)

Parameter	Symbols	Units	Analytic model	Simple model	Complex model	Complex including powerassist
Inertia front wheel + unsprung mass of suspension as a function of the vertical axis of rotation	$J_{uF}$	$\text{kg m}^2$		1.7	1.7	1.7
Stiffness exponential friction model	$k_{Fr\ rack}$	N/m		1600000	1600000	
Upper and lower limit static friction force	$F_{Fr\ rack}$	N		$\pm 150$	$\pm 150$	
Stiffness friction model steering column	$k_{Fr\ C}$	Nm/degree		12	12	
Upper and lower limit static friction force entire steering column	$M_{Fr\ C}$	Nm		$\pm 0.2$	$\pm 0.2$	

\*\* Both tyres of an axle

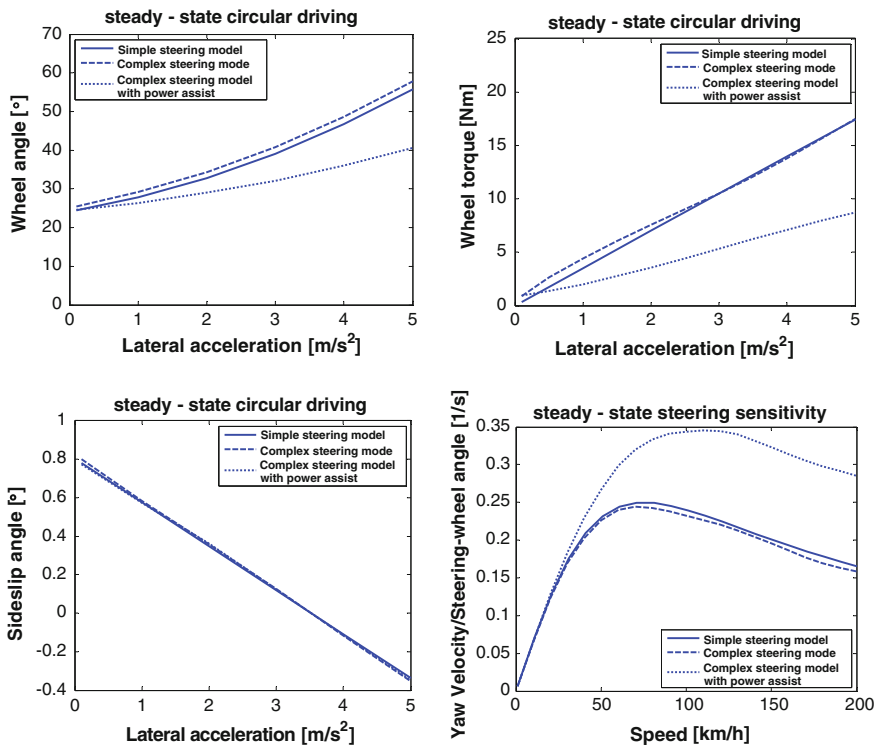


**Fig. 5.10** Influence of steering friction and power-assist on driveability during steady-state circular driving (a–c: constant radius  $R = 100$  m, d lateral acceleration =  $4 \text{ m/s}^2$ )

## 5.2 Basic Dynamic Steering Design

In the early development stages of a front-driven car the most important steering parameters, for example, the steering ratio, can be defined by using the linear theory of the single track model, valid now up to about  $0.4 \text{ g}$ . Once this car design is achieved, wheelbase, mass and its distribution as well as the cornering stiffness of the front and rear axle are at least approximately known.

### 5.2.1 Steering Axis Design: Steady State Self-aligning Torque

The steering-swivel axis describes the axis of rotation of the steered front tyre without considering lateral or longitudinal forces (see Chap. 4). It is assumed that this axis changes only slightly for low forces, then the geometrical conditions

**Table 5.3** Car and steering parameters

Parameter	Symbol	Units	Car 1	Car 2	Car 3	Car 4	Car 5	Car 6	Car 7	Car 8	Car 9	Car 10
Car mass	m	kg	1700	1500	1700	1700	1700	1700	1700	1700	1700	1700
Wheelbase	l	m	2.8	2.8	2.5	2.8	2.8	2.8	2.8	2.8	2.8	2.8
Track FA	$l_F$	m	1.4	1.4	1.25	1.12	1.4	1.4	1.4	1.4	1.4	1.4
Track RA	$l_R$	m	1.4	1.4	1.25	1.68	1.4	1.4	1.4	1.4	1.4	1.4
Yaw moment of inertia of the car	$J_z$	$\text{kg m}^2$	2600	2600	2600	2300	2600	2600	2600	2600	2600	2600
Cornering stiffness in front	$C_{\alpha f}$	N/rad	220000	220000	220000	220000	200000	200000	220000	220000	220000	220000
Cornering stiffness behind	$C_{\alpha H}$	N/rad	220000	220000	220000	220000	220000	220000	220000	220000	220000	220000
Actual cornering stiffness <sup>a</sup> in front	$C_{\alpha f,\text{eff}}$	N/rad	119438	119438	119438	119438	110063	121286	127615	115860	138715	
Actual cornering stiffness <sup>a</sup> behind	$C_{\alpha R,\text{eff}}$	N/rad	220000	220000	220000	220000	220000	220000	220000	220000	220000	220000
Constructive castor	$r_T$	m	0.02	0.02	0.02	0.02	0.02	0.02	0.018	0.02	0.02	0.02
Pneumatic Trail	$r_P$	m	0.04	0.04	0.04	0.04	0.04	0.04	0.04	0.04	0.04	0.04
Full castor	$r$	m	0.06	0.06	0.06	0.06	0.06	0.06	0.058	0.06	0.06	0.06
Kinematic steering ratio	$i_S$		15	15	15	15	15	15	15	15	15	15
Steering gear ratio	$I_G$	mm/rev	50	50	50	50	50	50	50	50	50	50
Pinion radius	$r_P$	m	0.007957747	0.007957747	0.007957747	0.007957747	0.007957747	0.007957747	0.007957747	0.007957747	0.007957747	0.007957747
Steering arm length	$r_L$	m	0.119366207	0.119366207	0.119366207	0.119366207	0.119366207	0.119366207	0.119366207	0.119366207	0.119366207	0.119366207
Torsion bar stiffness	$C_T$	Nm/degree	2	2	2	2	2	2	2	2	2	2
Torsional stiffness torsion bar	$C_T$	Nm/rad	115	115	115	115	115	103	115	115	103	115
Torsional stiffness axle mounting	$C_R$	Nm/rad	40000	40000	40000	40000	40000	40000	40000	40000	40000	40000
Steering stiffness	$C_S$	Nm/rad	15678	15678	15678	15678	14685	15678	18234	14685	22526	
Power assistance ratio	$A_S$		1	1	1	1	1	1	1	1	1	2

<sup>a</sup> Both tyres of each axle

**Fig. 5.11** Steering wheel angle as a function of lateral acceleration (constant radius R = 100 m)

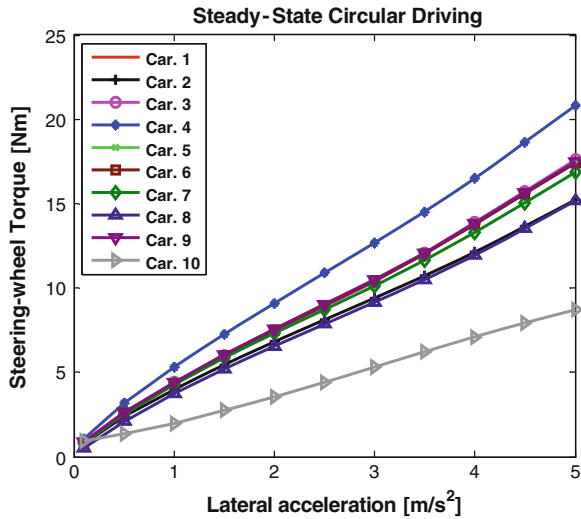
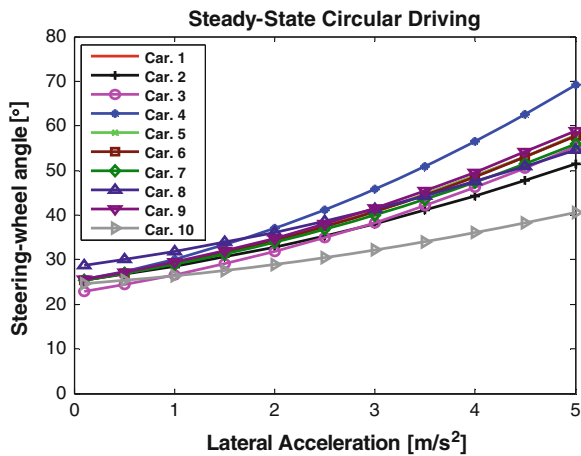


**Fig. 5.12** Steering wheel torque as a function of lateral acceleration (constant radius R = 100 m)



allow to compute the static righting moment at the front tyres (steering torque  $M_S$ ) according to Mitschke (1972) as follows:

$$M_S = m_F \cdot g \cdot \delta \cdot \left( r_0' \tan \sigma - (r_\tau - f_R \cdot r_{dyn}) \tan \tau \right) \quad (5.40)$$

with

$$r_0' = r_{stat}(\tan \sigma + \varepsilon_V) + r_0 \quad (5.41)$$

**Fig. 5.13** Lateral acceleration/Steering wheel angle as a function of Vehicle Velocity (lateral acceleration =  $4 \text{ m/s}^2$ )

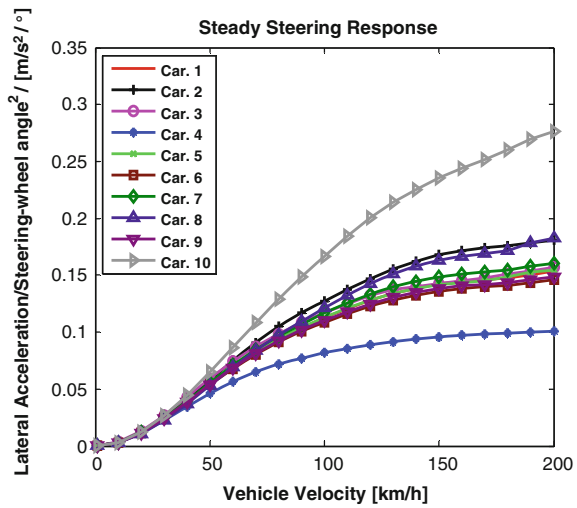
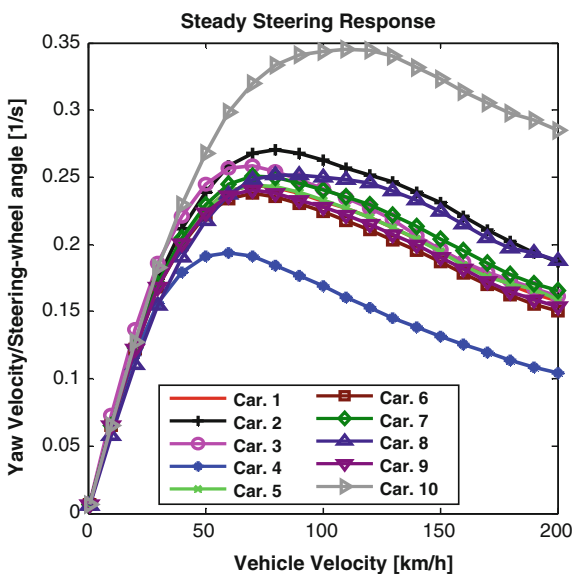


**Fig. 5.14** Yaw Velocity/Steering wheel angle as a function of Vehicle Velocity (lateral acceleration =  $4 \text{ m/s}^2$ )



Using the steering moment, frictions at the steering axes and the steering system, the steady limit of the steering angle can be assessed, beyond which the steering self-aligns at low speed, i.e. without a lateral force resulting from a lateral acceleration.

### 5.2.2 Determination of the Stability Factor

The stability factor is computed from the self-steering gradient as a function of the wheelbase:

$$K = m \cdot \frac{C_{zR,eff} \cdot l_R - C_{zF,eff} \cdot l_F}{C_{zR,eff} \cdot C_{zF,eff} \cdot l^2} \quad (5.42)$$

A particular significance is attributed to the effective cornering stiffness at the front axle (quasi-steady, Pacejka 2006), because the qualities of axle design, steering, roll stiffness of the spring suspension, and roll-steer effect act together.

$$C_{zF,eff} = \frac{C_{zF}}{1 + \frac{l}{l_R} (\varepsilon_{\varphi,F} \cdot C_{zF} + \Delta\varepsilon_{V,\varphi,F} \cdot C_{zF}) \frac{h}{C_\varphi} + (r_\tau + r_P) \frac{C_{zF}}{C_S}} \quad (5.43)$$

$h$	distance of the centre of gravity from roll axis
$\varepsilon_{V,\varphi,F}$	rolling steering factor at the front axle
$\Delta\varepsilon_{V,\varphi,F}$	portion of camber as a result of rolling
$C_\varphi$	roll stiffness
$r_\tau + r_P$	mechanical and pneumatic trail
$C_S$	bottom-top steering stiffness.

In modern car design the effective cornering stiffness may be approximated as follows (see also Eq. 5.28):

$$C_{zF,eff} \approx \frac{C_{zF}}{1 + (r_\tau + r_P) \frac{C_{zF}}{C_S}} \quad (5.44)$$

The significance of castor offset, cornering stiffness of the front axle and “bottom-top” steering elasticity is evident. Depending on the desired self-steering effect, the nominal cornering stiffness may be decreased at the front axle down to a half, with mixed tyres, i.e. narrower tyres at the front axle, even down to a third.

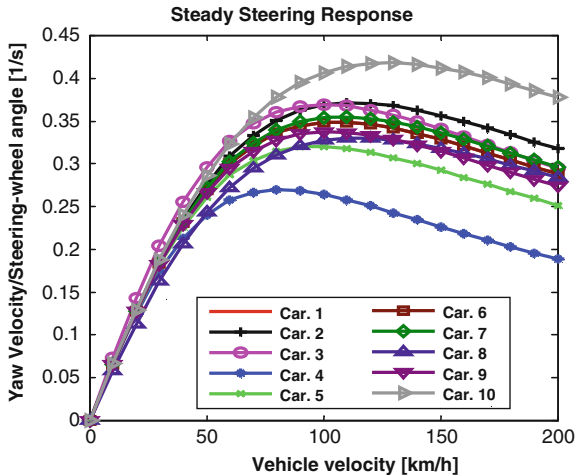
### 5.2.3 Steady State Yaw Gain and Steering Sensibility

A car should respond neither too strongly nor too weakly to steer-angles. The stationary yaw gain serves as a steady assessment quantity.

$$\frac{\dot{\psi}}{\delta_H} = \frac{1}{i_S l} \frac{v}{1 + Kv^2} = \frac{1}{i_S l} \frac{v}{1 + \frac{v^2}{v_{ch}^2}} \quad (5.45)$$

The yaw gain of modern cars is the highest between 100 and 120 km/h (see Fig. 5.15). According to Weir and diMarco (1980), the optimum range is about

**Fig. 5.15** Stationary yaw gain of the car variants (analytic steering model)



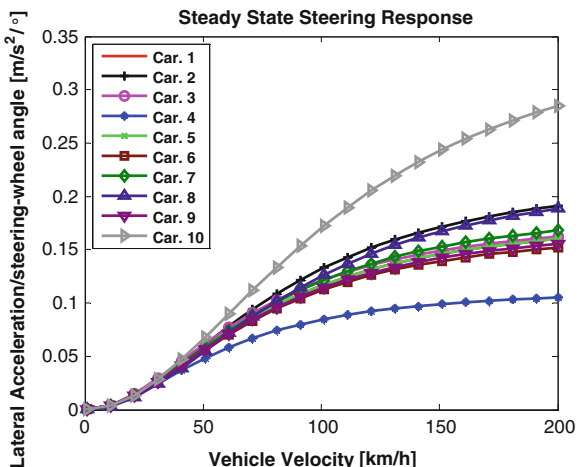
0.3 1/s at 80 km/h. This is used to determine the steering ratio around the middle position with a desired self-steering effect (Eq. 5.45).

This range ensures that a too fast car does not generate a too high lateral acceleration. This lateral acceleration as a function of the steering wheel angle input (steering response) is calculated as follows:

$$\frac{a_y}{\delta_H} = \frac{1}{i_S l} \frac{v^2}{1 + \frac{v^2}{v_{sh}^2}} = \frac{\dot{\psi}}{\delta_H} v \quad (5.46)$$

Figure 5.16 shows this lateral acceleration gain as a function of speed. It is evident that the lateral acceleration gain increases further, in spite of the drop of yaw gain over speed.

**Fig. 5.16** Steady state steering response of the car variants (simple steering model)



### 5.2.4 Steering-wheel Torque/Lateral Acceleration Gradient (Steady State)

In addition to the static self-aligning moment which predominates at low speed, a dynamic self-aligning moment overlaps at higher speed. The gain of this self-aligning moment at the steering wheel, of particular meaning for the steering feel, should not be too low or too high.

The steady-state of the wheel torque/lateral acceleration gradient is:

$$\frac{dM_H}{da_Y} = \frac{m_F \cdot r}{i_S} \frac{\left(A_S - a_Y \frac{dA_S^2}{da_Y}\right)}{A_S^2} \quad (5.47)$$

Optimal values, beginning at the zero position, are 2 to 3 Nm/m/s<sup>2</sup>. An additional friction torque at the steering wheel or column of approx. 0.1 to 0.5 Nm should also be considered.

### 5.2.5 Frequency Response Wheel Torque/steering wheel angle

Besides the optimal steering paths and the gain of the steering wheel torque over the lateral acceleration, there are further characteristics which are significant for the ideal adaptation of the steering behaviour to the driver. First, there is the quasi-steady increase of the steering-wheel torque over the steering-wheel angle, the steering stiffness.

The frequency response acc. to Mitschke and Wallentowitz (2003) is as follows:

$$F(s) = \frac{\text{steering wheel torque } (s)}{\text{steering wheel angle } (s)} = \left(\frac{M_H}{\delta_H}\right)_{\text{stat}} \cdot \frac{1 + T_{z1}s + T_{z2}s^2}{1 + \frac{2\sigma_f}{v_f^2}s + \frac{1}{v_f^2}s^2} \quad (5.48)$$

with:

$$T_{z1} = \frac{m \cdot l_R^2 + I_Z}{m \cdot v \cdot l_R} \quad (5.49)$$

$$T_{z2} = \frac{I_Z}{c_{zR} \cdot l_R} \quad (5.50)$$

$$\left(\frac{M_H}{\delta_H}\right)_{\text{stat}} = \frac{m \cdot l_R \cdot r}{i_S^2 \cdot l^2} \frac{v}{1 + (v/v_{ch})} \quad (5.51)$$

As with the response to steering wheel angles, the curve of the steering-wheel torque should not significantly deviate from the quasi-steady curve for common steering frequencies.

A significant phase has a negative effect on the subjective steering evaluation. Acc. to Hill (1987), the subjective rating decreases by approx. two points when a steering frequency of 0.5 Hz and a 20° phase shift occurs.

### 5.2.6 Free Control Stability

Driving stability is usually determined with a fixed steering wheel (fixed control). Safe driveability requires, in addition, that a wheel which is left alone (free control) or even turned and then left alone should not suffer a build-up of the coupled yaw steering vibration and any noise should fade away.

The simplest calculation is made in a single track model (two degrees of freedom), complemented by the equilibrium of torques around the steering axes, according to Braess (1967). A more precise assessment is possible according to Segel (1966). Figure 5.17 shows how the steering-wheel is suddenly left alone after a steady cornering of 4 m/s<sup>2</sup>. The return depends very much on inertia and dampings or frictions. The simple steering model without friction takes much longer to fade away, thus friction, damping and inertia have to be considered during tuning. Electromechanical systems help to ideally design these returns by applying special functions.

### 5.2.7 Natural Frequency and Damping of the Steering

Döhring (1961) explained already that the steering elasticity and, hence, the natural frequency of the steering at a steady steering angle are crucial for the accuracy of the car and its wheel shudder. A recent publication by Mouri et al. (2007) expanded the topic to the extent that the movement of the wheel could be optimised with regard to the desired steering feel. Figure 5.18 shows that the

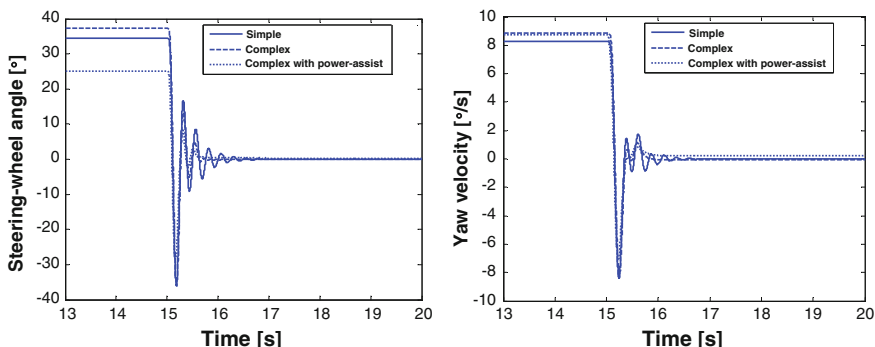
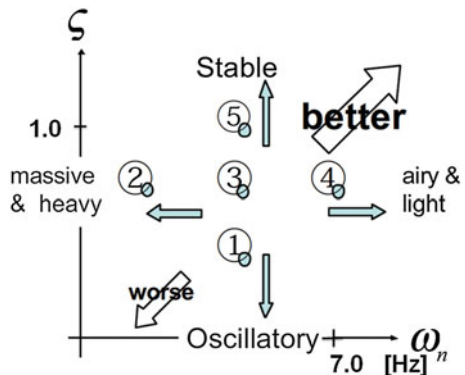


Fig. 5.17 Return of modern cars

**Fig. 5.18** Perception of the steering feel as a function of natural frequency and damping (values assessed at a fixed steer-angle)



associated values of the natural frequency are in the range of 6 to 7 Hz while the damping is between 0.8 and 0.9.

### 5.2.8 Minimising the Self Steering due to Uneven Braking Forces at the Front Axle

While the steering design matters primarily for the lateral dynamic driving, additional effects result for the longitudinal dynamics. One example is the  $\mu$ -split braking with different braking forces at the front axle. The negative scrub radius, automatically inflicting a steer-angle, can minimise the developing yaw moment and the resultant traction loss of the braking car. A simplified assessment is described by Braess (1965) and a more detailed one by Braess (1970).

For front-wheel-drive cars, a negative scrub radius is commonly used. Other cars implement rather small values. With EPS steering system, it is possible to generate additional torque to compensate the steering wheel torque from the driver (see Chap. 19). This superposition steering can achieve the countersteering movement without any interference of the driver.

### 5.2.9 Stable Steering Braking System

The separation of the brake circuits increases the safety, if any part of the braking system should fail. The developing yaw moment can be compensated by the negative scrub radius (Heissing and Ersoy 2007) if a diagonal arrangement is chosen so that one front tyre is always braked (Braess and Seiffert 2007). This arrangement may be regarded as a mechanical preliminary stage for the modern electric interconnected subsystems.

### **5.2.10 Influence of Aerodynamics on Driveability**

Any modern car has an aerodynamic lift that affects the two axles differently and, hence, the loads and the trim (Hucho 2005). In general, the lift alters the lateral acceleration potential and the self-steering effect, i.e. it impacts the hazard of under- or over-steer. A strong rear lift reduces the driving stability in the upper speed range, a lift at the front axle reduces the steering-wheel torque, causing the steering to “go free”, i.e. to lose steering precision. As a consequence, the front lift coefficient should be less than 0.1, at least for strongly motorised cars with higher top speed.

### **5.2.11 Front-wheel Drive Vehicles**

Front-wheel drive cars differ in various aspects of the self-steering effect from rear-wheel drive cars (see e.g., Krummel et al. 1981; Gillerspie and Segel 1983).

- significantly higher front load throughout,
- impact of the drive moment on the steering for inclining structures and, for asymmetric axle drive shafts, even when driving straight,
- direct influence of the driving forces on the yaw moment when a steering angle applies,
- indirect influence of the driving forces on the lateral force of the tyres and self-aligning moments.

All these effects and their influence on the lateral vehicle dynamics (self-steering effect, change of load in corners, low road friction etc.) and on the steering behaviour (steering forces, steering returnability etc.; Krummel et al. 1981) have to be taken into account. The drive power of front-wheel driven car was significantly increased during the last decades. Reducing the interfering force arm was helpful in designing axles (Heissing and Block 2001; Simon et al. 2009). Some other measures include controlled differential locks and further torque-influencing systems. (Frömming et al. 2009; Wakamatsu and Nishimori 2010).

## **References**

- Braess HH (1967) Beitrag zur Stabilität des Lenkverhaltens von Kraftfahrzeugen. ATZ 1967:82–84  
 Braess HH (1965) Beitrag zur Fahrtrichtungshaltung des Kraftwagens bei Geradeausfahrt. ATZ 67:218–221  
 Braess HH (1970) Theoretische Untersuchungen des Lenkverhaltens von Kraftfahrzeugen. FISITAKongress 1970, Paper 17.1.B  
 Braess HH (1975) Ideeller negativer Lenkrollhalbmesser. ATZ 77:203–207

- Braess HH (2001) Lenkung und Lenkverhalten von Personenkraftwagen—Was haben die letzten 50 Jahre gebracht, was kann und muß noch getan werden? VDI-report no. 1632
- Braess HH, Seiffert U (2007) Handbuch Kraftfahrzeugtechnik. Vieweg + Teubner Verlag: Wiesbaden 2007, p 581
- Decker M (2009) Zur Beurteilung der Querdynamik von Personenkraftwagen. Dissertation, Technische Universität München 2009
- DIN 70000 (1994) Fahrzeuggdynamik und Fahrverhalten. Berlin: Deutsches Institut für Normung
- Döhring E (1961) Über Wirkungsgrad und Elastizität von Automobil-Lenkgetrieben, ATZ Jahrgang 63, Heft 3, S. 75–77
- Döhring E, Becker JF (1973) Die Lenkunruhe der McPerson-Achsen. ATZ Automobiltechnische Zeitschrift 75(5):155–162
- Dödlbacher G, Gaffke HG (1978) Untersuchung zur Reduzierung der Lenkungsunruhe. ATZ Automobiltechnische Zeitschrift 80 (1978) 7/8, pp 317–322
- Frömming L, Henze R, Küçükay F, Apel A (2009) Querverteilung des Antriebsmoments bei Frontantrieb. VDI-report 2086:335–348
- ISO 4138 (2004) Passenger cars—Steady-state circular driving behaviour—Open-loop test Methods. 3rd edn. 2004-09-15
- ISO 7401 (2003) Road vehicles—Lateral transient response test methods—Open-loop test methods
- ISO 8855 (1991) Terms for road vehicle dynamics and road holding ability
- Gillerspie TD, Segel L (1983) Influence of front-wheel drive on vehicle handling at low levels of lateral acceleration. IMechE, Road Vehicle Handling, No. C114/83, pp 61–68
- Heissing B, Block M (2001) Fahrwerk und Antriebstrang. Der neue A4, special edition ATZ/MTZ, pp 84–96
- Heissing B, Ersoy M (2007) Fahrwerkhandbuch Grundlagen, Fahrdynamik, Komponenten, Systeme, Mechatronik, Perspektiven
- Hill R (1987) Correlation of subjective evaluation and objective measurement of vehicle handling. EAEC, Strasbourg
- Hucho W-H (2005) Aerodynamik des Automobils, 5th edn. Vieweg Verlag, Wiesbaden
- Kraaijeveld R, Wolff K, Vockrodt T (2009) Neue Testprozeduren zur Beurteilung des Fahrverhaltens von Pkw mit variablen Lenksystemen. ATZ Automobiltechnische Zeitschrift 111(3):124–129
- Krummel J et al (1981) Fahrverhalten und Lenkung bei Frontantrieb. 50 Jahre Frontantrieb. VDI Bericht 418:245–252
- Mitschke M (1972) Dynamik der Kraftfahrzeug. Springer, Berlin
- Mitschke M, Wallentowitz H (2003) Dynamik der Kraftfahrzeuge, 4th edn. Springer, Berlin
- Mouri H, Kubota M, Horiguchi N (2007) Study on effects of transient steering efforts characteristics on driver's steering behavior. SAE-Paper 2007-01-0823, Warrendale 2007
- Neureder U (2001) Modellierung und Simulation des Lenkstranges für die Untersuchung der Lenkungsunruhe. ATZ Automobiltechnische Zeitschrift 103(3):216–224
- Nozaki H (1985) The effects on steering system rigidity on vehicle cornering characteristics in power-assisted steering systems. JSAE-Rev 4
- Pacejka HB (2006) Tyre and vehicle dynamics, 2nd edn. Butterworth Heinemann, London
- Pfeffer PE (2006) Interaction of vehicle and steering system regarding on-centre handling. Thesis University of Bath, Bath
- Pfeffer, PE, Harrer M (2007) On-centre steering wheel torque characteristics during steady state cornering, SAE-Paper 2008-01-0502, Warrendale 2007
- Pfeffer PE, Harrer M, Johnston DN (2008) Interaction of vehicle and steering system regarding on-centre handling. Veh Syst Dyn 46(5):413–428
- Post JW (1995) Modeling, simulation and testing of automobile power steering systems for the evaluation of on center handling. Thesis. Clemson University, Clemson
- Riekert P, Schunck TE (1940) Zur Fahrmechanik des gummibereiften Kraftfahrzeugs. Ingenieur Archiv, vol 11, Heft 3, 6.1940, pp 210–224

- Segel L (1966) On the lateral stability and control of the automobile as influenced by the dynamics of the steering system, transactions of the ASME. J Eng Ind 88:283–295
- Simon M, Frantzen M, Gerhards T, David W, Jagt PVD (2009) Front wheel drive with 300 PS—Is it Possible? RevoKnuckle—Development of a Driven Front Suspension for a 300 PS Sports Car. Chassis.tech. München
- Wakamatsu K, Nishimori T (2010) Driving torque transfer system for FWD with steering wheel compensation. FISITA Paper F2010D022
- Weir DH, Dimarco RJ (1980) Correlation and evaluation of driver/vehicle directional handling data. SAE Paper 780010, Warrendale 1980
- Zschocke A (2009) Ein Beitrag zur objektiven und subjektiven Evaluierung des Lenkkomforts von Kraftfahrzeugen. Dissertation, Karlsruher Institut für Technologie

# Chapter 6

## Acoustics and Vibrations

Stefan Sentpali and Rupert Hintersteiner

Acoustics and Vibration technology for car development has gained significance and made major progress over the last few years. Sound patterns and volume of noises, as well as frequency and volume of car vibrations have to be considered while the car is being developed. Noises perceived as unpleasant should be very faint while warning noises have to be loud enough to meet certain safety standards. In addition, the noises of middle class and superclass cars are ‘designed’ in such a way that they correspond to what the customers expect. This is also true for any noticeable vibrations. The driver is in contact with the wheel and feels any vibrations occurring there at all times. The design of these vibrations of the steering wheel, including mounted parts and body, with regard to comfort is a major task. How acoustics and vibrations are perceived is an increasingly important argument for the decision to purchase.

The steering assumes a central role among the mechatronical systems, substantially influencing the fahrgefühl. Steering systems are some of the most powerful mechatronics in car construction, but they are also among those emitting the strongest noise. The relationship of acoustic  $P_{acoustic}$  and mechanical power  $P_{mechanical}$  can be estimated as a proportional function of the acoustic efficiency  $\zeta_{acoustic}$ .

$$\zeta_{acoustic} = \frac{P_{acoustic}}{P_{mechanical}} \quad (6.1)$$

---

S. Sentpali (✉)

Munich University of Applied Science, Munich, Germany  
e-mail: stefan.sentpali@steeringhandbook.org

R. Hintersteiner

Audi AG, Ingolstadt, Germany  
e-mail: rupert.hintersteiner@steeringhandbook.org

A range of  $10^{-8} \leq \zeta_{acoustic} \leq 10^{-4}$  is valid for most mechatronics systems. If the acoustic efficiency is known, it is possible to compute the sound power level  $L_W$  in dB.

$$L_W = 10 \lg \left( \frac{P_{acoustic}}{P_0} \right) = 10 \lg \left( \frac{\zeta \cdot P_{mechanical}}{P_0} \right) = 10 \lg(\zeta) + 10 \lg \left( \frac{P_{mechanical}}{P_0} \right) \text{ (dB)}$$

$P_0 = 10^{-12}$  [Hearing threshold in Watt]

(6.2)

More precise assessments require empirically gained level equations or emission values from artificial sound sources (ETS values) in compliance with the VDI directives (Verein Deutscher Ingenieure = Association of German Engineers).

## 6.1 Interfering and Operating Noise

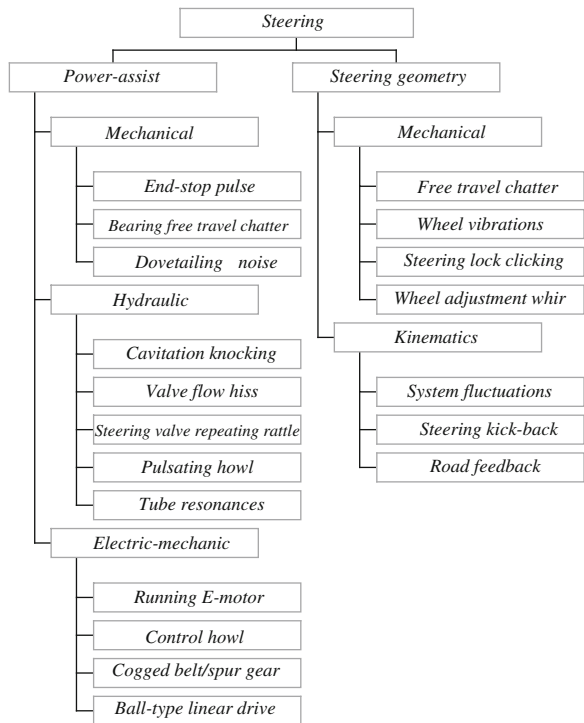
For acoustics it is useful to distinguish steering noise by operating and interfering noise. The systems are classified either by degree of influence by the driver or by operating time and exposure time of the noise emission. One premise is whether a steering function can be deliberately turned on by the driver or is activated automatically by the system. Deliberate or direct operations produce operating noises, heard, e.g., when the steering lock or the steering control is used. Noise emissions resulting from unconscious or indirect operations are interfering noises. An example would be the rattling that occurs when driving on bad roads or during parking. The driver will subjectively accept operating noise more than interfering noise, after all, there was a deliberate action and the resulting emission is learnt or even an expected feedback. The objective of car development complies with that. To achieve high-quality sound, the operating noise over time may be audible but not irritating and any interfering noise must be inaudible. A car brand may distinguish itself by its acoustics quality only though proper engineering of the operating noise. Table 6.1 shows typical steering noise symptoms in the crossover of operating time and type of noise.

### 6.1.1 Sound Sources of Steering Systems

A controlled power-assist may be either hydraulic, electric-hydraulic or electric. Active steering with hydraulic steering-assist can produce any kind of hydro- or vibroacoustic phenomena. The emission is usually related to the load. A classification of the phenomena is shown in Fig. 6.1. It is classified per influence of construction groups or design details on the noise, assisted by the type of

**Table 6.1** Classification of the noise symptoms of steering systems

	Operating noise (conscious direct influence by the driver)	Interfering noise (unconscious indirect influence by the driver)
Operating time (long)	Steering control (hum, crackling, grinding)	Coil spring (grinding) Parking (sing, hiss, squeal, rattle, hum)
Operating time (short)	Steering lock (click) End-stop (bang, hoot)	Gearbox pressure part (rattle) Free travel of the gear (rattle) Hydraulic return line (cavity rattle)

**Fig. 6.1** Sound and vibration sources of steering systems

power-assist and the structure of the steering geometry. The phenomena are classified as either “mechanical”, “hydraulic”, “electromechanical” or “kinematic”, corresponding to the main sources of noise. The sound flow through the system is not only governed by the source but also by the place, the transmission path to the interior and the kind of excitation.

Volume, pitch and pulse are determined by the respective free dynamic forces and their physical nature. Any rotating parts produce a harmonic behaviour. The resulting rotational noise consists of fluctuations of the alternating force per rotation  $Z$  (1st harmonic), the rev  $U$  and the ordinal  $n$ , being an integer multiple

(harmonics). With such harmonic phenomena, the noise behaviour is very much dependent on rev. Typical ordinal noises of hydraulic power-assistance systems arise from the pressure pulses of the pump while those of electric systems originate in variations of the magnetic attraction.

$$f_{nord.} = Z \cdot n \cdot \frac{U}{60} \text{ (Hz)} \quad (6.3)$$

U in 1/min

The amplitudes of the harmonic orders pass the full range of frequencies as the rev changes. Broadband noises are generated by the grinding of bearings, covers or overcritical pressure release in the hydraulic steering valve. The operating noise is mostly an overlapping of many noises and their variations.

### **6.1.2 Electric Steering Systems**

Recording the emitted sound pressure level of an electric steering system while steering, and disassembling the amplitude curves over time by frequencies, both help to generate a diagram of a characteristic curve family according to Fig. 6.2.

Now the individual components—the partial sound sources—can be recognised. They are allocated to the ordinals from the gear ratios of the electric motor and the gearbox. The actual condition of the emissions has to be known to reduce them by low-noise design. Once the sound sources are sorted by volume and interfering frequency band, an action plan for car construction can be developed, arranged by the same priorities. Adjust the design by the sound flow present, see the example in Fig. 6.3. Possible secondary actions may be assessed at virtually every component boundary. For example, this could mean one inserts viscous damping, installs an elastic decoupling or applies local impedance materials at the boundary layers. Any change that directly reduces the noise excitation is called a primary action, examples include avoiding inexact power measurements, discontinuities or dead times of the control.

### **6.1.3 Hydraulic Steering Systems**

The noise sources of hydraulic systems are mainly of hydraulic nature. Only the alternating pressure overlaying the static pressure produces audible or noticeable vibrations, also called pressure pulsation, as shown in Fig. 6.4.

The origin of pressure pulsations are fluctuations of the volumetric current and their interaction with hydraulic impedances. These are generated by local masses of oil volumes and the volume storage capacity, as well as the resonance lengths of the tube systems. Tuning and optimising of the acoustics has to be done in the full system (Fig. 6.5). For this purpose, mount the complete subsystem on special

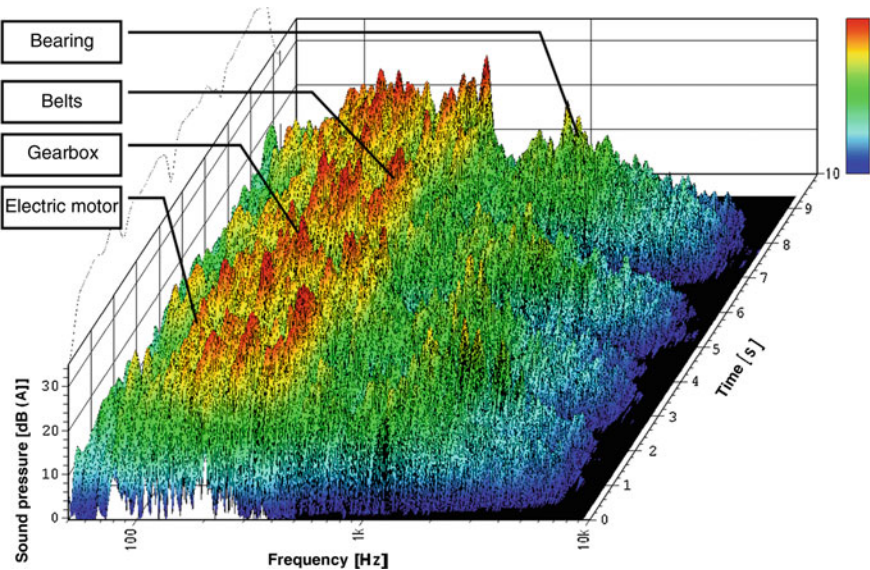


**Fig. 6.2** Sound emission spectrum of an electric steering system

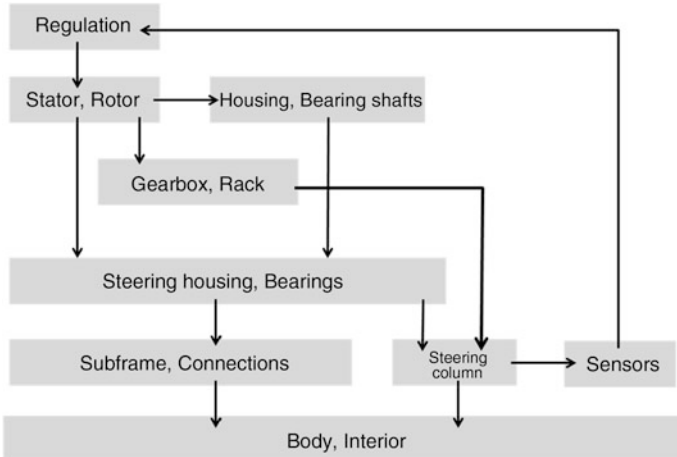


**Fig. 6.3** Sound flowchart of an electric steering systems with electric motor excitation

component test benches. When running independent acoustic evaluations of component systems, maintain the correlation to the full car. The dynamic forces or structure-borne sound accelerations are recorded at all the interfaces. Any lacking mounting impedances are either computed or measured in space according to their phase relationships in time. Assess the acoustic immissions by settling the

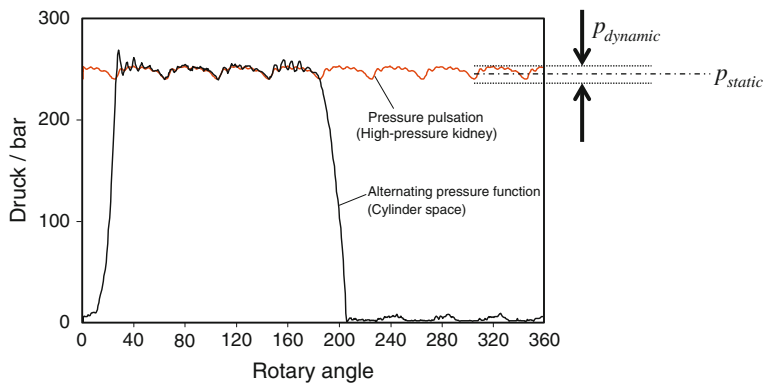
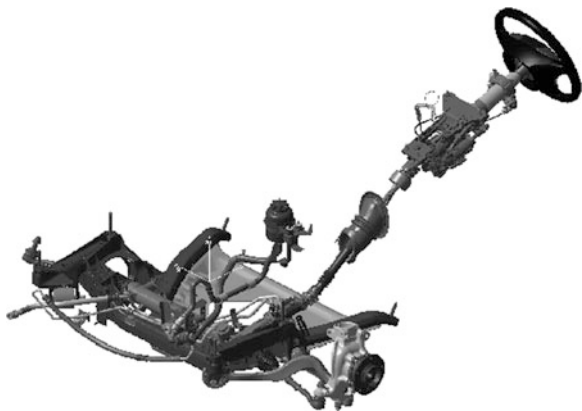


**Fig. 6.4** Overlapping of static and dynamic pressure pulsation of a hydraulic pump

**Fig. 6.5** Steering components for mounting on a system test bench



measurement values of the component against the virtual body. If temporal data are the basis, the result can be made audible and disclosed to a subjective audit by a jury. Acoustic optimisation in the projected car includes air noise emission; structure-borne sound excitation of the pump-, body-, fluid- and tube-sound transmission behaviour of the hydraulic tubes; free travels of dovetailings and shafts; and the implementation of isolating system bearings.

A high priority is the tuning of the high-pressure tube, also called the tuning of the stretch tubes between high-pressure pump and steering valve. Execute these tests on system test benches. Limit the test set-up to the hydraulic components and their arrangement as given by the available car space. Insert plastic pipes of various lengths and diameters and positions of throttles into the stretch tubes. These resonators may reduce noise by much more than 40 dB. The share of the throttle positions ( $x$ ) is  $<20$  dB, see Fig. 6.6.

Table 6.2 gives typical noise phenomena and the required remedy. Beside the parking noise that originates mainly from the howling pump, hissing sounds may

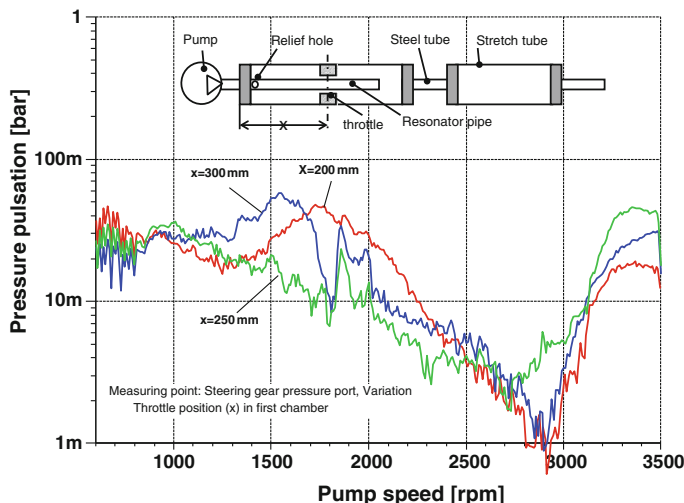


**Fig. 6.6** Variation of throttle position during workbench tuning of a stretch tube

**Table 6.2** Classification of noise phenomena of steering systems

Phenomenon	Cause and remedy
Pump howling	Minimise pressure pulsation at the steering gear by tuning panels and resonators in the stretch tube
Steering rattle	Unstable control circuit, due to high demands to steering rev and pressure, optimise the valve gradient and increase volume in the return line
Steering chatter	Hydraulic chatter due to cavitation enforced by off-road excitation, tune the panel positions and the back pressure in the return line to the tank
Steering hiss	Overscritical pressure release in the valve, tune the back pressure by panel(s) in the return line
Infiltration of structure-borne sound	Acoustic short circuit of the rubber stoppers of the suspension at too high static load, design the softness of the rubber and the best attachment site with a high input impedance

be heard just before the steering stop which are the result of overscritical pressure release across the control edge of the steering valve. Overscritical pressure release drives the flow speed at the valve edge to the speed of sound, creating an overlapping blast of very high acoustic power. This noise may be clearly reduced by increasing the back pressure in the return line or by a gradual pressure release across several panels arranged in a row. Integrating one or more such panels can avoid the hiss completely. If more than one panel is used, geometric graduation of the cross sections is recommended.

Note, however, that panels and throttles will raise the circulation pressure and, hence, the energy consumption. Rattling noises may occur if the wheels are

quickly turned to low friction values. Hydraulic chatter is the result of cavitation behind the steering valve, e.g., when a speed bump is passed over during circular driving.

## 6.2 Stability

The acoustic contribution of individual components in the steering depends on the nature of the problem or excitation. Hydraulic chatter and steering rattle are phenomena of hydraulic steering that result from the stability of the power-assist. Both phenomena can be well controlled by the design of the return lines and by adjusting the magnitude of the steering valve gradient. However, the application engineer is facing a conflict here: robust system designs that are robust with respect to steering rattle are more sensitive to hydraulic chatter and vice versa.

### 6.2.1 *Hydraulic Steering Clattering*

Passing speed bumps or bad roads generates peak-shaped excitations of the wheel and its transmission by the gear rack into the hydraulic cycle of the full system. This can produce a chatter of the mechanical free travel of the rack, and from cavitation in the hydraulic runback to the tank, behind the steering valve. It is classified by cause as a hydraulic chatter, subjectively indistinguishable from mechanical chatter and sporadically appearing without any immediate action of the driver. This chatter is obviously interfering noise and should be suppressed below audibility. The complicated mechanical and hydraulic processes in a steering system whenever the wheels receive a peak excitation are illustrated in the similarly complicated sound flowchart in Fig. 6.7.

Circular driving produces hydraulic clatter when bumps are crossed at 5–20 km/h. Hydraulic/mechanical interaction cause this excitation to send powerful pressure and volumetric current fluctuations into the tube system, particularly into the runback system (Fig. 6.8).

Pressure peaks in a not optimised hydraulic runback can rise to 100 bar when crossing a bump, just by cavitation. Figure 6.9 reveals the quick pressure drop in the low-pressure range up to the vapour pressure limit and the subsequent high pressure peak, audible inside the car as chatter. The pressure at the steering gear output drops significantly in the volumetric flow lows. The hydraulic liquid evaporates and after a short time condenses instantaneously. This excites the components to vibration. Tuning the dynamic volume gain and the back pressure in the runback avoids this noise by connecting a hydro-acoustic capacity to the steering valve at the outlet side.

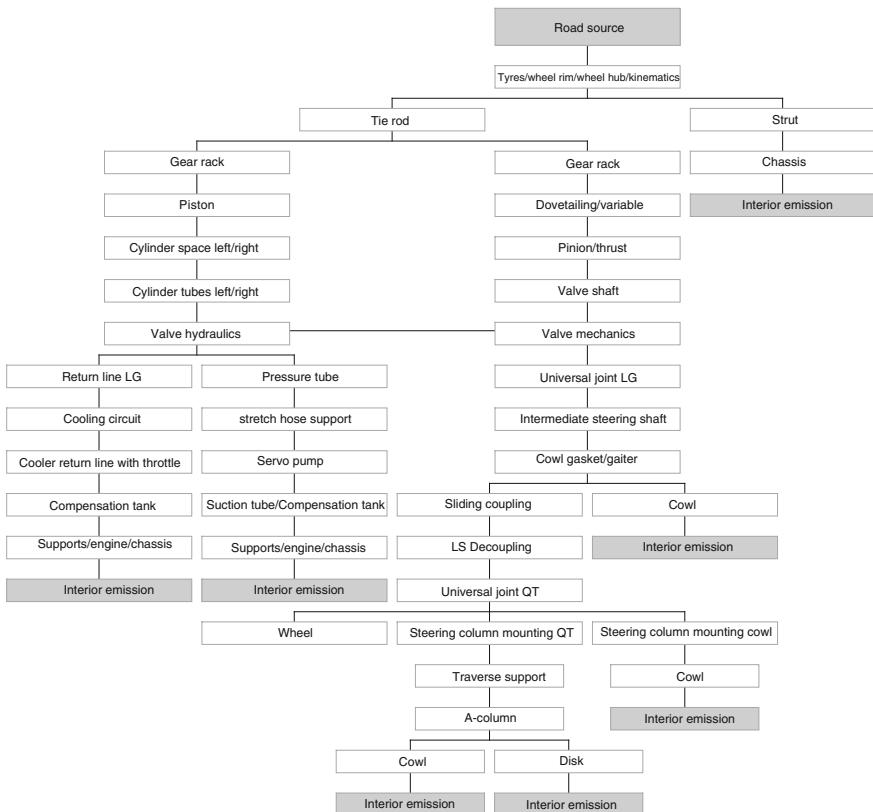


**Fig. 6.7** Sound flow during excitation from off-road driving or bumping

With high-capacity steering systems as they are found in sports saloons, this hydro-acoustically acting impedance may render the automatic control system unstable, which is evident from rattling vibrations at maximum cornering.

### 6.2.2 Steering Rattle

Parking produces varying radial forces, exciting a vibration of the steering, due to the discontinuity in the friction curve of the wheels on the road when static transits to kinetic friction. Hence, especially weakly damped systems on low friction roads are inclined to rattle. All the hydromechanical steering may vibrate. The main contribution is made by the pulsating oil volume in the elastic runback. If the dynamic volume storage capacity of the hydraulic runback into the oil tank is decreased, the amplitudes will be significantly lower (Fig. 6.10).

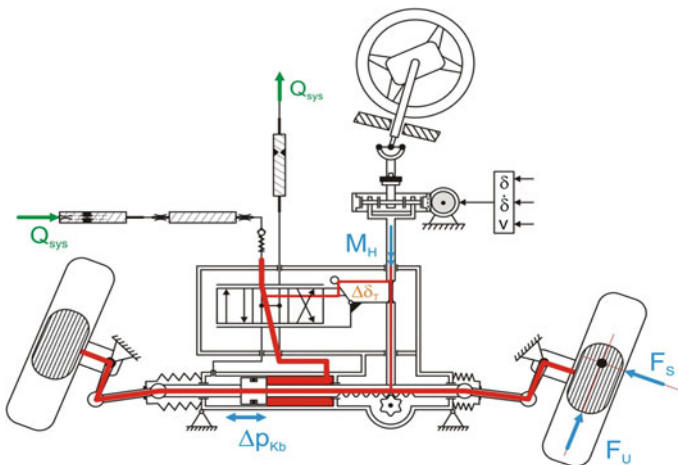


**Fig. 6.8** Functional diagram of the hydraulic cycle of a steering

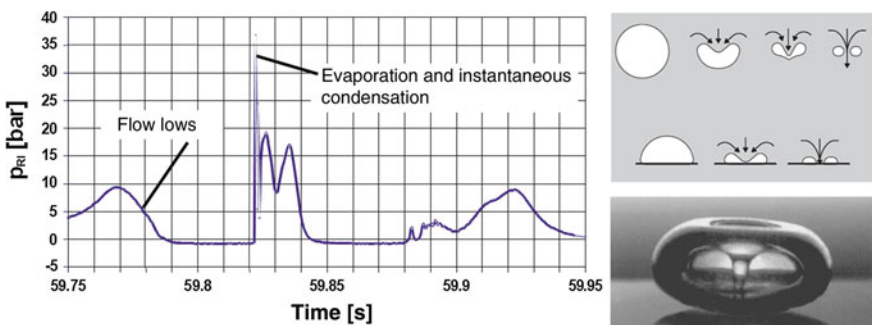


**Fig. 6.9** Pressure curve and graphic depiction of the cavitation peaks of hydraulic chatter

Indeed, sufficient dynamic storage volume is required to prevent a pressure drop below the vapour pressure and, hence, the hydraulic steering chatter phenomenon. Figure 6.11 shows examples of how a fuel return line is optimised. The ideal length of the volume storing runback stretch tube is determined during a test drive. Progressive volume increase as a function of the back pressure is adjusted by the material and inherent stiffness of the flexible tubing. The material stiffness is the result of the dynamic modulus of elasticity that applies to the system of rubber and fabric in the tube, the inherent stability is determined by oval cross sections.

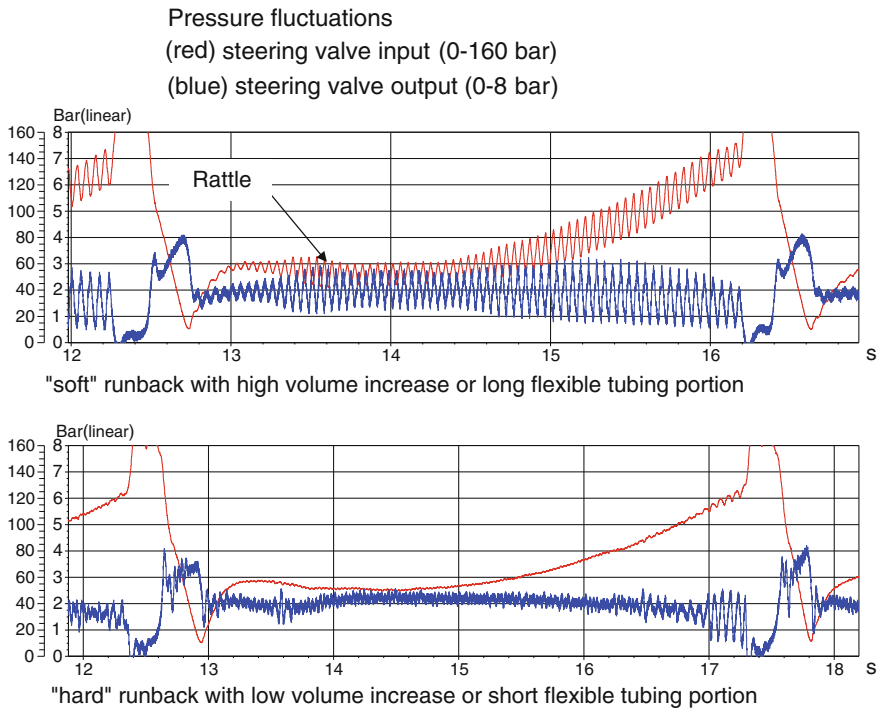


**Fig. 6.10** Pressure curve in the hydraulic runback with “soft” and “hard” flexible tubing material

### 6.2.3 Steering Wheel Nibble

Perceptible vibrations at the wheel may be classified in a similar manner as the subjective distinction of noise by operation and interfering sound (Table 6.1). The same is true here: if the oscillations at the wheel correlate with the steering or driving manoeuvre deliberately initiated by the driver, then this is an artificial signal feedback. Subjectively, the driver of a sports car will even expect it as feedback from the road. The opposite is the steering wheel nibble (SWNs), resulting from rotations in the frequency range of 10–30 Hz at medium speed. The complete steering system of wheel, column, gear, wishbones and trailing arms including wheel guidance and tyres may vibrate. The rotary oscillation in the wheel that can be amplified by resonance excitation is perceived as extremely annoying and makes the driver feel unsafe. The amplitudes are limited by the system damping and the friction of the wheels on the road. On account of low amplitudes in the wheel there is neither an interference with the steering behaviour nor are the oscillations relevant for safety. Any SWNs, however, are immediately

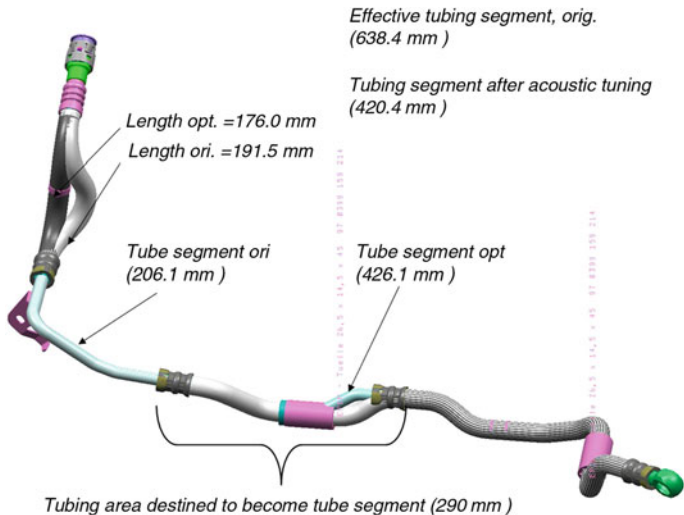


**Fig. 6.11** Optimisation of a fuel return line to avoid (hydraulic) steering chatter and rattle

reported to the customer service and can produce high warranty costs for the manufacturers. Two different SWN phenomena are distinguished by driving cycle:

- The free rolling SWNs develop from imperfections of the wheel at loadless straight driving. Its causes are dynamically alternating forces from imbalances, tyre force fluctuations or wheel eccentricity.
- The braking-excited SWNs develop during braking at medium speed, due to thickness variations of the brake disk. They produce an oscillating braking torque at the wheels and excite the wheel to a rotary vibration, transferred by the steering kinematics.

Lateral movements need to be eliminated before measuring rotary oscillations. A phase-related difference measurement by means of two tangentially arranged acceleration sensors is used (Fig. 6.12).

The acceleration amplitude of the rotary oscillations  $a_{SWN}$  derives from the absolute value of the complex vector sum according to

$$a_{LDS.} = \left| \frac{\vec{a}_1 - \vec{a}_2}{2} \right| \quad (\text{m/s}^2) \quad (6.4)$$

The phase position of the tyres has a major influence on the SWN amplitudes. There may be amplitudes up to  $5 \text{ m/s}^2$  (Fig. 6.13). Their cause is the kinematic and elasto-kinematic design of the steering geometry that transforms the gear ratio from the wheel to the steering wheel.

**Fig. 6.12** Sensor array to measure the rotary oscillation amplitude SWN

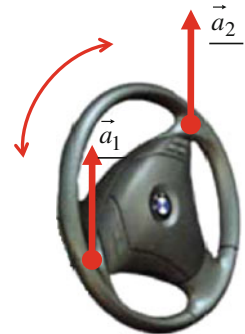
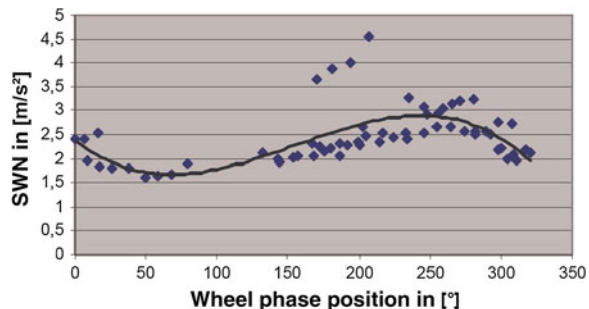


**Fig. 6.13** SWN as a function of the wheel phase position at a brake pressure of 10 bar  
Source Nowicki et al. (2005)



SWNs are avoided by suitably tuning the system components and their kinematic relations. The prime motivation is to avoid a match of the excitation frequency and the system's natural frequency at medium speed. When the system-immanent resonance is traversed outside of this operation cycle, there must be enough damping in the steering. Some steerings allow to vary damping and natural frequency by differently stiff wishbones. Figure 6.14 shows the amplifying function over the excitation frequency for different wishbone versions.

### 6.3 Structure-Borne Sound Transmission in Hoses and Cables

The acoustic description of material properties of limp components is mostly used for hydraulic stretch tubings of the power-assist and the loading condition of the pressure pulse transmission. In addition to this hydro-acoustic perspective, the following chapter discusses only the structure-borne sound transmission of limp flexible tubings. Beside the natural noise of the pump, a structure-borne sound

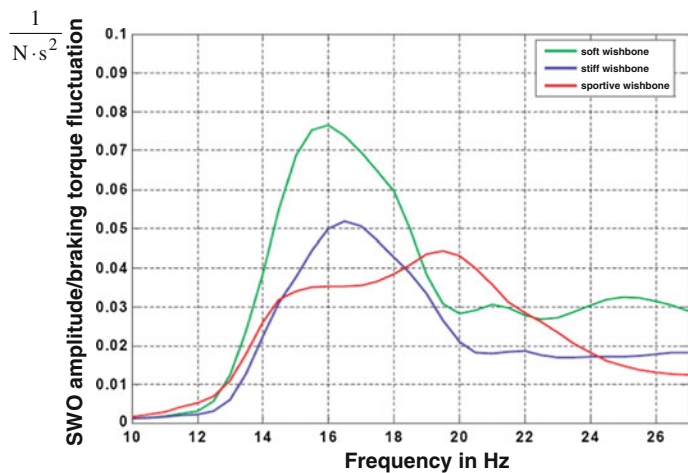


**Fig. 6.14** Transmission function of the braking torque fluctuation for differently stiff wishbones; *Source* Nowicki et al. (2005)

emission of the engine orders will occur if the pump is fastened to the engine, this sound is transmitted to the car structure by the high-pressure flexible tubing.

### 6.3.1 Superposition of Structure-Borne Sound Waves

The structure-borne sound wave transmission is an overlay of the dominant modes of the dilational, torsion and bending waves (Fig. 6.15).

Particular technical interest is devoted to the dilational wave. This quasi-longitudinal wave imposes a strain on the material elasticities in longitudinal, radial and tangential direction along the tubing, on account of its radial contraction. An insulating design of hoses may dampen the noise by as much as 40 dB—a far from negligible secondary sound path in the overall car acoustics.

### 6.3.2 Acoustically Acting Material Parameters

The elasticity of the tubing wall decisively influences the structure-borne sound-wave speed and its damping. The design of dimension and layout and the complex modulus of elasticity

$$\underline{E} = E + iE\eta \quad (6.5)$$

are important acoustic characteristics of the material.

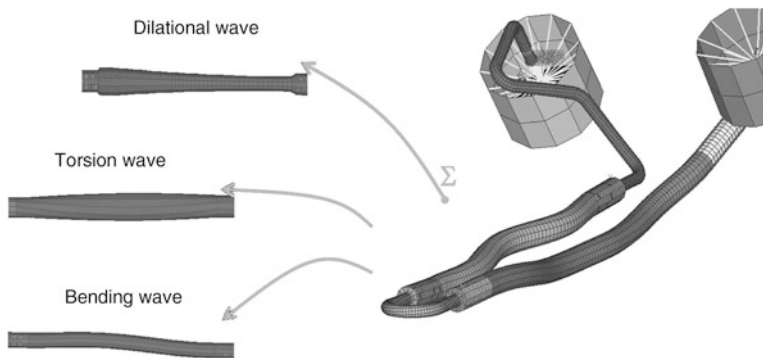


**Fig. 6.15** Dominant overlaid wave forms

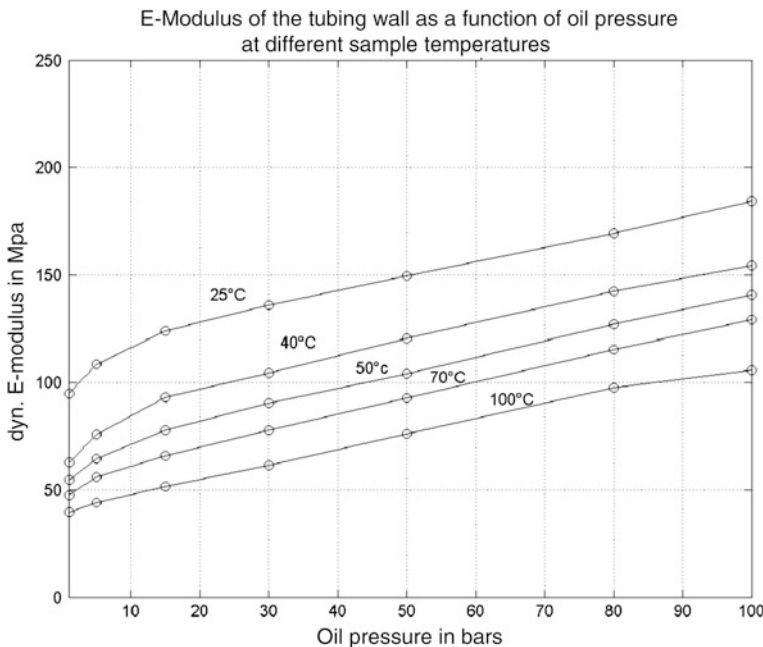


**Fig. 6.16** Dynamic modulus of elasticity of an oil pressure tube

High-pressure tubing is isotropic up to an oil pressure of 30 bars. Only at higher pressure will the modulus of elasticity become increasingly dependent on orientation and position. The radial and tangential E-modulus are coupled via the oil only for the dilatational wave. A linear relation between the modulus of elasticity at medium oil pressure and the material temperature is assumed (Fig. 6.16).

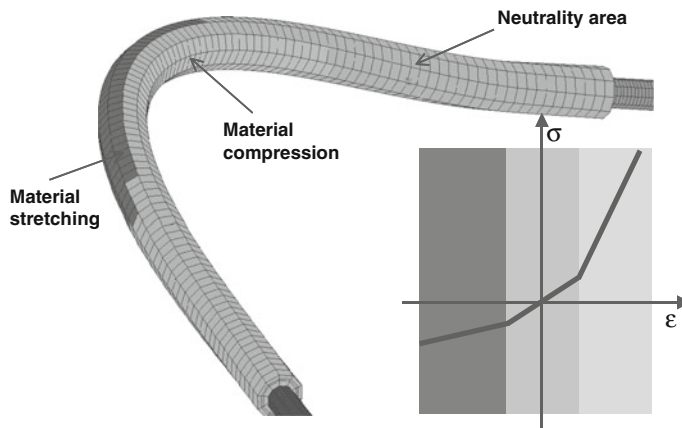


**Fig. 6.17** Stress pattern in a bent tubing

### 6.3.3 Reduction of the Noise Transmission by Bending

Flexible tubing is also used to compensate angular discontinuities, height differences or engine movements between two components. For bent mounting, the outer perimeter of the neutral fibre is exposed to a tear (material stretching) and the inner perimeter to compressive stress (material compression). This ‘trielastic’ behaviour increases the E-modulus acting at the tubing wall (Fig. 6.17).

The result is a rise of the wave speed at shrinking bending radii, proportionally raising the natural frequencies of the standing structure-borne soundwaves (Fig. 6.18).

The dilatational wave speed is empirically described by 6.6. The coefficient  $a$ , the exponent  $k$  and the dilatational wave speed  $c_{DW0}$  are determined by testing on a tube test bench.

$$c_{DW}(R) = \sqrt{c_{DW,\infty}^2 + \left( \frac{a \cdot c_{DW,0}}{\left( \frac{R}{R_0} \right)} \right)^2} \quad (6.6)$$

$$c_{DW,\infty} = \lim_{R \rightarrow \infty} c_{DW}(R) \quad (6.7)$$

$$c_{DW,0} = 1 \text{ m/s}, R_0 = 1 \text{ m} \quad (6.8)$$

Longitudinal excitation triggers a lateral force that becomes effective with increasing bending radius, on account of the bending angle. The curve of the lateral force initiates a bending torque triggering the bending waves. Correspondingly, lateral excitation triggers torsion waves.

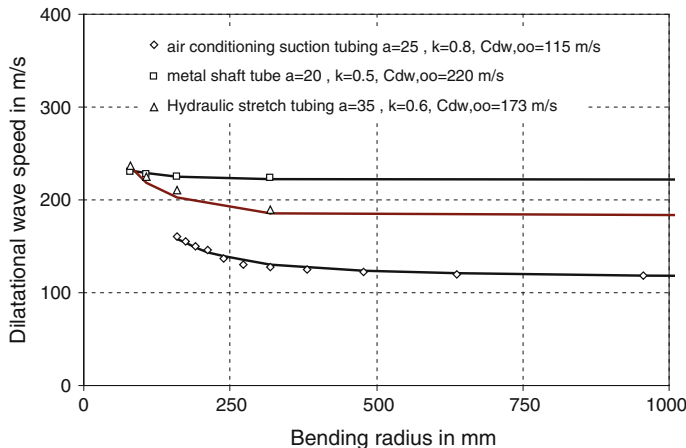


**Fig. 6.18** Influence of bent flexible or metal shaft tubings on the dilatational wave speed

## 6.4 Steering Column and Wheel—Design of Vibrations

The last important link of the steering chain, the steering wheel, is a kind of indicator for vibrations in the driver's hands. This chapter describes the design of the steering and its components to meet the high demand for comfort, including diminishing oscillations of the wheel, that are generated by vertical and lateral vibrations of the steering column. Any oscillations of the steering wheel from excitations by the car or the road from idling up to  $v_{\max}$  of the car are minimised. Figure 6.19 indicates that the body is excited by engine movements via its bearings or by wheel imbalances or potholes via the front and rear mountings. The car cross beam, a structuring component that bears the compartment, and the steering column transfer the vibrations to the steering wheel.

### 6.4.1 Design Strategy

The following facts need to be observed when designing the vibrations of compartment parts that are going to be integrated into the body, like car cross beam, steering column, steering wheel, air-conditioning etc.:

- Avoid superimposing frequencies of the main components by generating a mode map.
- Set target frequencies for components in the car.

The design strategy has to pay particular attention to the steering column and steering wheel.

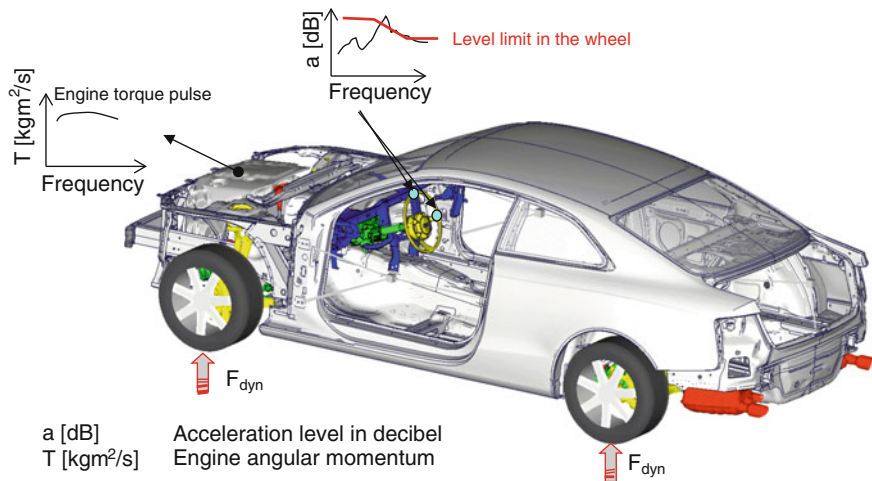


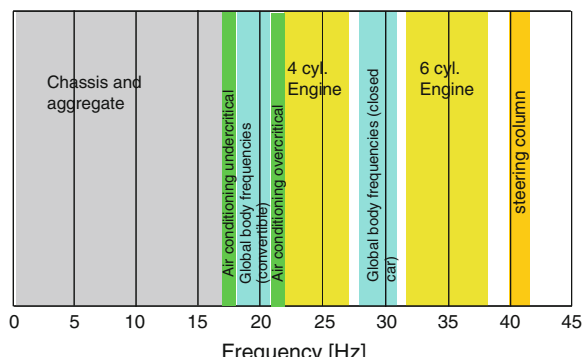
**Fig. 6.19** Excitation by road or car

Some premium manufacturers aim for supercritical natural frequencies of the steering column, i.e. the excitation frequencies at idle running and any possible wheel imbalance at maximum speed are less than the eigen frequency (natural frequency) of the steering column, avoiding superimposition and resonance. A high structural stiffness of the components helps to keep vibration levels at the steering wheel low. The possibility to absorb vibrations of critical engine/gearbox combinations by an ev. absorber mass acting inside the wheel is available, see Sect. 6.4.5 for details.

Other car manufacturers prefer an undercritical steering column that passes its structural eigen frequency when the engine is started. In most cases this requires an ev. absorber in the steering wheel.

Figure 6.20 represents a mode-map for the popular 4 and 6 cylinder engines, showing an eigen frequency of the steering column of  $\geq 40$  Hz that is overcritically designed with regard to the idling speed.

**Fig. 6.20** Mode-map to place the eigen frequencies of components in the car



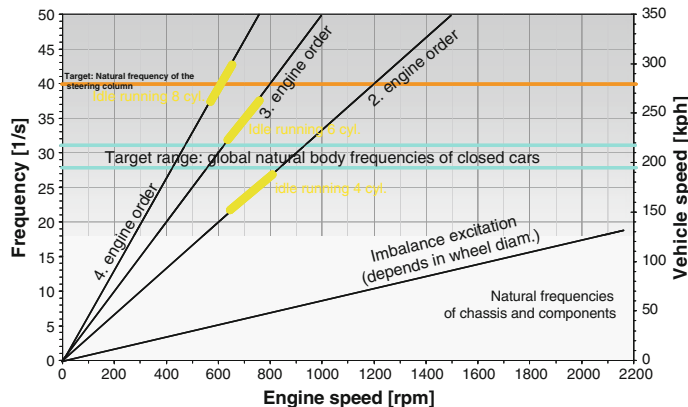


**Fig. 6.21** Engine speed over excitation frequency and speed

Once the natural frequencies of the single components are known, they can be implemented in the car in such a way that no unfavourable superimpositions, that would cause the steering wheel to oscillate, can appear. Mode-maps help to arrange the single components and their desired eigen frequencies in the car.

For example, the compartment module strategy of some manufacturers who implement the whole compartment as a single module allows for ways to install the air-conditioning with an eigen frequency of approx. 15–22 Hz. The global body modes of a convertible are typically found in this frequency range as well. A torsional excitation of the body can provoke the air-conditioning to resonate, raising the levels and causing perceptible vibrations of the wheel in this frequency range. It is desirable to place the air-conditioning either supercritically or undercritically to the global torsion eigen frequency of a convertible.

8-cylinder diesel engines are exciting at the 4th engine order. Their idling speeds are at about 620 rpm, which is higher than those of petrol engines, therefore the eigen frequency of the steering column of 40 Hz is no longer higher than the excitation frequency of idle running. These engines often require a wheel absorber.

Figure 6.21 shows the range of the excitation frequency for 4-, 6- or 8-cylinder engines at idle running, including the corresponding engine order, and the wheel imbalance excitation over speed.

#### 6.4.2 Target Eigen Frequencies of Components and Car

This chapter discusses target eigen frequencies of components for supercritically designed steering columns with a eigen frequency  $\geq 40$  Hz and no wheel absorber. Figure 6.22 shows all immediately involved structural components of a compartment which are essential to reach the eigen frequency of the steering column.

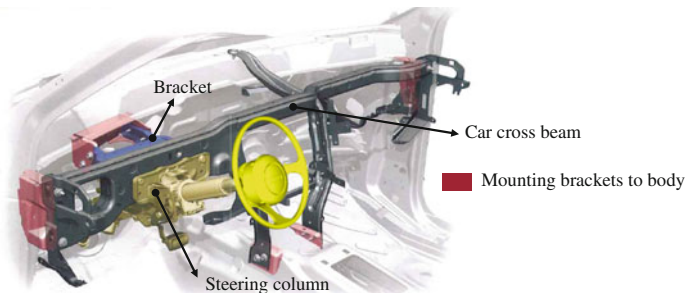


**Fig. 6.22** Structural components relevant for the eigen frequency of the steering column including connection sites

These are the car cross beam, also called instrument panel support or compartment cross beam, as well as the following components: steering column, mount, steering wheel and body, including their local mounting brackets.

Except for the body, all these components are developed by ancillary companies, together with the car manufacturer (Hintersteiner et al. 2008). A steering column manufacturer will discuss the requirements for the eigen frequency of a steering column in Sect. 10.3.4. The target frequencies for components and sub-components, some of which are shown in Fig. 6.23, can be gained from benchmark examinations with a huge number of eigen frequency measurements at steering columns and their rigid mounts, supported by finite elements models.

Measurement series reveal that the eigen frequency of the steering column of benchmark cars will drop in comparison to the eigen frequency of the steering column in the rigid mount by about 10 Hz (see also Sect. 10.3.4). Half of this drop is due to the elasticity of the car cross beam and the other half to the influence of the body, including its local stiffness at the corresponding screw connection places towards the car cross beam. This distinction was supported by a huge number of calculation results.

The construction states System level and Subsystem level, shown in Fig. 6.23, apply a steering wheel substitute mass (test disk) to achieve a standardisation in the early project phase. This reduces logistics and development times for the suppliers of steering column and car cross beam. Knowing the influence of an actual steering wheel on the respective construction state is of great importance for the understanding of the eigen frequencies and the corresponding objective. Applying a steering wheel instead of the much stiffer substitute mass in the subsystem level helps to measure or compute much lower eigen frequencies.

The manufacturers facilitate reaching the target frequency by determining the local static and dynamic body stiffness at the screwing places of the body consoles shown in Fig. 6.22 and by comparing them with target values (Hintersteiner 2008).

	Assembling condition	Frequency target
	Vehicle level (trimmed body)	40 Hz
	System level (cockpit)	47 Hz on rigid mount
	Subsystem level (steering column)	50 Hz on rigid mount
	Components level (steering wheel)	80 Hz on rigid mount

Fig. 6.23 Components and subcomponents with target eigen frequencies (Hintersteiner 2008)

### 6.4.3 Calculation Models and Load Cases

Calculation models supporting construction and finite elements models (FEM) of the trimmed body and the full car are shown in Fig. 6.24. The Trimmed body FEM represents a body fully equipped with component masses but without the components Chassis, Wheels, Engine, Gearbox and Exhaust system.

In the early development stage, the Full car FEM is approximated by a Trimmed body FEM to test the components developed in collaboration with suppliers—such as, for example, steering column, steering wheel and car cross beam—to see whether the specifications were met with regard to the eigen frequency of the steering column. The Full car FEM allows to analyse the additional modes of aggregate and chassis and to minimise the vibration levels relative to calculation variants.

Eight loading conditions are used to assess the eigen frequency of the steering column in the car. The loading condition “Driving Point Response” (inertance) serves merely to find the position of the eigen frequency of the steering column. An equivalent measurement is carried out by hitting a pulse hammer vertically and laterally on the steering wheel rim.

The loading condition “Frequency Response” is used to assess the transmission behaviour. This allows for the analysis of the vertical and lateral acceleration response of the steering wheel up to 50 Hz by relative comparison of calculation variants. An equivalent measurement is carried out with electric-dynamic shakers or a 4 axis hydropulse test rig.

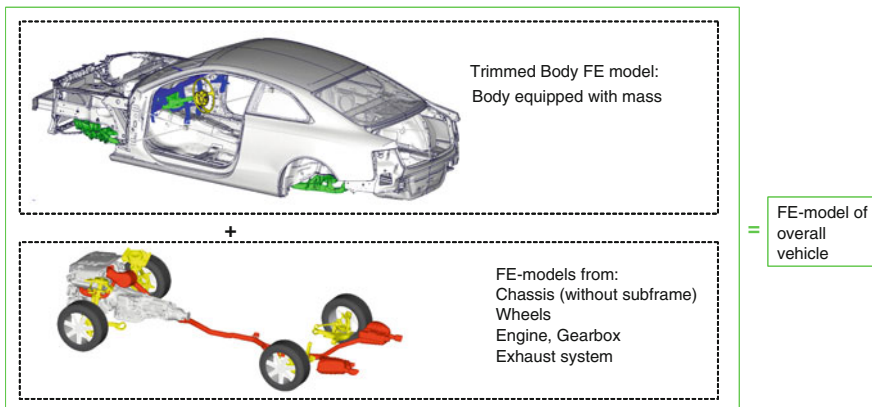


**Fig. 6.24** Finite element models of the trimmed body and the full car

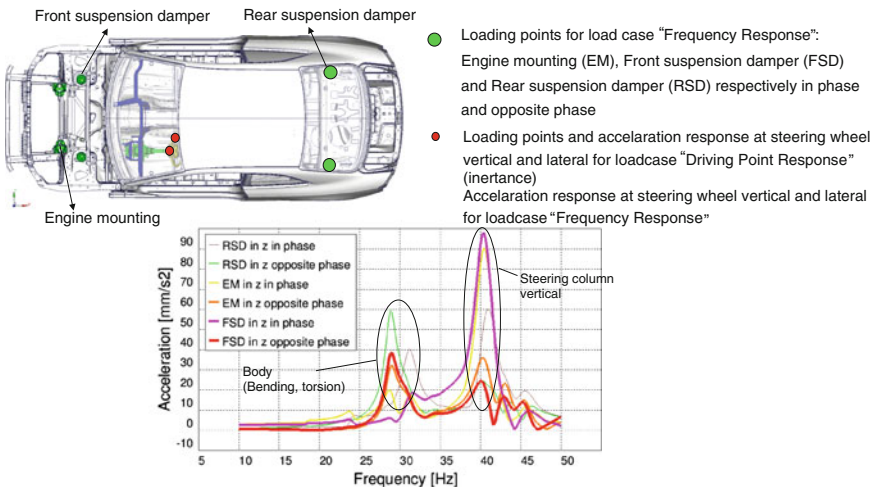


**Fig. 6.25** Standard load cases to assess the eigen frequency of the steering column and the transmission behaviour, with calculated result of the load case "Frequency Response"

Figure 6.25 shows a result of the load case "Frequency Response". A dynamic standard force of 1 N is excited, both in-phase and opposite phase, at the left and right engine mounts, the rear- and the front suspension dampers. The curves show the vertical acceleration response of the steering wheel in ( $\text{mm}/\text{s}^2$ ). The acceleration levels in (dB) were evaluated to compare arithmetic variants. Similar curves are plotted and analysed for the lateral acceleration levels at the steering wheel.

**Table 6.3** Effects of steering column parameters on the on-board eigen frequency

Steering column parameter	Eigen frequency of the steering column in the car after on-board eigen frequency of the steering column
Mass of the steering column	-0.15 Hz/kg
Steering column position (length adaptation)	-0.8 Hz/10 mm

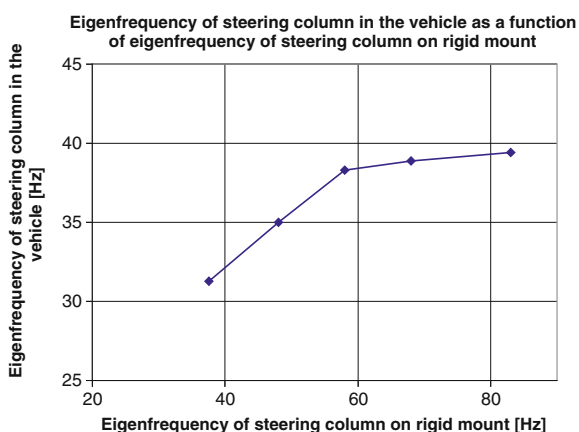
#### 6.4.4 Parameter Studies

This chapter discusses arithmetically the effect of different parameters of the steering columns and steering wheels on the on-board eigen frequency of the steering column. Target on-board eigen frequencies of the steering column apply to the extreme case, i.e. the steering column is fully extended. The height of steering columns can be adjusted, beginning at the central position, by about  $\pm 30$  mm along the column and by about  $\pm 25$  mm crosswise. When its eigen frequency is measured, the 4 end positions are evaluated by arithmetic models: both fully extended and for the height which represents the lowest natural frequency value (extreme case, depends on construction). Table 6.3 lists the effects of the column position and the total mass of a steering column on the on-board eigen frequency of the steering column.

Figure 6.26 shows the on-board eigen frequency (vehicle level) as a function of the eigen frequency of the steering column in the rigid mount (subsystem level). This curve, gained for a specific arrangement of car cross beam and body, shows that the on-board eigen frequency is saturated at an eigen frequency in the rigid mount of about 57 Hz. Higher frequencies in the rigid mount are not efficient any more, so that the car cross beam and the body in white consoles have to be stiffened to realise a 40 Hz steering column on-board.

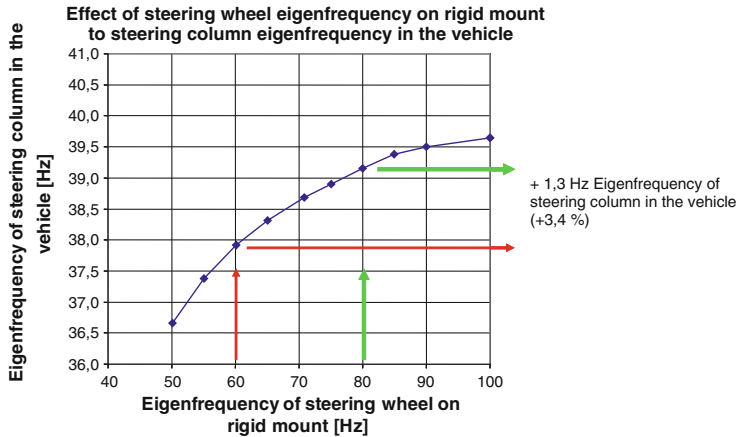
Table 6.4 shows the effect of the steering wheel parameter mass on the vertical on-board eigen frequency.

**Fig. 6.26** Vertical dynamic natural frequency of the steering column on-board as a function of the natural frequency of the steering column in the rigid mount



**Table 6.4** Effect of the steering wheel parameter mass on the *vertical* on-board eigen frequency

Steering wheel parameters	Effect on the natural on-board frequency
Mass of the air bag	-0.4 Hz/100 g
Mass at the steering wheel rim	-0.7 Hz/100 g

**Fig. 6.27** Influence of the eigen frequency of the steering wheel in the rigid mount on the on-board eigen frequency of the steering column

The mass of the steering wheel rim itself and the mass spread on it, such as foam surrounding, rim heating and rocker switches, are very sensitive to the on-board eigen frequency at 0.7 Hz/100 g.

Figure 6.27 shows the influence of another steering wheel parameter, the stiffness of the steering wheel in the rigid mount (component level), on the on-board eigen frequency of the steering column. It is raised by 1.3 Hz when the eigen frequency of the steering wheel in the rigid mount is increased from 60 to 80 Hz. Above 90 Hz, the curve levels so much that the on-board eigen frequency of the steering column cannot be increased much further.

#### 6.4.5 Steering Wheel Absorbers

As discussed in Sect. 6.4.1, steering wheel absorbers can be used to absorb vibrations in cars with critical engine/gearbox combinations. Diesel engine and/or automatic gearbox vehicles may optionally have a steering wheel absorber inserted for a supercritically designed steering column as well. Possible reasons are the high indicated pressure in diesel engines and the direct connection to the automatic

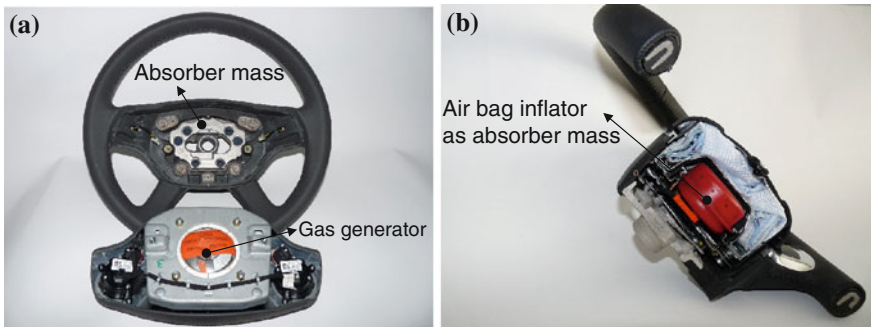


**Fig. 6.28** Potential vibration absorbers in the wheel: **a** additional mass, **b** gas generator of the airbag

gearbox, set on Drive position when the car is at rest and the brake pedal is pushed. This may cause vibrations at the steering wheel.

Figure 6.28 shows two steering wheels by different manufacturers with integrated absorbers. A conventional steering wheel absorber with an additional mass of 440 g is applied in Fig. 6.28a, the steering wheel in Fig. 6.28b applies the gas generator of the air bag as a 400 g absorber so that no additional mass is required.

The gas generator in Fig. 6.28b is elastically mounted on a radially implemented elastomer, as opposed to steering wheels without absorber function where it is screwed in rigidly. The absorber mass in Fig. 6.28a is fixed to the floor of the steering wheel rim by four cylindrical or prismatic elastomer pins.

The tuning of a steering wheel absorber in the full car is controlled by different measurement series during development. Absorber eigen frequencies of 24–36 Hz are measured at typical steering wheel sets. One compares the acceleration response of the steering wheel rim in vertical (“12 o’clock”, normal to the steering column axis) and lateral direction (“3 o’clock”, transverse to the car), for engine idle running and for excitation on a 4 axis hydropulse test rig, both in-phase (bending excitation) and opposite phase (torsion excitation), with the steering column either retracted or extended. Figure 6.29 shows the results of such a measurement series with an extended column.

These measurement series allow the recommendation of an absorber eigen frequency of 32 or 34 Hz. The level reduction at the steering wheel rim of approx. 5–10 dB, shown in Fig. 6.30, requires a 34 Hz steering wheel absorber according to the analysis of a full car simulation.

Acceleration levels at the steering wheel can be reduced by approx. 10 dB when applying a steering wheel absorber during idle running and driving, because of the excitation about the axes. Vibrations at the steering wheel may be visibly and, for the passenger, subjectively perceptibly reduced.

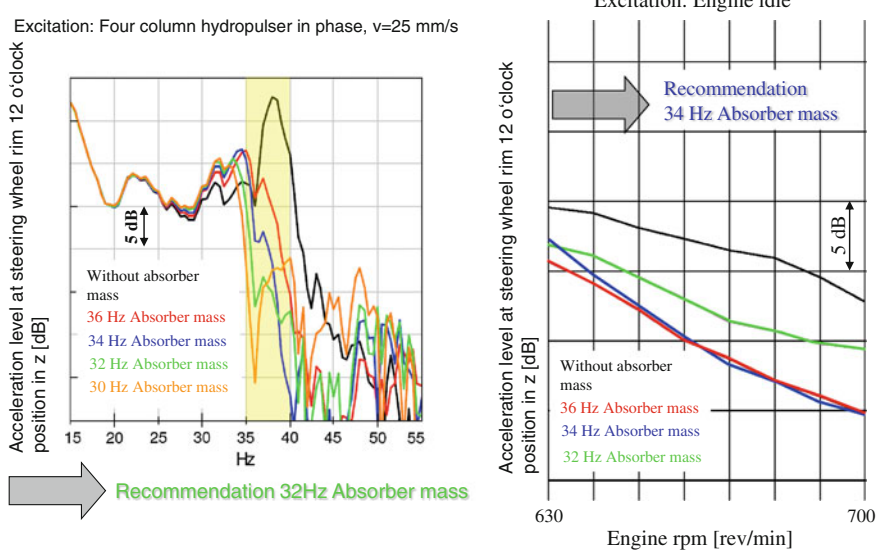
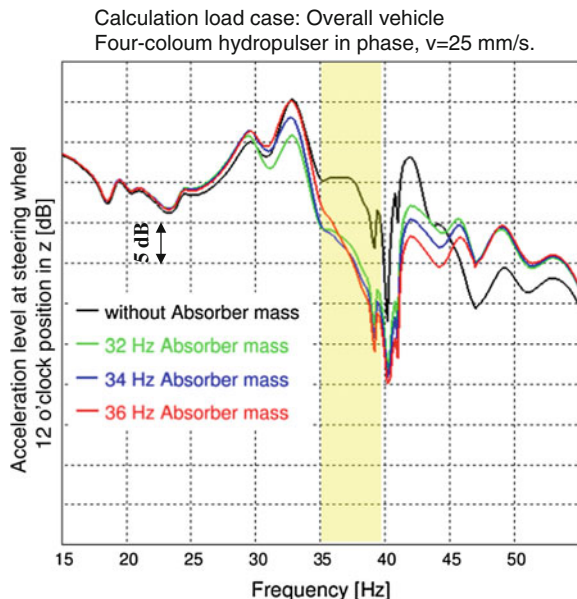


**Fig. 6.29** Measured levels at the steering wheel rim in *vertical direction* without absorber and with different absorber eigen frequencies

**Fig. 6.30** Computed levels at the steering wheel rim, *vertical direction*, without absorber and with different absorber eigen frequencies



## 6.5 Conclusion

The design of steering column and steering wheel, the car cross beam and the body with the screw consoles towards the compartment module is an important task with regard to the vibrations in a car. Persistent contact with the steering wheel allows the driver to feel the vibrations there.

Concerning idle running and road excitation, the design of the on-board steering column allows its eigen frequency to be designed either supercritically or undercritically. To avoid excitation of the steering column by components in the compartment, such as the air-conditioning, a mode map is used to distinguish eigen frequencies of the components and excitation frequencies.

Besides the global target eigen frequencies of the bodies loaded with mass, that were defined during development, targets for the local mounting stiffness at the body consoles screwed at the car cross beam of a compartment, need to be defined.

If there are still complaints about vibrating steering wheels from test drives, a steering wheel absorber to reduce these vibrations (amplitudes) for critical engine/gearbox combinations can be applied.

Target eigen frequencies are defined for the ancillary companies of components like steering wheel, steering column or car cross beam. These targets derive from a huge number of measurement series and analysed simulations. A steering wheel substitute mass serves the manufacturers of steering columns and car cross beams as a tool of standardisation.

Stable and non-vibrating driving is made available for all car drivers in any driving condition by the structural design of the components, as described in this chapter, that are relevant for steering wheel vibrations (steering wheel, steering column, car cross beam and body).

## References

- Hintersteiner R (2008) Steering wheel vibrations—from the requirements in the vehicle to the requirements of the individual components. *Steering Tech*, Munich
- Hintersteiner R et al. (2008) Funktionale Auslegung der Karosserie. Der neue Audi Q5, ATZ special edition
- Nowicki D, Bestle D, Strasser G (2005) Symposium Reifen Fahrbahn der TU Wien

# **Chapter 7**

## **Steering-Feel, Interaction Between Driver and Car**

**Manfred Harrer, Peter Pfeffer and Hans-Hermann Braess**

Steering-feel, from German *lenkgefühl*, is a driver's subjective sensation upon steering a vehicle. This steering-feel derives from the perception and assessment of steering behaviour and thus the drivability; it embodies the interaction between car and driver. The drivability generally consists of a vehicle's response to the driver's input, as well as external interferences, such as crosswind or uneven road surfaces. The steering behaviour is part of the overall drivability, and describes vehicle response to steering input as well as interferences. The optimization of the steering-feel is one of the main tasks in the development of driving dynamics. Quantitative assessments of handling, in particular the self-steering effect of passenger cars, had already begun in the late 1930s (Olley 1938). Yet, steering-feel was, and still is, almost always subjectively assessed and optimized exclusively by experienced test drivers. This is mainly due to the fact that the drivability and handling of a vehicle are so dependent on the steering-feel. The need for objective parameters with which to measure steering-feel has become increasingly important, especially with the growth of *digital prototypes*. Although some of these parameters have already been compiled, conflict still arises on the subject; on one hand, due to differences in philosophy concerning the construction and design, and on the other, due to ambiguous boundaries between *authentic* and *artificial* steering-feel, especially when considering driver-assist systems.

---

M. Harrer (✉)

Dr. Ing. h.c. F. Porsche AG, Porscheplatz 1 70435 Stuttgart, Germany  
e-mail: manfred.harrer@steeringhandbook.org

P. Pfeffer

Munich University of Applied Science, Munich, Germany  
e-mail: peter.pfeffer@steeringhandbook.org

Hans-HermannBraess

Ehemals BMW AG, Munich, Germany

This chapter will discuss the essentials of steering-feel. The basic relationship between command behaviours will also be explained. Furthermore, the specifics of a subjective assessment of *steering-feel* and of objective measurements of *steering behaviour* will be presented. Finally, parallels between the subjectively perceived steering-feel and objectively measured steering behaviour will be depicted.

## 7.1 Steering Behaviour and Steering-Feel

Unlike the dynamic driving behaviour of a vehicle at or near limit, which few drivers ever encounter, customers can easily experience steering-feel in the low-to-medium range of lateral acceleration every day. A chassis designed for agility combined with a precise steering system is the foundation for providing an intense driving experience. Good steering-feel requires the steering behaviour to be influenced by a balanced interaction between the torque and angle of the steering wheel, as well as the resulting degree of vehicle reaction.

Chassis development is vital to providing symbiotic drivability and steering behaviour. It takes the collaboration of a large number of experts with the knowledge and proper grasp of the driving experience to achieve a balanced calibration. Detailed subjective assessments and adjustments are the main focus of their work. Objective techniques for assessing the steering behaviour are used to actively support the subjective adjustment process.

The character of a car is fundamentally influenced by the steering behaviour and the corresponding steering-feel. The purpose is to develop a perfectly co-ordinated steering behaviour, marked by the equilibrium of driving safety, comfort and performance. Excellent driving ergonomics, intuitive handling and unambiguous response are also crucial.

A typical characteristic of the steering behaviour is a vehicle's response to cornering when influenced by lateral acceleration. This is where the driver can experience vehicle dynamics most clearly and emotionally. Cornering can be classified in three groups: The On-center area with initial steering input, a linear area of the driving dynamic including the increase of steering angle, and finally, the transition up to the limit. A linear function of steering angle and vehicle response up to high lateral accelerations is desirable, as well as a gentle but unmistakable indication when approaching the limit. The driver should be made aware of the approaching limit through a reduction of vehicle response, requiring a disproportional increase of steering angle input (understeer), as well as through a drop in steering torque.

The range of longitudinal and lateral acceleration in everyday driving situations is generally called the dynamic performance range, determined by driver, car and road. Figure 7.1 represents the relative frequency of different lateral acceleration values observed on different road types by a standard driver.

Note that during these standard driving conditions most lateral acceleration values fall under  $2 \text{ m/s}^2$ . Typical lateral acceleration values are lowest during

**Fig. 7.1** Lateral acceleration parts (standard driver)

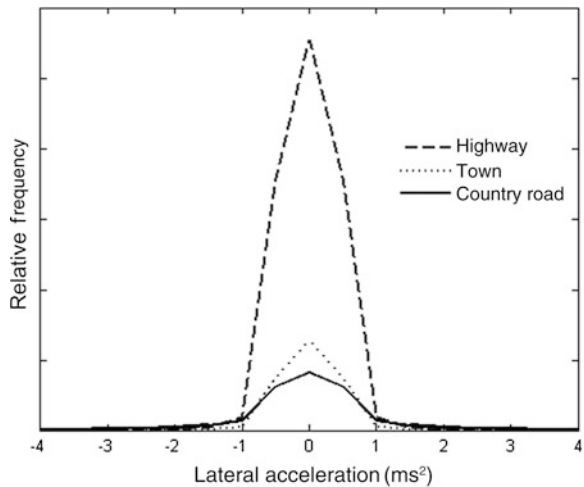
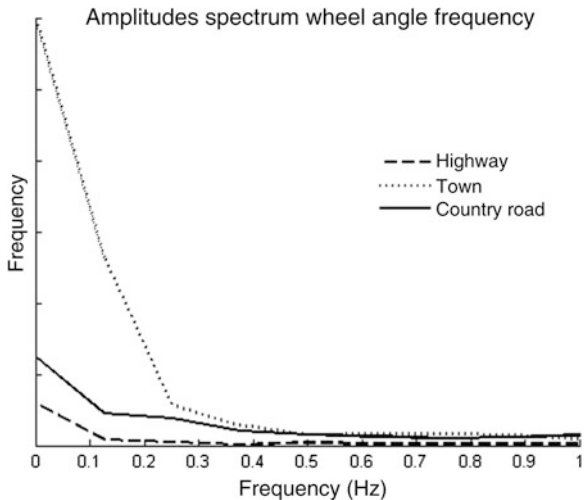


**Fig. 7.2** Frequencies of steering wheel angles (standard driver)



highway driving, followed by city driving. The driver determines this dynamic range, taking into account experience, risk, and demands for comfort, keeping in mind that the chassis has a far greater stability range in dry road conditions. This means that lateral acceleration ranges up to approx.  $4 \text{ m/s}^2$  are of particular interest when applied to the objectification of steering behaviour. This is the dynamic range that influences lower range dynamics in standard, daily driving.

It is evident from Fig. 7.2 that the frequency of any steering angle on different road surfaces lies far under 0.5 Hz. Extreme situations, such as sudden evasive maneuvers or double lane changes, produce much higher frequencies. For this reason, modern steering systems are designed and tested up to at least 3 Hz.

However, such high frequencies are rarely met in everyday situations of a standard driver. It is evident from this that steering-feel becomes particularly important in low frequency steering processes.

## 7.2 Steering-Feel

Steering-feel is a result of the direct interaction of driver and car through the steering wheel. The steering system fulfils two functions; as an actuator that the driver uses to initiate a change of direction, and as an important source of sensory information on driving condition and vehicle response. Steering-feel is the driver's subjective sensation of steering control, vehicle response, and haptic feedback. This also includes the driver's perception of the dynamic performance of the vehicle upon steering (steering behaviour). It can be defined as follows:

Steering-feel is the complete optical, kinesthetic, and haptic sensations of the driver while steering a car, resulting in a complex, subjective experience.

In many publications the concept of steering-feel is confused with steering behaviour, drivability, or handling; this will be avoided here. Nor can the steering-feel be psychologically interpreted as an emotion such as fear or joy (Wolf 2008). The course control from which the steering-feel develops can be visualized as a closed control circuit, known as the *driver/car control circuit* (Fig. 7.3), that describes this interaction. In order to optimize the stability and agility of the control circuit, the car must be able to adapt to the driver's skills. The quality of the steering system, the chassis, and the tires is essential here. Controlling the direction requires the driver to actively guide the car, taking into account the feedback of the driving state.

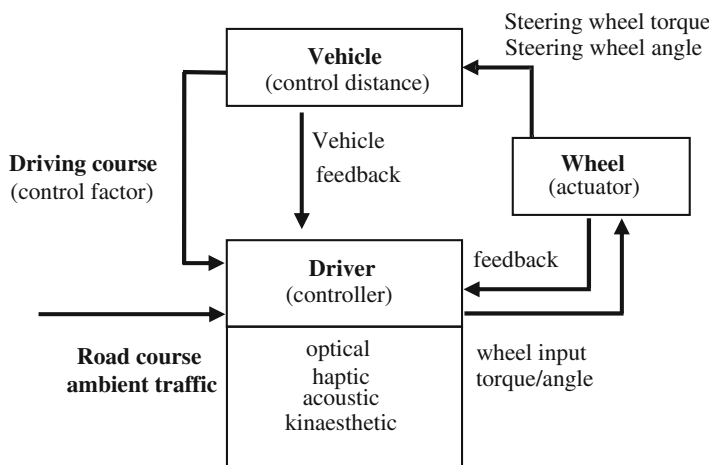


**Fig. 7.3** Driver/vehicle control circuit

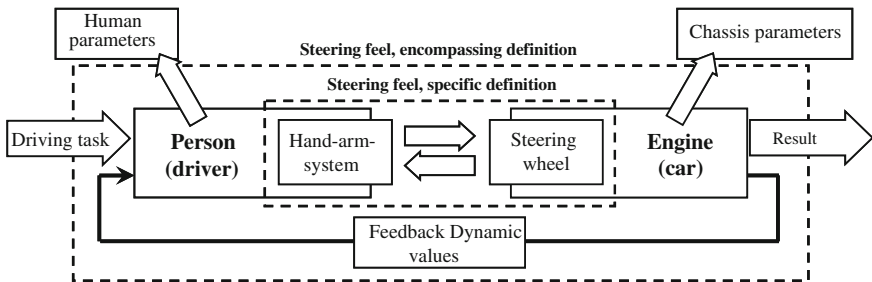


**Fig. 7.4** Steering feel in a specific and in an encompassing definition, Wolf (2008)

### 7.2.1 Guidance Behaviour

A good guidance behaviour is defined as the vehicle's tracking and road holding ability through an ideal steering effort from the driver. In other words, good guidance behaviour means that a deliberate change of direction through steering input must produce the expected result immediately, controllably, and regardless of speed. Naturally, these qualities must also apply under all loading, road, and weather conditions. The guidance behaviour and the resulting steering-feel may be distinguished as steering-feel in a specific and in an encompassing definition (Braess 2004) (Fig. 7.4).

In a narrow view, steering-feel predominantly concerns the given steering angle, the perceptible steering torque, and the relationship of each to speed. The main focus is on the haptic perception at the steering wheel.

A broader definition of Steering-feel considers not only the sensation through the steering wheel itself, but the total dynamic reaction of the vehicle to steering inputs. Besides the haptic feedback, the vehicle response is mostly perceived optically and kinesthetically.

Steering angle, torque, and a reliable drivability at high speed are important to achieve the desired steering behaviour and thus, the desired steering-feel over the entire speed range. Furthermore, it is important to avoid any obvious non-linear effects, for example around the steering midpoint, or a too narrow margin when transitioning into the possibly unstable limit areas of the vehicle.

### 7.2.2 Response Behaviour

The response behaviour is the ability to transmit information on changes in steering load, rolling resistance, or latitudinal and longitudinal forces through fluctuations in steering wheel torque. The response behaviour is divided into beneficial and interfering information, transmitted to the driver through the tire/wheel subsystems, front axle, steering gear, and ultimately, the steering column.

Beneficial information is, as the name suggests, beneficial when trying to implement a change in direction. One important example of this would be an unambiguous indication of the front wheel friction limit. In this case, a jump of the friction should alter the righting moment at the tire and influence the steering torque through the steering wheel.

Interfering information, such as a change of resistance at the wheels as a result of uneven road surfaces, produces an interfering torque about the steering axle, which is subsequently passed on to the driver via the steering column. These effects are desirable up to a certain level (by frequency and amplitude) to maintain some connection between driver and road. This behaviour should be more pronounced in sport cars than in vehicles designed for comfort which should deliver higher isolation from these interferences. Periodical interferences, like braking power fluctuations and wheel imbalance do not provide any useful information and should be suppressed as much as possible, or completely isolated so that driving is not affected (Groll 2006).

### 7.2.3 Requirements of Ideal Steering Behaviour and Steering-Feel

Optimal steering behaviour and the resulting steering-feel implies that a car must respond to steering input with an indiscernible delay and that the righting force at the steering wheel should be precisely distinguishable from the central steering position and rise steadily and noticeably to high lateral accelerations. A clearly distinctive center point is required for precise, linear driving, as well as an automatic steering return whose return speed adapts at the exit of the corner in order to prevent oversteer. A high dynamics setting for fast maneuvers is also required in combination with feedback on the driving and road conditions, without any impacts or oscillations transmitted through the steering wheel. Low wheel torques and angles are necessary for parking to fulfil the expectations of comfort.

These requirements can be summarized by the following prime targets:

- **Steering precision** by a distinctive *center-feeling*; instantaneous response to steering input; synchronous behaviour of steering angle input, steering torque increase, and vehicle response
- **Steering comfort** through steering wheel torque that is adapted to particular driving situations; low steering angle required for parking, cornering, and handling; automatic steering return with an adapted angular velocity of the steering wheel
- **Steering feedback** of driving state and road information in a balanced relationship with possible interfering variables
- **Steering dynamic** sufficient for quick maneuvering, for example, during a sudden evasive maneuver

To achieve the ideal steering behaviour, the quality and interaction of many subsystems such as tires, axle and elastic kinematics, roll stabilization and body rigidity, as well as the constraints, such as aerodynamics must all be considered.

### 7.3 Evaluation Methods for the Steering-Feel: Objectification

After this discussion of the requirements for an ideal steering-feel, possible assessment techniques will be now described. These techniques allow the subjective assessment results of steering-feel and the vehicle properties to be combined (Schimmel and Heißing 2009). ‘Objectification’ is understood as the assessment technique which turns subjective driving perceptions into objectively measurable characteristics or parameters.

#### *Characteristics-Based Correlation Analysis*

Characteristics-based correlation analysis is the most established technique and is already used in many publications. This technique facilitates the extraction of characteristics (objective parameters) from standardized maneuvers. Subjective ratings are mostly gained by experienced test drivers during separate assessment drives, using different rating systems. The recorded objective parameters are then compared to the subjective ratings by means of a correlation analysis, utilizing the experience of experts and publications. Typical results of this technique were published by Norman (1984), Dettki (2005), Harrer (2007), Zschocke (2009).

The advantage of this technique is the transparency and the ability for validation. However, the extra effort of gathering high-quality data and subjective ratings is a disadvantage.

#### *Vehicle Model Based Objectification*

Like the characteristics-based correlation analysis, the vehicle model based objectification uses a correlation analysis to link objective parameters with subjective ratings. However, the objective parameters are not gained from measurements at the car but rather from a car model directly used for correlation with the vehicle parameters. This car model is first populated with data from several driving maneuvers, which are also used to gain subjective ratings from the driver. Costly car measurements are avoided. The identification of the model requires more effort, however. Additionally it needs to be checked whether or not the model illustrates the drivability of the car extensively enough. This technique has been used in the publications of Kobetz (2004), Meyer-Tuve (2008), Schimmel and Heißing (2009).

### *Objectification of a Standard Driver*

Objectification of a standard driver does not require the identification of a car model, but of a driver model. This technique assumes that the driver's control matches the vehicle properties, compensating for possible deficits. The standard driver's identified parameters are then correlated with the subjective ratings from actual drivers. These tests can therefore be carried out in driving simulators and with non-standardized driving maneuvers as well, since the driver, rather than vehicle behaviour, is modelled. Evaluations applying these techniques were published by Henze (2004), Schimmel and Heißing (2009). According to Schimmel and Heißing (2009), the human driving performance can be only vaguely represented, preventing a specific analysis of the drivability and, hence, the car.

Some useful objective parameters of drivability and steering-feel have been obtained mostly with the help of the characteristics-based correlation analysis, in spite of certain shortcomings.

## 7.4 Subjective Evaluation of the Steering-Feel

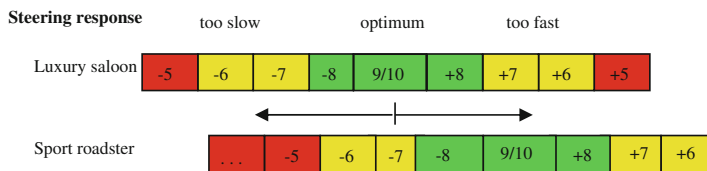
A subjective rating has been established in the car industry for the past decades, and has remained one of the most powerful instruments for assessing and tuning the drivability and steering behaviour of cars. However, the steering-feel is also subjectively assessed to gain data for further correlation analysis of objectification. The driver assumes the task of guiding the car and of observing it. Psychologically, a subjective rating always faces intraindividual (different conditions of one assessor) and interindividual variation (different conditions of various assessors). Constant driving conditions are, however, essential for a subjective rating of the steering qualities of automobiles. The steering qualities should be primarily assessed by experienced test engineers who have a distinctive feel for the OEM-typical drivability and are able to carry out maneuvers and ratings in a reproducible and reliable manner (Pfeffer and Schalz 2010).

Figure 7.7 shows essential rating criteria of the steering-feel. The previously mentioned qualities of an ideal steering behaviour, such as precision, comfort, feedback and dynamics, are represented by the individual rating criteria. The rating criteria are assessed by means of a rating system, the “10-point scale”, an established standard in the car industry. The objective is reached when 8 points were assigned to a rating criterion. 9 and 10 points are usually used only to assess especially outstanding handling features, i.e. when a rating criterion of a car clearly surpasses the established state-of-the-art, which generally is only achieved through more complex axle designs or chassis control systems. Figure 7.5 shows the described rating system.

A sufficient distinction of the subjective ratings is achieved when they are related to the vehicle class. It is understandable then, for example, that the highest rating of the response behaviour will require a much different vehicle response

	Classification	Rating	BI
Start of evaluation	Car corresponds to industrial standard	outstanding excellent very good good satisfying just enough	10 9 8 7 6 5
	Car below industrial standard	Not enough customer complaint stranded vehicle safety hazard	4 3 2 1

**Fig. 7.5** Assessment plan—rating index (Heissing and Brandl 2002)



**Fig. 7.6** Divergent optimum of different car classes

from a sedan than from a sports car. Figure 7.6 specifies the shift of the best rating as a function of the car class.

The individual rating criteria from Fig. 7.7 are assessed by point rating and critique, which provides additional information for every rating criterion as well as reasoning behind potential drops below the best rating.

The rating criteria from Fig. 7.7 will be explained in more detail in the following.

#### *Steering Wheel Torque Level When Parking*

A lower required steering wheel torque input is generally expected when parking, providing more comfort (less effort for the driver). The steering wheel torque should remain constant over the whole range of steering angles.

#### *Steering Wheel Torque Curve When Parking*

Here, it is assessed whether steering wheel torque oscillations are dependent on steering wheel angle. This phenomenon, known as torque ripple, can be caused by universal joint effects of the intermediate shaft.

Subjective Steering Feel Assessment					
Evaluator:		Driven distance:		Date:	/ /
Vehicle Type:		Reg. number:		Configuration num.:	
Steering Construction:		Method of Assistance:			
Tires:		Air Pressure:	bar (Front),	bar (Rear)	
		Load:	kg (Front),	kg (Rear)	
Remarks: _____					
Assessment Criteria		AI	SC		
optimal					
Parking	1 steering torque level 2 steering torque progression	<input type="checkbox"/>	too low undulated	<input type="checkbox"/> <input type="checkbox"/> <input checked="" type="checkbox"/> <input type="checkbox"/> <input type="checkbox"/>	too high
Steering torque on-centre	3 low speed (80km/h) +/- 15° 4 high speed (120km/h) +/- 10°	<input type="checkbox"/>	too low too low	<input type="checkbox"/> <input type="checkbox"/> <input checked="" type="checkbox"/> <input type="checkbox"/> <input type="checkbox"/>	too high too high
Steering torque off-centre	5 low speed (80km/h) +/- 50° 6 high speed (120km/h) +/- 30°	<input type="checkbox"/>	too flat too flat	<input type="checkbox"/> <input type="checkbox"/> <input checked="" type="checkbox"/> <input type="checkbox"/> <input type="checkbox"/>	too steep too steep
Holding torque during cornering	7 at 80-100 km/h	<input type="checkbox"/>	too low	<input type="checkbox"/> <input type="checkbox"/> <input checked="" type="checkbox"/> <input type="checkbox"/> <input type="checkbox"/>	too high
Centre feel	8 at 80 km/h < 5° 9 at 120 km/h < 5° 10 at 160 km/h < 5°	<input type="checkbox"/> <input type="checkbox"/> <input type="checkbox"/>	too weak too weak too weak	<input type="checkbox"/> <input type="checkbox"/> <input checked="" type="checkbox"/> <input type="checkbox"/> <input type="checkbox"/>	too strong too strong too strong
Steering friction	11 at 80-120km/h	<input type="checkbox"/>	too low	<input type="checkbox"/> <input type="checkbox"/> <input checked="" type="checkbox"/> <input type="checkbox"/> <input type="checkbox"/>	too high
Steering response	12 from the middle (80km/h) 13 under lateral acceleration.	<input type="checkbox"/> <input type="checkbox"/>	too slow too slow	<input type="checkbox"/> <input type="checkbox"/> <input checked="" type="checkbox"/> <input type="checkbox"/> <input type="checkbox"/>	too fast too fast
Straight-driving correction effort	14 at 80-120km/h			<input type="checkbox"/> <input type="checkbox"/> <input checked="" type="checkbox"/> <input type="checkbox"/> <input type="checkbox"/>	too high
Steering precision	15 at 80-120km/h	<input type="checkbox"/>	imprecise	<input type="checkbox"/> <input type="checkbox"/> <input checked="" type="checkbox"/>	
Feedback / Benefit	16 at 80-120km/h	<input type="checkbox"/>	Inadequate	<input type="checkbox"/> <input type="checkbox"/> <input checked="" type="checkbox"/> <input type="checkbox"/> <input type="checkbox"/>	pronounced
Feedback / Disturbance	17 on straight-ahead drive 18 under lateral acceleration	<input type="checkbox"/> <input type="checkbox"/>		<input type="checkbox"/> <input checked="" type="checkbox"/> <input type="checkbox"/> <input type="checkbox"/> <input type="checkbox"/>	excessive excessive
Steering angle demand	19 during parking 20 low speed (80km/h) 21 high speed (120km/h)	<input type="checkbox"/> <input type="checkbox"/> <input type="checkbox"/>	too small too small too small	<input type="checkbox"/> <input type="checkbox"/> <input checked="" type="checkbox"/> <input type="checkbox"/> <input type="checkbox"/>	too large too large too large
Steering returnability	22 on full lock	<input type="checkbox"/>	too slow	<input type="checkbox"/> <input type="checkbox"/> <input checked="" type="checkbox"/> <input type="checkbox"/> <input type="checkbox"/>	too fast
Remaining angle	23 from full lock 24 low speed (50km/h) 25 high speed (80km/h)	<input type="checkbox"/> <input type="checkbox"/> <input type="checkbox"/>		<input type="checkbox"/> <input type="checkbox"/> <input checked="" type="checkbox"/> <input type="checkbox"/> <input type="checkbox"/>	too large too large too large
Steering angular speed	26 during parking	<input type="checkbox"/>	Inadequate	<input type="checkbox"/> <input type="checkbox"/> <input checked="" type="checkbox"/>	

Fig. 7.7 Questionnaire for the subjective steering assessment (Harrer 2007)

### *Steering Wheel Torque at the Center*

Steering angle input out of straight driving may vary as a function of speed. The driving and holding force as a function of speed are rated for low lateral accelerations. A steering force is desired that has a tolerable level at any speed, giving the driver the feeling that the steering will always automatically center.

### *Center Feeling—Centering*

The centering of a straight driving car is rated. The car is stimulated by very small steering angle inputs to observe at which steering angles and torques the car will start to respond and whether the steering wheel (released) will fully right its initial position (straight driving). A perfect centering is desired that leaves no impression of backlash or hysteresis.

### *Steering Wheel Torque Curve*

The steering wheel torque level is assessed when cornering or through sinusoidal and random steering angle input. The torque curve as a function of the angle and the resulting vehicle response are rated. The steering wheel torque should slowly but steadily increase as a function of the lateral acceleration, until approaching the limit. An increasing torque as a function of speed supports the driver with direction changes as well.

### *Steering Wheel Torque When Cornering*

The steering wheel torque with constant-radius cornering is rated. The level of the torque should adapt to speed and lateral acceleration. A clearly perceptible anchor point that requires a noticeable increase of the steering wheel torque when steering under lateral acceleration should be present.

### *Response Properties upon Straight Driving*

Applying small steering wheel angles to straight driving serves to assess the proper structuring of the vehicle movements (yawing and lateral). The first period after the articulation is of special interest when the vehicle response develops and transitions into the semi-steady state driving. The angle inputs can be either sinusoidal or random. The goal is an ideal structuring of the vehicle response as a function of the steering wheel angle. No impression of elasticity, backlash, or large hysteresis should develop.

### *Response Properties under Lateral Acceleration*

When steadily cornering, the desired driving radius is widened or reduced by overlapping another steering wheel angle (positive/negative). The timing function of the subsequent vehicle response after application of steering angle and the further gain or fade of vehicle response (lateral or yawing) are all assessed as well. The first period after applying a steering angle is again of particular interest,

i.e. when the vehicle response is changing. The goal is an un-delayed proportional gain or fading of the vehicle response as a function of the steering wheel angle input. No impression of elasticity, backlash, or large hysteresis should develop, either.

### *Straight Driving*

Directional stability, impact sensitivity and the standard effort to hold course are assessed. Impact sensitivity refers to the impact of changing road resistance and side forces, as well as axle effects and aerodynamic influences at high speed. The objective is to develop high directional stability and, thus, course holding with little effort.

### *Accuracy*

The vehicle response, synchronous to the steering angle, and the effort to hold course during cornering are assessed over the full speed range. The objective is precise handling to follow the road easily and fluently, with little corrective effort.

### *Feedback of Useful and Interfering Information*

The communication of useful or interfering information through slight changes of steering wheel torque and angle is assessed. This haptic information is more or less pronounced depending on the car class (driver/road connection). Sports cars should give the driver as much information about the driving and road condition as possible. High-frequency oscillations of the steering wheel and impacts of all kind that might restrict the driver's control should be considered interfering information and suppressed as much as possible.

### *Steering Wheel Angle Demand During Parking*

The objective is to develop the lowest possible requirement for steering wheel angle during parking. Full steering-lock should be achieved with as few steering wheel rotations as possible.

### *Steering Wheel Angle Demand When Lane Changing*

The required steering wheel angle to achieve medium lateral acceleration should be low, according to car class.

### *Steering Return*

When turning, proper righting speed, steady return of the steering wheel, and small remaining angle (angular difference between central position and actual position of the steering wheel) is required.

### *Remaining Angle After Cornering*

The angular difference (final position after cornering and central position of the steering wheel) at different speeds is assessed when the steering wheel is released and cornering transitions into straight-line driving.

### *Steering Dynamics*

Torque peaks of the steering wheel or discontinuities of the power-assistance with sudden jerks of the wheel or sinusoidal steering are assessed. This effect is called catch up. The objective is to achieve a very high steering dynamic while maintaining constant power-assistance.

## **7.5 Objective Evaluation of the Steering Behaviour**

Recent car development has seen an increasing demand for clear and reproducible descriptions of drivability and steering behaviour of automobiles. The goal of objective car testing is to describe the handling and steering qualities independent of the driver and to gather parameters for objectification. A very large number of objective test processes have been published. Note that each of the mentioned maneuvers represents the steering and handling qualities of a car only in a specific driving condition. Only the inclusion of many different maneuvers will yield a complete image of the steering behaviour.

### **7.5.1 Measuring Equipment**

Measurements are established by applying defined steering angles and determining the motion of the vehicle. The steering angle may be applied either by a test driver or, preferably, by a steering machine—in particular during *Open-Loop* maneuvers.

Important parameters include steering angle and torque that can be recorded by the appropriate sensors in the steering wheel itself and/or the steering machine. The response variables, such as yaw speed and lateral acceleration, are recorded on a gyro-stabilized platform. In addition to the minimum extent of these measurements, specific variables of the steering system as, for example, the rack stroke or tie rod force are often determined as well. Table 7.1 gives an overview of the measurement systems to objectively evaluate the steering qualities of a car. The recommended accuracies are determined as well.

**Table 7.1** Measurement systems to record steering qualities

Sensor	Measured variable	Measuring range	Measuring accuracy
Measured wheel	Wheel angle	−500° to +500°	±0.1°
	Wheel torque	−15 to +15 Nm	±0.01 Nm
Optical distance laser	Rack path	−100 to +100 mm	±0.1 mm
DMS	Tie rod forces	−25 to +25 kN	±1 %
Correvit	Longitudinal speed	0–70 m/s	±0.01 m/s
	Lateral speed	−20 to +20 m/s	±0.01 m/s
Gyro-stabilised platform	Longitudinal acceleration	−25 to +25 m/s <sup>2</sup>	±0.01 m/s <sup>2</sup>
	Lateral acceleration		
	Vertical acceleration		
	Rolling angle	−90° to +90°	±0.1°
	Pitching angle	−90° to +90°	±0.1°
	Yawing angle	−180° to +180°	±0.1°
	Yaw speed	−300° to +300°/s	±0.1°/s

### 7.5.2 Driving Maneuvers

Driving maneuvers for objectively measuring the steering behaviour may be basically classified as *Closed-* and *Open-Loop* maneuvers. In a Closed-Loop maneuver, as, for example, a lane change, the driver assumes the control and observation of the car, operating and responding individually to fulfil the defined task. By contrast, during the Open-Loop maneuver, a steering angle is applied by the test driver or the steering machine regardless of the vehicle response. This is the only way to gain objective parameters that are independent of the driver. The following overview (Fig. 7.8) lists the recommended Open-Loop maneuvers to record the steering behaviour.

#### Weave Test

The weave test generates characteristics to assess the steering-feel and the steering precision around the central position. During this test, the steering angle oscillates sinusoidally with constant amplitude and frequency at a set vehicle speed. The lateral acceleration and yaw speed response variables are of particular interest, as well as steering torque and angle. A detailed test description is found in the ISO 13674-1 standard. The use of a steering machine with constant amplitudes and frequencies of the steering angle is recommended. The on-center steering behaviour may best be characterized by amplitudes between 2.5° and 10° and frequencies between 0.2 and 0.5 Hz.

#### Step Input Test

The step input test helps to characterize the transition from straight driving into constant-radius cornering. When driving straight, the car is brought into a circular path by applying a ramp-like input of the steering angle. The yaw speed and lateral

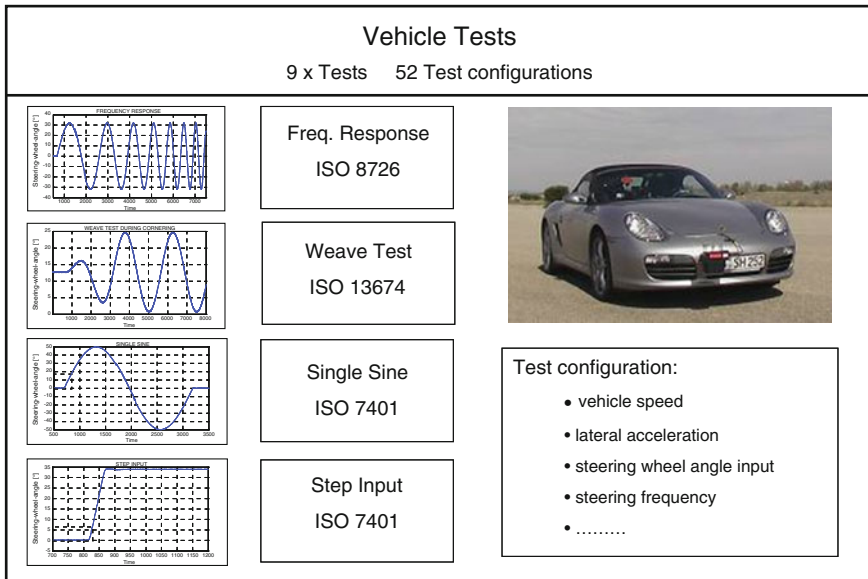


**Fig. 7.8** Objective vehicle tests

acceleration response variables, response times, and the achieved steady-state values are used for analysis. For a detailed test description and the prime rating criteria, see the ISO 7401 standard. According to these recommendations, the steering angle may be varied to achieve different steady lateral accelerations.

#### *Single Sine Test*

The purpose of the single sine test is to describe the transient drivability of the car by means of a sinusoidal steering angle input. This test is described in ISO/TR 8725. The steering angle input and the vehicle response of this test are based upon double lane changes. During this test, the steering angle input and the vehicle response variables are of special interest. The comparison of the highest absolute values of the angle-to-torque ratio and the vehicle response yields other important data to objectively describe the steering behaviour. As in the aforementioned tests, the input angle may be varied.

#### *Frequency Response Test*

The frequency response is measured to describe the transient behaviour in the frequency range. At a given speed, the car is prompted out of linear driving by a sinusoidal steering angle input. The steering frequency is continuously increased from approx. 0.1 Hz to approx. 3 Hz at constant amplitude. During this test, magnitude of vehicle response and any phase development as well as yaw speed and lateral acceleration as a function of the steering angle are of particular interest.

For the prime rating criteria, see ISO 7401. The steering angle may be varied to achieve different lateral acceleration values.

### ***7.5.3 Automated Data Processing***

The goal of dynamic measurements is the objective comparison of different cars or car configurations. Different maneuvers and variations of the test parameters such as angle amplitude, steering frequency, and vehicle speed are required for a full description of the drivability. In addition, each test must be measured several times for results to be reproducible. Hence, a test series often means the analysis of a massive set of measurements. For accurate evaluation of a measurement, various delays in the measurement sequence and the sensor positions must be considered. In addition, the data must be filtered as needed to correct the offset. Automated data processing is recommended on account of the massive amount and complexity of the tasks.

#### *Considering Delays*

The signals in the various measured variables shift due to implemented pre-filters as well as sensor and amplifier periods in the measurement sequence. In particular, the time difference between fast and slow measuring channels must be taken into consideration. These differences, especially with high-frequency steering angle inputs, must be considered to avoid distortion of the phase response. If the measuring data is used to validate simulation models, correction of the signal times is essential.

#### *Conversion to a Reference Point*

According to the ISO 15037-1 standard, the vehicle motion magnitudes should be converted to a reference point, independent of loading. The standard suggests that this reference point be centered in the wheelbase, at height of the center of gravity at standard dry weight. Since the sensors cannot usually be placed at this point, measurements are recorded at another measuring point. Conversion to the dedicated or a selected reference point allows the comparison between different cars.

### ***7.5.4 Objective Parameters***

Objective parameters are characteristics taken or computed from the measured and processed signals or simulations, such as amplitude values, gradients, delays, etc. Finding objective parameters is described in the following by means of the weave test. The adjustment of objective parameters in Open-Loop tests takes place in a similar manner.

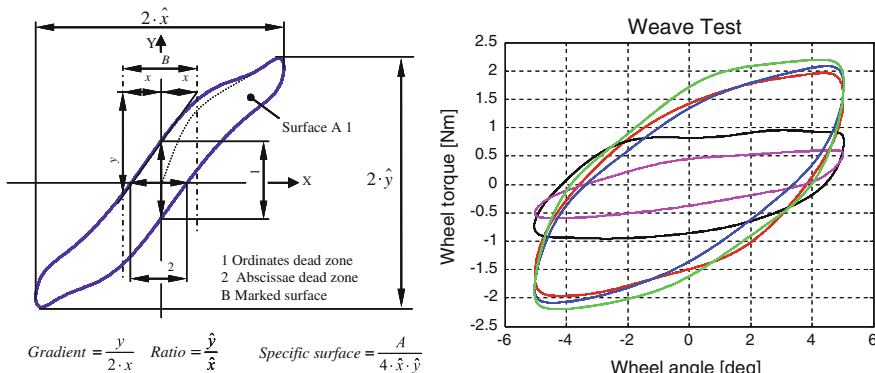


**Fig. 7.9** Objective parameters—example weave test at 0.25 Hz and 80 km/h

For an objective description of the On-Center steering qualities, the weave test is the most important. The goal is to achieve a steady-state driving condition during the application of constant, sinusoidal steering angles. Pairs of various measured variables are entered into a Cartesian coordinate system in order to compute objective parameters from steering angle, steering torque, lateral acceleration, etc. data with respect to time. Each pair of variables generates corresponding hysteresis curves from which objective parameters are derived (Fig. 7.9). Many objective parameters of the weave test are described in the ISO 13674 standard.

A validation of the measurement results requires a minimum number of repeated measurements to enable the assessment of the objective parameters with respect to distribution and variation. The distribution of an objective parameter is defined as its standard deviation from a mean value in a measurement series at identical conditions. The data is given in percent, where a small value of the distribution allows conclusions to be drawn on reproducibly measured parameters. Variable analysis helps to determine whether different test configurations differ significantly or only by accidental deviations. A variable analysis is essential for the statistical reliability of the objective parameters.

## 7.6 Correlation and Regression Analysis

Statistical techniques like correlation and regression analyses are needed to establish a connection between subjective ratings and computed objective parameters. The correlation analysis examines the connections between dependent and independent variables. Dependent variables of dynamic analyses are always subjective ratings. The independent variables are represented by objective parameters. The resulting correlation coefficient values show the statistical significance of the connection between dependent and independent variables.

Regression analysis additionally determines the connection between both variables by means of a mathematical function.

Easy correlation and regression analysis techniques have been useful to analyze the steering behaviour of cars in the linear range of driving dynamics. Here, the focus is on determining linear connections between subjective ratings and objective parameters. The requirements of a successful analysis are the compliance with various mathematical constraints (e.g., normal distribution of the sample size). Using the dummy variable technique, the above-mentioned correlation and regression methods can be extended to cover not only the analysis of single cars within a car class, but also of different cars across various classes. These regression models helped to establish that rating criteria relating to the steering torque level are independent of the respective car class (Harrer 2007). This means that the objective parameters concerned have nearly identical physical values for attaining ideal ratings in every car class. However, a rating criterion to describe the vehicle response on steering inputs is very much dependent on the respective car class. Attaining an ideal steering behaviour therefore requires different physical values of the objective parameters for each individual car segment.

## 7.7 Target Ranges for Ideal Steering Characteristics

Much effort has been invested into the objectification of drivability and steering behaviour. The weave test and the frequency response test are considered very significant for the objectification of the steering behaviour.

Table 7.2 gives value ranges for typical ideal steering behaviour during the weave test. The rating criteria and the proper objective parameters reveal a high correspondence throughout the mentioned publications. The rating criteria are explained in Sect. 7.4. The value ranges are distinct for sedans and sports cars, as long as a distinction of the car segment is feasible.

The frequency response test helps to determine the transmission of the yaw response on a corresponding steering angle input. This test primarily facilitates the assessment of the rating criteria Response power and Response properties over time at low-frequency steering angle inputs. An excerpt from the frequency response test is the Weir and DiMarco diagram (1978). It depicts the stationary yaw gain over the equivalent delay time. This delay time is computed by the frequency at which the phase response between yaw rate and steering angle corresponds to a phase angle of 45°. The following Weir and DiMarco diagram (Fig. 7.10) gives value ranges for currently built models.

This chapter has shown that there are already various objective target value ranges available to design steady or non-steady steering behaviour. Other qualities when, for example, approaching the limits of the driving dynamics, or the distinction of useful and interfering information, have not yet been established, however.

**Table 7.2** Weave test—collection of some value ranges for an ideal steering behaviour (Norman 1984; Dettki 2005; Harrer 2007; Zschocke 2009)

Rating criterion	Objective parameters	Value range for ideal steering behaviour
Wheel torque around the central position	Wheel torque gradient at a wheel angle = 0° Wheel torque at a lateral acceleration of 1 m/s <sup>2</sup>	From 0.3 to 0.5 Nm/° From 2.5 to 3.5 Nm
Centre point	Wheel torque gradient at a wheel angle = 0°	From 0.35 to 0.45 Nm/°
Steering friction around the central position	Wheel torque gradient at a lateral acceleration of 0 m/s <sup>2</sup> Hysteresis amplitude wheel torque at a wheel angle = 0°	From 2.5 to 3 Nm/(m/s <sup>2</sup> ) From 0.5 to 1.5 Nm
Required steer-angle during double lane change	Yaw rate at a wheel angle = 20°	Saloon: 0.30–0.32°/s Sports cars: 0.25–0.28°/s
Response (directness) from the central position	Yaw rate gradient at a wheel angle = 0°	Saloon: 0.20–0.30 1/s Sports cars: 0.30–0.35 1/s

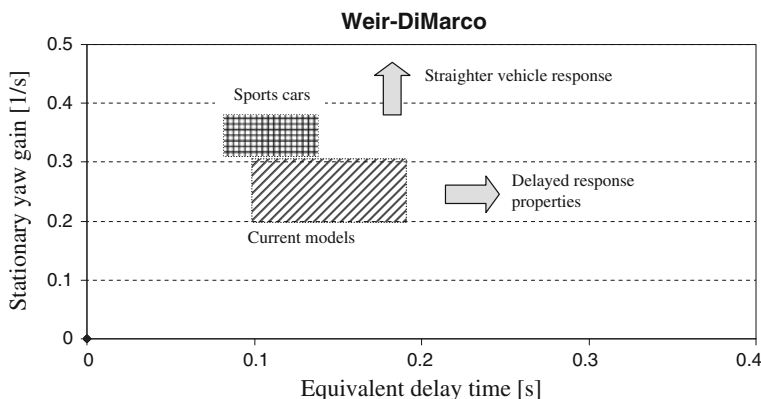


**Fig. 7.10** Weir and DiMarco diagram (modified)

## References

- Braess HH (2004) Die schwierige Übung des richtigen Kurses. Frankfurter Allgemeine Zeitung, 11 May 2004, Frankfurt am Main
- Dettki F (2005) Methoden zur objektiven Bewertung des Geradeauslaufs von Personenkraftwagen. Dissertation University, Faculty Mechanical Engineering, Stuttgart
- Groll von M (2006) Modifizierung von Nutz- und Störimformationen am Lenkrad durch elektromechanische Lenksysteme. Dissertation, University Duisburg-Essen
- Harrer M (2007) Characterisation of steering feel. Thesis, University of Bath, Department of Mechanical Engineering, Bath
- Heissing B, Brandl HJ (2002) Subjektive Beurteilung des Fahrverhaltens. Vogel Buchverlag, Würzburg

- Henze R (2004) Beurteilung von Fahrzeugen mit Hilfe eines Fahrermodells. Dissertation, Braunschweig, Universität (TU), (Schriftenreihe des Instituts für Fahrzeugtechnik, vol 7). Shaker Verlag, Aachen
- Kobetz C (2004) Modellbasierte Fahrdynamikanalyse durch ein an Fahrmanövern parameteridentifiziertes querdynamisches Simulationsmodell. Dissertation, Wien, Universität (TU). Shaker Verlag, Aachen
- Meyer-Tuve H (2008) Modellbasiertes Analysetool zur Bewertung der Fahrzeugquerdynamik anhand von objektiven Bewegungsgrößen. Dissertation, TU Munich
- Norman KD (1984) Objective evaluation of on-center handling performance. SAE Technical Paper 840069. Warrendale
- Olley M (1938) National influences on American passenger car design. In: Proceedings of the institution of automobile engineers, vol 32, pp 509–572 June 1938
- Pfeffer PE, Scholz H (2010) Present-day cars—subjective evaluation of steering feel. In: Proceedings of 1st international Munich chassis symposium, Munich, 8–9 June 2010
- Schimmel C, Heissing B (2009) Fahrerbasierte Objektivierung subjektiver Fahreindrücke. In: Tagungsband: Subjektive Fahreindrücke sichtbar machen IV, Haus der Technik, Expert Verlag, Essen
- Weir HD, Dimarco RJ (1978) Correlation and evaluation of driver/vehicle directional handling data. SAE Technical Paper 780010
- Wolf HJ (2008) Ergonomische Untersuchung des Lenkgefühls an Personenkraftwagen. Dissertation, TU Munich
- Zschocke AK (2009) Ein Beitrag zur Objektivierung und subjektiven Evaluierung des Lenkkomforts von Kraftfahrzeugen. Dissertation, University of Karlsruhe, Institut für Produktentwicklung

# **Chapter 8**

## **Layout of Steering Systems**

**Sina Brunner, Manfred Harrer, Manuel Höll and Daniel Lunkeit**

### **8.1 Basic Design of a Steering System**

Excellent driving and steering feel can be achieved only by a sufficiently precise steering system. Therefore, on the one hand, the design of a steering system has to be able to transfer high forces while on the other hand achieving little free travel, few elasticities and low friction in the movable parts. In addition, the steering system, supported by its power-assistance unit, should be able to realize sufficient steering dynamics. Adhering to these constraints is the only way to enable quick and precise steering of a car. In the following chapters the basic functional design of steering systems and the aspects of steering power and friction will be discussed in more detail.

#### **8.1.1 Rack Force**

The steering rack forces occurring from parking are crucial for the dimensioning of a steering system. The overall displacement force of the rack is the sum of the left and right tie rod forces. Essential influences on the level of the rack force at

---

S. Brunner (✉) · M. Harrer · M. Höll · D. Lunkeit  
Dr. Ing. h.c. F. Porsche AG, Porscheplatz 1 70435 Stuttgart, Germany  
e-mail: [sina.brunnger@steeringhandbook.org](mailto:sina.brunnger@steeringhandbook.org)

M. Harrer  
e-mail: [manfred.harrer@steeringhandbook.org](mailto:manfred.harrer@steeringhandbook.org)

M. Höll  
e-mail: [manuel.hoell@steeringhandbook.org](mailto:manuel.hoell@steeringhandbook.org)

D. Lunkeit  
e-mail: [daniel.lunkeit@steeringhandbook.org](mailto:daniel.lunkeit@steeringhandbook.org)

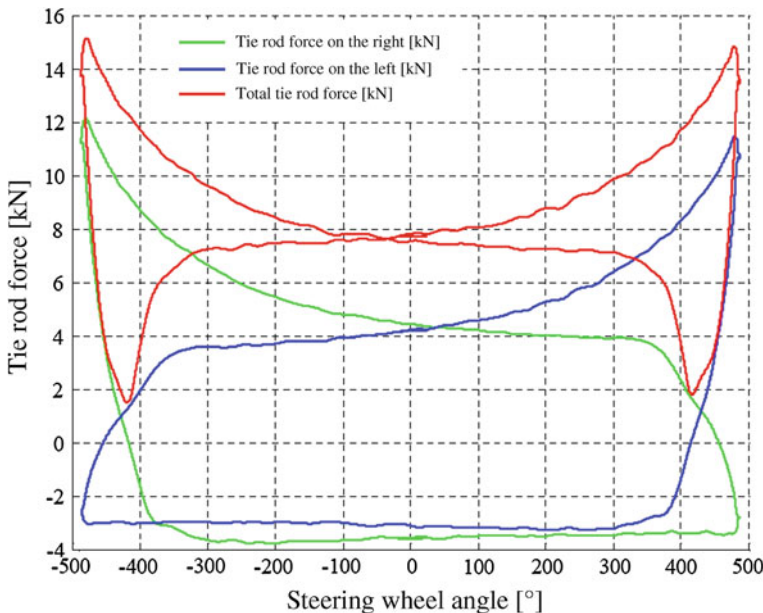


Fig. 8.1 Parking force measurement

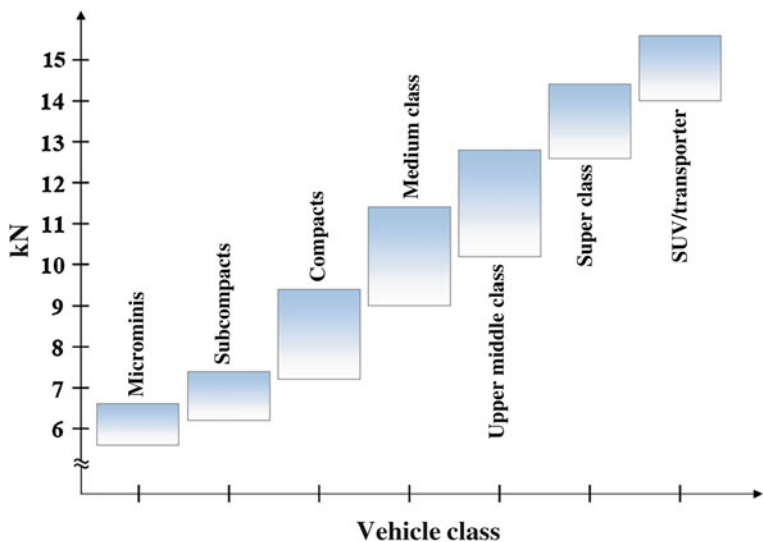
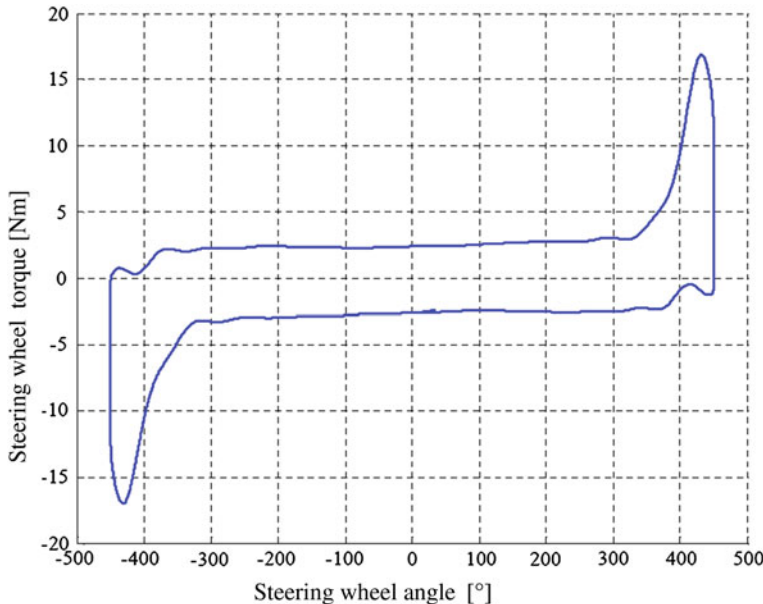


Fig. 8.2 Rack forces over vehicle class

parking are the axle kinematics, the front axle load, the size of the tyres, the air pressure in the tyres and the friction value of the road surface.

Figure 8.1 shows the results of such a parking force measurement. In this example, the highest rack force is 15 kN, achieved at the highest rack stroke or



**Fig. 8.3** Steering wheel torque when parking (undersized steering system)

steering wheel angle. The mentioned influencing factors demonstrate that the rack forces rise with increasing car size or weight. For this reason Fig. 8.2 shows the rack force ranges occurring among different vehicle classes.

### 8.1.2 Steering Wheel Torque

The steering wheel torque effort depends essentially on the design of the valve characteristic (for hydraulic power steering) or the applied software parameters (for electric power steering). The servo force of the steering actuator should be high enough so that it is possible to produce the desired steering wheel torque constantly over the entire steering wheel angle range when the car is at rest, taking into account the highest occurring rack force.

The steering wheel torque level, depending on the integrated steering system and its tuning, is located between 2.5 and 6.0 Nm in modern standard cars.

The servo force of an undersized steering system is not sufficient to turn across the full steering wheel angle range without demanding a higher effort from the driver. These circumstances are depicted in Fig. 8.3. In this example, the driver has to manually compensate a too low servo force by a higher steering wheel torque beyond a steering wheel angle which is higher than, say,  $\pm 350^\circ$ .

### 8.1.3 Steering Dynamics

The displacement dynamics of the steering actuator, as a function of the applied rack force, is crucial for a high steering wheel angular velocity (rate) that does not display any notable increase of the steering wheel torque. If the steering system is undersized, any quick manoeuvres will perceptibly raise the steering wheel torque.

It can be assumed in principle that the faster a manoeuvre is performed, the higher the perceptible steering wheel forces and torques will be. It is easy to identify the highest accessible steering wheel angular velocity, or rate limit, in a car at standstill by applying a sinusoidal steering wheel angle with an amplitude of about  $\pm 60^\circ$  while the steering wheel frequency is continuously raised up to 3 Hz. The steering wheel angular velocity and wheel torque are then rising functions of the steering wheel frequency. The rate limit is achieved when the steering wheel applied torque is approximately 50 % above the original steering wheel torque (Fig. 8.4).

The dynamic limits of a steering system may rarely be reached in everyday driving, yet sufficient steering dynamics can be crucial in a critical situation, such as in a sudden evasive manoeuvre. Therefore the required specifications of a steering system always define a steering rate limit as a function of rack displacement and force. Figure 8.5 shows a representative curve of the steering wheel rate limit. The presented default is limited by certain constraints. For example, the maximum permissible increase of the steering wheel torque upon reaching the steering wheelrate limit needs to be defined. For hydraulic power steering systems,

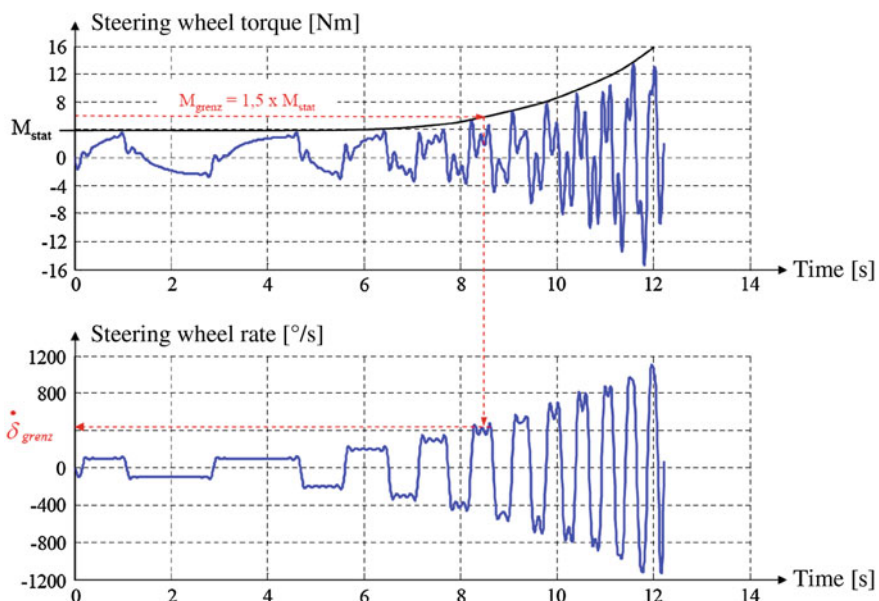


**Fig. 8.4** Determining the steering wheel rate limit

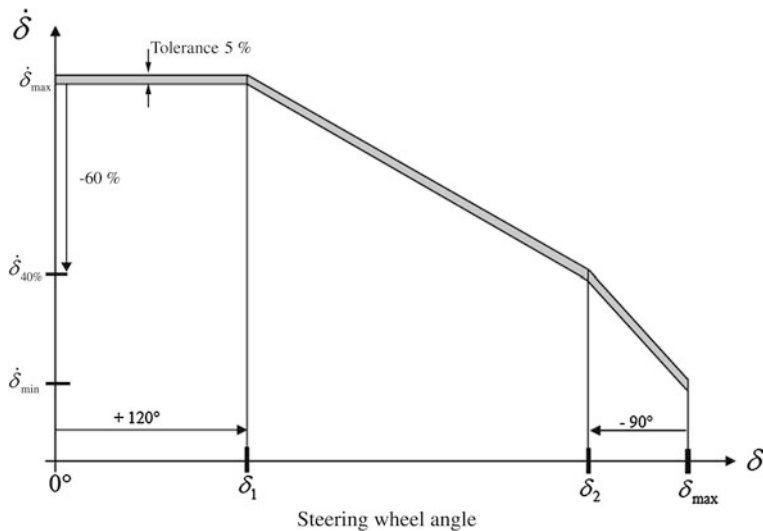


**Fig. 8.5** Default steering wheel rate limit

a default value of the available oil transport volume at the corresponding pressure is vital. For electric power steering systems, the system temperature and the highest voltage and current values applied to the ECU is defined.

### 8.1.4 Steering Power

The mechanical steering power can be computed from the required steering wheel angular velocity or rack speed and the resultant rack force. Figure 8.6 shows the power hyperbolas as a function of force and speed of the rack. Significant operating points of a typical SUV are indicated as well. Electric power steering system requirement specifications often use the mechanical steering power as a measure of the displacement dynamics.

### 8.1.5 Steering Friction

The mechanical friction is an important factor in the design of steering systems. Steering friction determines the driving and steering response of a car and, hence, the subjective perception of steering feel. Rack-based steering system designs cause a lot of Coulomb friction, originating from the sliding motion of the rack relative to bearings and gaskets. The high number of rotating mechanical parts in an electric power steering system generates a system friction which is higher than that of an hydraulic power steering system. The effects of the gear friction may be either negative or positive, depending on its nature and level.

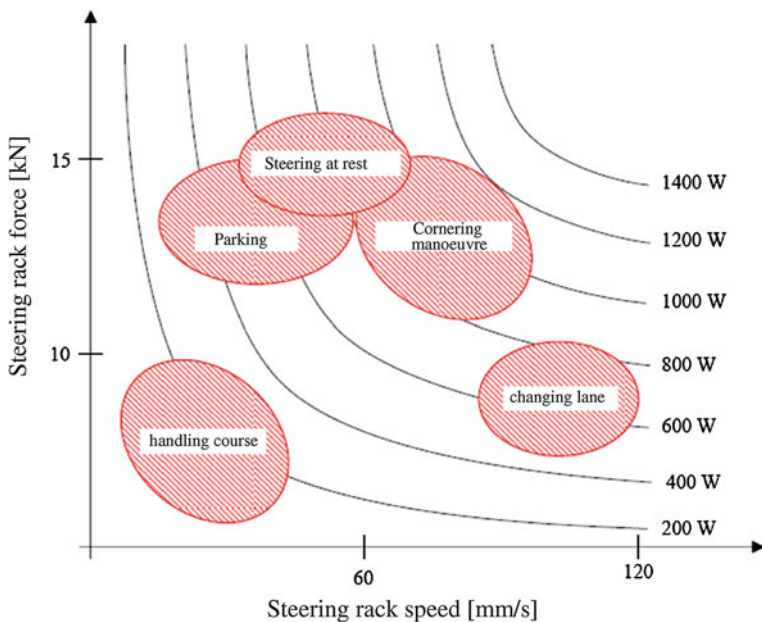


**Fig. 8.6** Mechanical steering power of an SUV (example)

### 8.1.5.1 Negative Features of Steering Friction

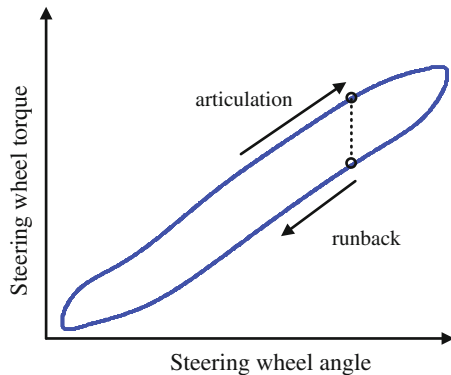
Ergonomic studies show that higher Coulomb friction in a control device reduces the human ability to control the device. It is evident that friction then also affects the precise dosage of steering movements, especially close to the centre point of a steering system, when the hydraulic or electrical power-assistance is low. In addition the so called stick-slip effect (transition from static to sliding friction), resulting from too high system friction when steering out of the centre point, should be avoided.

At low speeds, too much friction in the steering system will also reduce the car's self-aligning ability after cornering. Furthermore, the feedback of the steering system is affected by higher friction. Useful information about the current driving situation and road condition is accordingly reduced by friction.

### 8.1.5.2 Positive Features of Steering Friction

Friction in the steering system produces a hysteresis-like response of the steering wheel torque over the steering wheel angle. This hysteresis response is compulsory for precise cornering of a car. In a steady cornering it will generate an operating point with a notable rise of the torque when the steering wheel angle rises and a distinct drop of the torque when the angle lessens. This enables the precise adjustment of the steering wheel angle (Fig. 8.7). A high friction coefficient in the steering system will

**Fig. 8.7** Hysteresis of steering wheel torque over angle (steady sinusoidal alternating steer)



also support the suppression of interferences. Bumps and periodic excitations like wheel imbalances, fluctuations of the braking forces, etc. are damped accordingly. Any disturbances in the steering wheel can be reduced by higher friction.

There are two useful methods to determine the steering friction. The first method measures the displacement force of the rack, moving at a steady speed. The input shaft of the gear is free. A curve of the force over the rack displacement is the result. The amplitude of the displacement force increases as a function of the displacement speed.

Electric power steering systems, when passive (servo unit is shut-off), display higher displacement forces than hydraulic steering systems. At low ambient temperatures, the displacement force of an electric power steering system is also rising significantly in comparison to that of a hydraulic power steering system. Figure 8.8 shows the resulting modulating curve of the displacement force. This

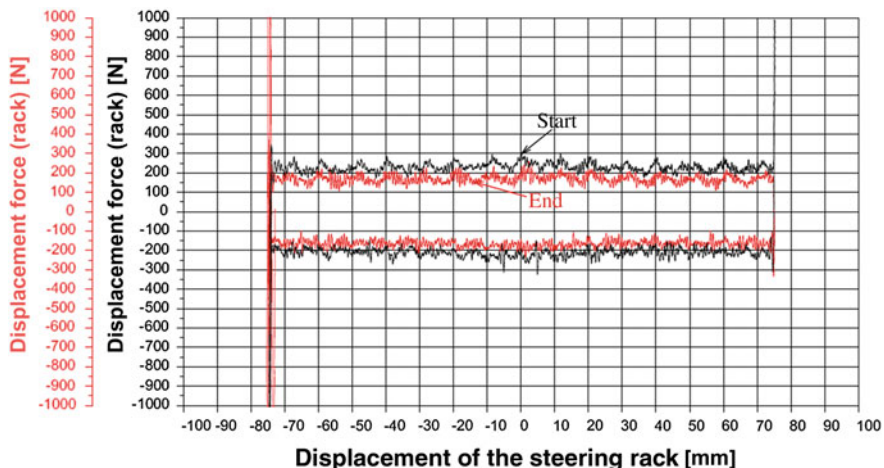


**Fig. 8.8** Displacement force measurement, EPS, 10 mm/s, before and after 80,000 km on the road

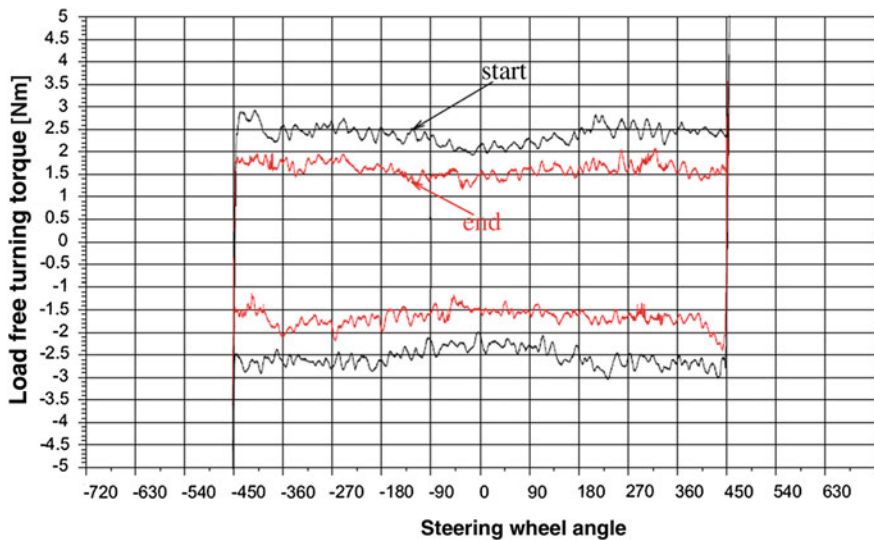


**Fig. 8.9** LFTT measurement, EPS, before and after 80,000 km of continuous running on the road

effect is caused by unwinding the pinion on the steering rack with varying cog engagements.

Another method to determine the steering system friction is to measure the steering wheel torque along the complete steering range without any external loads. In this case the input shaft of the gear is rotating at a steady speed and the rack is free of any external loads. The measurement yields the load free turning torque (LFTT) over the angle of rotation (Fig. 8.9). The same physical effects occur as when measuring the displacement force. The friction of the gear and the corresponding permissible limit values are usually specified when the car is new. A significant drop of the steering system friction during the cars lifetime cannot be avoided, it is due to wear and the jiggling in the steering system. After running for 300,000 km, a drop by half of the original value of the displacement force is not uncommon. Nevertheless, after an initial phase of a few hundred kilometres, the friction level should stabilise and be kept stable as long as possible.

## 8.2 Response Characteristics of Steering Systems

Response characteristics of steering systems can be distinguished by the conversion of torques at the steering wheel into forces at the rack and the conversion of forces at the rack into torques at the steering wheel. These two directions of transmission are generally unequal, i.e. knowing about one direction does not permit unequivocal deductions on the other direction, or its reconstruction. This fact does not initially appear very significant and it was marginalised in the past.

Yet deeper theoretical discussion of this relationship may help the developer of steering systems to answer many questions that can matter for their practical development. The following sections are meant to sensitise the reader for the subject by an introduction into the response characteristics of steering systems. Particular attention is paid to the differences arising from the technological switch from hydraulic to electrically assisted steering systems.

### 8.2.1 *Steering Response (Guidance Response)*

The driver's tasks in driving a vehicle can be interpreted as controlling the lateral and longitudinal dynamics of a car. Steering allows to focus on lateral guidance. The driver is sensor, filter, controller and actuator at once.

A conventional control system is generally adhering to the following criteria: stability, robustness, set point sequence and constraints to the available actuating power. Any system needs at least one actuating variable and the proper sensors to enable a suitable feedback which may serve to meet the controlling task. The set value steering wheel angle is generated by the driver, based on available sensors, for example: balance, eyes, ears, but also haptic perception of the steering wheel torques and accelerations. When generating a set value, any person will automatically avoid impossible actuation tasks, so that the controlling person, when skilled enough, can push the car to its physical limits.

Driving errors—so to speak: instabilities—occur when the driver has misjudged and transgresses the physical limits. The driver has misjudged when the mental model of the vehicle dynamics is insufficient or when the sensors for the mental model are sending delayed or wrong signals to the computing brain.

In this comparison the steering system, as an HMI, is fulfilling two tasks. On the one hand, it is the element that transmits the actuating variable, the steering wheel angle, set by the driver, via the steering gear and axle kinematics to the tyres. On the other hand, the steering system has to report haptic signals to the driver, e.g., to make statements about the contact of the tyre with the road or the forces present between tyre and road. As mentioned at the beginning, these two tasks of the steering system adhere to different directions of transmission. Their requirements can be deduced straight from our comparison. The transmission path steering wheel-to-road should be supported by the steering system in such a way that the actuating power provided by the human driver is sufficient to cover even the highest frequency range available. This bridges the gap to the steering wheel rate limit, relevant in system design, and the underlying power requirements to the system. In the transmission path from road to steering wheel or rather rack-force to steering wheel torque any changes to the force have to be reported to the driver in such a way that the useful content of this excitation can be fully exploited while the interfering content is suitably suppressed. This case is called good steering response.

## 8.2.2 Steering Feedback Response (*Response behavior*)

The preceding discussion shows that steering response may be interpreted as the conversion of varying forces and therefore speed and acceleration at the rack into variations of torque and therefore rotational velocity and acceleration at the steering wheel.

A suitable measure to theoretically study the transmission qualities of different steering systems is to define them within their free punch and to examine them then for minor variations around their neutral position. Needlessly complicated models of non-linear system qualities can thus be preliminarily avoided without limiting the general validity of the resulting statement. Next, the identified connections may be extended to non-linear systems, so that the reader may comprehensively examine the subject. A systematic procedure to evaluate the steering response will be presented in the following, beginning with a model of an hydraulic power steering system and continuing with a model of an electric power steering system.

### 8.2.2.1 Steering Feedback Response of Hydraulic Power Steering Systems

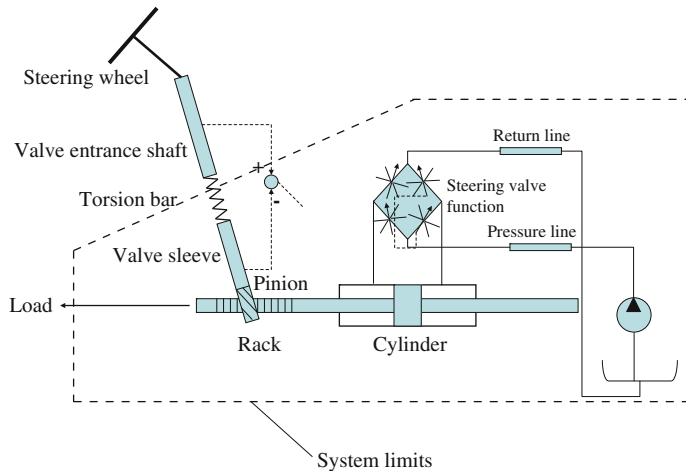
In general one has to distinguish between the feedback response of an active and a passive power steering system. An active power-assist is present when the driver initiates any steering process or is already continuing a quasi-stationary steering process. The steering system is passive when the driver does not change the course at the observed point of time. Which characteristic of the steering system is prevailing at which given time depends on the kind of power-assist and the respective system state. First, the passive feedback response of hydraulic power steering systems will be discussed.

Figure 8.10 shows the basic parts of a hydraulic power steering system, separated from the car. The design of axle kinematics and steering column is subject to different prevalent requirements than the steering system itself. Hence, the steering system will be discussed separately from steering column and axle kinematics. A detailed description of the hydraulic power steering system will not be given here, see the further chapters of this book. In the following, the steering system should be assumed as clamped at the torsion bar. This leads to an oscillatory system which can be well examined with the help of Bode's diagram.

To derive Bode's diagram for the oscillatory system steering, the equations of motion for the significantly simplified model are established. This yields the generic equation:

$$m\ddot{x} + d\dot{x} + cx = F(t) \quad (8.1)$$

Here,  $m$  is the mass of the rack and the hydraulic oil column. The damping of the system is represented by  $d$  and the stiffness of the steering system by  $c$ .  $F(t)$  are the



**Fig. 8.10** Basic diagram of a hydraulic power steering

forces, varying over time and acting on the rack from the outside,  $x$  is the position of the rack. Using the Laplace transform with the initial condition  $x(0) = 0$ , the transfer function for this SISO (single input single output) system and its representation in the Laplace area are at once derived:

$$G = \frac{X}{F} = \frac{1}{ms^2 + ds + c} \quad (8.2)$$

The analogy of the Laplace and the Fourier transforms allows to substitute the Laplace variable  $s$  by the complex number  $j\omega$ . This yields a complex frequency response that describes the response characteristics of the moving pinion as a function of the excitation at the rack. Separating this complex transfer function into its absolute value  $|G|$  and its phase  $\angle G$  and plotting both over the frequency results in a representation of absolute value and phase response of the examined system. Logarithmic scaling of the abscissa and scaling of the absolute value response at the ordinate in decibel (dB) yields Bode's diagram.

The absolute value response of Bode's diagram shows that for a given frequency  $f$ , an excitation at the rack has to be multiplied with the factor  $|G|(f)$  to receive the corresponding effect at the torsion bar. If the excitation at the rack is normalised to the value 1, the effect on the torsion bar is equal to the value  $|G|(f)$  for the frequency  $f$ . The frequency that allows to mark a drop of 3 dB in the absolute value response is called the corner frequency  $\omega_E$ . In contrast, the phase response signifies at which angular deviation the result of an excitation at the rack follows this actual excitation. This relationship is easy to explain using a pointer diagram.

The pointer diagram in Fig. 8.11 shows a snapshot of the excitation-to-effect ratio on the left side. The length of the pointer is '1'. This means that the absolute value response of the frequency response has an amplification of 1 at this point.

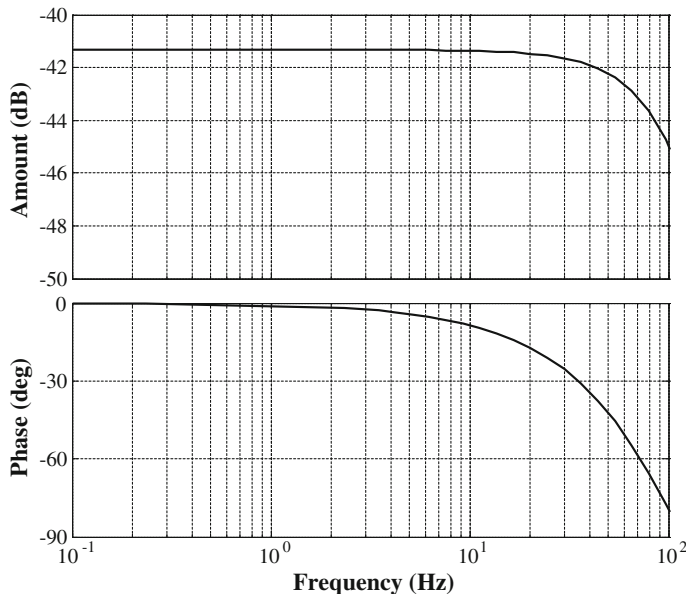


**Fig. 8.11** Bode's diagram of the passive hydraulic power steering

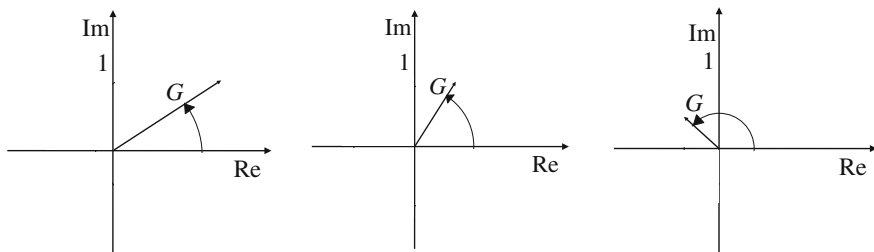


**Fig. 8.12** Pointer diagram of the response characteristics

The angle between pointer and abscissa of the first quadrant is the phase angle of this snapshot. The length of the pointer  $G$  and the phase angle between pointer and abscissa are changing according to the frequency of the revolving pointer.

Bode's diagram (Fig. 8.12) allows to see very quickly that higher frequencies will lower the excitation-to-effect amplification as the phase angle is growing (the angle is measured in mathematically positive direction). The curve shown is also called a low-pass filter. Studies of the human perception of steering torques have revealed that the sensory threshold for torque fluctuations is at 0.5–0.8 Nm (Burschardt 2003), depending on the actually applied steering wheel torque. This information allows to individually detect a changing torque at the torsion bar for any fluctuation of the force at the rack that occurs at a given frequency.

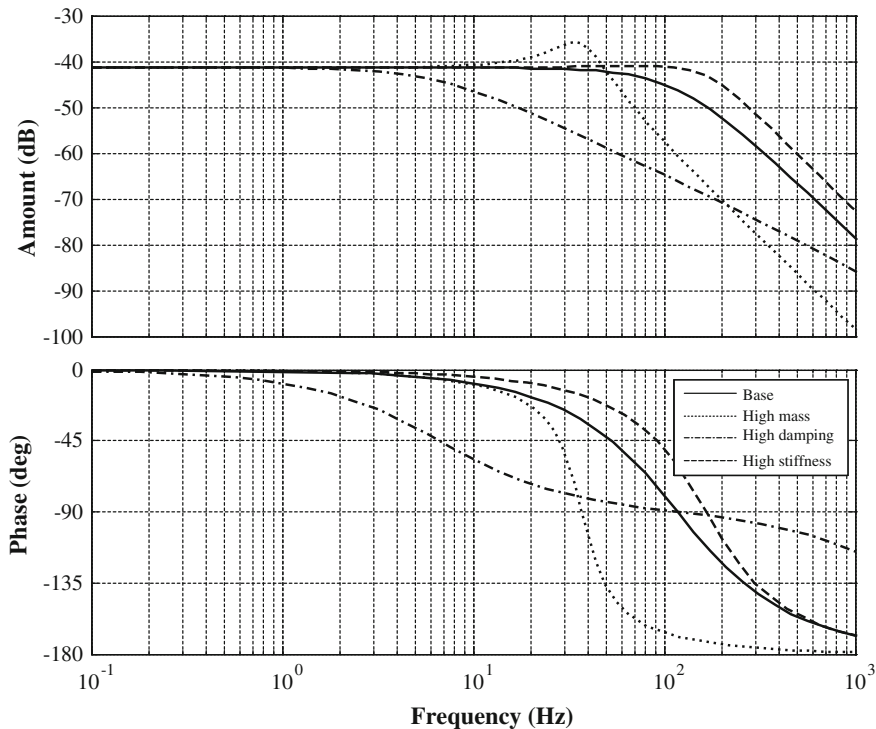


**Fig. 8.13** Bode's diagram of the hydraulic steering with modified parameters

The displayed frequency response is also called a 2nd-order lag element or a PT2 element. The structure of such a frequency response permits making statements about the meaning of the parameters in Eqs. 8.1 and 8.2. Consider that, according to the theory of oscillations, the proper motion of a vibrating system can be described by its damped natural frequency, being a function of the non damped natural frequency and the damping ratio. The non damped natural frequency is a function of system stiffness and mass, while the damping ratio is a function of damping constant and mass. Figure 8.13 shows the same steering system for different parameter settings. For reference purposes, the basic response characteristics, without modified system parameters, is shown again by a continuous line. The finely sketched curve of the frequency response shows that more mass  $m$  shifts the corner frequency towards the left, towards lower frequencies (reciprocal connection between non damped natural frequency and mass). At the same time, the damping ratio of the system drops (reciprocal connection between damping value and mass). A higher damping constant  $d$  (depicted by the chain-line curve) lowers the level of amplitude peaks at the resonance frequencies, shifting the corner frequency towards the left, towards lower frequencies. A higher torsion bar stiffness (approx. total stiffness)  $c$ , however, raises the corner frequency (coarsely dashed curve).

The frequency content found in hydraulic power steering systems is usually sufficient to supply any useful data that the driver may need. Actually, it is more likely that a hydraulic power steering system is perceived as too bumpy. This means that the full content of useful data is present, but the amount of interfering information is so high that the driver would perceive it as irritating.

The passive system response is prevalent, especially on a straight course, on account of the slowly climbing characteristic curves of the assist power around the centre point of the steering system. If some assisting power is already present, e.g., during a steady-state circular drive, the component of the assist unit will dominate with increasing power-assist. Ignoring the lag response of the assist unit, the servo power is diminishing the torque that the driver has to apply and, besides, has the effect to stiffen the overall system. In other words, the general amplification over the observed frequency range is less and the corner frequency is shifted towards higher frequencies.

### **8.2.2.2 Non-Linear Enhancement for the Description of Hydraulic Power Steering Systems Feedback**

The features discussed so far are based on the analysis of linearised systems. A real steering system is subject to significant non-linearities, though. On the one hand, there is the inherent friction, on the other hand, there are effects from the variable rack ratio or the non-linear valve characteristics. All non-linear qualities of a steering system listed above are essential tuning parameters, relevant for the steering feel. For example, when a variable rack ratio is used, the steering wheel angle required to produce a corresponding steer angle at the wheels is higher around the centre point of the steering than near the end stops. This design is sensible because high-speed driving concurs preferably with small steer angles, and a less direct rack ratio of the steering will make the vehicle respond less nervously. Low-speed driving often requires high steer angles, though, e.g., for parking. A more direct gear ratio is more advantageous here. The variable rack ratio, hence, is designed so that the steering wheel torque build up as a function of the rack travel will follow a degressive characteristic curve. This indicates for the response characteristics of the steering system that big steer angles will impair the stiffness of the overall system. This may not sound very plausible at first, but it can be explained as follows:

The stiffness resulting from the torsion bar and that from the power-assist unit are acting in parallel, so that their effects on the overall system stiffness can be examined separately. The torque at the torsion bar is set by the product of the difference angles between pinion and steering column and of the torsion bar's rotational stiffness.

$$M_{DS} = c_{DS} \cdot \Delta\delta = c_{DS} \cdot \left[ \delta_{LS} - \frac{2\pi}{i}x \right] \quad (8.3)$$

$M_{DS}$  is the torque at the torsion bar,  $c_{DS}$  is the rotational spring rate of the torsion bar,  $\delta_{LS}$  is the steering column angle,  $i$  is the variable ratio between pinion and rack and  $x$  is the displacement of the rack. The stiffness of the examined system results from the torque at the torsion bar, changing with the position of the rack. This can be computed by:

$$\frac{dM_{DS}}{dx} = c_{DS} \cdot \left[ -\frac{2\pi}{i} \right] = c_{var} \quad (8.4)$$

$c_{var}$  is here the variable stiffness of the system, shown as a function of the variable rack ratio. Big steer-angles produce a high ratio, so that the system stiffness is small, while small steer-angles concur with a small ratio, hence, the system stiffness is high. There is a similar relationship for the generally progressive assist power characteristic curves of the rotary disk valves. Here, however, the nonlinearity is found in the hydraulic power assist, progressively rising with the torsion bar torque. Hence, the total stiffness of the system is higher when there is a higher torque at the torsion bar. In any real steering system, both effects apply simultaneously and, depending on design, with different intensities. Only the superposition of these relationships can, therefore, be observed at a car or test bench.

Figure 8.14, top left, shows the response characteristics of a hydraulic power steering system with rising assist power. The continuous line represents an unassisted system. The assist power rises by the following sequence: finely dashed, dashed-and-dotted, coarsely dashed. It is obvious that the corner frequency of the frequency response will move to the right as the assist power rises, while the absolute value will lessen. Only the changing absolute values are relevant, because the corner frequency is far beyond the frequency range that is relevant for the driver. Hence the conclusion is permissible that the driver's resolution of excitations at the rack will drop as the assist power rises. This relationship does not substantially change in the frequency range that is relevant for drivers even if the lag from the hydraulic power assist unit is included, see Fig. 8.14, top right.

The lower left diagram shows as well that the total stiffness of the system lessens when the gear ratio becomes more direct, the corner frequency shifts slightly towards the left and raises the absolute value of the transmission. The lower right diagram shows a combined representation of variable rack ratio and progressive assist power characteristic curve, including any lags of the actuators.

The steering gear friction is also very non-linear, producing the hysteresis qualities of the steering system. It can be adjusted to some extent, to reduce the steering's sensitivity to the torque applied by the driver. Then the car will not respond to any ever-so-slight change of torque by the driving hands, and the steer-angle can be precisely set. The steering system friction is composed for a major part of dry friction and for a lesser part of viscous friction. For the response characteristics of the steering system, this means that the rack will not move before its friction is overcome, thus the torque at the torsion bar will not change. Minor fluctuations of the forces at the rack cannot be resolved at all, before this detection

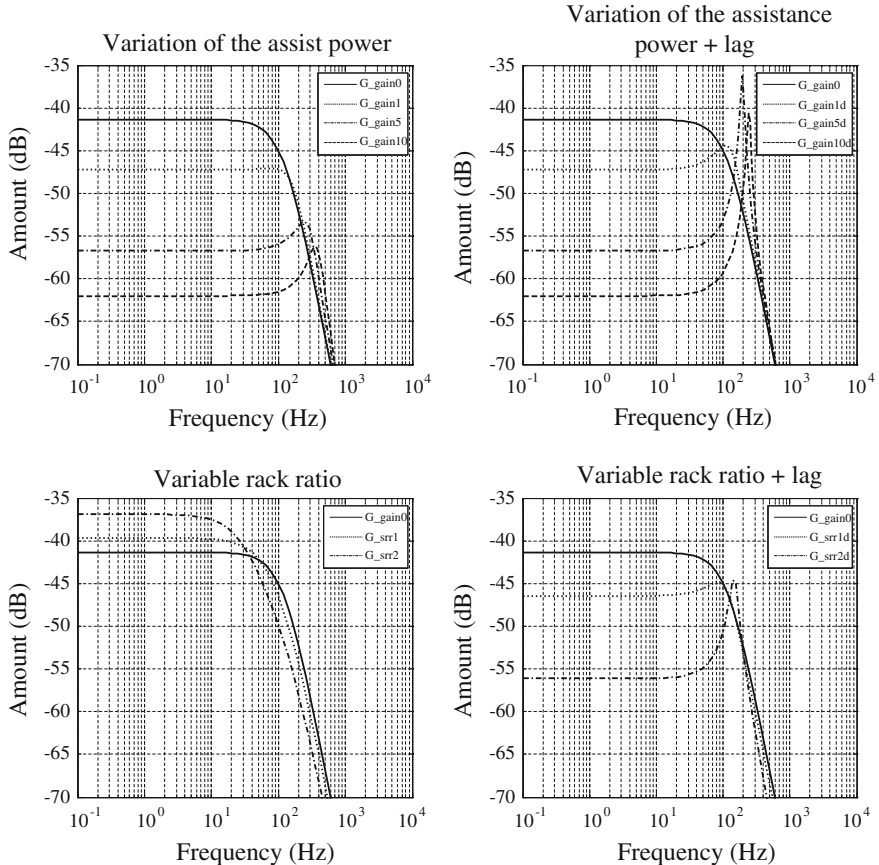


**Fig. 8.14** Bode's diagrams on different non-linear influences in the response characteristics

threshold is passed. This can be told from Bode's diagram by a corresponding reduction of the absolute values in the absolute value's response.

The preceding discussion reveals that many parameters of a steering system affect the response characteristics of useful and interfering data. In spite of the huge number of, sometimes complex, parameters, it is still possible to describe the response characteristics of a hydraulic power steering system in general without loss of generality. The cut-off frequency of any relevant feedback to the driver is in the range of 20–30 Hz (Brunn and Harrer 2004). This, together with the figures in this subsection, permits concluding that any hydraulic power steering system can be designed so that the maximum amount of useful data is available to the driver intrinsically.

The philosophy of the individual steering system development engineer decides how to set the parameters to permit the desired system response.

### 8.2.2.3 Feedback Response of Electric Power Steering Systems

#### Feedback

Analogous to the hydraulic power steering system, the response characteristics of an electric power steering system will be examined and discussed in this section. A steering system with an axis parallel brushless DC motor is shown in Fig. 8.15 as one example of a possible electric power steering system to be used in the following discussions.

As before, when the hydraulic power steering was discussed, the system boundaries refer only to the main elements of the steering system, including the pinion with torque sensor and torsion bar, the rack with its transmission gear and a BLDC motor with ECU.

The electric power steering system can also be modeled as a mass oscillator, if the torsion bar is assumed again as clamped tight.

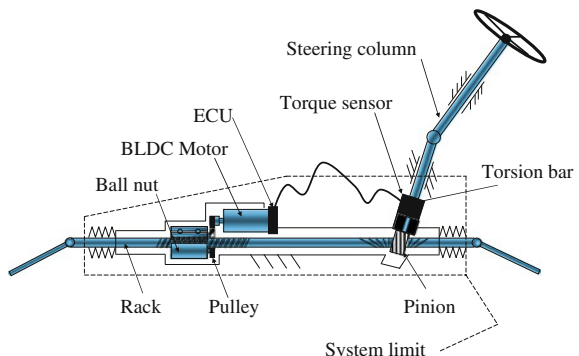
To simplify the derivation of the frequency response, the same generic equation of motion that was applied to the hydraulic power steering system (cf. 365 Eq. 8.1) is used. Note that secondary elasticities in the steering gear are ignored, while the rotational moment of inertia from the and the rotor shaft of the BLDC motor are added to the translating mass of the rack. This is achieved, e.g., by deriving the substitute mass for the moving rack from the energy equation of the overall system. The kinetic energy of the (axis-parallel electric power steering system) APA-EPS is derived from:

$$T_{EPS} = \frac{1}{2}mv^2 + \frac{1}{2}J_{KGT}\omega_{KGT}^2 + \frac{1}{2}J_{BLDC}\omega_{BLDC}^2 \quad (8.5)$$

Now  $m$  is the mass of the rack and  $v$  is its velocity,  $J_{KGT}$  and  $J_{BLDC}$  are the moments of inertia of the recirculating ball nut and the rotor shaft, their angular velocities are  $\omega_{KGT}$  and  $\omega_{BLDC}$ . Using the transmission ratios for the velocities:

$$\omega_{KGT} = \frac{2\pi}{i_{KGT}} v \quad (8.6)$$

**Fig. 8.15** Basic sketch of the axially parallel electric power steering (APA EPS)



Here,  $i_{KGT}$  is the transmission ratio of the recirculating ball nut in  $m/rev$  and  $i_R$  is the dimensionless gear ratio. This yields the kinetic energy of the EPS as a function of the rack velocity:

$$T_{EPS} = \frac{1}{2} \underbrace{\left[ m + J_{KGT} \frac{4\pi^2}{i_{KGT}^2} + J_{BLDC} \frac{4\pi^2 \cdot i_R^2}{i_{KGT}^2} \right]}_{m_{Trans}} v^2 \quad (8.7)$$

The substitute mass can be read from that as  $m_{Trans}$ . Standard transmission ratios are 0.006–0.010  $m/rev$  for the ball nut and 2.0–3.5 for the belt drive. The moment of inertia for the rotor is approx.  $1e-4 \text{ kg m}^2$  and for the recirculating ball nut approx.  $1e-3 \text{ kg m}^2$ . Ratios and moments of inertia of this magnitude yield substitute masses of 900–1800 kg. This indicates a considerable influence on the response characteristics of electric power steering systems, considering that the mass of the rack is only 2.5–3.5 kg.

At this point, the frequency response, familiar from Eq. 8.2, can be used with the computed substitute mass. Figure 8.16 shows the effects on the response

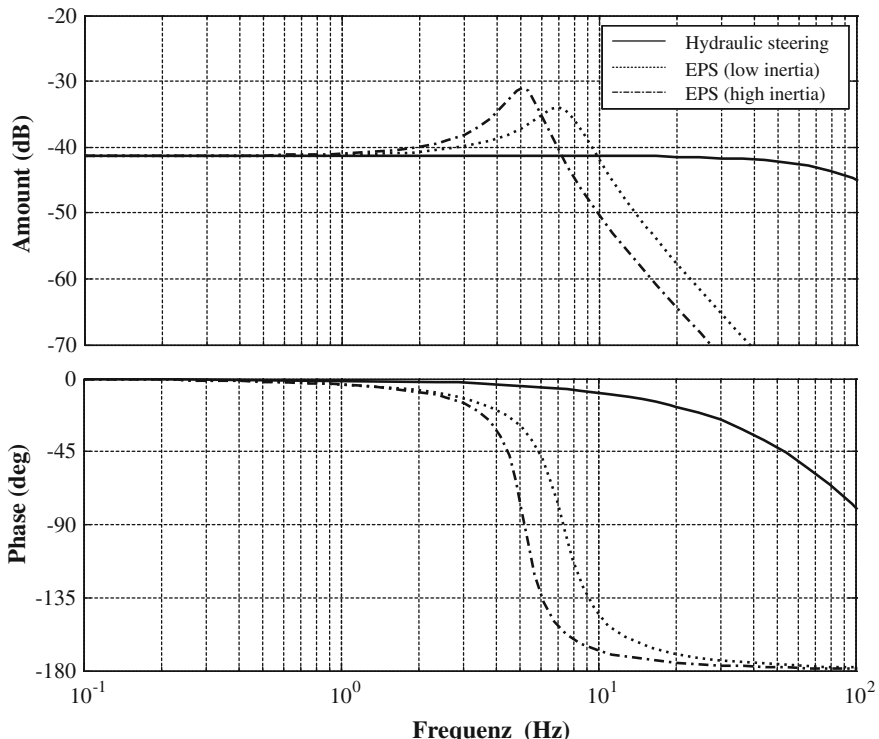


**Fig. 8.16** Bode's diagram of a passive electromechanical power steering

characteristics for a system with low (EPS-low inertia) and high (EPS-high inertia) substitute masses in comparison to a hydraulic power steering system, using Bode's diagram for the passive systems.

It is easy to see that an electric power steering system has considerable shortcomings in the passive response characteristics, compared with a hydraulic power steering system. The corner frequency of both examined EPS versions is much less than 10 Hz. Neither of the two systems provides the full frequency content of useful information to the driver. The reason can be deduced from the derivation of the frequency response. The inertia of the recirculating ball nut and the rotor produce an additional mass at the rack that shifts the corner frequency so much towards the lower frequency range that the developing mechanical low-pass filter eliminates a significant part of the response. Note, however, that some manufacturers welcome this quality of electric power steering systems, because interfering variables are suppressed by the same order of magnitude.

As in a hydraulic power steering system, the passive response characteristics are usually prevalent in electric power steering systems, too, when driving straight. The reason is that no power-assist is required when the car is not cornering. This effect is welcome, because the switch from hydraulic to electric power steering systems is not only motivated by more functionality but also by less energy consumption. The power-on-demand principle provides assist power to the system only when required. However, electric power steering systems often have active steering functions, that can be active even when the driver gives no steering input. This may be true, e.g., for a lane-keeping or a parking-assist system. Still, note that the actual response of the steering system for these functions is subordinate or the active intervention of the steering system is minor. Hence, it is still legitimate to say that the passive system response to straight driving will in most cases dominate the response characteristics of an electric power steering system.

This means in turn that the response behaviour of actively assisting electric power steering systems, i.e. during a manoeuvre, will be substantially affected by the assist power demand of the steering system. The assist power for the driver is realised in these systems by a feedback control system or at least by an advanced forward control approach. There are different approaches with different effects on the response characteristics of the individual active systems. Whatever the control strategy, the response of actively assisting systems depends a lot on the matching application modules, i.e. the reference defaults of the respective system and the parameters applied. One popular way is to provide application modules for the general assistance, the centre point feeling, the hysteresis, additional damping and an active steering return. Often, all these functions are in a more or less intertwining manner dependent on each other and the corresponding states of the steering system and the car. One example is the general assistance of the steering system as a function of the torsion bar torque, varying with the cars speed. This is not the only reason why the assist power provided by the steering system is rather non-linear. It should be obvious that it is not possible to make any really general statements on the response characteristics of an actively assisting electric power steering system. Yet to improve the reader's understanding of the present

dependences, it seems useful to focus on just one of the most common ways to build an EPS.

One of the most frequent approaches to realize an electric power-assist is an assist power that is provided proportionally to the torsion bar torque.

Figure 8.17 compares EPS and HPS response characteristics at different assist rates, assuming a nearly perfect control with short time lags. The effect of this kind of assist power default resembles the hydraulic power-assist very strongly.

This means that the assistance unit has the effect of an additional stiffness on the system. The first diagram of Fig. 8.17 compares an EPS and an HPS in passive states. The subsequent diagrams 2–4 (2 = weak assist, 3 = medium assist, 4 = powerful assist) repeat the comparison for successively higher assist powers. It is evident that, as already seen for hydraulic power steering systems, this kind of electric assist power also features a corner frequency that is shifting towards higher frequencies when the assistance rises, while the amount of forces at the rack converted into torques at the torsion bar is diminished. Indeed, in an electric power steering system, this process is based on a much lower corner frequency of the passive system. It may be added without further discussion of the subject that electric power steering systems per default suffer a higher friction than hydraulic systems. Hence, what was said for the HPS is true here as well: the system friction

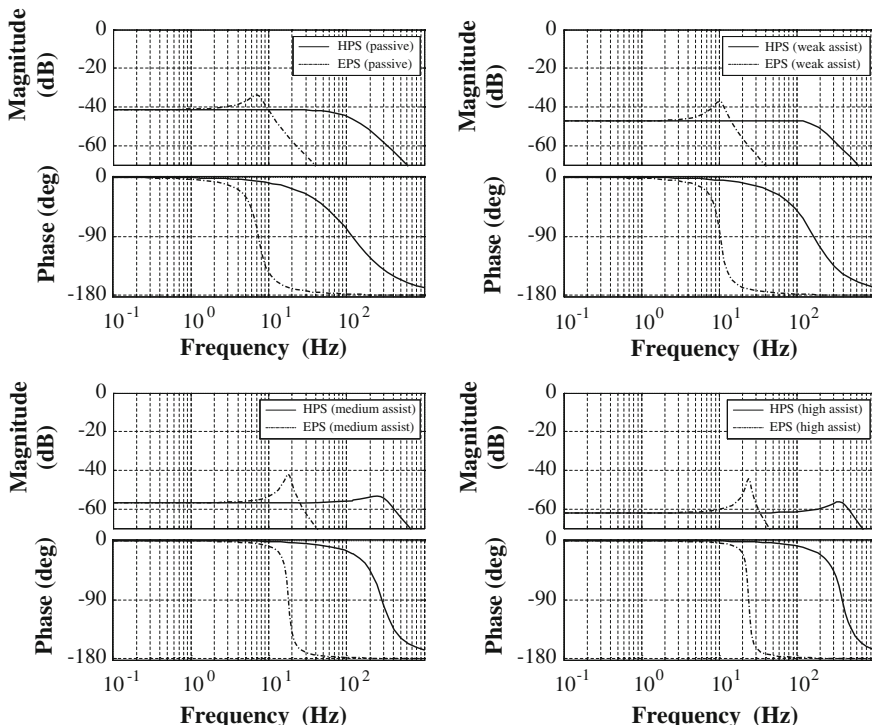


**Fig. 8.17** Bode's diagram of EPS and HPS for rising assist powers

of the steering has to be overcome before the rack starts to move at all. This effect is accompanied by a corresponding rise of the detection threshold at the rack. The variable rack ratio reduces the system stiffness, slightly decreasing the corner frequency, while the absolute value in the amplitude response is rising, as in hydraulic systems.

To conclude, the discussed problem of an insufficient passive response can be avoided. Using advanced control approaches and matching application modules, the lacking passive response may to some extent be substituted by an active response. Approaches are still in the development phase, however, though close to mass production. At best, the full frequency content can be provided to the driver as useful data. If the response characteristics of such systems have to be defined more exactly, as in the discussed example, the applied control approach and the matching application modules have to be known. Only then can a design-to-feedback approach help an electric power steering system to meet the highest requirements for its feedback qualities and even supply the full scope of active steering functions.

## References

- Brunn P, Harrer M (2004) Objektivierung der Lenkungsrückmeldung. VDI Fortschritt-Berichte, 12(580):67–79
- Burschardt B (2003) Synthetische Lenkmomente. VDI Fortschritt—Berichte, Reihe 22, No. 12. VDI Verlag, Düsseldorf
- Heissing B, Ersoy M (2007) Fahrwerkshandbuch. Vieweg+Teubner Verlag, Wiesbaden
- Stoll H (1992) Fahrwerktechnik: Lenkanlagen und Hilfskraftlenkungen. Vogel Buchverlag, Würzburg

# Chapter 9

## Steering Wheel

Markus Walters

### 9.1 Introduction

The driver perceives the steering wheel as one of the first parts inside a car. It is one of the most important interfaces between man and machine, because the steering movements are initiated at the steering wheel and the driver receives a direct response on the driving situation.

Because of its exposed position inside the car, the steering wheel has to meet plenty of additional requirements. It is a part of the driver's restraint system, meaning that corresponding safety and legal regulations have to be met and verified by slide and crash tests. Furthermore, the steering wheel has become a designed element, merging into the general look of the interior and bearing, for example, trade name or logo of the manufacturer.

The steering wheel has assumed a huge number of operation controls in recent years, e.g., to control on-board computer and radio, navigation or gearbox functions. Displays and function lights are implemented. Bus systems for the communication between steering wheel and vehicle enter the steering wheel electronics on this behalf.

### 9.2 Subassemblies

Many customers, particularly in the premium segment, demand more individualization, generating an ever greater variety. In addition, the various markets supplied by the manufacturers require further differentiation. The steering wheel as well is

---

M. Walters (✉)

Dr. Ing. h.c. F. Porsche AG, Porscheplatz 1 70435 Stuttgart, Germany  
e-mail: markus.walters@steeringhandbook.org

**Fig. 9.1** Porsche sports steering wheel with shift paddles



much affected by this individuation. Often, a huge amount of supplemental equipment is offered for the basic version that may be distinguished by technical and stylistic requirements (Fig. 9.1).

Some technical versions are:

- Multi function switch (e.g., car computer or navigation controls)
- Gearbox operating switch (e.g., paddle switch)
- Steering wheel heating
- Displays (e.g., upshift recommendation, functional displays).

Stylistic differences are marked by:

- Colours
- Materials
- Decorations
- Varnished or electroplated surfaces.

The shown example of a version tree (Fig. 9.2) helps to clarify the differentiation and variety of versions. 50 steering wheel versions develop in this example from a number of colours, decorations and technical varieties, like multi function or heating.

The basic structure, the foam body with the steering wheel rim, the horn function and the airbag are within the basic scope of a steering wheel (Fig. 9.3). This basic scope and additional elements, like switches or decorations, will be discussed in the following.

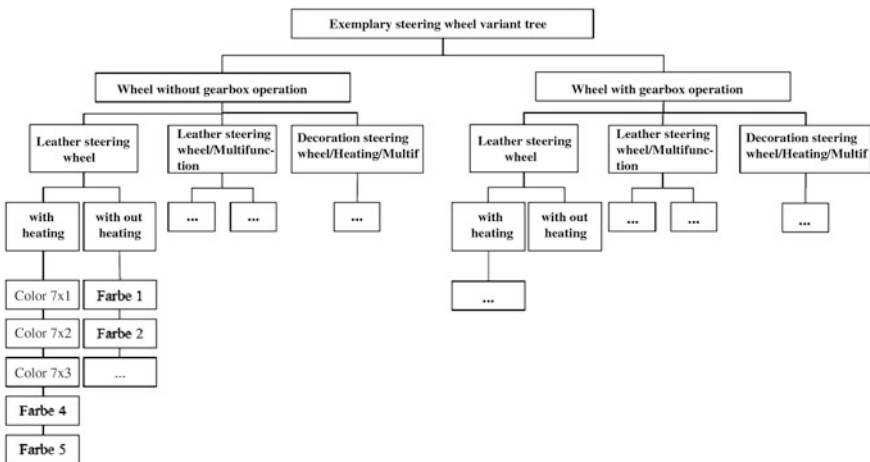


**Fig. 9.2** Version tree of steering wheels (example)



**Fig. 9.3** Exploded view of a steering wheel (Porsche 997 II). *Left to right* basic structure-steering wheel corpus-steering wheel cover with horn function-airbag

### 9.2.1 Basic Structure

The basic structure is the fundamental scope of a steering wheel. It establishes the supportive structure to meet the crash and operational safety requirements, it manifests a connection to the steering column, it serves as a base for bolting elements and generates the basic structure for corpus and rim, hence, of the steering wheel design.

Steering wheels are safety parts, in a frontal crash, when the airbag is triggered, they are exposed to high loads by the driver. In addition, the driver releases

steering and supporting forces into the basic structure that have to be endured permanently.

The design of the basic structure can decisively impact the natural frequency and the steering wheel's mass moment of inertia.

Weight requires basic structures to be made from light metals, like aluminium or magnesium (mainly die-cast). Magnesium is prevalent these days, due to the benefit of weight (Fig. 9.4).

Basic structure design has to include the above-mentioned aspects of crash, operational safety and natural frequency. In the case of a crash, the steering wheel should be able to absorb a high amount of energy, but it must not break. The energy is absorbed mainly by distorting the lower rim area. This is realised by a suitable design of the spokes and a connection to the hub floor. The lower spoke(s) is/are weaker than the upper spokes, to achieve this effect.

An engine or steering wheel imbalance can produce interfering excitations at rest or during a drive. The steering wheel needs to have a natural frequency of  $>65$  Hz, to meet the demand for a steering resonance (e.g., 40 Hz), essentially combined from the natural frequencies of the frame, including the connections to the car body, the steering column and the steering wheel. The design of the hub floor and the connection of the spokes are essential for this design of the full steering wheel. If the hub floor is not stiff enough, the idling vehicle may display a shivering steering wheel. Additional metal sheet inserts may be molded in to stiffen the hub floor. Another significant way to obtain the natural frequency is the connection of the airbag.

A steering wheel's mass moment of inertia is commonly raised by implementing additional weights as far away from the center of mass as possible. The steering wheel rim of the basic structure is the natural choice. There are different options to introduce the mass into the rim.

**Fig. 9.4** Basic structure. *Top left* rim, *top right* hub. *Bottom left* hub floor, *bottom right* spokes





**Fig. 9.5** Basic structure compound and basic structure with rim insert. *Left* round tread-moulding nodes-group basic structure. *Right* steel insert-basic structure with rim insert

One version has an U-shaped rim, into which the die-cast steel inserts are implemented and crimped. The advantage of this option is that the casting does not need additional effort and a multi-use mould can be used.

Another option is the immediate casting of tubes or round full treads (mainly steel). The steel tread in the spoke areas is surrounded with the die-casting, so that it leaves the mould as one part. This is called the basic structure compound.

Which option is chosen depends on the available manufacturing facilities and the philosophy of the manufacturer (Fig. 9.5).

Most connections to the steering column are implemented either by internal toothing or by a hex socket. The socket is implemented right into the tool, while a toothing is produced either by clearing after casting or by an additional, already cleared steel jack which is inserted into the die-casting tool and is cast-in, together with the rest.

The kind of connection depends on the vehicle's properties, such as steering column, structure space and electronics modules.

### 9.2.2 Rim and Corpus

The layout of a steering wheel corpus is primarily determined by design, albeit ergonomics and haptics matter when the rim is shaped. The geometry of the rim often distinguishes between sporty and convenient steering wheels. Some of the sporty attributes are a rim that is flattened underneath or thumb supports. Every vehicle manufacturer has its own philosophy with regard to cross sections and diameters of a rim. The scope encompasses oval to circular and thin to thick rims.

Manufacturers in the Far Eastern and American markets prefer plastic *back covers* for the corpus (die-cast parts) which are bolted onto the basic structure. The steering wheel rim is previously made by foaming, separate from the corpus.

Foamed steering wheels are almost exclusively sold at the European market. Corpus and rim are produced in a foaming process. The basic structure is laid into a foaming mould and foamed in situ with water-driven polyurethane (PUR) integral foam. To make coloured steering wheels, the PUR integral foam is dyed. A colour is introduced into the mould before foaming (in-mould covering) to improve the surface quality and to maintain the stability against light. Different grains are made in the foaming tool according to the manufacturer's specifications. This grain is introduced into the tool by etching. Foaming of the steering wheel copies the grain to the surface.

### **9.2.3 Horn**

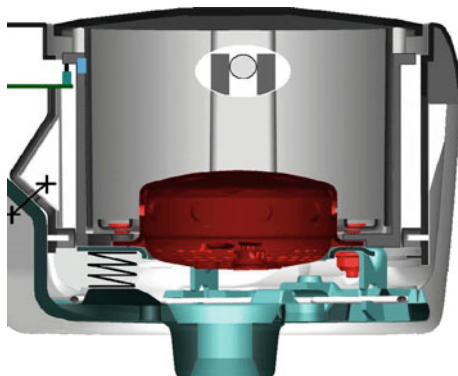
Current requirements to a horn system include not only a warning against danger but other factors as well, for example, the moderation of the horn forces, the precise definition of the horn's travel, the even shape of the joint between steering wheel and airbag module, reliable operation for the whole service life and little space filled by the parts of the horn.

Horn systems operated by an axial movement of the airbag module are preferred for automobiles. The airbag module is held in position by compression springs. It has to be pressed against the spring tension until the contact in the module support is closed (*floating horn*). Its advantage against horn buttons integrated into the steering wheel is the central position of the airbag module and the wider user surface. In dangerous situations and in any steering position, the driver will intuitively locate the horn and use it safely.

#### *State-of-the-art*

The common feature of almost all the marketed *floating horn* systems is the tilting of the airbag module when the horn is used. This tilt requires a wide gap between the airbag cover and the steering wheel, contrary to the demand for lesser gap widths. Several (usually 3–4) contact positions are needed to make sure that the horn contact is closed all over the surface of the airbag when the horn is pressed. The position of these contacts is quite vital, especially when the airbag module is big and has long spoke bedding-ins. In this case, the contacts are placed very far outward, so that the horn will not travel too much when it is operated near the edge of the airbag. Moreover, with tilting airbag units, it is hard to achieve any even horn actuating forces, because of the different lever ratios (pressure point vs. contact position).

**Fig. 9.6** Contactless horn with linear guiding of the airbag. (Source TRW). Magnet-hall sensor-chip-horn spring



#### *Linearly guided horn system*

Linear guiding excludes tilting the activated airbag module and presents a uniformly looking joint to the viewer. Furthermore, an even actuating force is established across the whole cover by linear guiding, the position for detecting the activation can be freely chosen, the horn travel tolerance is more controllable.

This kind of horn guidance suggests a contactless signalling by one single transducer (Fig. 9.6).

The physical principle is based on detecting the travel of the airbag module and evaluating it with a Hall sensor. The generated Hall sensor signal is processed by the steering wheel ECU and transferred to the vehicle ECU by a LIN BUS.

One big advantage of a contactless horn, due to the Hall sensor, is the absence of wear from the contact positions that otherwise would result from mechanic abrasion and electrical discharge sparks. Nor will the contact positions be sooted or oxidised, because the sensor is a closed system. This is also a great advantage for the service life tests (e.g., *coke test*). The Hall sensor is proof against short circuits, and this is another advantage against conventional horn buttons. Extraneous magnetic fields are eliminated by the system, preventing any external release.

#### **9.2.4 AirBag and Crash**

Safety is gaining importance for the car industry, both due to the persistently developing legal demands of different car markets (Europe, the USA, Asia) and due to crash cases that are relevant for consumer protection. The protective effect of the driver's airbag has to be provided within 30 ms, to meet the different requirements. The best possible restraining effect for passengers of any size has to be achieved as well. A test series with different fastened dummies is needed, as, for example, the 50 % dummy (average citizen), the 5 % dummy (light small woman) and the 95 % dummy (big heavy man). Examine also any wrong, unbelted loading

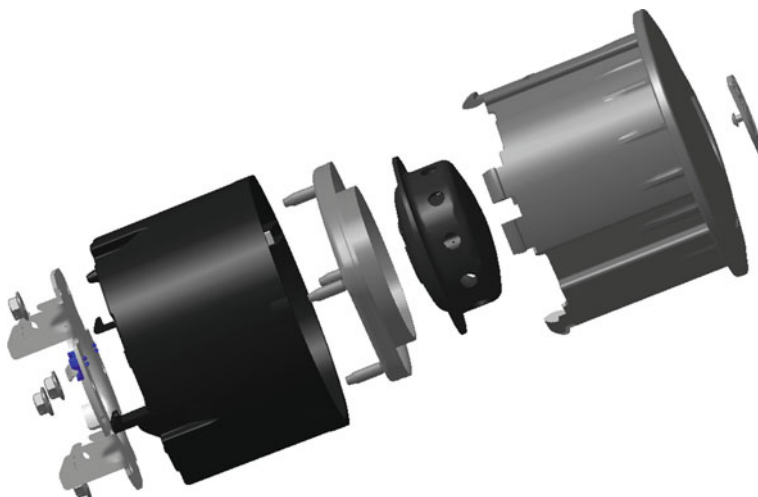


**Fig. 9.7** Airbag, exploded view (airbag not shown). *Left to right* bracket plate with bolt connection-generator support-airbag bracket plate-emblem-gas generator-airbag cap

conditions, the *OOP or Out of Position cases* on-board. These OOP loading conditions must not permit any danger to issue from the airbag system. These requirements/functions of the airbag have to be guaranteed for 15 years, across the whole temperature range of  $-35$  to  $+85$  °C, according to the manufacturer.

Figure 9.7 shows an exploded view of an airbag with the essential parts.

#### 9.2.4.1 AirBag Cover

Other than meeting requirements of design, the airbag cover contributes a lot to the restraining function of the airbag. If the airbag is ignited, e.g., by a frontal crash, the airbag cover will release the airbag in a controlled manner. This controlled opening/tearing of the airbag cover is due to tear lines on the inside cover, targeted reduction of the material strength that have been determined and optimised in a huge number of simulations and tests. A flaw of reducing the material strength, though, is that the tear lines may unintentionally show on the cover top, and that is undesirable because of the exposed position of the steering wheel. Therefore, the design of the airbag cover and the choice of the process parameters need particular attention.

#### 9.2.4.2 AirBag

Below the airbag cover is the airbag. The airbag consists of polyamide fibres, woven into a tissue, to be used either coated or uncoated. The firmness of the tissue

is influenced by the thread. Other versions are airbags with inner rebound tape or tear seams. The rebound tapes reduce the unfolding travel and provide for the best positioning of the airbag in front of the driver. The driver is ideally protected by the airbag when it unfolds during a crash as quickly as possible and into the right position in front of the driver. This is controlled by how the airbag is folded and the way the airbag is stored into the cover, over the gas generator. When a crash pushes the driver into the airbag, the air must be vented to reduce the impact energy and to catch the passenger. A flow-off exhaust in the airbag will do. The volume of air escaping from the airbag can be set by position, size or number of openings. This permits controlling the energy absorption. Upon specifying the size of the openings, all relevant loading conditions and dummy sizes are considered.

#### 9.2.4.3 Gas Generator

The gas generator has to inflate the airbag very quickly with the required amount of gas. Chemical generators with solid propellants are chiefly used on the driver's side. The propellant is accommodated in tablets inside the gas generator. The gas for filling the airbag is generated by a reaction of the propellant with the ambient air. Azidous propellants were used until the 1990s. All generators are now operated with azide-free propellants, due to higher concerns for environmental protection.

The bridge fuse is activated by the vehicle sensors, so that the ignition pill can initiate the fuel combustion. The gas required to fill the airbag is generated in the sudden burning of the solid propellant. The combustion produces very high temperatures in the furnace chamber (up to 1,000 °C, in some gas generators). The generated gas flows through the filter sieve of the generator nozzles, at high pressure, to fill the airbag. Its quick expansion and various diversions reduce the temperature in the airbag to an unproblematic level. The gas can escape again by the flow-off exhaust in the airbag (Fig. 9.8).

2-stage gas generators are often used to adapt the performance. They allow splitting the generator power, e.g., to assign 70 % of power to the first stage and 30 % to the second stage. It is possible to ignite only the first stage, both stages at once or first and second stage in succession, according to the severity of the accident and the passenger's position. For loading conditions fastened *in position*,



Fig. 9.8 Cross section of a gas generator (left 1-stage, right 2-stage). (Source TRW)

the severity of the accident has a major part in the performance characteristics of the airbag. In the OOP case, if the driver is too close to the steering wheel, the power of the airbag can be reduced (ignite only the 1st stage) to lower the risk of injury—the passenger's position is thus accounted for. If only the first layer was fired upon an accident, then the second layer has to be fired after 100 or 200 ms as well, by means of a discharging ignition, so that it will not pose any hazard to the rescuing forces.

The mounting of the airbag module at the steering wheel may alternatively apply a bolt connection or a *snap-in*. The snap-in system applies hooks at the airbag module that grip into the immobile snap-in unit at the steering wheel, establishing a connection between the parts. The *snap-in* connection facilitates the assembly, because the airbag module is simply pressed into the steering wheel, using little time for mounting. A bolt connection applies two bolts to immobilise the airbag module at the steering wheel. The assembly of the bolt connection takes more time than the *snap-in* solution. The slower mounting is outweighed by less susceptibility to noises, e.g., by road excitation.

### 9.2.5 Multi Function

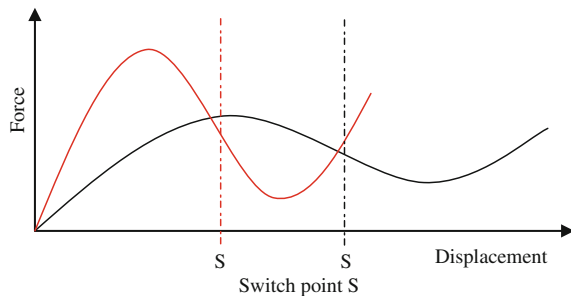
As indicated before, the steering wheel is accepting more and more electric functions and elements. One of the most widespread elements that should be mentioned is the multi function switch, e.g., for operating the car computer or the navigation system/radio. Gearbox operation/manual selection of automatic or double-clutching gearboxes is often relocated into the steering wheel. A few other functions are cruise control operation, steering wheel heating and additional displays. The transmission of functions from the steering wheel to the car is playing another role, according to the number of elements to be switched.

#### *Switch elements*

Upon operating the multi function switch (MFS), the driver receives primarily an acoustic and haptic feedback that the desired function was triggered. The keys are equipped with symbols and some are illuminated, to facilitate safe operation. The contact system and, hence, the currents and voltages to be switched are selected according to electric specifications, taking service life and temperature into account. The market supplies various micro switches that feature different haptic criteria, such as silicone switch mats whose layout can follow haptic criteria.

An essential argument for the choice of a switch element is how the haptics of the switch are specified. The haptics can be plotted in a force/displacement diagram, to indicate how the switch of a caliper will feel. A switch system is designed on account of such a force/displacement diagram (Fig. 9.9). The red line indicates a succinct circuit which is the typical design for a short stroke caliper. The black

**Fig. 9.9** Force/way diagram.  
(Source TRW)



characteristic curve is a harmonious circuit which is commonly produced using silicone switch mats.

The acoustics of a switch are usually not physically specified and have to be optimised in close co-operation between vehicle manufacturer and switch/steering wheel supplier. The switching operation should give a resounding and succinct sound. Audible low noises from sound bodies, like hollow cavities, or metallic secondary sounds, like the sounding of a spring, should be avoided. Different materials are sometimes used to produce the caliper stops.

Three ways to mount translating switches are preferred for steering wheels: the linearly controlled caliper, the unilaterally suspended caliper and the rocker caliper (Table 9.1).

#### *Transmission of functions steering wheel/vehicle*

A clockspring is a swivelling contact transmission that establishes the electric contact between the rigid cable harness in the steering column and the rotating electronics in the steering wheel. The flexible cables, rolled up into spirals, have to follow the steering wheel in both directions. Higher demands for convenience require more functions to be operated at the steering wheel. However, the number of functions that can be possibly transferred by a clockspring is limited, due to the limited space between steering wheel and column.

**Table 9.1** Comparison of switch concepts

	Linearly controlled caliper	Unilaterally suspended caliper	Rocker caliper
Advantages	<ul style="list-style-type: none"> <li>• Steady switch behaviour</li> <li>• Little use of space in X and Y direction</li> </ul>	<ul style="list-style-type: none"> <li>• Controlled system</li> <li>• Best solution for small spaces</li> </ul>	<ul style="list-style-type: none"> <li>• Controlled system, suitable for small spaces</li> </ul>
Disadvantages	<ul style="list-style-type: none"> <li>• Costly guidance tuning</li> <li>• Big use of space in Z direction</li> </ul>	<ul style="list-style-type: none"> <li>• No possibility for operation and lighting above the axle</li> </ul>	<ul style="list-style-type: none"> <li>• Operation and lighting above the axle is not possible</li> <li>• Fixing the zero position is difficult</li> </ul>

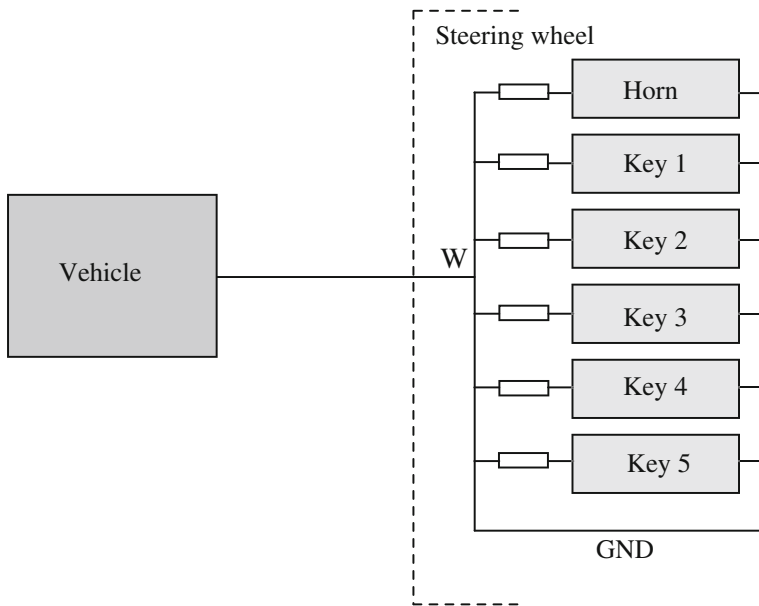


**Fig. 9.10** Voltage-coded transmission system block diagram. (Source TRW)

Two different techniques are used to transmit signals between steering wheel and car: power coding and bus systems.

#### *Voltage-coded signal transmission*

Each caliper of a voltage-coded system connects the voltage to ground by a resistance. Depending on which caliper is closed, the signal will be transferred by the clockspring to the vehicle, with its own resistance value. This is also called parallel data transfer (Fig. 9.10).

#### *Transmission by bus systems*

Specified data systems are generally applied in vehicles, e.g., CAN, FLEX-RAY, MOST and LIN BUS. Master/slave systems are often used in sensor and steering wheel applications, to establish the BUS performance within the financial budget. Taking these factors into account, the LIN BUS is often used for the vehicle/convenience functions interface.

The LIN BUS transfers the complicated functions of the steering wheel controls, for example, the multi function switches, the horn etc., to the steering shaft switch module. The steering wheel functions are processed by a micro controller (slave) and then sequentially transferred to the switch module (master) by only three lines (LIN, V<sub>CC</sub>, GND; Fig. 9.11). The transmission systems are compared in Table 9.2.

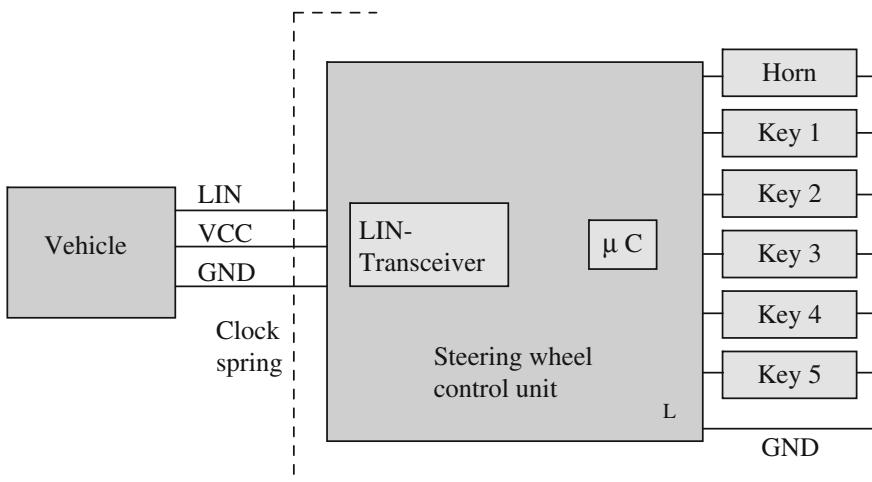


**Fig. 9.11** Diagram LIN bus transmission system. (Source TRW)

**Table 9.2** Comparison of transmission systems

	Voltage-coded signals	LIN BUS
Advantages	<ul style="list-style-type: none"> <li>• Cheap version</li> </ul>	<ul style="list-style-type: none"> <li>• Bus voltage equal to car battery voltage</li> <li>• Capable of diagnostics</li> <li>• Indefinite number of functions</li> </ul>
Disadvantages	<ul style="list-style-type: none"> <li>• Limited number of functions</li> <li>• Susceptible to temperature</li> <li>• Not capable of diagnostics</li> </ul>	<ul style="list-style-type: none"> <li>• Higher expenditure for development</li> <li>• More need of space</li> </ul>

### 9.2.6 Foam, Leather and Decorations

A steering wheel made of polyurethane foam is often integrated into the basic versions of lower or medium priced cars. A huge amount of extra equipment is further offered for individuation, for example, leather or wooden rim surfaces. A number of materials is available for the steering wheelskin (leathering):

- Grained steering wheel leather
- Smooth leather
- Perforated leather
- Alcantara
- Combinations of perforated and smooth leather
- Split leather
- Artificial leather.

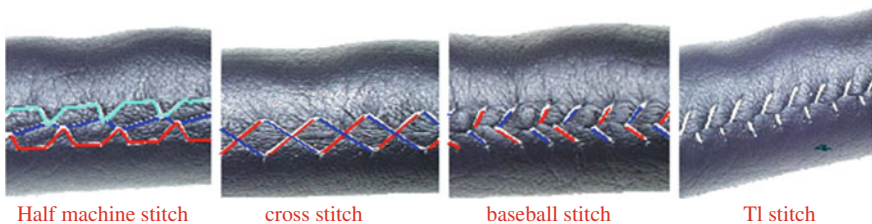


**Fig. 9.12** Kinds of stitch. (Source TRW)

And for the decorations:

- Wooden applications (burr walnut, ash, birch etc.)
- Carbon
- Aluminium optics
- Piano varnish
- Metal surfaces.

Cowhide is used as a steering wheelskin, adapted for application at the steering wheel rim by special tanning procedures. The leather is 1.2–1.4 mm thick. Only the back parts of the cowhide are suitable, because the neck and belly areas have folds and the stretch values of the material are unsteady. After punching out the unwound steering wheel strip, it is drawn by hand over the rim, fixed with glue and finally manually sewn. There are different stitches (e.g., half machine stitch, TI stitch, baseball stitch, cross stitch) to satisfy the customer's taste. Alcantara is applied in the same manner (Fig. 9.12).

Wooden decoration surfaces can be produced by different methods. The predominant materials are preformed GRP shells or die-cast plastic shells covered with a wooden veneer of only a few tenth of a millimetre thickness. Both halves of the shell are stuck together over the steering wheel rim and varnished several times by spraying or hot dipping. Intermediate grounding may be useful between the individual varnish layers, after the last layer, the varnish is polished if a high-gloss effect is desired. The application of decorative wood or carbon surfaces is very demanding and requires a lot of manual labour.

### 9.3 Requirements for Components and Assembly

The main requirements for a steering wheel are classified as design, technical realisation and optics, haptics and ergonomics. As for design, there are important features like the vehicle segment (e.g., sporty or luxurious), arrangement and number of switch elements, steering wheel diameter, steering wheel height and number of spokes. Free view on the dash and the vehicle segment are important for the choice of the steering wheel diameter. Small diameters, e.g., 360–370 mm or less, are mainly reserved to sporty vehicles, diameters of 380 mm and higher are

used for other segments. The number of spokes at a steering wheel may vary between 1, 2, 3 or 4.

The technical layout of steering wheels has to consider three factors: energy absorption upon impact, natural resonance to avoid unintentional vibrations and the mass moment of inertia. These requirements may often conflict, so that the best possible compromise has to be found. Very stiff steering wheels are ideal to meet the specifications of the natural resonance, but they impair the flexibility and, hence, the energy absorption during a crash. The mass moment of inertia directly affects the weight of the steering wheel and the natural resonance. The insertion of a vibration absorber can then be necessary. It is accommodated in the steering wheel or the gas generator of the airbag module is installed in a floating mount. Mounting and fastening of the airbag module has further effects on the natural resonance of the steering wheel. Bolt connections are then preferable against *snap-in* solutions. The actuating force of the horn should stay the same over the whole operating surface, and it should not be too high. The force is in a range of about 20–50 N, according to steering wheel and manufacturer. If the force is too high, the convenient use suffers, if it is too low, the airbag may unintentionally produce noise/rattle or *honk on its own* during driving.

The approx. 60 l airbag in its unit needs a suitable stacking space, and this can again affect the height of the steering wheel or its whole package. If the airbag clearly exceeds the rim, the OOP requirements may be hard to meet, that is why the airbag cover should not rise more than, say, 10 mm above the steering wheel rim.

## 9.4 Testing and Protection

Steering wheel and driver's airbag are parts of the overall restraint system, hence, they are also tested during slide and crash tests. Perform a test series at different speeds and offsets. The market to be supplied (USA, ECE, other) is very crucial for the scope of tests. Test any parts in advance, before a steering wheel/airbag enters expensive slide or crash tests.

Simulations help to establish the first basic design, before parts are mounted. Operational safeties and ECE-R12 are simulated for the layout of the basic structure, various puff-up and crash cases are computed for the airbag.

With the knowledge of the simulation and the design of the parts, the simulated tests are verified on the real parts, then one advances to mass production. Many different materials and surfaces are arranged inside the steering wheel in very little space. They are checked for endurance, environmental impact and quality. The ESD/EMV, long-term load and, if needed, the illumination of all electrical and electronic components is tested, first in the steering wheel and then on-board.

The steering wheel is in the driver's sight and reach at all times, much attention is therefore devoted to appearance and processing. In particular, the steering wheel should give a harmonious picture in terms of colour. The colours of the various

surfaces (PUR foam, leather, varnished surfaces) should therefore match with each other.

But the test on-board is as crucial.—How does the steering wheel feel when driving, is its rim too thick or too thin, are there any irritating contours felt when the steering wheel slips through the hand? How are pressure points of switches arranged, especially gearbox calipers? How are the general ergonomics of the steering wheel assessed, are switches within the driver's reach or hard to access?

### **9.4.1 Airbag**

To ensure the functioning of the airbag for more than 15 years, the following tests are carried out.

#### **9.4.1.1 General and Crash Requirements**

**Puff up/test at rest** The effectiveness of an airbag module is shown in static puff-up tests. No parts of the airbag may cause injury to the passenger during this test. Neither may the airbag burst, blow or come loose of the mounted airbag, either partially or completely. All airbag seams except for the tear lines must be closed.

**Electromagnetic compatibility/interference voltage resistance** Prove the electromagnetic compatibility to prevent airbag ignition from high-frequency electromagnetic fields.

**Gas concentrations** A chamber test serves to determine the gas concentration after ignition of the airbag in the vehicle interior.

**Crash requirements** The steering wheel/airbag has to be compliant with the following laws, among others:

- FMVSS 203
- FMVSS 208
- ECE-R 12
- EC 74/297
- ECE-R 94.

#### **9.4.1.2 Environmental Simulation**

The airbag should efficiently protect the passengers for at least 15 years. Environmental simulations are executed to ensure this. Suitable test methods simulate rapid ageing of the component. Table 9.3 gives an example of the scope of an airbag test before release.

**Table 9.3** Airbag tests

Serial number	Test programme for ambient simulation of the airbag module
1	Drop test
2	Mechanical shocking
3	Dust test
4	Vibration load with temperature
5	Climate change test
6	Salt spray test
7	Solar simulation
8	Thermal shock test
9	Puff-up behaviour at $-35^{\circ}\text{C}$ , room temperature and $85^{\circ}\text{C}$
10	Gas concentration
11	Tank test at $-35^{\circ}\text{C}$ , room temperature and $85^{\circ}\text{C}$
12	Airbag test
13	Reserve units

**Drop test and mechanical shocking** Airbag units can be exposed to high stress already during transport, handling and assembly. Drop tests simulate an accidental impact of the airbag during handling. They are carried out with mechanical shocking, defined impacts and hits. They mainly simulate the stress of transport, loading and driving.

**Dust test** Dust gathering over service life can cause parts of a car to fail. Dust loads are classified mainly by two causes of failure: the abrasion effect and the dust's ability to store humidity. To check these effects, the components are exposed to a predefined dust concentration in a chamber. This test is performed after mechanical shocking and before the vibration test, so that esp. the abrasive effect can be examined.

**Vibration load with superimposed temperature** Vibrations are transmitted by the chassis into body, steering column and further into the steering wheel and the driver's airbag. Over service life, such vibration loads can damage some parts, for example, by causing fissures or ruptures. In addition, resonances can expose a part to much higher loads. Therefore, the airbag is submitted to a vibration load. Cars and their parts have to withstand a broad temperature range, therefore a temperature is superimposed during this vibration test.

**Climate change test** Different coefficients of expansion when different materials are used can cause mechanical stress in a part. The climate change test helps to detect these effects.

**Salt spray test** The results of thawing salt in winter or sea salt in coastal areas are examined with the aid of the salt spray test. Salts can deposit at low temperature and in dry air, rising temperatures and humid air cause it to penetrate through openings, which may trigger chemical failures. The salt spray test is carried out as the final climatic test.

**Solar simulation and thermal shock test** The solar simulation serves to control the ageing of plastic (polymer) airbag covers exposed to ultraviolet rays. The solar simulation is followed by a thermal shock test, to detect any material changes or fissures that could prevent the airbag cover from proper tearing.

After the environment simulations (Table 9.3, serial numbers 1–8), the airbag modules have to meet the following requirements: Puff-up behaviour, Gas concentration, tank test, Airbag test and Reserve units. The appearance of the airbag cover (visible tear lines) has to be in pristine condition (see Table 9.3, serial no. 9–13).

The integration of electronics like multi function switch, switch paddles, steering wheel heating or displays forces the steering wheel to meet *electromagnetic compatibility* (EMC) requirements. The interaction of electric devices by electromagnetic fields and their technical and juridical background are stipulated in ECE R-10 (=95/54/EC) and 95/56/EC.

## 9.4.2 Steering Wheel

### 9.4.2.1 Operational Safety

A number of operational safety requirements are defined for the steering wheel that vary for each manufacturer. The following tests shall give an overview of the most current requirements. Some manufacturers may apply supplemental or divergent tests, they will not be discussed here.

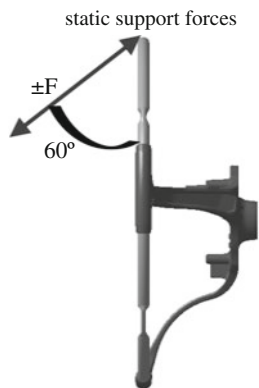
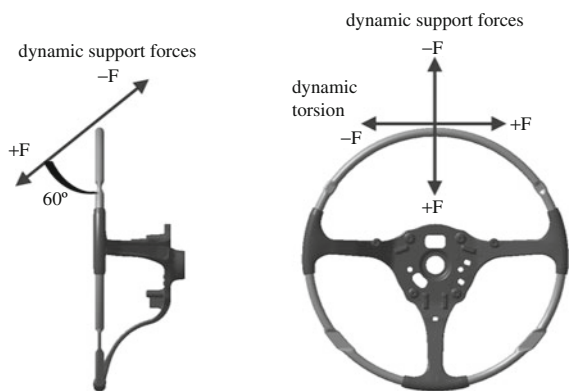
#### *Static strength*

The static strength is examined by pull, push and torsion tests. The pull/push test is performed by determining the support forces. For this test, the steering wheel is clamped tightly to the hub and a force is applied to the middle of the rim segment at an angle of 60°. First 500 N are applied to observe the beginning of plastification, then 700 N to observe the displacement. The elastic and plastic deformation of both force levels are recorded as a percentage of the rim diameter, any developing tears are a criterion for failure. The force is raised in an additional parts test until the steering wheel ruptures or an overall distortion of 20 % occurs. The permissible elastic and plastic deformation is defined by the respective vehicle manufacturer (Fig. 9.13).

The torsion resistance is examined when the rim is tightly clamped, a torque of 250 Nm is applied to the hub. The plastic deformation after discharge should be <3°, no tears or fissures may develop.

#### *Dynamic strength*

By analogy to the static strength, a dynamic test of the support forces is performed by testing the steering wheel against at the hub, a force is applied at 60° in the middle of the rim segment. A pull of the steering wheel with 300 N (towards the driver) and a push with 100 N is applied at a test frequency of 1–3 Hz. 180,000 changes of load with a survival probability of 50 % have to be achieved.

**Fig. 9.13** Static strength**Fig. 9.14** Dynamic strength

Any tearing, loosening screws or a load figure of 360,000 changes are defined as criteria to pass the test (Fig. 9.14).

The load direction of the dynamic torsion test is tangential to the central line of the rim, the point for applying the force is the middle of the rim segment. The steering wheel is solidly clamped at the hub. A force of  $\pm 250$  N is applied to the steering wheel at a test frequency of 1–3 Hz, the same load figures and finishing criteria apply as for the examination of the dynamic support forces.

#### *Identification of the natural frequency*

The natural frequency was established before by the finite element method, and is now verified by fixing the steering wheel on a *rigid mount* as it would be in the car, including the original steering column and screw connections. The mass of the supporting table should be 20–50 times higher than that of the examined part. The part is excited slightly with an impulse hammer. Free vibration develops. The two signals are recorded, both by the impulse hammer and by an acceleration receiver

mounted at the part. The resonance frequency is then acquired. The measurement is performed for all vehicle co-ordinates x, y and z.

#### *Identification of the mass moment of inertia*

A steering wheel's mass moment of inertia is determined at the middle of the hub from the time cycle around the bearing point. To test the steering wheel, it is mounted on a torsion rod and excited to vibrate. The time of the vibrations is measured and converted into a mass moment of inertia.

### **9.4.2.2 ECE-R12**

This regulation applies to the behaviour of automotive steering equipment, concerning the protection of the driver in a frontal collision.

This law stipulates that two tests have to be carried out for the release and registration of the steering wheel: the body block test and the head impact test.

#### *Body block test*

In a body block test, a sample (torso) with a defined mass of 34–36 kg and a speed of at least 24.1 km/h impacts the steering wheel. The highest force horizontal/parallel to the longitudinal axis may not exceed 11,110 N. The body block test can be carried out on a simplified bench, if the test bench the steering wheel is mounted on meets the same geometrical requirements and has a higher fatigue strength than a vehicle front end, and if this is requested by the manufacturer and approved by the technical service. If the vehicle is equipped with an airbag, the test is performed when the airbag is filled. If the car has an adjustable steering column, the steering wheel is positioned according to the standard position defined by the vehicle manufacturer (usually the middle of the height and length adjustment). The stiffest spoke and the most pliable part of the rim are checked as impact points of the steering wheel. For any other positions, check with the technical service.

#### *Head impact test*

In the head impact test, a hemisphere with a mass of 6.8 kg and a diameter of 165 mm is flung at the steering wheel at a speed of 24.1 km/h. The deceleration upon the sample's impact on the steering wheel may not exceed 80 g accumulated over 3 ms, or 120 g maximum force. The steering wheel has to be vertical to the impact direction. As in the body block test, a simplified test bench may be used. The following positions are tested: steering wheel centre, the contact point of the stiffest or strongest reinforced spoke at the inner edge of the rim, the centre of the shortest, not reinforced spokeless part of the rim upon touching the head form and, on request of the permit authority, a point representing the *worst case* at the steering wheel.

The above-mentioned forces of 11,110 N and the most powerful deceleration of 120 g are defined as finishing criterion of either test. No sharp or rough edges may develop nor any parts turned towards the driver that would increase the risk of injury.

#### 9.4.2.3 Environmental Simulation, Varnish Test, Electroplating Test

##### *Environmental simulation*

An environmental simulation is carried out to check materials, components or subassemblies for resistance against environmental influences. A realistic test would take 15 years to cover the whole vehicle life. The environmental simulation helps to model accelerated ageing, applying suitable methods like higher temperatures, higher energy input or superposed climate (dampness, heat).

A test series is performed on the semi-finished products, foam, leather or decoration surface. One checks for foam hardness, leather thickness, abrasion resistance of the leather or decoration, thermal resistance, ignition response and a huge number of other criteria.

In addition, three essential tests are performed at the steering wheel: the climate change test, the calorific storage and the solar simulation.

The climate change test covers 60 cycles of 12 h each, applying temperature and humidity. The temperature shifts from  $-35$  to  $90$  °C and the relative humidity from 30 to 80 %.

The highest temperature reached at the on-board steering wheel is approx. 100 °C. To check this temperature, calorific storage is used. For this test, the steering wheel is stored at 105 °C in an air oven for 504 h.

Solar simulation means that the on-board steering wheel is exposed to an irradiation of  $830 \pm 80$  W/m<sup>2</sup> for 240 h.

##### *Varnish and electroplating test*

If any varnished or electroplated parts are used in the steering wheel or at the operating surfaces, these are checked according to the specifications.

Varnished surfaces require, for example:

- Varnish adhesion (grid cut)
- Scratch resistance
- Thermal resistance
- Climate change test
- Ageing under hot light
- Emission response
- Surface resistance against media
- Cream resistance
- Wear.

Electroplated surfaces are checked for the following criteria:

- Adhesion strength
- Scratch resistance
- Thermal resistance
- Thermal shock resistance
- Thermal change resistance
- Climate change test

- Corrosion resistance
- Surface resistance against media
- Cream resistance.

### **9.4.3 Controls/EE**

#### *EMC/ESD*

*Electromagnetic compatibility* (EMC) defines the technical and juridical basis of the mutual influence of electric devices by their intrinsic electromagnetic fields.

Although the steering wheel does not really count as an electric component, the implementation of multi function switches, gearbox operating switches, steering wheel heatings or displays may turn it into a product which is subject to the EMC directives. The legal requirement for vehicles and individual parts with regard to their electromagnetic tolerance are regulated by ECE R-10 (=95/54/EC) and 95/56/EC.

#### *Key endurance run and environmental impacts*

To establish the reliability of operating keys for the entire vehicle life-time, key endurance runs are performed at normal, freezing and hot temperatures. The mechanical and electric functions are monitored and force/displacement measurements are used to evaluate the haptics in comparison to the original state before, during and after the test.

The switches are submitted to other tests, like electric stress (e.g., excess voltage, short circuit or reverse polarity), mechanical stress (e.g., vibrations, shock, free fall), climatic and thermal stress (e.g., humid heat, thermal shock), chemical stress by liquids (e.g., cleaning agent, spirit) and dust. Key symbols are examined for the positioning of colours and the intensity of lighting.

## **9.5 Modularisation, Trends of Development, the Future**

Esp. vehicle manufacturers of the premium segment offer a high degree of individuation to their customers, generating a huge number of steering wheel versions. Many versions can be realised simply by modularising the subassemblies. Modularisation can be seen at the example of a Porsche steering wheel. Four steering wheel covers, six foaming moulds and one additional display create a huge number of versions to select from, since all these parts can be combined.

Driver's airbag units are continuing to become smaller and more compact, with the purpose to maintain an airbag size of approx. 60 l. Furthermore, the airbag systems are more commonly adaptively designed, combined with one- or two-stage gas generators. The significant mass of the gas generator is used more and more often as a vibration absorber (see also [Chap. 6](#)).

The advent of camera-based assistance systems on-board to recognise, e.g., traffic signs or a departure from the lane, led to the more common use of vibration cassettes (imbalance motors) in the steering wheel that actively excite the steering wheel when the lane is left, to warn the driver (LDW—Lane Departure Warning). Various warnings or speeds can be indicated by the steering wheel, e.g., in the rim.

The inclination towards on-board individuation is growing, requiring individual material concepts for the steering wheels (e.g., electroplating, PVD coating, carbon, decorations, stone, open spokes with visible basic structure) and additional switches, e.g., for chassis settings or warning displays.

# **Chapter 10**

## **Steering Column and Intermediate Steering Shaft**

**Jörg Hauhoff and Ralf Sedlmeier**

### **10.1 Introduction**

The basic function of steering column and intermediate steering shaft is to establish the mechanical link between steering wheel and steering gear. The steering wheel and the torsion bar of the steering gear are linked in such a way that any rotation initiated at the steering wheel will be converted almost without loss or backlash. Torques issued from the steering gear are likewise converted to the steering wheel. The connecting elements, steering column and intermediate steering shaft, hence, affect the driveability and the perceptible contact with the road. Beside this basic mechanical function, there are now various other demands to both subassemblies. Among the components discussed here, from the driver to the front axle, the steering column primarily assumes the role of supporting the upper steering shaft. It consists of a shaft that interfaces with the steering wheel, which is composed of one or more parts, and of the intermediate steering shaft. This design is called a rigid steering column, it transfers merely the steering function but does not allow adapting the position of the steering wheel. Such systems have become rare and limited to very few segments, on account of their considerable deficits. Racing cars are an exception, because performance is more important than convenience here.

In the next stage of development, the steering column also permits positioning the steering wheel relative to the driver. One distinguishes tilt and vertical/longitudinal adjustment. Both mechanisms can be implemented either separately or combined, the latter being the more common method. For example, gate systems of manually adjustable steering columns enable a combined relative

---

JörgHauhoff (✉) · R. Sedlmeier  
Willi Elbe Gelenkwellen GmbH & Co. KG, Tamm, Germany  
e-mail: joerg.hauhoff@steeringhandbook.org

R. Sedlmeier  
e-mail: ralf.sedlmeier@steeringhandbook.org

movement between the vehicle-fixed case and the jacket tube. Electrically adjustable steering columns are driven by one or two motors and use independent mechanisms to generate both shifting movements. Parallel use of the drives adjusts tilt and length simultaneously, so that any points within the shifting range can be accessed by a nearly straight motion. The challenge is to provide a great shifting range of the steering wheel, while using little space for the column.

Once the driver has set the best ergonomic position, the movable part of the adjustment has to be reliably locked with the stationary casing. Manual steering columns can be locked by positive or non-positive systems, sometimes even by combined systems. It is important that the locking mechanism has to lock and unlock smoothly while generating high clamping forces. Electrically adjustable steering columns lock as a rule by autolocking drive systems.

Steering columns can also make a considerable contribution to safe driving. They are then called safety steering columns, and if the car crashes and the driver is hitting the airbag, they give way in a predefined manner. Beyond a specific, mechanically adjustable force level, a mechanism is triggered which permits moving those parts of column and steering wheel that enter the passenger area towards the front end of the car. Together with safety belt and airbag, they are systems that may generate space important for survival. The level of the force/travel characteristic curve in particular, the tolerance width of the characteristics and the response of the mechanism define the effectiveness of this system. The trigger can be either passive or active. A passive trigger is activated by the impact of the driver, overload elements like mole pins will usually break. An active trigger is operated at need by an ECU evaluating sensor signals. Pyrotechnic triggers are most often used in this case, because of their high-speed response.

Other functions of the steering columns are:

- to accept mechanical or electric locks for theft protection,
- to mount steering shaft switches (indicators, windshield wipers, multi function switches),
- to position clocksprings (airbag) and/or rotary angle sensors,
- to integrate torsion dampers or friction bearings to dampen vibrations,
- to accept superimposing gearboxes, see [Chap. 16](#).

One distinct challenge in the technical layout of the steering column is the requirement for space, stiffness and weight. There are perceptible elasticities which can become apparent, e.g., when the driver enters or leaves the car, and there are very high requirements to the 1st natural frequency of these systems, being a measure of the ability to transmit and possibly to amplify vibrations from external excitation. Exciters may be the engine, auxiliary units or the road. [Chapter 6](#) is exploring this in more detail.

Intermediate steering shafts represent the link between steering column and steering gear. The most basic configuration is a one-piece cardan shaft with two universal joints. Modern systems have a high density of performance to transfer high static or dynamic forces, even in very limited space. Intermediate steering shafts are adjustable, i.e. they dispose of a length compensation in which the shaft

can be separated, if necessary, so that it will not penetrate into the engine compartment when the drive unit is assembled. This compensation also serves to even out any tolerances or elastic distortions from dynamic stress or to compensate the movement along the steering column. Joints and compensation have no backlash and little friction. Prestretch the bearings of the universal joints in a defined manner and provide them with precise fits. The length compensation may be achieved by implementing splined shaft treads, using dividing layers that can easily slide. Other kinds of implementation are:

- Constant-velocity joints
- Drivelines with up to four joints and corresponding intermediate bearings
- Bearings and gaskets for cowl breakthroughs
- Length compensation with crash function.

## 10.2 Subassemblies

Steering column and intermediate steering shaft can be configured either as one common module or as separate parts. The column consists of the driveline carrying the torque (upper steering shaft) and the adjustable unit. There are two kinds of implementation, distinguished by the operation mode of the adjustable unit:

- Manually adjustable steering column
- Electrically adjustable steering column.

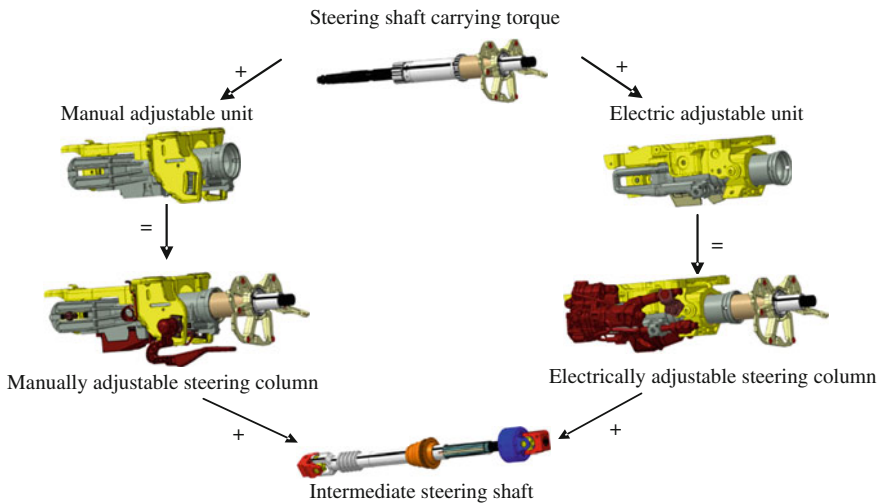
The intermediate steering shaft is linked to the steering column and establishes the connection with the steering gear.

Figure 10.1 shows the most basic implementation of a modular system for manually and electrically adjustable steering columns and shafts. Both column types can be configured by combining them with a manually or electrically adjustable unit, beginning with the upper steering shaft.

The variety is considerably increased by different drivelines (e.g., with or without lock) or special implementations of the adjustable units. If the corresponding shaft is part of the scope of delivery, the variety multiplies with every type. Typical shaft versions are separate implementations for e.g., right-hand, left-hand steering or four-wheel-drive vehicles.

### 10.2.1 Upper Steering Shaft

The upper steering shaft in Fig. 10.2 is connected to the steering wheel and the intermediate shaft. The interfaces are positive connections which are preloaded by screwing. Some available standard connections are splines, double or multiple corner connections, they are made in such a way that the possible assembly is unequivocal. This design ensures that steering wheel and shaft are aligned in a



**Fig. 10.1** Modular structure of steering column and intermediate steering shaft

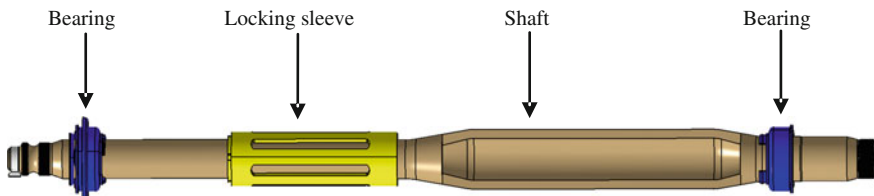


**Fig. 10.2** Upper steering shaft, Porsche 911

pre-defined position. The driveline is mounted without backlash on preloaded supports in the jacket tube.

The shaft of the steering driveline may be either hollow or full. Additional functions are:

- Integration of the upper crash element and length compensation
- Fixation of the indicator reset cam
- Fastening of the locking sleeve to adjust the steering lock.

### 10.2.2 Manually Adjustable Steering Column

The representation in Fig. 10.3 shows different types of manually adjustable systems. The left system (BMW 5) has a conventional gate duct in both main directions, the right system (Porsche 911) is lifted and tilted by a wing and a slider.

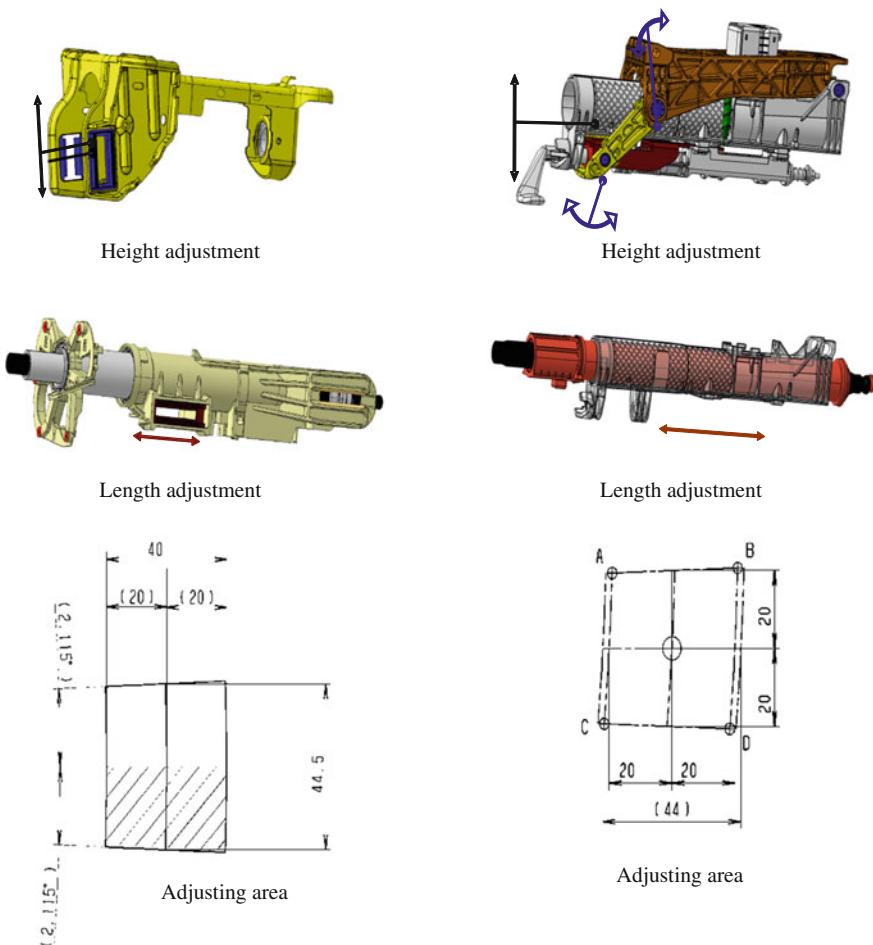


**Fig. 10.3** Manual steering column adjustment (left BMW 5, right Porsche 911) with adjusting area

The length is adjusted by moving the jacket tube. Although both systems clearly differ by kinematics, the shifting range is quite comparable, featuring 40–44 mm of travel in either direction. On account of the lever ratios, the change of tilt can be neglected for these systems. These adjustable units have in common that vertical and longitudinal adjustments are positively locked by interlocking elements.

### 10.2.3 Electrically Adjustable Steering Column

For these adjustable units, kinematics that are modified from the manual adjustable unit are used, see Fig. 10.4. The length is adjusted by an axial movement of the jacket tube, similar to the manual adjustment, but height and tilt are shifted by the

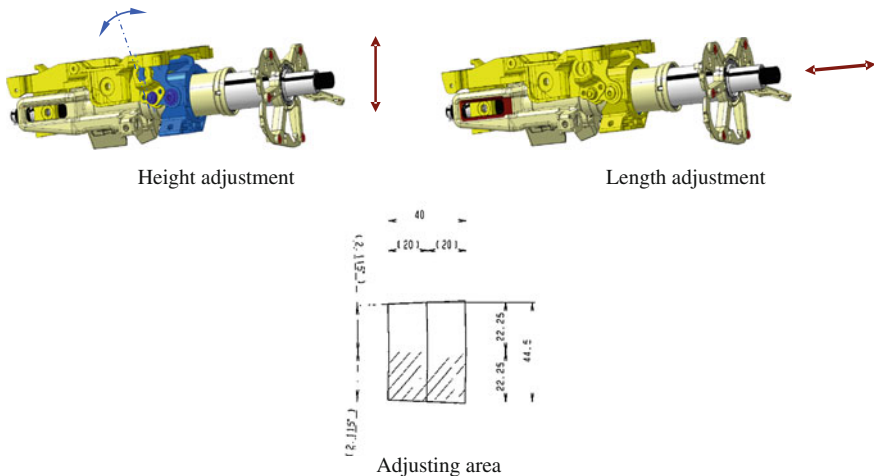


**Fig. 10.4** Electric steering column adjustment (BMW 5) with adjusting area

tilting movement of a wing. This is necessary because of the active direction of the electrical drives. The requirements for shifting range and steering wheel tilt are the same as for the manual adjustment.

#### 10.2.4 Intermediate Steering Shafts

The intermediate steering shafts of Fig. 10.5 are specifically configured parts which can differ a lot even within the same vehicle series, depending on the vehicle's configuration (e.g., right-hand driver, left-hand driver or four-wheel-drive vehicles). According to the arrangement of the steering shaft, constant-velocity joints, i. e. centred double joints, can be used instead of normal universal joints for right-hand drivers. Advantages of this configuration are the higher permissible working angle,  $>45^\circ$ , the nearly suppressed asymmetry and the known gimbal error.

The implementation of the length compensation has to distinguish the following requirements:

- Length compensation to compensate tolerances of the shell or assembly
- Length compensation to adjust the length of the steering column, for columns with a one-piece shaft without length compensation
- Length compensation with defined crash response.

The steering shaft with corrugated tube shown is part of a separate intermediate steering shaft. Separate shafts are often used to provide space for assembling the engine. The steering shaft with corrugated tube consists of transformed cross sections of different wall thickness, this creates a defined displacement response for discrete force levels in the range of moulded shafts.



Intermediate steering shaft with 2 universal joints + length compensation



Intermediate steering shaft with 2 centred double joints + length compensation



Steering coupling with corrugated tube



More piece I-shaft with top mount

**Fig. 10.5** Intermediate steering shafts

The multipart intermediate shaft consists of three joints and a top mount, fastened at the cowl. A sliding fit (orange), fastened above the top mount, bears the cowl gasket. In addition, this shaft has a tube-shaped torsion absorber (blue).

According to the kinematics of the front end, it may be necessary to use combinations of the configurations shown here. These also consist of shafts with combinations of single and double joints.

The state-of-the-art of intermediate shafts is to make them from non-corroding aluminium alloys or from steel. Extreme requirements to the permissible operation temperature, especially when met with high stakes for corrosion prevention, may suggest the use of stainless steel shafts.

#### 10.2.4.1 Gimbal Error and Centre Point

When a simple, bent universal joint is used, the gimbal error or degree of uniformity becomes relevant. Kinematics requires the output angle to follow the input angle asynchronously. It deviates in a sinusoidal curve, progressively with the deflection angle  $\alpha$ . The ratio of the derived angular velocities jitters around the gimbal error  $\Delta i$ . The power balance  $P = M \omega$  has to be fulfilled at the input and output side of the almost losslessly rotating universal joints, hence, the ratio of rate and torque can be computed from the rotary angle  $\varphi$  of the universal joint acc. to Eq. 10.1. A sinusoidal conversion of the rotation of rev and torque with twice the frequency of the joint (2nd order) is the result.

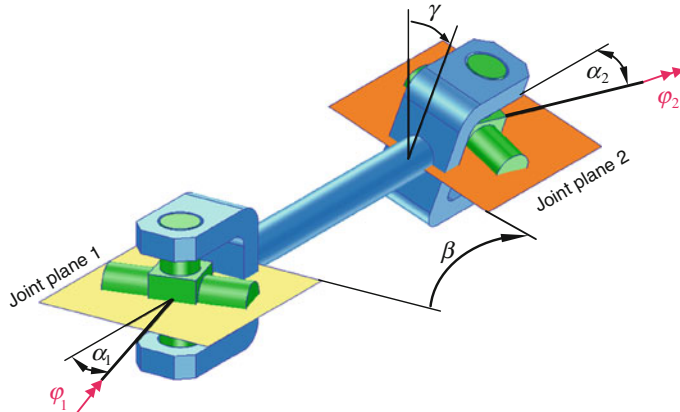


**Fig. 10.6** Shaft of a 2-piece joint chain, arranged in space

$$i = \frac{\omega_{Output}}{\omega_{Input}} = \frac{M_{Input}}{M_{Output}} = \frac{2 \cdot \cos(\alpha)}{2 - \sin(\alpha)^2 [1 + \cos(2 \cdot \phi_{Input})]} \quad (10.1)$$

Another result of the power balance is that the overall ratio of a chain of several joints is derived for every rotational angle from the multiplication of the individual ratios. The relative angular positions of the joints, called offset angles, produce different curves of the overall ratio from that, and they may differ significantly in phase and level of the gimbal error.

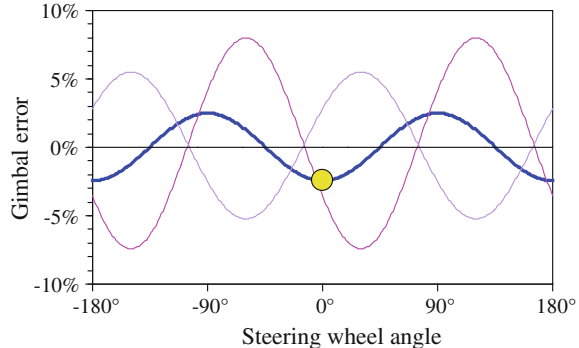
Assuming that the torque at the steering gear  $M_{Output}$  for turning the tyres will remain steady, the gimbal error in Eq. 10.1 corresponds exactly to the jitter of the steering wheel torque which the driver feels at his or her hands.

Two joints with equal working angles allow to fully compensate the gimbal error. Mounting space will most often prevent such an arrangement. Hence, in the usual case of two or several joints that are not bent in the same plane, an attempt is made to adjust the freely eligible offset angles  $\gamma$  in such a way that there is as little asymmetry left as possible, taking easy mounting into account. A chain of two joints bent in space, typical for steering shafts, is shown in Fig. 10.6.

The transmission ratio  $i$  of a steering with two joints is a function of the working angles  $\alpha_1$  and  $\alpha_2$ , the angle between the joint planes  $\beta$  and the offset angle  $\gamma$ . The plane of each joint is stretched along the axes of rotation of the accompanying drive shaft and driven shaft. Duditza describes the mathematical relationship of the ratio of the rotational angles  $\varphi_1$  and  $\varphi_2$  by Eq. 10.2.

$$\tan(\varphi_2) = \frac{\cos\alpha_2 (1 + \tan^2(\gamma - \beta)) \tan(\varphi_1)}{\cos\alpha_1 (1 + \cos^2\alpha_2 \cdot \tan^2(\gamma - \beta)) - \sin^2\alpha_2 \cdot \tan(\gamma - \beta) \cdot \tan(\varphi_1)} \quad (10.2)$$

**Fig. 10.7** Gimbal error and centre point



The transmission ratio is lowest if  $\gamma = \beta$ . In this case:

$$\tan(\varphi_2) = \frac{\cos\alpha_2}{\cos\alpha_1} \tan(\varphi_1) \quad (10.3)$$

If  $\alpha_1 = \alpha_2$ , then the movements are synchronous, hence  $\varphi_1 = \varphi_2$ . For any  $\alpha_1 \neq \alpha_2$ , the remaining asymmetry is used to improve the driveability. The minimum of the gear ratio (centre point) is then set on straight driving, so that an additional centring develops around the zero position. Symmetrical, slightly higher torques are then required for steering. At the same time, the ratio of steering wheel angle to steer-angle of the steering wheels is highest.

Figure 10.7 shows the joint degree of uniformity for a steering shaft of two phase-shifted joints, represented by thin lines. They overlay to create the full asymmetry, plotted in blue, so that the gimbal error is lowest and the centre point is found at the straight position of the tyres. The position of the centre point is indicated by a yellow dot.

A phase shift of the centre point by  $90^\circ$  would mean that straight driving was less stable. The torque would symmetrically drop from the zero position. An offset of  $45^\circ$  has a similarly negative impact, because the steerability to the left or right would be markedly different. On account of these relationships, the kinematics are analysed very carefully, because the driveability is significantly influenced by the arrangement of the joints. Target values of the asymmetry are less than 3 %.

## 10.2.5 Parts of the Subassemblies

### 10.2.5.1 Adjustable Units

The adjustable units enable the driver to change the position of the steering wheel relative to the driver's seat and, hence, to assume an ergonomic position. The adjusting can be driven either by hand or servo motors which can be activated by a switch. Two-way adjustable units are becoming prevalent even in small vehicles,

while the more complex and more expensive electrically adjustable columns so far are a standard equipment only in the upper middle class and higher.

### Manual Locking

The mobile part of the adjustable unit is locked at the stationary housing by the driver's hand moving a swivelling or pushable lever. Hence, the shifting travel required and the level of the actuating force are important parameters for convenience. The operating force should be steady and very low, while undesired loosening from vibrations or motions of the car has to be avoided. A perceptible snap-in point should give a feedback to the driver that the system is locked. High locking forces are welcome to prevent the steering wheel from slipping in a crash.

Predominantly, a rotation of the lever is converted by a ramp into an axial movement of a clamp piston, bracing the jacket tube with the stationary housing. The discrepancy between comfortable shifting and safety requirements is tentatively solved by variable ramp inclinations that become flatter with higher lock angles. Low friction at the ramp increases efficiency and clamp force, friction-type materials, grease or rolling elements are used for this reason. Non-positive and positive locking mechanisms are used, as in Fig. 10.8.

The non-positive locking mechanisms build up the hold forces by friction, depending on the clamp force. Their main advantage compared to positive locking mechanisms is that they can be continuously shifted. They often have a rib package whose hold force increases with each additional interstice. However, the rib packages raise the system cost and the needed space. They also make high demands to evenness and finish of the rib surfaces. Hence, they are sensitive to dirt and corrosion that deteriorate the surface.

In positive locking mechanisms, splined segments interlock to transfer high hold forces, regardless of the clamp force. Their main advantage is that they need less space. The splines can be shifted only by an integer multiple of the cog division, hence, only defined steering wheel positions can be set. Smaller splines at lower distances permit a finer division, but they transfer smaller hold forces. Too slightly inclined splines are no longer retained by self-retention. The greater and

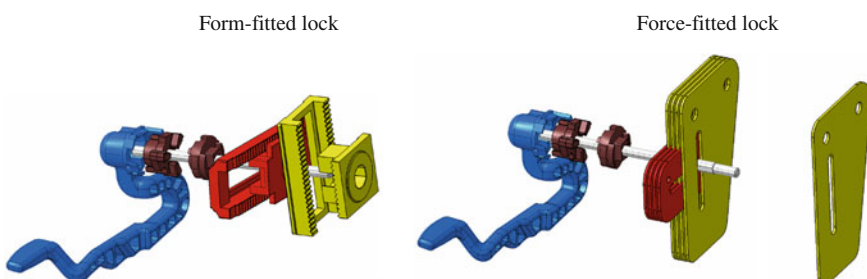


**Fig. 10.8** Positive and non-positive locking mechanisms

pointier the splines are made, the more stroke is required to separate the cog segments. The steep ramps needed increase the lock forces. The possibility of head/head positions of the splines is typical, preventing their mating. These appear more frequently, the bigger the ratio of cog head radius to cog division is designed. In this case, the lever cannot be locked until the driver has changed the steering wheel position. In spite of a huge number of concepts, no mechanism could prevail at the market which would efficiently prevent the splines from blocking.

Thus the specific advantages and disadvantages of positive and non-positive locking mechanisms suggest an individual choice for each vehicle. Both non-positive and positive locking mechanisms are widespread today.

### Electric Drive Unit

Mechanically commuting permanent-magnet DC motors with internal rotors are used to drive electrically adjustable steering columns, providing high economic efficiency and reliable technology. The motors are operated by an ECU and can be equipped with sensors to detect the shifting, usually measured without physical contact by using the Hall effect. Measuring the travel avoids touching the end stops that could produce noise and load peaks—even the risk that the friction-retained spindles drives might block.

There are either two motors to drive either movement axes, or one engine is operated by a switch gear. In this case, the two driving axes cannot operate simultaneously, and this results in longer driving times. A step-up gear changes the motor rotation into an axial translation. The parts of the shifting mechanism may not give way under the high loads of a crash and, hence, must be retained by friction. Worm gears are common, see Fig. 10.9. In this application (BMW 5), the drive is an engine with a switchable gearbox. The spindles can be either rigid or flexible to realise the necessary kinematics.

The adjusting movements are either initiated at the driver's will or controlled by convenience electronics. The memory function, for example, returns on ignition

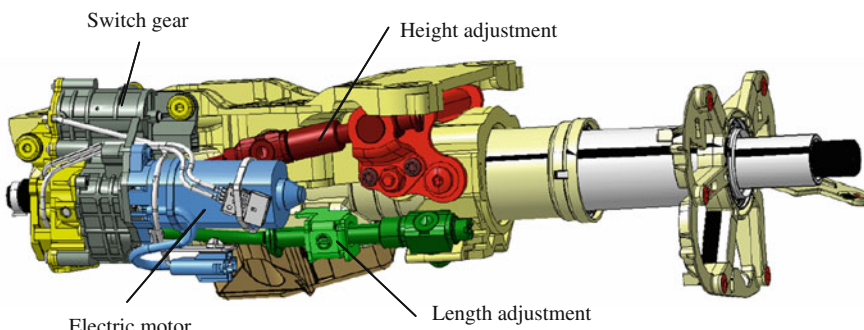


**Fig. 10.9** Drive unit of an electrically adjustable steering column (BMW 5)



**Fig. 10.10** Noise test in the production line

to its last position when the driver has changed, or the Easy Entry function will move the steering wheel into a limit position to ease climbing into the car. Thus adjusting is regular and compelling, even at very low temperatures, and this makes particular demands on the design. The requirements for service life and qualities at extreme temperatures are higher than those for mechanical shifting equipment.

One major challenge is the meeting of the noise requirements. The motors are inevitably close to the driver and well audible, particularly as the vehicles of the relevant classes are becoming less noisy. Interfering noise has to be avoided and the sound level limited, the sound pattern has to appeal as well and should not change under changing operating conditions. The steering wheel load is either stressing or relieving, according to the direction of the motor, the two shifting directions in most cases need different transmission ratios and temperature effects are inevitable. Therefore, the uncontrolled motors are running at different revs and can sound differently. Serial scattering can excite resonances in the car which are perceived as interfering noise.

The use of RPM controlled engines is uneconomical, the manufacturers therefore try to maintain the noise quality by decoupling the motors and measuring throughout the series. The drives in the power flow cannot be linked too softly, because of the requirements for crash and stiffness. Complex tests are therefore common. Subjective tests by listening are accompanied by measurements of the noise at the motors and the shifting equipment. Structure-borne sound receivers record spectra to be analysed, so that resonance positions of the vehicle can be considered, too. Figure 10.10 shows the noise test accompanying the full series.

#### 10.2.5.2 Upper Steering Shaft Including Jacket Tube

The jacket tube, in which the spindle is mounted swivelling in its bearings, is positioned by the adjustable units. The jacket tube of modern steering columns is

not tube-shaped any more, but it is an aluminium or magnesium die-cast part of complicated shape, including parts of the locking mechanism, the steering lock or the crash function.

The spindle bearings are specially developed, maintenance-free and low-friction roller bearings without clearance, due to preliminary tension; most often they are needle, four-point ball or angular contact ball bearings. Rev and bearing loads from steering are low. Development is therefore focussing on isolating noises, optimising the structure space, sealing and easy assembly, not to mention reducing costs.

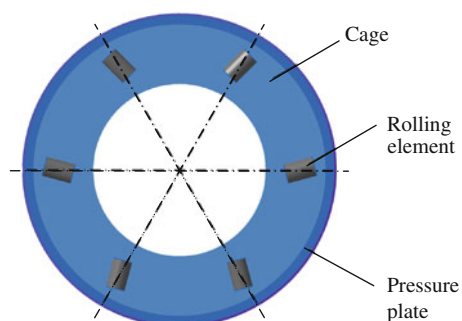
Optionally, special friction bearings may be used to dampen rotary oscillations of the steering wheel, see Fig. 10.11. They are non-standard axial needle bearings, having crossed rolling elements that do not roll precisely but slide in addition. The friction moment required to achieve the desired damping is adjusted by a predefined axial tension which is applied, for example, by a corrugated spring.

The spindle often has a length compensation which permits a linear expansion for axial shifting and retraction of the steering column in a crash case. This most often concerns synthetic-coated cog shafts, because the steering torque has to be converted by the length compensation.

In the case of an overloaded steering wheel, a safety steering column, together with the part of the shaft that is near the steering wheel, moves away from the driver. This possibility has to be taken into account during the concept phase as an integral part of the adjustable unit. The legal requirements for driver's safety cannot be met without a safety steering column, all new vehicles in the great industrial nations are therefore equipped with them. Seat belts are not obligatory everywhere, and legal requirements for crashes have to be observed even if the driver is not buckled up. The energy-absorbing effect of the seat belt is lost then, hence, the interaction of airbag and safety steering column is most important. Common systems have parts of an adjustable unit that are retreating on sliders or outer tubes retreating into a jacket tube. Figure 10.12 shows the plan of the BMW 5. This system has lower accelerated masses and does not need more space.

A snap-on element may be found on the steering shaft that can be engaged by a locking cam to prevent theft. The locking mechanism is integrated into the jacket tube. Electrically operated locking mechanisms are replacing the conventional

**Fig. 10.11** Fundamental roller bearing orientation of a friction bearing



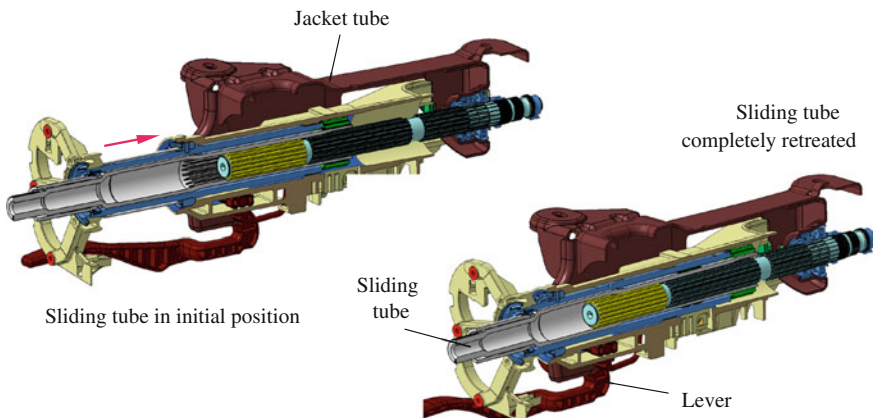


**Fig. 10.12** Collapse system of the safety steering column BMW 5

mechanical steering locks. The increasing electrification of vehicles permits realising a cheaper theft prevention by electronic locks. These systems will displace the locking mechanisms from the steering columns.

### 10.2.5.3 Crash Elements

All safety steering columns have a crash element that upon retreating generates a defined force opposing the airbag. Without this opposing force, the airbag could not unfold its protective effect. All passive safety parts, like airbags, seat belt, seat belt limiter and crash element, are precisely tuned to low backing values for the driver. Hence, the safety steering columns have to meet highest requirements for functions and their reproduction. The crash function may be required only once, but it must be reliably available, even after many years of operation.

Different force/displacement characteristic curves of the crash element are possible, see Fig. 10.13. Long absorption paths are basically favourable. In the closely occupied compartment, though, the space required by the retreating parts often cannot be kept available as desired. Steady or progressive characteristic curves with force levels between 1 and 10 kN and an absorption path of 60–120 mm are common. Demands for good reproduction enforce very low scattering of the force/displacement characteristic curves. Hence, concepts prevail that apply a material which is deformed or torn. High energy density at low costs is achieved this way.

Deforming crash elements exploit the low scattering range of the elastic module of metals. Their shapes are manifold. Wires and metal sheet strips of different cross sections are known which are either unwound or bent by rolls. Their cross-sections can extend or shrink along the absorption path to alter the force. Figure 10.14 shows some typical designs.

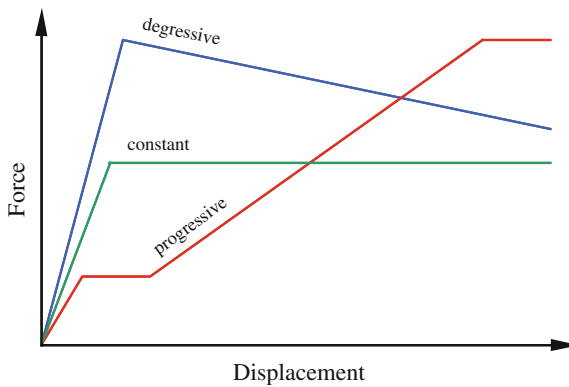


**Fig. 10.13** Qualitative characteristic curve of an absorber

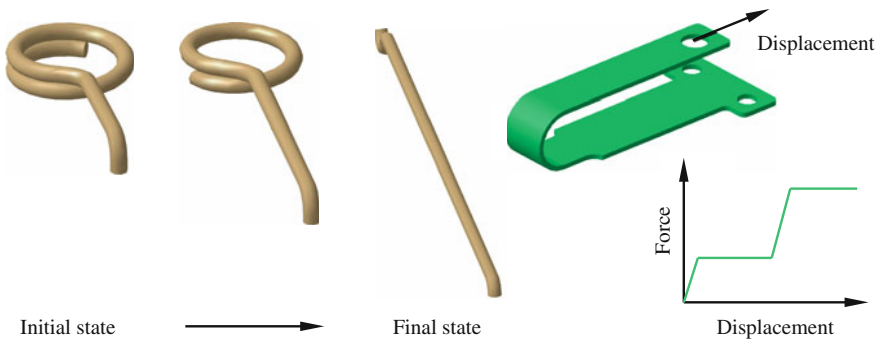


**Fig. 10.14** Metal crash elements (wire and metal sheet strip)

Deforming crash elements show wider scattering when the force is high, because friction effects are unavoidable. The production process may include batches of varying material parameters that require a calibration of the sizes and extensive quality-protecting measures.

Crash absorbers exploiting reproducible rupture processes occur in many shapes as well. There are metal bodies with rupture lines of less sturdy material that act like the seals of cans, but there are also tube-shaped GRP (glass fibre reinforced plastic) or CFRP (carbon fibre reinforced plastic) parts which are very light. The impact of friction and variations of the material batches is here much lower.

Figure 10.15 shows a GRP tube that was torn into strips by a ring with a defined contour. The characteristic curve is created by a variable number of internal tissue layers. The curves of GRP parts scatter very little, see Fig. 10.16. They are resistant to ageing and corrosion and need no additional space, because they disintegrate.

The alternate use of several crash elements for different crash scenarios is still rare. On ignition they can be selected by the crash sensors to take account of the

**Fig. 10.15** GRP absorber after crash

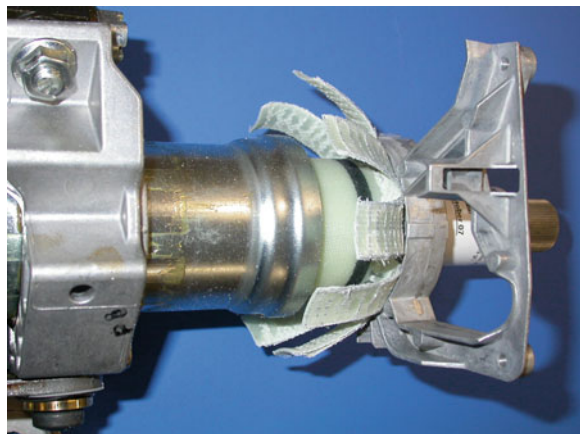
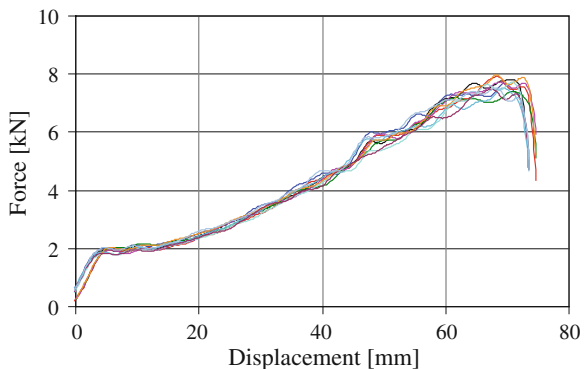


**Fig. 10.16** Scatter range of a GRP absorber



driver's stature, or by pyrotechnic switches that are triggered by the crash situation. They raise the price of the steering column adjustment considerably and assume parts to detect a crash, hence, up to now, they are used only if adhering to legal crash regulations is impossible without these adaptive parts. Indeed, stricter legal requirements may promote their spreading in the future.

A huge number of other concepts has been patented that supply adaptive functions and in addition use the complex qualities of special materials like shearing silicones or magnetisable fluids. They could not prevail, because of the high production costs.

#### 10.2.5.4 Joints

Modern steering shafts in cars are virtually exclusively equipped with universal joints. The versions shown in Fig. 10.17 are classified as universal joints or centred double joints, used as a constant-velocity joint with least degree of uniformity.

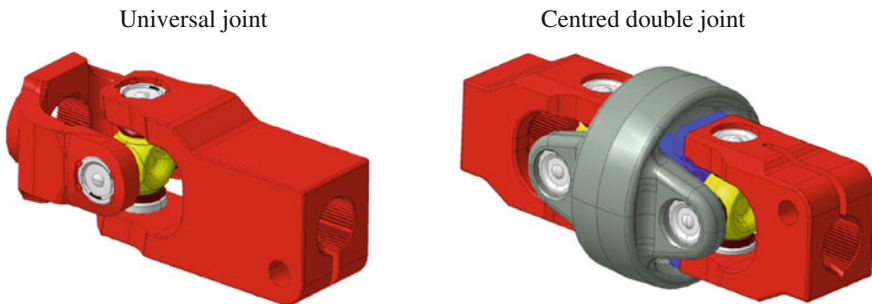


**Fig. 10.17** Joints for intermediate steering shafts

Double joints without centring are sometimes also used, but with an additional external top mount. All universal joints have a high power density and a very good efficiency of >99 %. Moreover, economic production is important. The particular kinematic effects of the dissimilar transmission can support the steering behaviour to a certain extent. Steering drivelines consist of various combinations of universal and double joints.

The use of sphere-controlled constant-velocity joints is kinematically possible, but not favoured for passenger cars, for reasons mentioned above.

### Universal Joints

The universal joint in Fig. 10.18 consists of a cross-pin set and yokes, shown in red.

The basic construction of the cross-pin set contains a case-hardened cross-pin with processed treads on the trunnion and the four bushings. The bushings are needle bearings with a board on either side. Tolerances of the treads, bushings and flanges in narrow tolerance zones  $\leq$ IT7, so that the steering movement is transmitted without backlash. The bushings are chosen according to application, with different strength, surface coatings or grease.

Added static seals, mounted tightly to the cross, protect the bearings against contamination with impurities and against leakage of grease. Standard sealing materials are NBR, HNBR and silicone. The bushings are preloaded by squeezing them into the yokes, axially to the cross-pin. Force and displacement are controlled during assembly. According to the design of the cross-pin set, a sliding fit is implemented between the axial contact surfaces of cross-pin and bushing. This reduces friction and pretension. The standard area of application of universal joints is a working angle of up to  $35^\circ$ .

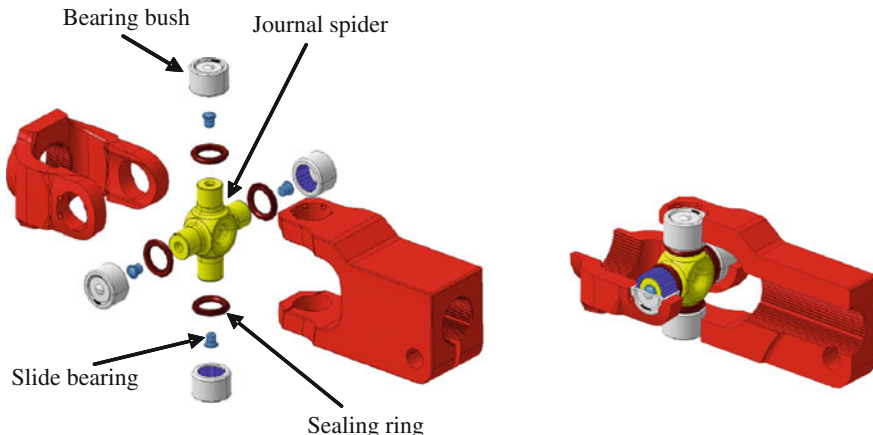


**Fig. 10.18** Universal joint

#### Centred Double Joint

The centred double joint in Fig. 10.19 consists of two universal joints whose phase is shifted by  $90^\circ$ . The centre bearing makes sure that within a defined area, the working angle at the simple joints is equal, guaranteeing their synchronisation. The guides of the centre bearing are positively and non-positively attached to the flanges, so that the centre ball is axially arranged and guided on the centring pin. The centre bearing is exposed to high loads and can generate typical vibrations and noises, because of the 2nd order bearing load. Therefore, use and arrangement are adapted to each vehicle. These joints can be used up to a working angle of approx.  $45^\circ$ .

#### 10.2.5.5 Length Compensation of the Intermediate Steering Shaft

The following designs of the length compensation are known:

- Length compensation with slip joint
- Length compensation with crash function.

The length compensation with slip joint allows adjusting the length of the shaft at a very low and steady force level, Fig. 10.20. The quality of the toothings is so precise that the longitudinal movement has a defined force of approx. 20 N. For example, aluminium or steel splined shaft treads compliant with DIN 5480 may be coated with modified plastic and fitted to the hub by means of suitable processes. Tread length and extent of the compensation are selected so that level and scattering of the displacement force across the displacement travel can be kept very low. Approx. 10 % of the peak displacement force may be achieved. The treads are smooth and without backlash.

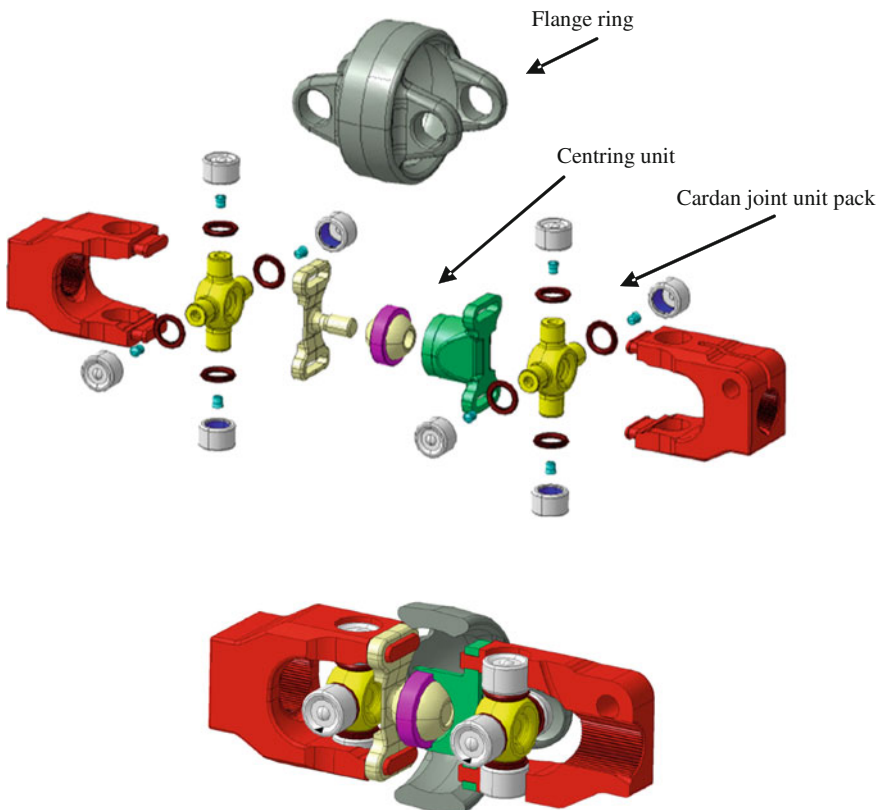


**Fig. 10.19** Centred double joint

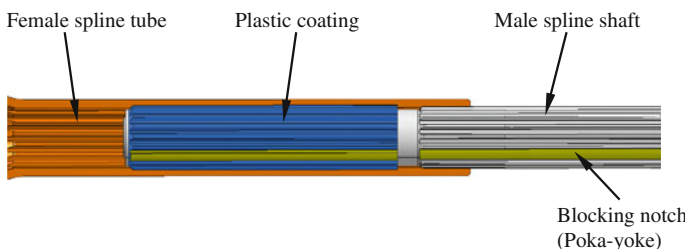
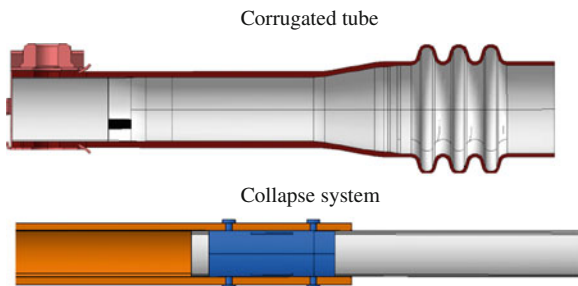


**Fig. 10.20** Length compensation for tolerance offset/longitudinal adjustment

Backlash and dogleg are not permissible. According to the tribological pairing and the application, these systems may be lubricated for a lifetime. A temperature range of  $-40$  to  $+250$  °C can be covered by a suitable choice of materials. Optionally, the systems are additionally sealed with bellows or lip seals.

**Fig. 10.21** Length compensation for crash function



The tread, including for example a block cog, is aligned for unequivocal assembly and for the rotatory adjustment of shaft and hub or the corresponding joints. Some applications require a limit stop to ensure that shaft and hub cannot be separated. This principle of length compensation is also used in the upper steering driveline.

The length compensation with crash function in Fig. 10.21 cannot be moved during standard use. The deformation of the front end by a collision with an obstacle can push the steering wheel through the steering shaft into the passenger compartment. This movement can directly endanger the driver or complicate the interaction of safety parts, due to the malpositioned steering wheel. To avoid this danger, the spindles of safety steering columns have parts that slip or fold under high load. They are mostly placed near the front axle. Corrugated tubes and telescoping systems prevail on the market.

A corrugated structure serves to achieve a high transferable torsion torque with a small folding force. Aluminium and steels with high yield strength and elongation are used to avoid brittle cessation of the corrugated tube under extreme load. If the corrugated tube would break, the vehicle could not be steered any more. The wall thickness of the corrugated areas is approx. 1.2 mm.

Collapse systems have tear elements that shear beyond a defined force threshold. After a break, the shaft retreats with low force into the hub. These systems need less space for distortion. Torque transmission and distorting force can be adjusted virtually independent from each other. The energy absorption is lower than with corrugated systems.

#### 10.2.5.6 Dampers

Steering column and intermediate steering shaft transfer torsional and longitudinal vibrations of the front axle to the steering wheel. For adjusting defined transfer functions and decoupling, suitable dampers are integrated into the upper steering shaft or into the intermediate steering shaft. Typical implementations are represented in Fig. 10.22: pipe-shaped tube-in-tube absorbers (left) or flexible couplings (right).

Tube-in-tube systems have an elastic absorber between internal and external yoke. The characteristic curve is essentially determined by geometrical and

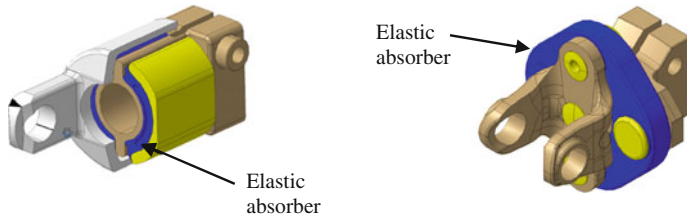


**Fig. 10.22** Torsion damper (tube in tube/flexible coupling)

material parameters. The torque transmission is stabilised by the internal contour striking an end stop after a defined rotary angle. These absorbers are very compact, showing good decoupling performance under axial stress.

Flexible couplings consist of an elastomer and fibre alloy. Different characteristic curves can be combined by choosing suitable elastomers and fibres. The fibres are arranged in loops to support the elastomer, they successively assume the transmission at higher loads. For some application profiles, flexible couplings may also be provided with mechanical stop units. At low working angles, they assume the function of joints. The transmission ability is here supported at need by internal centre bearings.

Some selectable damping materials can withstand temperatures as high as 175 °C. The characteristic curves of these systems are very progressive. The requirements to stiffness, damping and transfer function are absolutely specific for each car and have to be tuned individually.

The following quasi-static characteristics are typical for torsion dampers:

- Torsional stiffness 2–4 Nm/° at ±5 Nm
- Torsional stiffness 5–8 Nm/° at ±50 Nm.

### 10.3 Testing Steering Column and Intermediate Steering Shaft

To recognise faults of a steering column early on and to exclude any danger of the vehicle passengers before the start of the series production, the demanded features of the steering column are described in the specifications and the scope of tests is defined that is necessary for their verification. The check of the endurance strength and the assessment of features relevant for the customer have the highest priority. In spite of huge progress in numerical simulations, not all the acting physical effects can be modelled precisely enough, so that the test of the steering column is demanded by car manufacturers and will remain obligatory.

The engineering strength of the adjustable units is proven on the one hand by static load tests. There are tests under operation load which have to be endured without malfunctions, and there are tests under extreme and abusive loads which

must not reveal any defects that would impair the safety. On the other hand, durability tests are carried out with a substitute mass for the steering wheel. For electrically adjustable steering columns, they include tests under extreme temperatures and humidity, performed in climatic exposure test cabinets. These tests cannot be cut short substantially, because of the possible warming of the parts. The electric parts are not designed for a 100 % active period either, they need time to cool down. Hence, durability tests take several weeks and cause high costs.

Essential requirements like crash resistance or noise quality can be checked on-board, so that the test has to be performed in co-operation with the vehicle manufacturer.

### **10.3.1 Transmission Capability**

Steering shafts are safety parts, because any failure renders the vehicle uncontrollable. Therefore, high standards are applied to maintain the ability to transmit the steering torque. This ability is monitored by comprehensive tests in the development stage and by regular checks in series. The engineering strength is verified by continuous testing under equivalent dynamic loads, while the part qualities under extreme loads are evaluated in quasi-static tests.

#### **10.3.1.1 Static Strength**

Trying to steer when the steering wheel is blocked by the kerb can apply much higher torques at the steering column than driving. The steering column is also loaded with high forces and torques from misuse if the steering lock is broken open. Though damage from such misuse is permissible, the vehicle must remain controllable.

The steering columns are turned without radial force and with a blocked steering wheel to assess these extreme situations. The criteria of Table 10.1 apply.

**Table 10.1** Criteria to proof the static strength

Operation load 150 Nm	No functional interferences No plastic deformations No drop of the preload of the screws No cracks or ruptures
Misuse load 250 Nm	No functional interferences relevant for safety No plastic deformations relevant for safety No inadmissible drop of the preload of the screws No cracks or ruptures
Rupture behaviour	No rupture without deformation Test cancelled at 350 Nm without rupture

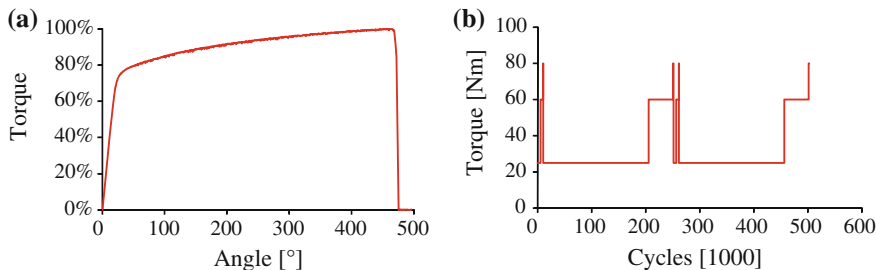


**Fig. 10.23** Static and dynamic transmission ability

### 10.3.1.2 Dynamic Strength

The dynamic engineering strength test examines the fatigue response of the steering columns. The test is made on oscillating test benches in stretched position or circulating in situ.

The circulation test provides a rotary angle, initiated at the steering wheel attachment with a defined torque, while a suitable counter torque is applied at the gearbox attachment to load the steering driveline. Each manufacturer provides different load-cycles for this test, featuring limit loads of 40–80 Nm, the higher load is applied to simulate usages like steering at rest without engine. A statistically qualified excess of a required number of load-cycles is demanded, no cracks or loosened screws may occur.

Figure 10.23 shows typical characteristic curves of the static and dynamic strength. The static curve plots the typically distinct flowing line until rupture. The right figure shows an example of a load group for the dynamic test. The service life test is cancelled when the necessary number of cycles is achieved, because these tests will often take several weeks, and the usage of the complex test facilities is expensive.

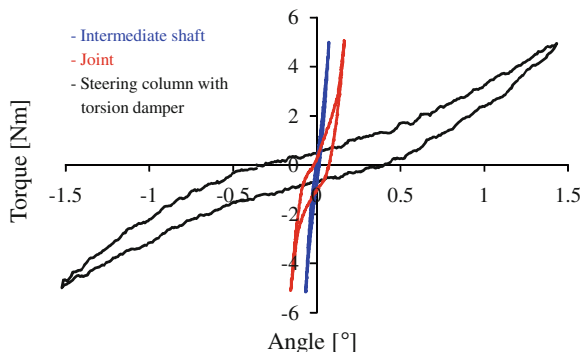
### 10.3.2 Stiffness

A highly torsion-resistant steering column is desirable for direct response and good feedback of the steering. Unfortunately, negative effects like the unfiltered transmission of interfering impulses to the steering wheel are then amplified, and they have to be suppressed by integrated torsion dampers, as described in Sect. 10.2.5.6.

Free travel in the steering is undesirable, because it evokes an indifferent steering feel, esp. around the central position of the steering. Free travel is easily recognizable from horizontal curves in the torque/rotary angle diagrams.

The stiffness is measured analogously to the static strength test. The same test facilities may be used. Special test facilities with more sensitive sensors are often used as well, because the load torques are lower during the stiffness measurement,

**Fig. 10.24** Stiffness curves of a column with torsion damper, joint and intermediate shaft



at approx. 6 Nm. The stiffness of the driveline may be measured in stretched position or in mounted position.

The joints—and the torsion damper—are the least stiff parts in the steering driveline. The stiffness of the joint is primarily marked by the yielding of the cross-pin. It cannot be arbitrarily increased without widening the required construction space. Figure 10.24 shows the characteristic curve of the parts and the steering driveline.

### 10.3.3 Durability Tests for Adjustable Units of Steering Columns

In the durability test, the limits of the shifting range are cyclically approached as often as a vehicle service life of approx. 15 years may require. For manually adjustable steering columns, hydraulically or pneumatically operated test facilities are used, for electrically adjustable steering columns, the motors are actuated. Higher loads are applied at the end stops. A typical part of the shifting cycles is carried out under extreme climatic conditions in climatic exposure test cabinets, to simulate the influence of the seasons. Figure 10.25 shows the schematic construction.

For every cycle, the locking mechanism of manually adjustable steering columns is operated. Optionally, the blocked steering column is loaded with a force to improve safety. For electrically adjustable steering columns, extreme situations of the electrical drive are simulated. Malfunctions can be detected after a drop of power or a breakdown by short circuit currents, when the drive is blocked.

The inevitable wear modifies the qualities of the steering column. However, no ruptures, cracks or other inadmissible losses of the introduction force may appear after the test. The steering column must operate and be without backlash. Changes of the operating forces or the noise response have to stay within the tolerance margins.

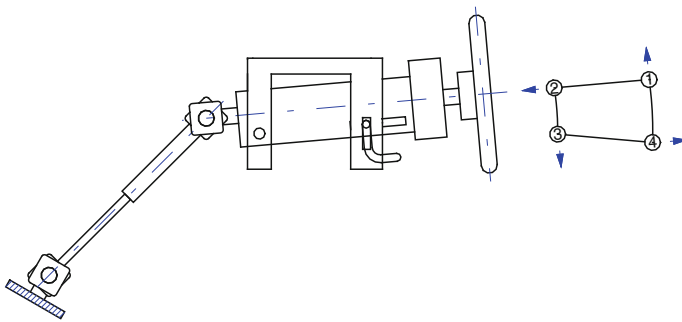


**Fig. 10.25** Experimental set-up of the durability test

### 10.3.4 Dynamics

Very stiff steering columns and high natural frequencies are demanded to improve comfort. Better steering feel and crash qualities are paired with preventing vibrations of the steering wheel. Vibrations can not only be caused by the driven wheels, but the air-conditioning, auxiliary units and the idle running of the engine can trigger bending self-oscillations of the steering shaft, as well. This demand for high stiffness causes a problem, because thick walls oppose the demand for low weight, compact size and small operating forces.

#### 10.3.4.1 Requirements of the Steering Column

The position of the lowest bending natural frequency of the on-board steering column is vital. It is measured by stimulating the steering wheel with an acceleration sensor. The stiffness of the contact areas, the weight of the steering wheel and the shaft and the qualities of the steering column are the main variables, described overall in Chap. 6. Raw bodies or steering wheels are not available during the early development stage, hence, the lowest value of a rigidly mounted adjustment is specified in the technical requirements and measured with a solid substitute mass instead of the steering wheel. Different steering column concepts for different vehicles can be better compared this way. Changed lever ratios modify the frequency values when adjusted, therefore the adjustable unit has to be shifted into the least favourable position. Most of the time this is the lower extended steering wheel position.

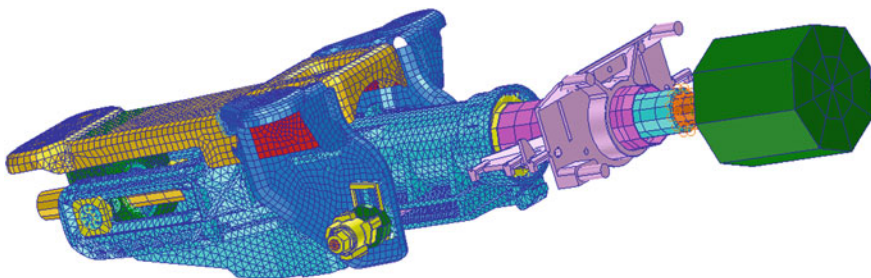
The soft screwing on-board lowers the natural frequencies; the values measured at the rigid mount are therefore always higher. Requirements for different vehicles and manufacturers may vary. Different directional stiffness can also mean that the requirements for the vertical and horizontal vibration direction will deviate from each other. Values  $>45$  Hz are typically demanded for the natural frequencies in a rigid mounting.

### 10.3.4.2 Analytic Identification/Measurement of the Dynamics

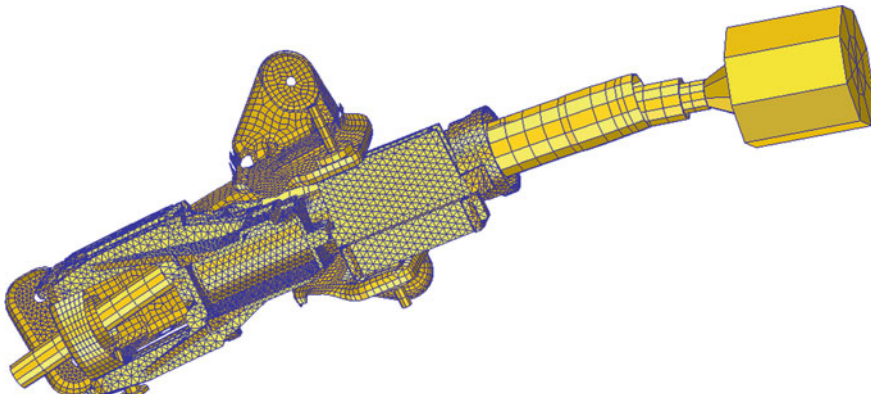
The natural frequencies can be computed by the finite element method during the conceptual phase. Figure 10.26 shows the model of a mechanical steering column adjustment. While the part stiffness is represented precisely enough by the elementing, suitable modelling of the contact points between the individual parts is crucial for the quality of the model. If any possible degree of freedom is too limited, the model is too stiff and the computed values are too high.

Figure 10.27 shows the first computed natural mode. The natural modes can be analysed beside the natural frequencies. Critical areas with big distortions can be made less critical by structural measures like ribbing or thickening.

The computed results can easily be checked by measurements if the stiff screwing points of the model are suitably represented. There is no ‘rigid mount’ in reality, though, therefore the mounting has to be very stiff. Solid mounting in steel is used. The measurements are carried out with an acceleration sensor as in Fig. 10.28.



**Fig. 10.26** Finite elements model of a mechanical steering column adjustment



**Fig. 10.27** The first natural bending mode of a mechanical steering column adjustment

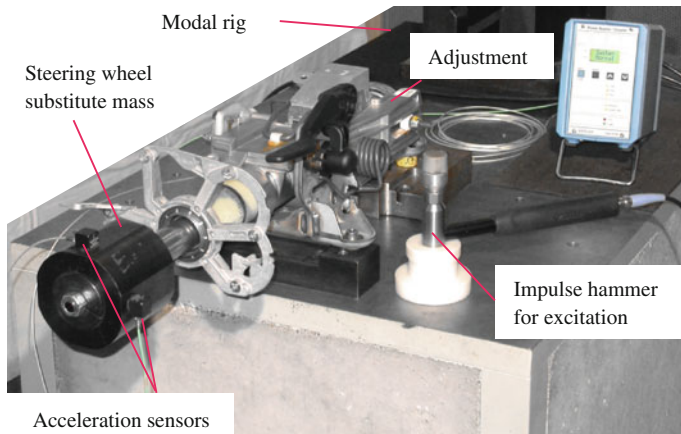


**Fig. 10.28** Test equipment for measuring natural modes

The vibration is commonly excited by an impulse hammer by whose help the excitation force can be measured. This makes sense in particular for steering columns that feature preloaded sliding guides, taking off at a specific force level. The loss of stiffness makes the measured natural frequency a function of the excitation force. This would not be true for strictly linear systems.

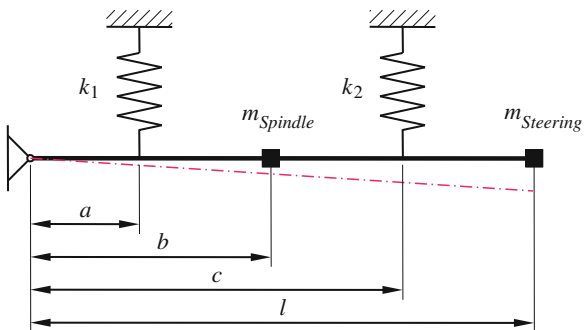
Faulty measurements may occur in reality when the test equipment has a natural frequency which is close to the measured frequency. This phenomenon is also present when the mass of the base is many times higher than the steering column. Hence, the bases are mounted floatingly, and their natural frequencies are far below the first measured frequency. A correlation between calculation and measurement allows validating the FEM model without knowing the characteristics of other vehicle parts. Then the validated model can be used by the vehicle manufacturer for insertion into the full vehicle model.

#### 10.3.4.3 Parameters of Influence

The stiffness of the adjustable equipment is determined by design, geometry of the parts and material qualities. The stiffness of the steering column bearings and the steering spindle at which the steering wheel is mounted is playing an essential role. A simplified model may be found in Fig. 10.29. The bearing stiffness and the yielding of the spindle are summarised by the stiffness coefficients  $k_1$  and  $k_2$ .

An evaluation of the lowest natural frequency  $f_0$  for the simplified model results from the energy method acc. to H. G. Hahn: Technische Mechanik, 2nd edition, Hanser 1992, p. 283 ff./33

**Fig. 10.29** Simplified model of a steering spindle suspension



$$f_0 = \frac{1}{2 \pi} \sqrt{\frac{k_1 a^2 + k_2 c^2}{m_{Spindle} b^2 + m_{Steering} l^2}} \quad (10.4)$$

The denominator contains a dominant mass of the steering wheel with higher weight and bigger rocker arm; it lowers the natural frequency. The influence of the spindle's mass is ten times lower. Only high stiffness can compensate the influence of the steering wheel. This impairs the use of a light metal spindle, because the low elastic module lets the stiffness drop for the same size of the spindle. Reducing weight by using high-strength steels with low wall thickness affects the natural frequencies negatively, too, because their elastic module is not higher.

Clearance, which can appear at contact areas where relative movements occur upon shifting, is a critical problem. Even the smallest gap can cause a significant drop of the frequency values, therefore the absence of clearance has to be guaranteed. High pressure or a large contact ration factor is not possible, because of the high operating forces involved. Therefore it was tried to spring-load sliding contacts, to prevent the sliding partners from taking off.

### 10.3.5 Crash Characteristics

#### 10.3.5.1 Steering Spindle

As described in Sect. 10.2.5.2, corrugated tubes and telescoping collapse systems are prevalent crash systems. They transfer the necessary steering torque and permit wide displacement during a crash. Both systems considerably differ in their crash qualities, although they serve the same purpose.

Figure 10.30 shows a buckled corrugated tube after the buckling test on a pull/push test bench. Cracks or ruptures are undesirable test results, even if the corrugated tube is buckled by 90°. Such buckling experiments are carried out for purposes of quality control.

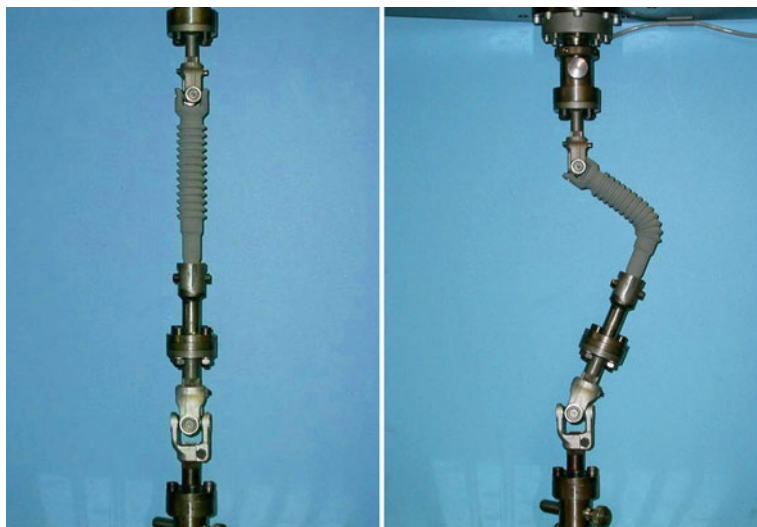


**Fig. 10.30** Corrugated tube (before and after the buckling test)

**Table 10.2** Qualities of corrugated tube and collapse systems

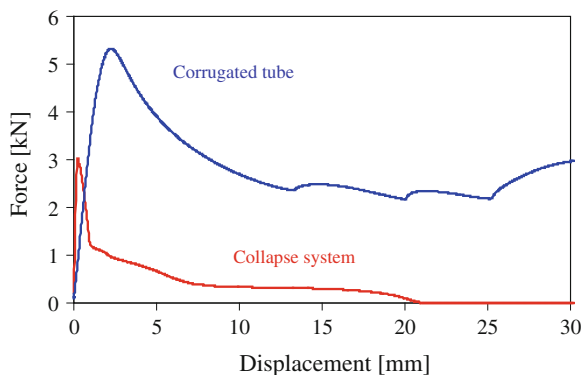
	Corrugated tube	Collapse system
Buckling direction	Radial	Axial
Force when breaking off	Higher	Lower
Adapting the force threshold	Heavier	Lighter
Radial force influence	Lower	Higher
Torsional stiffness	Lower	Higher
Cost	Low	High
Influence of the steering wheel torque on the buckling force	Low	High
Energy absorption	High	Low

Tough materials with distinctive flow behaviour are used. Steels do no display any distinctive hardening under high distorting speed, so that a pressure test at distorting speeds above 100 mm/min. will yield meaningful results.

A telescoping steering spindle does not buckle, but retreats instead. A defined force has to be exceeded before it is lower than that of the corrugated tubes. When tuning the crash qualities, demands for easy retraction and high transferable torques are causing trouble.

Table 10.2 compares the qualities, typical characteristic curves may be compared in Fig. 10.31.

**Fig. 10.31** Qualitative characteristic curves of corrugated tube and collapse system



### 10.3.5.2 Steering Column

Crash qualities of safety steering columns are tested in sled or vehicle tests under real conditions. Damage to vehicles or subassemblies with crash-relevant parts is recorded on these complicated test benches, and the crash performance is evaluated, based on retention values, measured on crash dummies. In a vehicle crash taking about 200 ms, the steering column is strongly loaded for a short time. There are other failure mechanisms than in static load tests, especially for brittle materials. These tests are not suitable for development and quality assurance testing because of long lead times, high technical complexity and high costs. Since the entire restraint system is evaluated, inferring on a single component such as the steering column adjustment is difficult.

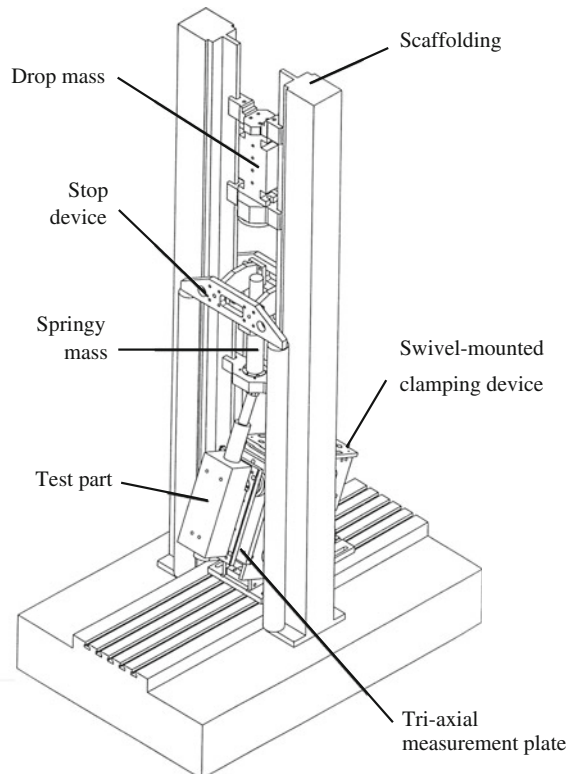
The assessment of the steering column properties is carried out by the Willi Elbe company in a substituted test at a drop tower, see Fig. 10.32.

A drop mass falls onto a spring-loaded mass, simulating the airbag, which is located between the drop mass and the test sample. A friction spring with absorbing properties is used. A heavy load roller is mounted on the steering wheel attachment so that the steering shaft can roll upon retraction. The adjustment is based on a hinged device to receive the reaction forces at the measuring plate with three triaxial piezoelectric force members. The test parameters (weights, angles of inclination, spring/damping characteristics) help to control the kinetics of the retraction and to approach nominal values.

One proceeds as follows:

- Validate the numerical simulation model of the steering column, using first drop tower results, under given conditions. A validated simulation model was developed for the test equipment.
- Identify the crash loads and the distance in the vehicle simulation and/or an on-board measurement. The validated model of the steering column is used for the simulation.
- Identify the drop tower parameters with the drop tower simulation model in such a way that the real loads and distance are very closely represented.

**Fig. 10.32** Drop tower for module test



- Validate these parameters in the drop test and define the parameters for the quality control.

The drop test does not precisely illustrate the on-board dynamics. Other than a quality control during manufacturing, layout and test of the parts for strength and displacement are already possible in the development stage.

### 10.3.6 Displacement Forces to Adjust the Steering Column

These are the forces to move the steering column and the intermediate steering shaft. In an electric drive unit, displacement forces are indirectly felt by noise or the service life of the electric drives.

The mechanical drive unit on the other hand, sends a direct response to the driver. The displacement forces merge from the adjustment unit's force and the length offset in the upper steering driveline. The displacement force in the upper steering driveline can be transferred by analogy to the length offset of the intermediate steering shaft. Essential parameters are

- force and
- uniformity of the displacement force.

Other than straight selected matings of the sliding fits and, if necessary, their grease, stick slip effects are of particular importance, because they can generate creaking noise and jerking motion sequences. Stick slip appears most frequently in areas of mixed friction at low speed. Based on lab measurements, the position of the system on the Stribeck curve can be found and favourably influenced—towards liquid friction—by using suitable lubricants.

Figure 10.33 shows the curve of the displacement force using a length compensation with an easy-going splined shaft tread. Symmetry of moving in and out and the scattering during a cycle reveal a well tuned system.

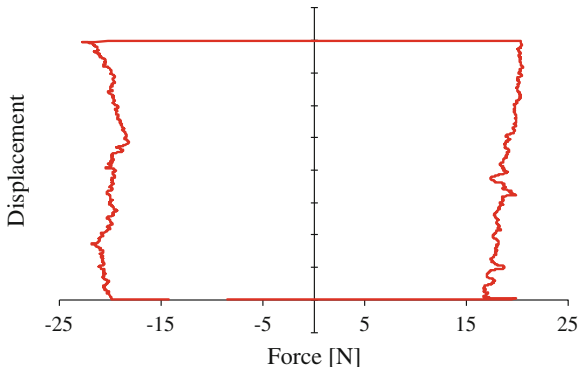
### 10.3.7 Temperature

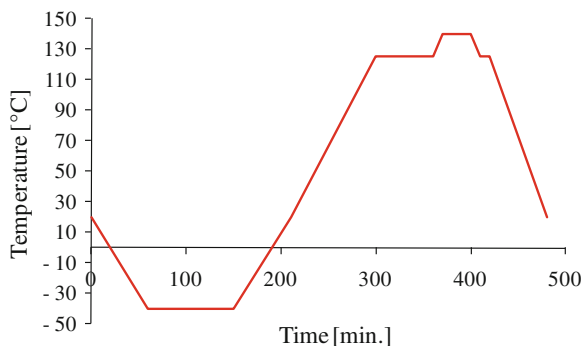
Steering parts in the passenger and engine compartments can be exposed to extreme temperatures of  $-40$  to  $250$  °C. Beside the mentioned corrosion effects, the following effects have to be controlled:

- Influence of relaxation and retardation when using plastic parts
- Avoiding noise and/or clearance by different coefficients of expansion
- Temperature influence on static and dynamic strength, esp. for aluminium, stainless steel and plastic
- Suitability of lubricants in roller bearings of the cross-pins and the length offset.

By analogy to the corrosion test, the temperature groups are used as shown in Fig. 10.34. They illustrate the operating temperatures and the heating phases at rest. Torsional durability and wear tests are also checked under temperature and humidity to verify the structure.

**Fig. 10.33** Displacement forces length compensation



**Fig. 10.34** Climate test cycle

### 10.3.8 Corrosion

Steering columns and intermediate steering shafts are exposed to very diverse conditions, on account of their installation on-board. While the steering column in the interior primarily has to withstand temperature and humidity, the intermediate steering shaft suffers from much higher exposure. The exposed position in the engine compartment may cause extreme loads:

- High peak temperatures
- Wide temperature ranges, heating and quenching by foam
- High air humidity till saturation/condensation
- Contamination with salted water and abrasive media
- Petrol, diesel, oils, polyurea etc.

These effects can cause corrosion. Convenience may be lost by heavy moving of the length offset or, e.g., wear of the bearings, but corrosion including structural damage of the torque-transferring parts has to be avoided as well.

The resistance against corrosion is examined with standardised tests, like the salt spray test (e.g., 720 h) and the climate change test, or with test cycles that are specifically designed for the vehicle. Recording the specific effects in advance is tricky, in spite of comprehensive attempts to standardise, therefore, dynamic corrosion tests that subject whole vehicles or areas to dynamic tests in climate chambers are often used. This test is made with accelerated cycles to gain a useful statement on the corrosion resistance after approx. 6 weeks of testing.

Intermediate steering shafts are often made of corrosion-proof 6-aluminium alloys, to avoid corrosion. Higher long-term temperatures of approx. 150 °C force the use coated steel systems or stainless steel solutions, due to a recrystallisation of the aluminium which reduces the strength. One needs to ensure that the coatings have a very good adhesion, high ductility and low thickness. The range of the used coatings covers wax and multi-layer protection systems.

In addition, mechanical protection systems, such as bellows, protective caps and renderers/seals are used.

## 10.4 The Future

Steering columns in vehicles of the higher compact category and up have set a high standard for ergonomics and safety by their basic technical qualities and safety features. With regard to these criteria, there will of course be more advanced requirements in the future, e.g., for the extension of the adjusting range. Concerning vehicle safety, one essential contribution will be the tuning of the overall system of vehicle, airbag and safety belt with tensioner even more sensitively. A comparison of available crash systems still reveals distinct differences in responding properties and controllable characteristic curves, as well as in the tolerance range of absorber characteristic curves. As in almost any other segment, weight will assume essential meaning, and these requirements have to be cost-efficient. Basically, it is to be assumed that the steering column will be integrated even further into the weight-bearing structure of the vehicle, rather than being added onto the support tube as an additional part. Steering column and pedal mount will probably be integrated with the cowl and the support tube.

The requirements of intermediate steering shafts for the defined qualities of joints and length compensations will be even more precisely specified in the future. Characteristics of stiffness in the zero passage and hysteresis widths are more frequently described as distinct parameters, requiring higher effort of production and quality control. Temperature and corrosion resistance have achieved a technological maturity that can no longer be economically improved. A future target will be the logical insertion of aluminium parts, taking into account high-strength alloys resistant to temperature. Also, the requirements for crash systems between the joints will increase. The tendency that was already discussed for the steering column will basically repeat here.

The authors believe that there will be conventional steering columns as well as intermediate shafts in the next vehicle generations. Compensation with By-Wire systems is not yet feasible, even though technically possible.

# Chapter 11

## Mechanical and Hydraulic Gears

**Johannes Hullmann, David James, Alois Seewald,  
Eduard Span and Alexander Wiertz**

### 11.1 Definition of Rack-and-Pinion Gears

The family of steering equipment covers hydrostatic steering systems, recirculating ball-with-nut gears, manual rack-and-pinion steering and rack power steering. The final steering system mentioned has a rack-and-pinion gear which transforms the rotation of the steering wheel into the translation of the rack and again into the steering movement of the tyres.

Table 11.1 shows a classification of steering system designs. The classifying features of the various models chosen are active principle, drive, primary gear, force introduction and integration. The naming of the steering and the corresponding abbreviation complete the presentation.

In a manual rack-and-pinion steering the parameters are the wheel angle and the wheel torque, which is initiated at the steering wheel and transformed by the dovetailing components, pinion and rack, into rack force and rack shift. Beyond these mechanical variables, no further energy is supplied to the manual rack-and-pinion steering to move the rack.

---

J. Hullmann (✉) · A. Seewald · E. Span · A. Wiertz

TRW Automotive, Livonia, MI, USA

e-mail: johannes.hullmann@steeringhandbook.org

A. Seewald

e-mail: alois.seewald@steeringhandbook.org

E. Span

e-mail: eduard.span@steeringhandbook.org

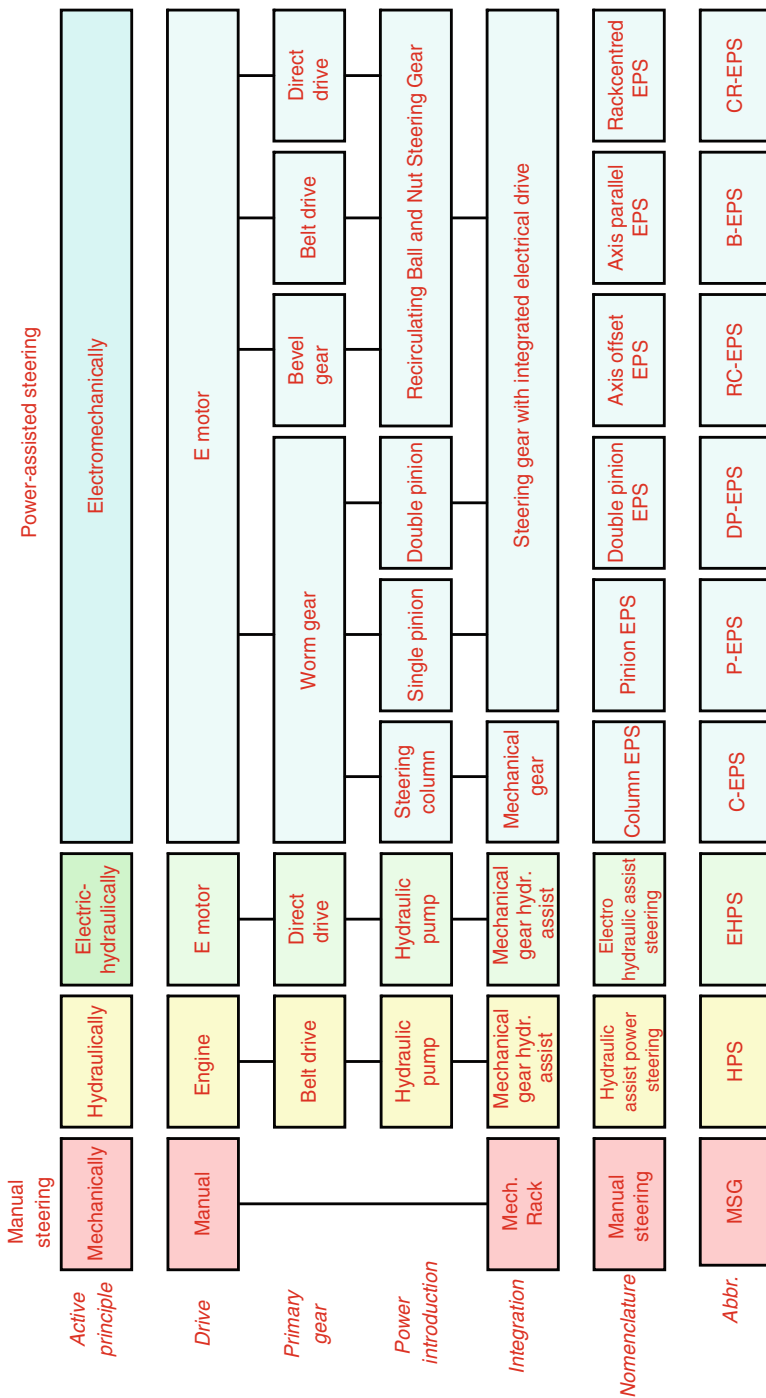
A. Wiertz

e-mail: alexander.wiertz@steeringhandbook.org

D. James

Tohop Steering Technology GmbH, Indianapolis, IN, USA

e-mail: james.david@steeringhandbook.org

**Table 11.1** Classification of steering designs

The rack power steering works essentially by the same principle, but an ‘assistant’ supports the driver’s steering activities. This assistant can be either hydraulic, electric-hydraulic or electromechanical. In an electromechanical rack-and-pinion steering, for example, the assistant moving the rack is an electric motor which allows contributing a suitable energy supply by means of an additional power-assist gearbox. A hydraulic assistant is a pump, powered by the internal combustion engine, that supplies the steering system. In contrast to both, the steering system of the electric-hydraulic version is decoupled from the internal combustion engine, and the hydraulic pump is driven by an electric motor. The structures these power steerings have in common, is that the existing wheel torque is exploited to control the assistant. The base for receiving the wheel torque is usually a torsion bar which allows activating the steering valve of hydraulic and electric-hydraulic steering, or a suitable twisting angle in the torque sensor of the electromechanical steering. The manual steering has no torsion bar.

This chapter will first discuss the mechanical rack-and-pinion gears, either driven by hand or by the above-mentioned power-assist gearbox, separated from the mechanical rack-and-pinion gear.

## 11.2 Applicability/Pros and Cons

Manual rack-and-pinion steering and rack power steering are almost exclusively used in vehicles with independent suspensions at the front axle. These are passenger cars of almost any vehicle class, as well as light commercial vehicles.

A direct comparison of the recirculation ball with nut gears that had once been widespread in these vehicle classes, too, shows the pros (+) and cons (−) in Table 11.2. Rack-and-pinion steering has replaced the recirculating ball gear in

**Table 11.2** Comparison between rack-and-pinion steerings and recirculating ball gears

Assessment criterion	Rack-and-pinion steering	Recirculating ball gear
Freedom of action	+	−
Efficiency	+	−
Bumpiness	−	+
Steering elasticity	+	−
Stroke limitation	+	−
Tie rods—radial forces	−	+
Usability with rigid axles	−	+
Drop of the full ratio over the wheel angle	−	+
Complex structure	+	−
Space required	+	−
Production costs	+	−
Weight including steering linkages	+	−

almost any vehicle with independent suspensions of the front axle, because of the lower steering elasticity, less need for space, less weight of the full steering system and lower production costs. The cons of the rack-and-pinion steering—less damping of externally excited power pulses (bumpiness), the curve of the steering ratio and the lateral forces from the tie rods—are compensated by constructive measures.

## 11.3 Kinematic Differentiating Features of Gears

The first basic criterion for the kinematic distinction of the gears is the on-board position of the wheel, distinguishing left-hand or right-hand driving. To supply all the markets, both versions are developed and offered for most vehicles in Europe. In the easiest case, if the structure of the vehicle permits it (package), the gear of either version is laid out symmetrically to the longitudinal axis.

In addition, there are special versions of sports or racing cars that feature a central steering wheel. They will not be discussed here any further.

### 11.3.1 Position of the Gear in Relation to the Front Axle

The on-board positioning of a gear in relation to the front axle provides four basic options, depending on whether the rack axis of a gear (gear axis) and the steering triangle of steering arm and tie rod are in front of or behind the front axle (see Figs. 4.19, 4.22, 4.23 and 4.24).

Most cars with front-wheel drive and laterally arranged engine/gearbox unit feature both gear and triangle behind the front axle. This arrangement enables easy integration of the steering column into the vehicle package. On the other hand, an unfavourably high thermal load will often accompany this arrangement, because the exhaust system is close to the gear.

Standard-driven vehicles preferably have both gear and steering triangle in front of the front axle. This avoids conflicts in the package between the longitudinal drive unit and the lateral gear, and the steering column can be easily guided past the engine.

Gears and steering triangles are rarely arranged at different positions (e.g., gear behind the front axle and steering triangle in front of the front axle; see Chap. 4, segment 4).

The position of the steering triangle gives ultimately the direction of the rack's motion upon steering, therefore it is essential for the dovetailing design, defining the way the pinion dovetailing is inclined.

### 11.3.2 On-board Gear Interfaces

The majority of vehicles has a steering mounted on a separate subframe that is in turn mounted to the body. Since the wheel suspension at the chassis is at least partially joined to this subframe, there is a stiff connection between steering and front tyres. This creates a basis for precise steering, even under the influence of high lateral forces in the wheels. Furthermore, the subframe is acoustically decoupled from the car, so that less chassis noise is transmitted by the gear into the body.

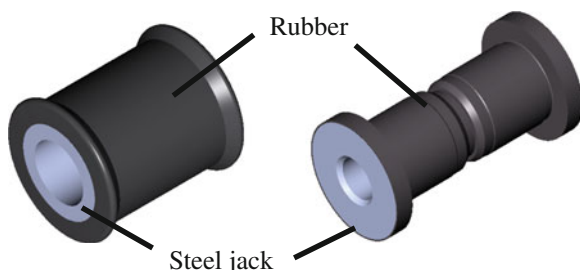
In addition, there are vehicles whose steering is separated from the front axle and directly joined to the body. This mounting is often given by the package, for example, in cars with front-wheel drive and longitudinal engine in front of the front axle (example: any Audi A6 older than 2011). Sometimes the steering is directly mounted at the engine bulkhead, i.e. the separation between engine and passenger compartment, this is a very cost-efficient solution. If any acoustic setbacks of this arrangement cannot be accepted, they are compensated by additional measures, such as damped tie rods and elastic mounting of the gear at the engine bulkhead.

The mounting points can be either rigid or flexible, i.e. by means of silent blocks or rubber mountings. A rigid arrangement provides highest stiffness of the steering system, but it has setbacks in acoustics and bumpiness. Rubber mountings offer the chance to tune the response and damping characteristics of the steering and to achieve the best compromise for the vehicle in question.

A rubber (metal) mounting consists in principle of a jack, usually made of steel, that is vulcanised into a rubber body. It acts like a progressive spring and provides the kind of damping that is native to rubber. Lateral and axial stiffness, as are necessary for the respective application, and the desired damping parameters are identified by means of vehicle simulations and road tests. Figure 11.1 shows typical one-piece and two-piece versions of rubber mountings.

The number of fastening points can vary from at least two, used to precisely adjust the on-board gear, up to four or more, which enables precise, controlled elastokinematics, together with the properly tuned rubber mountings.

**Fig. 11.1** Typical rubber mountings as one-piece and two-piece edition



### 11.3.3 Adjustment of the Gear Case

The co-ordinates of the main points of a rack-and-pinion gear—more precisely: the points of the axial joints at the tie rods, the lower universal joint of the steering column and the junction point of the rack and pinion axis—are given by the package of the full vehicle, as shown in Fig. 11.2. Therefore the pinion case can be turned outward or inward from the car's central plane. An inward orientation of the pinion case, vertical to the rack axis, would be unusual, though. It is chiefly found in racing vehicles.

### 11.3.4 Tie Rod Interfaces

Depending on how the two tie rods are connected with the rack, there is a distinction between a rack-and-pinion steering with central tap and others with end tap at one or both sides. A rack-and-pinion steering with end tap at both sides has the inner joints of the tie rods (axial joints) screwed directly onto both ends of the rack. This configuration is the current state-of-the-art, Fig. 11.3.

It merges high stiffness with low weight, because the rack axis is passing through the points of both axial joints. Torsion torques in the rack develop only from lateral forces from the tie rods which are a function of the tie rod angle (see also Fig. 11.2). The rack of a mechanical gear for standard strokes can be short, so

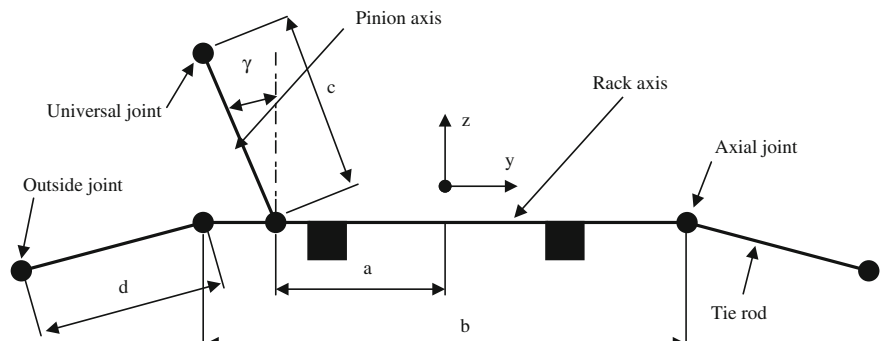


**Fig. 11.2** Typical outlines of a rack-and-pinion gear



**Fig. 11.3** Mechanical gear with end tap on both sides (Renault Scenic 3)

usually there is enough space for it in the package. Rather long tie rods can be used which display low torsion angles even at full deflection and rebound of the front axle, so that low lateral forces are applied to the rack. A rack-and-pinion steering with central tap has only one mounting point for both tie rods, and it is in the centre of the car, if the steering is set on straight driving. This steering model is rarely used in new applications, on account of the weight and the required space (see also [Sect. 11.9.1](#)). Short gears with end taps on one side are not used any more, either. They had been very compact, so that they could be mounted on the driver's side. By analogy with a gear with central tap, the tie rods were mounted at one end of the rack, while the other side remained free. This construction was suitable for purely manual steering with correspondingly low tie rod peak forces.

### ***11.3.5 Kind of Gear Ratio***

The stroke of the rack during one turn of the pinion is called the gear ratio of a rack-and-pinion gear. This means that for a higher gear ratio (more stroke per turn of the pinion), the whole steering ratio on-board will drop (wheel-angle-to-steer-angle ratio). A high gear ratio means that there is less effort for a wheel angle, for example on curvy roads or when cornering in the city. On the other hand, a high gear ratio complicates the exact adjusting of very small steer-angles, for example, when slight corrections of the straight course should be carried out at high speed. Moreover, a high gear ratio produces high steering forces in a manual steering and high power-assist torques in electromechanical steering systems.

The majority of gears produced has a steady gear ratio. If it changes as a function of the wheel angle or the rack stroke, this is called a variable gear ratio. This variability can be either constant, rising or falling with increasing wheel angle on different sections. This suggests a solution of the above-mentioned problems. The gear ratio curves of manual and mechanical rack-and-pinion gears are dropping with rising steer-angles, to counteract the kinematic rise of the wheel torques. There are also M-shaped (rising-falling) versions which merge this quality with a low gear ratio during straight driving. Typical steering ratios of different versions are compared in [Fig. 11.20](#). For relevant differences, resulting gear ratio curves, layout criteria and ways to produce a variable gear, see [Sect. 11.5](#).

## **11.4 Design and Main Components of a Mechanical Rack-and-Pinion Gear**

Some essential components of a mechanical rack-and-pinion gear that are important for the steering are shown in [Figs. 11.4](#) and [11.5](#):

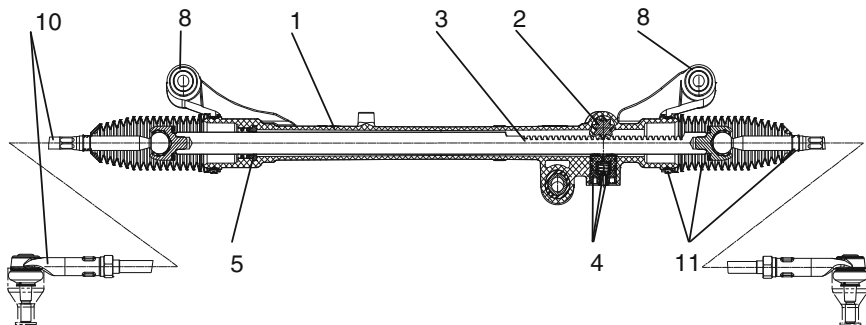


**Fig. 11.4** Cut of a mechanical rack-and-pinion gear

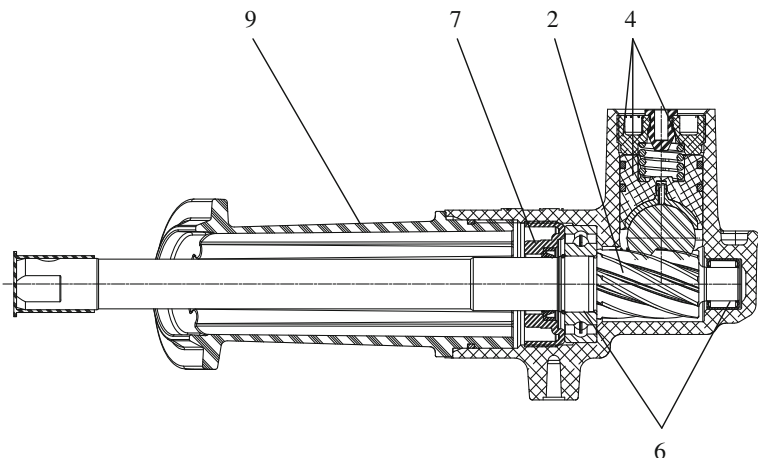


**Fig. 11.5** Cut of the pinion case of a mechanical rack-and-pinion gear

1. gear case
2. pinion
3. rack
4. rack yoke elements, including spring and adjuster bolt of the free travel
5. rack bushing
6. upper and lower roller bearings of the pinion
7. upper pinion screw to secure the axial mounting of the pinion
8. joining elements to receive and mount the gear case on-board
9. gear case gasket towards vehicle interior, near the junction of the pinion to the column (use depends on the on-board implementation of the gear)
10. tie rods (inside and outside joint)
11. gaiters including coupling clamps.

### 11.4.1 Gear Case

The gear case receives and joins all the components of the gear. It is either rigidly or elastically mounted at the vehicle by rubber mountings (see Fig. 11.1). The case has the additional task to accept any steering forces present, transmitted as wheel torques, and any forces acting from the tyres on the rack via the tie rods. Other functions are the limitation of the stroke and the reception of the end stop forces.

One-piece and two-piece gear cases are the most common designs. They are described in more detail in the following.

#### 11.4.1.1 One-Piece Gear Case

The one-piece type is the most common one. For an example, see Fig. 11.6. This version of a gear case consists of die-cast aluminium and offers the following benefits: The flanges to mount the gear case in the car are made right in the casting process. This technique also allows adding holders and mounts. The die-cast aluminium case is light and requires no costly welding or additional surface cover, unlike steel parts.

A few typical die-cast aluminium materials for gear cases are GD AlSi9Cu3 and GD AlSi12Cu. A listing of proper characteristics is shown in Table 11.3. The sand-cast G-AlSi7Mg0.3 and its mechanical qualities are also given in the table, as it is often used in prototype building and for small numbers of pieces.

#### 11.4.1.2 Two-Piece Gear Case in Composite Design

The two-piece version has a pinion case of aluminium and a rack case made of a steel pipe, see Fig. 11.7. The parts of the case are connected by grouting both components or by casting around the steel pipe during the die-casting process. The flange at the pinion case that mounts the gear case to the vehicle is shaped during the casting process. At the steel pipe, the case is joined either with a holder welded to the pipe or with an aluminium flange that is cast around the pipe. A very cheap way to mount a two-piece case to the vehicle can be realised with a separate securing clip and a rubber insert at the steel pipe.

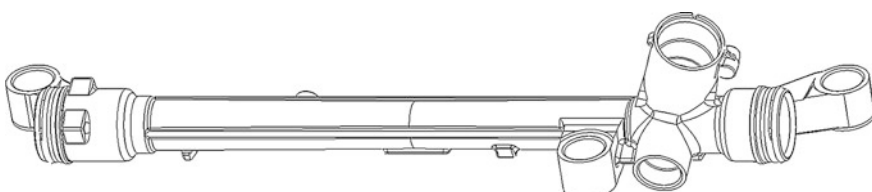
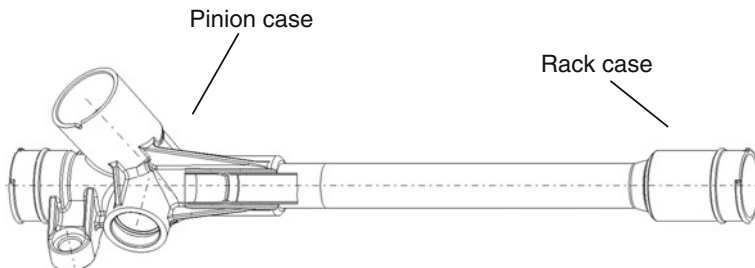


Fig. 11.6 One-piece gear case from aluminium die-casting

**Table 11.3** Typical aluminium die-cast and sand-cast materials and their mechanical parameters

	GD Al Si 9 Cu 3 Die casting	GD Al Si 12 Cu Die casting	G Al Si 7 mg 0.3 Sand casting (T6)
Tensile strength (N/mm <sup>2</sup> )	240–310	220–300	230–310
Yield strength (0.2 %) (N/mm <sup>2</sup> )	140–240	140–200	190–240
Stretch (%)	0.5–3	1–3	2–5
Brinell hardness (250 kg, 5 mm)	80–120 HB	60–100 HB	75–110 HB

**Fig. 11.7** Two-piece gear case in composite structure

One advantage of this two-piece implementation, compared with the one-piece aluminium case, is less space needed for the steel pipe, on account of the lower thickness of the wall. Nevertheless, the steel pipe needs a separate galvanic or varnished surface protection.

### 11.4.2 Steering Pinion

The pinion is connected to column and wheel by the intermediate steering shaft, and it is dovetailing with the rack. Therefore the main task of the steering pinion is to transform the rotation of the steering wheel into a translation of the rack.

#### 11.4.2.1 Pinion Bearing

One common arrangement of the pinion bearing of mechanical rack-and-pinion gears is a lower needle bearing, which is floating, combined with an upper deep groove ball bearing, which is fixed, that is axially mounted with the pinion, Fig. 11.8. The upper ball bearing and the pinion are again mounted in the gear case by the upper pinion screw, without axial free travel. The bearing therefore supports the axial dovetailing forces which develop from the usual diagonal dovetailing of

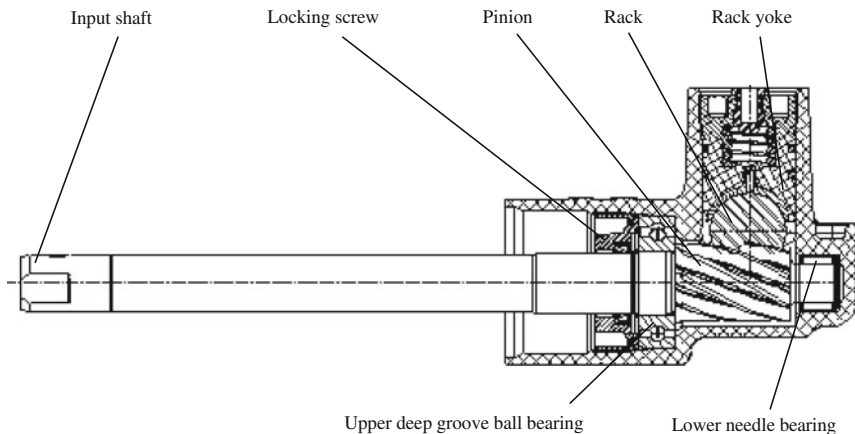


**Fig. 11.8** Pinion bearing arrangement with deep groove ball bearing (*top*) and needle bearing (*bottom*)

pinion and rack. It also bears the radial dovetailing forces and those forces which act from the tie rods about the rack on the pinion, together with the lower needle bearing.

This typical pinion support by means of deep groove ball and needle bearing is complemented by the less common variety with two angular contact ball bearings, see Fig. 11.9. In this case, an angular contact ball bearing is arranged both above and below the pinion dovetailing. The two bearings receive axial and radial forces synchronously. This version of a pinion bearing has not prevailed, because the costs of the parts are higher.

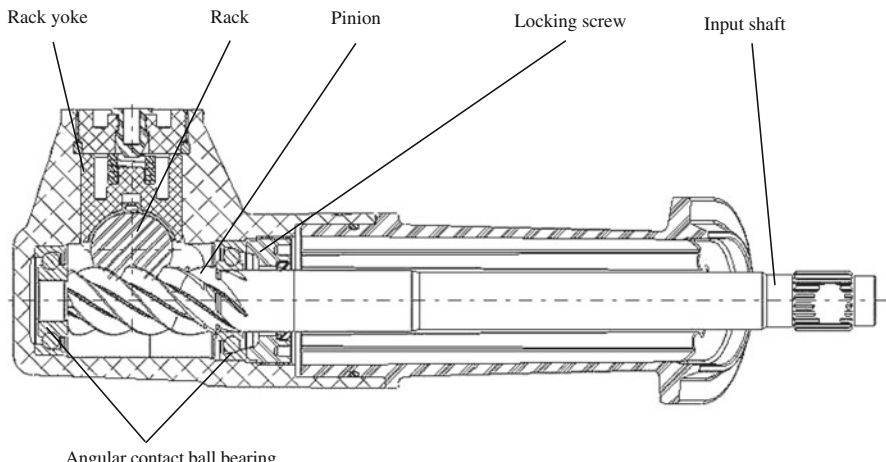


**Fig. 11.9** Pinion bearing arrangement with two angular contact ball bearings

### 11.4.2.2 Implementation of the Pinion Dovetailing

The steering pinion is usually toothed askew to achieve more dovetailing coverage when interacting with the rack dovetailing. This ensures that more than just one cog is dovetailing and that even dovetailing and uniform torque transmission between pinion and rack is maintained. Mechanical gears are basically designed with big dovetailing modules, so that the cogs are firm enough, on account of the high steering torques to be transferred.

Common manufacturing methods for the pinion dovetailing are the most often applied hobbing and the less common gear-tooth forming. There are high requirements for the run-out deviation of the pinion dovetailing (up to  $40 \mu\text{m}$ ) to achieve a steady frictional curve over the rack stroke with low free travel of the rack yoke.

### 11.4.3 Rack and Rack Guide

The rack has the task to convert a rotation, given by the steering wheel on the pinion, into a translation of the rack and the attached tie rods about the dovetailing between pinion and rack. The rack has to transfer the highest applying steering forces and tie rod forces in axial and radial direction. Diameter and material of the rack belong therefore to the main layout criteria of a rack-and-pinion gear. Primarily, the rack should be sufficiently resilient against bending to resist the high lateral forces that the tie rods may issue. Typical materials of racks and their mechanical qualities are shown in Table 11.4.

The rack is generally made of a round-bar steel. The dovetailing is made either by forming or by machining. To optimise the weight, it is partially or entirely hollowed out. There are also versions of racks for which a pipe is transformed according to Sect. 5.5. The making of racks is described there in more detail.

#### 11.4.3.1 Rack Guide

The translation of the rack is enabled by two bearings. Opposite the steering pinion is the rack passing into a plain bearing bush (see Fig. 11.4) that receives the lateral forces of the rack in radial direction.

**Table 11.4** Typical rack materials and their mechanical qualities

	SAE 1040 C40-C43	EN8C	37CrS4 41CrS4
Tensile strength ( $\text{N/mm}^2$ )	640	695	775
Yield strength (0.2 %) ( $\text{N/mm}^2$ )	440	495	620
Stretch (%)	19	17	13

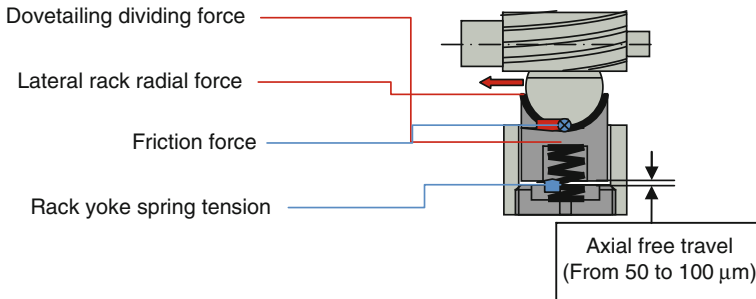


**Fig. 11.10** Forces acting on the rack yoke and the axial free travel

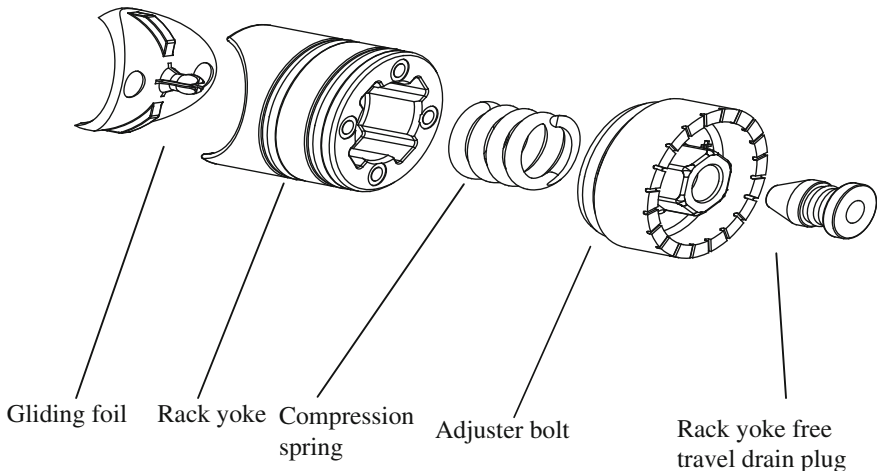


**Fig. 11.11** Construction of the rack yoke assembly in the gear case

The rack is guided on the side of the dovetails between the pinion and a spring-loaded rack yoke, see Figs. 11.4, 11.8 and 11.9. The rack yoke almost completely surrounds the diameter of the rack on the side that is turned away from the pinion (looking at the cross section) and presses the rack dovetailing against the pinion dovetailing by means of a compression spring, without free travel, if possible. The rack yoke is guided in a case drilling without free travel. Thus the bearing also enables the reception of the lateral rack forces in radial direction. Figure 11.10 shows the forces acting on the rack yoke, combined of the dovetailing dividing force, the lateral rack force and the rack yoke spring tension. Reliable functioning of the rack support is commonly ascertained by an axial free travel of the rack yoke between 50 and 100  $\mu\text{m}$ . The structure of the rack yoke and its components is shown in Fig. 11.11.

This bearing constellation reduces the movement of the rack to two degrees of freedom: the desired translation and a possible undesirable roll of the rack around its longitudinal axle. The contact area between the dovetailing of pinion and rack

along the pinion's axis is rather long, so that a rolling movement will push the rack away from the pinion. First, the spring pretension has to be overcome, then, the rack yoke spring has to be compressed, until the rack yoke touches the adjuster bolt. Consequently, the possible rolling movements are limited to a range which does not affect the function of the gear.

#### 11.4.3.2 Rack Yoke

The rack yoke has to perform the following functions during gear operation:

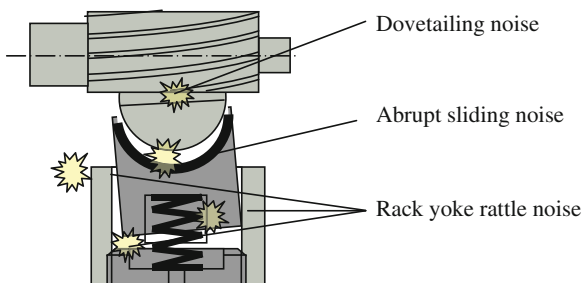
- Establish a plain bearing of axial rack strokes without free travel
- Establish a dovetailing between pinion and rack without free travel or noise
- Support radial and axial dovetailing dividing forces between pinion and rack
- Support tie rod forces at the pinion
- Compensate dovetailing tolerances between pinion and rack from manufacturing
- Tune steering qualities by varying the frictional mating between rack and rack yoke
- Suppress mechanical noise.

#### Construction of the rack yoke

To meet the requirements, the following construction of the rack yoke assembly is prevailing in reality. The rack yoke is a rounded plain bearing element which is axially moving in an appropriately sized gear case drilling. The depiction of the rack yoke in Fig. 11.11 shows that there is a plain foil at the rack which is fixed at the rack yoke and allows a low-friction movement of the rack. To achieve radial damping of the rack yoke, one or two O-rings can be integrated, they are fitted into corresponding grooves. The compression spring and the adjuster bolt enable a safe support of the rack. The drilled hole, made into the adjuster bolt to directly observe the free travel of the rack yoke, can be sealed with the drain plug after measurement.

Figure 11.12 shows potential noise sources in the system of the rack support by the rack yoke. This constellation can produce rattle under certain loads, like varying tie rod forces (for example, in a journey over uneven cobblestones) or

**Fig. 11.12** Potential noise sources in the dovetailing and rack yoke area



when movement of the rack reverses ('reverse knock'). This noise should be fully prevented by suitable measures.

To avoid noises of the rack yoke, one aims at as little radial and axial free travel of the rack yoke in the case drilling as possible.

The radial bearing clearance results mainly from the accessible tolerance margins for the outer diameter of the rack yoke and the inner diameter of its drilling. It depends on the chosen way these diameters are processed and on the mating of materials, because different thermal expansions require measures to prevent the rack yoke from blocking.

The axial bearing clearance is given by the adjuster bolt for the rack yoke clearance that ultimately represents a stop unit for the rack yoke, preventing further movement. Here again, the free travel should be as low as possible. Still, note that an insufficient rack yoke clearance entails a powerful rise of the friction in the rack, which the driver will perceive as very unpleasant and may interpret as a blocked rack. Hence, the rack yoke clearance has to be adjusted in such a way that it can also compensate the permissible deviations of the cog treads of the rack and the pinion, the run-out deviation of the pinion and the permissible static sag of the rack, beside the already mentioned tolerance and stretch differences. The permissible tolerance of the mentioned parts are therefore integrated into the definition of the rack yoke clearance. A clearance of up to  $100 \mu\text{m}$  is generally common. It is measured during the adjustment of the bolt straight through a drilling in its centre. After setting the clearance, the drilling is sealed in the bolt with the drain plug.

Optionally, an integrated O ring can be added to the adjuster bolt in the contact zone to the rack yoke, so that the noise in this area is further damped, if the operation of the steering should cause the rack yoke to strike on the adjuster bolt.

Possible rack yoke materials are aluminium, zinc-aluminium alloys, sintered metal or plastic. The friction contact surface of metal rack yokes to the rack consists of an additional foil of plastic or composite metal with bronze and PTFE support. The different sliding materials, combined with the pretension of the rack yoke spring, enable a tuning of the friction at the desired level. In general, one aims at very low friction to provide a good steering feel to the driver. At the same time, the steering has to damp any disturbances and vibrations acting from the outside; a defined friction is contributing to this. However, all sliding materials have in common that the difference between sliding friction and static friction should be as low as possible, this avoids stick-slip effects and resulting noise or abrupt movements of the rack during small steering corrections.

The friction contact surfaces of the rack yoke are adapted to the rack according to its geometry in the dovetailing area, i.e. semicircular, Y or V (see [Sect. 11.5.5](#)). Using Y or V rack yokes prevents the rolling of the rack due to the dovetailing for the most part.

## Rack yoke tuning

Altogether, the rack yoke and its parts allow tuning the steering qualities, damping mechanical noise and rack vibrations and optimising the steering response. Structural factors are the level of the rack yoke spring tension, the sliding parameters of the contact surface of rack yoke and rack, or their friction coefficient, the free travel of the rack yoke bearing and the insertion of O-rings in the perimeter. These factors affect response, damping and noise of a mechanical gear and can within limits influence the steering qualities.

Changes in the area of the rack yoke are often used in practice to damp noises and vibrations which are recognised only late in the process of development, without having to essentially modify the gear.

### 11.4.3.3 Rack Bushing

The rack bushing—the second rack bearing of a mechanical gear, beside the rack yoke with pinion—is a sliding fit which supports the lateral forces from the tie rods in the rack and ensures that the translation of the rack is low-friction and free of noise. In some applications, the rack bushing also assumes the function of the end stop, limiting the rack stroke.

Mechanical rack gears and gears for pinion EPS most often feature plastic sliding fits, versions of sintered metal are less common. By analogy with the contact area of rack and rack yoke, the desired friction can be adjusted by choosing the material mating. To counteract rattling noises, two O rings are sometimes applied at the outer diameter of the rack bushing of plastic sliding fits. This facilitates good noise damping. With the help of these O rings, some further damping of axial rack movements can be achieved for small stroke movements as well. In addition, sudden radial load impulses are damped by this kind of bearing. An example of a plastic rack bushing with two O rings is shown in Fig. 11.13.

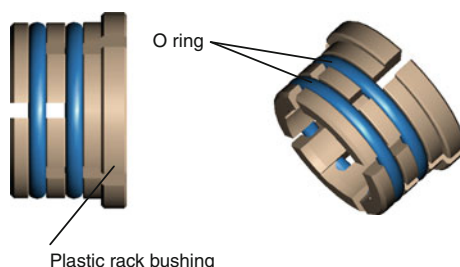


**Fig. 11.13** Rack bushing with two O rings

## 11.5 Dovetailing and Gear Ratio

The purpose of the dovetailing design is to include different limiting criteria, like high load-carrying capacity, high efficiency, low noise and high bending strength of the rack. Some of the individual measures generate opposing effects, demanding a compromise. For any given rack diameter, one tries to achieve the highest possible overlapping of profile and jump. The remaining cross section may not be weakened too much, otherwise the bending strength of the rack will be impaired. Constant and variable gear ratio are distinguished.

### 11.5.1 Constant Gear Ratio

The use of gears with constant gear ratio (CGR) is widespread in the car industry, where customary steering is concerned. The historical reason is the easier production by broaching. Broaching is acknowledged as an established manufacturing method for ‘common’ rack dovetailing, and it is most often applied; sanding and milling the dovetailing belong to the less widespread processes.

The full ratio of a consistently translated gear is computed from the centre gear ratio and the steering axis geometry of the vehicle. Consequently, the choice of a suitable gear ratio is a compromise between the preferred ratio in the centre area (or ‘straight ahead’ position), the desired manoeuvrability of the vehicle and the full number of steering wheel rotations, stop unit to stop unit.

The possibility to individually adapt the steering qualities by a variable gear ratio is a comfortable solution to find the best compromise for layout and adaptation of a steering system.

With regard to rules for the dovetailing design, the CGR is a special case of the variable gear ratio, so that the layout criteria discussed in the following sections also apply to CGR dovetailing.

### 11.5.2 Variable Gear Ratio

The above-mentioned manufacturing methods are not applicable for variable dovetailing with a flank geometry changing over the stroke. Hence, racks with variable dovetailing in mass production are either hot or cold transformed.

Dovetailing with variable gear ratio (VGR) uses a helical pinion, just like the CGR versions. The flanks of the rack cogs are bent, so that the same angles of the engaging cogs are present at any time of engagement. The left side of Fig. 11.14 shows the front cut through rack and pinion dovetailing. In the distance of the pitch circle diameter  $d_1$ , the cogs of the rack have a frontal division  $pt1$  (normal division to the pinion axis) and a related engagement angle. If the engagement angle rises,

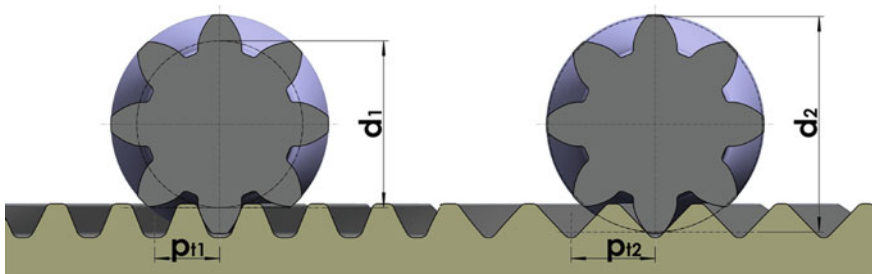


**Fig. 11.14** The different pressure angles of the pinion for different pitch circle diameters

the contact lines are shifted towards the head of the respective pinion cog. The right side of Fig. 11.14 shows a rise of the engagement angle in the front cut. Accordingly, the contact lines between pinion and rack cogs are separated by the pitch circle diameter near the cog heads of the pinion. The chamfer angle  $\beta_{z2}$  of the rack dovetailing turns into  $d2$  when the pitch circle diameter is large, because the chamfer angle of the pinion cogs rises with the diameter.

Figure 11.15 shows the different chamfer angles of the pinion for different pitch circle diameters. Under the influence of a small engagement angle and assuming an ‘installation angle’  $\gamma$  of the gear, the axial division  $p$  of the rack cogs is:

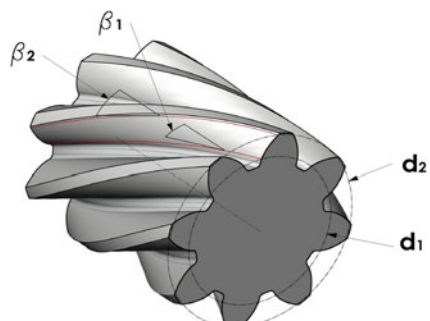
$$p1 = p_{t1} * \cos(\gamma + \beta_{z2}) / \cos(\beta_{z1}) \quad (11.1)$$

The gear rack travel  $S_y$  per steering wheel rotation (‘slope’ or ‘C factor’) is, using the number of the pinion cogs  $n$ :

$$s_y = p1 * n \quad (11.2)$$

As a result of the variation of the engagement angle (in the normal cut) of the rack cogs, the chamfer angle  $\beta_z$  and the module  $m$  are non-constant (cf. Fig. 11.15).

**Fig. 11.15** Different chamfer angles with different pitch circle diameters of the pinion



### 11.5.2.1 History of the Development

Variable gear ratios (VGR) are in use for sphere circulation gear since 1963. The development of the gear rack with variable dovetailing has lasted substantially longer. Although the first patents were submitted already in 1955, the actual development began with the patent of Henry Merritt in 1964. With Merritt's implementation a spur gear pinion was mounted in 90° angles to the gear rack. This kind of variable gear ratio offered only a very small rise of the gear ratio of approx. 8 % in comparison to the basic gear ratio.

After different other patents for variable dovetailing and suitable advancements, Arthur Bishop introduced the modern variable gear ratio of a gear rack by means of his patented diagonal-interlocked evolving pinion. This kind of gear ratio was first applied within the scope of a mechanical gear for the Isuzu Piazza which came onto the Japanese market in 1981. The gear was produced in Japan by the gear manufacturer Jidosha Kiki Company (JKC). At this time, ZF also began with the use of variable gear ratios in the Opel Ascona, Ford Sierra, in the BMW 3 series (E30) and in the Fiat Daily 1985.

The initial areas of application were mostly limited to the reduction of the steering expenditure close to the steering stop unit. In the 90 s the variable gear ratio was used increasingly in the area of hydraulic steering. The first-time use of variable transmission ratios in connection with electrically powered steering column systems occurred in 2001 from TRW in the Fiat Stilo and from Koyo-Seiko with the Saturn Vue.

### 11.5.3 Applications

Gear racks with variable gear ratio became popular to master the conflicts in the gear ratio layout and to open new possibilities. Although the first applications were focussed on supplying enough gear rack force without exceeding too much influence on the manoeuvrability, later solutions concentrated upon the need for improved dynamic qualities and ergonomic advantages.

#### 11.5.3.1 Applications for the Steering System

The first applications of the variable gear ratio concentrated primarily upon the mechanical advantage for the steering system. The whole ratio of a VGR steering system drops when the front wheel angle rises towards the stop unit. This phenomenon is a result of the actual steering arm radius  $r_L$  which decreases by rotation of the front wheels from the straight ahead position to the full steer-angle. The gear ratio at increasing steer-angles can be reduced by the variable implementation while retaining a high whole steering ratio.

### Mechanical gear—diminished torque

A basic challenge for the engineers of steering systems was to find a compromise for the steering ratio in the centre area of mechanical gears. It should limit the increase of the steering loads when the greatest steer-angle was approached and reduce the number of wheel turns to a satisfactory level. This task is complicated by rising axle and steering loads, caused by the chassis geometry.

Reducing the gear ratio for partially offsetting the higher loads during parking allows maintaining a higher gear ratio in the central position. This leads to a lower number of steering wheel rotations in comparison to a CGR system. Using a VGR in classical mechanical gears became less common during the past years. The latest application of a rack with variable dovetailing for a mechanical gear was found in the Smart, the MRR Roadster. The gear ratio course of the mechanical steering in this vehicle is shown in Fig. 11.16.

In contrast to hydraulic and gear rack-supported electromechanical gears, mechanical gears can be built smaller, however, on average they suffer higher pinion moments and load cycles. This results in increased forces in the dovetailing which can lead to wear problems. In this case, special attention needs to be paid to the cog sag and the contact tensions in the dovetailing.

### Power-assisted gear—reduced power consumption

Power-assisted CGR systems often do not have enough power to move the rack into the stop position with the required steering angular velocity. High weight of the front axle, high steering loads or limited power of the power-assistance can be blamed.

A limited power supply can also be ascertained for some column- and pinion-supported EP systems. These systems are integrated into most vehicles with smaller front axle loads, when space and costs are crucial.

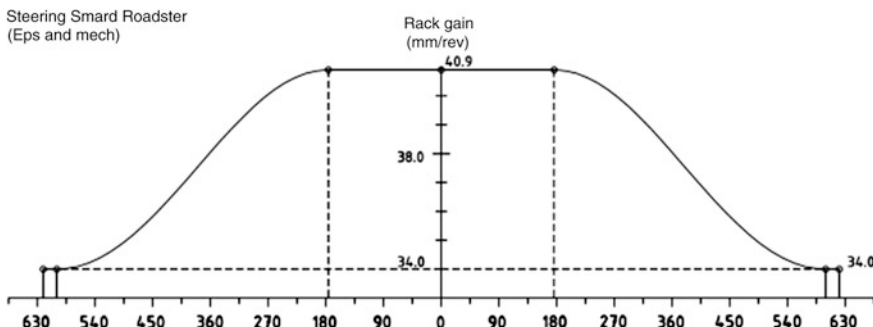


Fig. 11.16 Gear ratio course of the mechanical gear in the Smart Roadster. (Source Daimler)

The kind of variable dovetailing which is used for column- and pinion-supported EP systems resembles the gear ratio used in manual gears. They correspond to each other by a gear ratio that is lower farther away from the centre. The same favourably reduced pinion torque is achieved by this measure as in the manual gear. The loads on the dovetailing are, as expected, still higher in this kind of gears than in other models, because the whole driver and power-assist torque acts on the dovetailing of rack and pinion.

One purpose of the design of hydraulic or electric-mechanical rack systems is to limit the rack in its movement to the stop unit position. This reduces the power consumption and keeps it within the specified effective output of the power-assist system.

In all cases, the demands to the variable gear ratio can be plotted as a function of the steering geometry. The power and torque consumption of the power-assist system is thereby limited.

### 11.5.3.2 Driver Application

Power-assisted systems together with a VGR simplify car driving by suitable tuning. Advantages like easier parking, less high-speed nervousness or improved dynamic response of the vehicle are some of the characteristic features.

#### Ergonomics

In contrast to the reduction of the gear ratio with increasing steer-angle discussed above, a rise of the gear ratio is also conceivable, if the power-assistance is sufficient. The popularity of power-assisted systems allowed using the mechanical VGR for increasing the rack gain beyond the ratio desired at the central position towards the stop unit. The number of wheel turns, end stop to end stop, could be significantly reduced by that. This facilitates low-speed manoeuvres and parking. At the same time, there is less response to low corrections at the wheel during high-speed straight driving.

The change of the gear ratio increase usually began at a pinion or wheel angle between  $30^\circ$  and  $90^\circ$  and ended at a highest gear ratio at the angular range of  $180^\circ$ – $270^\circ$ . The driver can hardly discern this change of the rise, but its benefit is that the number of whole wheel turns, end stop to end stop, can be reduced to three or less. This prevented untimely tiring when driving in the city or on bendy roads, and it significantly promoted safe driving by the better manoeuvrability of the vehicle in such situations.

The first time this kind of variable dovetailing was applied was in the Ford Sierra in 1985. The use of this kind of gear spread only slowly during the 1990s, but it is common among higher-class vehicles of the 21st century. This solution also prevails among SUVs, because these cars have a rather high rolling axis, so

that a direct, concentric gear ratio could produce instabilities (cf. Baxter and Heathershaw 2002).

Till the end of the 90s, the number of suitable processes to manufacture high-precision VGRs rose, so that these systems are now commercially accessible to all manufacturers of gears.

### Vehicle dynamics

The development of the CGR had progressed till the beginning of the 21st century, and further benefits could be used. The economic VGR was made purely with the driver's needs in mind. The demand for a much higher rack gain within a shorter travel of the rack was rising. This enabled improving the vehicle's dynamic driveability.

The introduction of the Active Front Steering (AFS) by BMW in the series 5 of 2003 has shown that a change of the steering ratio improves the yaw rate response at low to medium speed clearly, even though the costs are high. The AFS system uses a mechatronical steer-angle superposing system to provide a VGR depending on speed. The angle-sensitive VGR can be called a not quite comparable, but cheaper alternative, according to Heathershaw (2004).

A relation between speed and the limits of the corresponding steer-angle change was first examined in the middle of the 1950s by Arthur E. Bishop at a conventional vehicle. On this basis, taking into account the typically generated lateral acceleration of 0.2–0.5 g, an angle-sensitive VGR could be made that had almost approached the characteristic curve of the yaw rate found for vehicles with a speed-sensitive VGR system. Since such a system is not speed-sensitive, it is very important that the gear ratio in the 'straight ahead' position is accordingly indirect, so that the high-speed steering feel is as expected.

The purpose of this measure is to make the change of the steering ratio discernible by the driver. This approach deviates from the principles of an 'ergonomic' VGR. A rack gain of 25–50 % over the medium VGR and, typically, between 90° and 120° of the first wheel turn is achieved by this principle. The quite large changes of the rack gain produce a high curvature of the rack cogs and their flanks, putting high demands to the accuracy of their shape.

The described kind of VGR was first used by Daimler in 2008, in the SL, SLK and CLC series within the scope of the Daimler "Direct Steering". Proper implementations of the gear ratio, the whole gear ratio and the variable dovetailing are shown in Figs. 11.17, 11.18 and 11.19.

#### 11.5.3.3 Special Applications

VGR gears can be used as well for combined requirements, for special gear ratio purposes or for the correction of asymmetries in the steering geometry.

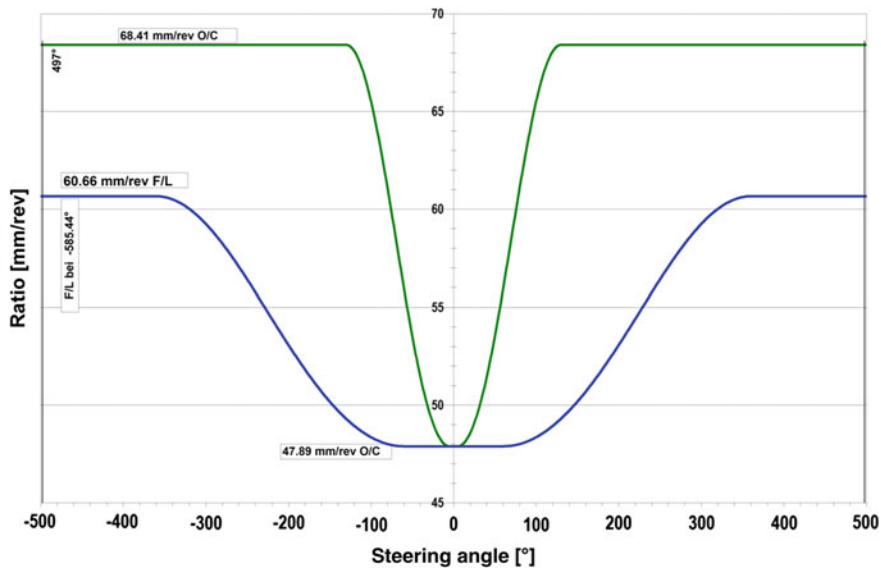


**Fig. 11.17** Gear ratio of a standard VGR steering (blue) in comparison to Daimler's 'direct steering' (green) in the Mercedes 2009 ML class. (Source Daimler)

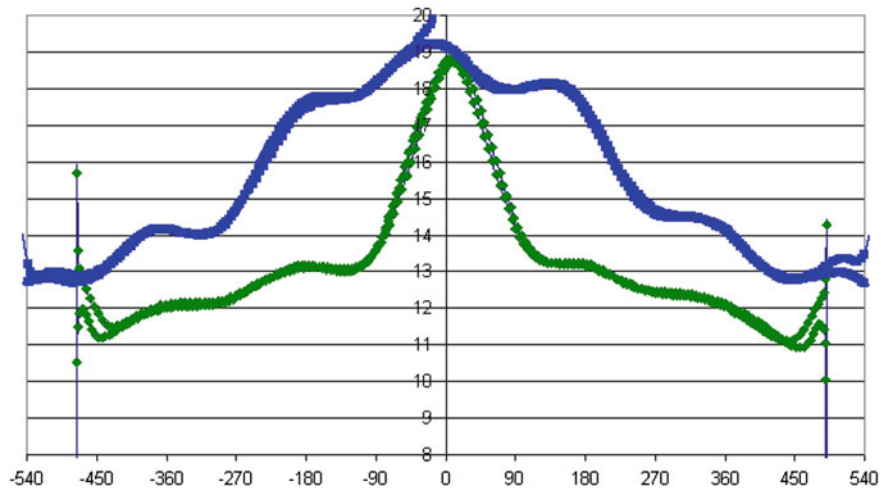


**Fig. 11.18** Whole steering ratio of a standard steering with VGR (blue) in comparison to Daimler 'direct steering' (green) in the Mercedes 2009 ML class. (Source Daimler)

### Combined applications

There are applications which demand a combination of driver- and system-related requirements for a VGR. The introduction of a driver-related VGR can be used for



**Fig. 11.19** Bishop VGR—dovetailing of the Daimler ‘direct steering’ in the Mercedes 2009 ML class. (Source Daimler)

a rack gain between central area and highest steer-angle (stop unit position). As discussed before, this produces a too high power consumption of the power-assist system. An overloading of the power-assistance can then only be remedied by reducing the gain until the end stop position.

To meet these sometimes opposing requirements, some manufacturing processes enable two or more gear ratio changes within a dovetailing. The restrictions to construction and production of a variable dovetailing set the highest and lowest gear ratio level for a dovetailing. The highest gear ratio is selected for the area beyond the centre. The lowest ratio is either in the centre position or in the area of the end stop position (or in both of these areas, if the ratios are equal).

An example for three ratios in one VGR is the M-curve VGR of the Opel Corsa of 2006. Its name is derived from the M-like shape of the gear ratio curve. Renamed the ‘Progressively variable steering’, the M-curve VGR was used for the sports models of the Opel Corsa 2006. Proper M-curves of the steering ratio and gear ratio are shown in Figs. 11.20 and 11.21. In addition, Fig. 11.20 compares the characteristic curves of a CGR and a VGR.

#### *Asymmetrical and special steering ratio purposes*

The VGR can be used to solve problems related to the steering geometry as well. One particular challenge is the occasional deviation of the steering ratio from the

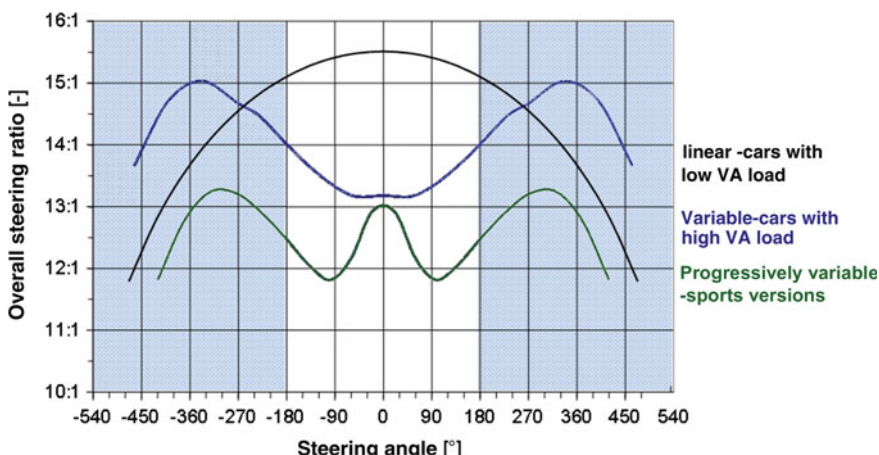


**Fig. 11.20** Steering ratios in the Opel Corsa: CGR for petrol car, VGR for diesel and ‘M-curve’ VGR for ‘progressively variable steering’. (Source IKA-RWTH)

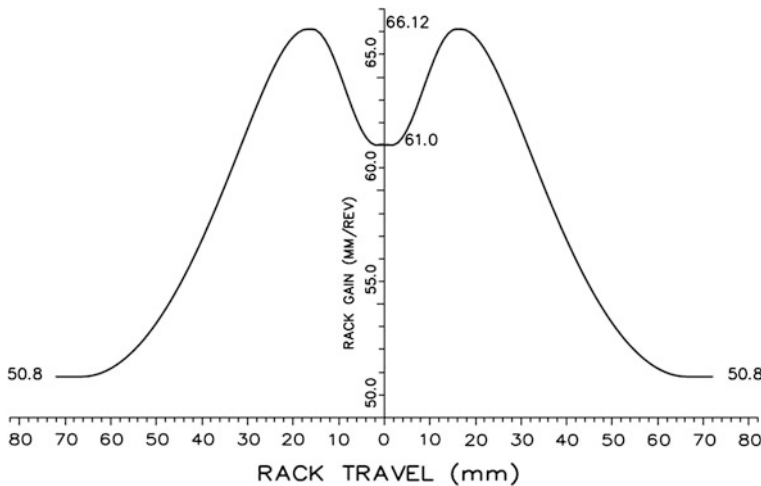


**Fig. 11.21** Gear ratio of the Opel Corsa M-curve VGR for the progressively variable steering. (Source IKA-RWTH)

desired curve. A VGR that adapts to a nominal curve can be developed based on the central gear ratio and the steering geometry, within the mechanical limits of the system.

Some steering geometries are distinctly asymmetric, despite the use of a CGR or a symmetrical VGR. This produces an asymmetrical steering ratio curve. In this case, an asymmetrical VGR is used to offset the asymmetries, so that a quite symmetrical steering response can be achieved.

#### 11.5.4 Technical Limits

A variable steering ratio is achieved by changing the standard engagement angle of the engaging rack and pinion cogs. The theoretical least and peak gear ratios are defined for a specific pinion module when the least and peak values of the engagement angle are set in the normal cut as upper and lower limits.

A conventional CGR version has a dovetailing optimised for contact engagement, stability, friction, tooth root stress and firmness. This task is more complicated for a VGR, because a satisfactory design has to be found for any normal engagement angle used in the VGR's pinion geometry.

##### 11.5.4.1 Size of the Rack Gain

The absolute limits for a rack gain are defined by the production process. Nevertheless, some limits are also due to the product development which defines the

'constraints'. Early developments intended a least engagement angle of only 14°. These low angles have two shortcomings, though: One is a trend to wedge under load, i.e. the dovetailing of the pinion wedges together with the cogs of the rack, and this can cause excessive friction and high wear. The other is the higher accuracy of the cog flank surfaces required when the engagement angle is reduced, to achieve the same accuracy in vertical engaging. Concerning the rack gain and the cog engagement, the vertical portion has to be controllable in any case of deviation, because vertical deviations of the surfaces have a considerable impact. The horizontal component contributing to the rack gain is less important. Reducing the engagement angle entails higher requirements for accuracy but limits a further gain of the rack ratio. As a result, a lower limit of the normal engagement angle of 20° is used in reality.

The upper limit of the engagement angle is defined by the gear application. The helical pinion transfers forces on the cogs of the rack which can be divided into axial, transversal and vertical vectors. Accordingly, the general purpose in designing a rack-and-pinion steering is to maximise the axial component of this force, in particular for CGRs. Figure 11.22 compares pinion force vectors with low and high dovetailing engagement angles.

Variable dovetailing always sees deviations occurring at the cogs of the rack with regard to these force vectors. One tries to minimise the vertical force vector when higher pinion loads shall be transferred. A high vertical force component will also see high forces acting on the rack support and the rack yoke, provoking high friction loads. Due to these considerations, rack yoke contact surfaces with low friction coefficients are used for rack-and-pinion systems with high vertical force components (see Sect. 11.4.3.2).

#### 11.5.4.2 Contact Lines

The engagement angle also influences the length of the contact lines between the pinion and the rack cogs, a measure of the dovetailing quality. This is described by

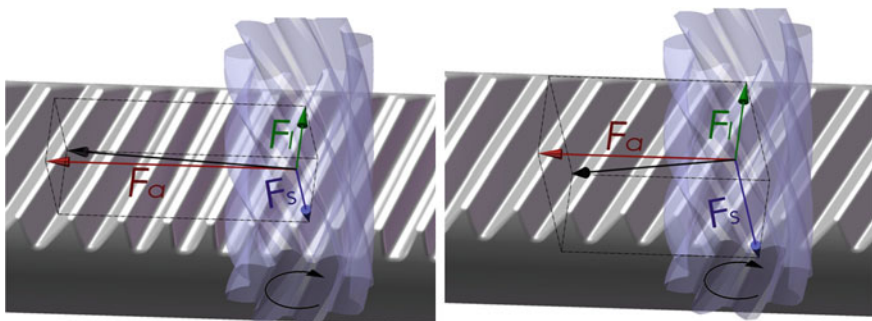


**Fig. 11.22** Pinion force vectors with low and high dovetailing engagement angle

the overall engagement  $\varepsilon\gamma$ , the total of tread engagement  $\varepsilon\beta$  and jump engagement  $\varepsilon\alpha$ , which results from the helical dovetailing. The whole engagement supplies the average number of cogs in contact. The theory of dovetailing calculation for involute gears is documented in DIN 3960.

A typical tread engagement decreases quite quickly when the normal engagement angle rises, while the jump engagement rises only minimally.

Different full engagements are used as standards for different kinds of steering systems. Concerning VGR design, it is ensured that these standards are observed.

Hence, a bigger gain of the gear ratio uses a bigger dovetailing area than a constant gear ratio, to maintain adequate full engagement. Implementing the desired rack gain may require compensating the reduced tread engagement by a bigger jump engagement (due to a bigger dovetailing width), to receive a satisfactory function.

#### 11.5.4.3 Stability and Noise (NVH)

The power between pinion and rack dovetailing is transmitted along the contact lines. Two or more cogs are usually in contact. If the pinion is turned and the rack is driven, the contact lines move along the rack cogs. As long as there is always at least one contact force vector of a contact line acting on each side of the rack dovetailing's axis of rotation, the rack is prevented from rolling. In this case, the active torques of the contact force vectors have the same amplitude and opposite directions. Figure 11.23 shows how the contact lines of adjoining cogs move when the pinion is rotating. This rotation shifts the contact lines and their resultant forces.

Pinion geometry, engagement angle, chamfer angle of the pinion cogs and the distance of the rack dovetailing to the axis of rotation can cause conditions in which all the contact forces generate parallel torques around the rack's axis of rotation. The rack is then in an unstable state and inclines to slight turns around its

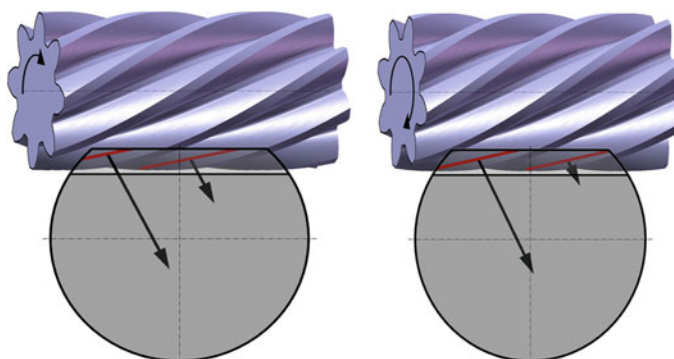


**Fig. 11.23** Contact line movement of adjoining cogs when the pinion rotates

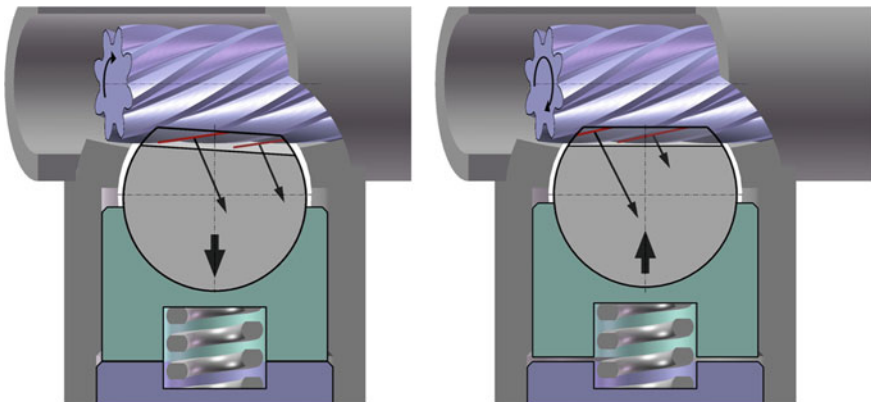


**Fig. 11.24** Rotation of the rack by unstable contact line vectors and a shifting rack yoke (*left*), stable contact line vectors (*right*) upon full pinion contact and rack yoke clearance

axis of rotation. The rack is supported in the gear case by a rack yoke pressing its dovetailing against the pinion dovetailing. As was discussed in Sect. 11.4.3.2, the rack yoke clearance enables the offset of the dovetailing tolerance and permits a slight rolling of the rack under high loads.

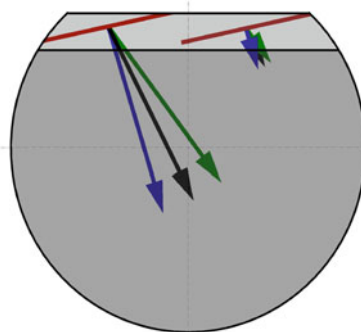
Figure 11.24 (left) shows the field line vectors that cause the instability and thus the turning of the rack. The spring-loaded rack yoke is pressed against the adjuster bolt attached in the gear case. When the pinion turns on, the next cog is engaged and an offset torque is created around the rack axis (see Fig. 11.24 on the right). The rack turns back into the initial position of the full engagement, restoring the rack yoke clearance. Except for all the other forces that are acting on the rack in this case, the movements described in this unstable state can contribute to a noise in the gear [sic! Why “except” (mit Ausnahme)?]. The change of the torques in the engagement kinematics can also produce transmission errors in the rack gain and changes in the axial rack force.

A short engagement distance of rack cogs and pinion or rack cogs with a higher axis of rotation are indicators for an unstable dovetailing engagement.

Figure 11.25 shows that the sliding friction between the surfaces of the rack and pinion dovetailing affects the angle of the contact force vector. The pinion torque (on the driver’s side) produces a greater vertical component of the contact force vector (shown in blue), while the rack force from the tie rods generates a lesser vertical component (shown in green). The result reveals a higher risk of unstable engagement and, hence, expectable noise from excitations of the chassis. The power flow from the road, as for example upon road kickback, should be considered more critically than the power transmission from the driver.

Using a VGR means that the engagement geometry has to change. Therefore, it is ensured that minima and maxima of the gear ratio curve do not make unstable dovetailing engagement more likely.

**Fig. 11.25** Effect of the friction on the contact line vector forces (unstable situation during recoils [green])



### 11.5.5 Manufacturing Processes

Since VGR racks were introduced in 1981, many different processes have been used in serial production. The main requirement for a suitable standard process is to make a dovetailing with three-dimensionally curved, non-prismatic cogs. Vertical and transversal curvatures should be possible. High curvatures of surfaces or 3D shapes require more accuracy and quality of the dovetailing.

The first process, introduced by JKC, Japan, in 1981, was a combination of hot forging, deburring and cold stamping. Although this process was used for lots with few pieces for more than two decades, it suffered a significant decarbonisation of the cog surfaces as a result of the hot forging, and that interfered with the wear-resistance. Low service life of the tools and the risk of imprecise adjustment of the parts during calibration added to the disadvantages of this production mode.

Only three processes for making variable dovetailing are still in use.

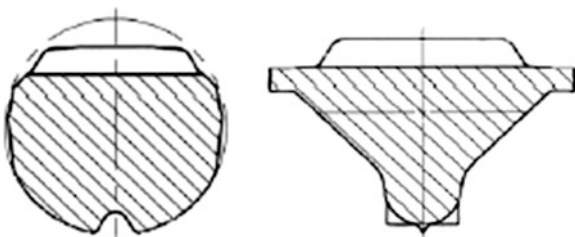
#### 11.5.5.1 Rotary Swaging

Rotary swaging was developed by a collaboration of ZF Friedrichshafen and Heinrich Schmid AG in early 1980 and implemented in production after 1985. A circular movement of the upper cog tools generates a gradual reshaping of the material. This circling is limited to a swinging parallel to the rack axis, to produce the rack dovetailing. The basic material is submitted to a special soft-annealing process to achieve the desired reshaping without fissures. At the same time, the blank is covered with a graphite lubricant to extend the service life of the tool.

This kind of production leads to excessive displaced material gathering in burrs on the flanks of the dovetailing, that need to be removed in a subsequent step. If a humpback rack (D-form rack) is made, material is machined away before reshaping, to avoid any distortion of the rack during the swaging process. The cold solidification of the rack's surface is exploited to compensate the low firmness of the raw material.

The described process can be used to make humpback racks or Y racks. Figure 11.26 compares the cross sections of both rack backs as an example.

**Fig. 11.26** Typical swaged rack cross sections. (Source Heinrich Schmid AG)



An offset of the swinging of the upper cog tool has to be considered during the construction of the tool. This limits the highest curvature of the cog flanks that can be achieved with this tool, a curvature needed nowadays for the dynamic implementation of a VGR.

### 11.5.5.2 Semi-hot Forging

To handle the decarbonisation problem, semi-hot forging was introduced by James N. Kirby Ltd. and Bishop in 1982, though calibrating and cold stamping were necessary parts of this process, too.

Bishop introduced a semi-hot forging process for Y racks in 1984; it did not need calibration any more. In the following years, this approach was further pursued, until at last a new process became available in 1994. The first VGR rack forged by this process, without burrs, was used in the mechanical steering of the Fiat Punto series.

A single forging process is sufficient to produce the VGR dovetailing at a temperature of 700–800 °C. This manufacturing method now allows achieving a high curvature of cogs and flanks with the required accuracy. In comparison to other processes, a good surface structure is achieved, internal tension is avoided and decarbonisation of the cog flanks is prevented. This process, which requires no further treatment steps in the cog area, provides a high precision shaping of the dovetailing, enabling the highest possible gear ratio range and the fastest possible rack gain.

Bishop developed this process, and the first variable dovetailing at a humpback rack was forged in 2005. The new process allowed producing a bigger variety of cross section shapes to widen the dovetailing, larger cross sections (in comparison to the shaft area) and all kinds of D, Y or V rack backs in the dovetailing area. Figure 11.27 presents typical semi-hot forged rack cross sections.

As described in Sect. 11.5.4.2, a significant rack gain often requires bigger and broader cogs to achieve a contact engagement which is favourable for the application. Bishop's semi-hot forging process enables the making of racks with dovetailing widths of up to 115 % of the rack diameter.

Before the actual forging, the blank is heated, and after forging, it is cooled down to produce the desired material properties. An exact monitoring of the heating and cooling is essential. All common chemical compositions and states of

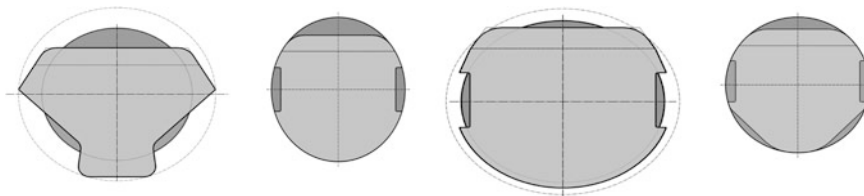


**Fig. 11.27** Typical semi-hot forged rack cross sections. (*Source* Bishop Steering Technology Limited)

**Fig. 11.28** Examples of D and Y ‘ActivRak™’ racks



delivery can be forged out of steel now, a fact which is very beneficial with regard to the currently more frequent EP systems. Figure 11.28 shows examples of recent D and Y rack cross sections with variable dovetailing.

### 11.5.5.3 Pipe Reshaping

A different approach to making racks was pursued in Japan during the mid-1980s. A reshaped pipe was taken as a blank to develop a lightweight version of a rack. The material in the middle of conventional ‘solid’ racks, near the rack axis, contributes to the rack’s weight, but little to its bending strength. Hence, this material is in many cases removed by deep drilling to reduce the weight, at least in the non-dovetailing area of the rack. Making racks from pipes is therefore an elegant solution, weight and efficiency of use being the prime motivations.

In contrast to rotary swaging or semi-hot forging, as described above, pipe reshaping is achieved by inserting spikes on the inside. The pipe is preformed to increase the wall thickness in the cog area at some local places. Then the pipe is fixed between stamps, the desired cog form is contained in one half of the stamp. Several cold spikes (up to 16) are pushed successively through the pipe, to press the material gradually into the cog tools. Figure 11.29 shows a cutaway view with the pipe rack in the dovetailing area.

**Fig. 11.29** Typical pipe rack cross section, here of a Mazda 6



The material necessary for pipe reshaping contains less carbon than most other rack applications that commonly have a content of 0.30 %. The pipe is fully hardened and tempered after shaping and treating, so that it receives the necessary bending strength. However, the surface resistance is lower than that which competitive processes and materials might achieve.

The pipe reshaping process was first used for CGR gears in hydraulically driven power steerings. But VGR dovetailing can also be made by this method. However, the cog width is then much lower in comparison to the forging processes, because the rack material the cogs are made from has to be pressed from the inside of the pipe outward into the cog mould. Accordingly, bigger pipe diameters have to be selected in order to achieve comparable widths and accuracy of the cog shape.

## 11.6 Requirements of a Mechanical Rack Gear

This chapter discusses the general requirements of function and firmness of mechanical rack gears, proven by bench tests. Before the actual test, the gear is submitted to a startup process, to anticipate any potential sagging effects and to support the test results.

Tests checking essential functional aspects of the gear are already carried out as soon as the gear is assembled in the production line. More extensive tests are performed at typical, randomly selected parts from a batch of gears (auditing). Firmness, wear and environmental tests on the other hand, are part of the development programme. After the release for series production, they will only be repeated at defined time intervals (e.g., once per year) as accompanying tests.

### 11.6.1 Functional Requirements of Gears

All function tests are carried out at a gear without tie rods in built-in position at room temperature ( $20^\circ \pm 5^\circ$ ). Some vehicle manufacturers, upon defining the

functional requirements, make a distinction between the comfort area, with a steering wheel angle of  $\pm 180^\circ$  or a rack path of  $\pm 25$  mm around the central rack position, and the remaining dovetailing area.

### 11.6.1.1 Rack Yoke Clearance

Although the limitation of the highest rack yoke clearance (e.g.,  $100 \mu\text{m}$  max.) is in fact an indirect functional requirement, it is crucial for other functional requirements or the friction and noise response of a rack-and-pinion gear (see also Sects. 11.4.3.2 and 11.5.4.3). The widest clearance is usually defined at the central position of the rack and measured by a suitable drilling in the adjuster bolt or the yoke cover. A linear receiver records the relative movement of the rack yoke against the gear case. The reference point for the rack yoke clearance is set by driving the rack yoke into touch with the cover, a deflection torque of 5–10 Nm without lateral forces around the longitudinal axle of the rack is applied. The unloaded rack yoke then rebounds, and its relative movement is recorded by the linear receiver, resulting in the value of the rack yoke clearance, see Fig. 11.30. This clearance can also be recorded as a function of the rack's position. If the values are very small, then a rising friction at the rack is likely. If, by contrast, the upper limit value of the clearance is surpassed, there is a risk of steering rattle in the car.

### 11.6.1.2 Steering Pinion Torque

To measure the steering pinion torque, a rotation without tension or free travel and with constant rev is applied at the input shaft. There are no loading elements at the

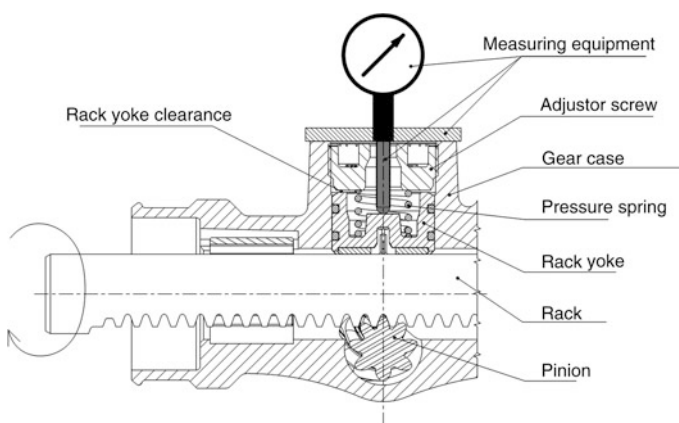


**Fig. 11.30** Identifying the rack yoke clearance by applying a deflection torque without lateral forces to the rack

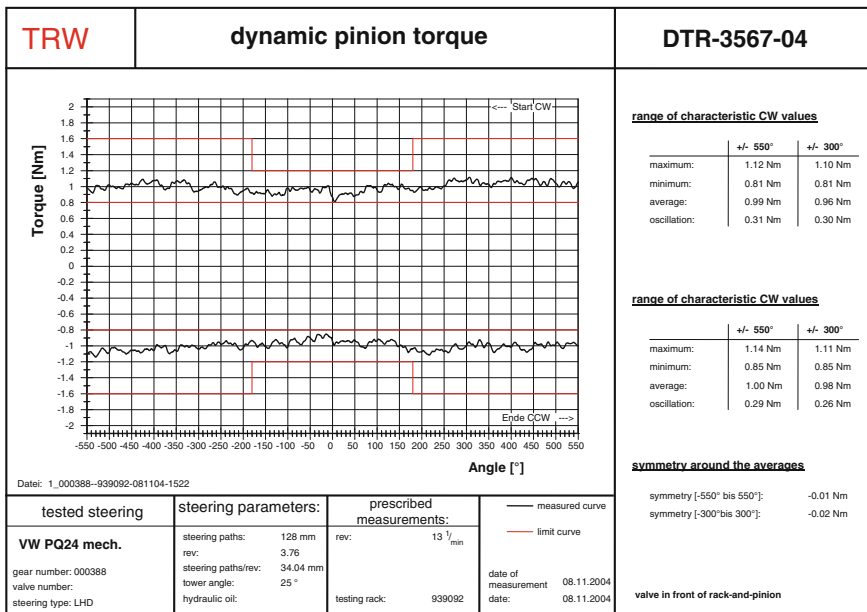


**Fig. 11.31** Pinion torque of a mechanical rack-and-pinion steering

rack, so that it moves freely. The rotary angle and the torque at the input shaft are recorded over a measuring cycle.

As the minimal and maximal values of the rotary torque and its oscillation over the stroke are predefined, the test is counted as failed if these values are surpassed. A typical value of the pinion torque is in the range of 0.8–2.0 Nm, commonly achieved when the pinion has a rev of 15 rpm. Figure 11.31 shows the result of a measurement of the pinion torque, moving left or right and remaining inside the specified range. The highest permissible pinion torque that the specification of this steering permits is accordingly marked in the image and should be less than 1.2 Nm in the comfort area while staying below 1.6 Nm beyond the comfort area.

### 11.6.1.3 Rack Displacement Force

A linear drive is attached to the rack strainlessly and without free travel. There are no additional loads at the input shaft, so that the shaft moves freely when the rack is shifted with a steady displacement speed of 5–10 mm/s, according to specification. Rack forces of 150–350 N are permissible. The rack travel and the rack force is recorded over the measuring cycle. If the highest measurement value of the displacement force exceeds the defined limit value, the test is considered failed. If demanded, the oscillation of the displacement force is evaluated as well.

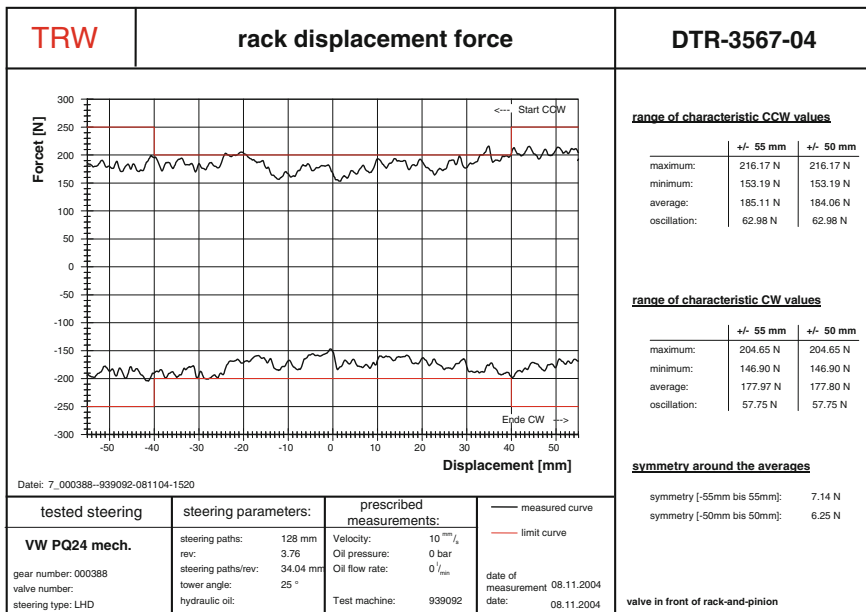


**Fig. 11.32** Rack displacement force of a mechanical rack-and-pinion steering

The rack displacement force of a mechanical rack-and-pinion steering is applied over the rack path in Fig. 11.32. In this case there were values of up to 200 N permitted for the central area of the rack; 250 N may be achieved in the outer dovetailing area. The rack displacement forces of mechanical gears are usually a little higher than those of rack-supported power-assisted gears. The reason is that all the rack forces of mechanical gears are directly transferred over the pinion/rack link. High input steering torques generate high forces in the dovetailing, the major part of which is acting on the rack yoke. The high pre-tension of the rack yoke demanded thereby and a gliding foil corresponding to the forces influence the rack displacement force.

#### 11.6.1.4 Efficiency

Some vehicle manufacturers require information about the efficiency of the gear, distinguishing direct and indirect efficiency. For the direct gear efficiency, one observes the conversion from the rotating input shaft into the translation of the rack, i.e. the ratio of rack force to pinion torque achieved as the pinion is moving. For indirect efficiency, also called reset efficiency, the movement transferred by the chassis on the rack is examined, i.e. the quotient of accessible pinion torque and rack force at the moving rack is computed. The direct efficiency established from the rack shift of a typical mechanical rack-and-pinion steering is shown in Fig. 11.33.

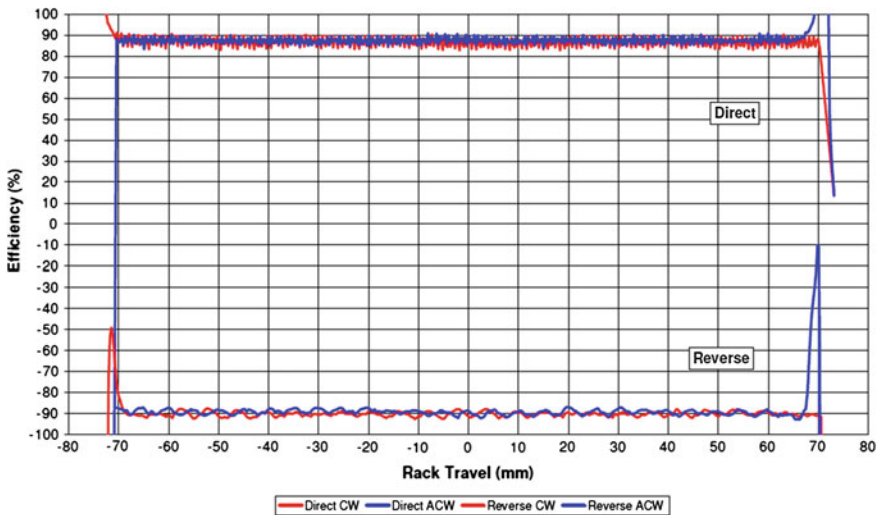


Fig. 11.33 Direct and indirect efficiency of a mechanical rack-and-pinion gear

The result confirms the standard values for the direct efficiency of a mechanical rack-and-pinion gear which, according to the load, are found in the area of 85–92 %. The indirect efficiency of the mechanical gear is often a little lower; this depends on the dovetailing design.

#### 11.6.1.5 Noise (NVH) Requirements

The general Noise, Vibration, Harshness (NVH) requirement of a mechanical rack-and-pinion gear is the ‘absence’ of any annoying rattling noise. Hence, steps to avoid noise are considered already during the design of the gear. Calculations and simulations support these considerations. As soon as the first prototypes are available, hardware examinations on the test bench follow. The gear is fixed on the test bench and realistically loaded. Responses according to frequency and excitation amplitude occur at the bearing points of the rack which are then evaluated for their practical relevance. If there is any need for improvement in the area of the rack yoke, remedial actions as discussed in Sect. 11.4.3.2 may be examined and implemented as, for example, the change of rack yoke clearance and spring stiffness or the insertion of O rings. A successful tuning is confirmed in the vehicle test.

#### 11.6.2 Strength Requirements of the Gear

Examination of the static and dynamic strength is decisive for the strength requirement.

### 11.6.2.1 Static Strength

The static strength of a mechanical rack-and-pinion gear is confirmed chiefly by the ‘fracture torque test’ and the ‘Charpy impact test’.

#### Fracture Torque Test

The focus of this test is the check of the rack’s static strength, pinion and case. The parts are tested until failing by applying a torque to the input shaft both ways, without any lateral force, while the rack is blocked. The test is passed if at least one defined torque level was achieved before the torque drops and the part in the steering fails. The requirements are usually in the range of 250 Nm.

#### Charpy Impact Test

The impact is directed onto the gear by a tie rod above the ball pivots of the outer joint. The position of the tie rod corresponds to the built-in location at full deflection. The rack is fully extended on the load side. The moment of inertia of steering column and wheel is applied by a substitute mass at the input shaft. The requirements to the gear are met if the full effectiveness was proven for each load layer and no part has fractured.

### 11.6.2.2 Dynamic Strength and Wear Test

Parking and wear tests are carried out within the scope of testing the dynamic strength.

#### Parking Test

The parking test is a bench test which applies high rack loads, to simulate the service life load of a gear within a short time. This test is an important part of the test programme for mechanical rack-and-pinion steering, because it yields statements on service life for almost all the parts. The input shaft is driven over the rack stroke with constant speed. A test load equivalent to the highest operation load of the steering opposes the rack’s direction of movement. Equal operation loads are applied at both outer joints, right and left. At the end stop, the axial joint touches the gear case. The torque at the input shaft is raised to the prevail torque and kept at this value. Then the rotation of the input shaft and the direction of the load at the tie rods is reversed.

## Wear Test

The wear test is performed on a test bench that simulates the service life load of the gear in a rather short time, because of the level of the initiated forces and torques. Primarily, parts like pinion, rack, bearings and the internal fouling of the gear are tested by abrasion.

The input shaft is driven against a test load at the rack, the speed should be constant over the rack stroke. The test load is applied to the outer joints of the tie rod and the input shaft of the steering. At the end stop (stroke end position), the axial joint touches the gear, enabling a gain of the torque. When the peak torque is reached, the rotation at the input shaft and thereby the direction of the rack force is reversed.

If after the wear test the functional values of the steering do not correspond to the given specification any more, the test is failed. A rack yoke clearance of 0.5 mm or higher also produces a fail result of the test.

## **11.6.3 Environmental Requirements of the Gear**

Environmental requirements are met if the salt spray test and the dirt water test were passed in an environmental simulation.

### **11.6.3.1 Salt Spray Test**

For the salt spray test, a steering is sprayed with different NaCl solutions, compliant with DIN ISO 9227. The following requirements apply:

- no base metal corrosion
- absolutely water-tight
- effective after the test.

### **11.6.3.2 Dirt Water Test**

This test is performed at a completely assembled steering which is repeatedly driven against either end stop by turning the pinion. This test includes two operating modes, consisting of spraying the steering and a subsequent dry run. For spraying, the whole steering including the tie rods is sprayed with dirt water at zero pressure. The dry run heats the gear with hot air. After the test, the gear has to be absolutely sealed, as in the salt spray test.

## 11.7 Design Verifications and Product Validation of a Rack-and-Pinion Gear

The release procedure and the tests to be finished for release are parts of the specifications. The releases occur at important points of the development programme.

The entire release procedure is coordinated with the customer (OEM), before the gear supplier is selected. This release procedure becomes a compulsory part of the specifications. Only steerings that passed all the tests described in the test specifications can receive an internal product release from the steering manufacturer.

The purposes of these tests and the requirements of the respective samples are discussed in the following.

### 11.7.1 Concept Verification

The purpose of this test is to verify product features qualitatively (the product may be used without safety risk) and quantitatively (the demands of the specifications are kept). The concept verification (CV) phase is marked by loops in the development, finished when the design is ultimately fixed.

### 11.7.2 Design Verification

The purpose of the design verification (DV) tests is to corroborate product features of samples made with substitute tools. These tests confirm that the product design matches the demands for quality. The tests are carried out after the final definition of the design, no further loops will be passed.

### 11.7.3 Product Validation

The purpose of the product validation (PV) test is to ratify product features of samples in series production (industrial manufacturing). When the samples are made, the parameters of the later series production have to be observed precisely. This includes the manufacturing of parts, assembly, machines and tools used, procedure sequence and quality control.

The PV test (and the DV test) are conceived to check the product features concerning

- Static strength
- Dynamic strength
- Wear-resistance and
- Environmental resistance.

The size of the applied test loads depends on the operation loads expected for the product. The release programme is passed when all requirements of the relevant test standards were met within the defined scope of validation.

### **11.7.4 Accompanying Test**

The purpose of the accompanying test is a random check of product features which cannot be monitored by the quality control during production. These features are commonly described in the generic product specification. The quality of the supplied parts and the stability of the assembly process are controlled by these tests. Hence, the samples have to be made compliant with the defined and released process parameters.

## **11.8 Hydraulic Steering Systems**

The hydraulic power-assisted rack-and-pinion steering is an advancement of the manual steering into which additional elements were introduced to amplify the rack force. Figure 11.34 shows that it consists of a mechanical part, very similar to the mechanical rack-and-pinion steering described in Sects. 11.4 and 11.5, and a hydraulic part including the components for force generation (cylinder/piston), steering (valve) and transmission of the auxiliary energy (transfer lines and hydraulic connections).

The effective rack force of this steering model is generated by a superposition of mechanical and hydraulic force:

$$F_R = F_{mech} + F_{hydr} = \frac{M_H}{r_{Pi}} + \Delta p_C(M_H) \cdot A_C \quad (11.3)$$

### **11.8.1 Objectives**

#### **11.8.1.1 Reducing the Steering Forces**

The main argument for the development of power steering was the reduction of the necessary steering forces, esp. when the vehicle is at rest, to improve the driver's

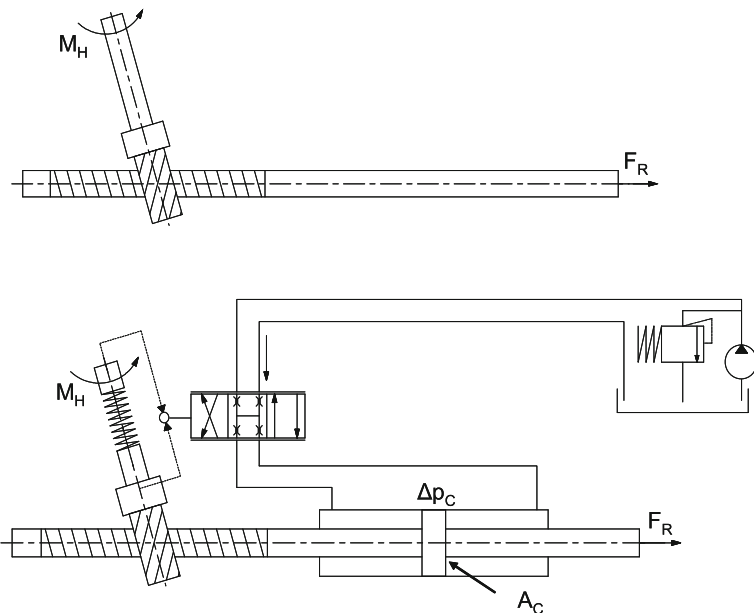


**Fig. 11.34** Design comparison of mechanical and hydraulic steering

convenience. The demand for this discharge of the driver has grown with rising front axle loads and the resulting higher rack forces of the steering.

### 11.8.1.2 Reducing the Steering Ratio

The possibility to reduce the steering ratio was also exploited early on. For manual steerings, it has to be high, so that the steering forces are kept convenient for any driver and within the scope of the registration regulations (ECE regulation R79). Such a design often prevents fast changes of course at low speed, because the driver is not physically capable of applying the necessary wheel angles fast enough. The reduction of the steering ratio in power steerings improves the steering convenience and safety, because, for example, quick evasive manoeuvres in city traffic are better supported. The tendency to further reduce steering ratios or to employ VGRs that are dropping beyond the central position of the rack is ongoing and has become an important objective for power steering.

### 11.8.1.3 More damping of the steering system

Another purpose is to increase the damping of the steering system for various appearing vibrations and to suppress interferences initiated in the steering system by the road. One particular objective is to integrate the additional elements that

some mechanical gears may need into the power steering, so that the add-on costs of the power steering are partially compensated.

#### 11.8.1.4 More Freedom in the Design of the Chassis

A power steering is standard equipment in most vehicle classes, hence, the possibility to avoid compromises in chassis design in favour of lower steering forces is exploited as well. This concerns, e.g., the definition of the castor and the choice of the tyre thickness.

#### 11.8.2 Necessary Changes in the Vehicle Opposed to Manual Steering

The package of the hydraulic steering has to accommodate some additional components by which the gear loses compactness (see Fig. 11.35). One is the steering valve on the input shaft, extending the least distance between rack axis and attachment of the gear to the intermediate steering shaft. Furthermore, the steering cylinder has to be arranged in the extension of the rack axis or parallel to it.

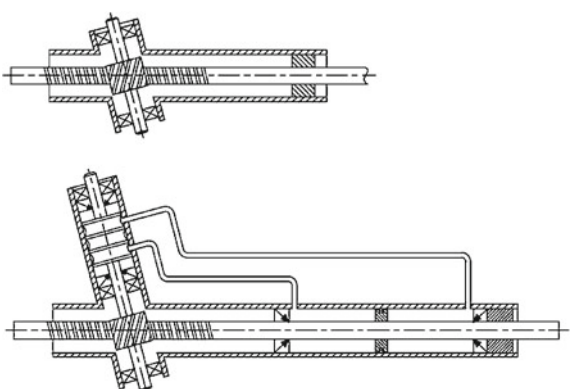
The auxiliary power supply, either a part of the secondary drive unit of the internal combustion engine or an electrically driven engine/pump aggregate, and its connection to the power steering by pipes and hoses, entails more profound changes.

On the other hand, compromises in the design of the front axle geometry in favour of low steering forces are not required any more.

#### 11.8.3 Necessary Changes in the Gear Opposed to Manual Steering

The gear is designed for much higher operation loads. This is needed because of the generally higher steering forces resulting from the design of the front axle

**Fig. 11.35** Comparing packages of manual and hydraulic gears



geometry. Even more significant is a change of the driver's behaviour who steers much more often when the vehicle is at rest, i.e. when the rack forces are high, because any power steering will facilitate this without trouble. Yet some components of the gear, like dovetailing or pinion bearing, are less stressed by driving, because they are loaded only with lower torques applied by the driver. Hence, the design of the strength of these components is focussed on a few or a single peak load which may appear during abuse situations like a kerb impact or accidents in which even the highest possible power-assistance is insufficient and a major part of the rack force will transfer into the mechanical part of the steering.

#### ***11.8.4 Specific Features of Hydraulic Gears for On-board Use***

No servicing is intended for the hydraulics of the steering system—apart from a regular check of the oil level within the scope of a general vehicle inspection, to avoid failure from minor leakage. This places high demands on the sealing system of the steering hydraulics.

Other than with a manual steering, the safety concept of the power-assisted steering system also has to consider a failure of the power-assistance. The formal requirements are met by a mechanical driving of the steering wheel to the front wheels and by a proof of low enough steering forces if the power-assist fails, compliant with EU regulation ECE R79. It is ensured as well that the driver can handle a vehicle with failed power-assist safely enough, even in real traffic situations, and that any failure is indicated early on.

### **11.9 Constructions and Components of Hydraulic Gears**

The function of a power-assisted rack covers the following aspects:

- Solid or elastic attachment of the gear case to the vehicle (mainly at the sub-frame which takes up the front axle)
- Defined mounting points of the axial joints of both tie rods at the rack in a fixed distance
- Translation of the rack, parallel to the Y axis of the vehicle co-ordinate system (transverse axis)
- Defined gear ratio between rack translation and input shaft rotation
- Defined mounting point for the steering column at the input shaft of the gear, so that its position and the orientation of the input shaft allow the observation of the specifications for the attachment to the steering wheel (package, free running, uniformity of the gear ratio)

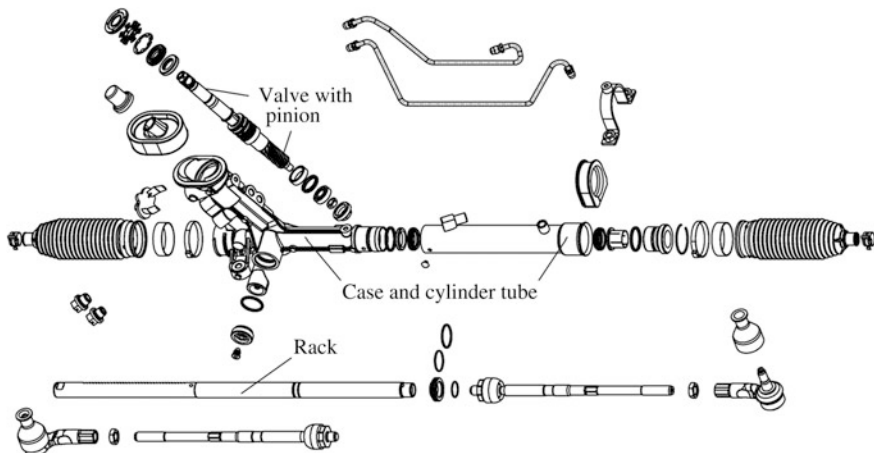


**Fig. 11.36** Main components of the hydraulic rack-and-pinion steering

- Integration of the steering hydraulics which receive the wheel torque applied at the input shaft and its translation into an assisting force in the direction of the rack.

Figure 11.36 shows an exploded view of a typical gear, the main components are labelled.

Many components are similar to those of the mechanical gear: pinion, rack yoke, rack, bushing, case and gaiters. They were already discussed in Sect. 11.4. This chapter therefore only discusses the additional components of hydraulic power steerings, based on the general construction of a rack-and-pinion steering: steering cylinder, steering valve and connections.

### 11.9.1 Configurations

Various configurations were developed to adapt the gear to the package and front axle geometry of the car, differing chiefly by the arrangement of the steering cylinder.

#### 11.9.1.1 End Tap

This configuration, shown in Fig. 11.37, is characterised by the continuous rack which is dovetailed on one half (mechanical part of the gear) and designed as a piston rod with piston on the other half (hydraulic part of the gear). The respective axial joints of the tie rods are joined at their ends. This is currently the most common version.

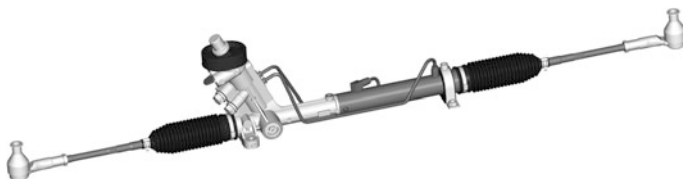


**Fig. 11.37** Hydraulic rack-and-pinion steering with end tap

This configuration of the steering is compact and of low weight; it facilitates a stiff joining of the wheels, because the rack also joins both tie rods without further components and because the tie rods transfer the force into the gear without any offset into the rack axis. Left- and right-hand drive version can often be built by mirroring the steering at the middle of the rack, ultimately exchanging the mechanical and the hydraulic part. The rather short remaining length of the tie rods can be a shortcoming of this arrangement. It is defined by the distance of the steering arms at the wheels and by the total length of the rack. Big bending angles of the tie rod joints can result from deception and rebound of the front wheels, entailing a high lateral force as a part of the tie rod forces transferred to the rack; this has to be considered when designing their strength. On the other hand, large toe-in changes over the spring path of the front wheels can result, forcing compromises in the design of the chassis geometry.

However, a suitable design of the chassis can apply short tie rods favourably to reduce the steering ratio for high steer-angles even further.

### 11.9.1.2 Central Tap

This configuration, shown in Fig. 11.38, also consists of a mechanical and a hydraulic part which are connected by a continuous rack. The tie rods, however,

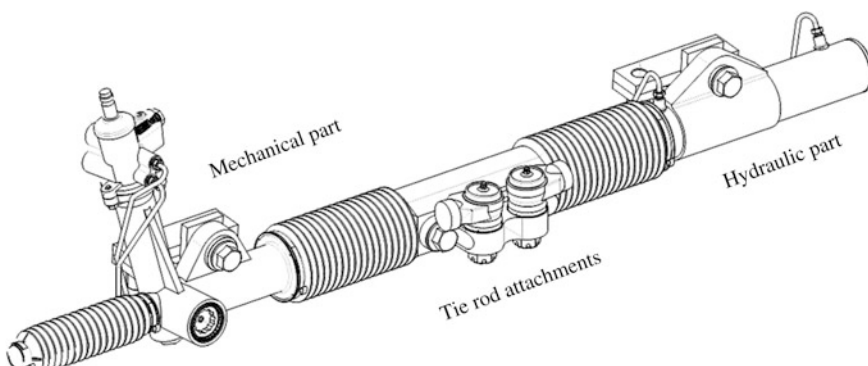


**Fig. 11.38** Rack-and-pinion steering with central tap (tie rods not shown)

are mounted outside of the axis in the middle of the rack, between the mechanical and the hydraulic part.

The advantage of a possibly larger tie rod length is countered by higher construction expenditure and weight. In the 1980s and 1990s, when power steerings were offered as extra equipment for lower vehicle classes, this construction allowed installing a compact and light manual gear with one-sided tap (short gear) and a power-assisted gear with central tap in the same vehicle, without further adaptation of the mounting or the tie rods. This design is avoided in new constructions and was lately used only in some all-terrain vehicles, in which advantages of long tie rods for the chassis geometry are more apparent, on account of very long spring paths.

### 11.9.1.3 Parallel Auxiliary Cylinder

The parallel arrangement of the steering cylinder to the rack axis developed from the desire to use a power steering in a chassis that was originally made for a manual steering, without essential changes. A differential cylinder is connected to the steering case, so that the piston rod is parallel to the rack and coupled to its end by a connecting element. The cylinder is an independent unit, the steering case is modified chiefly to accept the steering valve. One shortcoming of this construction is the different effective piston surface in the two cylinder chambers, resulting from the fact that on one side of the piston, the piston rod covers a part of the piston's surface. If the same rack force is desired, different pressures have to be applied according to the steering direction, this needs to be observed during valve design. Because of the axial offset, the piston rod transfers bending torques into the rack, and the connecting element is charged with high loads, too. The weight is then higher than that of a gear with end tap, and efforts for assembly and costs are higher, too. The advantages are a possibly longer tie rod and a basically higher flexibility of the package, because the steering cylinder can be arranged in different positions inside the gear case. This configuration is not used any more in passenger cars if the whole platform is equipped with power steering.

Heavy-duty vehicles, though, feature prototypes of a similar configuration, shown in Fig. 11.39. They should be used if the still widespread rigid front axle



**Fig. 11.39** Prototype of a parallel gearbox for heavy-duty vehicles

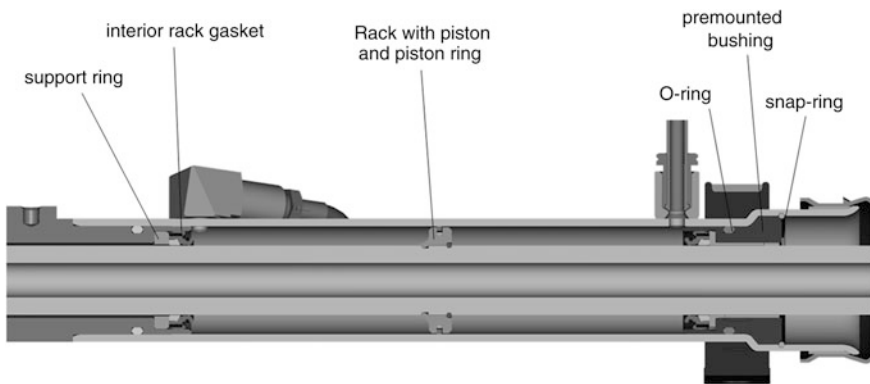


**Fig. 11.40** Assembly pipe and rack

with recirculating ball-with-nut gear and steering linkage is substituted with an independent suspension with rack-and-pinion steering. However, the axial joints are then attached at both sides of the hydraulic cylinder, and the mechanical part of the steering including the rack is arranged in parallel.

This design enables quite long tie rods which are useful to achieve large turning angles of the front wheels ( $>55^\circ$  for the inner wheel) while maintaining Ackermann's condition to a great extent. Both features are necessary to provide a small cornering circle even for a long wheelbase and to make it usable in practise. The reduction of the whole steering ratio can be limited until the full angle of the wheels is achieved. That is desirable for heavy-duty vehicles, so that enough power-assist is available over the whole steering path, while the gear is very small and light.

The configurations in the following chapters refer to steering systems in the preferred design, the end tap.

### 11.9.2 Cylinder

The cylinder of a power steering contains all the parts for supplying an assist power by hydraulic means. The parts are shown and labelled in Fig. 11.40.

In addition, the cylinder includes one or several outside mounting points for on-board mounting. In power steering, the bushing of the rack is placed into the cylinder area to establish a very wide distance between the two bearing points in the steering.

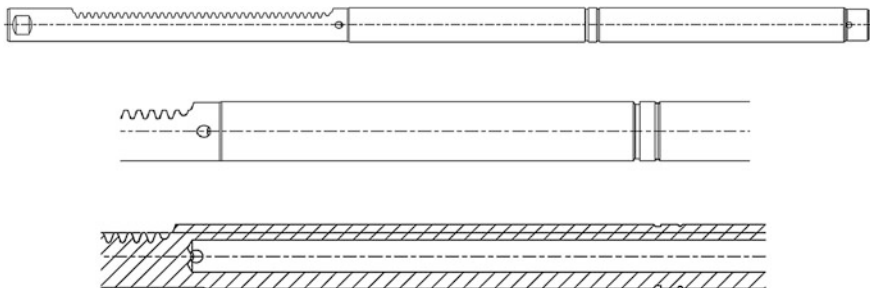


**Fig. 11.41** Rack with concave drillings and piston groove

### 11.9.2.1 Rack in the Cylinder Area

The rack in the cylinder area has the following functions:

- Bearing the piston and the piston forces
- Sealing the cylinder space and the rack gaskets
- Bearing externally transferred longitudinal and lateral forces with low elasticity
- In most configurations: Air pressure compensation between both spaces, surrounded by the gaiters, when the rack is moving.

Racks are mostly made of corresponding round bar steel in one piece—two-part assemblies are seldom used for mechanical or hydraulic applications. To reduce weight and to permit the mentioned airflow, the rack is drilled hollow across the whole length or at least in the hydraulic area (see Fig. 11.41). When the mechanical section including the dovetailing is finished and a radial groove is introduced into the rack to fasten the piston, it is ground in the whole hydraulic area to achieve a sufficient surface finish for the rack seals, which may not be impaired by the further production process.

The same requirements apply to the layout of the rack strength as to mechanical steering systems. They result esp. from the fact that the rack is a critical part in safety issues that has to maintain a solid connection between the guided wheels and a controlled movement along their longitudinal axis under any circumstances. The area critical for the strength is generally near the dovetailing, towards the middle of the rack, hence, no particular requirements need to be observed for the hydraulic section of the rack. Yet, overall, the rack has to be laid out with more strength than a manual steering would provide. One reason is the wider length of the rack which allows for higher bending torques when lateral forces are introduced at their ends. Another is the higher potential rack forces, particularly in abuse situations like kerb impacts. They are caused by a combination of hydraulic peak support and extremely high steering wheel torques (they can amount to more than 100 Nm). Even in this case, the rack may not suffer plastic deformation that would affect its easy motion in the gear.

### 11.9.2.2 Pistons with Piston Ring

The piston is made from a rotary steel part, the piston ring consists of a PTFE compound (filled with bronze or graphite), produced by sintering or extrusion, then it is twisted and cut to length.

Together, they have the following functions:

- Hydraulic separation of the two cylinder spaces with least internal leakage
- Transmission of the hydraulic forces to the rack.

Figure 11.42 shows piston and piston ring in the mounted state, joined to the rack.

The sealing of the cylinder chambers is a primary task of the piston ring. The gap (approx. 0.1 mm) between the outer diameter of the piston and the inner diameter of the cylinder pipe is closed by the piston ring. It is located in a groove of the piston whose depth allows it to perform compensating movements. Since the outer diameter of the piston ring is wider than the cylinder pipe and there is the biasing force of the O-ring under the piston ring, a static contact pressure is generated to prevent the fluid from flowing over the piston ring when the pressure rises quickly (blow-by effect).

The actual sealing effect, however, results from a contact pressure, applied by the fluid pressure. The piston ring is pressed against the corresponding groove flank, and the O-ring exerts a radial force on the inner diameter of the piston ring. A required prerequisite for meeting this task is constant free access of the fluid to the O-ring. During rapid mutual pressurisation it may happen that the piston ring will touch the turning point of the groove flank and prevent direct access of the pressure medium to the O-ring. Then the pressing force for sealing is not produced, which can cause leaking. Therefore, grooves are made at both sides of the piston ring, to keep the hydraulic connection to the O-ring upright (Fig. 11.43).

The gap between piston ring and piston groove should allow the ring to move. If the ring is too wide, however, it will move during a change of the pressurised side (e.g., by reversing the steering direction) from one contact surface of the groove to the other. This first delays the pressure buildup in the cylinder chamber, then releases it with a steep gradient when the piston ring has achieved its final position and the sealing begins. This causes sound impulses in the hydraulic system, these are clearly audible in the vehicle and are unacceptable.

**Fig. 11.42** Assembly rack with piston and piston ring

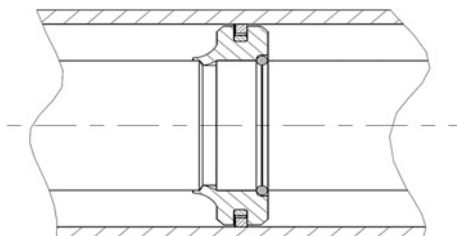
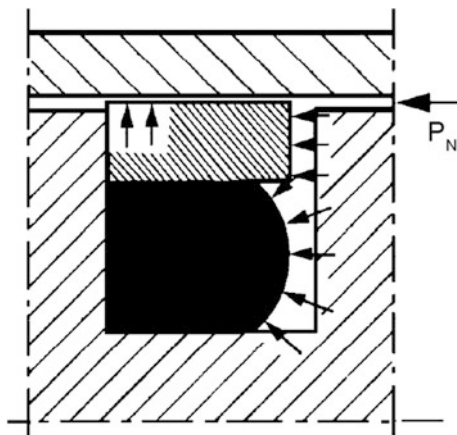


**Fig. 11.43** Effect of the fluid pressure on piston ring and O-ring



The gap between the outer diameter of the piston and the inside diameter of the cylinder pipe prevents the piston from touching the cylinder wall, even if the rack bends under lateral force. But under lasting influence of high pressure and high temperature, the material of the piston ring is able to creep through a too wide gap (oil temperatures up to 120, 140 °C are possible in individual applications), so that the piston ring extrudes into the gap, loosing its sealing capabilities.

There are different ways to attach the piston to the rack. They have in common that material from the inner diameter of the piston is transformed by pressing into a radial groove on the rack. The piston disposes of a collar with low wall thickness at its inner diameter, either on one side or on both sides. This collar is radially deformed by pressing with a corresponding matrix, by rolling out or by swaging hammers into proper grooves on the rack, establishing a positive connection. If the piston has a collar only on one side, then the other side will be supported by a retaining ring which lies in a rack groove.

Basically, the piston has to be able to transfer the hydraulic peak forces into both directions without moving relative to the rack. Otherwise its motion would generate sound impulses in the hydraulic system, similar to those described for the piston ring.

### 11.9.2.3 Rack Gaskets and Sealing System of the Cylinder

The main function of the rack gaskets is to seal the hydraulic area of the cylinder pipe reliably, under any possible condition, to prevent leakage for the whole service life. The gaskets should further ensure that no air is sucked from the space within the bellows into the cylinder. This can happen during extreme steering movements at high rack speed, when low pressure is generated in a cylinder chamber, because the volumetric flow extracted by the pump is below the

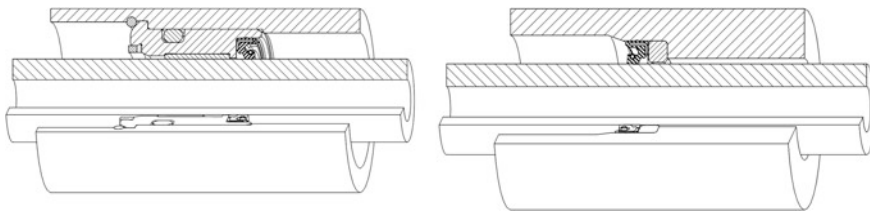


**Fig. 11.44** External and internal installed rack seal

changing volume of the chamber. Another common and, for this effect, critical situation occurs when the vehicle is mounted and the front wheels are swivelled while the engine is switched off.

Figure 11.44 shows installed rack seals. The left figure displays a seal pressed into the rack jack, as it is inserted at the end of the hydraulic cylinder (external rack seal), the right figure shows a seal pressed into the steering case on the border between the mechanical and the hydraulic part of the gear (internal rack seal).

#### Configuration of a rack seal

The rack seal consists of a metal body which establishes the strength to resist pressures of 120 bar and more. This body is moulded with a rubber mixture in such a way that the sealing elements in the outer and inner diameter receive their shape.

The used rubber material has to establish the compatibility to the used hydraulic oil, it needs to be sufficiently strong at high temperatures and sufficiently flexible at low temperatures. At the mating face to the rack high abrasion resistance and low friction is also required, this avoids stick-slip effects and any resulting audible seal squeaking.

#### Interface at the external diameter

The seal at the external diameter is pressed into the case or jack. To establish sealing at this point, the press fit has to be configured for sufficient radial pre-tension of the mating face, the seal seat has to be machined with narrow tolerance margins and it needs a defined surface structure. A too rough surface could cause the outer seat of the seal to wear or shear off upon assembly. A too smooth surface could mean that in spite of correct size, the press fit of the seal could fail and be pulled out of its seat when low pressure is applied in the corresponding cylinder chamber. This occurs when the steering system is filled and in some operation modes. A large enough wedge-face supports the seal if the cylinder chamber is pressurised. A supporting plastic ring integrated into the seal often serves this purpose.

### Interface in the inner diameter

At this interface relative movements between sealing lip and rack may occur. It is laid out so that it leaves only a thin oil film for lubrication behind when the rack moves out, and this oil film can be fully retaken when the rack moves in. The radial pretension is established by combining three effects, see Fig. 11.45.

First, some 50 % of the whole radial force is issued by the spiral spring integrated into the seal, when it is widened to the rack diameter during assembly.

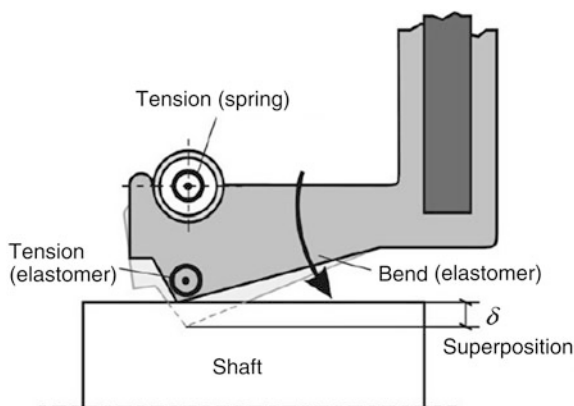
Second, the perimeter of the sealing lip is widened during assembly, too, contributing some 40 % of the whole radial force as an elastomer tension.

Third, there is an elastomer bend section (approx. 10 % of the whole radial force, all data given for ambient temperature) which results from the bend (bend angle 7–12°) of the diaphragm surface when it is pushed onto the rack.

In addition to the static radial force, the pressure admission flow generates a radial force part on the sealing lip which rises proportionally to the pressure, because the sealing lip is not vertically oriented to the rack, but turned at an angle into the cylinder space. The diaphragm surface is distorted under rising pressure, so that in addition to the primary sealing lip, acting in the static state (0 bar pressure above atmospheric), the sealing lips on the base or the diaphragm surface on the rack are touching and supporting the sealing (see Fig. 11.46).

One particular difficulty in the layout of a seal is the required high flexibility of the mating face during radial movements of the rack. The bearing plan of a rack-and-pinion steering (guide about rack yoke and steering pinion) is the reason that the rack moves radially under lateral force, relative to the seal, and it rolls, for example, due to radial dovetailing forces between rack and steering pinion. The sealing lip has to follow these movements and make sure that a sufficient radial pretension is maintained around the whole perimeter of the rack—otherwise oil will leak out in such situations. This is most difficult in extreme cold start situations, because then the elastic mixture loses its flexibility. Further, one needs to

**Fig. 11.45** Static preliminary tension of the rack seal on the rack



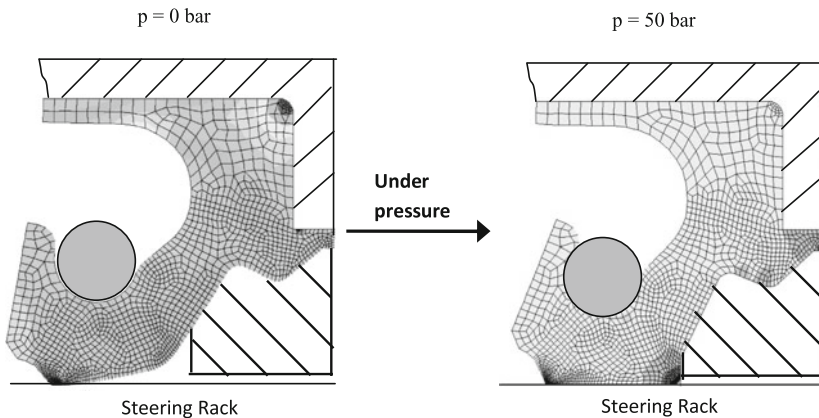


**Fig. 11.46** Function of the rack seals

ensure that these movements entail no overstretching of the elastic body, because it will otherwise lose its mechanical strength and fail early under pressure (penetration wound).

#### Integration of the seal in the gear

The internal rack seal which separates the hydraulic from the mechanical section is used directly at an accordingly shaped place in the steering case.

The external rack seal is implemented into the rack jack. Then the outer diameter of the rack jack is sealed with an O-ring against the cylinder pipe.

In general, the maximum working pressure of a rack-and-pinion steering is limited by the rack seals. A very high pressure is aimed at, because then the required rack force can be generated with a small piston surface, allowing for the layout of a low volumetric pump flow, which is favourable with regard to energy consumption and thermal load of the steering system, beside advantages for package and weight. Above a limit of approx. 140–150 bar, however, the risk of steering failure due to leakage rises for conventional seals within the intended service life.

#### 11.9.2.4 Cylinder Pipe with Connections

The cylinder pipe has many tasks:

- Surround the cylinder space with sufficient pressure resistance
- Supply hydraulic connections to link the cylinder chambers and the transfer lines to the steering valve
- Bear and seal the rack jack

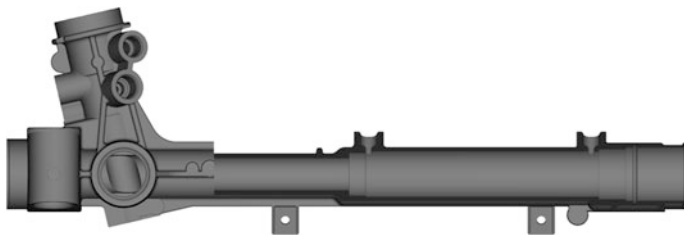


**Fig. 11.47** Gear case as an integral case

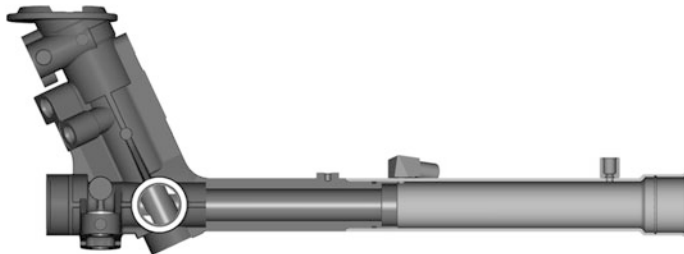


**Fig. 11.48** Gear case with pipe/case connection

- Supply mounting points for the gear
- Bear other individual mounting points, for example, for a heat shield
- Join the seal bellows.

Two configurations are common, shown in Figs. 11.47 and 11.48.

First is the cylinder pipe, an integral part of the steering case, made of die-cast aluminium (integral case). The mounting points of the gear, hydraulic connections and other mounting points can be integrated into the mould. Like the valve area, the cylinder area has to be fully machined.

Second is a separate pipe, most commonly a steel pipe, pressed onto a short gear case containing input shaft and valve. The inside of the pipe receives its inside diameter and the required surface finish without further treatment by a process called calibrating, it consists of pushing a steel sphere with defined diameter through the pipe. For the hydraulic connections, however, the cylinder pipe has to be drilled first, and then corresponding connecting pieces have to be welded to the pipe. Mounting elements are welded at the pipe, too, bearing the risk of welding distortion of the pipe, which would not be acceptable in the cylinder area. In general, the combination of gear case and pressed steel pipe is cheaper than the integral case. The latter also puts high demands to the available die-casting technology, limiting the scope of potential manufacturers. However,

depending on the number and complexity of the parts to be welded at the steel pipe, the integral case can also be cheaper, in addition to the lower weight of this configuration.

### 11.9.3 Rotary Disk Valve with Input Shaft and Steering Pinion

The steering valve is, from the technological point of view, the core of the hydraulic power steering. Today it is always a rotary disk valve and has the following tasks:

- Maintain a mechanical through-put from the input shaft to the steering pinion
- Connect both cylinder chambers with the inlet and runback of the hydraulic supply
- Record the wheel torque introduced by the driver and identify the course
- Adjust the hydraulic pressure depending on the acting wheel torque and direct the pressure into the cylinder chamber corresponding to the course.

The steering valve is connected to the driver by the steering column and the steering wheel, and esp. the level of the current power assist, i.e. the pressure directed from the steering valve into a cylinder chamber is clearly felt. Therefore, the steering valve has to build up the driver's support in a predictable, repeatable and steady way, with low hysteresis and without lag. This means that the requirements for precision of the steering valve parts are high.

The parts of the gear are shown and labelled in Figs. 11.49 and 11.50, both assembled and in an exploded view.

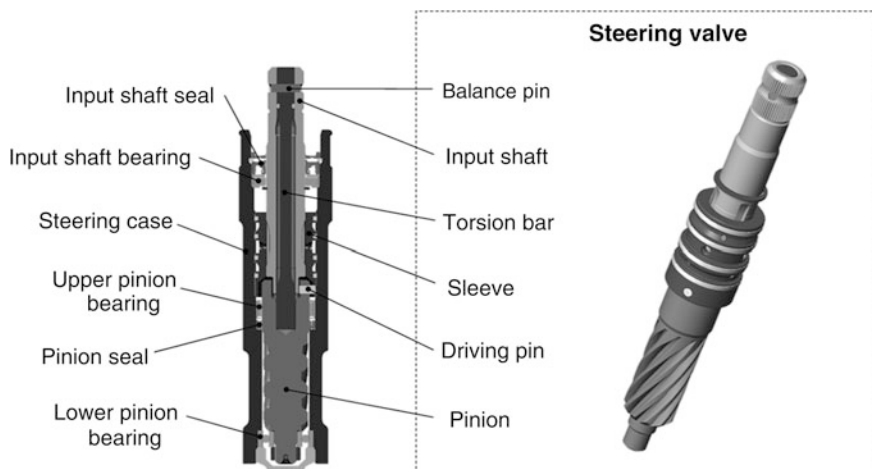


**Fig. 11.49** Steering valve ZSB with naming of the parts

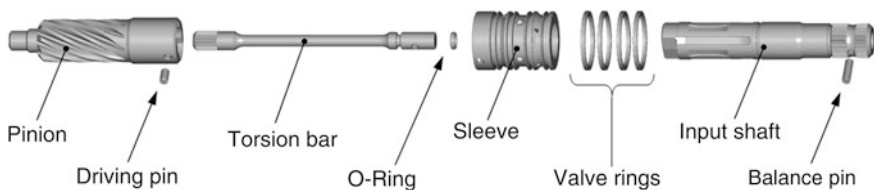


**Fig. 11.50** Parts of a steering valve in explosion representation

### 11.9.3.1 Steering Pinion

The steering pinion is very similar to the version in mechanical gearboxes. Its support however, is right above and below the dovetailing area in the case, so that reaction forces are not transmitted from the dovetailing into the steering valve. The mechanical coupling of the input shaft is maintained both by a torsion bar whose end is pressed into the body of the steering pinion, and by end stop surfaces for the input shaft, that limit the peak torsion of the torsion bar, which represents a mechanical overload fuse.

Furthermore, the steering pinion disposes of a mating face for a shaft-lip type seal, to seal the valve chamber arranged right above or below the upper steering pinion support, so that the support is either inside the hydraulic chamber and runs wet or is outside and runs dry.

### 11.9.3.2 Torsion Bar and Overload Fuse

The torsion bar connects input shaft and steering pinion axially, so that they have a defined position to each other. It also causes a relative twist between input shaft and steering pinion as a function of the steering wheel torque, which is used to control the power assist and its direction. Its layout has to maintain an exactly defined torsion spring stiffness which is primarily determined by diameter and length of the choke. It has an influence on the required steering wheel torques (more stiffness = more steering forces) but also a profound impact on the steering feel and the feedback of the steering—these facts are discussed in more detail in Sect. 11.10. Within the scope of the greatest possible angle difference between input shaft and steering pinion, defined by their respective stop surfaces, the torsion bar has to be permanently rigid. Endangered cross sections are near the choke and near the O ring groove.

The torsion bar is pressed into a drilling at one end of the steering pinion. At the other end it is connected with the input shaft usually by piercing both crosswise and securing them with a pin. The valve is mounted into a hydraulic balancing stand which models the surroundings of the gear near the steering valve. The steering pinion is fixed onto the mounted sleeve, and the operation of the valve is simulated by moving the input shaft. Then the valve characteristics for a clockwise and a counterclockwise torsion are recorded. Finally, the input shaft is moved into

a position in which the valve indicator is symmetrical for both rotational directions: the hydraulic centre. That is, a twist out of this position around a certain angle, clockwise or counterclockwise, will produce the same pressure. In this position, the input shaft is connected with the unloaded and tension-free torsion bar, e.g., by drilling and pinning. By this process, called the balancing of the valve, it is ensured that pressure is not driven into one cylinder chamber without wheel torque and that the pressure builds up, according to the wheel torque, symmetrically into either rotational direction.

### 11.9.3.3 Sleeve with Valve Rings

The sleeve is one of two parts representing the function of the steering valve (see Fig. 11.51). It is solidly connected with the steering pinion in the rotational direction, however, it can follow an angular or axial offset between the surrounding input shaft and the steering pinion within certain limits. On the outside, the sleeve has three radial grooves that create three chambers, separated by the valve rings, once they are installed into the case. The middle groove is connected with the inlet of the hydraulic supply by drillings in the case, the upper and lower groove are connected with one of the cylinder chambers.

The valve rings are almost identical with the already described piston rings in terms of function and resulting requirements, material and configuration.

Inside, the sleeve is cylindrical. Axial grooves are implemented at a certain distance from the end of the sleeve which have sharp, right-angled edges at the rim. They adopt the valve function in their interaction with the grooves and control edges of the input shaft (see Sect. 11.9.3.4). The remaining cylindrical sections of the inner diameter without grooves, and the corresponding surfaces of the input

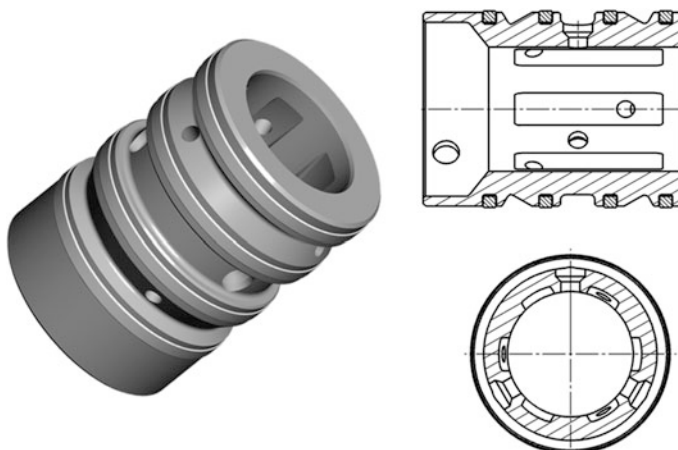


**Fig. 11.51** Sleeve with valve rings

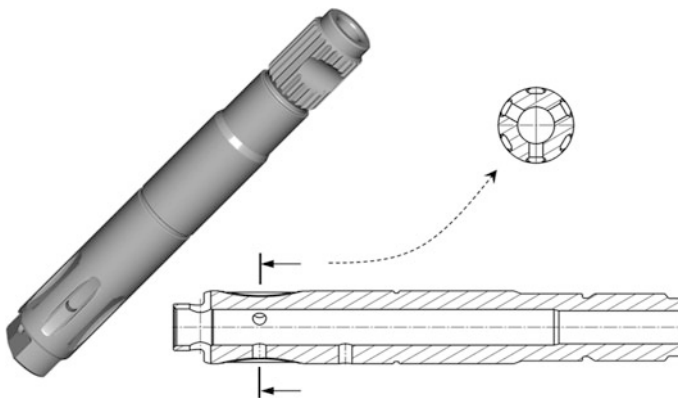


**Fig. 11.52** Input shaft

shaft sealing this valve area by a gap, are as narrow as possible. Hence, high demands are made to the treatment of the cylindrical inner diameter, both with respect to the sizes with very low tolerance margins and with respect to the surface finish.

#### 11.9.3.4 Input Shaft

The input shaft is the second part of the steering valve. It has the purely mechanical function of transferring the wheel torques, either from the pinning into the torsion bar or from the end stop surfaces into the steering pinion, it is shown in Fig. 11.52.

The inside of the input shaft is drilled hollow. The hollow cavity of the version shown here is connected by lateral drillings to runback grooves and the valve chamber beyond the sleeve, whose section in turn is connected by a case drilling to the runback of the hydraulic supply. On the outside, the hollow cavity is sealed by an O ring between input shaft and torsion bar.

In the actual valve section, the input shaft is the counterpart of the sleeve with a high-precision cylindrical outer diameter and axial grooves. Their edges, called control edges, are provided with an exact structure, either by sanding several facets or by stamping a certain form of the control edges. The curve of the power assist over the wheel torque is determined by this structure, as described in Sect. 11.10.1. The contour near the sleeve and the sleeve itself seal the high-pressure area by narrow gaps, as described above. At its upper end, the input shaft is supported to take up the lateral forces initiated by the steering column. A radial oil seal seals it against its surroundings (Fig. 11.53).

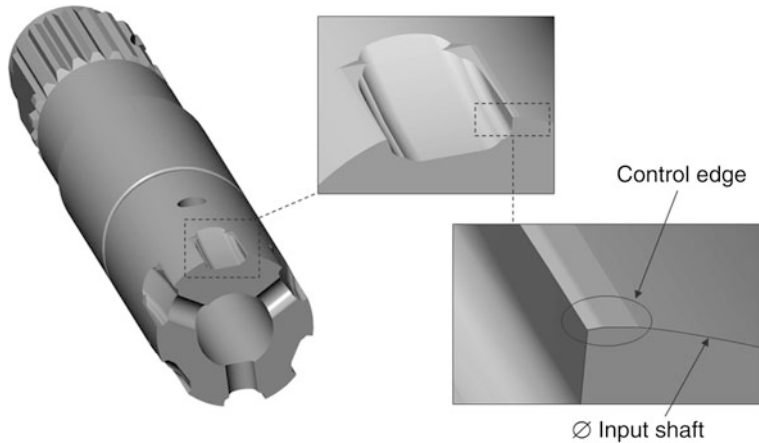


**Fig. 11.53** Cut view of an input shaft with control edge

#### 11.9.3.5 Configuration Forms

Many versions of the described valve configuration were developed to solve special problems, mostly for packaging. They are not widespread, because these versions cause add-on costs or negative concomitants like more friction, and they are not required if the car is properly designed. Alternative valve designs (star valve, coil valve) have been fully displaced by the rotary disk valve as well.

However, two kinds of valve housings are still distinguished, see Fig. 11.54.

The easier form, the cartridge valve, has a valve housing which is a part of the complete steering case. In this version, the lower pinion bearing is fixed. The outer

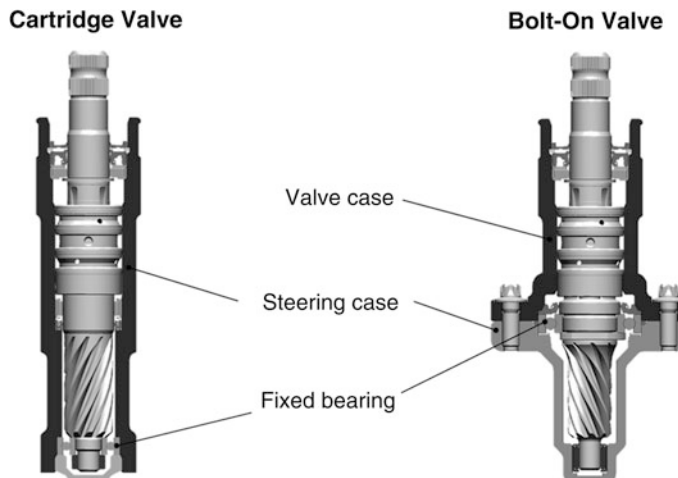


**Fig. 11.54** Cartridge valve (on the *left*) and bolt-on valve (on the *right*)

diameter of the pinion is limited by the inner diameter of the pinion seal which in turn is given by the outer diameter of the sleeve and the space required for the seal. The widest diameter of the pinion determines the biggest possible steering ratio (rack stroke per pinion rotation).

The alternative form, the bolt-on valve, is completely preassembled in its own valve housing and screwed on the steering case. The fixed bearing is the upper pinion bearing, attached between valve and steering case. The size of the pinion is not restricted by the sleeve in this configuration. A higher assembly effort and a greater number of individual parts are the setbacks.

#### ***11.9.4 Other Parts of a Hydraulic Gear***

Other parts which have to be added to a hydraulic gear shall be mentioned briefly, for the sake of completeness.

##### **11.9.4.1 Transfer Pipelines**

The task of the transfer pipelines is to hydraulically connect the valve section with the cylinder section individually for each cylinder chamber. They are usually made of low-diameter steel pipe and provided with different kinds of hydraulic connections at their ends, depending on the requirements of space and assembly.

The cross sections have to be selected in such a way that, despite quick steering movements and accordingly high volumetric flows in the transfer pipelines, there will be no high resistance to flow, esp. not when the fluid is cold and more viscous.

##### **11.9.4.2 Bellow Vent Pipe**

In contrast to the mechanical gears which admit a free air exchange between the compressed and the expanded bellow when the rack moves, the sealed cylinder area of the hydraulic steering has to be circumvented. Solutions establishing the exchange by an external connection of the bellows by means of a pipe have almost fallen out of use. The costs for the bellows rise, because of the required pipe connection (the bellow is no longer axially symmetric), the external pipe has shortcomings in the package and the air exchange system is prone to leakage during operation, potentially entailing long-term corrosion on the rack and subsequent oil leakage of the gear.

More often, the hollow drilling of the rack is used to enable the aerial exchange between both sides of the cylinder. This is made possible by a lateral drilling before the dovetailing and either another lateral drilling at the end of the rack or venting grooves introduced into the axial joint.

**Table 11.5** Some characteristics of hydraulic rack gears

Vehicle class	Compact cars	Compact category	Middle class	Van/SUV	Light utility vehicle
Front axle load (kg)	950	1,150	1,500	1,800	2,100
Maximum rack force (N)	7,000	8,500	11,000	12,500	15,000
Rack diameter (mm)	24	26	28	30	32
Piston diameter (mm)	40	42	46	48	52
Maximum working pressure (bar)	90–120				
Volumetric flow (l/min)	6	7.5	9	10.5	12
Rack stroke (mm)	$\pm 65$ to $\pm 85$				
Gear ratio	40–60 mm/rotations (sports car also 75 mm/rotations)				
Temperature	−40 to +120 °C (partially also +140 °C)				

### 11.9.5 Typical Characteristics of Hydraulic Gears

The layout of rack gears for passenger cars is always specific to the respective car platform. Specific features of the drive concept, the layout of the package or the definition of the chassis affect the requirements for the respective gear significantly. Therefore, there are major differences between the gears even for vehicles in the same class. This also concerns their characteristics.

Table 11.5 gives an overview of the representative characteristics of gears in the different vehicle classes.

## 11.10 Functionality of the Steering Hydraulics

### 11.10.1 Steering Valve: Principle of the Cutback

According to the terminology for hydraulic parts, the steering valve is a mechanically operated 4/3-way proportional valve with an open centre. This means that a continuous volumetric flow is transported by the hydraulic supply through the valve. The resistance to flow is least in neutral position. With increasing deviation, the resistance to flow of the valve increases steadily, and the flow pressure rises. At the same time, depending on the rotational direction, one chamber of the steering cylinder is connected to the inlet and the high-pressure levels there, the other one is connected with the runback and the low-pressure level prevalent there. The active principle of the steering valve is the specific cutback of a continuous volumetric flow.

As shown in Fig. 11.55, the configuration of the steering valve corresponds to that of a Wheatstone bridge. A pressure difference is generated by changing the resistances to flow of the bridges B1 and B4 or B2 and B3 in pairs. They are

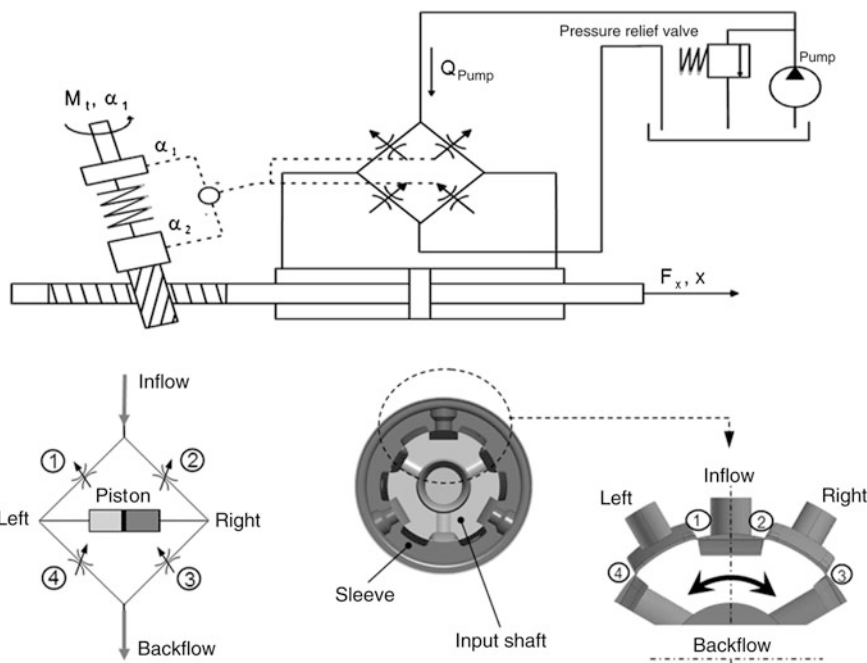


**Fig. 11.55** Diagram of the steering hydraulics

constantly passed by the hydraulics fluid and directed into both chambers of the steering cylinder. In real valves, there are several Wheatstone bridges in parallel, three of them are shown in the example. Only one bridge, i.e. a  $120^\circ$  segment of the valve cross section, is examined to understand the active mechanism in the valve.

The flow path of the hydraulic liquid in the valve is as follows: The fluid streams into the central ring channel on the outside of the sleeve. Drillings pass it on to the space between sleeve and input shaft, more precisely, to a place where the input shaft has an axial groove on its outer diameter while the sleeve has none on the inner diameter.

The fluid continues into a space where the sleeve has an axial groove on its inner diameter but the input shaft has none on the outer diameter (note: In the image below on the right, the hydraulic spaces are dark while sleeve and input shaft are bright). A sufficiently wide gap remains in the neutral position of the valve between both areas (bridge B1 and B3), because of the negative overlap of the valve, so that the fluid can flow over with little resistance. The volumetric flows split symmetrically between both possible directions of flow. Each of the grooves in the inner diameter of the sleeve is again connected by drillings to one of the ring channels in the outer diameter of the sleeve: the groove that is left in the image is connected to the upper ring channel and the right groove to the lower ring channel. The two ring channels are connected via the transfer pipelines with one cylinder chamber each: the upper ring channel with the cylinder chamber which

supports a steering movement to the left and the lower ring channel with the opposite chamber.

Next, the hydraulic liquid flows again into an area with a groove in the input shaft and without groove in the sleeve (bridge B2 and B4), again, there is little resistance in the neutral position because of the negative overlap.

In the form shown here, the grooves in the input shaft are connected by drillings to their hollow internal parts, so that the fluid is conducted to there. It flows axially to the input shaft into an area which is not covered by the sleeve, leaves by lateral drillings in the input shaft and returns by a drilling in the case and a connected runback into the tank. The state of the not actuated valve (central position) is shown on top in Fig. 11.56.

If the input shaft is torsioned relative to the sleeve, as shown in the figure, the cross sections change where the fluid is streaming from a groove in the input shaft to a groove in the sleeve, or vice versa. For example, if there is a counterclockwise torsion of the input shaft, the cross section of the bridge B1 grows, so that the fluids passes easier into the groove of the sleeve which is connected to the cylinder chamber supporting a steering movement to the left. The cross sections of the bridges B2 and B4 shrink, so that the respective volumetric flow passing over both bridges is hemmed in the same measure (symmetrical flow distribution). There is a corresponding back pressure in the space limited by these bridges, it is equal to the cylinder chamber pressure  $p_A$ . The bridge B3 then receives a wider cross section, so that the volumetric flow across this bridge can freely pass away into the tank. In this area, the pressure level is low and corresponds approximately to the tank pressure, and thus also to the pressure in the cylinder chamber B ( $p_B$ ).

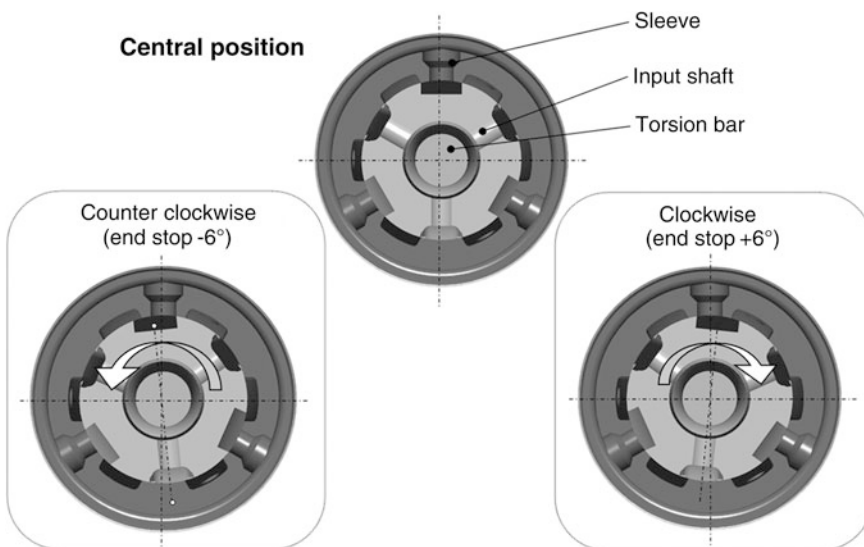


**Fig. 11.56** Cutaway view of the valve in the actuated state

The form of the control edges in the input shaft essentially determines the runoff cross section of the respective bridges as a function of the relative position of input shaft and sleeve, describing the valve curve.

The orifice formula serves well to compute the approximate pressure drop as a function of the runoff cross section:

$$Q_1 = B_1 \cdot \sqrt{pP - pA} \quad (11.4)$$

$$Q_2 = B_2 \cdot \sqrt{pA - pR} \text{ mit } pR \approx 0 \quad (11.5)$$

$$Q_3 = B_3 \cdot \sqrt{pP - pB} \quad (11.6)$$

$$Q_4 = B_4 \cdot \sqrt{pB - pR} \text{ mit } pR \approx 0 \quad (11.7)$$

$$B_i = CD_i \cdot A_i \cdot \sqrt{\frac{2}{\rho}} \quad (11.8)$$

Symmetry of the control edges:

$$B_2 = B_3 \quad (11.9)$$

and

$$B_1 = B_4 \quad (11.10)$$

Distribution of the volumetric flows:

$$Q_P = Q_1 + Q_3 = Q_2 + Q_4 = Q_R \quad (11.11)$$

The Eqs. 11.9 and 11.10 result in:

$$Q_1 = Q_3 \quad (11.12)$$

and

$$Q_2 = Q_4 \quad (11.13)$$

$$Q_2 = Q_1 - QA(\dot{x}_r) \quad (11.14)$$

With static rack:

$$\dot{x}_r = 0 : Q_2 = Q_1 \quad (11.15)$$

The Eqs. 11.11, 11.12, 11.13 and 11.15 yield:

$$Q_1 = Q_2 = Q_3 = Q_4 = \frac{1}{2} Q_P \quad (11.16)$$

Effective cylinder pressure:

$$\Delta p = pA - pB \quad (11.17)$$

From Eq. 11.4

$$pP = \frac{Q_1^2}{B_1^2} + pA \quad (11.18)$$

From Eq. 11.6:

$$pP = \frac{Q_3^2}{B_3^2} + pB \quad (11.19)$$

With Eq. 11.17:

$$\frac{Q_1^2}{B_1^2} + \Delta P + pB = \frac{Q_3^2}{B_3^2} + pB \quad (11.20)$$

Equations 11.9 and 11.16 yield for a static rack:

$$\Delta p = \frac{1}{4} Q_P^2 \cdot \left[ \frac{1}{B_2^2} - \frac{1}{B_1^2} \right] \quad (11.21)$$

Substituting Eq. 11.8 yields:

$$\Delta p = \frac{\rho}{8 \cdot CD} Q_P^2 \cdot \left[ \frac{1}{A_2^2} - \frac{1}{A_1^2} \right] \quad (11.22)$$

The valve curve is given as the pressure difference over the wheel torque, see Fig. 11.57. The relationship between wheel torque and relative torsion angle of input shaft and sleeve is given by the stiffness of the torsion bar. The outmost line which is recorded for increasing actuation of the valve, i.e. for rising pressure

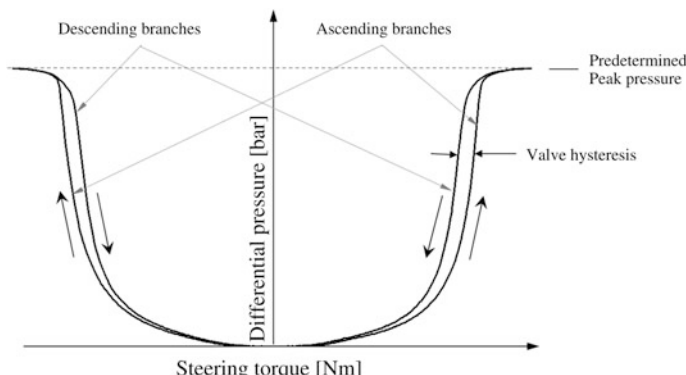


**Fig. 11.57** Example of a valve curve

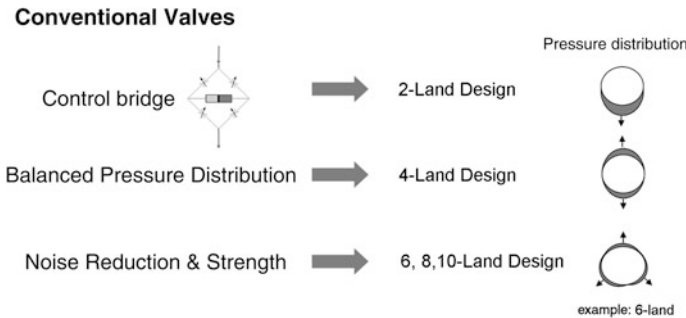


**Fig. 11.58** Number of the bridges and distribution of the pressure zones in the sleeve

(ascending branch) is authoritative for the examination of a measured valve curve. Friction in the input shaft moving relative to the sleeve and to the case produces lower wheel torques on the descending branch at the respective pressure. The difference between the ascending and the descending branch is the valve hysteresis.

Real valves have three or four bridges arranged in parallel, so that the volumetric flow splits evenly between them. On the one hand, this requires more precision in manufacturing the valve parts because the cross sections at each bridge have to be small to achieve the desired total cross section, and all bridges have to be precisely synchronised. On the other hand, there are two advantages:

- Segments with high flow pressure and low return pressure are alternating in the inside of the sleeve. As mentioned before, the gap should be narrowest between inner diameter of the sleeve and outer diameter of the input shaft to provide for least leakage, however, nothing may stick. The maximum deformation of the sleeve is less if it occurs in many, but small segments all around the valve, rather than in a few large segments (see Fig. 11.58). A higher number of parallel bridges allows designing a lower gap width, in particular for high-pressure valves.
- A higher number of control edges enlarges the hydraulically moistened perimeter. This enlargement improves the pressure energy drop. A lesser chance for cavitation is the result, valve hisses are suppressed.

The accuracy by which a desired valve curve may be achieved is strongly dependent on precise treatment of input shaft and sleeve.

### 11.10.2 External Influence on the Valve Indicator

The equations derived from the orifice formula to define the pressure difference in the piston over the actuation angle of the valve show the following dependence (assuming a constant flow coefficient):

- The pressure rises quadratically with the volumetric flow.
- The pressure rises quadratically with the shrinking cross section of the gap at the control edges.
- The pressure rises linearly with the density of the fluid.

De facto, the friction of the fluid in narrow cross sections has an influence as well, but it is not significant for driving and shall not be discussed here. One effect occurs at high viscosity of the fluid that increases the pressure difference in the piston with rising viscosity. In reality, this high viscosity is only present after a cold start, in particular when mineral oil is used as a hydraulic fluid. Their influence is well perceptible in the car (lower wheel torques), but short-lived, on account of the quick heating up of hydraulic power steering.

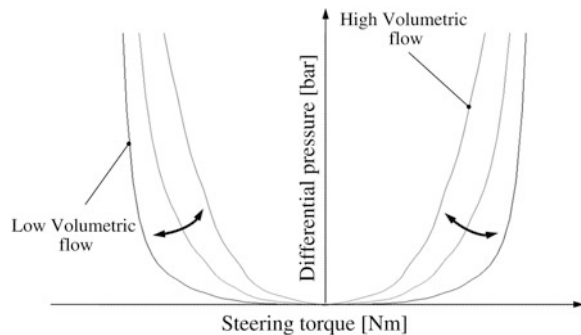
However, the density of the fluid varies only slightly with temperature and between different fluids during operation, so that there is no significant effect.

The valve curve is designed so that for a volumetric flow, which is assumed to be constant and transported by the pump, a given valve curve (pressure difference in the piston over wheel torque) is generated by adjusting the gap at the control edges as a function of the position of the valve, that belongs to the respective wheel torque. According to the treatment process (sanding or stamping the control edges of the input shaft), the accessible structures are limited. A change in size of  $1 \mu\text{m}$  would already alter the valve curve at the control edges measurably, therefore, the fine tuning of the control edges is carried out after a preliminary tuning in a simulation, applying an iterative process of making and testing.

Observing the given tolerance margins for the valve curve in serial production is not accomplished by monitoring the shape of the parts and by controlling it in the manufacturing process—already the required measurement of a corresponding number of parts is not feasible with the needed accuracy. At least, the valve characteristic of a mating of sleeve and input shaft should be measured during balancement and checked for observance of the tolerance margins before they are attached to each other. For some scattering widths, a hydraulic measurement of the parts against a reference part can make sense, so that input shafts or sleeves or both are classified, and then favourable matings are selected for balancement and mounting.

Installation in the gear changes the valve curve against its state during balancement. This is partially due to more friction at the input shaft (seal and support), partially also to minor tensions esp. between input shaft and sleeve that result from tolerance margins of the parts and the steering case. These tensions entail more friction and slightly change the relative position of the control edges of the input shaft to the grooves of the sleeve. As already mentioned, variations of  $1 \mu\text{m}$  have already a significant influence on the valve curve there, so that changes can result which, if they are systematic, may be corrected by corresponding corrections of the control edges and the balancement of the valve. However, a stiff valve assembly with little free travel and high rigidity is favourable, to lower the influence of outside factors affecting the valve.

**Fig. 11.59** Influence of the volumetric flow on the valve characteristic



Other than the interfering influence which has to be considered to keep the given valve indicator, there are also influences which can be used for a specific adaptation of the valve characteristic. It can be efficiently altered, for example, by a variation of the volumetric flow, based on a given shape of the control edge, see Fig. 11.59.

This effect becomes usable in pumps with variable volumetric flow, for example, to generate a speed dependence of the required wheel torques, providing low torques at low speed and high torques at high speed, to improve the control of the steering manoeuvres. In turn, a pump powered by the internal combustion engine has to transport a sufficient volumetric flow even at idling speed, to avoid an uncomfortable increase of the wheel torques at this operation point which is often used for parking manoeuvres.

### 11.10.3 Effects of Steering Movements: Volumetric Flow Splitting

So far, only the static case, without any movement of the rack, was considered in the examination of the valve indicator. If the rack is moved, the distribution of the volumetric flows in the Wheatstone bridge changes. A volumetric flow is taken from a place at the growing chamber (for example, between the bridges B<sub>1</sub> and B<sub>4</sub>) and added at another place by the shrinking chamber (for example, between the bridges B<sub>2</sub> and B<sub>3</sub>). These volumetric flows to and from the cylinder depend on the speed and surface of the piston.

Figure 11.55 shows an example: a movement of the rack towards the arrow at the speed  $x$  and against the load  $F_r$ . The valve is actuated according to the introduced load in such a way that the cross sections of the bridges B<sub>1</sub> and B<sub>4</sub> are widened and those of the bridges B<sub>2</sub> and B<sub>3</sub> are shrunk, so that  $p_A \approx p_P$  applies on the high-pressure side and  $p_B \approx p_R$  on the low-pressure side, i.e. the bridges B<sub>2</sub> and B<sub>3</sub> delimit the high-pressure area from the low-pressure area. Due to the symmetry of the control edges, the same volumetric flow  $Q_2 = Q_3$  is flowing. The hydraulic cylinder takes a volumetric flow  $Q_A$  from the volumetric flow  $Q_1$ , so that  $Q_2 = Q_1 - Q_A$  with  $Q_A$  depending on the rack speed  $x$ .

Equations 11.11 and 11.14 imply:

$$Q_2 = Q_3 = \frac{1}{2}(Q_P - Q_A(\dot{x}_r)) \quad (11.23)$$

$$Q_1 = Q_4 = \frac{1}{2}(Q_P + Q_A(\dot{x}_r)) \quad (11.24)$$

By analogy with the Eqs. 11.21 and 11.22,  $\Delta p$  is:

$$\Delta p = \frac{1}{4} \cdot \left[ \frac{(Q_P - Q_A(\dot{x}_r))^2}{B_2^2} - \frac{(Q_P + Q_A(\dot{x}_r))^2}{B_1^2} \right] \quad (11.25)$$

$$\Delta p = \frac{\rho}{8 \cdot cD} \cdot \frac{(Q_P - Q_A(\dot{x}_r))^2}{A_2^2} - \frac{(Q_P + Q_A(\dot{x}_r))^2}{A_1^2} \quad (11.26)$$

This means that for increasing rack speed, the volumetric flow passing the two closed bridges will drop. To maintain the same power assist, their cross sections have to be reduced, the valve has to be actuated further, meaning more manual power. If, finally, the complete volumetric flow is absorbed by the steering cylinder, no more volumetric flow is flowing through the bridges, there is no more pressure drop there, whatever the cross section of the bridges. In this case the power assist suddenly fails ('Catch-the-pump').

Steering systems with variable pump (e.g., EHPS) enable a recording of the steering wheel rate, which the volumetric flow of the pump may follow within the scope of its efficiency. This helps to compensate the described effect. Esp. EHPS systems can raise the issued volumetric flow by lowering the system pressure, so that a sudden failure of the power assist can be avoided. The power assist will only drop proportionally to the rising steering speed when the limit of the system performance is achieved.

#### 11.10.4 Valve Noises: Hiss

The principle of the valve demands rather high volumetric flows through narrow gaps. This is accompanied by a perceptible pressure drop in the fluid, entailing cavitation, if there is an overflow into the low-pressure area. HF hissing sounds develop, which are emitted as an airborne sound and as a structure-borne sound by the input shaft of the gear into the steering column. Whether airborne sound enters the passenger compartment depends on the installation position of the gear. The shape of the steering column determines whether structure-borne sound advances to the wheel and is emitted there as airborne sound.

The focus of gear development is on preventing the origin of noise. Attempts are made to achieve at least a very steady curve of the flow speed by corresponding design of the control edges. The given valve curve should be achieved by a shape

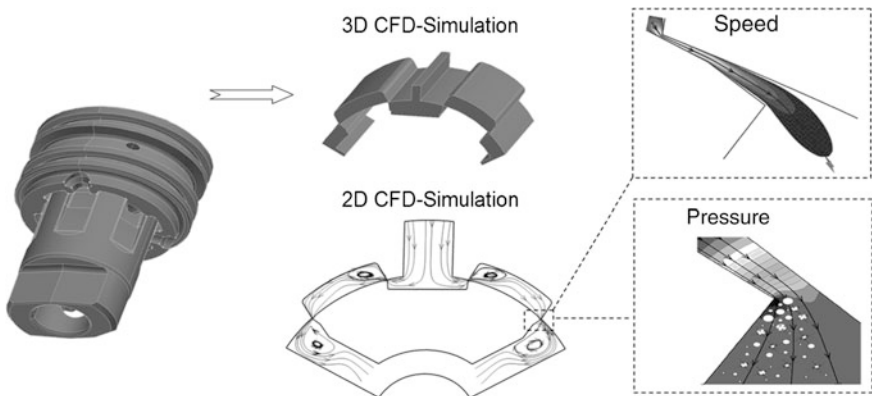


**Fig. 11.60** Fluid flow in the actuated valve—CFD simulation

of the control edge that generates the desired back pressure without zones of very high flow speed. The corresponding layout is supported by CFD simulations.

Figure 11.60 shows an example of the given 3D-geometry and the calculation results in the form of flow speed and local pressure profiles.

Another means to reduce hissing noises is a higher return pressure, e.g., the specific use of throttles in the tank connection of the valve or in the runback. The effect is a generally higher pressure level in the whole gearbox, reducing the likelihood for cavitation even at consistently high flow speed. On the other hand, hydraulic losses are a drawback of this measure, the volumetric flow has to be transported by the pump against a higher pressure level. In the end, this increases the fuel consumption of the vehicle and the thermal load of the whole hydraulic power steering, so that additionally, an engine oil cooler may have to be used, increasing the weight and the costs of the system.

To handle this problem, variable throttles were developed for the runback, these are controlled over the flow pressure. The effect of the throttle is thus limited to those situations in which cavitation can occur in the valve. This function can be integrated into the steering valve. This valve design is described in Sect. 11.11.4.

However, a complete elimination of the cavitation is not feasible. Therefore, a second approach is to keep the remaining noise away from the driver and the passengers.

### 11.10.5 Internal Leakage

Internal leakage denotes the volumetric flow which flows through the valve when it is fully actuated, i.e. closed. This happens only at certain pressures, most of the time at the peak system pressure. This volumetric flow cannot be used to do work

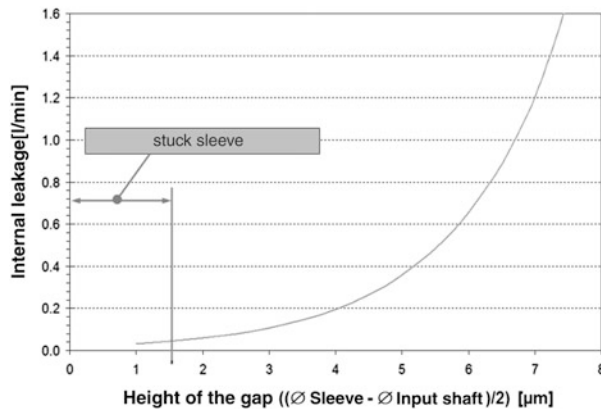


**Fig. 11.61** Effect of the gap heights in the valve on internal leakage

in the cylinder, it is therefore a loss to be avoided. However, in contrast to the external leakage, internal leakage does not affect the function of the gear but only its efficiency.

Internal leakage occurs at different places of the gear:

- At the control edges which leave a residual gap between input shaft and sleeve even in the completely actuated state to avoid a contact of both parts and thus the risk of sticking. Therefore the bridges cannot be completely closed, entailing a permanent overflow by the valve from the high-pressure to the low-pressure side.
- At the cylindrical mating faces of input shaft and sleeve that should prevent an axial escape of the fluid from the high-pressure area of the valve. A small gap has to remain again to avoid contact of both parts so that the valve would be stuck. Figure 11.61 shows the internal leakage as a function of the height of this gap.
- At the sealing rings between sleeve and valve housings which should prevent an overflow of the fluid from a ring channel of the sleeve with high pressure into a ring channel with low pressure or into the runback space of the valve housing. With corresponding layout and correct assembly this leakage can to be assumed to be zero.
- In the cylinder over the piston ring or the mounting of the piston by overflow of the fluid from the high-pressure side of the cylinder to the low-pressure side. This leakage path can also be neglected if layout and assembly are correct.

Especially high-pressure steering systems with pumps feeding only a little flow to conserve energy, such as electrically powered hydraulic steering, high internal leakage affects the efficiency of the steering system. Corresponding optimisation helps to lower the internal leakage below 0.3 l/min at 100 bars.

### ***11.10.6 Modelling (Position Control Circuit)***

The regulation-technical aspects of a hydraulic power steering can be modelled as a position control circuit. A steering wheel angle is applied by the driver and transferred to the input shaft. This steering wheel angle corresponds to a nominal position of the rack. The external rack forces are acting as disturbance variables, caused by righting moments at the wheels or drilling torques of the wheels when steering at rest.

If there is a deviation between nominal and actual position of the rack, the torsion bar is used to close the control circuit on two parallel paths. First, a force proportional to the deviation is mechanically transferred to the rack by means of the torsion bar and the steering pinion. The second path leads over the valve, guiding a certain pressure into the corresponding cylinder chamber to support the desired movement of the rack. In the quasi-stationary case, the level of the assist power is determined by the valve curve. If the rack force is sufficient, the rack moves towards its nominal position. Indeed, the valve, being a controller in this circuit, has no I portion, so that some deviation will always remain as a function of the applying external forces.

This explains that even a steering system follows control rules with corresponding natural frequencies and damping, in particular it has a stability limit. If that limit is crossed, vibrations occur in the steering system which are perceptible or audible. They are perceived by the driver as very disagreeable.

To precisely determine the stability limit, the dynamic behaviour of the steering system is modelled and complemented by the following parts and effects:

- masses, elasticities and damping of the different mechanically coupled subsystems
- non-linearities, such as the friction between quite moving parts
- capacities and inductances of the hydraulic system originating from stretching hoses under pressure and mass and flow speed of the fluid
- resistances to flow in the hydraulic system from throttles or orifices
- external factors, such as the control behaviour of the pump for varying pressures.

Hence, the parameter setting for the correct modelling of a steering system in the simulation is rather complicated and assumes intensive recording of the characteristics of the steering system in tests.

### ***11.10.7 Damping: Instabilities***

An essential factor for the stability reserve of the steering system is the gradient of the valve characteristic (pressure difference in the cylinder over wheel torque) which shows the amplification in the control circuit. In principle, it is desirable to lay out the valve characteristic in such a way that beyond a certain pressure, which

is never achieved during driving but only in a standing vehicle, the wheel torque rises as little as possible. This enables a good feedback of the steering to the driver in the operating range and, yet, quite low wheel torques during parking. On the hand, this would require a very large gradient of the valve curve, which entails instabilities in the steering system. Hence, in reality, one aims for a high gradient that is sufficiently far from the stability limit.

To lift the stability limit even further, it is also possible to increase the damping in the steering system. In the easiest case, a resistance to flow is introduced into the hydraulic system, e.g., a throttle in the runback line. It generates a resistance that is dependent on the volumetric flow and takes energy from the system to lower the amplitudes for a non-stationary curve of the volumetric flow. The pressing of all seals at their mating faces, reinforced by the higher system pressure, entails additional friction and dampening. The effect of the throttle is the bigger, the higher the back pressure. However, the limits are narrow, because the throttle losses decrease the efficiency of the steering system, increase the energy consumption caused by the steering system and load it very strongly with heat.

There is also the possibility to throttle the volumetric flow streaming out of the cylinder chamber (see also Sects. 11.11.3 and 11.11.4). A damping proportional to the rack speed results. In addition, there is less kickback of the steering system, i.e. the gear transmits less external force impulses to the driver, caused, for example, by road bumps. Mind that narrow limits are set here as well, because quick steering movements generate much higher rack speeds than would occur in an unstable situation, so that a throttle setting yielding sufficient damping will often intolerably limit the efficiency of the steering system in evasive manoeuvres.

## 11.11 Additional Hydraulic Systems

Additional systems for hydraulic steering are used to further improve its properties, based on the standard parts of the gear, both by resolving opposing target situations and by shifting the limits of the system beyond those of the standard layout.

### 11.11.1 Centring

The standard valve layout provides a power assist even for small wheel torques. However, in the region which is relevant for straight driving with small course corrections, the function of the hydraulic steering should be very similar to a mechanical steering. The standard valve design offers a driving of the input shaft to the steering pinion with very high stiffness, this is favourable for precise steering in the mentioned driving conditions. Nevertheless, this stiffness is defined by the torsion bar in the hydraulic steering. At the same time it has to permit a

sufficient relative torsion between input shaft and steering pinion to close the corresponding gaps in the valve, without applying too high wheel torques. A fundamental disadvantage of the hydraulic steering develops. The layout of a hydraulic power steering aims at using a very stiff torsion bar without raising the wheel torques for cornering or parking too much.

To solve this conflict, a centring torsion bar is used, as depicted in Fig. 11.62, both disassembled and assembled. A coarsely rigid driving is produced by a pretense unit parallel to the torsion bar, until the wheel torque surpasses the centring torque applied by the pretense unit. Then the input shaft starts to torsion relative to the pinion, and the additional righting moment is applied by the torsion bar.

The depicted system is an example of such a parallel unit. It consists of two rings, three calottes are introduced at angles of  $120^\circ$  into one of the facing sides. The rings are arranged in such a way that the calottes lie on top of each other and that a sphere lying in between them establishes a positive contact between both rings.

If both rings are torsioned relative to each other, the sphere moves up a ramp in both opposite calottes and presses the two rings apart.

One ring is connected to the sleeve of the valve and to the steering pinion by grouting. The other ring disposes of axial grooves in its inner diameter. These grooves correspond to axial grooves which are introduced, in addition, into the input shaft. The positive contact is again established by spheres running in the grooves between ring and input shaft. Therefore the rotation of the input shaft is transferred to the ring, while the degree of freedom required for an axial movement relative to the shaft is granted.

A centring force is exercised by a spring between the input shaft and the attached ring. It is transferred by the spheres to the ring fastened on the sleeve. A relative torsion between input shaft and sleeve and the attached rings converts

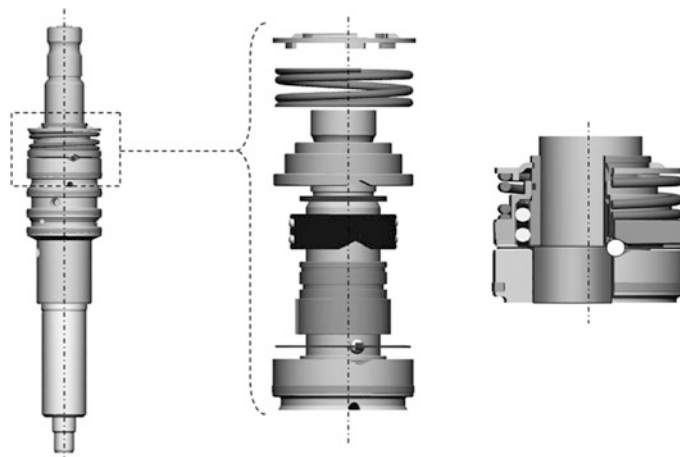
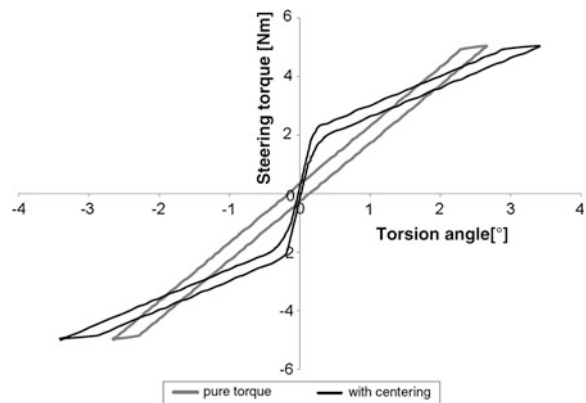


**Fig. 11.62** Centring by means of a spring-loaded axial rotary clutch

**Fig. 11.63** Wheel torque over angle of torsion in the comparison



the axial spring tension into a righting moment which acts with the righting moment of the torsion bar. In contrast to the torsion bar, this mechanic may use the shape of the calottes (ramp angle) and the pretension of the spring to set a torque which is (almost) rigidly transferred from the input shaft to the steering pinion, without relative torsion and, hence, without actuation of the valve. This results in the desired centring, shown in Fig. 11.63 where it is compared to a steering valve which has only a conventional torsion bar.

In addition, there is the option to choose spring stiffness and shape of the calottes so that the effective valve stiffness and valve characteristic are even more controlled, for example, by a degressive curve of the ramp angle.

There is also the option to use this mechanism for a parameterised steering that may be speed-sensitive. This is discussed in Sect. 11.11.2.

An additional system for centring permits separating the operation ranges of the valve for straight driving and cornering within certain limits and to optimise them individually. This reduces conflicts and increases the degrees of freedom by tuning.

By proper choice of the centring torque, the operation point of the power assist is set in such a way that the steering during straight driving is very precise. Then the torsion bar stiffness can be set lower, so that the wheel torques rise less steeply to the parking range with increasing rack force than in a conventional system. This improves the steering comfort in such situations.

Centrings for steering valves exist in many configurations which are also more compact, easier and cheaper than the version discussed here. Their effect is similar to the described solution.

## 11.11.2 Speed Dependence

Conflicts in valve tuning result from the vehicle speed, too. At very low speed and in particular when parking, the steering should be very smooth to provide the best

steering comfort, i.e. to offer high power assist for low wheel torques. At high speed, the support has to be much lower to maintain sufficient steering precision and to avoid accidental jerking around of the steering. Yet the full power assist should be available to the driver at need, for example, to keep control of the steering if a front wheel has left the road and rolls on a soft shoulder. In the layout of the vehicles, high-speed safety dominates esp. in Europe.

A speed-sensitive influencing of the valve characteristic grants a solution of this conflict and more parking comfort.

There are two basic technical concepts: Setting the volumetric flow in the steering valve allows, as described, a variation of the wheel torque. This principle is used only in systems which supply the gear according to demand by a variable pump.

There are other systems that vary the applying wheel torque beyond a certain relative torsion between input shaft and pinion, they set the effective stiffness of the torsion bar, in other words, they adapt to the respective driving situation: A low stiffness if high support is desired, a high stiffness if a driving with low elasticity is important.

A conventional torsion bar with very low stiffness is complemented with a parallel additional system in the construction, supplying an additional righting moment that can be controlled from the outside.

A central part of such systems is a mechanism that transform the relative torsion of the valve into a linear movement along the valve axis, as discussed in [Sect. 11.11.1](#) for the centring. The ring linked with the input shaft of the additional system is here a hydraulic piston, the reaction piston, with a piston ring dividing the space behind the valve drilling of the case into two chambers.

A spring sets a pretension of the system and a rigid driving at low wheel torques, as in the centring system. Beyond this torque, the valve is actuated. The torsion bar is not very stiff, so that the mechanically generated righting moment rises only little. The actuation of the valve raises the flow pressure. This pressure is diminished by a driven magnetic valve and fed into the chamber between the reaction piston and the input oil seal. The axial force generated by the pressure on the reaction piston generates the main part of the righting moment in the valve.

The magnetic valve creates a fixed ratio between flow pressure and reaction pressure as a function of electric power. This allows to set different righting moments by modifying the flow through the magnetic valve to a specific flow pressure.

Finally, an excess-pressure valve in the reaction chamber ensures that the wheel torques do not rise too high if the full power assist is required in extreme situations while the magnetic valve permits high reaction pressures at the same time. This is also a part of the safety concept which adjusts the characteristic curve at the highest reaction effect if the additional system has failed. Then the high-speed response of the steering can be set while the driver is able to achieve the maximum pressure without applying too high manual torques.

Figures [11.64](#) and [11.65](#) show this system and the possible variation of the valve curve.

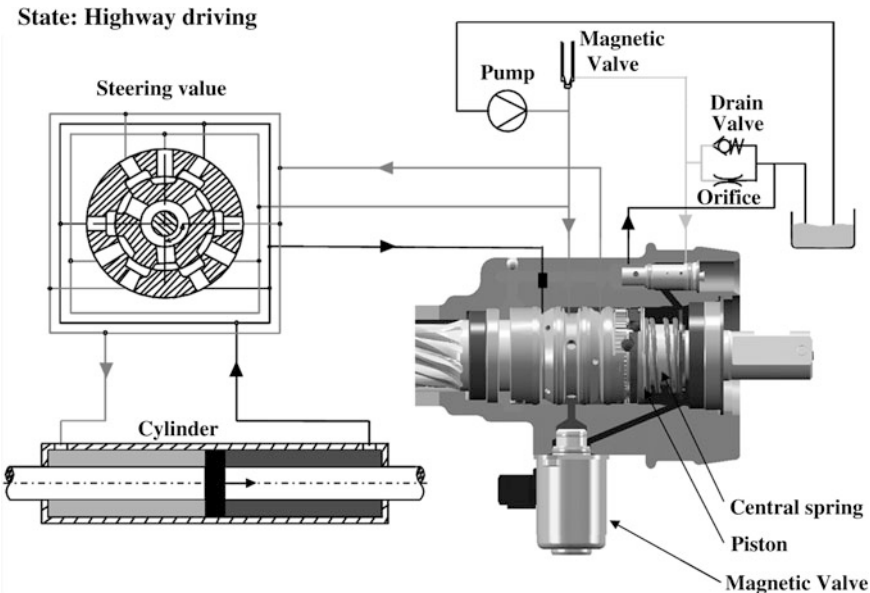
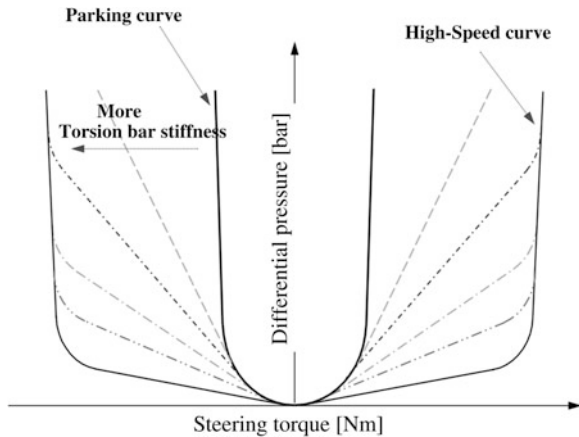


**Fig. 11.64** Representation of a system with hydraulic reaction

**Fig. 11.65** Valve characteristic of a system with hydraulic reaction



It can be seen that the valve characteristic can be divided into three areas. Around the middle position, the pretension of the centring spring acts, so that no power assist builds up. At higher wheel torques, the cylinder pressure over the wheel torque rises about linearly, its gradient depends on the electric power of the magnetic valve. The characteristic curve with the lowest wheel torques (often called parking characteristic [no translation found]) uses only a low reaction pressure to prevent the reaction piston from lifting. For the characteristic curves with a more level gradient, a steep increase of the gradient is then observed beyond

a certain wheel torque. A further rise of the reaction pressure is prevented by the excess-pressure valve in the reaction chamber.

This design provides the most freedom in valve layout by tuning the shape of the control edge at the valve, the torsion bar stiffness, the shape of the calotte, stiffness and pretension of the centring spring, the excess-pressure valve in the reaction chamber and the ratio of reaction pressure to flow pressure. This is opposed by a considerable additional expenditure of parts for the valve and the whole steering system, in particular the magnetic valve, its electric connection and an ECU, to supply it with power according to the given parameters, such as the driving speed.

More internal leakage occurs, because the volumetric flow in the reaction chamber is taken from the inlet. This additional leakage rises with the reaction pressure and has to be considered during the layout of the hydraulic pump.

A more simple system falls back on the same mechanics, but pressurises the piston from the other side. Here the space between reaction piston and input oil seal is directly connected with the runback. The exhausting fluid from the valve, though, is still dammed up by an electrically adjustable throttle valve, before it can flow away into the steering runback. The centring spring is powerful in this system. The reaction piston generates an opposing force to the centring force of the spring, as a function of the back pressure caused by the electrically adjustable throttle valve.

The variation of the valve curve is achieved mainly by a change of its dead band. The setting for high speed does not dam up the runback, and the full centring force of the spring acts. For parking, the centring force of the spring is almost completely eliminated. However, the slope of the valve characteristic is also determined by the torsion bar stiffness and, in addition, by the form of the calottes. It cannot be varied.

This system is a little cheaper because it does not fall back on an adjustable pressure converter but only on an adjustable throttle. Its disadvantage is the accumulation of the whole volumetric flow in the runback, resulting in higher losses and more heating of the system in driving situations when only low wheel torques are aimed at.

### **11.11.3 Damping Valves**

This additional system has the purpose to reduce the steering kickback when force impulses are initiated from the outside. This happens, essentially by integrating a steering damper into the rack-and-pinion steering, as was occasionally used in steering systems with a ball-recirculating gear with nut.

The cylinder and the rack with piston assume the supply of the power assist and the function of the identical parts of a steering damper. To receive a speed-sensitive damping, the volumetric flow leaving the cylinder chamber has to be throttled, so that a force develops against the direction of movement. However,

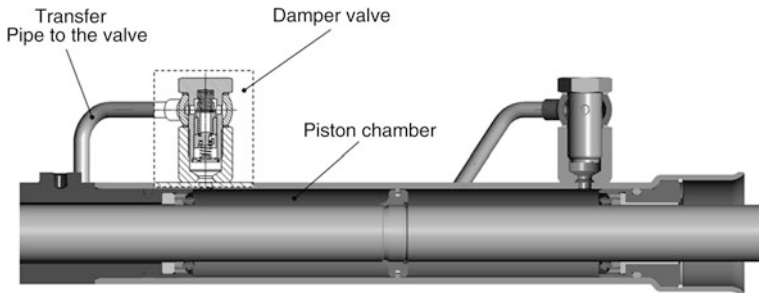


**Fig. 11.66** Cylinder with hydraulic connections and damping valve

the streaming volumetric flow may not be throttled to avoid cavitation and aeration in the cylinder chamber.

The following conflict results: An effective damping of external force impulses requires a cutback which would be so powerful that a desired quick steering movement could not achieve the required rack speed even when the peak pressure was issued into a cylinder chamber. Thus it would not support evasive manoeuvres accordingly. This has to be counteracted by limiting the pressure difference from the throttle with an excess-pressure valve.

Hence, a damping valve like in Fig. 11.66 is attached directly to the hydraulic connections of the cylinder and combines the function of three hydraulic parts:

- The check valve that allows fluids to stream unhindered
- The throttle which builds up a pressure dependent on the volumetric flow as the fluid leaves
- The excess-pressure valve which limits the peak back pressure caused by the throttle.

Figure 11.67 shows one example of a characteristic curve for a damping valve passed in damping direction.

#### 11.11.4 Steering Valves with Damping Qualities

Proper design enables integrating the functions of the damping valves into the steering valve to a great extent. Figure 11.68 shows the configuration of such a valve.

The purpose is to activate the throttle function only at need, i.e. when cornering, when the strongest kickback occurs.

At the same time such steering valves offer a solution for hydraulic instabilities in the steering system. The conflicts between damping in the steering system and efficiency and load, mentioned in Sect. 11.10.7, can be resolved this way. The throttles are activated only when instabilities can occur. The usual valve curves

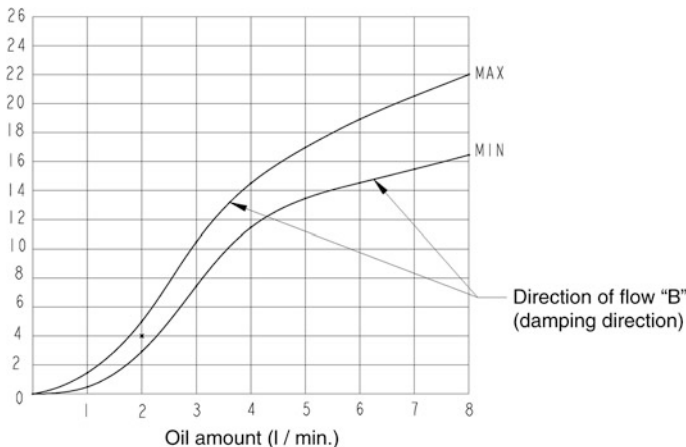


Fig. 11.67 Characteristic curve of a damping valve

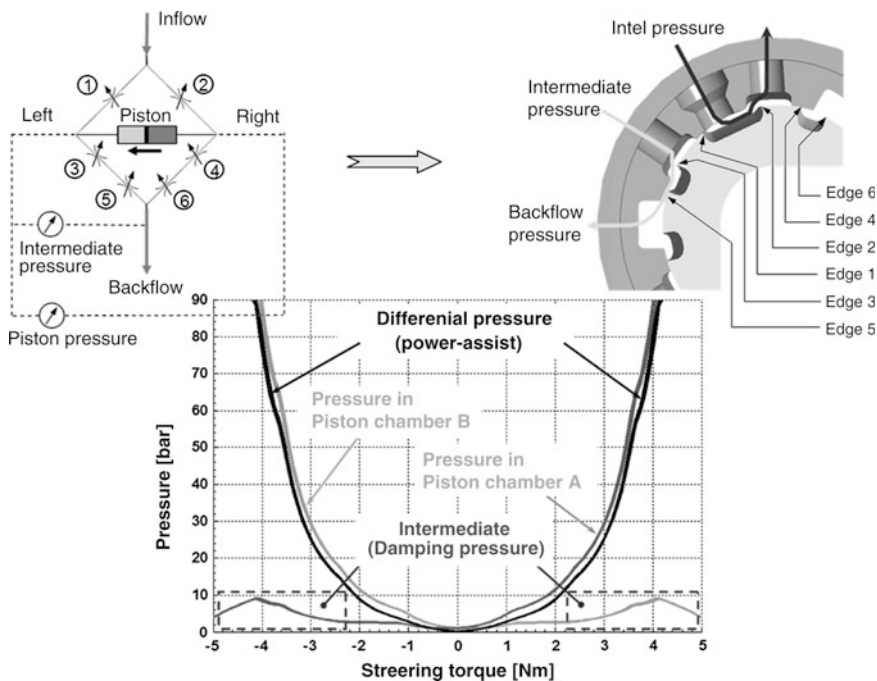


Fig. 11.68 Steering valve with defined damping by additional control edges

have a flat gradient around their neutral position, so that there is a sufficient stability reserve, even without additional measures. The biggest part of driving takes place here. Passing into the parking range, at high pressure, makes a gentle introduction of the throttle desirable.

This function can be integrated into the steering valve by an additional control edge pair, passed by the fluid before it leaves the valve and streams into the runback.

In the neutral position of the valve, these control edges leave a wide gap for the discharge of the fluid. If the valve is operated, the control edges on the high-pressure side close like those of a conventional valve, while those on the low-pressure side open even further. On the low-pressure side, the additional control edges reduce the cross section of the gap if the valve is strongly actuated. The discharging fluid is throttled. The throttle is not activated on the high-pressure side.

Therefore a slight counterpressure against the high working pressure in the accordingly pressurised cylinder chamber is generated in the opposite chamber. Its level depends on the applying volumetric flow. Since oil is squeezed out of the attached chamber as the rack moves, the volumetric flow rises proportionally to the rack speed, so that a speed-sensitive damping results from an instationary movement of the rack, effectively reducing the vibrations. The intensity of the throttle effect is controlled by the layout of the additional control edges.

### ***11.11.5 Pressure Limitation in the Rack-and-Pinion End Position***

An undesirable effect of hydraulic gears is the peak system pressure applying as the steering is held at the end position. The steering valve is fully modulated then and allows only a small volumetric flow to pass, while the pump works against the peak pressure and conducts almost the entire transported volumetric flow through the excess-pressure valve back into the tank.

This causes a mechanical load of the steering system by acting forces and pressures. It also causes a very quick heating of the hydraulic fluid. Especially in pumps driven by the internal combustion engine, the permissible maximum temperature of the fluid can be passed within less than a minute if very high engine speeds apply at the same time. Adjusting and maintaining this operation mode is ultimately an abuse of the car, but it cannot be excluded for the whole range of end customers, and is difficult to prove if the customer complains about a failing system.

Another problem develops because the driver suddenly imposes a high load for the pump when the steering is already at the end position, the valve is in neutral position (no applying wheel torque) and the driver steers towards the end position. If the engine is idling, the control of the idling speed cannot always compensate this sudden additional load fast enough—there is the risk that the engine shuts down as a result of the steering movement. This can be avoided by raising the idling speed. But this significantly increases the standard consumption of the vehicle, on account of the idle running phases which are frequent in the test cycle.

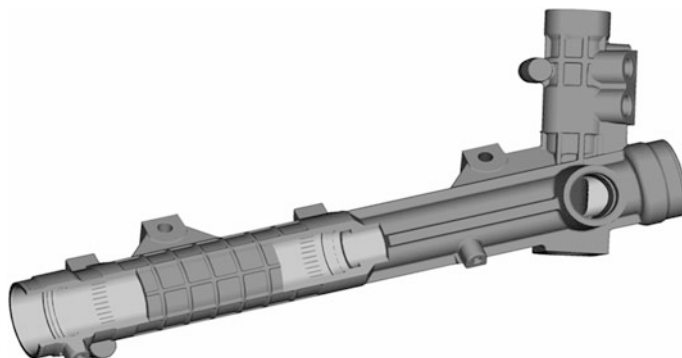


**Fig. 11.69** Cylinder with overflow grooves in the piston end positions

A practical solution of these problems is a pressure limitation at the end position. This is made by inserting overflow grooves into the cylinder near the end positions of the piston. They enable a leakage oil flow from the high-pressure side of the cylinder to the low-pressure side if the piston crosses them, see Fig. 11.69.

Depth and number of the grooves are set in such a way that all the volumetric flow given off by the pump is passing through them with the desired rest pressure. A very low rest pressure is aimed at. It is limited, nevertheless, by the need to provide a sufficient hydraulic rack force for steering the opposite way, away from the stop unit, so that the wheels are moving without additional wheel torques from the driver (manual steer). The required force is lower than that needed for steering towards the stop unit, because of the weight righting of the steering.

The thermal load of the steering system is significantly lowered by a pressure limitation at the end stop, so that additional engine oil coolers can be renounced in most cases. Part of the add-on costs for this system is thus compensated. Besides less loss at the end position, this is also an effect of better thermal absorption, because the pump does not conduct the hot hydraulic fluid directly to the tank, but through the pipes to the gear, then through the valve and both cylinder chambers and then through the runback to the tank. It can emit heat this way.

Another advantage is that noises from steering at the stop unit are reduced by the lower pressure. To be precise: mechanical noise from touching the end position and hydraulic noise which can be caused, otherwise, by the high pressure gradient. If this noise occurs in gears without pressure limitation with an annoying intensity it has to be eliminated. To do so, an additional elastic element between the end position in the gear and the axial joint of the tie rod is inserted.

A limiting factor for the application of such a system is the layout of the chassis structure. The righting moments applied by the axle at the full steer-angle are often very low, especially in vehicles with front-wheel drive. There is a risk that the remaining support is not sufficient to steer away from the end position at need. That is perceived by the driver as a subjectively unpleasant ‘sticking’ of the steering.

## 11.12 Ball-Circulation Gears with Nut/Utility Vehicle Steering Systems

### 11.12.1 Fields of Application

The ball-recirculating gear with nut is the traditional form of steering which converts a rotation of the steering wheel into a swivel of the steering arm which is transferred by the track and tie rods to the wheels.

This transmission by leverage is also the main advantage of their modern applications: vehicles whose guided axle is rigid are almost always equipped with ball-recirculating gears with nut. By a corresponding layout of the steering structure they permit mounting the gear to the frame and following the complicated spatial movements of the rigid axle with little kinematic repercussions on the steering system. This applies in particular for axles which are attached only by leaf springs.

However, a rack-and-pinion steering has to be connected solidly with the body of a rigid axle. This produces conflicts with package and steering kinematics and demands for a very loadable and highly flexible attachment of the steering column. The joints in the steering column have to cover a wide range of angles. Their length offset should have a very high stroke, so that the joints are able to follow any possible relative movement between the axle with gear and the frame or even that of a driver's cab that is elastically supported on the frame.

Nowadays, vehicles with rigid front axles are mainly found in two categories:

- cross-country vehicles destined for off-road service that should admit extremely high axle crossing
- utility vehicles of the middle and heavy class with permissible front axle loads of more than 2 t.

In typical configurations, either the gear is mounted to the body frame on the driver's side, the corresponding front wheel is connected by a track rod and both front wheels are connected by the tie rod (shown in Fig. 11.70), or the gear is placed in the middle of the car and both front wheels are coupled directly by tie rods.

No sufficiently large rack-and-pinion gears are available for coaches with independent suspension in the front axle. A steering quadrangle is usually used for applications in these and for the rare use of ball-recirculating gears with nut in passenger cars. One more track rod is sometimes used as a connecting element in coaches, on account of the driver being seated far in front of the front axle.

All arrangements have in common that they contain many elements which introduce friction and elasticities or even free travel into the steering system. They affect in general the steering feel and precise steering. Lots of leverage elements also indicate an expensive steering system, so that the ball-recirculating gear with nut was displaced by the rack-and-pinion steering wherever it is available as a feasible alternative.

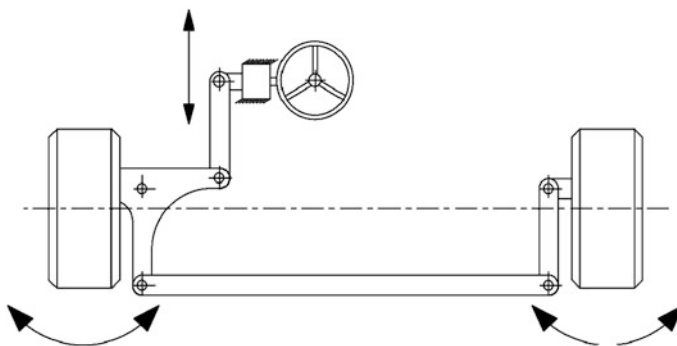


**Fig. 11.70** Connection between gear and front wheels in utility vehicles with rigid front axle

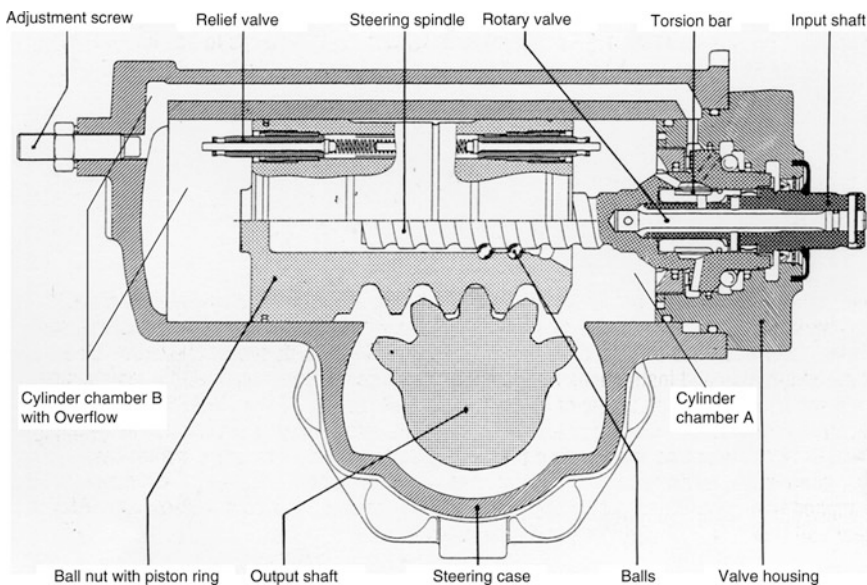


**Fig. 11.71** Ball-recirculating gear with nut in a cutaway view

### 11.12.2 Configuration of Ball-Recirculating Gears with Nut

Ball-recirculating gears with nut are produced only in an integrated module, so that the mechanical part of the gear and the hydraulic part are gathered in a common case. This module is also called integral steering or block steering.

The ball-recirculating gear with nut, of which Fig. 11.71 shows a sample cutaway view, can be separated into the following subassemblies:

- Valve with valve housing and input shaft
- Steering shaft, linked with the valve

- Ball nut and piston, linked with the steering shaft by balls
- Steering shaft with dovetailing segment.

The input shaft, linked with the steering column, and the valve are similar to shaft and valve of a hydraulic rack-and-pinion steering. It is another rotary disk valve with input shaft, sleeve and torsion bar. However, the valve is designed for much higher volumetric flows and higher working pressures, compliant with the purpose of the gear, so that, for example, the circulatory cross sections are wider and the walls of the sleeve are thicker.

There the spindle follows instead of the pinion, it is connected to the steering nut. A rotation of the spindle is converted into a translation of the ball nut and the positive connection between them is established by recirculating balls, so that the friction is low. The opposite end of the ball nut is a piston in a cylindrical part of the steering case. The cylinder chamber, located there, is connected by a channel in the case with the corresponding ring groove of the sleeve, while the other ring groove is connected directly with the whole remaining cylinder space. Waste-gate valves are in the ball nut, they are operated if the piston approaches the end position. They open a transfer canal, conducting fluid from the high-pressure side to the low-pressure side with a defined rest pressure (cf. [Sect. 11.11.5](#)). This avoids unrequired loads of the whole steering system when the steering is kept at the end position.

The movement of the ball nut is transferred by a dovetailing to the steering shaft and then produces a swivel of the tightly pressed-on steering arm at the outside of the case. The dovetailing has a constant or a variable gear ratio, according to the configuration of the gear.

### ***11.12.3 Comparison Between Ball-Recirculating Gear with Nut and Rack-and-Pinion Steering***

Resemblances between a ball-recirculating gear with nut and a rack-and-pinion steering are only found in the steering valve which is made in the same manner.

All together, the ball-recirculating gear with nut is much more robust and suitable for applications with hard conditions or that have to merge high reliability with a long service life, as, for example, utility vehicles, which are usually laid out for a road performance of 1 million km.

One reason for the high robustness is the sealing system with only one radial high-pressure oil seal at the steering shaft. The shaft is only rotating there and, hence, easier to be sealed than a rack with two high-pressure seals against which it is linearly moving. This allows for peak working pressures of 185 bars, soon to become 200 bars.

A ball-recirculating gear with nut offers a better damping against external impacts as well, chiefly because of the mechanical efficiency of the ball-recirculating gear with nut. It is higher for movements applied by the input

shaft than for repercussions of the ball nut, so that these are damped by more friction. Finally, the ball-recirculating gear with nut is more compact and, hence, suggests to cover a wide spectrum of vehicle applications with few standard products. Then any required individual adaptations are carried out in the design of the steering linkage and the support for the steering. This way, the financial benefits of mass manufacturing may be exploited even for specified applications which are built only in small numbers, as is common with some utility vehicle models.

This is opposed by drawbacks of the whole steering system. Including the required steering linkages, a steering system with ball-recirculating gear with nut is much heavier and, at least when build in great numbers, more expensive than a rack-and-pinion steering. The huge number of transmission elements between steering column and wheels and their elasticities and frictions at the joints affect the steering feel—a rack-and-pinion steering permits a more immediate perception of events at the wheels. These factors are important for passenger cars where the advantages of the ball-recirculating gear with nut are limited. That is why rack-and-pinion steerings are almost always used in passenger cars.

#### ***11.12.4 Technical Data and Parameters***

See (Table 11.6).

#### ***11.12.5 Additional Systems***

On account of the equal configuration of the steering valve, the respective systems for centring the torsion bar (Sect. 11.11.1) and speed-sensitive control of the valve characteristic (Sect. 11.11.2) are also found in ball-recirculating gears with nut. They are somewhat similar to the configurations for rack-and-pinion steering.

Valve designs that introduce specific damping into the gear (Sect. 11.11.4) can be transferred to ball-recirculating gears with nut as well. In utility vehicle applications, they are more important than in passenger cars, on account of the high power assist and the resulting high power of the valve.

Damping valves (Sect. 11.11.3) are not required, due to the mentioned damping qualities of the ball-recirculating gear with nut against external impacts. A pressure limitation at the end stop (Sect. 11.11.5) is already included in the standard layout. One special additional system found in gears for heavy utility vehicles with several guided axles is an option to connect an auxiliary cylinder.

Instead of designing large special gears for these vehicles, which are usually produced in quite small numbers, the required additional steering force is introduced by coupling an auxiliary cylinder to the steering linkage near the second guided axle, that is required anyhow. This cylinder is supplied over the steering valve, since the valve housing has hydraulic connections linked to the corresponding ring channels

**Table 11.6** Some parameters of hydraulic ball-circulation gears with nut

Vehicle class	Cross-country vehicles	Light utility vehicle	Moderately heavy utility vehicle	Heavy utility vehicle	Construction vehicles
Front axle load (t)	1.8	2.5	5.5	7.5	9.5
Maximum source torque (Nm)	1,200	1,700	5,000	6,500	8,500
Maximum working pressure (bar)	120		715–185		
Volumetric flow (l/min)	6	8	12	16	25
Swivelling angle output shaft	$\pm 90^\circ$ to $\pm 100^\circ$				
Gear ratio	Approx. 16:1 to approx. 26:1				
Temperature	−40 to +120 °C				

of the valve sleeve. This permits using the same gear that is found in cars with one guided axle, except for this small modification, and keeping the load of individual parts very low by distributing the power supply according to demand.

### 11.12.6 Dual-Circuit Steering

Heavy utility vehicles with very high front axle loads or two front axles may fail to observe the registration regulations for operation at power assist failure when the steering is used mechanically exclusively. The dual-circuit steering, whose schematic hydraulic diagram is shown in Fig. 11.72, maintains a sufficient volumetric flow of the steering oil supply even when one steering circuit has failed.

Normally only the pump powered by the internal combustion engine (1) is connected with the gear (4/5) by the dual-circuit transfer valve (6). A slight cutback of the volumetric flow in this valve helps to install a control pressure which actuates the valve against a spring into the displayed position. The runback leads over this valve into the tank as well. The tank has two separate chambers which are interconnected above the least level.

The auxiliary pump (2) is mechanically connected to the live axle, usually at the output shaft of the drive gearbox. This helps to ensure that the required volumetric flow can be provided even when the internal combustion engine has failed, as long as the vehicle moves. Normally, the transported volumetric flow is conducted by the dual-circuit transfer valve back into the tank (3). A slight cutback is present here as well. The developing back pressure is monitored to warn the driver if the second control circuit fails (he or she would not notice otherwise) and to request stopping the vehicle.

If the primary control circuit fails, there is no control pressure at the dual-circuit valve. Then the spring adjusts the valve in the second switch position. Now the gear is fed by the second control circuit, a leak loss over the main pump is prevented by the check valve (8). The driver is warned and asked to stop the vehicle.

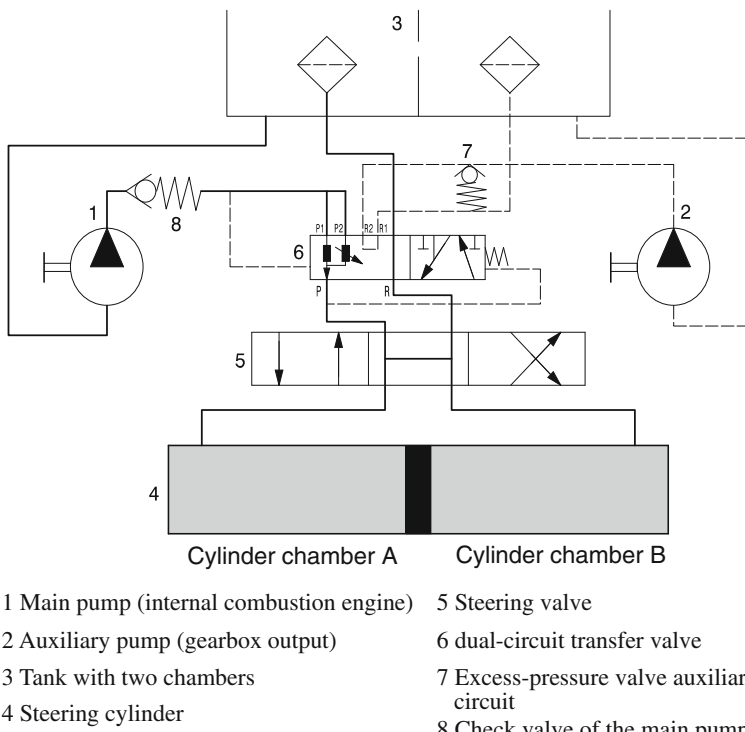


**Fig. 11.72** Scheme of a dual-circuit steering

The gear itself and all its parts are considered sufficiently failsafe, so that no further redundancy is necessary.

## 11.13 Requirements for a Hydraulic Gear

The general requirements for function and strength of hydraulic gears are, in the end, an extension of the requirements for mechanical rack-and-pinion gears with specific tests of the steering hydraulics.

Hence, only the additional requirements shall be discussed here.

### 11.13.1 Functional Requirements

The function tests are complemented by measurements of the valve characteristic and the internal leakage. Both were discussed in Sect. 11.10.

### ***11.13.2 Strength Requirements***

#### **11.13.2.1 Static Strength: Burst Pressure Test**

The static strength of the hydraulic system is tested by introducing a volumetric flow into the gear when the steering valve is closed. The flow is controlled in such a way that the pressure rises steadily. The gear has to remain tight, up to the peak working pressure including a safety reserve, and it has to stay fully functional. In addition, the burst pressure, i.e. the point at which a part of the steering hydraulics fails, has to lie above a certain limit value, say, at least three times the peak working pressure.

#### **11.13.2.2 Dynamic Strength: Pressure Pulsation**

The dynamic strength of the steering hydraulics is tested by generating pressure pulses in the gear. This may be done either by actuating the steering valve when the rack is blocked or by introducing a varying rack force. A high number of pressure pulses is desired, hence, the excitation should be high-frequency (5 Hz or more). The gear has to be fully operable after this test.

### ***11.13.3 Environmental Requirements: Cold Start Test***

An important quality of hydraulic gearboxes to be checked is the sealing under cold circumstances. As described, seals lose their flexibility when it is very cold, and they may not be able to sufficiently follow movements of the rack, the steering pinion or the input shaft any more. A cold start simulation test to check whether hydraulic oil is leaking under these conditions.

Down to a temperature of  $-20^{\circ}\text{C}$ , this must not happen at all. At lower temperatures, most tests run down to  $-40^{\circ}\text{C}$ , some millilitres of leakage are tolerable, according to the purpose of the vehicle.

## **References**

- Baxter J, Heathershaw A (2002) Bedeutung der Mittencharakteristik bei Hochgeschwindigkeitsfahrt. 11. Aachener Kolloquium Fahrzeug- und Motorenmechanik  
Heathershaw A (2004) Matching of chassis and variable ratio steering characteristics to improve high speed stability. SAE paper 2004-01-1103. SAE, Warrendale, Pa. 2004

# Chapter 12

## Tie Rods

Dirk Adamczyk, Wolfgang Kleiner and Dirk Maehlmann

### 12.1 Introduction

The tie rod connects the steering gear with the wheel carrier and transfers the gear stroke to wheel carrier and front wheel.

From the kinematic point of view, this is a crank mechanism, with the rack acting as a slider and with the wheel carrier acting as a rotating member (Fig. 12.1). The tie rod is the coupling member (Heißing and Ersoy 2007). At the same time, the stroke of the wheel has to be enabled. A three-dimensional movement develops; hence, the design of the mounting points of the tie rod as ball joints has to have suitable degrees of freedom. It is due to the lever ratios (length of the tie rod vs. distance of the tie rod mounting at the wheel carrier to the carrier's axis of rotation) and to the carrier's angled axis of rotation that the appearing angles are bigger at the wheel carrier than they are at the gear.

A common modern tie rod consists of an inner and an outer joint. The inner joint (near the gear) is also called the axial joint. The outer joint (near the wheel) is also known as the radial joint. Both joints are adjustably connected to each other. Most of the time, the joints should have low friction torques, to achieve good responsiveness of the chassis and low actuating forces.

---

D. Adamczyk (✉)  
ZF Friedrichshafen AG, Friedrichshafen, Germany  
e-mail: dirk.adamczyk@steeringhandbook.org

W. Kleiner · D. Maehlmann  
ZF Friedrichshafen AG, Dielingen, Germany  
e-mail: wolfgang.kleiner@steeringhandbook.org

D. Maehlmann  
e-mail: dirk.maehlmann@steeringhandbook.org

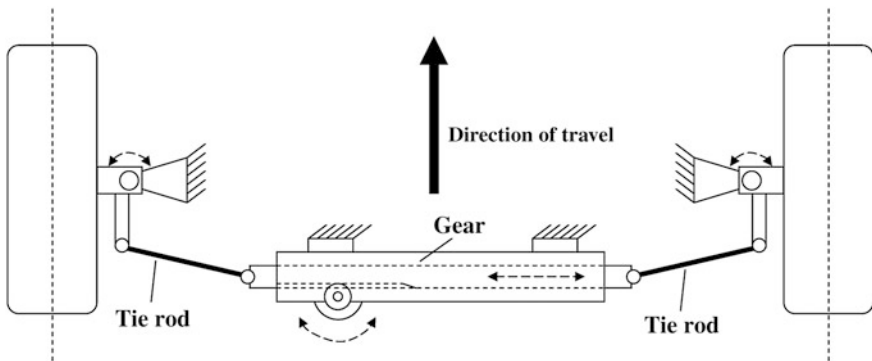


**Fig. 12.1** Interaction of gear, tie rod and wheel carrier. *Source ZF Lemförder GmbH*

## 12.2 Basic Variants

### 12.2.1 Tie Rods for Ball-and-Nut Steering

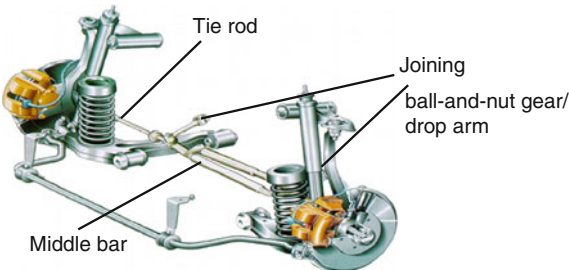
In the ball-and-nut gear, the turning of the ball-and-nut steering wheel is converted by a screw wheel with a spiral groove, in which the balls roll (Stoll 1992). The left and right tie rods are connected by a middle bar. The movement of the steering wheel is converted into a yaw and transferred to the middle bar. Space and costs restrict this structure today mainly to big commercial vehicles, when rack-and-pinion steerings cannot be used, e.g., because of the high loads. The rather slender middle bar will under certain circumstances be beneficial, too, e.g., with regard to ground clearance.

Figure 12.2 shows a front axle with a ball-and-nut gear. Tie rod implementations of this design are shown in Fig. 12.3.

### 12.2.2 Tie Rods for Rack-and-Pinion Steering

For passenger cars and transporters, this design is currently used most frequently, esp. because of its rather low costs (Fig. 12.4). Hence, the remainder of this chapter will only discuss this design in more detail; in any case, much of the content also applies to tie rods for ball-and-nut gears.

In rack-and-pinion steerings, the steering movement is transferred by wheel, gear and tie rods to the front wheel carrier and ultimately to the tyres. The tie rods are directly attached to the gear rack. In contrast to the ball-and-nut gear, here, the rack assumes the function of the middle bar as well. Moreover, the inner joint is protected by the gaiter of the gear, so that no distinct sealing system is needed.



**Fig. 12.2** Front axle and ball-and-nut gear. *Source ZF Lemförder GmbH*

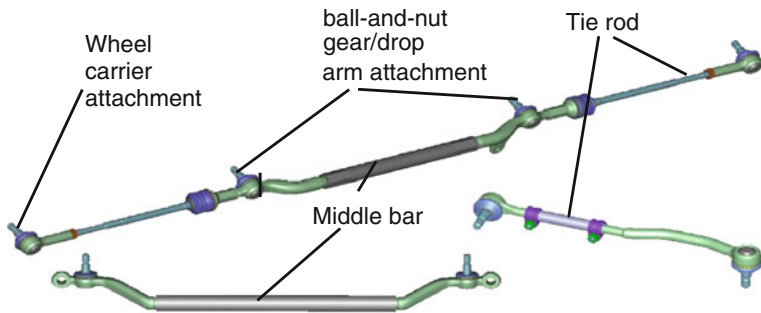


**Fig. 12.3** Sample structures of tie rods for ball-and-nut gears. *Source ZF Lemförder GmbH*

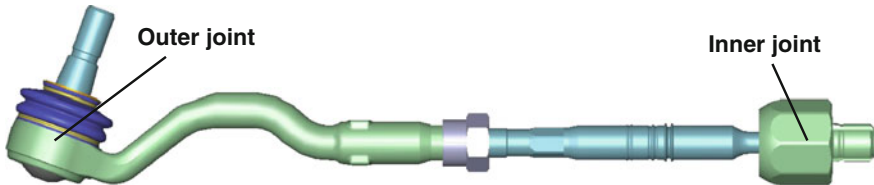


**Fig. 12.4** Sample implementation of a typical tie rod for passenger cars. *Source ZF Lemförder GmbH*

The whole design of a rack-and-pinion steering entails quite short tie rod lengths of 250–350 mm. Deflecting and rebounding of the wheel result in high tilting angles at the joints of both wheel and rack. These big angles cause high requirements on the design of the tie rods.

## 12.3 Tie Rod Joints

### 12.3.1 Inner Joint (Axial Joint)

The inner joint tilts in the steering process and during jounce and rebound, due to the arrangement of the tie rods at the rack, while the outer joint essentially tilts upon jounce and rebound but turns upon steering (Fig. 12.5).

The inner joint has a thermoplastic liner as its bearing element—the ball race; an additional elastomer ring is inserted here. The elastomer ring seen in Fig. 12.6 acts like a spring, counteracting free travel in the joint from overloading and wear of the ball race by readjusting itself. Loading capacity and robustness are thereby increased for the service life. The joint is sealed-for-life.

Ball stud and housing are mainly produced in cold forging. Cold forged parts improve the geometrical accuracy, so that only the ball of the ball stud has to be processed by additional machining, keeping the material allowance very low (Landgrebe et al. 2001). The ball stud has a gaiter support groove to accept the gear gaiter. The groove can either be coldly reshaped or machined in a separate

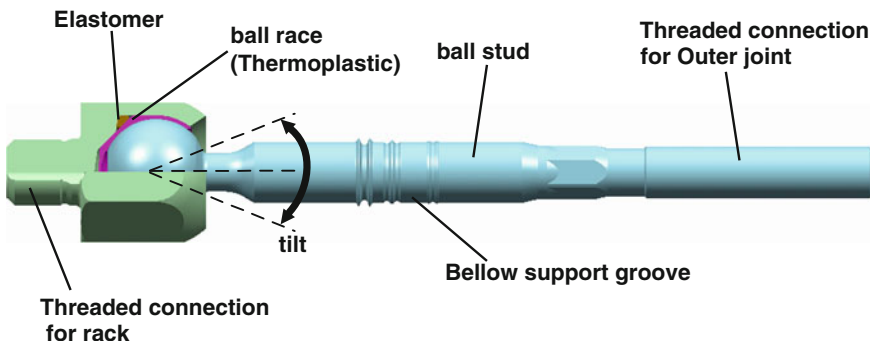


**Fig. 12.5** Rotary and tilting movement of an outside joint

**Fig. 12.6** Design of an inner joint. *Source* ZF Lemförder GmbH

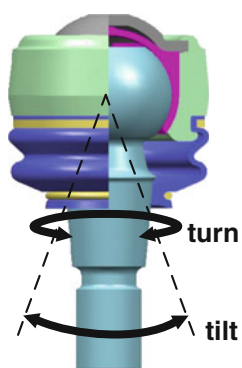
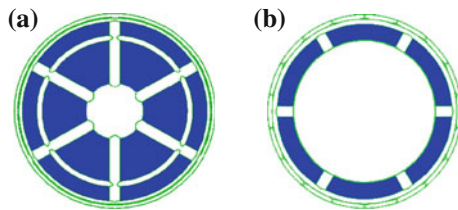


**Fig. 12.7** Effective surface of an axial tie rod bearing in push and pull direction. **a** Effective bearing surface towards pressure. **b** Effective bearing surface towards pulling direction (*joint opening*)



step (Fig. 12.6). In contrast to the sealing system of the outer joint, only a static sealing is necessary here; there is, hence, no relative movement between ball stud and gaiter in the sealed zone. During operation, the gaiter is stressed only by its own linear expansion. Only when the toe is adjusted by turning the pivot, the gaiter glides in the support groove.

The inner joint commonly requires a wider diameter than the outer joint. The resulting (effective) surface of a joint support is smaller towards the tie rod opening, and the tie rod can support less load in this direction. However, the inner joint is loaded just in the pulling direction of the ball stud, towards the housing opening (Fig. 12.7). By contrast, the outer joint is loaded vertically to the ball stud; accordingly, the resulting surface of the bearing is much bigger towards the load.

The joint housing and the bearing are protected against environmental influences by the gaiter. Hence, it has to meet only few requirements for surface protection, but the shaft of the ball stud is exposed to corresponding influences. A few common kinds of surface protection for ball studs of inner joints are, e.g., cathodic immersion painting (CIL) with a resistance of 240 h salt spray test, zinc iron (ZnFe) with 480 h and zinc nickel (ZnNi) with 720 h.

### 12.3.1.1 Ventilation Function of the Inner Joint

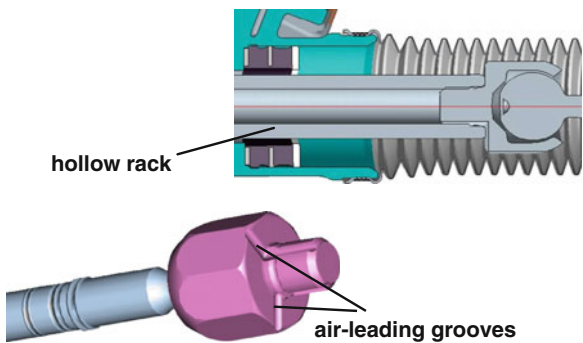
A steering movement compresses and relaxes the gaiter alternately on the right and left side of the gear. Without integrated pressure compensation, the enclosed air would produce high or low pressure in the steering gaiter. These different pressure ratios would subsequently cause leakages at the gear.

In the past, the function of the pressure compensation was maintained by linking both sides of the gear with separate air conduits.

An integrated function has been produced for some years, and ‘air-leading grooves’ are now introduced into the axial tie rod housing. These grooves may be part of the housing manufacturing, without additional expenditure, and they enable a pressure compensation across the hollow steering rack. A least overall cross section is necessary in the integrated state to allow for the pressure compensation. Three grooves will meet this demand perfectly. The resulting discontinuous thread can be safely made and screwed (Fig. 12.8).

Drilled ventilation holes in axial joint housings are still in use sometimes, instead of ‘air-leading grooves’; they require an additional step of housing manufacturing, though.

**Fig. 12.8** Air-leading grooves in the inner joint.  
Source ZF Lemförder GmbH  
**a** Hollow rack. **b** Air-leading grooves



### 12.3.2 Outer Joint (Radial Joint)

Figure 12.9 shows different versions of housings for outer joints. The housing design is substantially limited by available space, requiring either straight and simple or several times stepped housings for the outer joints. Bigger and broader wheels have restricted the use of straight housings to rare applications.

The structure of the joint and its interacting parts are shown in Fig. 12.10; this joint as well is sealed-for-life. It is joined to the wheel carrier by the ball stud,

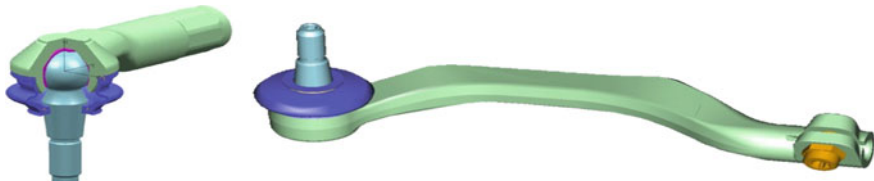
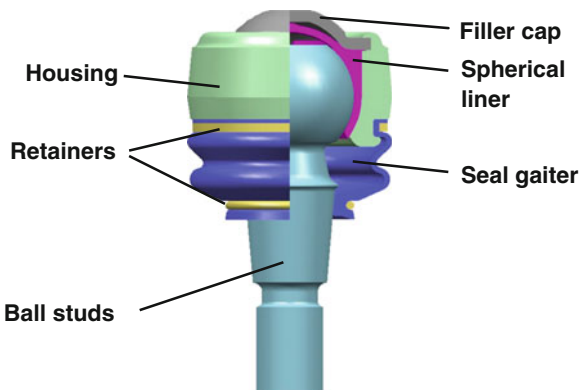


**Fig. 12.9** Design example of outer joints. Source ZF Lemförder GmbH

**Fig. 12.10** Construction of an outer joint. Source ZF Lemförder GmbH



mainly by means of a conical seat and screwing (see also Sect. 12.7). In contrast to the inner joint, the housing of the outer joint is chiefly made in hot forging.

Hot forging allows for complicated geometry, for example, stepped housings. However, the housing has to be machined later to achieve, e.g., the necessary tolerance margins in the bearing area. Simpler housings can be produced by cold forging. Coldly forged housings need hardly any machining; hence, they are cheaper.

The outer joint is exposed to powerful ambient influences, since it is close to the wheel. Hence, galvanic coating is increasingly common for surface protection, e.g., ZnFe and ZnNi.

The ball studs as well are coated more and more frequently to enable robust sealing (see Sect. 12.5.4).

## 12.4 Toe Adjustment

Axial joint and radial joint are connected by a shifting thread. It allows to adjust the toe of the wheels. The best adjustment of the toe serves to improve a stable straight course and to lessen tyre wear, among other things.

All the solutions shown in Fig. 12.11 are in use today, depending on function and assembly requirements. The toe adjustment is mainly automated, so that any of the mentioned screwing options may be chosen, in accordance with the assembly process of the vehicle manufacturer.

## 12.5 Requirements and Design

### 12.5.1 *Design Regulations for Tie Rods*

Basically, the sizing of tie rods observes a relationship between vehicle weight or axle load, rack force and joint sizes used. Figure 12.12 shows this relationship. The yellow area marks the transition zone. Apart from the outer forces acting on the tie rod or its joints, the joint size is mainly fixed by the greatest angles and the highest operating temperatures.

### 12.5.2 *Design of the Tie Rod with Regard to Component Strength*

The component strength is the most important feature of a tie rod. If it breaks, the active chain of the pull/push forces is interrupted, and de facto, the vehicle cannot

### Design solutions for the toe adjustment:

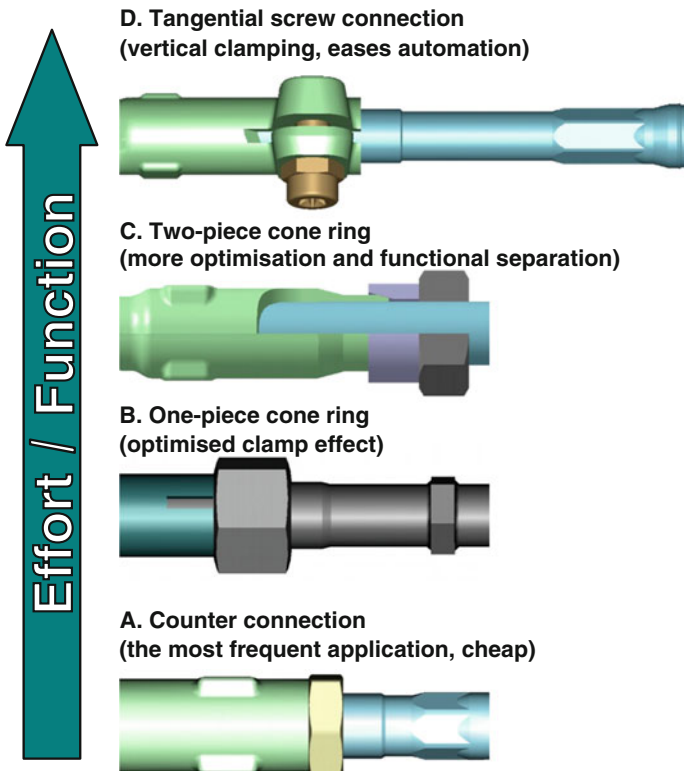


**Fig. 12.11** Designs of toe adjustment. Source ZF Lemförder GmbH

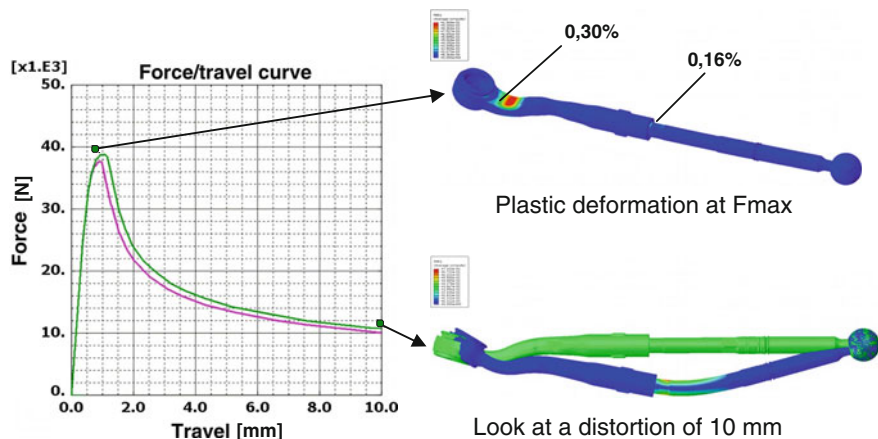
be steered any more. To prevent this from occurring, CAE methods are used for the design and the parts are controlled by extensive tests. The tie rods are validated first by means of FEA (Fig. 12.13), then test on physical parts and finally validated on-board. The loading conditions, distinguished by operation load, special events and abuse, are relevant for the design. The operation load must not permanently deform the metallic parts, but the loading conditions Special events and Abuse may tolerate or even welcome any remaining distortions (see ‘Damage chain’ in Sect. 12.9.1). Yet the mechanical link between gear and wheel carrier has to survive any loading condition.

Figure 12.14 shows the relationship. The red characteristic curve marks the load requirements. For the tie rod, they are deduced from the vehicle loads it is exposed to. The green curve above shows the stress-number curve of the tie rod which is accordingly above the load requirement. The sketched lines mark the beginning plastic deformation and, finally, the area in which the tie rod may or should snap.

The tie rod has to remain operable even under loads from special events. This is ensured by using high-strength, ductile materials for the relevant parts. Steels are

Vehicle class	Steering assistance force [N]	Allocation of the joint size		
		Outer joint	Inner joint	Ball size
Superclass	15000			
	14000			
	13000			
Upper middleclass	12000			
	11000			
Middleclass	10500			
	10000			
	9500			
Lower middleclass	9000			
	8500			
	8000			
	7500			
Compact cars	7000			
	6500			
	Outer joint	Ø22		Ø27
	Inner joint	Ø26	Ø29	Ø32

**Fig. 12.12** Relationship between vehicle size, steering assistance force and joint or ball sizes to be selected, Runge et al. (ATZ 10/2009)



**Fig. 12.13** Shows a simulation of a buckling force. Source ZF Lemförder GmbH

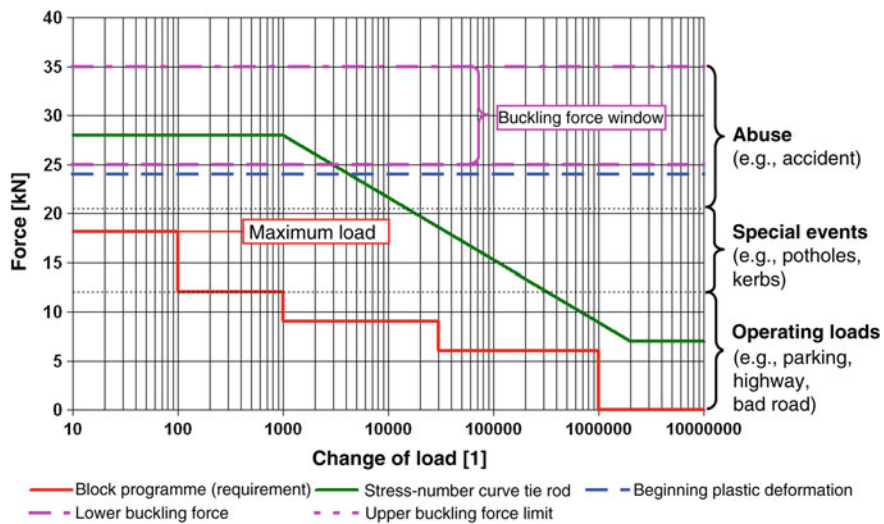


**Fig. 12.14** Relationship between the loading conditions operation load, special events and abuse.  
Source ZF Lemförder GmbH

used, but also aluminium materials, they are a lightweight alternative. Whether light materials are applicable, depends in particular on the free space on-board (see also Sect. 12.8).

### 12.5.3 Design of the Joint Bearing

Many modern passenger car joints have a plastic bearing liner made of a thermoplastic material (plastic with linear macromolecules, Menges 1970). In the operating mode, polyoxymethylene, or POM for short, enables a good compromise between the requirements for loading capacity, low movement torques, tolerance margins and zero backlash. Polyetheretherketone (PEEK) is used for very high temperatures. Composite materials and metal bearing liners are also used in special housings (Heißing and Ersoy 2007).

The choice of the proper bearing material is linked to the requirements of load and temperature (Fig. 12.15). One important layout criterion is the permissible surface pressure that the installed bearing liner can endure under temperature exposure without flowing. An excess of the permissible pressure can cause free travel in the joint when the car is driven. Free travelling joints usually strike by noise and free travel in the steering. The result are customer complaints during the main examination of the vehicle which can again cause repair sessions to exchange the joints or the tie rod.

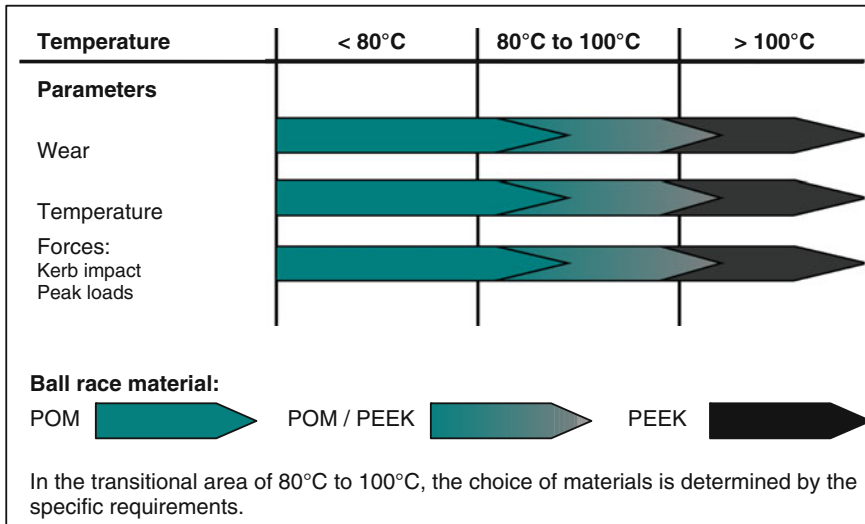


**Fig. 12.15** Bearing material as a function of load and temperature. *Source ZF Lemförder GmbH*

#### 12.5.4 Design of the Outer Joint Sealing

The joint sealing prevents dirt and water from entering the bearing. Penetrating water leads to corrosion in the bearing (Guy 1976). Dirt and corrosion mean more wear and can entail an untimely failure of the joint by free travel. This is the most frequent cause for failing joints. Hence, the design of the joint sealing is a core element of joint layout. Figure 12.16 shows the process of development for joint sealings.

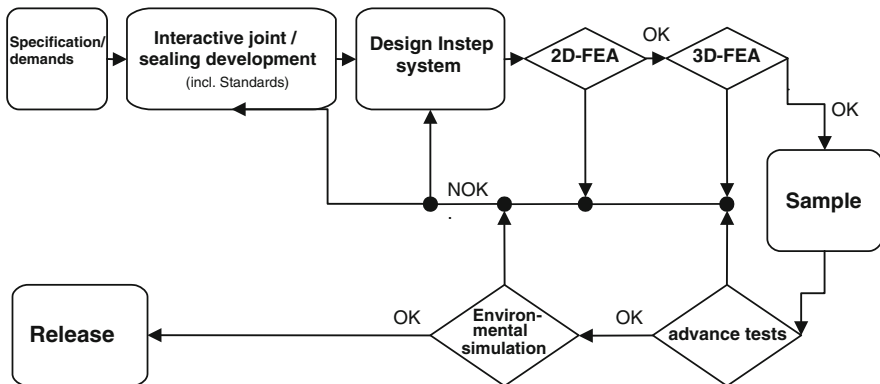


**Fig. 12.16** Design flowchart for a joint seal. *Source ZF Lemförder GmbH*

### 12.5.4.1 Requirements of the Joint Sealing

The joint sealing is subject to more complicated dynamic loads than shaft-lip type seals, resulting from the superposition of turning and tilting movements which the outer joint has to perform during the steering stroke and concurrent deception and rebound of the wheel. The rotary angles of the joint are approx.  $\pm 35^\circ$  and the tilting angles approx.  $\pm 30^\circ$ , depending on the design of the axle.

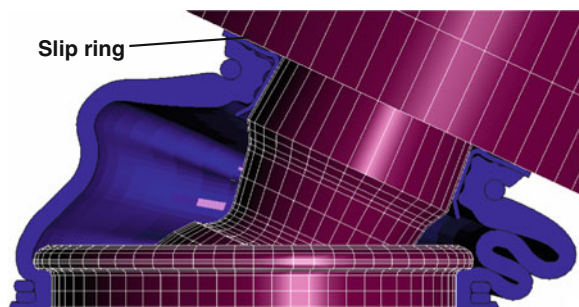
Implement a static sealing at the housing, the sealing is radially and axially gliding at the pivot. The dynamic sealing function is achieved here by the combination of radial and axial parts. The gaiter is exposed to superimposed stress from tilting and turning. This function is implemented by choosing a proper geometry and material. Elastomers are frequently used. The design is checked by FEA (Fig. 12.17). The sealing system is validated by running an environmental simulation in a test chamber and complemented by vehicle tests.

At rest, the particular requirement of the high-pressure cleaning is important; during a cleaning process, housing and pivot sealing have to withstand at least 80 bars.

CR is an elastomer that is frequently used for gaiters. A temperature range of  $-40$  to  $+80$  °C can be covered by standard quality CR. HNBR and others are used for higher temperatures till 100 °C.

Corrosive infiltration of sealing systems cannot be fully avoided, the sealing areas are therefore often corrosion-proof to ensure that the sealing function will be maintained for many years. Dynamic sealing at the ball stud is very important here. Different nitration procedures have prevailed. They provide the advantages of an abrasion-proof corrosion prevention (BMFT 1981). The ball itself may be coated, supplying additional strength. Slight infiltration of moisture will then not cause corrosion in the bearing. An alternate option to nitration is the use of additional construction elements, as, for example, a slip ring made of a material that is poor in corrosion. This slip ring is visible in Fig. 12.17.

**Fig. 12.17** 3D-FEA of a sealing system. Source ZF Lemförder GmbH



## 12.6 Damping/Decoupling

In particular housings, damping or decoupling functions are assumed by the tie rods. Undesirable vibrations are damped or decoupled by a damping or decoupling element (Stoll 1992). A decoupling function can be assumed by the inner joint, the outer joint or a separate element (Fig. 12.18).

*Advantage:* The spring designator can be designed according to requirements. The versions shown can maintain a damping function throughout the service life of the vehicle.

*Disadvantage:* Undesirable elasticities. Separate parts, leading to higher costs and weight.

## 12.7 Interfaces to the wheel carrier

Various manufacturing methods and materials are used for implementing wheel carriers.

A steel-forged wheel carrier establishes an ideal connection of the outer joint (see also Fig. 12.19). A conical connection is used here to connect the outer joint with the wheel carrier. Expenses and weight may also demand that wheel carriers are made of metal sheet, cast steel, cast aluminium or aluminium-forging technology (Vieregge et al. 1994). In these housings, pressed-in jacks and conical disks of high-strength materials are applied. They are able to accept the necessary

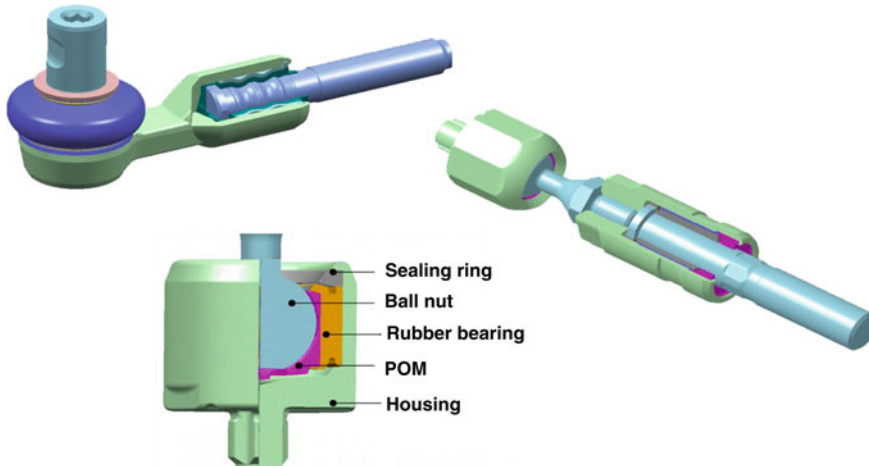


**Fig. 12.18** Options to integrate damping and decoupling in the tie rod. *Source* ZF Lemförder GmbH

**Fig. 12.19** Conventional cone connection, mostly in connection with steel-forged wheel carriers

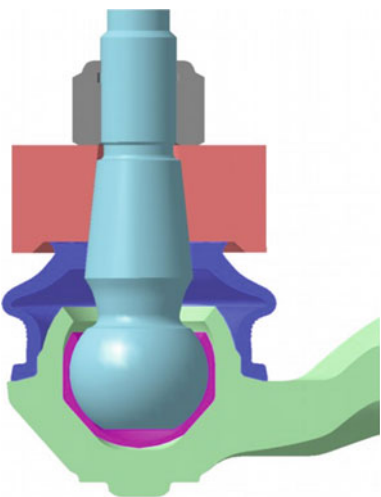
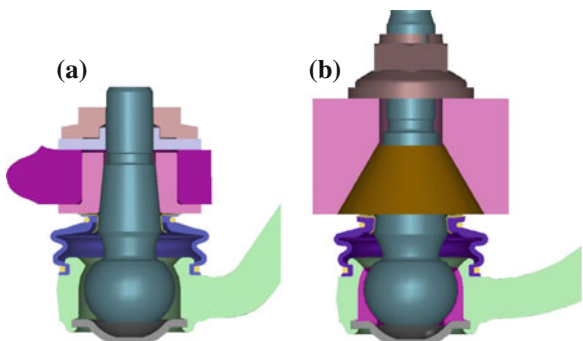


**Fig. 12.20** Screw connection of the outer joint with a lightweight wheel carrier.

Source ZF Lemförder GmbH

- a** Pressed socket,
- b** Taper connection



surface pressures and to transfer the dynamic operation loads. If the permissible surface pressure is exceeded, the screw connection loses its pretension, so that the screw may turn loose under dynamic stress.

Figure 12.19 shows a cone plug connection with a 1:10 cone for a steel-forged wheel carrier, while Fig. 12.20 shows solutions with pressed-in jacks and a level cone for a 1:1 cone for lightweight wheel carriers.

## 12.8 Lightweight Design

Lightweight chassis for passenger cars are marked by the reduction of the unsprung masses, applied in many parts.

This demand is also made to the tie rod, mostly at the outer joint. The housing of the outer joint offers the greatest potential.

**Fig. 12.21** Example of a lightweight tie rod. *Source ZF Lemförder GmbH*

Outer joint with aluminium forged housing



Aluminium forged alloys and suitable cast aluminium materials are in use. These materials feature the required high ductility and a very good resistance against corrosion. Hence, they need no additional coating.

The aluminium joint housing is designed durable, taking space and design regulations into account, by analogy with steel-forged housings. A direct comparison shows that lightweight materials require more space.

The example (Fig. 12.21) provides a weight reduction of approx. 30 %, compared with a steel implementation.

## 12.9 The Future

### 12.9.1 Overload Behaviour

Tie rods are quite cheap parts that can be exchanged by the service with little effort. Hence, the tie rod assumes in some cars a ‘sacrificial or safety function’. The buckling load of the tie rod is adapted to this function, so that the rather expensive parts, like gear and wheel carrier, are protected from damage by the buckling of the tie rod even during abusive driving. This is then the upper limit of the buckling load. The lower limit is determined by the forces applied in safe driving. A buckling force window is the result, inside of which the tie rod responds to an introduced load. The failure response with the sequence of failing parts (here: the tie rod fails before gear and wheel carrier) is also called a damage chain.

Not only compressive forces, but also tractive forces are transferred by the tie rod, hence, a buckling force window is not enough to protect the adjoining parts against overload if a manoeuvre is made under pull load (see Fig. 12.22).

Reliable overload protection needs to use a safety element. It is designed for an overload window of, say, 20–25 kN. If this load of the tie rod is achieved on-board (pull or push load), the safety element distorts in such a way that the tie rod is then permanently extended or shortened. The tie rod has to continue transferring steering forces when the safety element was activated, but it will do so with more free travel/changed length. The steering clearance/length modification is selected so that the driver will note the fault and visit a car service.

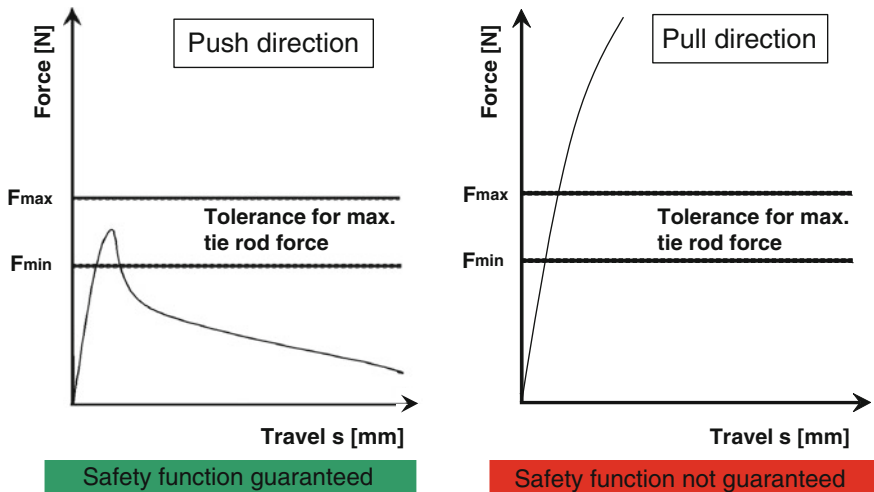


**Fig. 12.22** Buckling/pull load diagram. *Source ZF Lemförder GmbH*

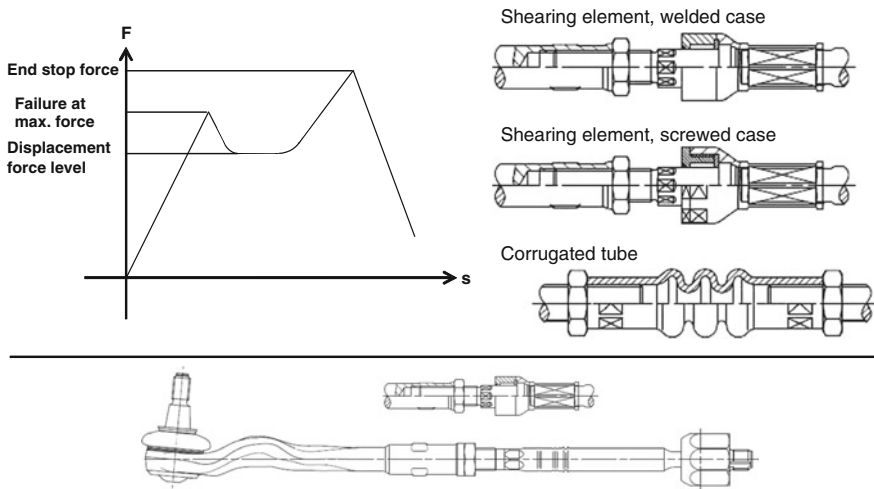


**Fig. 12.23** Function of the safety element and examples of different safety elements. *Source ZF Lemförder GmbH*

This progress towards the classical buckling force window safely protects the complicated systems gear and wheel carrier against overloads in push or pull direction.

The functionality of the safety element is shown in the diagram in Fig. 12.23 (ZF Patent 1991).

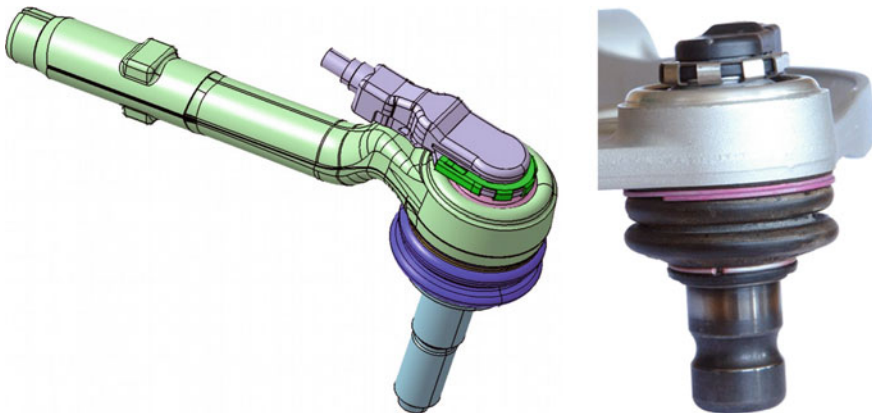


**Fig. 12.24** ZF LSM—sensor ZF Lemförder module. *Source* ZF Lemförder GmbH

### 12.9.2 Sensor Joint

A sensor located in the ball joint can record any movement of the joints (e.g., the tilting angle). This data helps to deduce the driving and vehicle condition, as, for example, the ride-height of the car or the deceleration velocity of the wheel. This data is required, e.g., for headlamp levelling, for the ride-height situation of air suspensions or for regulated dampers.

Different sensors are in use, some of which have to be integrated on-board by expensive belt leverages. Including all required mountings, this structure is rather heavy, consuming space and producing more inaccuracies in the signal chain. The actual sensors of modern solutions, e.g., for ride-height sensors, have a lower signal quality, due to the tolerance ranges of the mechanical auxiliary leverages and of their assembly, for example. Integrated joints avoid these additional inaccuracies.

Integrated joints entail a more compact and much lighter implementation, and the quality of the signal is better, saving up to 1.0 kg of weight in comparison to current sensors. The implementation shown below has an unchanged sealing and support system of the joint. The outside sensor records the force line of a magnet in the joint, using a non-magnetic cover. The magnet is integrated into the front side of the ball stud, unused for the joint function, and does not require any additional space.

Figure 12.24 shows examples of the ZF Lemförder sensor module.

## References

- BMFT (1981) Tribologie und Verschleiß  
 Guy A (1976) Oberflächenverfahren. University Florida—Korrosionsmechanismen

- Heißing B, Ersoy M (2007) Fahrwerkhandbuch, 201
- Landgrebe D, Hirschvogel M, Kettner P, Pischel W, Dahme M, Wondrak J, Nägele H (2001) Bibliothek der Technik Bd. 213, Massivumformtechniken für die Fahrzeugindustrie
- Menges G, Aachen TH (1970) Werkstoffkunde. Kunststoffe 15:88
- Runge W, Gaedke A, Heger M, Vähning A, Reuss HC (2009) Elektrisch lenken—Notwendige Effizienzsteigerungen im Oberklassensegment, ATZ 10/2009
- Stoll H (1992) Fahrwerktechnik, Lenkanlagen und Hilfskraftlenkungen
- Vieregge K, Adlof W (1994) Schmiedeteile: Gestaltung, Anwendung, Beispiele
- ZF Patent (1991): DE 39 15 991 C2

# Chapter 13

## Hydraulic Power Supply

Dieter Semmel

### 13.1 Servo Pumps

#### 13.1.1 Introduction

Hydraulically supported steering systems have been a standard of the car industry for many years, being state-of-the-art even in compact cars. The open centre steering system with a volumetric flow-controlled vane-type pump has prevailed against other possible steering systems, essentially because of its price. This steering system is questioned, though, by the very heated debate about energy conservation. Power-saving hydraulic systems are advancing, hence, because the power dissipation of a limited vane cell can no longer be neglected. These systems will be discussed in the following.

#### 13.1.2 Vane-Type Pump

This kind of power-assist pumps is the classical, most common type of pump (Fig. 13.1).

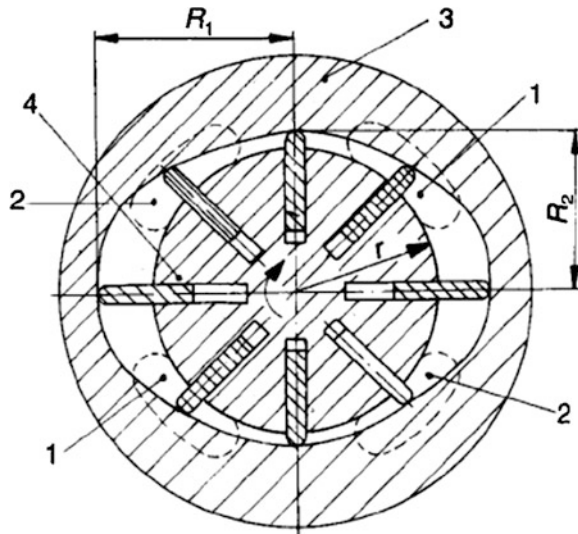
The function group of the pump basically consists of a rotor (4) with inserted movable wings and a cam ring (3). The rotor is turning in the cam ring, the wings are touching it due to the centrifugal forces in the slotted rotor. Separate chambers develop, whose volume changes when sliding along the cam ring. The oil volume sucked into any chamber is compressed when the chamber shrinks, and it is pressed out. A constant vane-type pump is designed for two strokes. The

---

D. Semmel (✉)

Dr. Ing. h.c. F. Porsche AG, Porscheplatz 1 70435 Stuttgart, Germany  
e-mail: dieter.semmler@steeringhandbook.org

**Fig. 13.1** Arrangement of a two-stroke vane-type pump



compressive forces developing in the rotor are compensated by the symmetrical arrangement of two inlet (1) and outlet kidneys (2), the bearing load remains low.

The transported volumetric flow rises proportionally to the pump rev. The characteristic curve of the volumetric flow of an on-board vane-type pump is usually descending. A dropping characteristic curve helps to lower the power-assist for high speeds (and, hence, a high pump rev). The volumetric flow is controlled by the limitation valve, shown in Fig. 13.2. The volumetric flow control is based on the principle that more flow through the throttle generates a more pronounced pressure drop at the throttle. The pin (4) follows the piston (1), moving with the pressure difference, because of the pretension of the spring (5). The flow cross section in the drilling of the sleeve (3) changes, this affects in turn the pressure difference and, hence, the size of the backflow cross section, released by the piston (1).

A typical dropping characteristic curve of a volumetric current is shown in Fig. 13.3. The position of the limiting point is clearly recognisable here.

The aim is to drive the pump at the limiting point across the whole rev range. This way, a steady power-assist level is maintained. Providing the highest volumetric flow is very important for the parking mode (low rev, low speed, high demand for steering activity).

The indicator for quality and efficiency of a vane-type pump is the volumetric efficiency, plotted in a characteristic curve of the volumetric flow over pressure for a specific operation point. An ideal pump would keep the volumetric flow constant for the whole pressure range, meaning that the gap losses in the pump would remain steady with rising pressure. Unfortunately, pump characteristics of that kind cannot be implemented, because the gap losses are rising with pressure, in

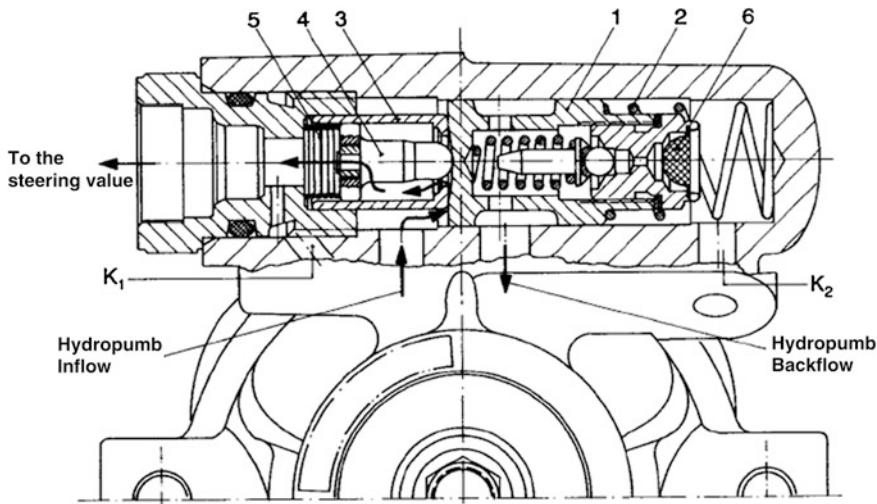


**Fig. 13.2** Limitation valve

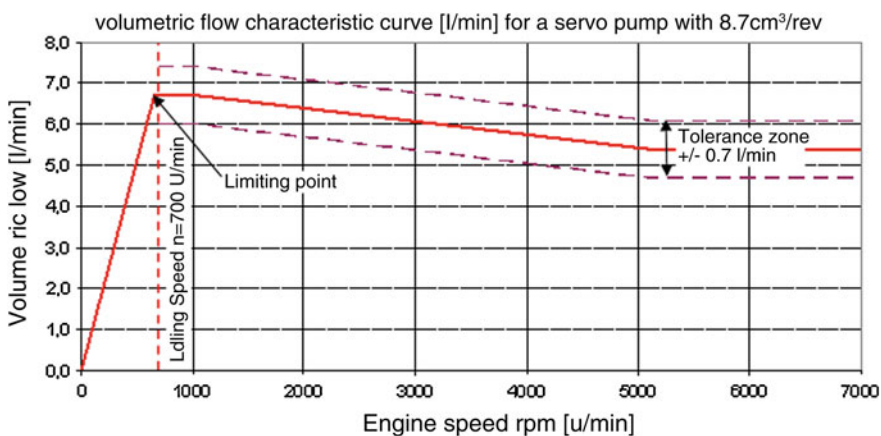


**Fig. 13.3** Volumetric flow characteristic curve of a limited vane-type pump

spite of pressure compensation in the pump. The characteristic curve in Fig. 13.4 shows a standardised curve of the permissible drop of the volumetric flow over the pressure range, representing an upper permissible limit curve. The size of the pump is considered in this depiction, too, because the volumetric flow is normalised to the geometrical flow volume.

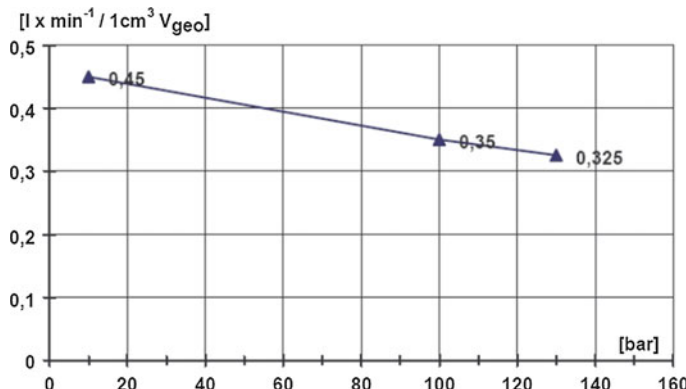


**Fig. 13.4** Limiting characteristic curve of the volumetric flow over pressure of a vane-type pump

### 13.1.2.1 Vane-Type Pumps with Bypass Valve for Energy Conservation

These pump models are sold by various manufacturers, using brand names like ECO, EV<sub>2</sub> (Fig. 13.5) or KEEPS.

The principle of these pumps is to reduce the energy consumption by lowering the circulation pressure in the steering system when the steering is passive, e.g., when driving straight. In an open centre steering, the circulation pressure arises from the permanent transport of the oil volume through the system. It can be controlled either by the pressure losses of the oil-carrying parts or by the present volumetric flow.

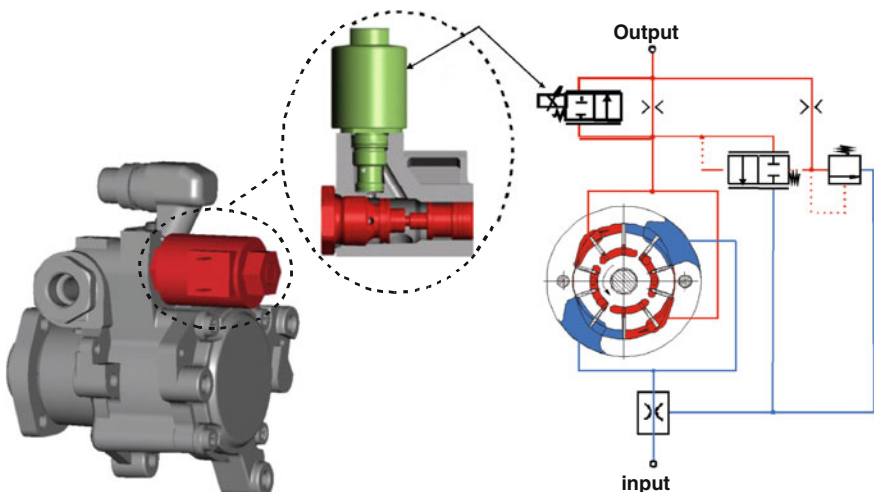


**Fig. 13.5** Arrangement of the steering pump with bypass valve (EV<sub>2</sub>) (IXETIC)

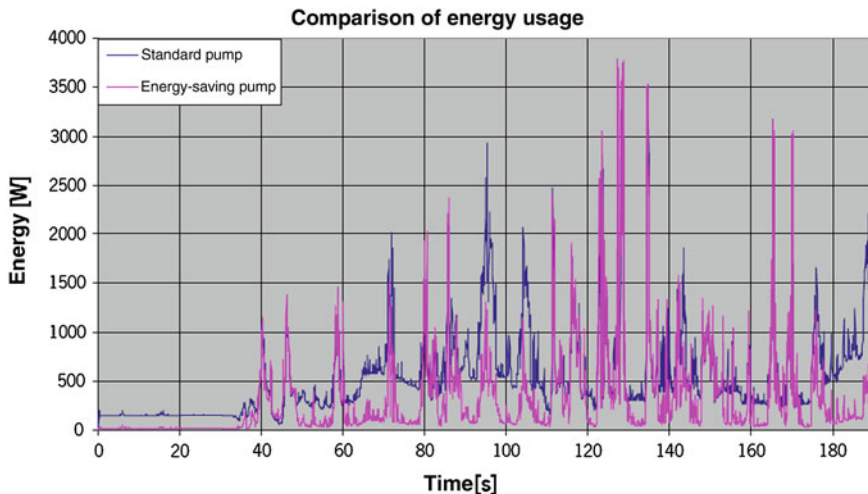


**Fig. 13.6** Comparison of the energy consumption of conventional vane-type pumps and with pumps with bypass valve

The circulating volumetric flow of this pump model is significantly lowered when a suitable bypass valve is used, so that the circulation pressure in the system drops. The limited volumetric flow and the used volumetric flow are transported in this pump against the present circulation pressure, hence, a considerable amount of energy is saved for high engine/pump speeds and low steering activity (e.g., straight driving on the highway).

Figure 13.6 shows the energy conservation potential in a driving cycle. The volumetric flow can be lowered only by a certain amount, according to the driven speed, so that no driving dynamics are lost. The actual energy conservation potential per manoeuvre is therefore quite low. Figure 13.6 also shows very clearly the reduced circulation pressure in the initial area without steering activity.

### 13.1.2.2 Variable Pump

Variable vane-type pumps are an advancement of the classical vane-type pump. The pump is able to generate only as much volumetric flow as is required for the steering system, due to the function of the variable pump capacity. The interior circulation of a volumetric flow in the limited area of a conventional vane-type pump is thereby avoided. Variable pumps are single-stroke vane-type pumps. The pump chambers are divided into suction and pressure chamber by an eccentric deviation of the cam ring, by means of a pressure balance. The deviation is designed according to demand, so that only the actually required oil volume is transported. When the idling speed operating point is reached, the variable pump transports a constant volumetric flow. A rising pump rev leads to an increasing

pump pressure which in turn leads to a pressure increase in the cam ring via the governing valve, reducing the eccentricity. The geometrical pump capacity decreases and overproduction of pressurised oil is prevented. A drop of the pump rev and a descending pressure gradient produce in turn a higher deviation of the cam ring, the geometrical pump capacity rises again.

The power input of a vane-type pump is approximated as follows:

$$P = V_{geom} \cdot n \cdot p \cdot 1.67 \times 10^{-3} [\text{W}] \quad (13.1)$$

$V_{geom}$  Geometrical pump capacity [ $\text{cm}^3/\text{U}$ ]

$n$  Pump rev [rpm]

$p$  Pressure [bar]

1.67 Unit correction value

In a conventional vane-type pump, the limited volumetric flow is preloaded on the pressure in the system, too. Very high power dissipations at high pump revs and system pressures are the result. The power input of a vane cell with  $12 \text{ cm}^3/\text{rev}$ , for example, may be 1,002 W for a circulation pressure of 10 bar and a pump rev of 5,000 rpm. These values correspond to straight driving on the highway without steering activity, the generated energy loss of 1 kW is converted into heat, which has to be removed via the steering engine oil cooler. The use of energy saving pumps is therefore an important help to reduce power dissipations, and the variable pump provides the highest potential savings (Figs. 13.7, 13.8, 13.9).

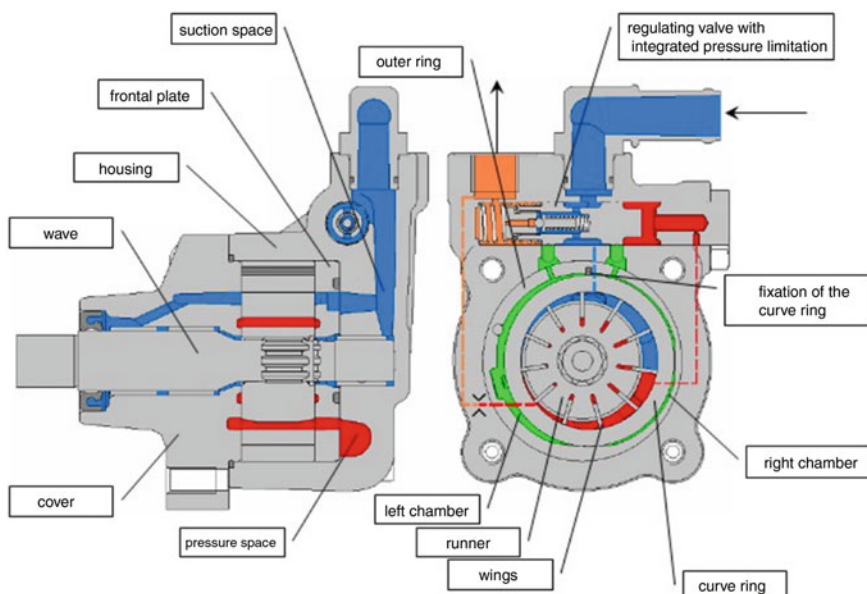
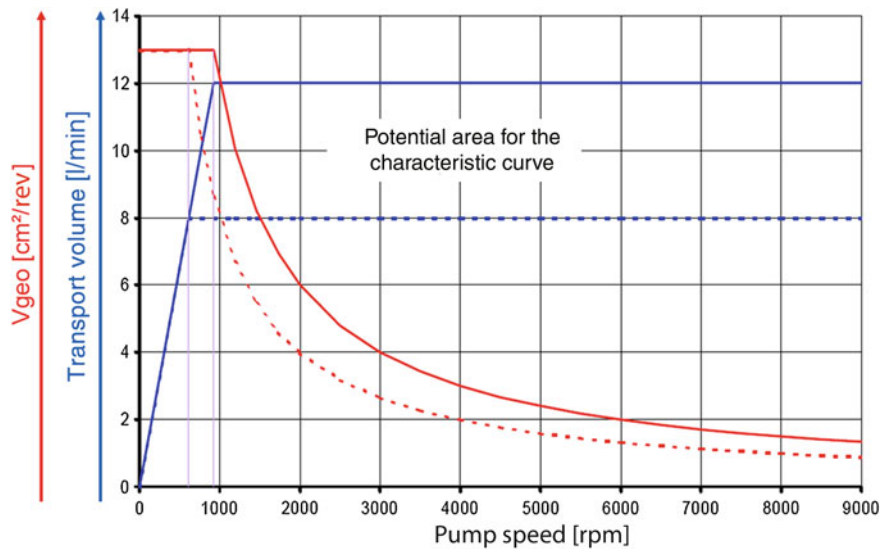
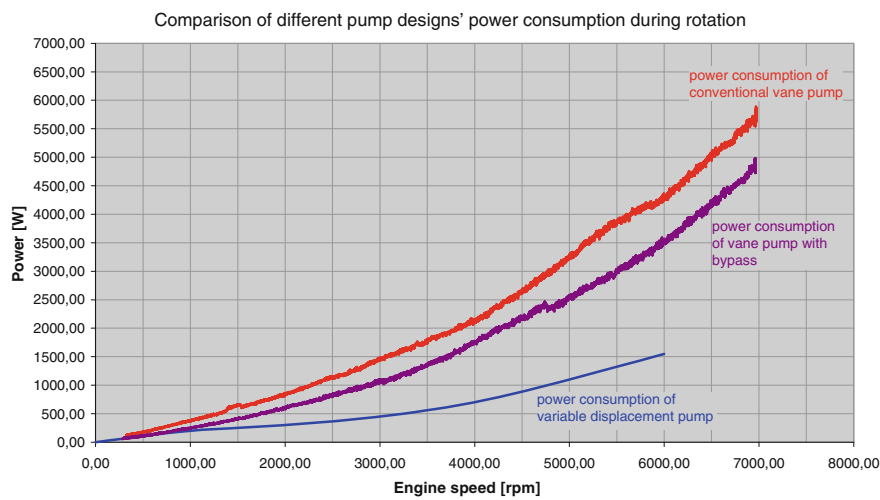


Fig. 13.7 Cutaway view of a variable pump. Source ZF Lenksysteme



**Fig. 13.8** Characteristic curve of the geometrical pump capacity and the volumetric flow over the variable pump speed



**Fig. 13.9** Comparison of the pump designs of a vane cell

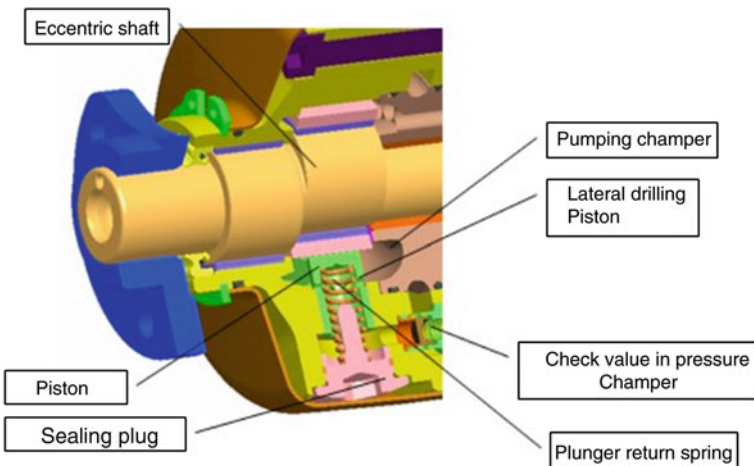


**Fig. 13.10** Detail, pump element of a radial piston pump

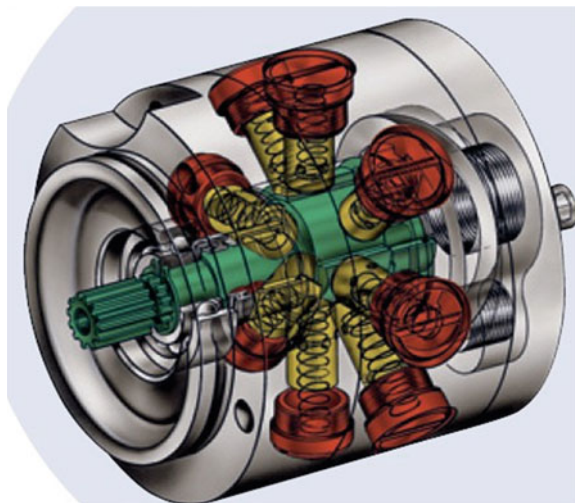
### 13.1.3 Radial Piston Pump

The radial piston pump consists of individual pump elements which are driven by a common eccentric shaft. The cylinder spaces are filled with oil through lateral drillings in the piston which connect to the oil-filled pumping chamber. In the transport stroke, these lateral drillings are closed at the lower edge of the respective cylinder, so that pressure builds up during the further stroke movement.

The benefit of this principle is internal suction control, i.e. the transported volumetric flow remains fairly constant across the whole pump rev range. This suction control results from the fact that higher pump rev reduces the time to fill the cylinder spaces. This reduction prevents complete filling of the space, the transport volume per pump stroke drops with increasing speed. On the other hand, the transported volumetric flow remains constant for the entire pump rev range. Therefore, in contrast to a limited vane cell, this type of pump requires no volumetric flow limitation; any losses from limitation are hence avoided. The radial piston pump can even be operated at very high pressure (200 bar), so that a broader application range is covered than with a vane-type pump (Fig. 13.10).

The disadvantage of a radial piston pump is its high price, due to complex manufacturing. Furthermore, the much inferior acoustics in comparison to the vane-type pump are noticeable. This is a flaw of the design, primarily resulting from fluctuating pressure as a result of the much lower number of pistons (commonly 7–8 pistons, according to pump size). A comparable vane-type pump with similar geometrical pump capacity has at least 11 wings, accordingly producing 11 displacement compressor chambers (Fig. 13.11).

**Fig. 13.11** Construction of a radial piston pump. *Source* ZF Lenksysteme



### 13.1.4 Tandem Pump

The tandem pump is a combination of vane cell and piston pump, providing an independent supply of two different hydraulic cycles (e.g., power steering and rolling stabilisation system) whose constraints with regard to system pressure may differ. Most rolling stabilisation systems are high-pressure systems with pressures of approx. 180 bar, but a vane-type pump cannot operate these economically. The vane-type pump is sufficient for the steering, though, as the highest accessible system pressures of a vane-type pump are approx. 150 bar. A combination of both pump types on one shaft yields the following benefits:

- less construction space by common use of the central plate of both pump types
- only one drive required in the auxiliary driveline of the engine
- less weight (Fig. 13.12).

## 13.2 Oil Supply and Oils

### 13.2.1 Oil Tank

Vehicles with hydraulic power-assistance need a servo oil tank to maintain a clean oil reserve in the steering system, compensating the volume and degassing and calming the medium. Filling the system is more difficult without a tank, too. Other functions of the servo oil tank are filtration, cooling and maintaining the supply of the steering system for any possibly applicable acceleration of the car.

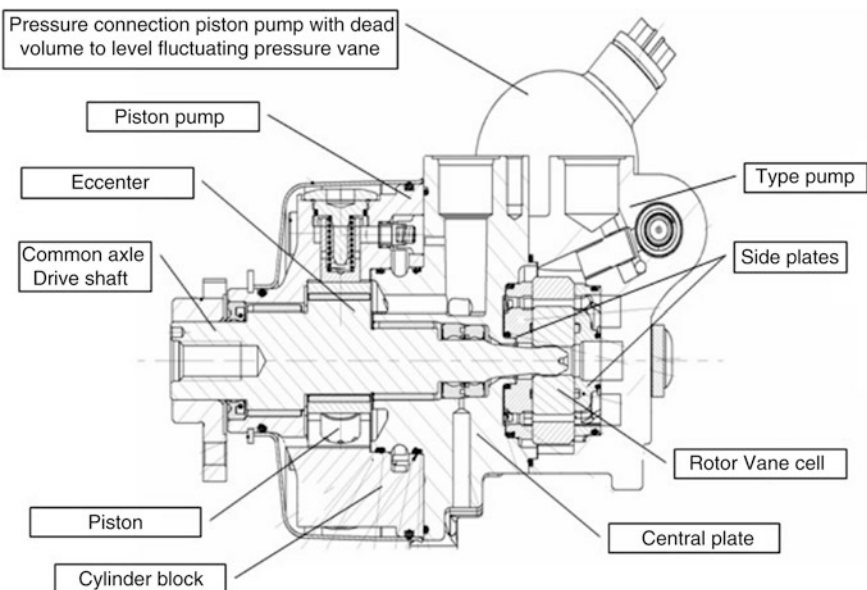


**Fig. 13.12** Cutaway view of a tandem pump (IXETIC)

### 13.2.1.1 Types

Servo oil tanks are now mainly made of plastic (PA), welded as die-cast parts or blow-moulded. These production methods have prevailed because of price and design. A filter element can be easily and safely integrated into the two-part construction (Fig. 13.13).

Servo oil tanks are classified as either pump-mounted or body-mounted configurations. The benefit of pump-mounted configurations is their short inlet pipe into the pump which is ideal designwise to avoid cavitation in the pump. The mounting of the servo oil tank to the pump is a disadvantage of this configuration, because it has to be shaped in such a way that HF aggregate vibrations do not produce ruptures in the tank. Pump-mounted servo oil tanks are also exposed to higher temperatures than body-mounted tanks, due to the proximity of the pump to the exhaust manifold.

### 13.2.1.2 Filling and Ventilation

Current series production steering systems are filled by vacuum filling. First, a filling quill is placed on the tank opening to generate a vacuum. This vacuum is maintained for some time to detect any potential leakage. If the values are within the defined range, the system is filled with pressure through the quill and leveled to

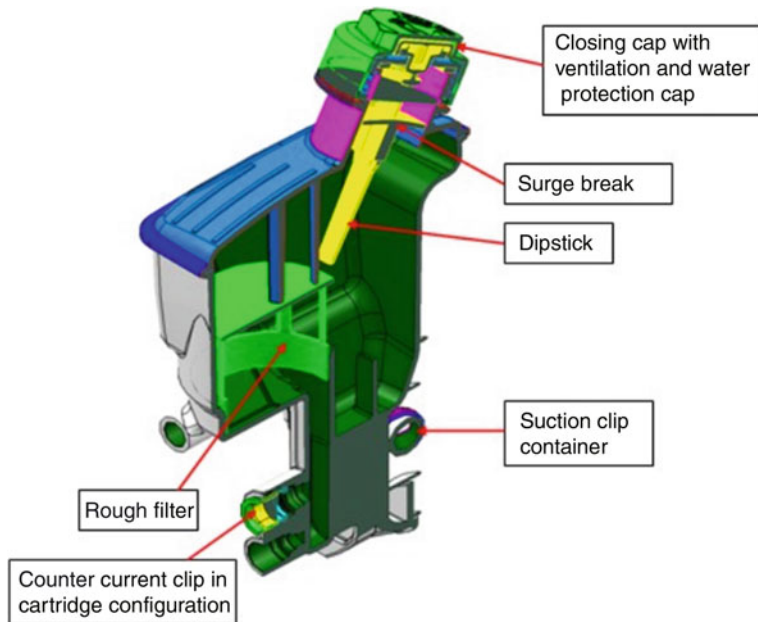
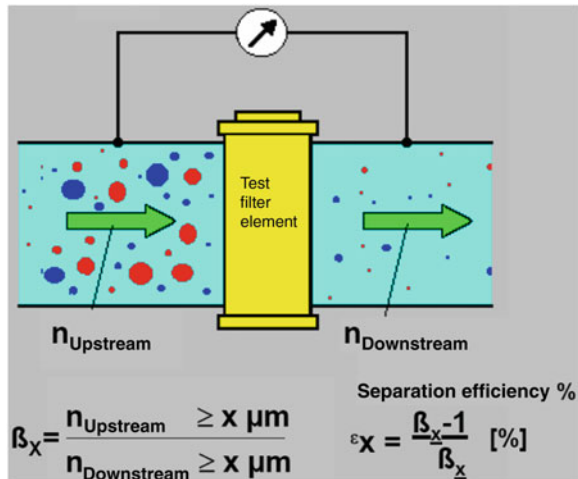


**Fig. 13.13** Construction of a pump-mounted servo oil tank

**Fig. 13.14** Connection of separation efficiency and  $\beta$  value (HYDAC)



maximum at the same time. Easy filling and subsequent ventilation of the system in a garage are enabled by operating the steering end-stop-to-end-stop while the engine is running. Steering systems can be ventilated in this manner very well. Then the level in the tank is checked.

### 13.2.1.3 Filtration

The filter configuration of power-assisted steering systems is always arranged as a runback filter in the tank. A coarse non-woven filtration with a mesh size of  $100 \mu\text{m}$  is sufficient for steering systems without servotronics (speed-sensitive change of the steering torque).

A fine filtration with a mesh of at least  $15 \mu\text{m}$  is absolutely necessary for servotronics steering systems. The design of these fine filters has to consider not only the mesh size but also the filter surface. These filters are also usually equipped with a bypass to prevent the filter element from bursting when the filter is polluted. The following features are observed when:

- original pollution in the system
- pressure loss of the cartridge, new and saturated
- pollution entering during service life.

### 13.2.1.4 Separation Efficiency

The separation efficiency  $\beta_x$  of a filter measures particle sizes and amounts which the filter is able to filter out. The  $\beta_x$  value indicates the capability of the filter element to separate particles of a specific size. Typical data for a hydraulic system are, e.g.,  $\beta_{12} > 200$ . The  $\beta$  value is higher than 200, according to the curve shown in Fig. 13.15, an almost complete separation is therefore possible. The index 12 means that all particles  $>12 \mu\text{m}$  are reliably filtered out. Figure 13.14 illustrates the connection between  $\beta$  value and separation efficiency of a filter element.

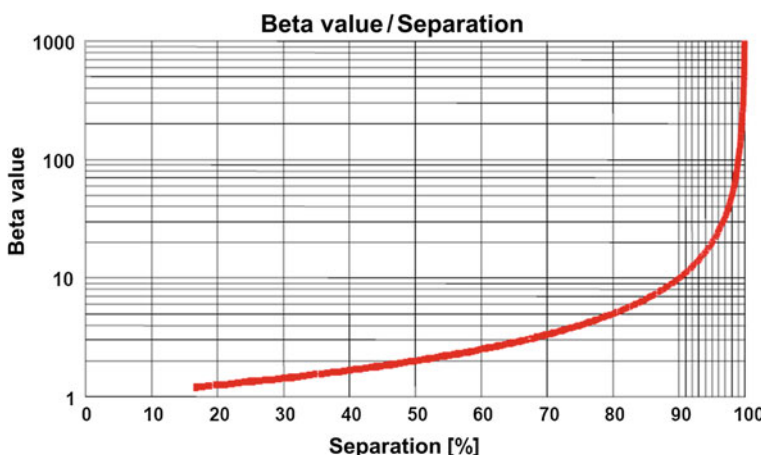


Fig. 13.15 Design of a filter element (HYDAC)

### 13.2.1.5 System Purity

Purity is very important for the safe function of a hydraulic system. System purity distinguishes between original dirt and impurity from the operation of the system. The purity of the single parts which enables safe functioning of the system is defined by the following parameters:

- whole amount of pollution in the respective component, in mg/oil-covered surface
- highest permissible particle sizes, 2D, in  $\mu\text{m} \times \mu\text{m}$
- defined special particles, inevitably resulting from the chosen manufacturing process, the defined amount does not impair the function of the system.

Typical purity data for hydraulic lines are:

- highest particle load: 1.5 mg per metre of line
- greatest particle size:  $200 \times 90 \mu\text{m}$
- exceptions: Number of special particles per metre of line length:
- not more than 25 hard particles  $<500 \times 200 \mu\text{m}$
- not more than 25 soft particles  $<2,000 \times 90 \mu\text{m}$  permissible
- no abrasive particles

#### *Testing methods to identify the system purity*

Basically, the method for a purity test of hydraulic parts has to be qualified to be compliant with VDA19/ISO 16232, i.e.

1. Blind value measurement
2. Decay curve with 10 % or other criterion
3. Double test

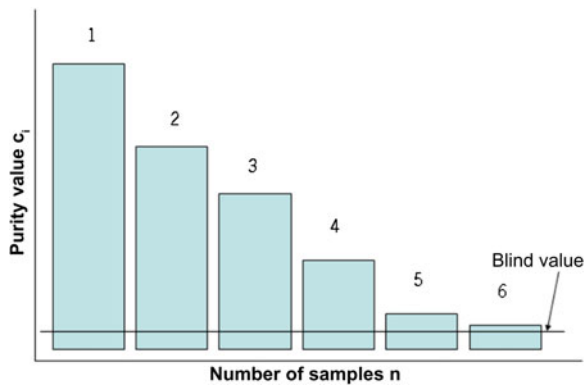
Concerning flushing time, preliminary treatment and flushing amount, the parameters are set so that the criteria for the decay curve are met. If the measured values deviate from the set points defined in the standards, then the test method is reevaluated. This qualification needs to be carried out before the first test. It is run in the defined scope at a sample component (or two of them, for a double test). The purpose of the qualification check is to ascertain the suitability of the used extraction process. Most extraction processes are indirect methods and aim at grasping as much of the particle pollution on the component as possible.

There is in principle no absolute way to determine the actually present particle load. Therefore, decay measures that should maintain the suitability criterion according to Fig. 13.16 are performed. Repeatedly checking the same part should identify a decrease of the particle pollution. The criterion for the suitability of an extraction process is the decay criterion, see Fig. 13.16.

Decay criterion:

$$c_n \leq 0.1 \times \sum c_i (n \leq 6)$$

**Fig. 13.16** Check of the decay criterion and the blind value



A sufficient decaying response to the extraction of pollution is present if after up to six subsequent checks of the same part, the final measured value is not higher than 10 % of the total of the measured values.

### 13.2.1.6 Design Under Lateral Acceleration

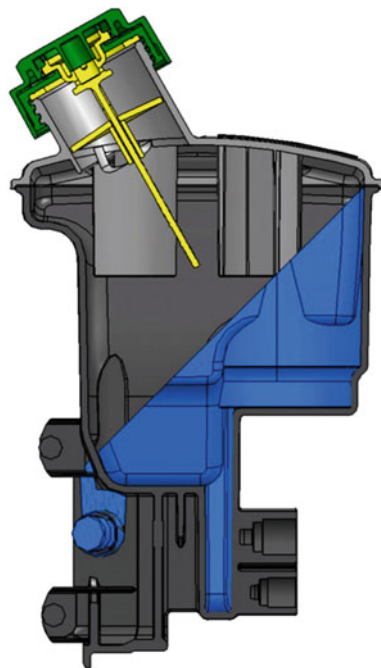
Manoeuvres that involve extreme lateral or longitudinal acceleration are critical for the design of the tank. One needs to ensure that the intake of air during such manoeuvres is avoided under any circumstances and that any escape of oil from the tank is safely prevented.

To do so, one makes a cross section of the tank at the slant of the present acceleration and at the level of the oil volume. It needs to be ensured that the suction neck is sufficiently covered, i.e. is under the oil level. The filling volume thus determined is the ‘min’ filling of the container. This is a purely theoretical design, hence, a sufficient safety distance for any sloshing in the car needs to be kept. If there is not enough safety distance, the tank needs to be enlarged or redesigned by clever integration of ribs in such a way that the suction neck is at any time sufficiently covered at any time. Finally, the theoretical design is confirmed on a centrifuge test bench before starting the system on-board (Fig. 13.17).

### 13.2.2 Steering Hoses and Tubes

Conduits in the steering system are essentially classified as high and low pressure conduits, applying both rigid tubes and flexible hoses. The high-pressure conduits connect the pump pressure output and the steering valve in the gear, low-pressure conduits are arranged in the complete runback system of steering valve–radiator–tank.

**Fig. 13.17** Liquid level in the tank at strongest braking



The following issues are observed when:

- avoid any pressure losses by sufficiently sizing the cross sections of the tubing
- sufficient acoustic decoupling of the overall system
- safe squeezing of the hose integration
- sealing of the overall system for the full service life.

### **13.2.2.1 High-Pressure Duct Including Screw Connection (Hose Types and Construction)**

It is of utmost interest that the stretch tube may serve in high-pressure conduits as an acoustic decoupling element. This is basically achieved by the design of the hose. A 10 % increase of volume should be achieved at peak pressure. How the tissue of the pressure carrier is made has an essential influence on the stretching response of the hose. Polyamides or aramide fibres are used most of the time. The thread angle influences the stretch response of the hose as well. Figure 13.18 shows a typical hose design.

Resonators or tuners are also used in stretch tubes. They are PTFE tubes with an inner diameter of approx. 6 mm and additional lateral drilling holes. The length of

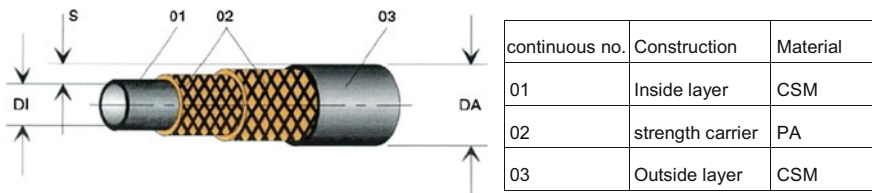


**Fig. 13.18** Hose construction of a stretch tube

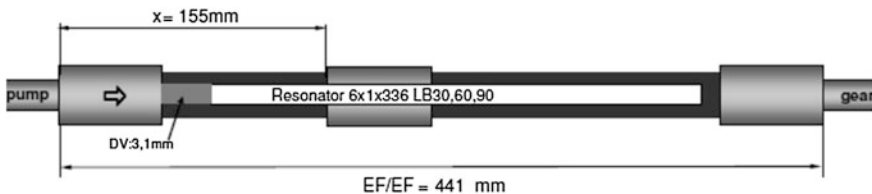


**Fig. 13.19** Resonator in the stretch tube

the tuner and the number of the lateral drilling holes are the main acoustic tuning parameters in the steering system (Fig. 13.19).

### 13.2.2.2 Screw Connections Of High-Pressure Lines and Stretch tubes

Overview on the standard high-pressure screw connections (Fig. 13.20):

Classical hydraulic screw connection for high-pressure applications; high loss of pressure, low accuracy of the position during assembly (Fig. 13.21).

Pressure screw connection in steering hydraulics systems; resistant to pressure up to 150 bar, little loss of pressure, very sensitive against rupture from vibrations (Fig. 13.22).

**Fig. 13.20** Ring neck screw connection

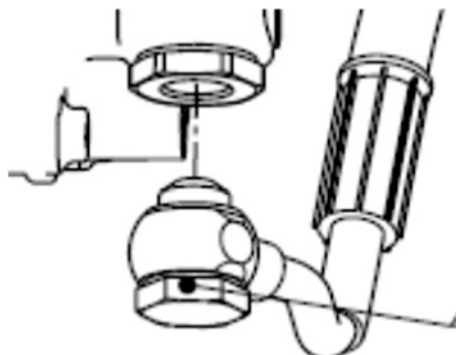


**Fig. 13.21** Saginaw screw connection

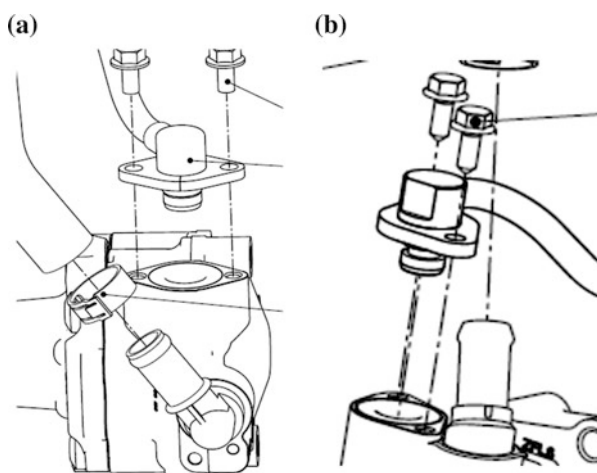


**Fig. 13.22 a and b** Flange screw connection

Universal screw connection for high-pressure applications with good accuracy of positioning, little loss of pressure, resistant to rupture from vibrations, needs much space.

### 13.2.2.3 Suction and Return Conduits

The suction and return conduits are low-pressure conduits. Accordingly, the hoses are much simpler than stretch tubes, the used elastomer can be less resistant to temperature than that of stretch tubes.

The return line from the gear to the servo oil cooler has acoustic significance as well. The purpose is to make the hose very soft, taking any possible cavitation effects from the steering system into account that may result from excitation at the tyres. Ideally, a small compensation volume which prevents cavitation from impacts at the tyres can be made available by proper design of the return line. Throttles that are effective against steering kickback are also used in the return line.

### 13.2.2.4 Acoustic Tuning/Noise Measures

A comparison of different stretch tube tunings at 80 bar follows (Fig. 13.23):

This representation shows very well how the acoustic behaviour of the hydraulic system can be influenced by a suitable choice of resonators, throttles and hose lengths. The purpose of any stretch tube tuning is to achieve the best possible damping for the least loss of pressure. Acoustic tuning targets mainly the low-speed range. This reflects situations like parking or driving at low speed, e.g., city traffic. Hydraulic noises are especially annoying here.



**Fig. 13.23** Pulsation curves of pump speeds and different secondary measures

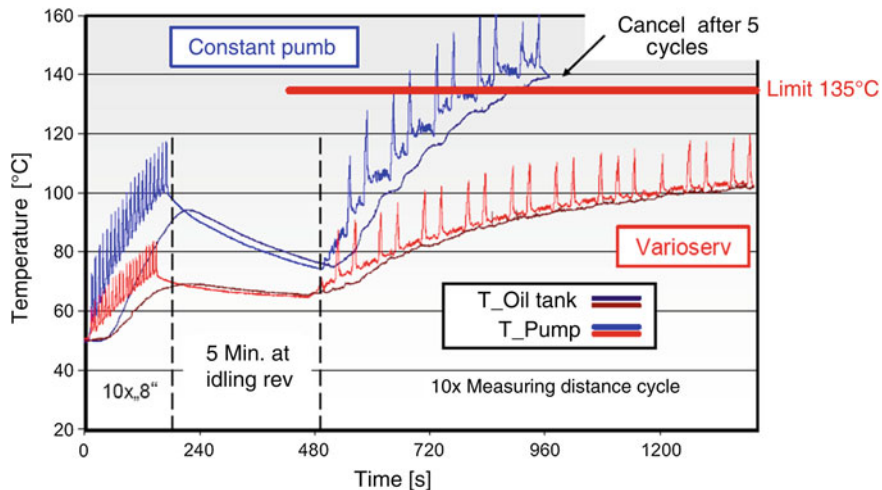


**Fig. 13.24** Temperature curve in the steering system, comparison of constant and variable pump

### 13.2.3 Cooling/Cooling Fronds/Cooler

The easiest kind of servo oil cooler is a simple cooling frond, integrated into the return line. This type of cooler is sufficient for steering systems with variable pumps or low steering power. Most vehicles with standard servo pumps and higher steering power already need a soldered cooler.

The most efficient form already need of cooling is an oil/water heat exchanger, because it also provides for a quick heating of the system at very low temperatures. There is no general rule for the need or size of a servo oil cooler, because this depends very strongly on purposes and constraints of the steering system. An important part of defining the size of a servo oil cooler is the notion that during a defined driving cycle that is passed several times, the temperature curve will be inert below the defined peak temperature. Figure 13.24 shows the influence of the used servo pump on the temperature response (Figs. 13.25, 13.26)

### 13.2.4 System Limits

The operational conditions of the car are vital for the hydraulic design of a steering system. A hard off-road passage with high steering forces and engine speeds is the worst case of operating conditions for vehicles in the SUV segment, especially since the vehicle has a very low cooling air flow, due to the low speed.

Driving manoeuvres on a round course are the worst case of operating conditions for sports cars. The vehicles are running at very high speed, the high cornering speeds are producing very high steering pressures. Impacts from

**Fig. 13.25** Soldered servo oil cooler

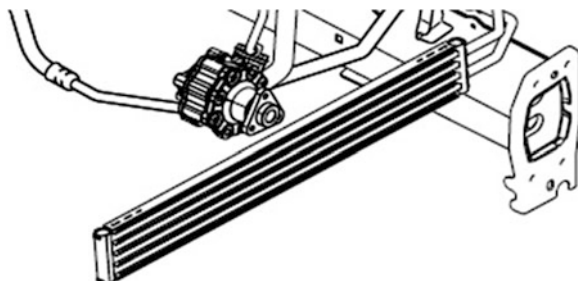


**Fig. 13.26** Oil/water heat exchanger



crossing ‘kerbs’ can even cause the steering system to switch to the pressure limitation for a short time, so that the hot pressurised oil in the pump is transported directly to the suction side. The steering system is even further heated up, if this lasts longer, failure from overheating may be the consequence.

A safe design of the steering system should never surpass a servo oil temperature of 120 °C during normal operation. Temperature peaks of 150 °C may occur for a short time, depending on the operation medium. Nevertheless, they should remain isolated events that should not add up to more than half an hour during the whole service life.

The system pressure of the steering is usually defined at an upper limit of 120 + 8 bar. This limit has also proved itself with regard to a suitable choice of stretch tubes, because the volume reception of pure high-pressure hoses is very limited.

### 13.2.5 Servo Oils

The preferred hydraulic oil used in steering systems is Pentosin. The earlier used oil ATF was almost completely replaced by Pentosin. The reason is Pentosin’s much higher stability with regard to temperature and viscosity across a very wide

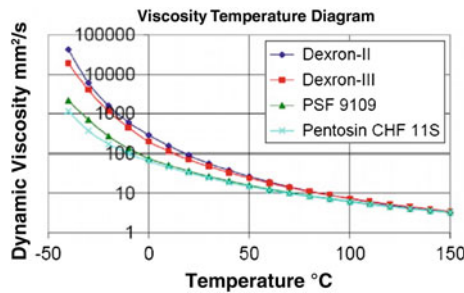


Fig. 13.27 Viscosity/temperature diagram for different servo oils

ISO-Code (nach ISO 4406)	Number of particles per 100ml	
	min	max
0	0,5	1
1	1	2
2	2	4
3	4	8
4	8	16
5	16	32
6	32	64
7	64	130
8	130	250
9	250	500
10	500	1000
11	1000	2000
12	2000	4000
13	4000	8000
14	8000	16000
15	16000	32000
16	32000	64000
17	64000	130000
18	130000	260000
19	260000	500000
20	500000	1000000
21	1000000	2000000
22	2000000	4000000
23	4000000	8000000
24	8000000	16000000
25	16000000	32000000
26	32000000	64000000
27	64000000	130000000
28	130000000	250000000

21 / 18 / 15 new  
 $>4\mu\text{m}$   $>6\mu\text{m}$   $>14\mu\text{m}$

21 / 18 / 15 old  
 $>2\mu\text{m}$   $>5\mu\text{m}$   $>15\mu\text{m}$

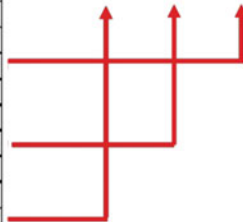


Fig. 13.28 Distinction of the purity classes

temperature range. The following curves compare different oils across the whole temperature spectrum. The advantage of Pentosin is most effective in the very low temperature area (Fig. 13.27).

Typical ranges of Application Beta-x>200		Filter delicacy x =	Recommended Oil purity classes								Pollution mass concentration	
			old purity class				new purity class				ISOMTD	Steel portion
- Stationary hydraulics	Drive closed cycle	NAS 1638	ISO 4406/91 2 5 15	ISO 4406/99 4 6 14	SAE AS 4059/01 4(A) 6(B) 14(C)						mg/l	mg/l
- Static hydraulics			3	- 12 9 15	12 9	5A 3B 3C					0,05	0,2
High-quality steering with servo-value cylinder		3	4	- 13 10 16	13 10	6A 4B 4C					0,1	0,35
Steering with servo-and proportional steering elements		5										
			5	- 14 11 17	14 11	7A 5B 5C					0,15	0,5
			6	- 15 12 18	15 12	8A 6B 6C					0,2	1
General mechanical engineering and static hydraulics with electrically operated valves	Hydrostatic cycle (T=90-115 °C)	10	7	- 16 13 19	16 13	9A 7B 7C					0,5	2
	Hydrostatic cycle (to Tmax = 90°C)	15	8	- 17 14 20	17 14	10A 8B 8C					1	4
Simple steerings with hand slide valves	Simple hydrostatic cycle	20	9	- 18 15 21	18 15	11A 9B 9C					3	10
			10	- 19 16 22	19 16	12A 10B 10C					5	18
			11	- 20 17 23	20 17	>12A 11B 11C					10	34
			12	- 21 18 24	21 18	>12A 12B 12C					20	68

Fig. 13.29 Recommended purity classes for hydraulic systems



Fig. 13.30 Accessible purity classes by way of supply of the hydraulic oil

### 13.2.5.1 Other Specifications

As discussed in the chapter ‘Filtration’, system purity is an essential criterion for the safe operation of a steering system. The basic purity of the used operation medium contributes essentially. The oil is divided into the following purity classes according to ISO (Fig. 13.28):

Figure 13.29 lists the current hydraulic systems, to facilitate the choice of the purity class required for safe operation of a hydraulic system with the recommended filtration. They shall serve only as a first indication, suitable tests have to ensure that the selected purity class is sufficient.

The basic purity of a hydraulic oil depends essentially on the way the oil is supplied. Barrel oil does not meet the requirements for a complicated hydraulic system with regard to its purity class. However, the purity class can be significantly raised by suitable filtration in the filling station. The classification of the purity class by kind of supply, shown in Fig. 13.30, is important for appraisal by the customer service, because different ways of supply are quite common here. A note on suitable filtration needs to be included in the customer service instructions.

# Chapter 14

## Electrically Powered Hydraulic Steering

Jochen Gessat, Alois Seewald and Dirk Zimmermann

### 14.1 Introduction

Electrically powered hydraulic steering was developed in the early 1990s from the demand for power-saving steering systems which can be controlled independently from the internal combustion engine. The capabilities of these systems has been successively expanded.

#### 14.1.1 Configuration and Functional Principle

Electrically powered hydraulic steering consists of a motor pump unit (MPU) which can be modularly combined with a steering gear, see Fig. 14.1. Other than the arrangement shown, a configuration can be chosen in which the MPU is directly mounted on the steering gear. This leads to a filled and tested compact system which has no more hydraulic interfaces during vehicle assembly. The steering gear is a standard hydraulic steering gear whose valve was adapted to the (lesser) volumetric flow of the MPU by an altered geometry of the valve control edge.

The MPU has a hydraulic part with external gear pump, hydraulic resonator and check/pressure relief valve, as well as an electric motor with ECU. It is screwed to

---

J. Gessat (✉) · A. Seewald · D. Zimmermann  
TRW Automotive, Livonia, MI, USA  
e-mail: jochen.gessat@steeringhandbook.org

A. Seewald  
e-mail: alois.seewald@steeringhandbook.org

D. Zimmermann  
e-mail: dirk.zimmermann@steeringhandbook.org

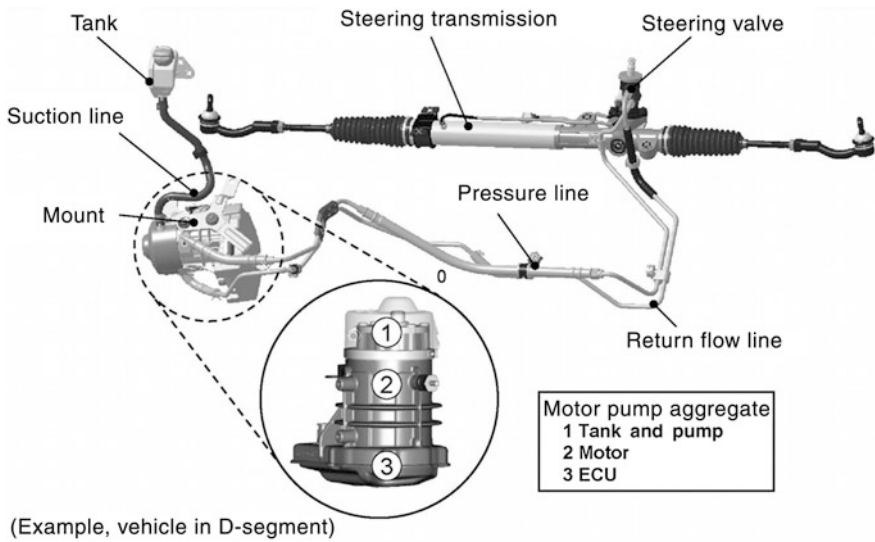


**Fig. 14.1** Electrically powered hydraulic steering (Source Fa TRW, D segment vehicle)

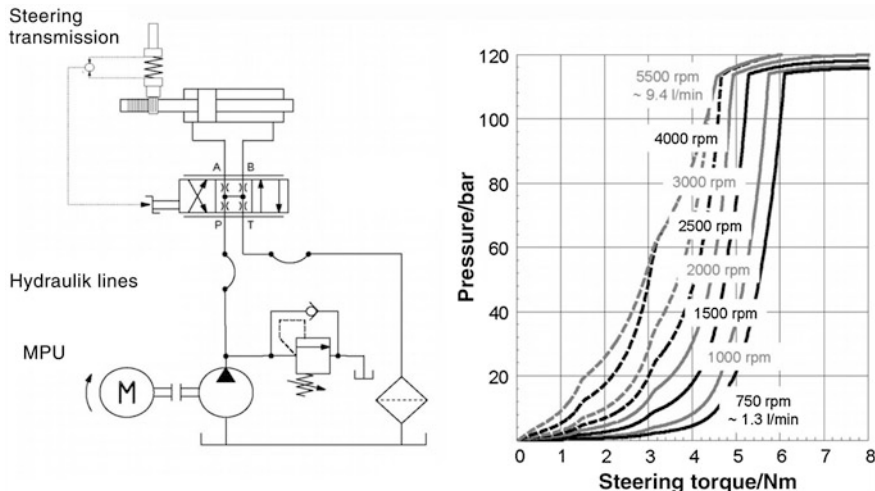


**Fig. 14.2** Hydraulic diagram and valve curves

the vehicle or to the steering gear, by means of brackets adapted to the application. The hydraulic connection to the steering gear is established by hoses.

Figure 14.2 shows the hydraulic diagram to illustrate the functional principle. The MPU is driven with the input parameters vehicle speed and steering wheel rate, providing the system's volumetric flow. If there is no steering wheel angle

sensor, the load is reported back to the MPU as a pressure converted into interior electric levels to control the rev.

The motor pump unit additionally contains the tank with an optional return line filter, the pressure relief valve (PRV) and the check valve. The PRV limits the peak system pressure and protects other parts against overload (e.g., hoses). It also limits the load torque of the engine and prevents stalling. The check valve is open when the steering is switched off, providing ventilation of the system. During service, when the steering is switched off and the vehicle is jacked up, the rack can be easily shifted, without any hydraulic pressure building up. In the fault case of a blocked pump, it provides for easier steering of the system, because the pump is circumvented. The hydraulic pipe system contains pipes and hoses on both the high- and the low-pressure side, to transmit energy and to improve the steering equipment acoustics. The steering gear consists of the steering cylinder and a 4/3 port directional control valve in rotary disk configuration with an open centre (open centre valve). When free of load, the flow is passing the valve with very little resistance. If the rack is loaded, a torsion spring (torsion bar) is twisted by the driver's steering torque. This generates a proportional torsion angle, shifting the valve, so that a pressure difference builds up which is keeping the load in balance. The torsion and, hence, the steering wheel torque depend on the valve's volumetric flow and also on the volumetric flow of the motor pump unit (see also chapter 'Hydraulic power steering'). If the volumetric flow rises, a lower torsion angle (less torque) will be sufficient to generate the same pressure difference in the steering cylinder that would apply when the volumetric flow was smaller. This effect is used to directly influence the steering feel as a function of vehicle speed.

Figure 14.2 shows (on the right) the course of the valve curve if the steering rack is not moving (5 l/min EPHS valve) for different nominal MPU volumetric flows (nominal revs). The disruption of the valve curve towards higher torques, seen here for higher revs ( $>4,000$  1/min) and pressures above 60 bar, is based on the volumetric flow/pressure characteristic curve of the motor pump unit, because the volumetric flow drops at higher pressure, cf. also Fig. 14.5 left (MPU characteristic curve). In this situation the unit does not achieve the defined nominal rev any more.

### 14.1.2 Steering System Classification

Electrically powered hydraulic steering is a semi-active electric steering that has a solid connection between steering wheel angle and tyre steer-angle. The assist torque is variable and determined by means of a steering diagram.

Though the auxiliary torque can be parameterized, as opposed to electromechanical steering systems, the direction is not reversible. This enables several comfort and energy functions, but no special torque functions like active tracking or automatic parking, because the electrical drive has no direct kinematic tie to the gear. Nevertheless, the decoupling has the benefit that the system needs less expenditure with regard to functional safety. Besides, the steering feel is not affected by the qualities of the electric motor (e.g., mass moment of inertia).

**Table 14.1** Steering systems and functions

		HPS conventional	EPHS	EPS
Steering system classification		Passive	Semi active	Semi active
Steering wheel angle—tyre steer-angle		Solid	Solid	Solid
Steering wheel torque—assist torque		Solid	Variable	Variable
In the direction of assist torque		Unidirectional	Unidirectional	Bidirectional
Energy consumption and CO <sub>2</sub>	Meeting demand and high efficiency	–	X	X
	Stop/start compatibility	–	X	X
	HEV, eV, compatibility FCV	–	X	X
Safety	Steering intervention and ESP ( $\mu$ -split, oversteer)	–	–	X
	Lane departure warning	(X)	(X)	(X)
	Lane keeping assistant	–	–	(X)
Comfort	Speed-sensitive power assist	–	X	X
	Controlled parking	(X)	(X)	(X)
	(Semi-)automatic parking	–	–	(X)

X System immanent

(X) requires additional components (e.g. video system)

Table 14.1 is an overview of important qualities in comparison to other steering systems. Note that functions like lane departure warning or controlled parking can be shown regardless of the steering system. They are standard equipment, e.g., of conventional hydraulic systems in superclass cars.

### 14.1.3 Application Examples

The use of EPHS began in compact cars and continued in superclass and sports utility vehicles, on account of the development of top-performance motor pump units. A universal applicability for passenger cars and light commercial vehicles has been achieved since, see Table 14.2. The main arguments for using this steering are energy saving, the absence of a pump drive in the internal combustion engine and new drive concepts (hybrid vehicles, electromobiles etc.).

## 14.2 System Descriptions

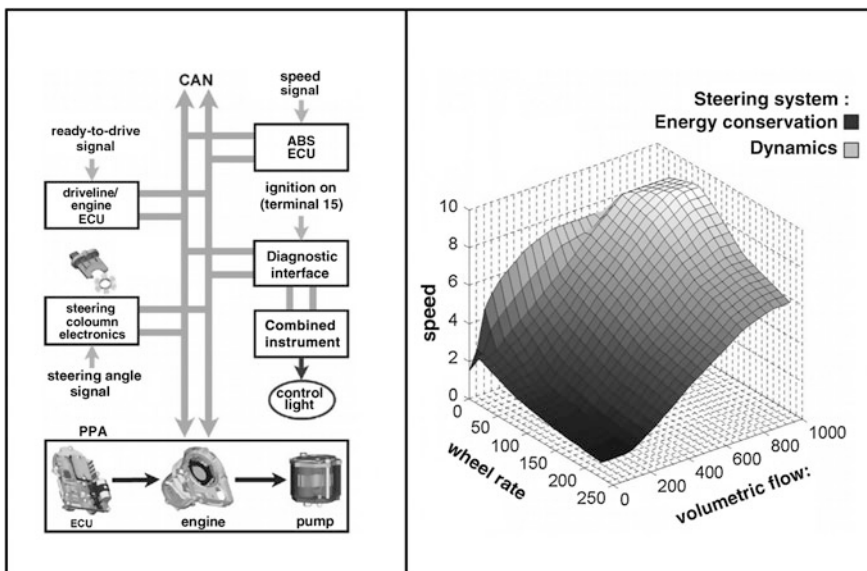
The possible system states shall be described first, beginning with a system overview. Then the system design will be discussed. Overall efficiency and power input are discussed at the end.

**Table 14.2** Vehicle classes and applications of motor pump units

Vehicle class	A/B	C/MPV	D/E	SUV	LCV (3.5 t)
<i>Example</i>					
Typical front axle load (kg)	960	1,090	1,200	1,400	1,800
MPU (W)	560	710	890	890	1,000
Max pressure (bar)	96 + 8	108 + 8	120 + 8	120 + 8	120 + 8
Max volumetric flow	5.7	7.8	9.3	9.3	12.0
Max current (A)	70	85	98	98	115
Standby current (A)	2.5	2.5	2.5	2.5	2.5
Nom. voltage (V)	13.5	13.5	13.5	13.5	13.5
Max assist power (kN)	7.6	10.6	14.5	16.0	18.0
Assist power at 540°/s & 50 mm/rev (kN)	5.7	8.5	10.9	10.4	11.6
Mechanical power at the rack (W)	428	638	818	780	870

### 14.2.1 System Overview

The motor pump unit is controlled by the car's CAN (high speed, 500 kbit/s), Fig. 14.3. A signal of the driveline is used to activate the steering. This can be, e.g., any data on the stable operation of the internal combustion engine or indicating the general readiness to drive, as is found, for example, in hybrid vehicles. The steering diagram, which illustrates the nominal rev of the motor pump unit and the power assistance as a function of different variables, commonly uses the vehicle speed and steering wheel rate.

**Fig. 14.3** System overview and steering diagram

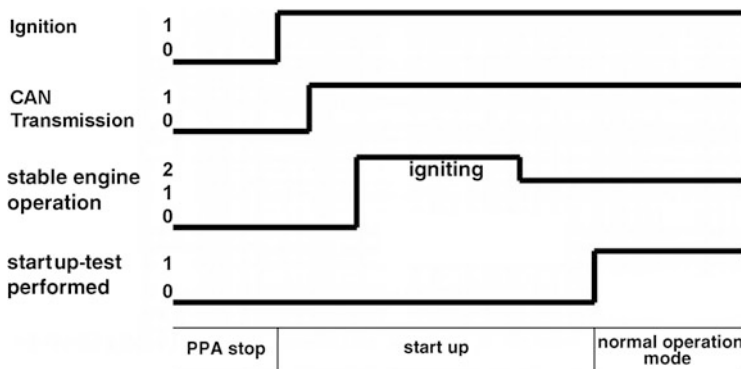


**Fig. 14.4** State diagram

It is also possible to control the power assist by other parameters, as, for example, the loading state of the vehicle, the oil temperature to compensate the changing viscosity or the steering wheel angle. Self protection functions and diagnostics are also implemented.

The system can assume different states or modes. Some of them are:

- system switched off
- system startup (wait for steering request)
- normal operation mode
- system shutdown
- relapse mode

Figure 14.4 shows how the system may be started and set to normal operation. The ignition signal wakes the system. When an internal test has ended, the internal combustion engine is running and CAN messages can be exchanged, the normal operating mode is achieved. A relapse mode (not shown here) can be assumed, e.g., when input signals of the motor pump unit are faulty or lacking. In this case, for example, the MPU can be driven at a steady medium rev to establish sufficient auxiliary support.

The steering feel is better if the hydraulic system is fed with some least volumetric flow. A least rev of the engine is the result: Standby revs of 750 to 2,000 1/min are available in technical configurations. The peak rev can be determined from dynamic requests, benchmark figures are between 4,000 and 6,000 1/min. This corresponds to a peak volumetric flow range of 1.5–12 l/min, according to MPU model. The reference value for the highest system pressure is 130 bar.

### 14.2.2 System Layout

The power design includes a steady state and a dynamic examination. Typical requirements for a power steering of passenger cars are between 400 and 900 W of

mechanical power in the rack, depending on the size of the car. The highest power consumption (battery power) currently permissible in 12 V on-board power systems is up to 120 A.

### 14.2.2.1 Steady State Layout

Motor pump units can be modularly combined with different steering gears. Different power classes of motor pump units can meet almost any vehicle requirements. The stationary system is in principle examined in two steps:

1. Based on the electric input power in the motor pump unit (power and voltage in the MPU plug) the hydraulic output (pressure and volumetric flow) is generated: Volumetric flow/pressure characteristics.
2. The hydraulic output (pressure and volumetric flow) serves to compute the mechanical output at the rack, taking into account the (small) part which the driver enters mechanically at the steering wheel.

In this approach all system parameters that are relevant for the power are examined. It is very important that the electric power supply is defined, i.e. which voltage is available at which power at which discharge point (input power). According to application, cable lengths, plug resistance, etc are considered. In principle, the described approach can be carried out the other way as well, e.g., the combination of parts (pump size, electrical engine) is deduced from the vehicle requirements.

Figure 14.5 shows how the force/steering wheel rate diagram is generated from the MPU characteristics. The pressure generates a force by means of the piston area, the volumetric flow enables the cylinder movement (filling of the moving cylinder). The calculation includes the power contributed by the driver.

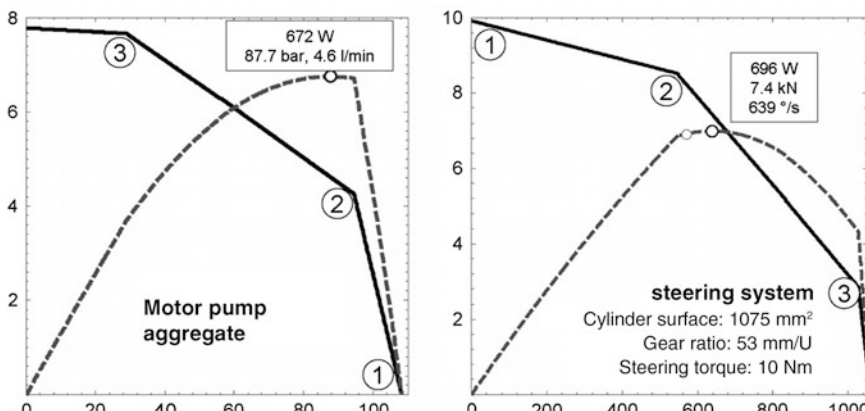


Fig. 14.5 MPU characteristic curve and mechanical steering power

### 14.2.2.2 Dynamic Layout Criteria

A consideration of the steady state system behaviour can lead to a false assessment of the steering power at higher steering wheel rates.

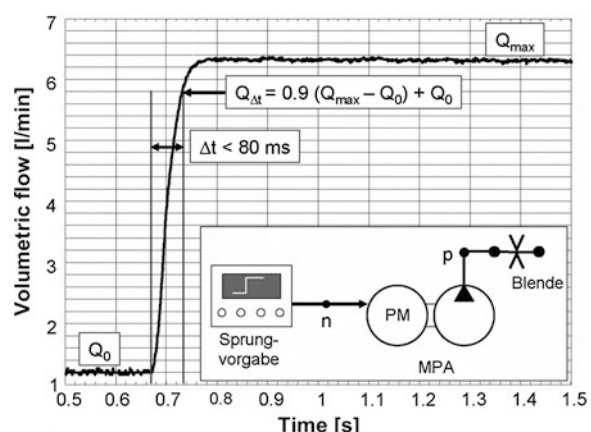
A dynamic steering process usually starts at zero and drives up to a high steering wheel rate. Several inertia effects and the control of the MPU (steering diagram) play an important part for the dynamic response. Some important parameters are:

- The motor pump unit has to power up from standby to peak rev (esp. mechanical inertia of the electric motor).
- A part of the volumetric flow is used up for the expansion of the hoses and is not available as a momentary useful volumetric flow in the valve.
- The valve is not in a fixed position but changes its effective cross sections during the steering process.
- There are lags in signal processing which are small relative to the mechanical time constants.

These effects can be accounted for if other qualities like the hydraulic capacities (hoses), the mechanical moment of inertia of the motor pump unit, as well as the steering map and signal processing times, are included in the design process. Then the highest steering wheel torque which the driver has to apply during an evasive manoeuvre can be used to assess the steering power.

The MPU is verified by measuring the step response against a hydraulic load (orifice). A step between the basic and the peak rev is given. It is equal to a step of the volumetric flow, when a pump with constant pump capacity is used. The time after which 90 % of the jump level, including the standby volumetric flow, is achieved is used as a criterion, see Fig. 14.6. This process is derived from the on-board load situation that also determines the choice of the orifice. If short enough step response times are given (e.g., 80 ms), the overall system is insensitive to the variation of other system parts, as, for example, hydraulic lines.

**Fig. 14.6** Dynamic system layout



### 14.2.3 Energy Consumption

First, important operation modes which concern system layout and potential energy saving are discussed. A discussion of the energy conversion from the internal combustion engine to the mechanical output and the electric power input of the steering follows. The often claimed potential energy or CO<sub>2</sub> saving is not an inherent quality of electric or EPH steering but follows from the substitution of an uneconomically working hydraulic pump. The terms efficiency and power input have to be specified before beginning the assessment of the energy.

#### 14.2.3.1 Efficiency

The term efficiency is used for steering against a load. It is the most important parameter in a system design that includes the definition of the electrical machine, because the limited electric input power, e.g., 1,300 W, should yield a very high mechanical output (e.g., for parking). For high forces, the efficiency of the valve-controlled cylinder drive is above 90 %. This is due to the fact that the valve is fully opened towards the cylinder connections, inflicting hardly any losses. The total friction force of all seals is also negligible relative to the generated forces, because of the good lubrication. Attainable pump efficiencies of approx. 90 % and the motor designs used allow the electrically powered hydraulic steering to achieve an as high overall efficiency as the electromechanical recirculating ball-with-nut gear. The highest attainable overall efficiency is not only a function of the parts of the steering proper, but it is also affected by secondary parameters, especially by the cable resistance, see Table 14.3. The typical position of the motor pump unit in rather cold surroundings affects the overall efficiency favourably (e.g., in the fender area), because the efficiency of the electric power pack decreases at higher temperatures. e.g., for ambient temperatures of about 100 °C, the efficiency near the internal combustion engine drops by approx. 4 %.

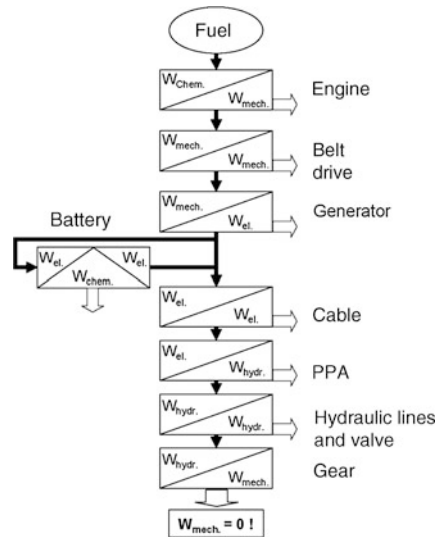
#### 14.2.3.2 Power Input and Energy Consumption

When driving straight, the efficiency is zero, because no mechanical power is requested from the rack. Then the least possible power input of the steering becomes the target of evaluation. This state is prevalent as a rule and even the only one present for assessing the kilometrage by the New European Driving Cycle

**Table 14.3** The cable resistance

Cable	Engine & ECU	Pump	Hydraulic lines	Valve	Gear with hydraulic cylinder	Overall efficiency
EPHS at 13.5 V, 85 A, 50 °C						

**Fig. 14.7** Energy flow during straight driving



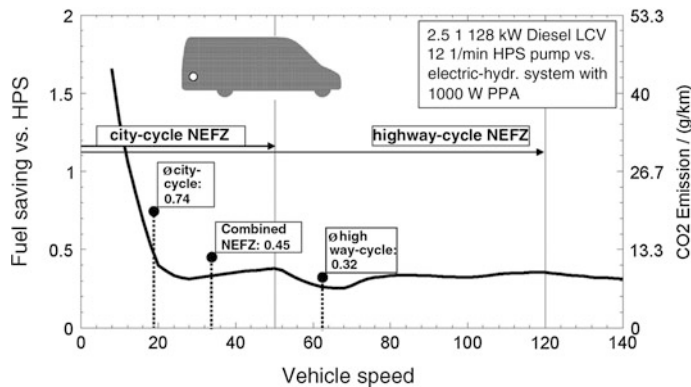
(NEDC) according to EC 715/2007, because there is no steering movement. Adding up the momentary power input ( $W$ ) yields the energy consumption (Wh or l) for a cycle with a certain length.

Figure 14.7 illustrates the energy flow of an NEDC, Table 14.4 shows the mean power inputs for the different parts (Bosch 2002). Note that in spite of the conversion into electric energy, the point balance for the EPHS or the EMS looks far better. The main reason is the quality of the hydraulic vane-type pump.

The substitution of the hydraulic pump by a motor pump unit can be evaluated with the help of a model calculation. One computes the power balance, taking into account all resistances and the diagram of the internal combustion engine. An arbitrary driving speed is chosen as an input value. It suggests a certain gear selection and, hence, combustion engine speed. The road resistances, i.e. the roll

**Table 14.4** Average power losses NEFZ in (W)

	EPHS	HPS
At the engine crankshaft	<60	>340
Belt drive	≤5	
Generator	≤15	30–40
Battery	≤5	Not applicable
Cable	≤5	Not applicable
ECU	≤5	Not applicable
E motor	≤5	Not applicable
Pump	≤5	>250
Hydraulic lines	≤5	30–80
Steering valve	≤5	30–80
Steering gear	0	0



**Fig. 14.8** Fuel and CO<sub>2</sub> saving

and air resistance, and the power input of the secondary consumers are considered. Using the involved efficiencies (e.g., generator, belt drive etc.) the performance is computed. This allows finding the current working point (rev, torque) of the internal combustion engine and to determine the input power and fuel supply per time. The potential saving is identified by computing the difference of two calculations, once with a hydraulic pump (HPS) installed and once with an EPHS. Figure 14.8 illustrates the lower consumption of the EPHS in comparison to the hydraulic steering as a function of vehicle speed.

Other reference points are the calculated driving cycle values that contain different vehicle speeds. Computations are usually complemented by roll test bench measurements, e.g., once with and once without a steering system, to evaluate its impact. The shortcoming of this method is that many measurements have to be made to resolve the effect of a few tenths of a litre per hundred kilometres. The least attainable power consumption of the motor pump unit depends slightly on the efficiency of the electrical machine, hence, the potential saving is almost fully dependent on the pump to be substituted and on the energy conversion by the internal combustion engine (switch revs, combustion engine characteristic). This somewhat lessens the potential saving for smaller pumps (or smaller vehicles).

### 14.3 Components

The main components of an electrically powered hydraulic steering are the steering gear, the motor pump unit, the fluid, feed and return line, brackets and accessories as well as sensors to record vehicle speed and steering wheel rate. The steering gear is described in Chap. 11 and will not be discussed again here.

### **14.3.1 Motor Pump Unit**

The motor pump unit consists, among others, of the main groups electric power pack, external gear pump and check/pressure relief valve, described in the following. The most powerful unit made by TRW will be described as an example.

#### **14.3.1.1 Main Requirements and Interfaces**

Concerning the use of the motor pump unit, important main requirements can be deduced immediately. They are adopted in the system architecture and the choice of parts.

(a) Vehicle integration

- low weight-to-power ratio or little need for space
- flexible arrangement or adaptation options of the mechanical, electric, signalling and hydraulic interfaces
- acoustically inconspicuous

(b) Mode of operation, reliability and safety

- high dynamic 1-quadrant operation, continuous mode
- typical service life of 8,000 h, approx. 300,000 km
- self-monitoring/diagnostics
- function safety ISO WD 26262, compliant with classification ASIL B

(c) Ambient conditions

- Class IP6K9K (dust isolation, vapour cleaner etc.) or IP6K7K (brief immersion, thermal shock), distinct by application
- ambient temperature range  $-40$  to  $140$  °C
- corrosion resistance 720 h salt spray test
- vibration and shock requirements up to 10 g, distinct by application

(d) Electric requirements

- on-board power supply voltage 9–16 V
- on-board power supply current  $I < 115$  A, distinct by application
- quiescent current for terminal 15 consumer  $I < 100 \mu\text{A}$
- reverse voltage protection.

#### **14.3.1.2 Electric Power Pack**

Electronics and motor are integrated into a single unit, an electric power pack, to serve reliability, more compact space and efficiency.

The application defines the fundamental structure of rotor and stator in a cylindrical configuration an inside rotor is most common. Basically, the five different structures indicated in Table 14.5 are suitable, each with their mentioned qualities, pros and cons. The motor designs ‘stepping motor’ and ‘asynchronous motor’ are not represented in EPH systems, though.

The first electro-hydraulic systems were integrated in compact or lower middle class vehicles. The applying requirements to power and convenience (acoustics) favoured direct current motors (DC) or brushless direct current motors (BLDC).

The expansion of EPHS steering to bigger vehicles with higher power and convenience requirements triggered the development of 3-phase permanent magnet synchronous motors with rare earth magnets. They allow achieving very low volumes or weight-to-power ratios. The weight-to-power ratio is about 40 % less than that of an asynchronous motor of the same power.

The BLDC version is predestined for this application, because the motor pump unit is constantly running to supply the standby volumetric flow. The rotor generates the magnetic field, the alternating field is generated by electronic commuting in the stator. The rotation is generated by alternate attraction and repulsion. The rotor is turning synchronously, following the rev of the alternating field. The rotor position can be detected by sensors (e.g., Hall effect pulse generator) or by computational methods (engine model, sensorless control), enabling a very robust and cheap configuration (Hofer 1998).

The electric power pack, Fig. 14.9, is electronically stabilised at its nominal speed in its field of operation. To properly exploit the electrical unit at higher revs, it is operated in a weakened field. This establishes a rev bandwidth of 750–6,000 1/min.

As the most powerful EPHS needs about 110 A at a full hydraulic output of 1,000 W, setting a limit to any 12 V vehicle electrical systems, the thermal management of motor and ECU is very important. Of consequence for the driver is the time the system can be used at high load or the time it can be kept at the end stop until a thermal protective mode is activated (critical time). Typically, the thermal constraints are defined in specifications, such as ambient temperature, permissible peak temperature and steering manoeuvre, e.g., the number of subsequent parking cycles.

Installing the motor in the hydraulic oil, i.e. using the fluid to cool the windings and the ECU, helps to extend the critical time considerably. This effect is due to improved convective transmission of heat (by a factor of 100 (!) relative to air) and the additional thermal mass (caloric capacity of the oil). Figure 14.10 shows the time to reach a critical temperature state in the electronics (e.g.,  $T_{\text{crit}} = 120^\circ\text{C}$ ) as a function of the ambient temperature (=initial temperature) for a parking cycle. At an initial temperature of  $92^\circ\text{C}$ , the requirement (200 s parking) is just about met by a dryly running motor pump unit. The wet running concept achieves a three times longer period for this constraint. The recorded measurement can also be interpreted as saying that the wet running motor pump unit can be used at an ambient temperature of  $T = 105^\circ\text{C}$  and yet meet the specification.

**Table 14.5** Inside rotor motor structures for motor pump units

Motor	SR	ASM	DCM	BLDC	PMSM
	Switched reluctance	Asynchronous motor	Direct current motor	Brushless direct current	Permanent magnet synchronous motor
Name	Stepping motor	Asynchronous motor	Direct current motor	Electronically commutated DC motor	3-phase synchronous motor
Supply	3 phases AC	3 phases AC	DC	DC	3 phases AC
Rotor	Metal sheet package rotor	Distributed rods, closed, die-cast aluminum rotor cage	Rotor winding, punched rotor metal sheet package	Ferrite magnets in metal sheet part	Rare earth permanent magnets (NeFeB)
Stator	Punched metal sheet packages, concentrated winding, open (single cog winding)	Punched metal sheet packages, distributed	Ferrite magnets in metal sheet part	Punched stand package, distributed stator winding (or single cog winding)	Segmented stator, concentrated winding, open (single cog winding)
Main advantages	Robustness/price	Robustness/price	Price, easy control	Price, easy control	Power density, efficiency, construction space, acoustics
Main disadvantages	Acoustic efficiency	Efficiency/space	Wear by mech. commutator, efficiency	Acoustics	Price (rare earth magnets), complex electronics
MPU application	Not applied	Not applied	Low cost applications/ compact car	Series application up to C segment	Premium high power up to D/E Segment and LCV

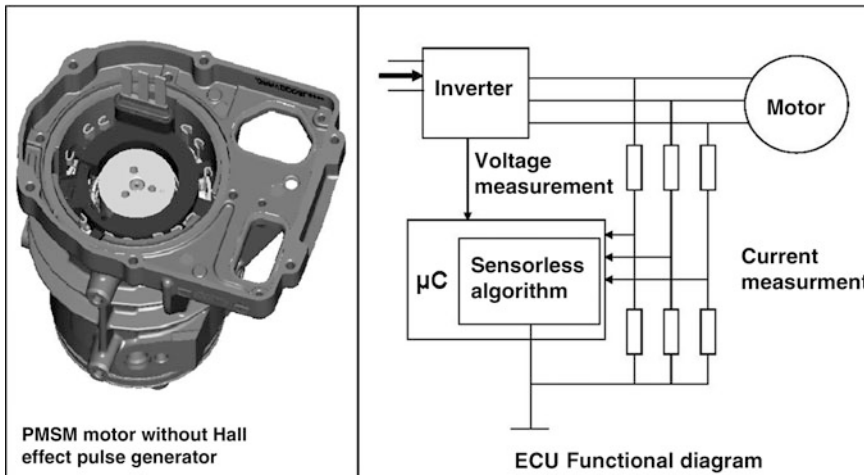


Fig. 14.9 Electric motor without sensor and ECU functional diagram

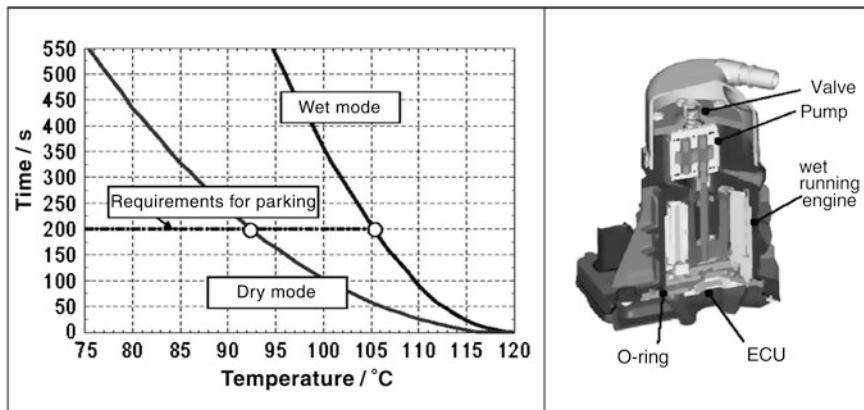
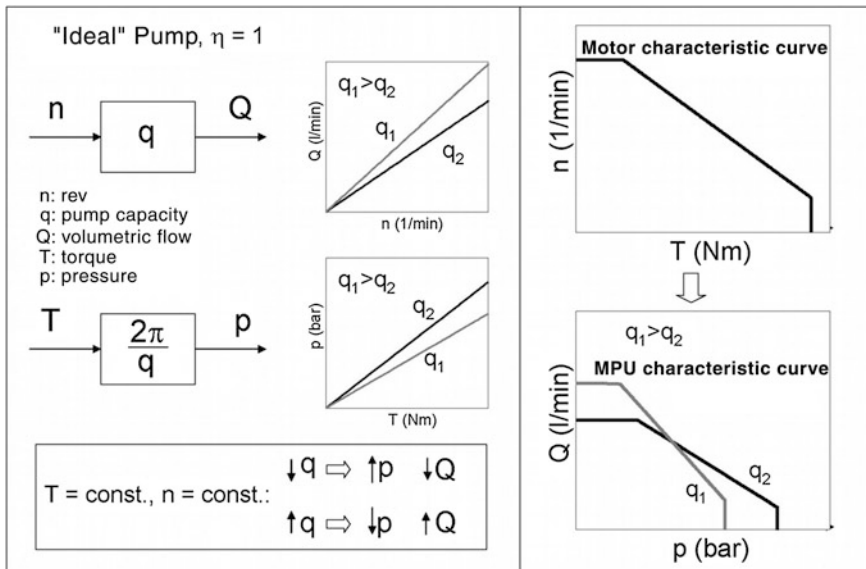


Fig. 14.10 Thermal quality of an MPU running dry or wet with full load

### 14.3.1.3 Pump and Valves

The pump converts the mechanical power of the motor into a hydraulic output of the motor pump unit. Figure 14.11 shows (on the left) the functional qualities in matching block diagrams for an ideal configuration without loss. The input values of the pump are rev and pressure, the output values are pump volumetric flow and pump drive torque. Note that the pump volumetric flow is proportional to rev and geometrical pump capacity ( $\text{cm}^3/\text{rev}$ ). The idealised configuration is not a function of pressure. To maintain a hydraulic pressure, defined by the load or the force at the rack, a torque is required that is inverse proportional to the pump size. For a



**Fig. 14.11** Block diagram MPU and characteristic curve design

given motor characteristic curve, the characteristic curve of the motor pump unit can be raised by the pump size (geometrical pump capacity) to high volumetric flows and pressures without changing the peak power.

Real configurations deviate from the ideal response with regard to the volumetric flow because of internal leaking (gap losses). This response is described by the volumetric efficiency as a function of rev and pressure. With regard to the torque, a (small) part serves to overcome the friction at axial and radial bearings. This is covered by the hydraulic-mechanical efficiency. Motor pump units integrate external gear pumps, because these are very robust, cheap and small (Ivantysyn 1993). Very high efficiencies can also be achieved by special manufacturing methods ( $\eta_{\text{vol}} \approx 97\%$ ,  $\eta_{\text{hm}} \approx 91\%$ ,  $\rightarrow \eta_{\text{total}} \approx 88\%$ ).

Figure 14.12 shows a configuration example of an external gear pump and its main parts:

- oil pump body
- gearwheel pair (straight or diagonal dovetailing)
- sealing elements (moulded seals or sealing plates)
- sleeve bearings (with or without bushings)
- lid

The gearwheel pair is supported in the sleeve bearings. This unit is placed into the body and shut off on both sides by the sealing elements and lids. The pressure load, rising across the perimeter towards the pressure side, produces a radial bearing load which is taken up by the sliding fit. Surfaces exposed to operating

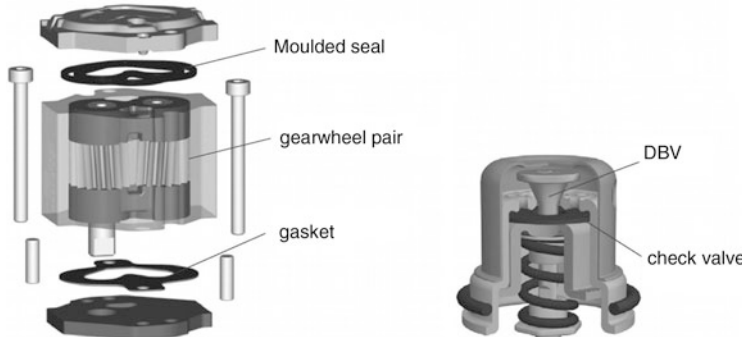


**Fig. 14.12** External gear pump, combined check and pressure relief valve (Source TRW)

pressure develop from the special design of the moulded seal in the region of the lids and sleeve bearings. Axial compensation is thereby achieved and proper sealing of the facing gearwheel surfaces is established.

The tooth gaps carry the liquid across the outside contour from the suction to the pressure side. The kinematics of meshing produce an asymmetry of the volumetric flow (pump pulsation) whose effect is compensated by secondary measures. The resonator, integrated into the MPU housing, and the use of special hydraulic tubes are some of them.

The peak pressure of the pressure relief valve is adjusted by the travel stroke. The check valve is realised by applying a flat valve body, see Fig. 14.12 on the right.

### 14.3.2 Hydraulic Pipe System

Just as with conventional hydraulic power steering, low-and high-pressure lines made of hose and pipe sections are used in EPHS systems. The higher requirements for the damping behaviour of the high-pressure line entails its more complex structure in an EPHS system. Hence, in the following, the focus is put on the high-pressure line.

#### 14.3.2.1 Main Requirements

The following list shows the main requirements for a high-pressure line of an electric-hydraulic power steering:

- hydraulic connection between pump and gear with very low circulatory resistance
- damping of the pump pulsation, i.e. diminished fluid noise

- damping of system vibrations
- flexible mechanical connection between motor pump unit and steering gear (reducing the structure-borne sound transmission, tolerance offset).

The mentioned requirements apply for any lines in hydraulic steering systems, more effort is necessary to dampen the pump pulsation in EPHS systems, though. The main reason is the variable rev of the electric motor which is adjusted regardless of the internal combustion engine speed. The rev of the electric motor rises, e.g., when parking at rest, to make enough volumetric flow available. In this case, the high-pressure line has to damp the pulsations of the pump across a broader frequency range. A conventional pump, powered by the internal combustion engine, would in this case run with a steady rev and only discrete frequencies (pump orders) would have to be damped.

#### **14.3.2.2 Configuration and Damping Principles**

On the outside, all high-pressure lines in steering systems are made in a similar manner. Sections of pipe and hose are alternately connected in a row. Impedance jumps at the contact points from different stiffness values of hose wall and pipe wall cause a reflection of the liquid waves, see Fig. 14.13. The constant reflection and the absorption effect of the hose wall damps the pressure waves.

In spite of this effect, there are always typical natural frequencies of the individual segments which reduce the damping. Hose installations or ‘tuners’ are used to achieve a broadband damping, to improve the damping response of the pipe system. There are two essential kinds of tuners: the first case is a PTFE tube and the second case is a steel spiral.

#### **14.3.2.3 Determination of the Damping Behaviour**

The damping behaviour of the hydraulic pipe system can be analysed independently from the car while the response characteristics are determined in a test, see Fig. 14.14. This reduces the test costs on the vehicle level considerably.

The response characteristics are described by the transmission matrix T. The matrix joins the vectors of pressure and volumetric flow pulsation at two points, e.g., beginning and end of a line. Pressure pulsation, volumetric flow pulsation and matrix terms are complex functions in the frequency range. The transmission matrix can be determined if pressure and volumetric flow are known at both points.

While the pressure pulsations can be measured directly, the volumetric flow pulsations in the examined frequency ranges cannot. Indeed, the pressure signals from two or more points of a line whose response characteristics are known allow deducing on the volumetric flow pulsation. Hence, the system is switched between two reference tubes, see Fig. 14.14.

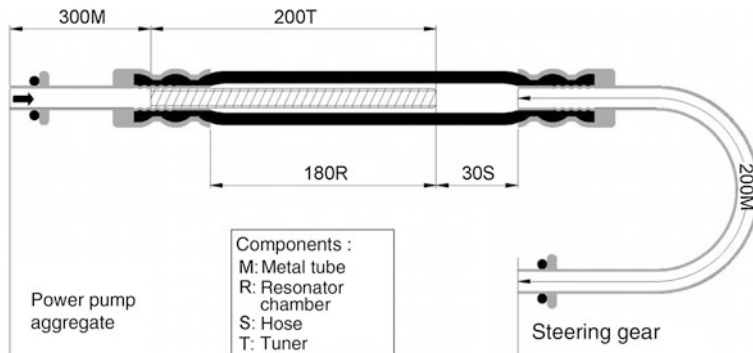


Fig. 14.13 Pipe system configuration—impedance jumps, tuners

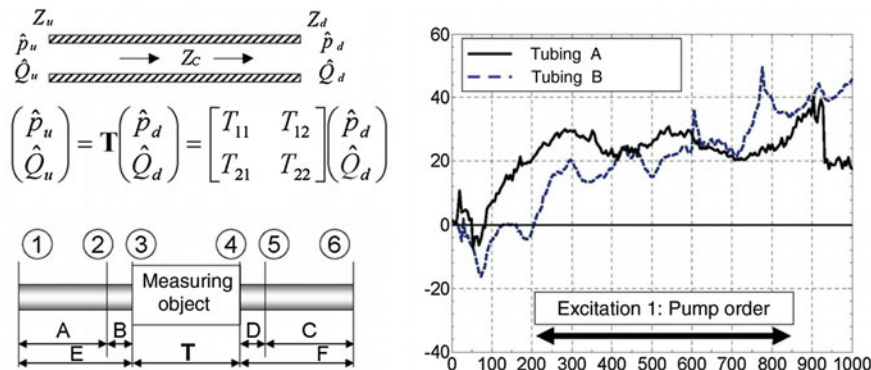


Fig. 14.14 Verification of pipe systems—response characteristics

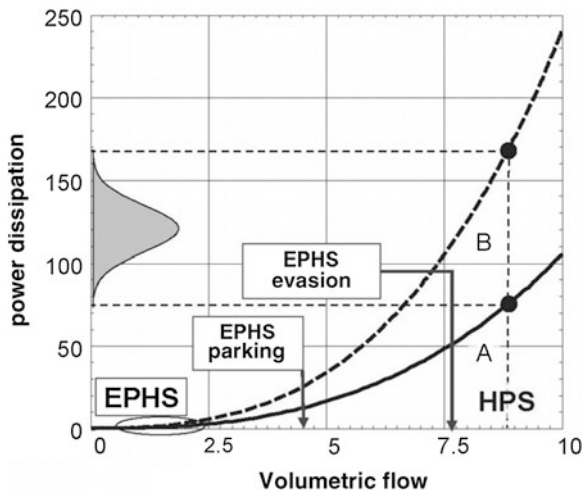
Then the terms of the required matrix can be identified as a function of the known transmission matrices of the reference tubes and the transfer functions of the pressure pulsations between the measuring positions 1 and 2, as well as 5 and 6.

A suitable measure of the quality of the damping is the element  $T_{11}$ . It represents the ratio of the pressure amplitude at the line entrance to the pressure amplitude at the line exit with an ideally closed end. The example shows a comparison of two pressure pipe systems. The pump frequency range is shown as well. Pipe system A has a much better damping and is therefore used on-board.

#### 14.3.2.4 Hydraulic Resistance

The pressure loss characteristics of the pipe system is non-linear. The pressure loss grows progressively with increasing volumetric flow, and as a result, the passive power dissipation rises disproportionately, see Fig. 14.15.

**Fig. 14.15** Verification of pipe systems—pressure loss



To minimize power consumption, the steering system should operate at about 2 l/min. This ensures that EPHS systems will have low

- power dissipation of the hydraulic pipe system (cf. HPS system),
- variation of the power dissipation when different pipe systems are used (cf. HPS system).

The latter aspect is important in particular because vehicle applications always require other technical solutions for tubing and acoustic tuning, due to the available space.

### 14.3.3 Other Components

#### 14.3.3.1 Sensors

The volumetric flow (or the MPU rev) is controlled by setting vehicle speed and steering wheel rate. In most cases, sensors are applied which are already on-board, such as the wheel speed sensor (ABS) or the steering wheel angle sensor of the electronic stability control (ESC).

#### 14.3.3.2 Fluids

Electrically powered hydraulic steering applies liquid ATF oils, e.g., Pentosin CHF 11 S or Total LDS H50126. They allow extending the operational temperature range down to  $-40^{\circ}\text{C}$ . Purity requirements are compliant with ISO 4406 18/16.

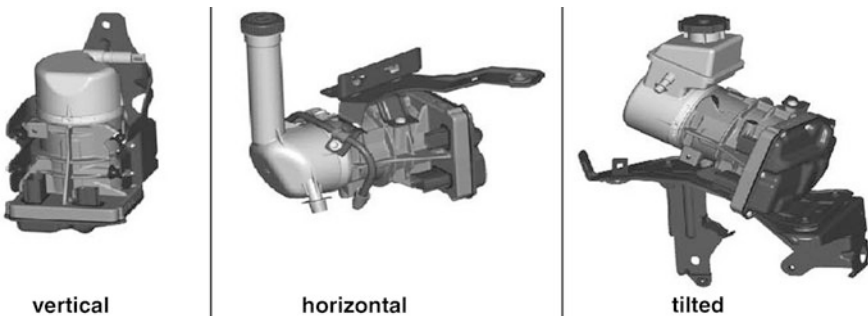


**Fig. 14.16** Adaptation to the vehicle environment—brackets and tanks (Bublitz 2010)

#### 14.3.3.3 Tanks and Brackets

Tanks and brackets are parts which are simple to adapt to the application. The motor pump unit can therefore assume almost any position in the available space. Figure 14.16 gives an overview of different standard applications.

## References

- Bosch (2002) Autoelektrik—Autoelektronik, Systeme und Komponenten, ISBN 3-528-13872-6  
Bublitz H (2010) Die elektrohydraulische Servolenkung als Lenkungstechnologie für Daimler Hybridfahrzeuge, 19. Aachener Kolloquium  
Hofer K (1998) Regelung Elektrischer Antriebe: Innovation durch Intelligenz. VDE Verlag, Berlin  
Ivantysyn J, Ivantysynova M (1993) Hydrostatische Pumpen und Motoren. ISBN 3-8023-0497-7

# Chapter 15

## Electric Power Steering Systems

Alexander Gaedke, Markus Heger, Michael Sprinzl, Stefan Grüner  
and Alexander Vähning

### 15.1 Introduction

A change of hydraulic systems to solely electrically operated steering systems (Electric Power Steering, EPS) has taken place in passenger car steering systems during the last years. The use of these systems was originally limited to small vehicles, because the power density of the electronic parts and the energy available from the on-board wiring was not sufficient to serve bigger vehicles and higher steering powers. New technologies enable the general use of EPS in the superclass now. Various EPS varieties have established themselves in the individual vehicle classes in the market (see Fig. 15.1). These systems will be described in Sect. 15.2 in more detail.

The advantage of electric power-assisted steering in comparison to HPS is that it is activated only when needed. This is called a power-on-demand system, i.e. energy is fed only when the car is steered. A rather low average energy consumption is the result, leading to better mileage and less CO<sub>2</sub> emission. Figure 15.2 shows the petrol and CO<sub>2</sub> reduction for a middle class vehicle with a 2.0 l petrol engine. Note that the savings in fuel consumption and CO<sub>2</sub> emission achieved in NEDC and by end customer driving are of a similar scale.

---

A. Gaedke (✉) · M. Heger · M. Sprinzl · S. Grüner · A. Vähning  
ZF Lenksysteme GmbH, Schwäbisch Gmünd, Germany  
e-mail: Alexander.Gaedke@zf-lenksysteme.com

M. Heger  
e-mail: Markus.Heger@zf-lenksysteme.com

M. Sprinzl  
e-mail: Michael.Sprinzl@zf-lenksysteme.com

S. Grüner  
e-mail: Stefan.Gruener@zf-lenksysteme.com

A. Vähning  
e-mail: Alexander.Vaehning@zf-lenksysteme.com

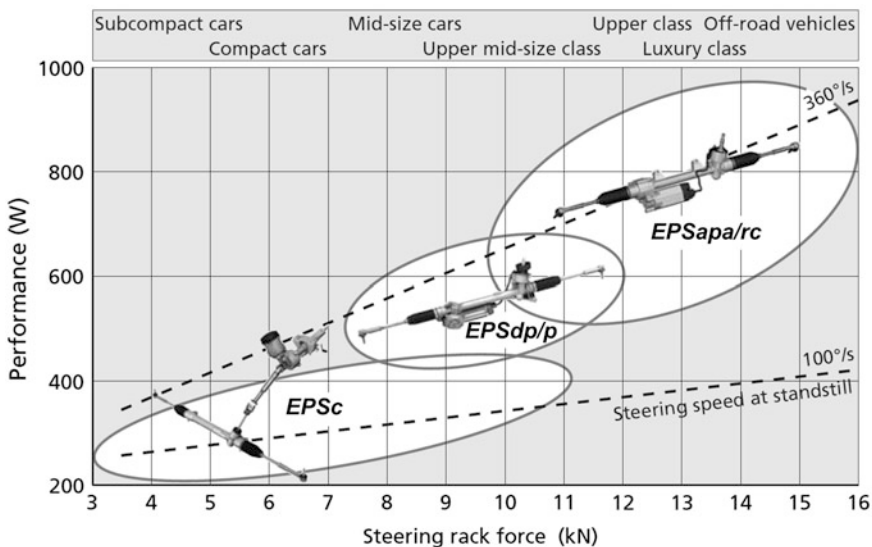


**Fig. 15.1** Operational areas of steering systems in different vehicle and power classes

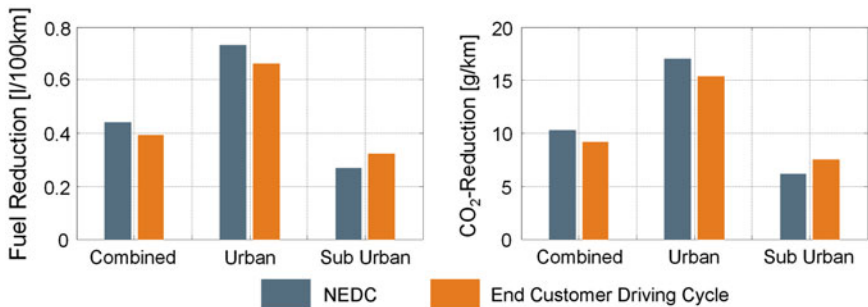


**Fig. 15.2** Saving of EPS in comparison to a conventional HPS. The results of the NEDC (New European Driving Cycle) and driving by the end customer are comparable. The measurements were taken at a BMW 320i

High requirements for less consumption and emission make the use of EPS indispensable in all vehicle classes.

Another advantage of EPS is the additional functionality that meets higher requirements for vehicle safety, ride comfort and driver-assist. Examples are, e.g., parking assistants that guide the vehicle automatically into a parking spot by intervention into the steering. Systems like Lane Departure Warning should be mentioned, too. They warn the driver by a superposed torque at the steering wheel when the lane is unintentionally left. Therefore, functions like Lane Departure Warning contribute to improving road safety. More functions will be found in Sect. 15.6.

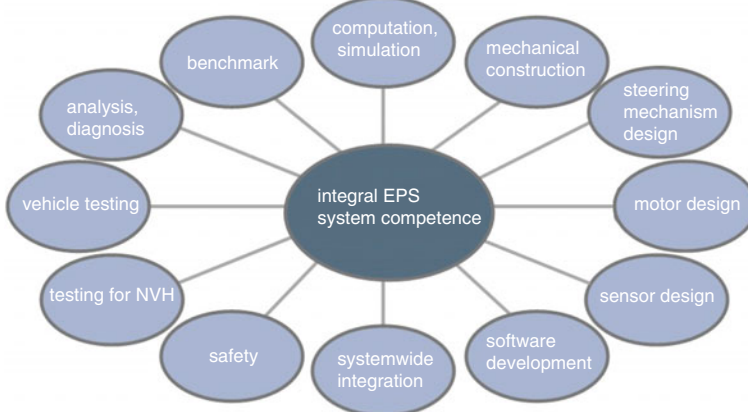


**Fig. 15.3** Scopes of EPS development

The development departments of the steering system manufacturers were facing new challenges in making EPS available in series. The development of such a complicated mechatronic system and the applying safety requirements demanded many new processes of development which had not been required for HPS up to now. Safety standards IEC 61508 and ISO 26262 should be specifically mentioned here (see Sect. 15.5).

With EPS, particular attention has to be paid to the acoustic response of the on-board system. Servo motors and gearbox layers of the EPS unit emit noise (vibrations) that had not been present before. They should not be perceived by the driver as annoying, hence, the development of every individual component and their on-board assembly has to consider the acoustic transmission paths. Simulation tools are used early on for doing so.

Figure 15.3 presents the various scopes of EPS development. The interaction of all the mentioned scopes is indispensable to develop an excellent steering system.

### 15.1.1 Analogies of EPS and HPS

This section will discuss the essential differences of the configuration and function of HPS and EPS units.

Figure 15.4 shows that the HPS has many individual parts (pump, hoses, gear etc.) that are usually assembled on-board, not before. Then the system has to be hydraulically filled and the connections tested for leakage.

The EPS, though, is supplied to the vehicle manufacturer as a complete and tested unit. Only the electric connection to the vehicle has to be established to start running the steering.

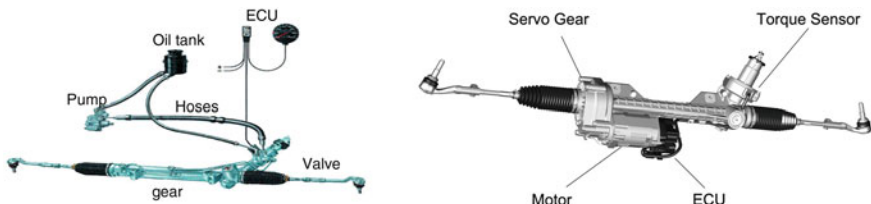


**Fig. 15.4** Less complexity in EPS in comparison to HPS. EPS requires no additional parts

The two systems differ in the generation of the power-assist as follows:

- **HPS** generate the power-assist in a hydraulic cylinder which is connected to the rack. A hydraulic pump supplies the cylinder with hydraulic energy. It is actuated by a rotary disk valve (see Sect. 11.3).
- **EPS** generates the power-assist by means of an electric motor whose force is fed into the rack or steering column by a servo gear unit. The electric motor is powered by the on-board wiring. The motor is actuated by power electronics integrated into the electric ECU of the EPS.

With both steering systems, the detection of the driver's intention is crucial for providing the required power-assist. The systems detect it as follows:

- in an **HPS**, a rotary disk valve is connected to a torsion bar. This component is accommodated in the steering driveline between wheel and gear. If the driver steers, the torsion bar is twisted and the rotary disk valve opens one way. Pressure is applied to one side of the hydraulic cylinder, and the power-assist is active. The level of the power-assist is a mechanical function of the valve characteristic (see Sect. 11.10).
- **EPS** uses torque sensors to identify the driver's purpose. As in the hydraulic system, a torsion bar is twisted when a steering movement is initiated (see Sect. 15.3.3). Now the required power-assistance is computed in the EPS-ECU using the measured torsion bar torque. It is a benefit that the power-assist characteristics can be changed by a software almost arbitrarily, no mechanical changes are necessary.

## 15.2 Designs of EPS Systems

### 15.2.1 EPSc: Column

The EPSc (Fig. 15.5) is the oldest EPS variety in regular use. It entered mass production as early as 1988, in a Suzuki Cervo (Stoll and Reimpell 1992). It was used at first only in minis and compact cars whose rack forces and steering powers are very low. Today, the EPSc is also used in middle-class vehicles. This became

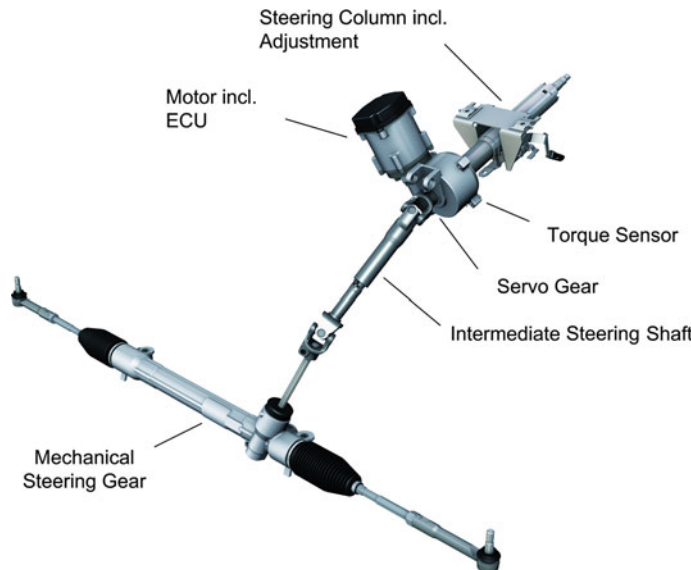


**Fig. 15.5** Electric power-assisted steering with power-assist unit in the steering column (EPSc)

feasible due to the use of new materials for power-assisted gears, steering columns and pinions that permit transmitting higher torques.

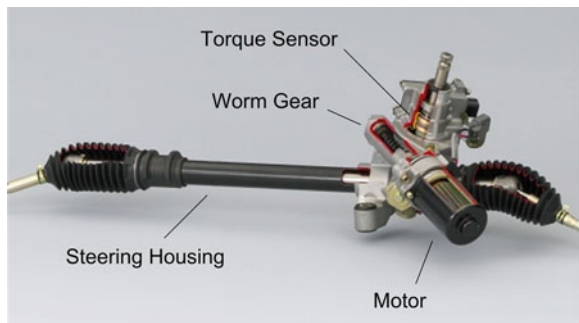
The power-assist unit of the EPSc is accommodated in the interior of the vehicle. This is favourable with regard to the environmental requirements. In the interior, the power-assist unit does not need to be watertight, for example. A lower temperature range of  $-40$  to  $85$  °C applies as well, while the engine compartment requires  $-40$  to  $125$  °C. Especially the high temperatures are a challenge for the electronic parts of the power-assist unit. A shortcoming of the interior is that the power-assist unit is placed very close to the driver and can be heard more easily.

The power-assisted gear of an EPSc is not a self-locking worm gear. The screw is mounted at the engine shaft of the electric motor, and the accompanying worm wheel is connected to the steering column. Other gearbox varieties are known, e.g., a belt gearbox or a direct drive. However, these do not appear in significant numbers on the market so far.

The forces of the power-assist unit are transferred along steering column, intermediate steering shaft and pinion, setting limiting factors for the highest accessible steering forces. A longitudinal adjustment of steering columns, for example, requires sliding elements in the steering shaft (see Chap. 10). For higher torques, they have to be laid out more sturdy and, therefore, more expensive. The easiest configuration of such sliding elements is a simple plastic slider. Higher transmission torque make expensive metal bearings obligatory.

A particular problem is the crash response of the EPSc, because the power-assist unit is in the upper steering column, near the driver.

**Fig. 15.6** EPSp by NSK company (Source Internet NSK Europe)



### 15.2.2 EPSp: Pinion

The power-assist unit of the EPSp is placed right at the steering pinion (Fig. 15.6).

The power-assist torque generated by the electric motor is transferred by a worm gear to the pinion and the rack. The system can achieve slightly higher steering powers than an EPSc, because the forces do not need to be transferred along steering column and intermediate steering shaft. Since the power-assist unit (engine and ECU) is near the EPSp in the engine compartment, it has to meet higher requirements for temperature, density and vibration than, e.g., an EPSc. These higher requirements also apply for the EPSdp, EPSapa and EPSSrc systems (Sects. 15.2.3–15.2.5).

The package possibilities of this system are limited, because the power-assist unit can be turned only around the axis of the steering pinion. Another problem is that the power-assist unit is near the driver's legs. Therefore, it needs to be ensured that the power-assist unit cannot penetrate into the space of the legs during a crash.

### 15.2.3 EPSdp: Dual Pinion

The power-assist unit of the EPS Dual Pinion is mounted at a second pinion (Fig. 15.7). This steering is very well suited for medium or upper middle class vehicles. The first standard use of such a steering occurred on the VW GOLF Platform in 2002.

The installation of the power-assist unit at the second pinion permits separating sensor unit and drive unit. Since the main drive pinion gear ratio is independent from the steering ratio, a power-optimising layout is possible. The additional system power is 10–15 % higher than that of an EPSc or EPSp.

The power-assist unit can be positioned by an accordingly tuned worm gear, individually turning 360° radial to the rack and main drive pinion axis (Fig. 15.8). This quality allows adapting the steering to very difficult installation space. A very good crash safety can be achieved by careful exploitation of the installation space.

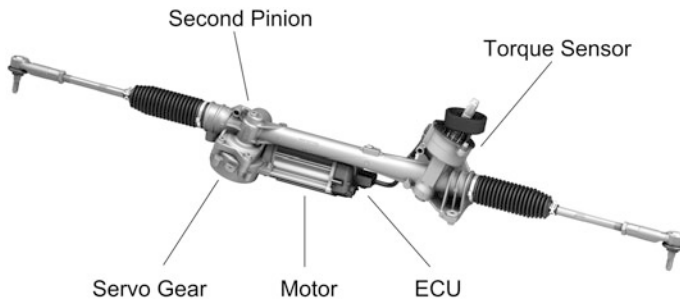


Fig. 15.7 EPSdp by ZF Steuersetze

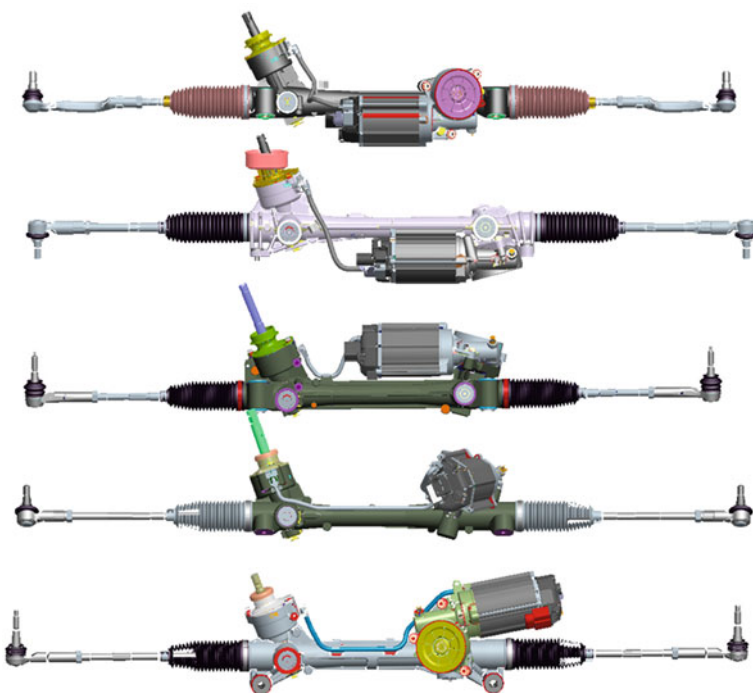
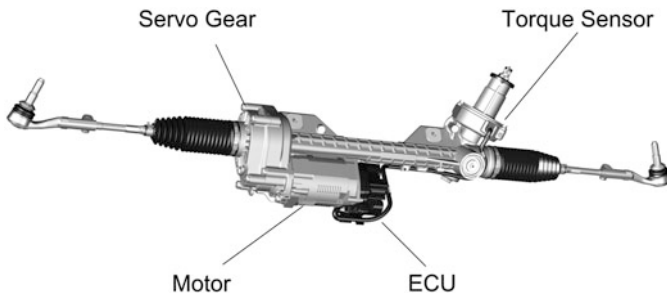


Fig. 15.8 Various examples of the EPSdp, the power-assist unit can be placed very flexibly. Therefore the steering can be best adapted to the available installation space

#### 15.2.4 EPSSapa: Axle Parallel

The EPSSapa (Fig. 15.9) with an axle-parallel drive is marked by low system friction and high efficiency. This steering is applied in dynamic sports cars, upper middle class cars, even in high load vehicles, for example, in cross-country



**Fig. 15.9** EPSapa steering by ZF Steuersysteme

vehicles and transporters. The first standard model to use the EPSapa was the BMW 3 in 2007.

In this steering model, the power-assistance is generated by the electric motor and transferred to the rack by a combination of ball screw and timing belt gearbox. The ball screw converts the rotation of the engine into a translation of the rack.

This gearbox model requires that the engine is arranged in parallel with the rack. The power-assist unit can then be turned arbitrarily around the rack, so that the installation space on-board can be perfectly exploited.

### 15.2.5 EPSSrc: Rack Concentric

The rack-concentric steering system uses a ball screw as a gear to convert the rotation of the engine into a translation of the rack. In contrast to the EPSapa, the ball screw is here directly driven by an electric motor. Therefore this steering system has one gearbox layer less than the EPSapa (cf. [Sect. 15.2.4](#)).

The concentric configuration requires a special servo motor with hollow shaft rotor, because the rack of the steering passes through the motor.

As mentioned above, the motor engages directly into the ball screw, and there is one gear ratio layer less. Since the multiplication is lower than that of the EPSapa, an electric motor that can produce higher torques is needed. If the power fed by the on-board wiring should stay the same, this can be achieved only by a larger motor. This means that in comparison to an EPSapa, the electric motor of an EPSSrc has to produce a twice as high torque at the same output power level.

Due to the concentric arrangement, the EPSSrc is very compact, yet this configuration has a disadvantage. All the previously discussed steering systems allow arranging the power-assist unit to some extent around the steering, enabling easier packaging. The motor of the EPSSrc and its ball screw can be shifted only slightly axially along the rack (Fig. 15.10).

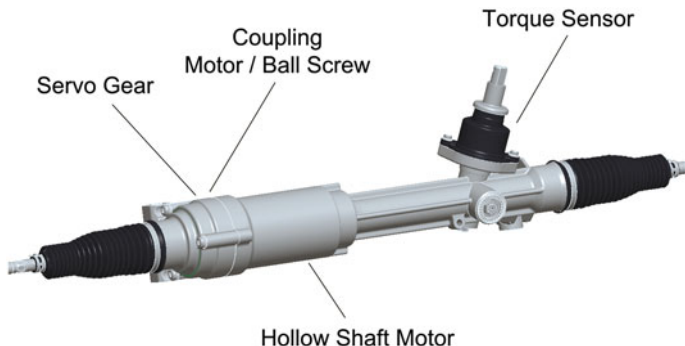


**Fig. 15.10** EPSrc, the hollow shaft motor is arranged concentrically around the rack

## 15.3 Subassemblies of the EPS

### 15.3.1 Power-Assisted Gear

The power-assisted gear establishes the connection between drive unit, wheels and driver. Hence, it is active right in the power flow of the EPS. Because of vibration, friction or inertia effects, the gearbox parts have to be considered in an assessment of the static and dynamic qualities of the overall system. Combinations of screws, ball thread, timing belt and rack-and-pinion gears (cf. Chap. 11) are used for EPS applications, according to the system version. As the gearbox configurations are always form closed, every input movement is allocated a unique output movement.

*Function* The main function of the servo gear unit is the transmission of the power-assist torque to the rack when the electric motor has provided it on demand. The rotation of the power-assist drive is converted into a translation of the rack. The different characteristics of the necessary output power and the available drive power generate a necessity to adapt the torque or rev level by the power-assisted gear for power transmission. The drive torques have to be amplified by a gear ratio towards the slow end, to generate the necessary rack forces while meeting the requirements of the power-assist drive with regard to costs, space or power demand. Accordingly big transmission ratios can be achieved by a combination of two gearbox layers.

An essential secondary function of the servo gear unit is a change of the axis of rotation. This concerns the position of the drive and driven axles in space, which is essential for size and shape of the space the EPS is installed in. A general division of gearboxes with parallel, intersecting or oblique axes of rotation is possible.

*Qualities of power transmission* In view of the power transmission, the EPS gearbox layers are mainly determined by their transmission ratio and their efficiency. The transmission ratio  $i$  is the ratio of input and output rev,  $n_{in}$  and  $n_{out}$ .

$$i = \frac{n_{in}}{n_{out}} \quad (15.1)$$

The loss of power in a gearbox layer,  $PV$ , is represented by its efficiency  $\eta$ . It represents the ratio of usable power  $P_{use}$  and supplied power  $P_{sup}$ .

$$\eta = \frac{P_{use}}{P_{sup}} = 1 - \frac{P_V}{P_{sup}} \quad (15.2)$$

*Technical requirements* In the following, the most important technical requirements of the power-assisted gear for EPS are listed:

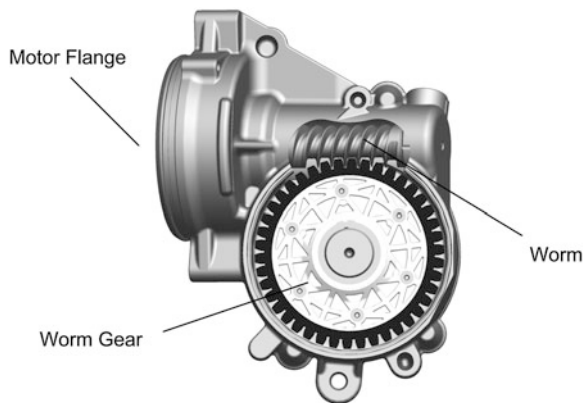
- high static and dynamic strength
- high safety against self-inhibition
- high loading capacity for operation and ambient conditions
- no servicing to maintain the effectiveness for the whole service life
- high efficiency to keep specified limit values for the input and output power of EPS systems
- low free travel to avoid an unstable steering torque curve during alternate steering or by dynamic rack force changes
- high stiffness and low moments of inertia as a basis for the best steering feel
- low weight, taking into account strength requirements and target costs
- low emission of structure-borne and airborne sound to avoid interfering noise and vibrations.

### 15.3.1.1 Worm Gear

Worm gears belong to the screw gears. The axes of screw and worm wheel do not intersect. The shape of the screw corresponds to a multi-stroke threaded bolt whose rotation drives the worm wheel, due to its screw-like shape, see Fig. 15.11. A big slip component is typical for the transmission of motion in comparison to spur gears, see also Niemann and Winter (2004). Noiseless and steady transmission of motion is possible. Nevertheless, the slip towards the contact line generates a higher loss of power. Therefore, the efficiency is lower in comparison to spur cut gears.

Worm gears are used in the EPSdp to transmit power between electric motor and main drive pinion. The steering column variety EPSc and the pinion variety EPSp apply a worm gear for power transmission as well. It is used to transfer the drive torques of the electric motor to the steering column. Worm gears allow for great gear ratios in a layer. For EPS applications, they are in the range of 15–30. The transmission ratio corresponds to the ratio of the number of worm wheel cogs to the number of thread gears at the screw.

**Fig. 15.11** Worm gear of an EPSdp. The variable arrangement of the screw in the perimeter of the worm wheel offers an additional degree of freedom to exploit the installation space in the best manner



A worm wheel with plastic gear rim is the most common tool to keep dovetailing noise and the wear of the cog flanks low for the whole service life. It cogs with a hardened steel screw. The gear rim, strongly loaded as a result of the high forces, is made out of high-performance plastics. To maintain a lasting zero backlash in the cog engagement, the screw can be put on to the worm wheel using a helical spring with a defined pretension.

### 15.3.1.2 Ball Screw Drive

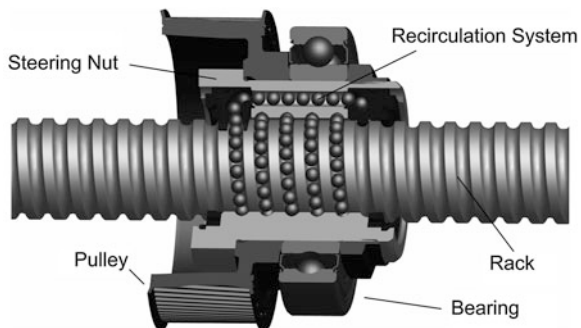
Ball screws transform the rotation of the electric motor in an EPSSpa or an EPSSrc system into a translation of the rack and vice versa. The application of ball screws in steering technology traces back to the ball-with-nut steering gear. Essential parts of the ball screw (KGT) are, acc. to DIN 69051-1 (1989), the ball thread spindle, the balls as rolling elements and the ball thread nut including the runback system and the seal elements, see Fig. 15.12.

Ball screws are favourable for converting rotation and translation because of the high mechanical loading capacity, the big attainable transmission ratios and the highly efficient energy transmission with little loss. Efficiencies of more than 90 % can be achieved.

The ball thread spindle of modern EPS systems is a part of the rack. The ball thread nut also called steering nut, is supported by means of a ball bearing. This bearing accepts the radial and axial forces applying during the operation. The axes of steering nut and rack are overlaid. The drive comes either directly (EPSSrc) or via a belt gearbox (EPSSpa) from the electric motor. The drive torque is supported by the rack near the pinion dovetailing. To reduce the resulting load of the steering pinion, the rack can be Y-shaped.

The principle of ball screws corresponds to that of a wedge which converts a translation through an inclined plane into a lateral movement and vice versa, see also Steinhilper and Sauer (2006). The sloped plane is a screwing line around the rack and inside of the steering nut. Balls are used as rolling elements to reduce the

**Fig. 15.12** Parts of the ball screw (EPSapa). This allows an efficiency-optimised power transmission also with the highest steering forces



friction and to transmit loads between the tracks of ball thread nut and ball thread spindle.

The slope  $h$  represents the distance by which the rack is shifted during one axial rotation of the ball thread nut. The slope of ball screws in modern electromechanical steering applications has a typical value of 5–10 mm. The slope helps to directly compute the transmission ratio of the ball screw:

$$i_{KGT} = \frac{2\pi}{h} \quad (15.3)$$

Layout and safety of ball screws are very demanding. Beside classical bench tests and strength computed by means of FEM analyses, NVH examinations are necessary as well, see Fig. 15.13.

### 15.3.1.3 Toothed Belt Drive

Toothed belt drives of the EPSapa transfer the assist power of the electric motor to the ball thread nut. The engine shaft (axle drive shaft) and the ball thread nut (driven shaft) are axle-parallel. The toothed belt drives for EPS applications consist of a

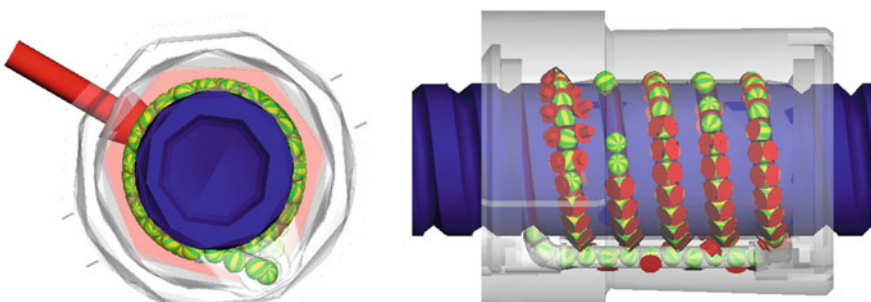
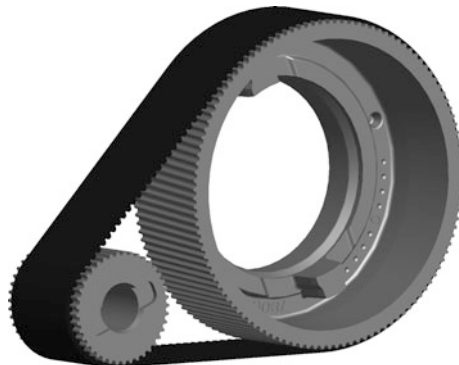


**Fig. 15.13** Multi-body simulation of ball screws for the inquiry of internal motion sequences. The simulation results serve as an early functional safety check

**Fig. 15.14** Timing belt gearbox of an EPSapa. The use of high-capacity treads and diagonal dovetailing allow for a better noise response



belt and two serrated pulleys, Fig. 15.14. The transmission ratio corresponds to the ratio of the diameters of the driven pulley  $d_2$  and driving pulley  $d_1$ :

$$i_{belt} = \frac{d_2}{d_1} \quad (15.4)$$

Current transmission ratios are in the range of 2–4.

Toothed belt drives belong to the shape-paired traction drives. The positive locking of the dovetailing between the belt and the serrated pulleys prevents slipping during the power transmission. At the same time, the necessary pretensions can be significantly reduced in comparison to other traction drives. Timing belts are also called synchronous belts, because of their synchronisation.

The free belt segments between the serrated pulleys are called empty span and tight span. The tension of the belt in the tight span is higher than its pretension when load is transmitted between the pulleys. At the same time, the belt tension in the empty span drops by the same amount. The belt always has to be loaded with a certain least tension, so that the belt is bedded trouble-free in the dovetailing of the serrated pulley. A correct belt pretension is vital for service life, noise response and good transmission of the belt. More noise can develop from amplified vibrations of the belt when its pretension is too low, see also Nagel (2008).

A basic sizing of toothed belt drives is stipulated by the standard ISO 5295 (1987). It can be used to approximately identify the required belt width for the safe transmission of the torque, as a function of the used belt tread, the power and the geometrical ratios of the gearbox. The detailed layouts that include the loading time as well, for example, have to be determined in close cooperation between belt and steering system manufacturers. The use of high-performance treads enables the highest power density, an energy-efficient transmission of motion and a better noise response. This can be further improved by diagonal dovetailing. The increased risk that, because of this, the timing belt might leave the serrated pulley has to be counteracted by means of flanged wheels.

High differences in temperature near the internal combustion engine and the resulting load of the timing belt may put tight constraints to the range of usable

belt materials. The temperature range of  $-40^{\circ}$  to  $+125^{\circ}\text{C}$  is a reason to use rubber elastomers as basis material of the timing belt. Fibreglass is used for the tensile member. It offers not only the best tensile strength but also low thermal expansion. Sinter materials are preferred for the serrated pulleys of modern standard EPS applications.

### 15.3.2 Electric Motor

#### 15.3.2.1 Overview/Comparison/Working Area

The power assist is supplied by the electric motor of the electromechanical steering system. It converts electric energy, fed in by the on-board wiring, into mechanical energy on demand. Sufficient power assist in all driving situations has to be provided through a good choice of the motor type and size. The electric motor is crucial for the steering feel and the driver's perception because of the direct mechanical connection to the steering wheel.

*Classification* (Lindner et al. 1999; Fischer 2006; Stölting and Kallenbach 2006) Electric motors can be classified by the type of motion as rotational engines and translational engines (or linear motors). Only rotational engines are used for EPS applications, because of easy configuration, high power density and uncomplicated control. They consist of a stationary stator and a swivelling rotor, concentric to the stator. Depending on how stator and rotor are arranged, they are further classified as internal and external rotor motors. The type of power feed distinguishes DC, AC, 3-phase and pulse motors. The three-phase AC motors, or polyphase motors, can be differentiated by the rev response of the rotor to the magnetic field of the stator as asynchronous and synchronous motors.

*Motor-power classes* Brushed DC motors with permanent magnets were originally used in the first EPS systems. They can be operated by a very easy control at the DC wiring of automobiles. The rising power demand of middle and large vehicle classes and the rapid development of microprocessor and inverter technology made brushless AC motors feasible, driven by a rectifier and field-oriented actuation.

*Operating range* The choice of a motor has to include the notion that a steering system is not operated at a steady nominal working point, for example, a steady rev or torque (cf. Sect. 15.4). A typical parking procedure with high steering forces has to be fed with the highest assistance force, up to a defined steering speed. The steering forces are much lower when driving, but then, higher steering speeds are required, e.g., for evasive manoeuvres.

Simply said, the operating range of an electric motor for EPS can be divided into a speed range with constant torque and another speed range with almost

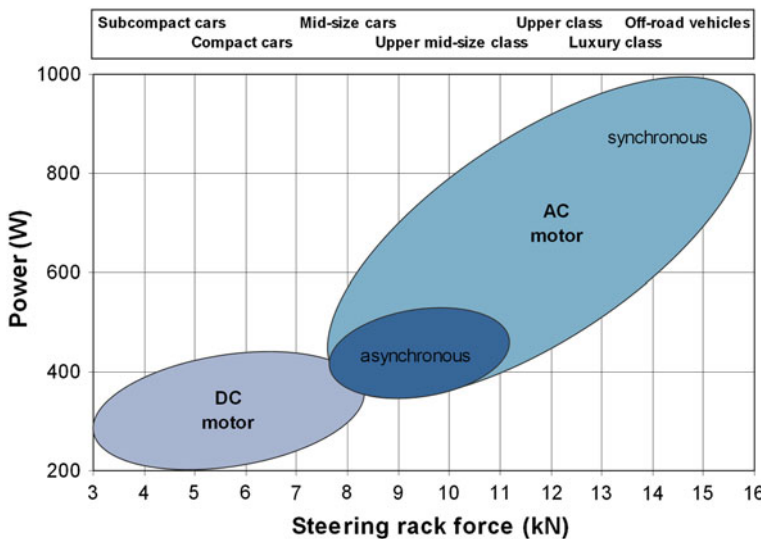


**Fig. 15.15** Sketch of the power demand of electromechanical steering systems to the electric motor and typical characteristic curves of current EPS motors

constant output power (Fig. 15.15). Taking a limited supply voltage and the highest permissible power consumption of the electric motor into account, some typical characteristic curves of motors of currently used EPS motors are shown in Fig. 15.15.

A comparison of the power demand with typical characteristic curves of motors illustrates the advantage of the 3-phase motors for the use in EPS, due to their wider speed range, achieved by field weakening (Stölting and Kallenbach 2006). The field weakening enables operating the motor above the nominal speed without having to amplify the input voltage or input power of the drive. The lesser available motor torque in the field weakening mode does not limit applications in electric power-assisted steering, because the required steering forces are dropping much at high steering speed.

Externally excited DC motors, permitting field weakening as well, are not used for EPS systems, because of their more complicated configuration and the still limited output power.

*Technical requirements* The main technical requirements for an electric motor for EPS systems are listed in the following:

- highest output power between 150 and 1,000 W as a function of the vehicle class (Fig. 15.16) to cover the peak capacity during parking and evasive manoeuvres.

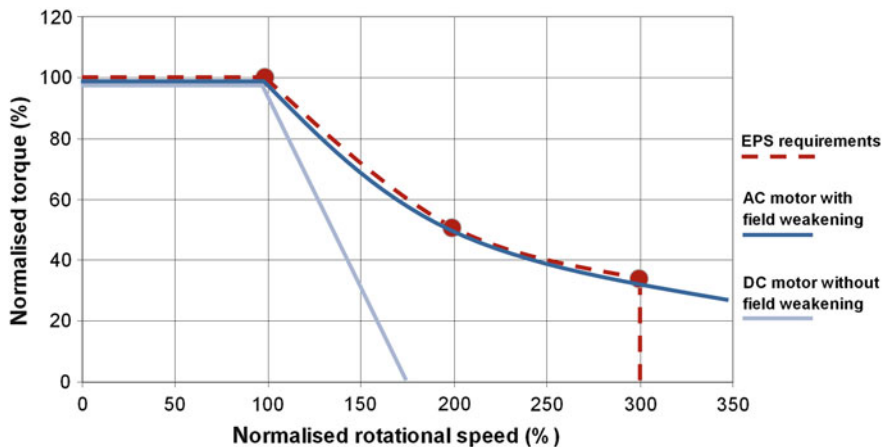


**Fig. 15.16** Operation range of different electric motors for electromechanical steering systems

- The highest output power has to be made available only briefly, because on average, steering forces are low and steering events are rare, so the longterm required output power is fairly low.
- wide operating range (M/n characteristic curve) with steady output power to supply high steering forces for parking and high steering speeds for evasive manoeuvres.
- very high power density and good efficiency, because the available space is small and the power from the on-board wiring is low.
- very high torques in the operation mode and low cogging torque to achieve a constant uniform steering force power-assist.
- very high engine dynamics serving a stable steering control, i.e. low electric motor response time and inertia.
- when using a PME engine: Special winding connections to prevent inadmissibly high brake torques from short circuits in the motor winding.
- quiet motor for a good acoustic response of the steering.
- solid configuration for the whole service life, because the steering is laid out as a maintenance-free system for the service life and no exchange of the motor is intended.
- low EMC disturbances to maintain reliable service of all electric vehicle systems, most relevant for mechanically commuting motors, because of brush sparking.
- high ambient temperatures, between +85 and +125 °C, according to installation place.
- high mechanical strength with regard to accelerations and vibrations.

### 15.3.2.2 DC Motor with Mechanical Commutator (see also Stölting and Kallenbach 2006)

The stator of mechanically commuting motors (DC motor) serves to generate a stationary magnetic field. This magnetic field can be generated either by permanent magnets or by a field winding (externally excited motor, inverse-speed motor, shunt-wound motor). The rotor consists of a core with grooves that accept the rotor winding. The power is supplied by a commutator/brush system which impresses the current as a function of the relative position of rotor and stator in such a way that a continuous rotation is the result. Therefore a mechanically commuting engine can be operated with DC power.

PME engines are essential for EPS systems, as discussed in Sect. 15.3.2.1. They can be actuated by very simply power electronics with two lines only, because of the absent field winding. The lack of a field weakness range is a disadvantage of this motor, because the PME DC motor to reach high revs is rather big. Since the motor torque is directly proportional to the impressed motor current, the torque control that is typical for EPS systems can be implemented with little control effort.

The rather bad cooling of the rotor windings and the high inertia of the rotor limit its use to low-power steering systems. The accessible power density of DC motors is lower than that of AC motors because of the loss and space demanded by the commutator. In addition, sufficiently low wear of the mechanical commutator/brush system and electromagnetic tolerance with the engine needs to be ensured (Fig. 15.17).

The motor housing is usually deep-drawn out of a simply sheet steel and contains a support for the engine shaft. Cheap hard ferrite is used for permanent magnets. They do not achieve the power density of rare-earth magnets like samarium-cobalt (SmCo) or neodymium-iron- boron (NdFeB). The magnets are glued or clamped into the motor housing and mechanically protected by an

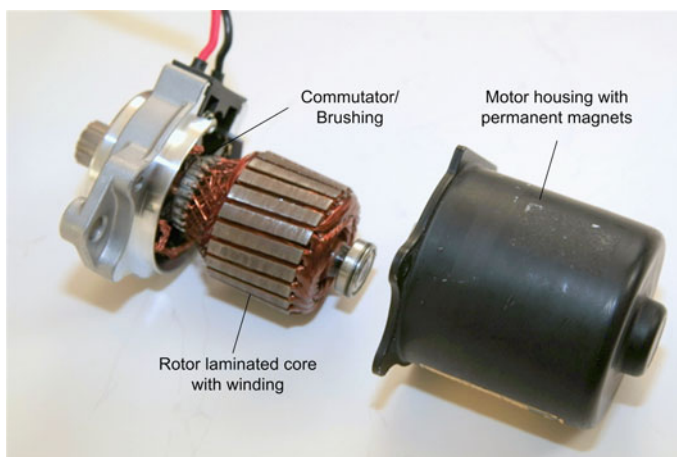


**Fig. 15.17** Typical EPS DC motor with mechanical commutator

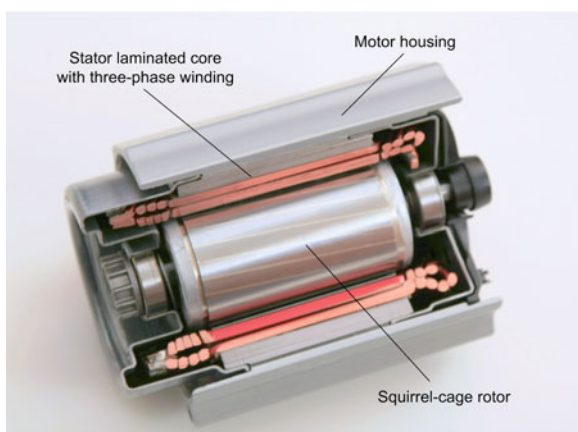
additional sheet-metal jacket. Motor housing and magnets represent the stator of the DC motor. The rotor consists of stacked and electrically isolated electric metal sheets to reduce iron loss from eddy currents and demagnetisation. To achieve low torque ripple and small cogging torques, the winding is distributed to as many grooves of a set rotor core as possible and connected to accordingly many commutator bars. The commutator is completed to a commutator/brush system with spring-supported carbon brush conductors. A cover bearing the brush system axially closes the motor housing. Typical DC motors for EPS systems are 4-pole engines with two or four carbon brush conductors and 22 commutator bars.

### 15.3.2.3 Asynchronous Motor

The asynchronous motor (ASM) is a three phase AC motor, distinguished by an extremely robust construction, high operational safety and high strain ability. This is achieved by the fact that the rotor is a squirrel-cage rotor, containing no additional parts like wire winding or magnets. A squirrel-cage rotor consists of conducting rods arranged in parallel with the shaft in a metal plate packet. They are short-circuited at the front by rings (squirrel-cage). The stator is usually equipped with a three-phase winding generating a rotating magnetic field. The rotating field induces currents in the squirrel-cage of the rotor which, obeying Lenz's law, counteract the source and therefore generate a torque on the rotor shaft (Fig. 15.18).

Due to the cooling of the stator winding and the ECU (piggyback ECU, cf. Sect. 15.3.4.1), a solid casting housing is used for the housing of the asynchronous motor shown above. The core with the stator winding is arranged inside. The three-phase winding is made of solid copper wire for a very robust motor construction, distributed across the perimeter of the motor. The rotor also contains a core, to reduce the eddy current loss. Aluminium moulded in its grooves make for the squirrel-cage. The air gap between stator and rotor has to be kept very small in this design, to achieve a low demand for a magnetisation current, hence, high

**Fig. 15.18** Configuration of a robust asynchronous motor



efficiency. This often leads to narrow manufacturing and assembly tolerance margins.

Asynchronous motors with squirrel-cage rotors cannot operate as generators, because of the missing magnetic excitement from a stator's magnetic field. Hence, no additional safety measures to shut down the motor power have to be included into EPS systems. The safety concept is much easier. Lacking a magnet, the motor is also marked by low torque fluctuations and is very quiet. Compared to mechanically commuting DC motors, asynchronous motors with higher current and power have a higher power density. In contrast to DC motors with permanent magnets, asynchronous motors can be operated with field weakening.

#### 15.3.2.4 Synchronous Motor

Like asynchronous motors, synchronous motors belong to the group of three-phase motors, operated with sinusoidally powered three-phase windings. The rotor consists of stratified electric metal sheet and serves to generate a magnetic field which is independent from the stator power. EPS motors apply permanent magnets for that (PME synchronous motor/PMSM). This permanent, non-inductive magnetic rotor causes the rotor to turn synchronously to the applying stator magnetic field, hence, the name synchronous motor.

Publications use the terms, brushless DC motor (BLDC) or electronically commutated motor (EC). This kind of motor is driven not by sinusoidal but by block-shaped currents. Including integrated power electronics and power sensors, it is used, for example, as a self-controlled engine for actuator drives in the automotive industry. It can be operated with DC power. Since an ideal, rectangularly impressed current does not exist in reality and the distribution of the magnetic flux density would have to be very high, these motors have a rather high torque ripple. Hence, only PMSMs with sinusoidally impressed current are used, for current electric power-assisted steering (Fig. 15.19).

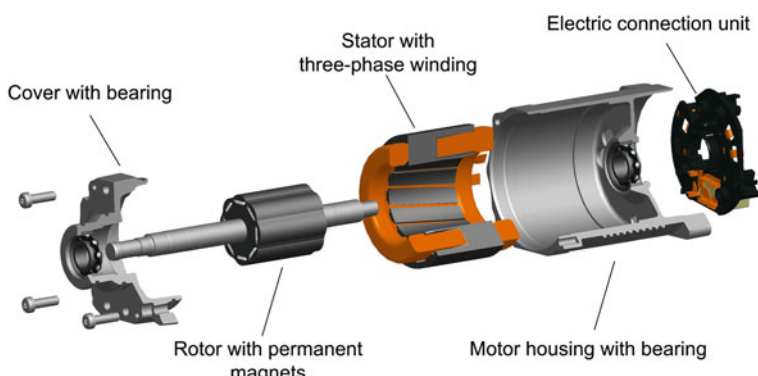


Fig. 15.19 Configuration of a synchronous PME motor (exploded view, cut in parts)

The stator of a synchronous motor is basically identical to that of the asynchronous motor. Instead of a distributed winding, a concentrated single-tooth winding is preferred for EPS systems. The spatial separation of different windings and corresponding connections help to avoid short circuits, reducing brake torques that might occur in the generator mode. Additional measures may be taken to disconnect the motor currents in a fault case, such as phase or star point separation, according to motor-power class and vehicle response.

Power drains and torque disturbances due to circular currents in the motor windings can be avoided by connecting synchronous motors in star-connections. The windings are distributed into different stator grooves. The stator grooves and the number of rotor poles define the motor topology. 6-, 8- and 10-pole engines with 9 to 12 stator grooves are often used for electric power-assisted steering.

Highly energetic rare-earth magnets of neodymium-iron-boron (NeFeB) are used as magnetic materials for the rotor. These are inserted in a very sturdy configuration as block magnets, either in individual bags of the core (embedded magnets) or on the surface of the rotor core as ring or segment magnets. Motors with surface magnets have an additional sleeve over the rotor to prevent the brittle magnets from splitting off (Fig. 15.20).

Because the motor torque of a synchronous motor depends on the strength of the stator and the rotor magnetic field and their enclosed angle, the machine is very well suited for field-oriented motor actuation. This allows driving the machine very precisely and dynamically. Modern synchronous motors can be operated in field weakening mode if the magnets are sufficiently powerful, hence, above the nominal speed. They supply the steady output power which is typical for steering applications across a very wide speed range (Sect. 15.3.2.1; Fig. 15.21).

Compared to the asynchronous motor, the PMSM is marked by a higher power density and better efficiency. A main source of losses are the ohmic stator losses which can be drained by the stator metal-sheet package and the motor housing. The synchronous motor has a lower rotor moment of inertia than DC and asynchronous motors. A chamfer of the rotor or stator helps to reduce the cogging torque to a level which is fitting for EPS systems.

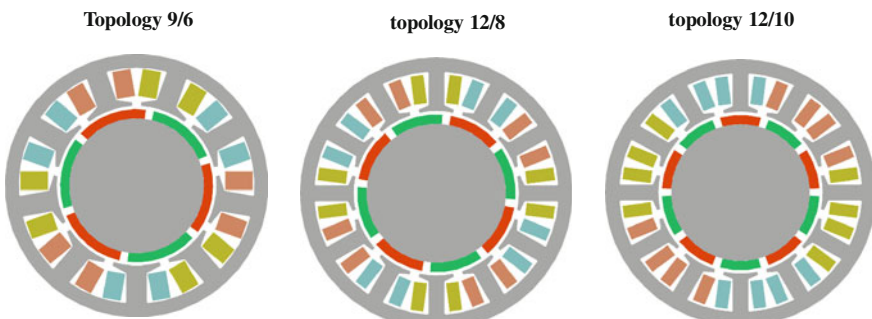


**Fig. 15.20** Motor topologies of PMSMs

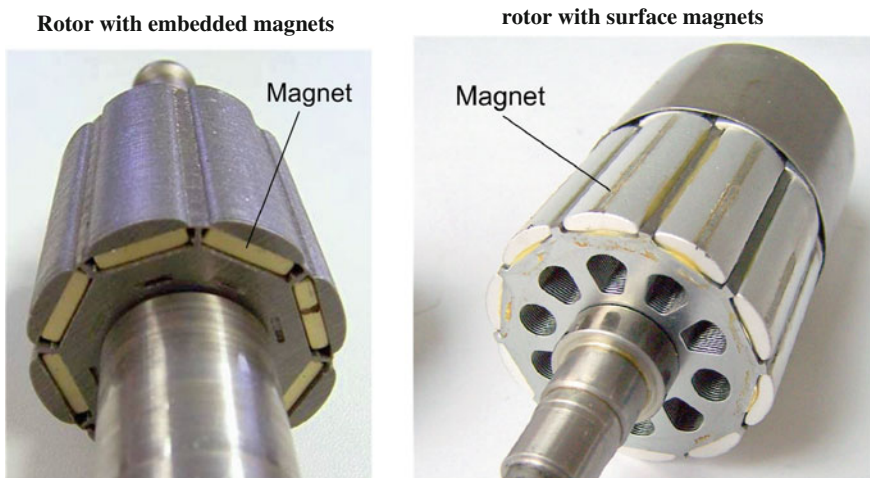


**Fig. 15.21** Rotor configurations of PMSMs

### 15.3.2.5 Position and Rev Sensors

If a DC motor with a mechanical commutator is used, no position or rev sensors are required for the actuation, because the individual motor windings are fed by the commutator.

Field-oriented actuation of polyphase motors is common, as it permits a very dynamic motor operation in a wide speed range. It needs additional sensors for the proper impression of the stator's currents and its magnetic field. The rotor speed is used for the field-oriented actuation of the synchronous motor and the rotor angle for that of the asynchronous motor.

#### *Technical requirements*

- without servicing or wear, therefore, touch-free measuring principle
- high resolution and accuracy
- high temperature range of  $-40$  to  $+85$  °C (interior) or  $-40$  to  $+125$  °C (engine compartment)
- high serviceable life and service life
- high reliability/availability, hence, redundant electronics for diagnostics capacity are common
- small size, easy configuration and assembly
- sturdy measuring principle with regard to fouling, vibrations, EM compatibility

Two different sensor designs for the position and speed sensors of polyphase motors have prevailed.

**Resolver** A resolver consists of a field winding and usually two receiver windings, enabling measuring the angle of a swivelling shaft. Exciter and receiver coil are magnetically coupled by a swivelling structure. The measuring principle is based

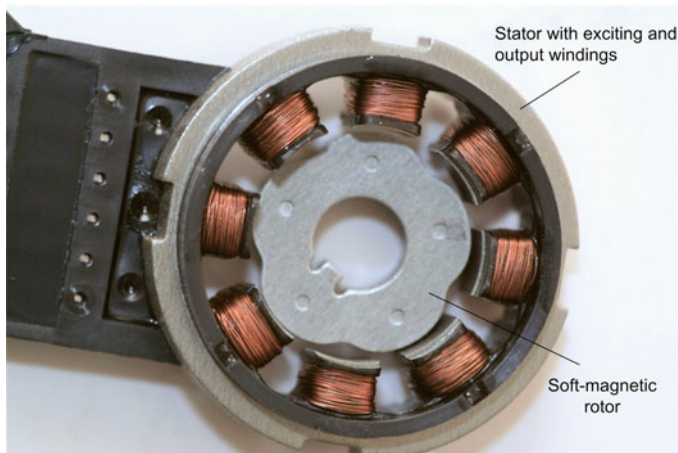


**Fig. 15.22** Configuration of a reluctance resolver for EPS systems

on the induction law and consequently works with alternating voltages and currents for excitement and analysis. The classical resolver has a rotating field winding and is supplied with power by brushes and slip rings. The receiver coils are turned by  $90^\circ$  and fixed in the case.

Modern resolvers of steering applications have field winding and receiver windings arranged on the stator. This allows measuring angles contact free and without electric signals supplied to the resolver shaft. The magnetic coupling that can be changed by the rotary angle is generated by a special soft-magnetic rotor structure (reluctance resolver) (Fig. 15.22).

In contrast to magnetic measuring principles, the absolute measuring range of a resolver can be adapted by a suitable stator and rotor configuration. The sensors can be adapted to the number of terminals of the used motors so that there is a higher angular resolution serving as input signal of the field-oriented actuation. The inductive measuring principle makes the resolver resistant against interferences by external stationary magnetic fields. They are suited for transmitting signals across medium distances (standalone ECU) and need no magnet material. In a favourable configuration, the rotor is squeezed as a core onto the engine shaft. The rather complicated electronics and signal analysis is unfavourable, because the carrier-frequency method needs a special demodulation. The rather complicated configuration of resolvers with stator carrier, wire-wound coils and rotor core needs a rather wide space. They are often more expensive than magnetic measuring principles.

**Magnetic angle sensors** The basic principle of a magnetic sensor is based on a permanent magnet generating a stationary magnetic field. This magnetic field passes one or several parts that are dependent on a magnetic field. Angle sensors

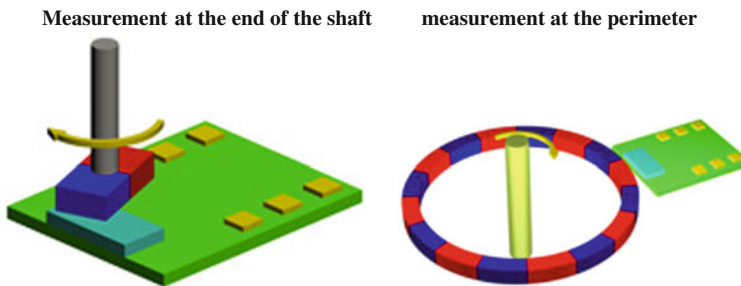


**Fig. 15.23** Measuring arrangements of magnetic sensors for position and rev measurement (Source Internet Sensitec)

are made by setting a transducer magnet on the shaft to be measured, for example, on the engine shaft, and arranging magnetic field sensors axially or radially.

Two different plans for EPS systems are in use. For measuring at the end of the shaft, a 2-pole magnetic tablet is used, for the perimeter measurement, a magnet ring (Fig. 15.23) is applied.

A measurement at the end of the shaft is preferred if the ECU is axial to the engine (cf. Sect. 15.3.4.1). This arrangement is favourable due to its compact package, because the evaluation sensors can be integrated into the EPS-ECU. No other parts like sensor case or electric connections are required.

The transducer magnetic field is analysed by Hall or magneto-resistive sensors. From an application perspective, the most important difference is the physical quantity that is measured.

The Hall sensor is based on a magnetic flux density measurement, i.e. the intensity of the magnetic field is recorded. A magneto-resistive sensor, on the other hand, measures the magnetic field curve, i.e. the orientation of the magnetic lines of the flux (MR sensors, Zabler et al. 2001). This dependence on the direction of the magnetic transducer field often suggests the MR sensors as the favoured solution, because the measuring accuracy does not depend on the absolute magnetic field strength and, hence, is independent of many parameters like temperature, ageing and mechanical tolerance margins.

A disadvantage of the widespread anisotropic magneto-resistive angle sensors (AMR) is the unambiguous measuring range of only  $180^\circ$ , because only the position of the magnetic field can be measured, but not its orientation or polarity. Hall sensors provide an unambiguous measuring range of  $360^\circ$ , but compared to MR sensors, they need a more sophisticated signal analysis and compensation for a precise measurement of the angle, because the mentioned parameters affect the measurement result. In future EPS applications the Giant MR effect might substitute the current AMR sensors, as it allows measuring an unambiguous angle for the full range of  $360^\circ$ .

### 15.3.3 Torque Sensor

#### 15.3.3.1 Requirements/Classification

One of the most important measured variables of EPS systems is the steering wheel torque initiated by the driver. It is measured at the input shaft of the steering system. Based on the measured steering torque, the required power assist is identified by the steering functions and control; the EPS motor supplies it to the driver. The quality of the steering torque measurement has an impact on the attainable steering feel, because the driver perceives it directly. Beside the functional requirements for measuring accuracy and resolution, the steering torque has to be measured with absolute reliability. Otherwise, if the measurement was faulty, the EPS motor might be unintentionally actuated and initiate an uncontrollable steering event.

The most important technical requirements for torque sensors of modern EPS systems are listed in the following:

- utmost reliability
- active torque measuring range of approx.  $\pm 10$  Nm
- high signal resolution and measuring accuracy
- high measuring dynamics and signal processing with little delay
- high serviceable life and service life
- interference-resistant, diagnostics-capable interface to the ECU
- temperature range  $-40$  to  $+85$  °C for interior applications (EPSc) and  $-40$  to  $+125$  °C for engine compartment applications
- Resistant to fouling, vibrations, wear.

The torque sensors can be classified by their mechanical configuration as sensors with or without mechanical torsion rod. The torsion rod of torsion-afflicted sensors convert the torque measurement into an angle measurement. The typical stiffness of a torsion rod in modern EPS systems is between 2 and 2.5 Nm per degree of torsion angle ( $2$  – $2.5$  Nm/ $^\circ$ ). The highest torsion is limited by a mechanical entrainment to  $\pm 5^\circ$  for the protection of the torsion bar.

Torque sensors can also be classified by the basic measuring effect, differentiating between measurement of the torsion angle, the surface strain and the torsion load.

Current EPS systems apply only sensors with torsion rod, because they permit high-precision and interference-resistant torque measuring. The following section will therefore discuss sensors with torsion rod first, then [Sect. 15.3.3.3](#) will specify the motivation and limits of the torsion-resistant torque measurement.

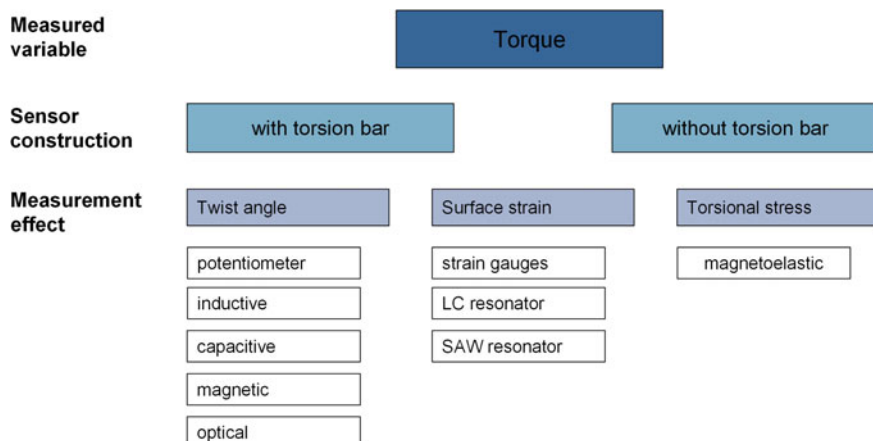
### 15.3.3.2 Sensors with Torsion Rod

Figure 15.24 shows an extract of potential principles to measure the steering torque in EPS systems. Sensors with torsion rod apply a great number of potentiometric, inductive, magnetic and optical sensors.

*Potentiometer measurement* The first EPS applied only potentiometer sensors which are very cheap because of their widespread use in industrial products and their simple configuration. These sensors are used only for low-cost systems in the compact car segment now. The main reason is that the measurement value may be blurred by wear of the not contact-free measuring principle, the limited mechanical loading capacity and the sensitivity to dirt.

The measurement is based on a slider potentiometer establishing an electrically conductive track by a sliding contact. The ‘measuring’ and, therefore, the electric resistance change as a function of the slider’s position on the resistance track. For safety reasons, torque sensor applications in EPS systems apply at least two resistance tracks and several parallel sliding contacts for the signal feed. The resistance tracks are made of conductive plastic and the sliders are shaped like brooms to reduce the wear.

A benefit of the potentiometer measurement is the ratiometric analysis. The measurement is independent of the absolute resistance value and temperature interferences. Moreover, the potentiometer measurement supplies a sufficiently big measuring effect, so that no additional amplification and processing of the signal is required. That’s why the temperature requirements are unproblematic. Some potentiometer torque sensors for EPS systems include an angle measurement to identify the current steer-angle.



**Fig. 15.24** Overview of fundamental measuring principles to measure the steering torque of EPS systems

Unavoidable wear and the resulting blur of the measurement values limit modern potentiometer torque sensors to an accuracy of  $\pm 3\%$  over their service life.

*Inductive sensors* Inductive sensors are a type of magneto-dynamic sensors, because the basic effect assumes an alternating magnetic field. The main advantage of the inductive measurement is its insensitivity against external media like dirt, oil and water. Inductive sensors can be reliably operated in adverse surroundings. That's why inductive sensors have chiefly prevailed for industrial measuring tasks, beside the potentiometer sensors. They are supplied in many different configurations and measuring arrangements (Zabler et al. 2001).

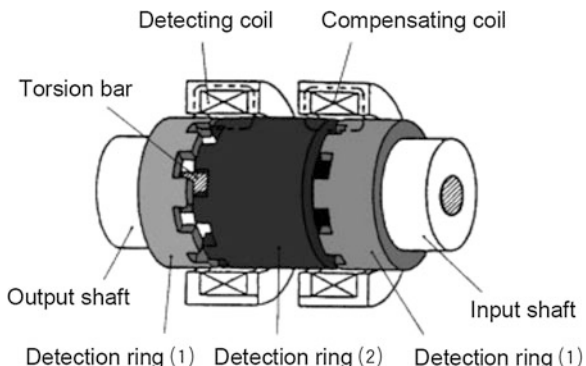
An example of torque measurement in steering systems is given by the measuring arrangement in Fig. 15.25.

The sensor is based on a system of coils which is driven by an oscillator. The voltage induced in a coil changes as a function of the torsion angle of the torsion rod. A first coil is arranged over two soft magnetic rings. Each ring is mechanically connected to an end of the torsion rod (Fig. 15.25 Detecting coil). Both rings have distinctive cogs along their perimeters. The effective air gap between both rings changes as a function of the turning of the cogs against each other. This alters the impedance of the coil and changes the voltage induced in the coil. A second coil (Fig. 15.25 Compensating coil) is used because the coil impedance depends on other parameters which are in turn dependent on temperature, for example. The compensating coil is arranged over a magnetic circle that is independent of the torsion angle and supplies a reference voltage which is subject only to ambient conditions and facilitates a compensation of various parameters.

The sensor configuration with wire-wound coils discussed above is complemented by inductive measuring systems with planar coils (Fig. 15.26). Suitable conducting paths on a board create transmitter and receiver coil. The rotor consists of an electrically conductive material and provides the magnetic coupling between transmitter and receiver coil.

An alternating current generates an alternating magnetic field in the transmitter coil which passes the rotor, inducing an alternating current. This rotor current leads

**Fig. 15.25** Example configuration of an inductive torque sensor for EPS systems [Source Internet Koyo (Yoshida 2002)]



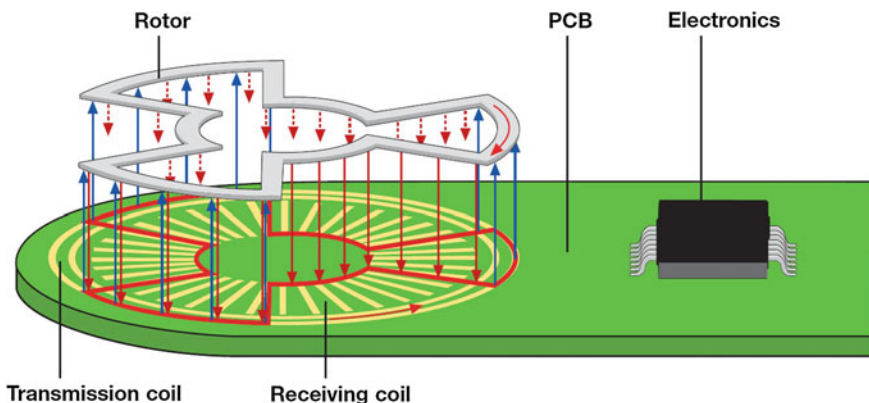


**Fig. 15.26** Example configuration of an inductive measuring principle with coils made of conducting paths (Source Internet Hella 2014)

to another electromagnetic field which induces a voltage in the receiver coil. The special shape and position of transmitter coil, rotor and receiver coil make the electromagnetic coupling between transmitter and rotor independent of the rotor's position, while the feedback from rotor to receiver depends on the rotor's position.

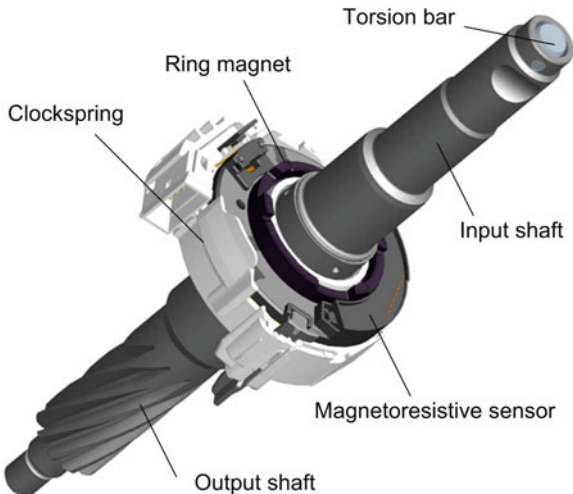
One transmitter and two receiver coils are commonly needed. If the voltage induced in the reception coils is compared to the source voltage (ratiometric signal analysis), the measurement is mostly independent of temperature and insensitive to mechanical tolerances. Such processes need no separate compensation coil and distinguish themselves by an easy configuration.

*Magnetic sensors* Unlike inductive sensors, magnetic sensors apply a static magnetic field which is generated by a permanent magnet and passes one or several sensor elements that are dependent on the magnetic field. As discussed in Sect. 15.3.3.1, the torque of sensors with torsion rod is determined by an angle measurement, hence, the same measuring effects can be exploited as in the magnetic angle measurement (cf. Sect. 15.3.2.5). The same qualities and choice criteria apply for useful magnetic sensors as for the magnetic angle measurement. For this reason, Hall and MR sensors have prevailed on the market for magnetic torque sensors.

The lower absolute angle measuring range of the MR technology ( $180^\circ$ ) in comparison to Hall measuring ( $360^\circ$ ) is no restriction for the application as a torque sensor, because for the applied torsion bars only a small torsion angle range has to be measured.

When a torsion bar with  $2 \text{ Nm}/^\circ$  and a measuring range of  $\pm 10 \text{ Nm}$  is used, an angle measuring range of  $\pm 5^\circ$  is required, for example. The torque measuring range may be modified by the applied torsion bar or by the number of poles of the transducer magnet.

**Fig. 15.27** Magnetic torque sensor with direct difference angle measurement by ZF Steuersysteme



In EPS applications, two basic measuring arrangements of magnetic sensors are currently used. The first configuration measures the torque directly via the difference angle of input and output shaft. Figure 15.27 shows that a multipolar magnet ring is set on one side of the torsion bar, and a magneto-resistive sensor is placed opposite of it and connected to the other end of the torsion bar.

This arrangement is favourable because of the immediate measurement by sensors in the torsion rod. Mechanical parts and assembly tolerances that might affect the measurement result are reduced to a minimum. If magneto-resistive sensors are used to measure the magnetic field, high-resolution and high-precision torque sensors can be built because of the typical field direction measurement (cf. Sect. 15.3.2.5) and ratiometric signal analysis. This depends very little on extraneous factors like temperature and ageing. The electric contacts of the sensor element, that is rotating in a steering event, is established by a clockspring whose length depends on the steer-angle range. During assembly, attention is paid so that the clockspring cassette remains in neutral position until the steer-angle is limited by the steering system to avoid any damage or tear. For that reason, a different configuration of a magnetic torque sensor without clockspring has been established.

The magnetic torque sensor without clockspring uses a magnet ring as a transducer magnet as well. However, the sensor elements for measuring the magnetic field are fixed in the case. A soft magnetic flow conductor couples transducer magnet and sensor element (cf. Fig. 15.28).

The flow conductor consists of two parts which are concentrically arranged over the transducer magnet and connected to one end of the torsion bar. The transducer magnet is right on the other end of the torsion bar. The position of the flow conductor relative to the transducer magnet and, therefore, the magnetic flux density in the flow conductor changes as a function of the applying torsion bar

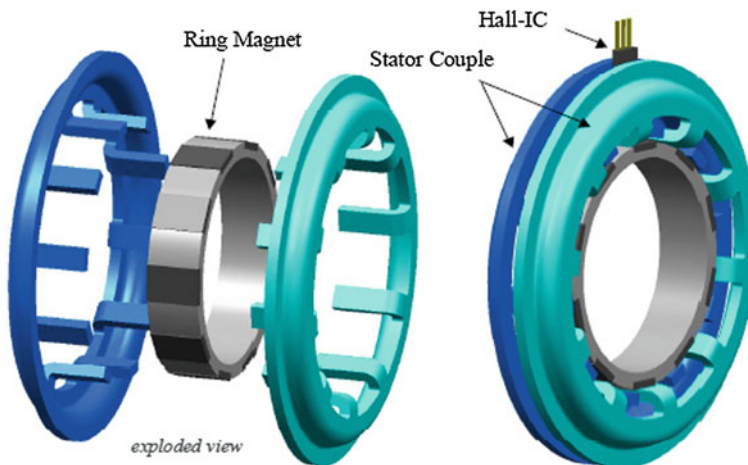


**Fig. 15.28** Magnetic torque sensor without clockspring for electric contacts (Jerems et al. 2004)  
(Source Valeo 2004)

torque. The flux density is measured by Hall sensors which are arranged at the perimeter between both parts of the flow conductor.

The process is based on an absolute measurement of field strength or flux density. Hall sensors and transducer magnets that can be calibrated and compensated for ambient temperatures are therefore required. The influence of parts and assembly tolerances on the measurement result can be reduced because the concentric magnetic field is accepted by the flow conductors across the full perimeter of the transducer magnet (integrating measurement). By comparison, the MR technology discussed before is a measurement of the magnetic field at a specific point. A high measuring accuracy with low hysteresis is achieved when during the design of the magnet circle close attention is paid to the choice of a soft magnetic material with low remanence and to a precise adjustment of the transducer magnet when the sensor is assembled.

*Optical sensors* Optical sensors consist of a light-emitting and a photosensitive component. Both parts are separated by a suitably structured component. The luminous flux from transmitter to receiver is influenced by the torsion angle of a torsion bar. A common configuration of optical sensors are incremental encoders, often used in automation for high-precision positioning tasks.

The optical measuring principle means that the sensors are very insensitive against electromagnetic disturbances (EMC). Filigree code disks and optical structures help to gain very high resolution. However, due to the very harsh conditions, and because of their sensitivity to dirt and limited mechanical load capacity, these sensors can only be used in limited circumstances. Moreover, such sensors supply only pulses for source signals which may be added up to a relative information on the angle. Such incremental sensors are not suitable as torque sensor,

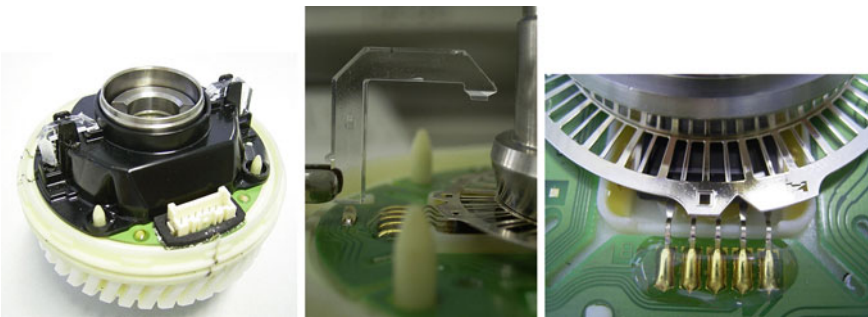


**Fig. 15.29** Optical torque sensor for EPSc systems (TRW)

because the angle difference of the torsion bar across the desired torsion range has to be unambiguously identified. Hence, the light intensity between transmitter and receiver is varied and evaluated with absolutely measuring sensors by one or more code disks. The following series of figures shows such a sensor (cf. 15.29).

The luminous flux generated by an LED is conducted by a fibre-optic light guide and two lead-frame plates, arranged over a torsion rod to an integrated photo-diode array.

The sensor in Fig. 15.29 is partially redundant, it has two independent optical measurement modules. Optical torque sensors are used only for EPSc systems at the moment because of the limited temperature range of optical semiconductor parts and the general sensitivity to dirt.

### 15.3.3.3 Torsion-Resistant Sensors

An important factor for a good steering feel is the stiffness of the complete steering driveline, between steering wheel and the guided wheels (cf. Chap. 3). A too low stiffness is often perceived by the driver as an inert and imprecise steering response, leading to frequent steering corrections. A too high stiffness may mean that impacts at the wheels, for example from bumps on the road, can be transferred undamped to the steering wheel. EPS systems currently tend towards a torsion bar stiffness of above  $2 \text{ Nm/}^\circ$ . Assuming a constant measuring range for the torque measurement, this leads to lower torsion angles and, hence, to higher requirements for the absolute resolution and accuracy of the used sensor measuring principle (angle measurement by torsion rod). For these reasons, many concepts and patents deal with the torsion-resistant torque measurement for EPS.

Classical strain gauges, as they are used in industrial measurement for measuring torques, are no option for EPS systems. Due to the fact that the filigree resistance foils are glued on the measurement shaft, which is unsuitable for large series production, and the often troublesome calibration needed, other solutions are researched.

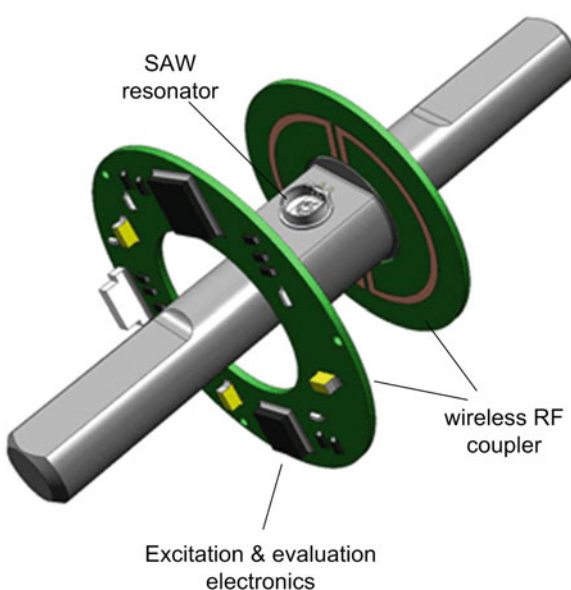
A measuring system which is also based on a surface strain of the measurement shaft is called Surface Acoustic Wave (SAW). The basis of the measuring principle are SAW resonators. One such resonator consists of metal electrodes on a piezoelectric substrate (quartz). Operated with an alternating voltage of suitable frequency, the piezoelectric substrate generates a mechanical vibration which spreads out along the material surface. External forces, e.g., from strain and compression lead to a change of the resonator frequency. The frequency change is therefore a direct measure of the applying torque. This process is sometimes used to control the tyre pressure of cars (Fig. 15.30).

A measuring principle which measures not the surface strain, but the mechanical load at the measurement shaft, is based on the magneto-elastic or magneto-strictive measuring principle. The altering magnetic field of a ferromagnetic shaft is measured here under torsional load (Fig. 15.31).

The magneto-elastic measuring sensitivity of common steels is very small. A sufficiently amplified measuring sensitivity can be achieved in some processes by also permanently magnetising the measurement shaft. Yet the sensitivity of a steering torque measurement is much lower than that of current torsion-afflicted sensors and requires additional insulation.

Another big challenge is to achieve a high measuring accuracy, in particular following the overload torque specified in Sect. 15.3.3.1. That is because overload protection by mechanical limitation of the torsion angle is not available. Hence, both described torsion-resistant processes suffer currently a wide hysteresis following an overload torque, which results from the measuring principle.

**Fig. 15.30** Design of an EPS-torque sensor based on a surface strain (Source Internet Transense Technologies)



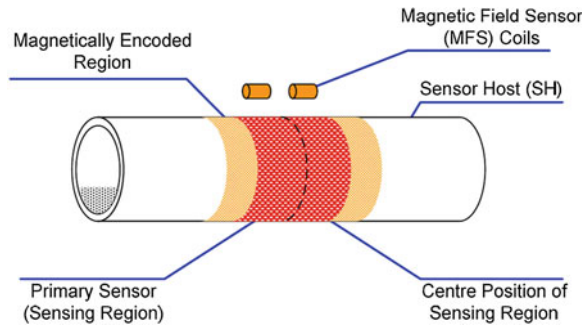


**Fig. 15.31** Simplified measuring configuration of a magneto-elastic torque sensor (*Source Internet NCT Engineering*)

### 15.3.4 ECU

ECUs for EPS basically include signal-processing electronics, to compute the currently required power assist, and power electronics, to feed the electric motor accordingly (Fig. 15.32).

Interior and engine compartment ECUs are distinguished by their location on-board. The following table lists the most important requirements for EPS-ECUs (Table 15.1).

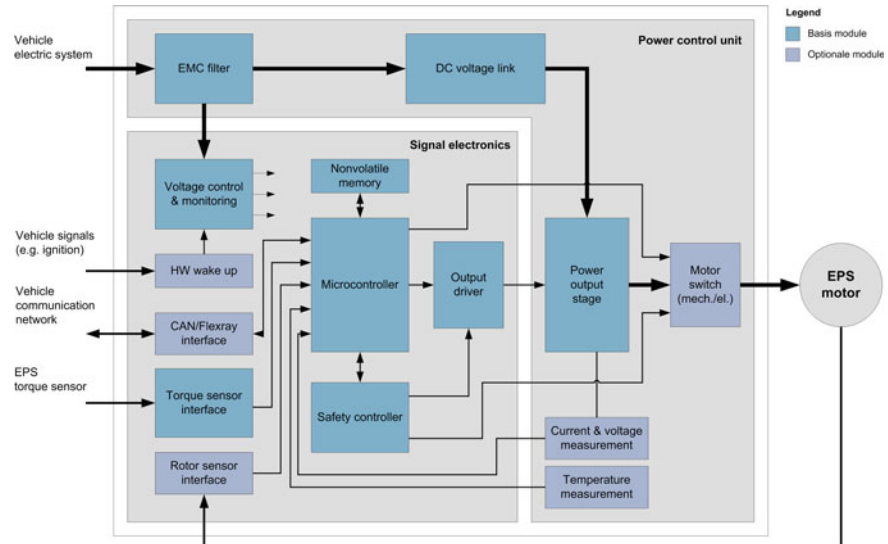


**Fig. 15.32** Simplified block diagram of an EPS-ECU consisting of signal electronics and power electronics

**Table 15.1** Requirements for EPS-ECUs for interior and engine compartment

On-board location	Interior	Engine compartment
Typical supply voltage	9–16 V	
Maximum closed-circuit power consumption	<250 µA	
Typical operating temperature	–40 to 85 °C	–40 to 125 °C
Thermo shock with flood water	No	Yes
Sealing requirements	IP5K0 dust-proof, no water protection	IP6K9 K dust-proof, jetting-resistant
Ambient resistance	Damp heat	Salt spray
Media resistance	No, only in special cases	Yes, different reagents
Mechanical vibrations	10–20 m/s <sup>2</sup> for body-mounted parts	
Mechanical shock	300–500 m/s <sup>2</sup> for body-mounted parts	
Electromagnetic tolerance	Immune against disturbances/irradiation. No interfering electromagnetic radiation Applied standards (excerpt): • Conduction disturbances ISO 7637 • Irradiated disturbances ISO 11452 • Radio disturbances IEC CISPR25	

### 15.3.4.1 Designs

ECUs are preferably arranged close to the EPS motor, to keep electric loss as low as possible (piggyback ECU). Internal loss develops in the connecting lines between the ECU and the electric motor of the EPS, they rise with increasing length of the line. The number and configuration of the electric contacts, as for example the plug-in connectors, have to be considered in computing the distribution loss as well.

The low level of distribution loss renders the piggyback ECU the common solution for any medium or high power rack-and-pinion power steering.

EPSc systems of the compact car segment may also apply standalone ECUs because of low power demand and limited space for installation. They are not arranged right at the steering but connected to the electric motor by lines of about 1 m in length.

Another drawback of standalone ECUs beside the mentioned distribution loss is the often too complex wiring of the motor and sensor connections. Additional parts like plugs and cable connections have to be used. Sometimes, additional measures are necessary to electromagnetically insulate the motor lines.

Figure 15.33 shows a piggyback ECU with axial mounting at the electric motor and internal electric connection.

High-current connections between electric motor and ECU can be made because of the axial mounting of the ECU, either by plugging, insulation-displacement connectors or welding. The position and rev sensors required in three-phase motors (cf. Sect. 15.3.2.5) can be integrated on the circuit board of the signal electronics, to achieve a measurement that is highly precise, immune to

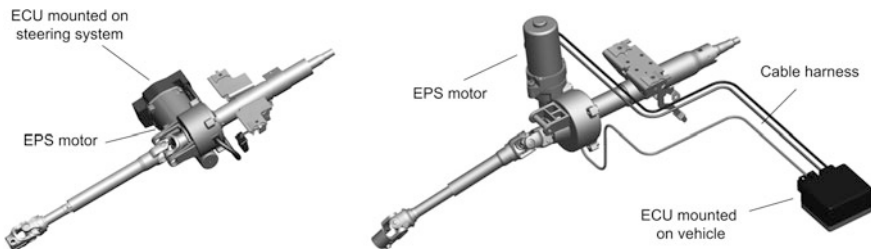


**Fig. 15.33** Typical configurations of an EPS-ECU as piggyback (left) or standalone version (right)

**Table 15.2** Current circuit boards for EPS-ECUs and their qualities

	Printed circuit board (PCB)	Thick film copper (TFC)	Isolated metal substrate (IMS)	Directly bonded copper (DBC)
Carrier material	Epoxide resin	Ceramics	Aluminium	Ceramics
Conducting material	Copper	Copper/silver paste	Copper	Copper
Conducting thickness (μm)	35–400	15–200	35–300	200–400
Electric conductivity	High	Low	High	High
Thermal conductivity	Low	Very High	High	Very High
Coefficient of expansion	High	Low	High	Low
Current load capacity	Medium	Medium	High	Very High
Mounting varieties	SMD, THC, on both sides	SMD ‘bare-die’	SMD	SMD, bare-die
Integration density	Medium	High	Medium	High

*SMD* Surface Mounted Device

*TFC* Thick Film Copper

*THC* Through Hole Component

*bare-die* Semiconductor component without case/unpackaged chip

interference and cheap. The axial mounting of electric motor and ECU is complemented with a radial mounting, common for EPS piggyback ECUs (Table 15.2).

Ceramic carrier materials and metal substrates are used as circuit boards of modern EPS systems, beside the conventional printed circuit technology on the basis of epoxy resin (e.g., FR4). Individual circuit boards and external ECU connections are usually connected by punched copper rails (lead-frames), moulded in plastic. Wire-bonding or laser welding establish the contacts between lead-frame and circuit board.

### 15.3.4.2 Signal Electronics

The signal electronics compute the power assist required in the current driving situation. The required sensor signals are read, made plausible and used to compute the power-assist torque of the EPS motor by means of control algorithms discussed in Sect. 15.6. A motor control generates the actuating signals of the power electronics from the requested power-assist torque.

Recent EPS-ECUs communicate with other vehicle control systems, like the Electronic Stability Programme (ESP) or the vehicle diagnostics, by bus systems. The CAN-bus, used in chassis applications most often with transmission rates of 500 kBit/s, is complemented with the Flexray bus, enabling transfer rates of up to 10 MBit/s. This interface helps to read data on the driving condition, as, for example, vehicle speed and steering wheel angle, and external steering interventions are set, for example, by the driver assistance systems.

The core of the signal electronics are modern micro-controllers with CPU, RAM, ROM and additional periphery like AD converters, timer unit and serial and parallel interfaces (Beierlein and Hagenbruch 2004; Table 15.3).

The micro-controllers are programmed in C, including some special program directives for automotive applications (MISRA-C Rules 2004). Real-time operating systems acc. to the OSEK/VDX standard may be used for the sequence control of functions, also providing services for network management and communication.

The power electronics are actuated by highly integrated electric switching circuits (ICs). They convert the pulse-width modulated signals (PWM) of the micro-controller into voltages that may serve to control the power semiconductor. Moreover, they provide all the required supply voltages and often include signal amplifiers to measure the motor power and functions to protect the power semiconductors.

Beside the steering functions, various fault detection and shutdown measures are implemented in the signal electronics. They monitor the correct function of all the subassemblies, and in the event of a fault, the system is set into a safety mode (see Sect. 15.5). The state-of-the-art is to monitor the correct programme processing of the micro-controller by the second independent safety controller. It can be either another micro-controller (mostly 8 bits) or an application-specific

**Table 15.3** Recent micro-controller characteristics of EPS

	Low performance EPS	High performance EPS
Architecture	Single $\mu$ C with 8/16 bits	Single $\mu$ C with 16/32 bits
Stroke (MHz)	16–32	32–128
Arithmetics	Integer	Integer and floating point
ROM (kByte)	16–32	256–1,024
RAM (kByte)	0,5–2	10–60
A/D converter (bit)	8	10/12
Interfaces	No	CAN or Flexray

integrated circuit (ASIC). Continuous monitoring checks the main computer for its time response and the contents of its arithmetic results. Other safety measures in the ECU are, for example, the monitoring of all the internal supply voltages and sensor signals and the issued actuation signals of the power output stage. In a fault event, the main controller and the safety controller can operate the electric switch-off channels (see Sect. 15.5.2.4). A switch-off channel can be a motor relay, for example. Upon a fault event, the power flow can be interrupted in the power electronics or in the e-motor to avoid unintentional brake torques by PME motors.

A fault management integrated into the software controls the registering, processing and storage of fault events. Any registered irregularities are identified and evaluated and suitable remedies are initiated. The remedies depend on the severity of the fault and may range from switching to redundant signals via switching off individual functions to shutdown of the complete power-assistance. The registered events are stored in a non-brief data memory, including a unique designator, for the subsequent vehicle diagnostics.

### 15.3.4.3 Power Electronics

The task of the power electronics is the control of the energy flow between on-board wiring and EPS motor. According to the motor-power class, modern EPS systems may feature amps of up to 170 A. The DC wiring makes voltage DC-links obligatory. First, the input voltage and the input current are filtered by inductances and condensers are filtered to meet the strict EMC requirements. The DC-link is made of several high-capacity electrolytic capacitors. Typical capacity values of the DC-link are 1,000 to 10,000  $\mu\text{F}$ , according to the EPS motor-power class.

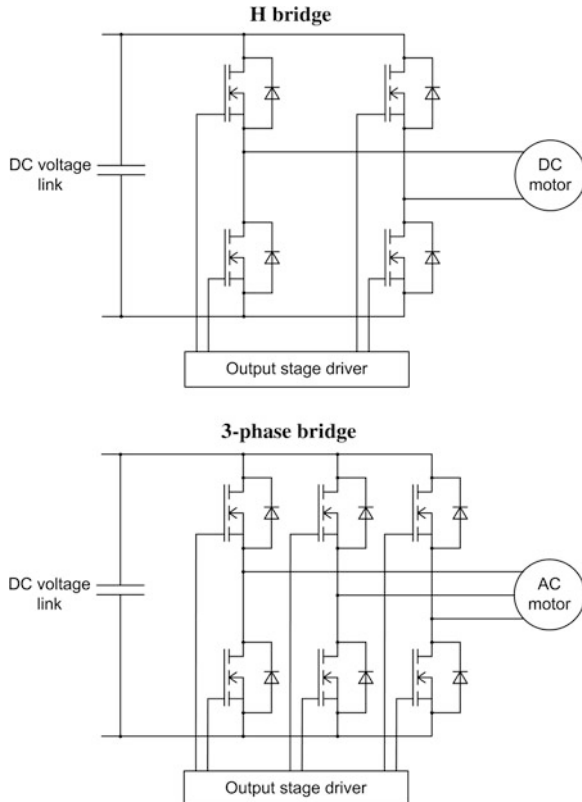
The actuation signals, provided by the signal electronics, are converted by a power output stage into suitable power for the EPS motor. The output stage consists of several power transistors in bridge connection. DC motors apply a h-bridge and three-phase motors a three-phase bridge connection.

Self-locking field-effect transistors (MOSFETs) are the only kind of transistors applied, marked by low-power control and low-impedance resistance in the switched-on state. IGBT transistors, as they are used in electric drives of hybrid vehicles, are not suitable for a 12 V on-board wiring because of their higher on-state power dissipation.

Modern power semiconductors can be operated at a chip temperature of 175 °C. At ambient temperature, they may conduct long-term currents of up to 200 A across a chip surface of 35 mm<sup>2</sup>. In EPS systems, these transistors are implemented either as housed parts on printed circuits or metal substrates or they are mounted on ceramic circuit boards without housing (bare-die). Sometimes, the complete bridge connection is one subassembly, moulded in plastic (Fig. 15.34).

The heat of power semiconductors is commonly dissipated by a metallic backplate connected to the steering case or the electric motor. The layout of the transistor cooling has to include on-state power dissipation as well as losses from switching, because a very high power dissipation can occur briefly. The dissipation

**Fig. 15.34** EPS power output stage for DC and three phase AC motors



may be reduced and the EMC requirements met by a compact assembly of all parts in the power flow, low-impedance mounting and connection, and a symmetrical assembly and layout of the components that should feature low inductance (Fig. 15.35).

## 15.4 System Design

### 15.4.1 General System Requirements

This chapter discusses the essential technical requirements of electromechanical steering (EPS) that have to be included into the system layout (see Chap. 3).

**Mechanical interfaces** The steering is connected on-board with the steering shaft and the wheel by the input shaft of the torque sensor. On the output side, the tie rods connect the mechanical interface to the guided wheels via the hub carriers. The steering is screwed to the axle carrier of the vehicle. The structure-borne

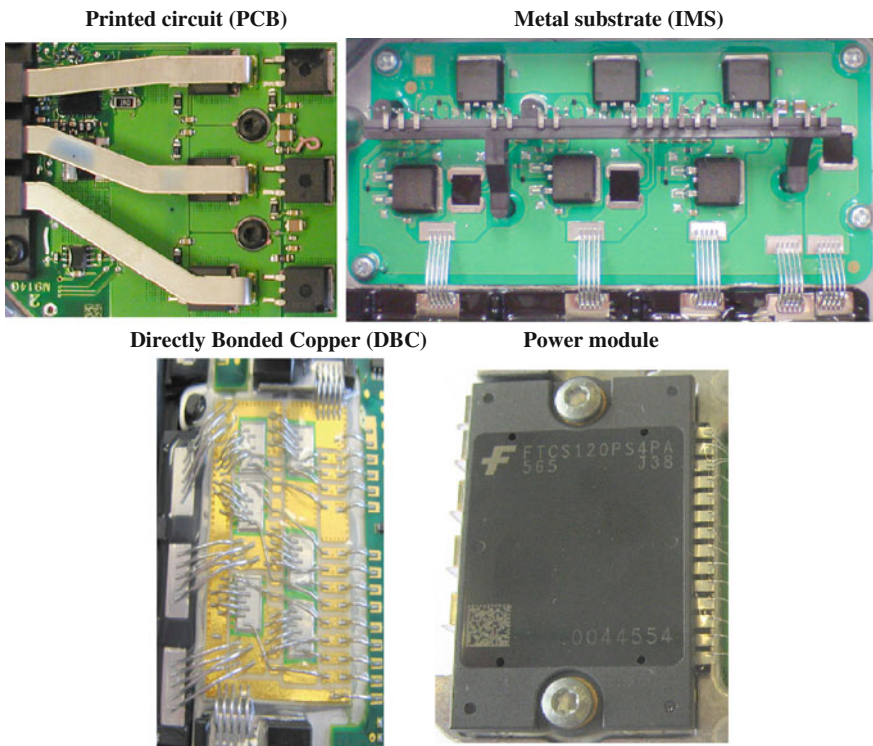


**Fig. 15.35** Configurations of EPS power output stage (PCB, IMS, DBC, module)

sound transfer may be reduced by supporting the axle carrier on elastic bearings (silent jacks).

*Electric interfaces* High-current plugs connect the steering system to the on-board wiring. Modern steering systems add a connection to the communication wiring of the vehicle. The ECUs dispose of another hardware input to activate the steering (terminal 15). Activation by the communication network (software Wake Up) is also possible. The supply voltage and the highest possible power consumption are specified by the vehicle manufacturer (Fig. 15.36).

*Power demand* The output power of the EPS system is defined by several working points. A working point is defined by the total tie rod force, the steering speed and the steering torque. At least three working points are usually specified (parking, slow travel, evasive manoeuvre). An important aspect of the power demand is its basic constraints, like design temperature and voltage and the number of repetitions (load group).

*Functional requirements* The essential function of an EPS system is the supply of power-assist on demand. Other functional requirements are described in Sect. 15.6.

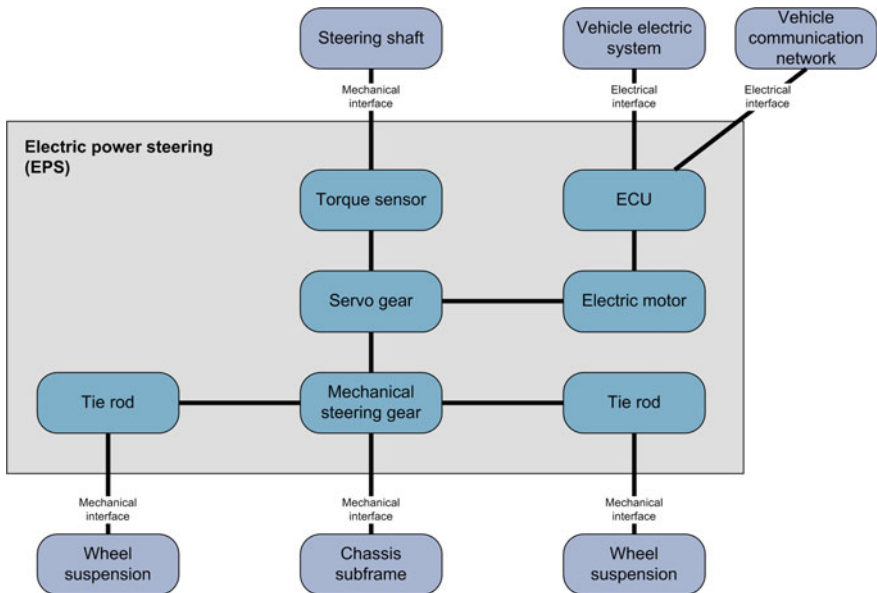


Fig. 15.36 Interfaces and parts of an EPS system

*Safety requirements* The electric power-assisted steering has to be laid out in such a way that a safety-critical state of the steering can be excluded during the serviceable life according to the state of the art. A safety-critical state is present when the vehicle response deviates from the normal state so much that the driver cannot keep control of the vehicle and a risk for body and life or real values develops (see Sect. 15.5).

*Environmental requirements* Environmental requirements are the whole structure of mechanical, electric, thermal, chemical, acoustic and other demands for the steering which are raised because of the on-board operation of the steering system (Table 15.4).

### 15.4.2 Design Parameters

The power of electric power-assisted steering is laid out along the power flow. The demanded output power and the available installation space of the steering serve to deduce the requirements for steering parts like rack, gearbox, electric motor, ECU and torque sensor. Depending on whether the EPS engagement is at the steering column or the rack, different kinematic relationships and degrees of freedom result in the system layout. All the following discussions assume stationary working points (uniform, not accelerated motion) and lossless parts.

**Table 15.4** Excerpt from the system requirements of current EPS systems

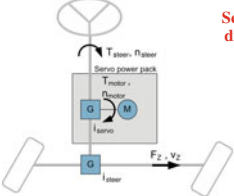
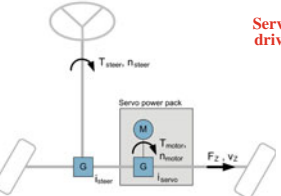
	Value range
Steering wheel angle range	$\pm 450$ to $\pm 650^\circ$
Steering wheel torque range with power-assistance	$\pm 3$ to $\pm 8$ Nm
Steering wheel torque range upon abuse	$\pm 200$ to $\pm 300$ Nm
Steering ratio (rack path per steering wheel rotation)	44–60 mm/rev
Peak tie rod force parking	$\pm 3$ to $\pm 16$ kN
Minimum steering wheel speed parking	$100\text{--}360^\circ/\text{s}$
Supply voltage	9–16 V
Maximum current bearing	$<120$ A
Temperature range	$-40$ to $+85$ °C for vehicle interior $-40$ to $+125$ °C for engine compartment
Serviceable life	15–20 years 5,000–12,000 active hours of operation 200,000–300,000 km of vehicle endurance
Acoustics	Sufficiently low noise generation has to be proved by objective test bench measurements at the complete steering system. The tests are coordinated between car and steering system manufacturer

*Specification of the output power* The output power ( $P_Z$ ) of an EPS system is fully described by information on the required tie rod or rack force ( $F_Z$ ) and the rack speed ( $v_Z$ ) according to Eq. (15.1). Vehicle manufacturers usually specify not the rack speed, but the steering speed at the wheel ( $n_{steer}$ ) and the gear ratio ( $i_{steer}$ ) (Eq. 15.2). A separate description of the power demand for different driving manoeuvres is favourable (Table 15.5).

*Choice of the steering system gear ratio* The gear ratio is defined as a ratio between rack path and steering wheel angle. The gear ratio is specified by the vehicle manufacturer, because together with the axle kinematics, it determines the steering characteristics of the vehicle (see Chap. 4). A direct gear ration of, say, 58 mm per rotation of the steering wheel, reduces the effort that the driver has to invest into steering. With a gear ratio of 44 mm/rotation, the required steer-angle for the same rack path would be higher by a factor 1.3. Direct gear ratios are preferred in order to reduce the effort for parking and to get a very agile steering response from the vehicle. Nevertheless, direct steering ratios cause appreciable lateral movements of the vehicle from small steering movements at high speed. That's why VGRs are sometimes used, because they allow perfecting the effort for parking, taking into account the driving stability at high speed.

*Choice of the servo ratio* The working point of the electric motor ( $M_{motor}$ ,  $n_{motor}$ ) is defined by Eqs. (15.2), (15.3) and (15.4) for a given output power at the rack

**Table 15.5** Kinematic connections of the different EPSEPS

Steering column EPS system (EPSc, EPSp)	Rack EPS system (EPSdp, EPSpapa, EPSrack)
 <p><b>Servo drive</b></p>	 <p><b>Servo drive</b></p>
$P_Z = F_Z \cdot v_Z \quad (1)$ $v_Z = i_{steer} \cdot n_{steer} \quad (2)$ $F_Z = 2\pi \frac{M_{steer} + i_{servo} \cdot M_{motor}}{i_{steer}} \quad (3)$ $n_{motor} = i_{servo} \cdot n_{steer} \quad (4)$	$P_Z = F_Z \cdot v_Z \quad (1)$ $v_Z = i_{steer} \cdot n_{steer} \quad (2)$ $F_Z = 2\pi \frac{M_{steer}}{i_{steer}} + i_{servo} \cdot M_{motor} \quad (3)$ $n_{motor} = i_{servo} \cdot v_Z \quad (4)$

$\delta_H$  [rad] Steering wheel angle

$\delta_H^*$  [rad] Pinion angle

$M_A$  [Nm] power assistance torque

$M_H$  [Nm] steering wheel torque

$M_S$  [Nm] kingpin torque (sum of)

$s_r$  [m] rack displacement

$i_s$  [-] overall steering ratio

( $F_Z$ ,  $v_Z$ ) and a given input power by the driver ( $M_{steer}$ ,  $n_{steer}$ ) over the servo gear unit. The symbol  $M$  represents the torque and the symbol  $n$  represents the rev.

The servo gear ration is selected in the tension zone between motor torque ( $M_{motor}$ ) and motor speed ( $n_{motor}$ ). The best system layout is found by varying the servo ratio with regard to positioning force or actuator speed. For example, for a given electric motor ( $M_{motor}$ ,  $n_{motor}$ ), a reduction of the servo gear ratio implies a lower rack force (Eq. 15.3) and a higher steering speed (Eq. 15.4; Figs. 15.37, and 15.38).

*Layout of electric motors and power electronics* The demanded working points ( $M_{motor}\ x$ ,  $n_{motor}\ x$ ) suggest the layout of the EPS motor. The power demand helps to define whether a DC or an AC motor is used (Sect. 15.3.2). This affects the requirements for power electronics (Sect. 15.3.4.3) and control engineering (Sect. 15.6). Then the electromagnetic motor design and the winding layout are defined, yielding the overall size and power input of the electric motor.

Essential layout criteria for the power electronics are the current load capacity and the cooling of parts. After possible power semiconductors and parts of the DC-link have been chosen, they are evaluated together with various mounting and connecting systems. The load of the high-power electronic parts with regard to voltage, current and thermal absorption is evaluated by simulating circuits and

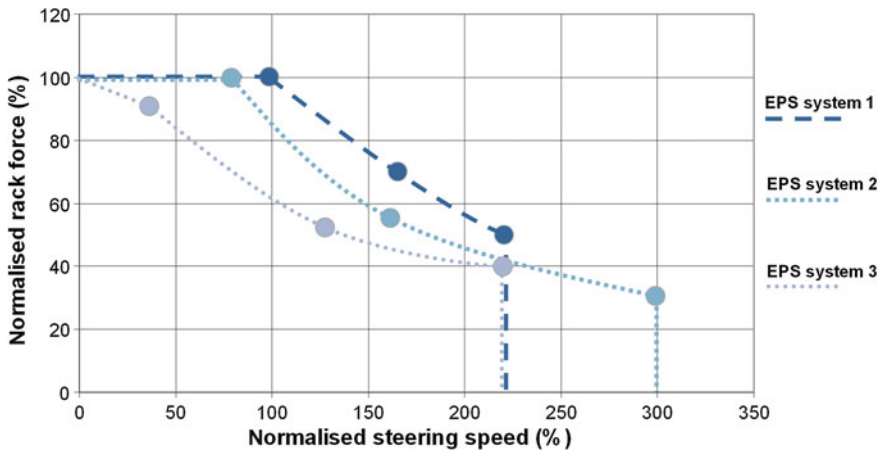


Fig. 15.37 Typical power demand of current EPS systems

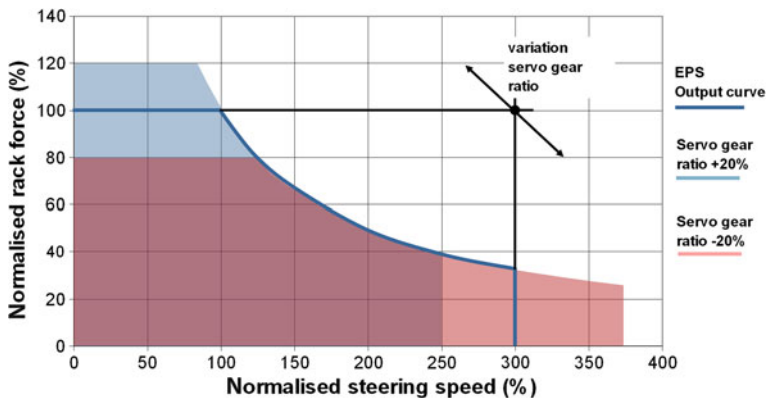


Fig. 15.38 Adaptation of the EPS operating range by varying the servo gear ratio

thermal response for different steering manoeuvres. The power consumption from the on-board wiring is verified.

*Constraints for the system layout* As mentioned before, the choice of the servo ratio defines the requirements for torque and rev of the electric motor. The servo ratio can be selected only within certain limits. For example, the permissible peak forces on the mechanical parts are limited because of their strength. This gives the least possible servo ratio. On the other hand, the servo ratio cannot be increased arbitrarily, because the engine speed will increase as well. Higher actuator speeds produce more noise in the mechanical parts, for example during the cog engagement of the servo gear units.

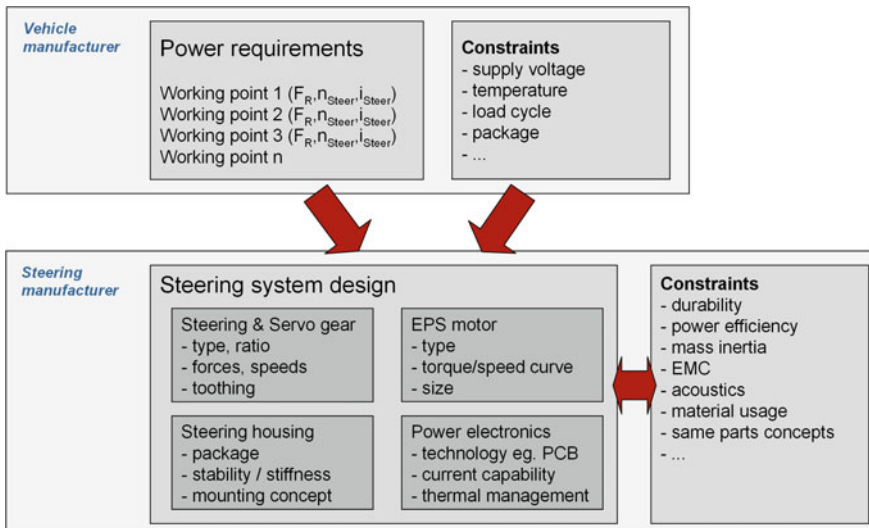


Fig. 15.39 Graphic representation of the power layout of EPS systems

The inevitable power dissipation of the parts, which also depends on their working points, has to be considered in the system layout as well. The overall efficiency of the steering has to be considered, as well as other technical functions as installation space, inertia and EMC, or even economic factors like material use and same-parts plans (Fig. 15.39).

### 15.4.3 Requirements for the Wiring System

The requirements for the electric on-board wiring can be taken from the mean power demand and the appearing power peaks.

*Mean and peak power demand* The power demand describes the electric power required from the on-board wiring as a product of supply power and consumed voltage.

Classical long-term consumers, for example, ignition control and fuel injection, have a higher mean power input than Power-on-demand systems, including electric power-assisted steering. An electric power-assisted steering needs an input power of less than 10 W in everyday travel. This comes mainly from the power consumption of the signal electronics. This is opposed by brief power peaks of 1,000 W or more during parking and turning manoeuvres.

Hence, only the peak power demand is relevant for on-board wiring requirements of EPS (Fig. 15.40).

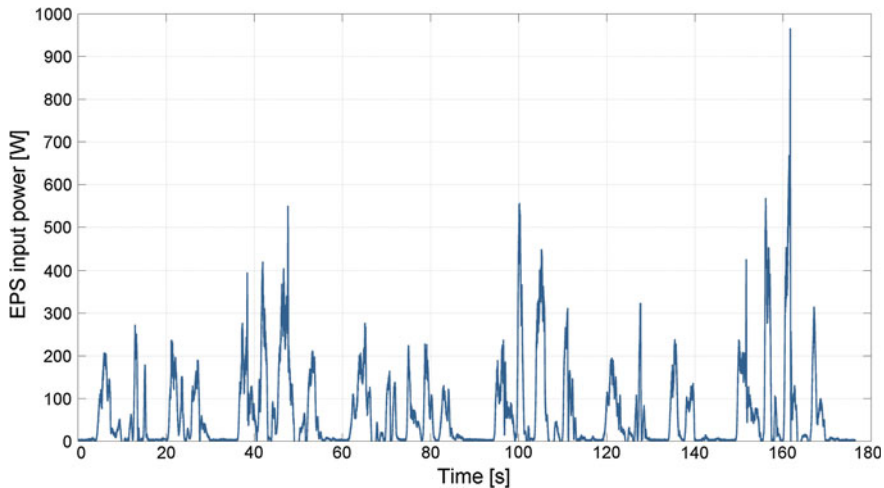


**Fig. 15.40** Measured input power of EPS during parking of a middle class vehicle

*Dynamic power demand* The mentioned absolute power and the need of the consumers for power over time are crucial for sizing the on-board wiring. Brief power peaks have to be covered by the battery, for example, because of the delay in generator control. That's why the upward current slope is relevant for electric high-power consumers, as is the peak current for the stability of the supply power (Bordnetzrückwirkung).

*On-board current repercussions* The on-board wiring of a car consists in principle of a generator for energy conversion, a battery for storage, lines for distribution and the attached consumers (Bosch 2002). State-of-the-art is still the conventional 12-V on-board wiring, often called 14-V on-board wiring. The generally advancing electrification of cars pushes the conventional on-board wiring to its limits with regard to power load and dissipation. Rising demand by the electric consumers and measures to reduce consumption and emissions further burden the components of the on-board wiring. For example, voltage fluctuations and power load in the on-board wiring are rising due to start/stop function and the recuperation of braking energy.

A pure 42-V on-board wiring, as it has been stipulated for a long time in ISO 21848, has not been introduced to the mass market till now. One reason is the huge investment that a conversion of all the on-board wiring parts and consumers would entail. Beside the known parts, like generator and battery, all the ECUs would have to be adapted to the new voltage, for example, including sensors and actuators.

*Energy management* If several electric consumers briefly need energy at the same time, a safe power supply of the consumers has to be maintained even in the worst case, when the generator rev is low or the battery is partially discharged. For example, a very high and brief power demand may occur during an evasive

manoeuvre with electric power-assisted steering and ESP intervention. Thus intelligent energy management systems are implemented in many modern vehicles. They coordinate the response of the involved on-board wiring components. Hence, an essential task of the energy management is to compare the power demand of the consumers to the power supply of the on-board wiring and to maintain balance. The battery charge is monitored as well as the energy distribution by demand and priority of consumers. For example, various standby and closed-circuit consumers are switched off when the vehicle is parked and the battery is low, so that the vehicle may be ignited again.

## 15.5 System Safety

### 15.5.1 Normative Code

#### 15.5.1.1 IEC 61508

The IEC 61508 is an international standard for the development of electric, electronic and programmable electronic (E/E/PE) systems (Bosch 2002). This standard developed in the field of process engineering or mechanical engineering, but it is not restricted to certain application areas, it may rather be considered a ‘fundamental standard’ for the development of systems relevant for safety. The standard was published with the title ‘Functional safety of electrical/electronic/programmable electronic safety-related systems’ and was divided into seven sections.

The whole safety life cycle is considered, including the concept phase, planning, development, conversion, introduction, maintenance, change and disposal/scraping.

Systems are relevant for safety when their failure indicates a considerable risk for persons or the environment.

The systems are arranged in safety integrity levels, or SIL. The range reaches from SIL1 to SIL4, with SIL4 making the highest demands to the systems. In the automotive industry, SIL4 is not relevant, the highest classification being SIL3. It has to be proved before mass production that the product meets the SIL requirements.

#### 15.5.1.2 ISO 26262

ISO 26262 (‘Road vehicles—Functional safety’) is a standard of electric/electronic systems relevant for safety, especially for the range of application in automobiles.

The standard was necessary because the IEC 61508 originated in facility building, made in small or very small numbers. Their potential dangers for persons

and environment were reduced by integrating external safety measures, such as protective screens or emergency shutdown strategies. Therefore, no detailed default requirements for the car industry could be taken from it.

The safety of automobiles has to be maintained by the correct configuration of the function, i.e. safety has to be an integral component of the product. In addition, specific features, such as mass production, which distributed development etc., have to be considered. Therefore, ISO 26262 was written on the basis of IEC61508. The first edition of ISO DIS 26262 is published on Nov 11, 2011.

There is a public draft, the ISO DIS 26262, in the process of coordination since 2009, the final international publication had been intended for 2011.

The safety integrity levels are divided by ASIL A to ASIL D (Automotive Safety Integrity level), ASIL D corresponds to the highest requirement level and is comparable with SIL3 acc. to IEC 61508. Requirements which are not relevant for safety are marked QM (quality measure) and are not addressed by ISO 26262 activities. Instead, they have to be treated by the processes of quality maintenance.

## ***15.5.2 Safety in EPS Applications***

### **15.5.2.1 Task of the Safety Concept**

The system has to be laid out in such a way that faults are safely controlled. The following options are conceivable:

- fault exclusion according to the state of the art, e.g., by suitable mechanical design
- exclusion of safety-critical fault consequences, e.g., by proving that the driver is not or only slightly affected
- fault detection by a suitable safety concept and taking down the system into a safe state sufficiently quickly (fail-safe principle).

The system risk or the safety integrity level (ASIL) is identified by a danger and risk analysis, first without considering safety measures. Then the system risk is reduced by developing a safety concept. The task of the safety concept is to implement safety measures to reduce the present systemic risk to a calculable, potential rest risk. The effectiveness of the safety concept is documented by a safety proof, see Fig. 15.41. The scope of proof is given by the safety integrity level (ASIL).

### **15.5.2.2 EPS Risk Classification**

The assessment of the systemic risk has to consider the range of application and the motor-power class of the EPS. Assessing the current steering systems for

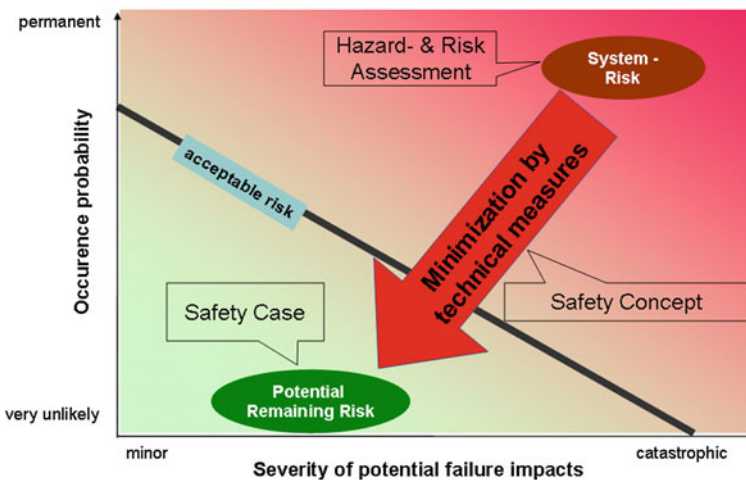


**Fig. 15.41** Safety concept to minimise the system risk

medium and superclass vehicles yields the following classification (risk graph from ISO/DIS 26262-3, rev. 2009-06-28):

- undesirable actuation of the servo motor → ASIL D
- heavy running of the steering system, e.g., by false actuation of the servo motor (not mechanical causes) → ASIL D
- sudden supply of the power assist, e.g., by unintentional relaunch → ASIL A
- failure of the power assist → QM.

The above classification classifies EPS systems as ASIL D. The protective purposes can be deduced directly:

- The steering system has to recognise faults that trigger an undesirable actuator function and change into a safe state according to the ASIL D requirements.
- The steering system has to recognise the faults that lead to heavy running of the steering system and change into a safe state according to the ASIL D requirements.
- The steering system has to prevent unintentional relaunch of the power-assist according to the ASIL A requirements.

There can be no safety integrity function for mechanical parts, therefore, faults have to be excluded from the mechanical design. This is ensured by the processes of mechanical development.

Constructive design has to exclude, e.g.:

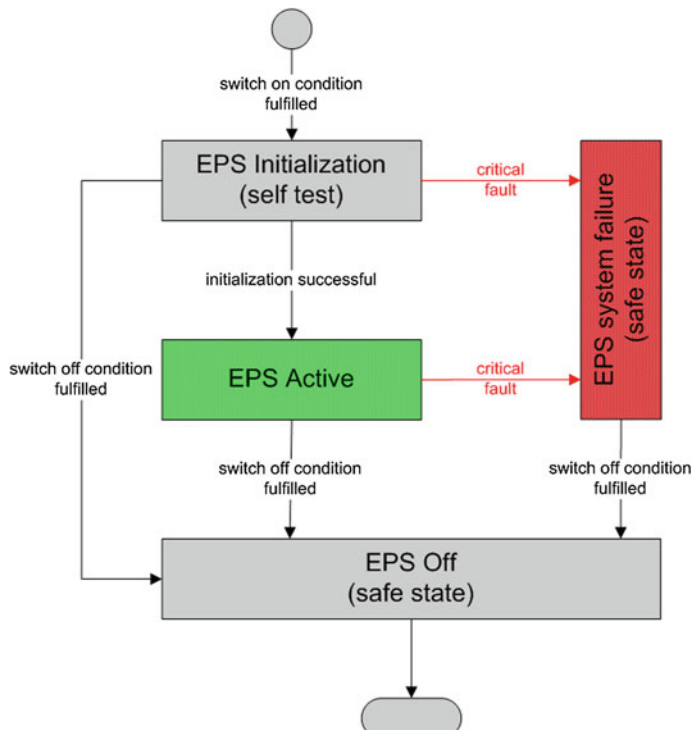
- loss of the mechanical contact between steering wheel and tyres
- heavy running of the steering due to mechanical causes.

### 15.5.2.3 Qualities of the Safe State

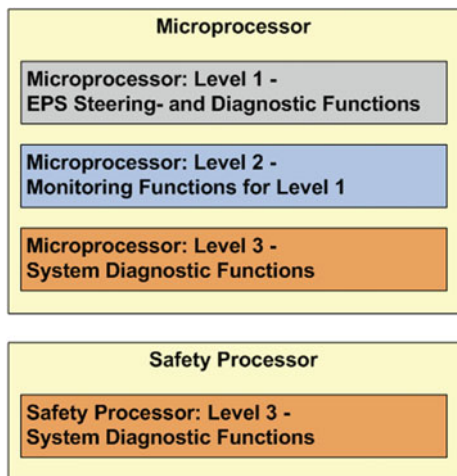
The safe state of an EPS steering can be defined by the following qualities:

- The steering system may not generate a power-assist.
- The safe state can be left only by switching off and on and successful initialisation of the ECU (see Fig. 15.42).
- The electric motor may not generate any torques above a safety-critical value (depending on vehicle and steering layout).
- The mechanical steering ability has to be maintained according to ECE R79 (UNECE 2005).

A power-assistance (state ‘EPS active’) may be generated only after successful, perfect initialisation. If a critical fault appears, the state ‘EPS system fault’ is immediately entered. The states ‘EPS off’ and ‘EPS system fault’ set the steering system into safe state. The switch-off channels (cf. Sect. 15.5.2.4) ensure that the safe state is reliably entered.



**Fig. 15.42** System states of the EPS system

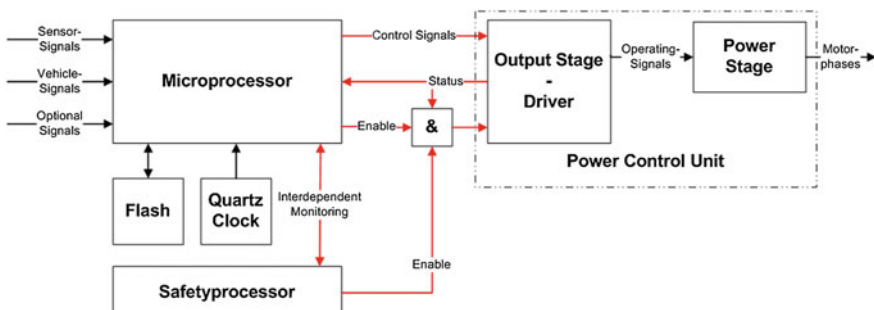
**Fig. 15.43** 3-level plan

#### 15.5.2.4 Switch-Off Channels

When a safety-critical fault is recognised, the system has to enter the safe state with the help of the switch-off channels within a fault tolerance time. The fault tolerance time is the time during which the system may accept faulty signals without entering a dangerous condition. This time is required for fault detection and the subsequent fault reaction. It depends on the layout of car and steering.

A reliable fault reaction needs switch-off channels that can be activated by diverse and independent ways.

The switch-off channels are activated by the microprocessor unit and additional hardware parts. These parts have to be selected in such a way that they supervise each other all the time. This ensures that the system can be transferred into a safe state. EPS applications use the power electronics as a switch-off channel. The control to deactivate the switch-off of the power electronics can for example look like in Fig. 15.44.

**Fig. 15.44** Block diagram of the EPS ECU with switch-off channel

In order to exclude undetected faults in the operation of the switch-off channels their effectiveness needs to be checked individually before activating the steering functions. Therefore, test routines are run before the initialisation phase. Only if the test result was positive, the system is released and enters the state ‘EPS active’ (cf. Fig. 15.42).

The ECU is designed in such a way that the EPS remains in the safe state when powerless.

The safety requirement to switch off the fault-afflicted system immediately and to transfer it in the safe state has to be compatible with the demands on quality. An essential quality characteristic is the availability of the power-assistance, i.e. the amount of time when the power-assistance is present, relative to the serviceable life for the whole service life.

$$v = \frac{(n - a)}{n} \cdot 100 \quad (15.5)$$

$v$  Availability [%]

$a$  Failure time [h]

$n$  Serviceable life for service life [h]

This means that from the quality point of view, it does not make sense to transfer the system immediately into the safe state after any fault event because not all faults are safety-critical to the same extent. Therefore, it is common to categorise the faults and to differentiate the system response. The following fault reaction strategies may apply:

- Limit EPS operation e.g., switch-off partial functions (restriction of the comfort)  
e.g., reduce the EPS assist power
- Switch to signal substitute values
- Transfer the system softly into the safe state, e.g., slowly reduce the power-assistance, then switch to the safe state.

### 15.5.2.5 Safety Measures for Subcomponents of the System

To analyse potential fault sources, it is sensible to decompose the system into its parts. The following subsystems can lead to undesirable actuation of the servo motor:

- fault in the external signals
- fault in the sensors
- fault in the microprocessor
- fault in the ECU (including power electronics and software)
- fault in the actuation.

Faults in the following subsystems can lead to a heavy steering

- fault in the engine (e.g., short circuits)
- fault in the ECU (including power output stage and software)
- fault in the actuation.

The fault consequences are classified as ASIL D with regard to ‘undesirable actuation of the servo motor’ and ‘heavy steering’. High requirements to the subsystems are the result, i.e. the necessary safety measures have to achieve an accordingly high diagnostic coverage.

### Monitoring of External Signals

The safety integrity of external signals depends on the respective vehicle manufacturer and the model varieties of the vehicles. The safety relevance of the signals read by the vehicle bus is evaluated by a systematic analysis.

If possible, the EPS functions are laid out so that no received signals may impair the safety. If this is not possible, then the steering manufacturer has to define suitable safety requirements for the concerning signals.

In addition, one or more of the following safety measures for external signals are common:

- monitoring time-out
- monitoring message counter
- monitoring check sum
- monitoring value range
- gap monitoring.

To improve the availability (see [Sect. 15.5.2.4](#)) of the power-assistance, it makes sense to switch external signals to signal substitute values upon a detected fault event, if possible. Although this can diminish convenience, for example through a higher required steering force, it entails no effects that are relevant for safety.

### Monitoring Sensors

The calculation of the desired power-assistance and the control of the servo motor need sensors (see [Sects. 15.3.2.5](#) and [15.3.3](#)). Malfunctions of the sensors immediately affect the resulting power-assistance, hence, a failure to meet the protective targets cannot be excluded if no additional safety measures are taken (see [Sect. 15.5.2.2](#)). Monitoring with accordingly high diagnostic coverage has to be installed, matching the sensor design and their signal transmission.

## Monitoring Plan of the Computer System

Generally, the EPS functions are computed on a microprocessor with a computer core. The high diagnostic coverage demanded by the SIL classification is often achieved by a 3-level plan to monitor this microprocessor. This plan has proved itself in E-gas and ESP applications. An intelligent hardware unit, called ‘safety controller’ in the following, is added as a further monitoring level. The implemented software functions are distributed on 3 levels (see Fig. 15.43).

The following functions are executed on **level 1**:

- the steering functions (e.g., sensor read, calculating output values, control of the steering actuators)
- the diagnostic functions for steering (monitoring and testing of system inputs, system outputs, sensors and actuators for specific steering functions)
- the comparison of level 2 and level 1 results (output values have to stay within a permissible tolerance range).

The following functions are executed on **level 2**:

- the diverse algorithms (significantly different algorithms to calculate the output values) for monitoring level 1 steering functions that are relevant for safety
- the comparison of level 2 and level 1 results (output values have to stay within a permissible tolerance range).

Level 1 and level 2 are installed on the microprocessor. The software of these levels can use different calculation resources of the microprocessor (integer unit or floating point unit).

The permissible tolerance range between the level 1 and level 2 results depends on the vehicle and steering layout and has to be gained from road trials in the target vehicle. Faults are purposefully set to identify the requirements and the effectiveness of the level 2 functions. The worst deviation of the output values computed from level 1 and tested on level 2 may only lead to a response of the steering system which can be safely controlled by the driver.

The system diagnostic functions are computed on **level 3**. These safety measures for software and hardware parts to maintain the system integrity are independent from the application. They include, e.g.:

- monitoring the storage areas
- operating the safety controller
- logical and temporal programming flowchart monitoring
- monitoring the operating system
- monitoring the software comparative algorithm (comparing the results from level 1 and level 2)
- testing the microprocessor core
- monitoring the microprocessor and the safety controller by means of a question/answer game.

Level 3 is split in two. One part is installed on the microprocessor and the other part on a separate safety controller. The results of the program parts are exchanged between microprocessor and safety controller by an interface.

If any of the three levels detects a fault relevant for safety, the system enters the safe state.

### Monitoring Power Electronics/Actuator

The electric motor to generate the power-assistance for EPS applications differs by power demand and cost requirements (see [Sect. 15.3.2](#)).

Malfunctions of the electric motor can immediately lead to the identified system risks (cf. [Sect. 15.5.2.2](#)), hence, monitoring with accordingly high diagnostic coverage needs to be provided.

To control the effects of undesirable actuations of the servo motor, the system has to be able to deactivate the power electronics fast enough. The deactivation of the power output stage is intended as a switch-off channel.

All electric motor concepts have to meet the requirements of the safe state (cf. [Sect. 15.5.2.3](#)) to prevent heavy steering.

The switch-off of the power output stage may not be sufficient for some electric motor concepts, because a fault event, e.g., a short circuit in the electric motor or in the power electronics may unintentionally induce voltages producing a current. This unintentional current generates motor torques opposing the steering purpose of the driver. In other words, unintentionally braking motor torques can be generated which can cause a heavy steering for some gear ratios of the electric motor to the steering wheel. Without safety measures for these situations, the mechanical steering ability may not be available any more.

The potential unintentional current has to be prevented either by the electric motor used or by additional measures. Some safety measures are:

- exclude motor and inlet short circuits in the design
- avoid currents in the fault case by additional parts (engine/power electronics)
- monitor power electronics/actuator.

### Safety-Related ECU Block Diagram

The ECU is responsible for executing the steering functions and all the safety functions of the EPS. The following parts are necessary:

- microprocessor, the core of the ECU
- safety controller for microprocessor monitoring (watchdog function) and for monitoring supply voltages
- non-volatile RAM to store non-volatile data
- quartz clock generation for the microprocessor

- output stage driver to control the parts of the power electronics of the output stage
- output stage to control the motor phases.

A block diagram of this configuration is shown in Fig. 15.44.

From the safety perspective, the hardware architecture is an enabled single-channel system which is controlled by a microprocessor. This unit is monitored by an independent safety controller, allowing good diagnostic coverage. The necessary means for the fault response are provided by the redundant control of the switch-off channels (release signal of the power electronics) which can be operated by the microprocessor, the safety controller or the output stage driver.

## 15.6 Steering Functions and Control

As discussed in the preceding sections, EPS disposes of an electric motor that feeds mechanical energy into the system. Now it is the task of the steering functions to feed this energy into the system on demand. On-demand means that the energy has to be fed in such a way that the driver's function of driving the vehicle is power-assisted in the best way possible. To meet this claim, the steering functions have to respond appropriately to the driver's intent and to the current movement of the steering system. The driver's intent is registered by the torque sensor. It measures the torque that the driver applies to the input shaft of the steering gear (see Sect. 15.3.3).

The movement state of the steering system is registered by an angle sensor. This signal can be measured by a steer-angle sensor at the steering column, or it can be computed by the rotor position sensor in the steering. The signal of this sensor is notably an absolute steering wheel angle.

The tasks of the steering functions in on-demand supply of mechanical energy can be classified as follows:

- actual steering functions
- control for the steering feel
- control of the electric motor

The torque is defined by the actual steering functions that the driver has to maintain or perform to guide the steering wheel. The response of the free steering wheel can be influenced by steering functions, too.

The control provides the proper supply of mechanical energy. As discussed above, it can be divided into two subclasses: the control for the steering feel and the control of the electric motor. The control for the steering feel assumes essential stabilisation tasks, so that the torque demanded by the steering functions is free of undesirable vibrations and other disturbances.

The control of the electric motor, on the other hand, is responsible for highly dynamic and precise supply of mechanical energy. The stabilisation and high

dynamics tasks are closely connected to haptics and acoustics of a steering system, so that any shortcomings significantly affect the system performance in these areas. Too low dynamics of the actuation may cause a too tough response, leading to inert handling of the whole vehicle. Insufficient stabilisation can be the cause of bad haptics, whether slight vibrations in the wheel or an audible system response. For the control of the electric motor, see the standard textbooks, such as Schröder (2009) or Stölting and Kallenbach (2006).

### 15.6.1 Steering Functions

Based on the control of the steering, it is the task of the steering functions to define the force that the driver perceives while guiding the steering wheel. This includes the static hold of the steering wheel and dynamic situations like steering in and out of a corner. In addition, the response of the free steering wheel is defined by the steering functions, up to functions like automatic steering for parking.

The steering functions have to cover many aspects, so that understanding is improved by a structuring of the steering functions according to their main purpose. The following distinction can be made:

- basic steering functions
- extended steering functions
- functions at vehicle level.

The basic steering functions are those functions which represent the familiar response of a HPS in an EPS. This response is complemented with the extended steering functions that use the specific possibilities of EPS. Finally, in a group with other vehicle systems, like sensors for measuring parking spots or a lane detection camera, functions at vehicle level can be implemented into an EPS.

#### 15.6.1.1 Basic Steering Functions

Within the scope of the basic steering functions, there are four essential functions:

- power-assistance
- friction compensation
- inertia compensation
- damping.

These basic steering functions may be made parametrisable according to speed. In the following, the impact of these functions is outlined and complemented with notes on the parametrisation as a function of speed.

## Power-Assistance

The most elementary and most important basic steering function is the power-assistance. Its task is to ensure that the driver does not have to support all the forces applying at the rack by the steering wheel, but that the EPS motor supports an essential part of these forces. How such a function is made and parametrised decides how the relative strengths at the rack are presenting themselves at the steering wheel and, hence, to the driver.

The impact of this function is obvious from the notion that, in a first approximation, there is a quasi-stationary force balance at the rack:

Rack force =  $i_{\text{steer}}$  torsion bar torque +  $i_{\text{servo}}$  motor torque (see Fig. 15.45). Here,  $i_{\text{steer}}$  is the conversion of torsion bar torque into rack force. The corresponding conversion of the motor torque is  $i_{\text{servo}}$ .

The torsion bar torque is the torque which the driver has to support at the steering wheel, the motor torque is the share of the power-assistance function.

A given value of the rack force can be offset by any combination of torsion bar torque and motor torque (see Fig. 15.46).

The choice of the distribution of torsion bar torque and motor torque decides how the steering feel is perceived by the driver and how much information about force changes can be resolved in the rack. The illustration shows one possible version. Plotting the motor torque over the torsion bar torque according to this diagram yields the power-assist characteristic curve known from hydraulics, see Fig. 15.47.

Information about the expectable feedback quality is gained from plotting the torsion bar torque over the rack force. A steep slope implies that minor changes of the rack force cause major changes of the torsion bar torque. This is perceived by the driver as a good feedback on road condition and bumpiness.

At low speed, especially at rest, the rack forces are highest. At such speed, a differentiated feedback about the road is unnecessary, hence, the power-assistance

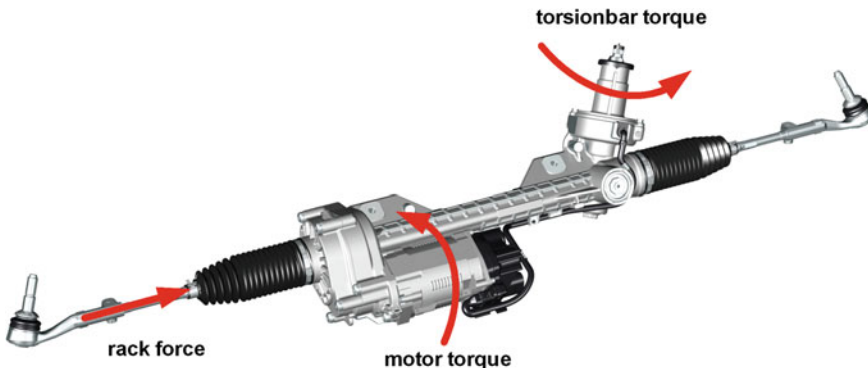


**Fig. 15.45** EPS with essential forces acting on the steering system. These forces keep a quasi-static balance

**Fig. 15.46** Balance of rack force and the sum of motor torque and torsion bar torque. The share of the torsion bar torque is enlarged for clarity

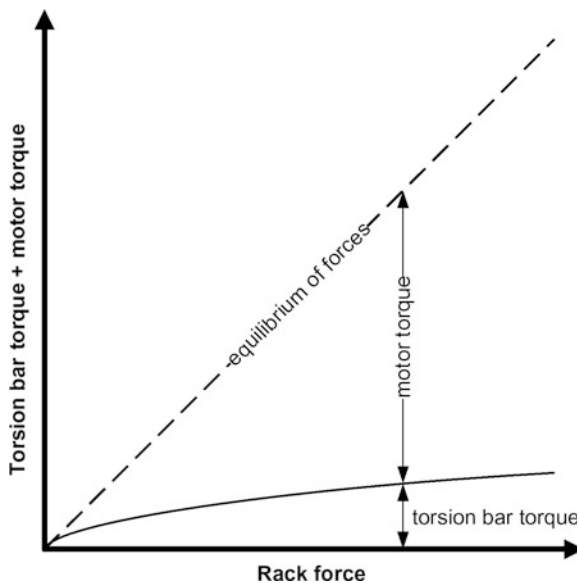
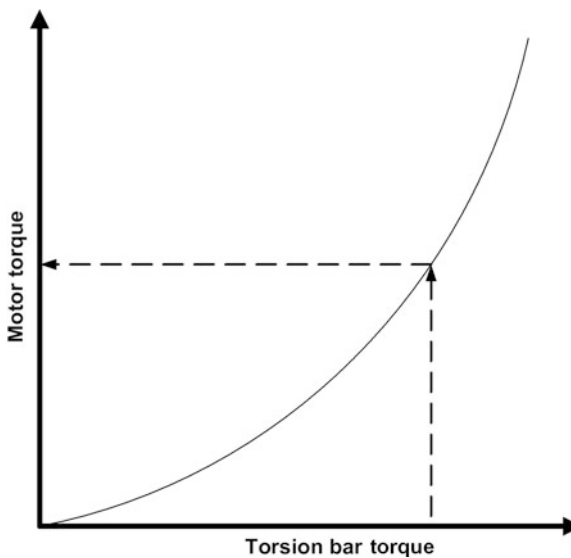


**Fig. 15.47** The power-assist characteristic curve shows the motor torque as a function of the torsion bar torque



can be applied in such a way that comfortable steering, end-stop-to-end-stop, is possible. Nevertheless, beyond the low speed range, attention is devoted to the representation of the lateral acceleration or the rack forces in the steering torque, so that the power-assistance has to be applied very differently. One challenge for the application is to create a harmonious transition between both requirements.

Returning to the force balance outlined above, one may notice that this model only applies under the assumption that the steering system is without friction or inertia. Any support of the movable parts of a steering is subject to friction, though, and the movable parts, esp. the rotor of the EPS, have an inertia. Thus the force balance does not fully apply as described. To match the assumptions as closely as possible, the effects of friction and inertia needs to be compensated.

### Friction Compensation

The task of a function for friction compensation is to reduce the effects of frictions in the steering with regard to the above-mentioned force balance. This can be achieved by supplying a suitable compensation torque as a function of the current movement state and the torque requested by the power-assistance.

A very simple friction compensation can be acquired by assuming a fixed amount of overall friction. This hypothetical friction moment is always applied in parallel with the current movement or, if the steering system is at rest, in the direction of the torque requested by the power-assistance.

Such a simple way of friction compensation is not very practical, though, because it is very susceptible to measuring noise and does not take changing friction into account. Frictions change esp. from ageing and, even more, because of varying temperatures.

The physical causes for friction in the steering system imply that friction compensation should not be parametrised as a function of vehicle speed.

### Inertia Compensation

Typical EPS gear ratios yield an inert mass of several hundred kilogrammes for the movable parts in the steering, relative to the rack. The force balance discussed above does not consider these inertia effects. This entails that dynamic excitations in the rack do not affect the torsion bar torque, and steering movements initiated by the driver always have to operate against this inert mass. A function for inertia compensation has the task to reduce these negative effects of inertia on the steering feel.

Again, a very simple inertia compensation is conceivable. The rotor acceleration can be gained from a differential quotient, based on a measurement of the rotor position or rotor speed of the EPS motor. The current rotor acceleration gained this way can be offset against the overall inertia to yield a corresponding compensation torque. Then it can be requested from the EPS motor in addition to the torque from power-assistance and friction compensation. Such a simple way of compensation is not very practical, though, because it is very susceptible to measuring noise.

The physical causes for friction in the steering system imply again that inertia compensation should not be parametrised as a function of vehicle speed, either.

## Active Damping

A friction- and inertia-compensated steering system responds very sensitively to disturbances in the force balance. Excitations from the road lead immediately to a violent acceleration of the system which is perceived by the driver as a kickback. Smallest changes of the moment that the driver applies to support the steering wheel produce powerful movements of the system and, hence, a very nervous steering response.

These undesirable qualities may be reduced by damping the steering system. In an EPS this is realised by a suitable steering function.

A simple way of a damping function requests from the EPS motor a torque that is oriented against the steering direction and proportional to the current steering speed. This way of damping contradicts the notion, though, that the driver's steering manoeuvres should be supported, so that a high-quality damping function has to be much more sophisticated.

A damping function should be parametrised as a function of vehicle speed. At rest, only the righting and the post-pulse oscillation of the steering wheel have to be suitably controlled. At high speed, adequate damping is necessary to prevent the steering wheel from overshooting and the car from fishtailing when the wheel is released in a corner.

### 15.6.1.2 Extended Steering Functions

Based on the already described basic steering functions, power-assistance, friction compensation, inertia compensation and damping, the EPS displays a steering response that is comparable to that of a classical HPS. Extended EPS functions are not included yet. This is achieved by extended steering functions.

## Active Return

The design of modern front axles generates a runback response which is often unsatisfactory, primarily in the low, in the low speed range. Sometimes the axle designs are laid out in such a way that the forces revert well before the mechanical end stop, pulling the steering further towards the end stop.

The task of the active runback function is to improve this response. The basic idea is that the EPS motor adds torques in the straight-ahead direction as a function of the steering wheel angle or the steering movement. Such a function has to guide the free wheel as well as the driver-controlled wheel into the straight-ahead position as desired.

A very efficient variety of such a function can be a wheel rate control, with the nominal steering speed being defined as a function of the steering wheel angle and the vehicle speed. If the peak torque that the function may feed is reduced as a

function of the applying hand torque, then the transition from free to guided steering wheel can be purposefully shaped.

### Directional Stability Correction

The always present slope of the road towards one side means that the steering wheel is typically not free of torques when it is running straight. The driver has to actively correct to prevent a drift of the vehicle down the slope, i.e. the steering wheel is turned around a small angle when driving straight. Directional stability functions can be applied to relieve the driver from such routine tasks.

If an active runback function is already present, it is obvious that its straight-ahead course could be slightly shifted. Ideally, the straight-ahead course should be shifted by an offset angle until the course-keeping driver can hold the steering wheel free of torques. The setting of the offset angle is crucial for such a function. Note that the offset angle is a dynamic variable. If the slope changes, the offset angle has to follow.

#### 15.6.1.3 Functions at Vehicle Level

A very specific steering feel, matching car and target group, can be achieved with an EPS by the basic and extended steering functions. In addition, the EPS can be integrated as an intelligent and integrated actuator into the context of functions at vehicle level. The role of the steering in the context of some functions at vehicle level will be discussed next.

### Park Steering Assistant

The park steering assistant is a function that does not expect the driver to steer, esp. during reverse parking in the kerbs (parallel parking). The driver's task is focussing on throttling and braking, while the vehicle electronics steer the vehicle accordingly. The necessary steering movements are gained from ambient sensors, e.g., ultrasonic sensors, identifying the parking spot and the position of the car relative to the parking spot and other obstacles.

The task of the EPS is to perform the requested steering movements. An internal steer-angle control may be used to achieve this, but not only the steer-angle proper has to be controlled by the EPS. A suitable interface to the involved functional units has to be provided, too. Then this interface and the control have to be secured by a whole series of monitoring functions. It has to be ensured that the interface cannot be accessed during a motorway journey, and an injury of the driver from intervention into the turning steering wheel has to be excluded, to mention only two examples.

### Driver Warning/Lane Departure Warning

A frequent cause for accidents on motorways is the unintentional departure from the lane. Often, tiredness or too little attention of the driver is the reason. To attain the attention of the driver when the road is unintentionally left, a vibration of the steering wheel, the driver warning, can be generated by the EPS.

Such functions survey the relative position of the car in the lane using an on-board integrated camera. If departure is imminent, the EPS receives the request to activate the driver warning function. Then the driver warning proper is generated by the EPS applying additional steering torques with suitable frequency and amplitude.

### Tracking/Lane Keeping System

A logical advancement of the driver warning function is continuous tracking. Tracking has the purpose not only to warn the driver, but to keep the vehicle in the lane by an active steering control.

Current legal stipulations have to be observed which do not permit autonomous tracking. As a result, the tracking function may assist only if the driver actually controls the steering wheel.

An important aspect is the design of the additional torques. Account has to be taken of the fact that the function should reliably guide the driver in the lane without appearing irritating or even patronising. The tracking function implies that the EPS has an interface to actively control the steering torque. Ideally, an additional torque is directly applied to the steering wheel by this interface.

The application of any additional torques can provoke safety-critical situations. Hence, this interface has to be limited and monitored properly. The limiting has to be made in a way that enables the driver to override the additional torques requested by the tracking at any time.

### Dynamic Steering Torque Recommendation

The functions of the dynamic steering torque recommendation is to try to motivate the driver to a specific steering movement by applying an additional torque. When braking on  $\mu$ -split, the driver can be animated by a short torque impulse to correct on time. The structure of the torque impulse is subject to the same stipulations as the additional torques of the tracking. The impulses are limited so that the driver can override them at any time and no safety-critical situations can develop.

## 15.6.2 Control Plans for the Steering Feel

The preceding section presented many different steering functions. All of them are based on an underlaid control for the steering feel, by whose help the steering torque that these functions requested is adjusted. Two basic approaches for this basic control of the steering shall now be discussed. The steering control approaches discussed in Sect. 15.6.2.1 convey the principle of the HPS to the EPS. The group of control plans described in Sect. 15.6.2.2 has given up this idea and perceives the EPS as a mechatronic overall system focussing on controlling the torque which the driver feels at the steering wheel.

### 15.6.2.1 Classical Control Plans

All classical control plans for the EPS have in common that they emulate the functions of an HPS. The basic functional principle of the HPS can be described as follows: a suitable assistance force is applied by the steering as a function of the force applied by the driver. There is no simple linear connection between the assistance force and the driver's force but a progressive connection, see Fig. 15.47. The force applied by the driver corresponds to the torsion bar torque.

From the point of view of control engineering, this structure may be interpreted as a P controller with variable gain and a set point of 0 Nm (see Fig. 15.48). The shape of the classical power-assist characteristic curves implies that the gain factor increases with rising deviation.

A stability analysis reveals that the closed control circuit is unstable. As a consequence, the P controller has to be extended by a stabilising component. How this stabilisation should be made and parametrised is know-how of the steering manufacturer. Two basic approaches are conceivable. The first approach is based on the idea to make the stabilisation so solid that the variable gain can be compensated by the power-assist characteristic curve. The second approach exploits the fact that the current gain is known. Thus the parameters of the stabilisation can be guided, e.g., by tables of the current gain. The resulting control circuit is shown in Fig. 15.48.

It is interesting that the steering feel is not the set point for the control but rather the resulting residual deviation of the P controller, i.e. the power-assist

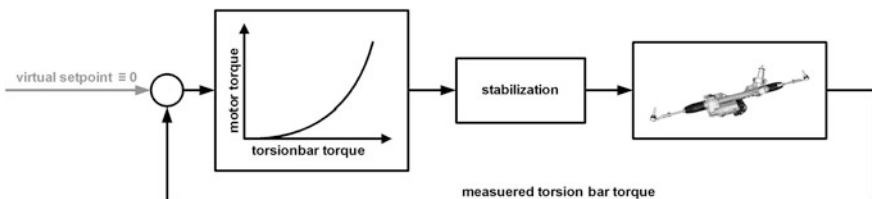


**Fig. 15.48** Control circuit with classical EPS control plan

characteristic curve. The control or stabilisation of the steering in these control plans is very closely related to the steering feel. An adaptation of the steering feel always means an intervention into the steering control. Examining the steering functions on vehicle level, that try to impress additional torques at the steering wheel, will show that the context of classical control plans does not contain a direct way of doing so. These qualities of the classical control plans have led to new control plans being developed, these allowed giving the driver's torque as a set point.

### 15.6.2.2 Control of the Driver's Torque

Considering the task to provide a control for the steering feel will quickly yield the following structure: The variable perceived by the driver, the torsion bar torque, is the control variable, the EPS motor torque is the set variable. The forces acting by tie rods and rack on the steering are interferences, just like the torques applied by the driver to the steering wheel.

Thus the task of the steering control disintegrates into two parts. The first task is the determination of the set point for the torsion bar torque, in other words, the application of the steering feel. The second task is the identification of the EPS motor torque required to adjust this torsion bar torque, i.e. the control of the torsion bar torque. There is thus a distinct separation between steering feel and steering control, with little interaction. This distinct separation of tasks and the structure of the control circuit are shown in Fig. 15.49.

Such a structure demonstrates that additional torques at the steering wheel can be added to the set point for the torsion bar torque (see Fig. 15.49) and then really set.

The design of the torsion bar torque control can exploit the full range of known control unit design methods. The control unit design with LQG/LTR by Henrichfreise and Jusseit (2003) may serve as an example. The most important requirements for the control are performance and robustness. The necessary robustness is profoundly defined by the standard dispersion of production, ageing and ambient influences, such as the ambient temperature.

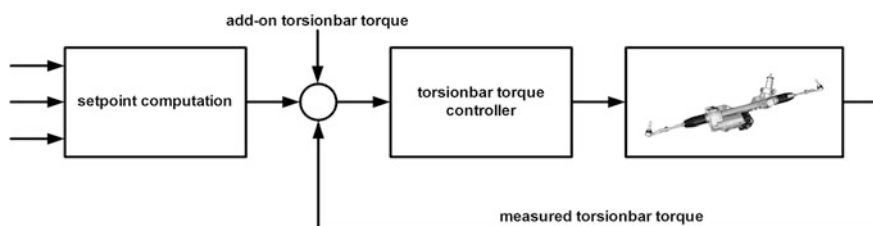


**Fig. 15.49** Control circuit of current EPS control plans based on the control of the driver's torque

A main problem of the set point calculation is how to illustrate the basic steering function of the power-assistance in these new control plans. A part of the answer is given by the basic force balance of the steering. Classical control plans define by the power-assist characteristics in what way the power-assist of the rack force should be distributed to motor torque and torsion bar torque. Now it is possible to directly set the torsion bar torque that is supposed to apply at a given rack force. However, the answer is incomplete, because the question how the rack force can be computed is still unsolved.

Immediate computing of the rack force on the basis of the basic force balance is not promising, because this addition of forces always includes friction and inertia effects as well. They lead to rack forces being computed either too high or too low. A potential method for direct computing of the relevant forces is found in Grassmann et al. (2003). Alternative approaches try to interpret the rack force as a lateral force or acceleration (Pfeffer and Harrer 2007), originating in the field of driving dynamics.

The friction and inertia compensation functions are basic steering functions which are no longer needed, because the control adjusts the set point right at the torsion bar, so that intervening frictions and inertia are automatically compensated. The other steering functions can be made as discussed in the section on steering functions. However, the torsion bar torque will replace the motor torque here, so that these functions draw closer to the driver, so to speak.

## References

- Beierlein T, Hagenbruch O (2004) Taschenbuch Mikroprozessortechnik. Fachbuchverlag, Leipzig
- Fischer R (2006) Elektrische Maschinen. Hanser Verlag, München
- Grassmann O, Henrichfreise H, Niessen H, von Hammel K (2003) Variable steerunterstützung für eine elektromechanische Servolenkung. 23. Tagung "Elektronik im Kfz", Haus der Technik, Liederhalle Stuttgart, 17–18 Juni 2003
- HELLA KGaA Hueck & Co (2014) Elektronik—Sensoren zur Positionserfassung. Technische Information
- Henrichfreise H, Jusseit J (2003) Optimale Regelung einer elektromechanischen Servolenkung. 5. VDI Mechatronik Tagung 2003, Innovative Produktentwicklung. Fulda, 07–08 Mai 2003
- IEC 61508 International Electrotechnical Commission, Functional safety of electrical/electronic/programmable electronic safety-related systems, Part 1–Part 7
- ISO 26262 International Organisation for Standardization (2011) Road vehicles—functional safety, Part 1–Part 10
- Jerems F et al. (2004) Sensor for modern steering assist systems. SAE 2004-01-1773
- Lindner H, Brauer H, Lehmann C (1999) Taschenbuch der Elektrotechnik und Elektronik. Fachbuchverlag, Leipzig
- Misra C (2004) Guidelines for the use of the C language in critical systems
- Nagel T (2008) Zahnriemengetriebe: Eigenschaften, Normung, Berechnung, Gestaltung. Hanser Verlag, München

- Niemann G, Winter H (2004) Maschinenelemente: Band 3: Schraubrad-, Kegelrad-, Schneckenrad-, Ketten-, Riemen-, Reibradgetriebe, Kupplungen, Bremsen, Freiläufe, 2. Auflage. Springer, Berlin, Heidelberg, New York
- NORM DIN 69051-1 (1989) Kugelgewindetriebe—Teil 1: Begriffe, Bezeichnungssystem
- NORM ISO 5295 (1987) Synchronous belts—calculation of power rating and drive centre distance
- Pfeffer PE, HARRER M (2007) Optimaler steerradmomentenverlauf bei stationärer Kurvenfahrt. VDI Berichte Nr 2014:2007
- ROBERT BOSCH GmbH (2002) Autoelektrik Autoelektronik. Vieweg Verlag, Wiesbaden
- Schröder D (2009) Elektrische Antriebe—Regelung von Antriebssystemen. Springer, Berlin, Heidelberg, New York
- Steinhilper W, Sauer B (2006) Konstruktionselemente des Maschinenbaus: Grundlagen der Berechnung und Gestaltung von Maschinenelementen. Springer, Berlin, Heidelberg, New York
- Stoll H, Reimpell J (Hrsg.) Fahrwerktechnik: Lenkanlagen und Hilfskraftlenkungen: Auslegung- und Beurteilungskriterien, Sicherheit, steerokinematik, steerübersetzung, steergetriebebauarten, Bauteile der steieranlage, hydraulische, elektrische, pneumatische und geschwindigkeitsabhängige Hilfskraftlenkungen. 1. Auflage, Vogel Buchverlag, Würzburg 1992–291 Seiten, ISBN 3-8023-0431-4
- Störling H-D, Kallenbach E (2006) Handbuch Elektrische Kleinantriebe. Hanser Verlag, München
- United Nations Economic Commission for Europe (UNECE) (2005) Control 79, steering equipment
- Yoshida K (2002) Development of Custom IC for EPS Torque Sensor, Koyo Engineering Journal English Edition E160, Nara
- Zabler E et al (2001) Sensoren im Kraftfahrzeug. Bosch Gelbe Reihe

# Chapter 16

## Superimposed Steering System

Mirko Reuter and André Saal

### 16.1 Introduction

The growing number of mechatronics options in the field of steering systems provides additional steering functions. One of them is the superimposed steering system. A heterodyne angle is added to the driver's steering input by a specific superposition of the steer-angle. This enables additional steering functions, for example, a VGR or steering dynamics and steering stabilisation functions. Combined with a superposed steering torque, functions that are otherwise reserved to steer by wire, such as freely programmable steering functions, may be enabled.

### 16.2 History

The first patent application for the angular superposition of a steering system was a US patent of the Ford Company from 1972 (Fig. 16.1).

It already contains the basic function of combining simultaneously a permanent mechanical driving with flexibly superposed steer-angles. This function is intended for potential further steering functions (crosswind compensation was mentioned, for example). The described functional principle corresponds closely to the active steering that was later introduced by BMW, see Fig. 16.2. An angle is superposed between drive shaft [steering shaft, 18] and driven shaft [steering spindle, 50] by

---

M. Reuter (✉) · A. Saal  
Audi AG, Ingolstadt, Germany  
e-mail: [mirko.reuter@steeringhandbook.org](mailto:mirko.reuter@steeringhandbook.org)

A. Saal  
e-mail: [andre.saal@steeringhandbook.org](mailto:andre.saal@steeringhandbook.org)

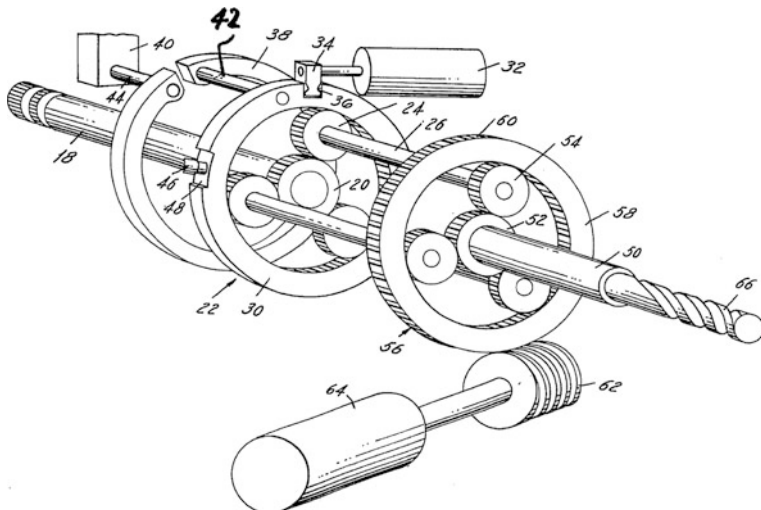


**Fig. 16.1** Patent sketch ford from 1972 [US 3831701]

twisting an annulus [60] of a double planet drive [24, 26, 54] coupled about the planet pinion carriers, see Fig. 16.1.

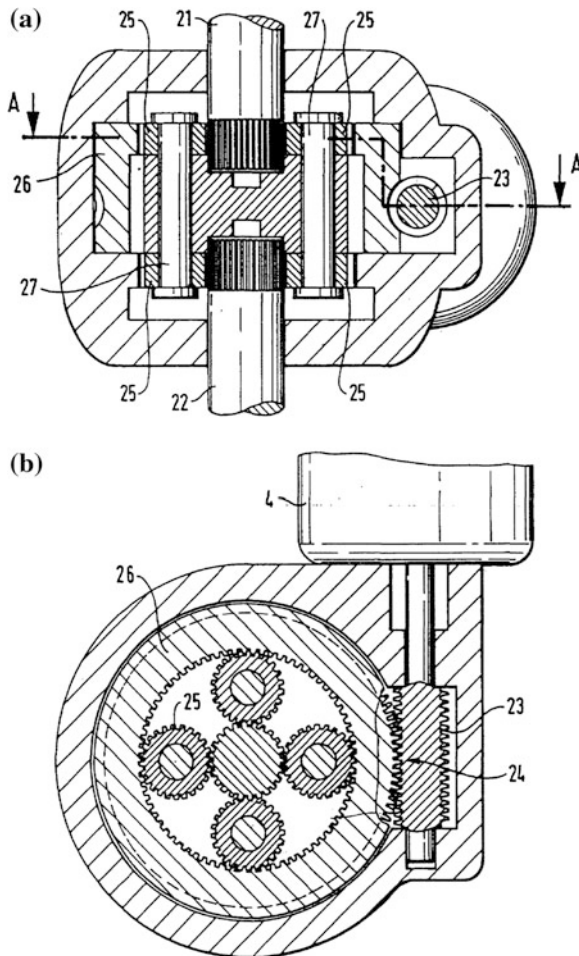
In spite of the patent application in the 1970s, this technology became manifest in standard cars only several decades later, because back then, the mechatronics were difficult to make and expensive. A few functions (VGR by wheel angle and vehicle speed) were introduced to some markets by Honda in 2000, applying a purely mechanical gear ratio adjusting equipment, VGS (Variable Gear Ratio Steering System) in the S2000 model (Shimizu et al. 1999). But this is not a superimposed steering system proper. The large-scale production of a superimposed steering system according to the definition was introduced by Toyoda Machinery Works (now JTEKT), Lexus, ZF-Lenkssysteme (ZFLS) and BMW as late as 2002.

### 16.3 Functional Principle

The function of the superimposed steering system can be developed in different basic manners. An additive movement of the steering gear or a relative movement between rack and tie rod (cf. EP 1637426 A1, DE 102 16130 A1) is conceivable, for example. But in reality, superposition by integration of a heterodyne gearbox in the steering driveline or the gear has prevailed so far.

The integration of this heterodyne gearbox allows superposing a freely controllable engine angle ( $\delta_M$ ) over the driver's steer-angle ( $\delta_H$ ). This adds an additional degree of freedom to the steering system on which this function is based.

**Fig. 16.2** Patent sketch  
Robert Bosch of 1990 [DE  
4031316C2]



A main feature of this superposition is that, in contrast to steer by wire systems, the mechanical coupling between steering wheel and front axle is not disrupted. The basis of this mechanism can be described by a simple equation:

$$\delta_{H*} = \delta_H + \delta_M \quad (16.1)$$

Stabilising and lane-keeping functions always need either a countertorque supported on the driver's side or an additional superposed steering torque to compensate the response. This is due to the torque balance in the heterodyne gearbox, necessary for the mechanical driving (Fig. 16.3).

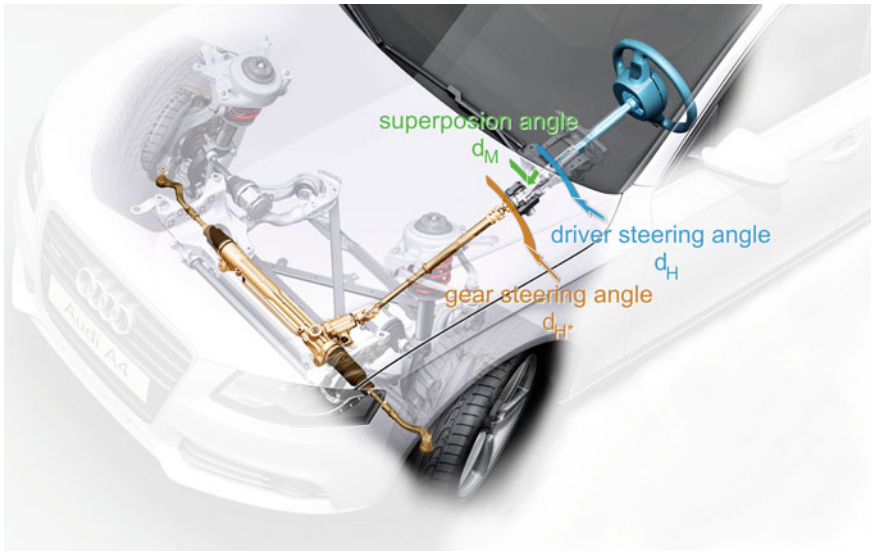


**Fig. 16.3** Functional principle of the superposition of angles

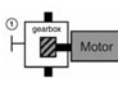
## 16.4 Configurations

All superimposed steering system actuators in use consist of an electronically commuted electric motor (brushless DC, for the basics of BLDCs, see [Sect. 15.3.2.4](#)) with accompanying position sensors, a heterodyne gearbox and a safety lock that locks the electric motor when powerless, blocking the additional degree of freedom in the gearbox. A direct pass between steering wheel and gear is thereby enabled. The market currently distinguishes three different superimposed steering systems by their principle. They differ primarily by the gearbox model used and by the position in the steering driveline.

Regardless of the used technology, the superposition in any system is represented by a gearbox with unequal gear ratio between added angle ( $\delta_M$ ) of drive ( $\delta_H$ ) and driven shaft ( $\delta_{H^*}$ ). This unequal transmission ratio generates a difference angle between drive shaft and driven shaft when the electric motor superimposes the angles. This is the base of all the other functions (Fig. 16.4).

### 16.4.1 General System Configuration

Other components and, in some systems, further adaptations to architecture and interlinking have to complement the heterodyne actuator so that a complete superimposed steering system is achieved.

variant	assembly area		
	steering gear	intermediate shaft	steering column
①			
②			
③			

**Fig. 16.4** Heterodyne systems from top to bottom: active steering (BMW-ZFLS), dynamical steering (Audi-ZFLS), variable gear ratio system (Lexus-JTEKT)

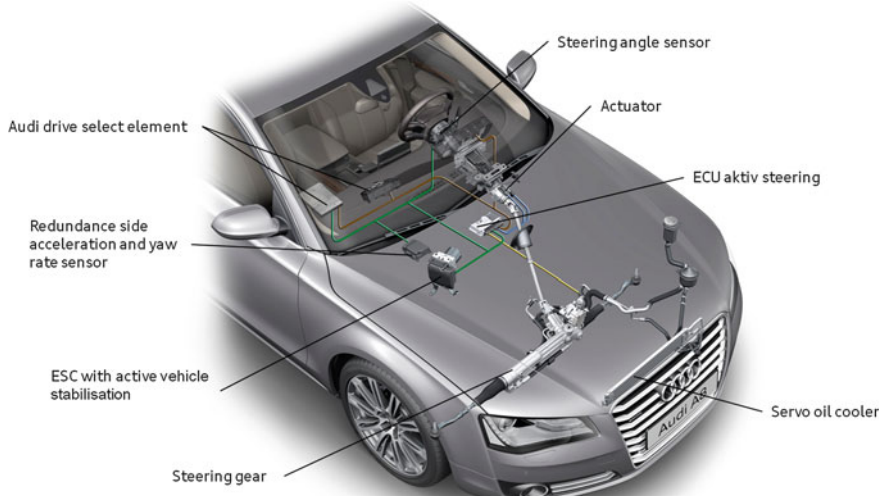


**Fig. 16.5** Superpositioned steering, example: Audi superimposed steering system

Figure 16.5 shows some components involved in such a system. The individual modifications are explained in the following chapters.

## 16.4.2 Actuators and Actuator Varieties

### 16.4.2.1 Audi/ZFLS Dynamic Steering

The actuator integrated into the steering column consists of an electronically commutating, permanently excited hollow-shaft synchronous motor that is concentric around the steering shaft (brushless DC). It includes position sensors, a harmonic drive gear box and a locking mechanism that locks the electric motor and, hence, the superposition when powerless, Fig. 16.6.

The concentric arrangement allows placing all rotating components (shafts, gearbox, engine and lock ring) in a stationary case, enabling a direct attachment to the upper part of the steering column. At the same time, this joining permits a modular arrangement, because the location inside the vehicle makes the system almost independent from any spatial restrictions in the engine compartment. Lower environmental requirements (e.g., moisture, temperature) for the actuators have to be met as well, while higher demands are made to the actuator acoustics and the crash response (Fig. 16.7).

The angular superposition of Audi's superimposed steering system is based on a harmonic drive. It combines a high reduction ratio (1:50) in compact size with a high torque capacity and torsional stiffness. For superimposing an angle, the electric motor turns the elliptic inner rotor (wave generator, WG). A flexible thin-section ball bearing (Flex Bearing, FB) deforms a thinly walled sun gear (flex-spline, FS) that is attached to the drive shaft of the steering (at the wheel), see

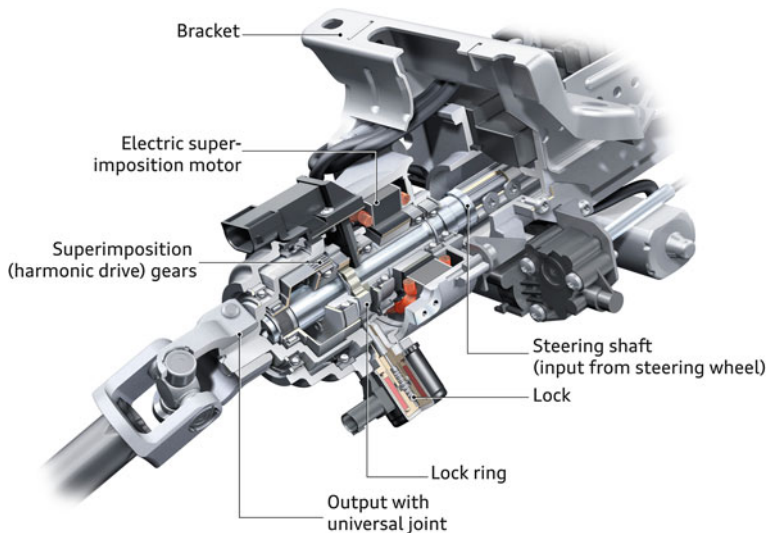


**Fig. 16.6** Cut-away view of the actuator in the steering column

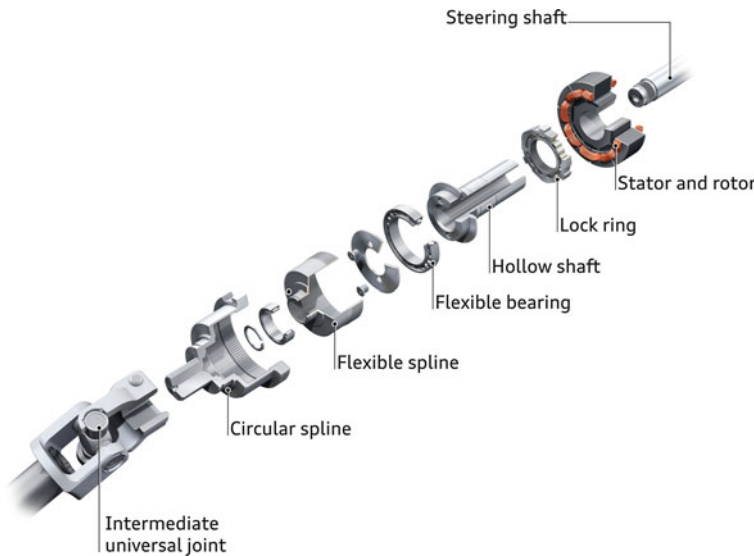


**Fig. 16.7** Exploded view of the parts of the actuator to illustrate the concentric configuration

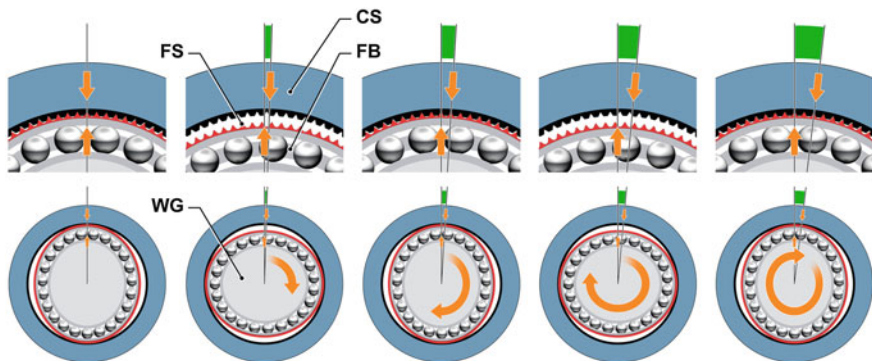


**Fig. 16.8** Functional principle of the harmonic drive

Fig. 16.8. The sun gear engages an annulus (circular spline, CS), attached to the driven shaft, on the vertical axles of the inner rotor's driving ellipse.

The different cog numbers of sun gear and annulus (at the steering gear) generate a superposition when the driving ellipse is rotating. An entire rotation of the driving ellipse produces a ratio of 100/102 cogs and a superposition of 7.2°.

The safety concept of the overall system involves a locking mechanism as a relapse level for serious system faults. It locks the engine shaft, removing the additional degree of freedom from the harmonic drive, so that the continuous mechanical driving of the gearbox from drive to driven shaft is maintained.

One shortcoming of arranging the actuators in the steering column is that interfering effects by the actuator (e.g., additional friction, repercussion and dynamic approach effects) cannot be damped or diminished by a hydraulic steering valve or the torque sensors of an EPS. This shortcoming affects any heterodyne system which is arranged in front of the steering valve or the torque sensor. Hence, these effects need to be reduced to a minimum by constructive and controlling measures.

#### 16.4.2.2 Active Steering BMW/ZFLS

The actuator integrated into the steering gear of this system is based on the superposition of angles by a double planetary gearbox that is placed into the gear between steering valve and pinion. The engine is connected to the gearbox, creating an additional reduction layer by applying a worm gear that is locked by a lock system when powerless, see Fig. 16.9. This way, the whole gear ratio between the electronically commuting, permanently excited synchronous motor (brushless DC) and the heterodyne gearbox is realised.

The superposition of the active steering is based on different gear ratios of the individual planet layers. When the planet pinion carrier, powered by the worm gear, turns, the planetary stage 1 on the sun gear of the drive shaft revolves with

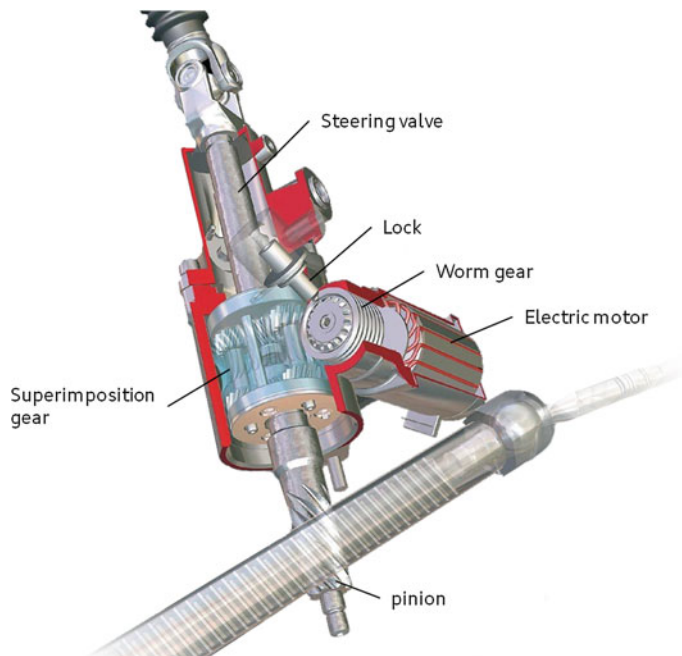
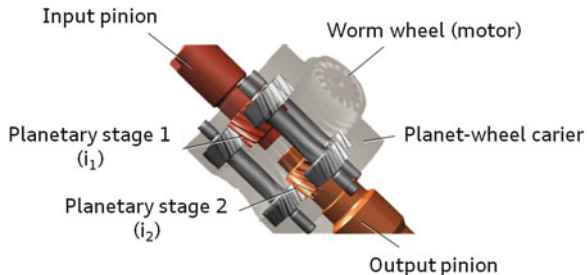


**Fig. 16.9** Cut-away view of the actuator in the steering gear. *Source* ZFLS

**Fig. 16.10** Functional principle of the superposition gearbox. Source ZFLS



the transmission ratio  $i_1$  (For example,  $i_1 = 15/12$ ). The rigid coupling passes the rotation directly to the planetary stage at the pinion. Now this rotation is transmitted to the drive shaft attached to the valve with the transmission ratio  $i_2$  (for example,  $i_2 = 13/14$ ), see Fig. 16.10.

In this example, each rotation of the planet pinion carrier turns the pinion shaft by 1.34 rotations relative to the drive shaft. Both planetary stages have to be spring-loaded, which may cause more friction in the gearbox, to keep potential free travel of the gear as low as possible.

In the safety concept, the self-inhibiting worm gear between engine and planet pinion carrier significantly reduces the undesirable back rotation in the passive state. Additionally, an interlocking slide spline locks worm gear, when it is deactivated. This enables the direct driving between steering valve and pinion. However, since the gear ratio is more direct in that state, one chooses an adapted steering ratio for the fault case when designing the overall system.

Arranging the actuators in the steering gear ('arrangement behind the steering valve (HPS) or behind the steering torque sensor (EPS)') allows damping—or at least reducing, for the sake of the steering feel—of some interferences of the actuators by the power-assistance of the steering (e.g., additional friction, repercuSSION and dynamic approach effects). However, a fundamental drawback of the planetary gearbox with several cog interventions is that the reset of the steering and the road feedback are decreased by the higher friction.

#### 16.4.2.3 Lexus/JTEKT VGRS

Like the dynamics steering, the VGRS (Variable Gear Ratio System) is based on a superposition of steer-angles by a harmonic drive, although a harmonic drive with double circular spline (CS) is used in this version. While the CS-D on the driver's side has 100 cogs, the CS-S on the side of the gear has 102 cogs. An offset of 2 cogs is generated for each full rotation of the electric motor, attached to the wave generator (WG), between driver and steering gear. Therefore the whole gear ratio between engine angle and heterodyne angle is 1:50, see Fig. 16.11.

The internal configuration of the other components is slightly different from Audi's superimposed steering system. Electric motor and locking mechanism are not hollow shafts but centrally arranged in the midst of a rotating overall case.

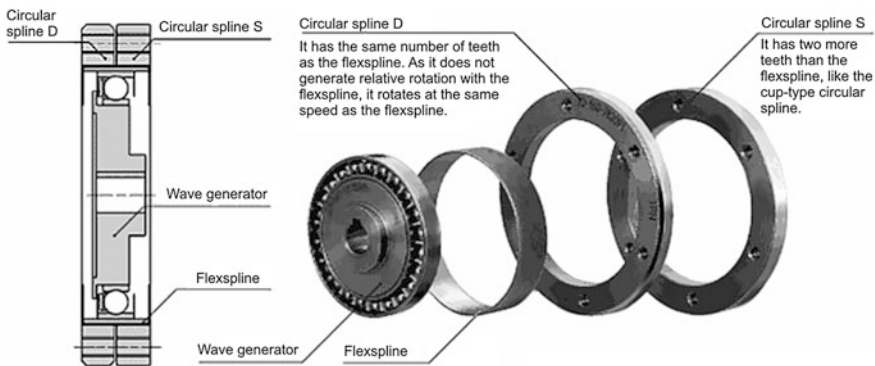


**Fig. 16.11** Source harmonic drive GmbH

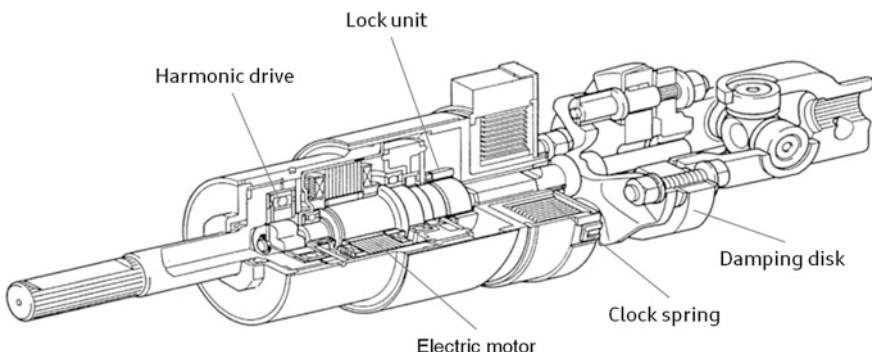


**Fig. 16.12** Cut-away view of the actuator in the steering column. *Source* Toyota

For this system, the power flow across the halves of the casings entails that the whole case is rotating with the steering movement, see Fig. 16.12. This requires sufficient free space on the side of the package.

On account of the arrangement in front of the steering valve or the steering torque sensor, measures to reduce repercussions on the steering feel are also integrated here. In comparison to other variants, an additional damping plate serving this purpose is integrated into this system between actuator and steering wheel. This reduces the haptic repercussions and the structure-borne sound transmission by the steering driveline, see Sect. 16.4.3.2.

Another type of this system by the manufacturer is now integrated into the steering gear, similar to the BMW-ZFLS system. The heterodyne unit, though, is still accommodated near the driver and in front of the steering torque sensor.

### 16.4.3 Adaptations in the Steering System

In a superimposed steering system, higher demands to the steering system design are set by the pinion rate, which may be higher during parking and evasive manoeuvres or because of the dynamic steering stabilisation interventions. These higher demands require a larger servo pump for hydraulic power steerings, to meet the higher demand for volumetric flows. Higher energy consumption of the larger pump often entails the installation of ECO controllers (ECO = Electrically Controlled Orifice; see Sect. 13.1.2.1). When the demand for steering is low (e.g., at motorway speed), the volumetric flow and the resultant circulation pressure may be reduced to save energy and fuel. The dynamic adaptation of the volumetric flow at medium and low speed (e.g., on country roads) enables the best steering performance.

Larger dynamics and volumetric flows often require additional adaptations at the tubing and the engine oil cooler.

Vehicles with electric power-assist also have a higher demand for power in the above-mentioned situations.

#### 16.4.3.1 Steering Ratio

The steering gear used is designed very directly to minimise the acoustic reper-  
cussion of the heterodyne system during parking and at low speed. The acoustics can thereby be improved, because relative to a symmetrical design of the steering ratio (Fig. 16.13a), there is less noise emitted (proportional to the heterodyne activity).

In the design of the steering gear ratio, however, the mechanical relapse level of a superimposed steering system must be controllable over the whole speed range, if a fault occurs. Any potential jumps of the steering ratio due to deactivation and the ability to control the whole steering ratio in the case a fault occurs, need to be considered.

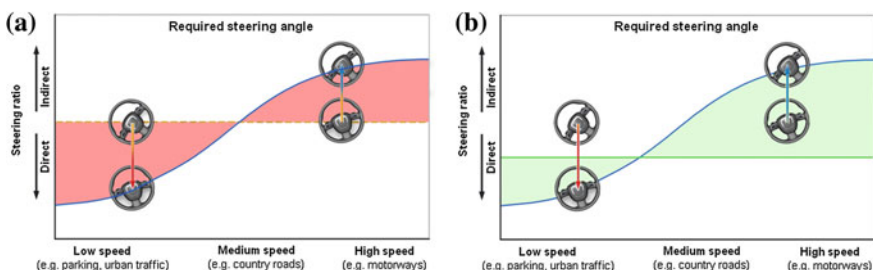


**Fig. 16.13** Acoustic design of the basis steering system. **a** Symmetrically. **b** Acoustically optimised

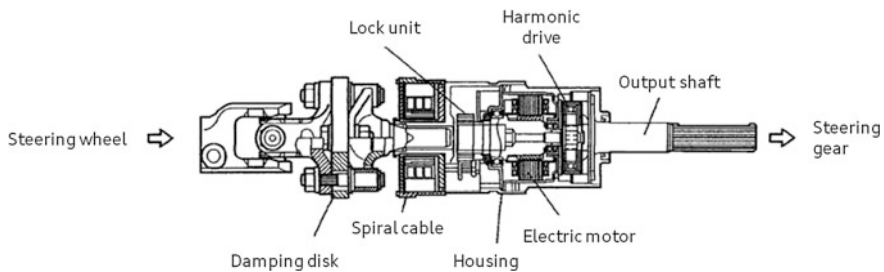


**Fig. 16.14** Acoustic decoupling by absorber disk in the steering column (JTEKT system, *source Lexus*)

#### 16.4.3.2 Adaptations to Meet NHV Requirements

The acoustic repercussion of the superposition is sometimes further reduced by installing absorbers in the steering column (e.g., ‘Hardy disks’) or entire enclosures of the actuators in the vehicle, Fig. 16.14.

The main purpose is to reduce the structure-borne sound transmission (absorbers) and the airborne sound transmission (enclosures).

A drawback of the absorbers is the resulting lower stiffness of the steering driveline that has a tendency to impact steering feel, steering response and steering precision. The integration of an enclosure, on the other hand, requires additional package space. Therefore, these secondary acoustic measures need to be considered in the context of the general requirements.

#### 16.4.3.3 Adaptations Due to Steering Stabilisation

The steering dynamics are high when a steering stabilisation is used and, hence, the necessary fault latent times are low. The stability control systems are adapted when steering stabilisation functions are added.

For example, in the implementation of Audi’s superimposed steering system, the sensors for steer-angle, yaw speed and lateral acceleration are redundant. This redundancy is necessary to provide the required reaction times in case of faults. Model-based monitoring of the input signals does not yet achieve the accuracy and latency time that would be necessary for fault detection.

#### 16.4.3.4 System Network

Using the functions of the superimposed steering system needs a complicated system network of different subsystems in the vehicle structure.

Figure 16.15 shows an example of a network of Audi’s superimposed steering system. Some functions are distributed to different ECUs and interlinked by

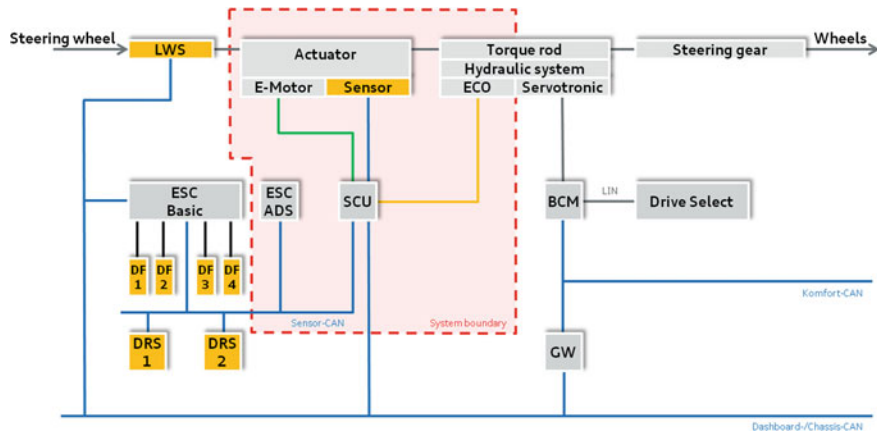


**Fig. 16.15** Network of the superimposed steering system, example: Audi superimposed steering system

several bus systems. The steering control unit (SCU) controls the actuators and coordinates the function of the dynamic steering, but the steering stabilisation functions are accommodated in the ESP. Both control devices are redundant via the sensor and dual-suspension CAN to ensure the necessary integrity of the exchanged signals, see Fig. 16.15.

Another component of the overall system is the body control module (BCM), which is the interface to individualise the dynamic steering by mode (drive select) and to control the speed-sensitive power-assist (servotronics).

## 16.5 Functions of the Superimposed Steering System

### 16.5.1 VGR

The possibility to freely control the angle of a superimposed steering system allows making steering ratio characteristics that significantly depend on the steer-angle or the car speed. This superposition of angles entails a perfect solution to the basic compromise between agility and handiness (direct gear ratio) and stability (indirect gear ratio) in a defined mechanical steering ratio. It is therefore possible to find a suitable gear ratio for every speed or requirement range. Three different typical speeds may be mentioned as basic corner points for the design of the steering ratio. These are parking and manoeuvring at low speed, the medium speed range (e.g., city and country road travel) and high speed (e.g., motorway travel), see Fig. 16.16.

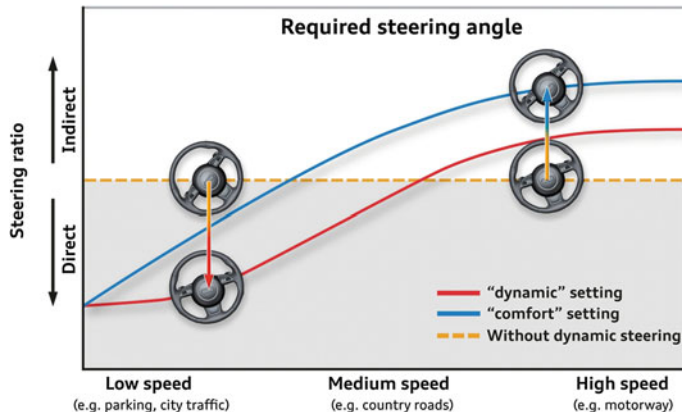


**Fig. 16.16** Principle curve of the steering ratio over vehicle speed

### 16.5.1.1 Low Speed

To facilitate parking and manoeuvring, the demand for a steering wheel angle in such situations is reduced to a minimum. The driver should be able to guide the car in the low speed range without shuffle-steering. The steering ratio in this range is designed very directly. However, the driver's adaptation to this gear ratio and the acoustic constraints need to be considered (see Sect. 16.4.3.1).

The whole gear ratio curve at low speed has the main purpose of reducing the driver's steering effort.

### 16.5.1.2 Medium Speed

In the medium speed range, the desired response with regard to handiness and agility can be achieved by the VGR. The yaw gain is typical for this agility. In contrast to a conventional mechanical steering, a superimposed steering system allows the yaw gain to build up much faster with rising driving speed, see Fig. 16.17. The results are better handiness and agility at medium range, and this can be sustained across a wide speed range, too.

### 16.5.1.3 Stability at High Speed

For the medium to high-speed range and bigger cornering radii, the steering ratio has to permit a quiet and gentle vehicle guidance. This condition can be realised by a much more indirect gear ratio than in the lower speed range.

For this driving response, the most important describing variable in the high-speed range is the gain of the lateral acceleration, see Fig. 16.18.

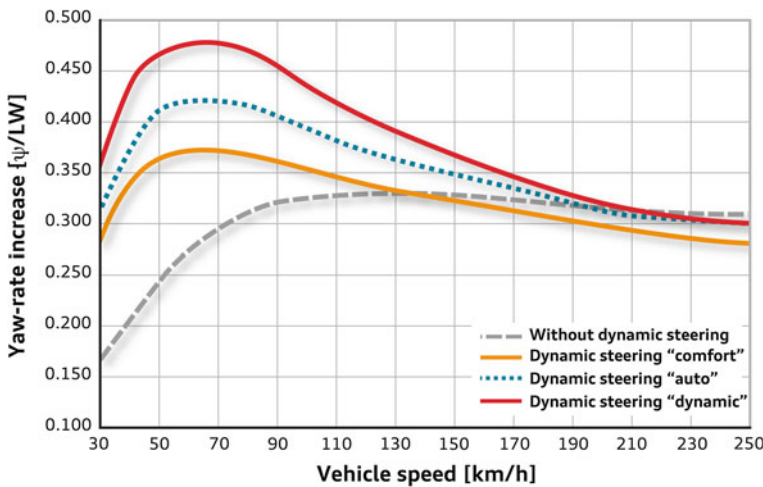


Fig. 16.17 Yaw gain with and without superimposed steering system

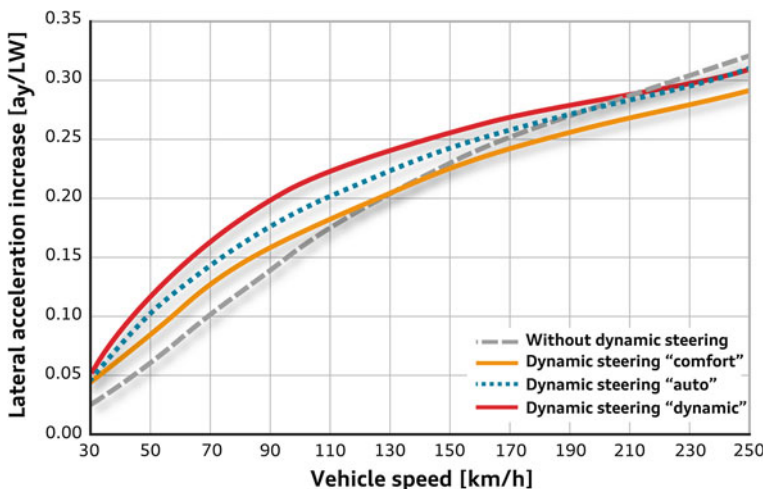


Fig. 16.18 Gain of the lateral acceleration with and without dynamic steering

The gain of the lateral acceleration can be considered a quantifying parameter of the vehicle response for changing the track at high speed. Hence, a lesser and steadier gain enables quieter and safer vehicle guidance, resulting in sturdier driveability. When the steering ratio characteristic curves are designed, special attention is paid to a harmonious transit between the requirements of the various speed ranges. This facilitates the driver's adaptation to the changed gear ratio.

#### 16.5.1.4 Varieties of Characteristic Curves According to the Driver's Request

Because the characteristic curves (steering ratio and support torque) of a superimposed steering system can be freely controlled, their individuation can be provided to the driver by a suitable operating element for controlling the vehicle response as desired. These characteristic curves should consider the above-mentioned design directives in different forms and weighting. They can significantly change the gain response of yaw and lateral acceleration, as the driver desires, see Figs. 16.17 and 16.18.

### 16.6 Steering Stabilisation

The steer-angle superposition permits active stabilising steering corrections that are almost independent from the driver. It can stabilise the vehicle in dynamically critical situations not only by triggering the ESP to brake individual wheels, but also by additional overlaid tyre steer-angles. Two main benefits are the result:

- The overall stability of the vehicle is improved by concurrent braking and steering interventions. This applies in particular to high speeds ( $>100$  km/h), because the superimposed steering system then offers obvious advantages in contrast to a brake stabilisation, on account of the very fast response time.
- In some less critical driving situations, braking interventions can be renounced in part or even completely, so that the vehicle stabilisation is more harmonious and comfortable. Less braking interventions mean that especially on roads with low friction (e.g., snow) but the same driving stability, the vehicle will drive perceptibly more agile than a car which is stabilised only by braking interventions (Fig. 16.19).

The effectiveness of stabilising steering interventions is generally dependent on the available useful steering performance. For the superimposed steering system, the gradient of the stabilising superposition angle can be considered a measure of this performance. Figure 16.20 shows that a rise of this gradient can significantly reduce the stabilising steering wheel angle that the driver has to add in unstable situations, and even the drop of speed during the stabilisation can be significantly lowered.

Indeed, it can also be seen that braking interventions are still necessary for yaw damping and lower speed, according to the degree of instability. To achieve the best agility and concurrent stability, the best distribution of the stabilisation torque on brake and steering is made by an arbitrating concept.

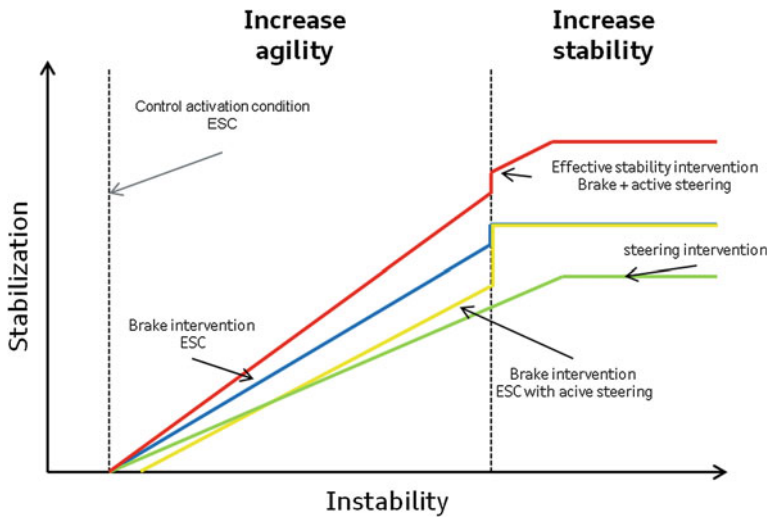


**Fig. 16.19** Stabilisation with and without superimposed steering system intervention

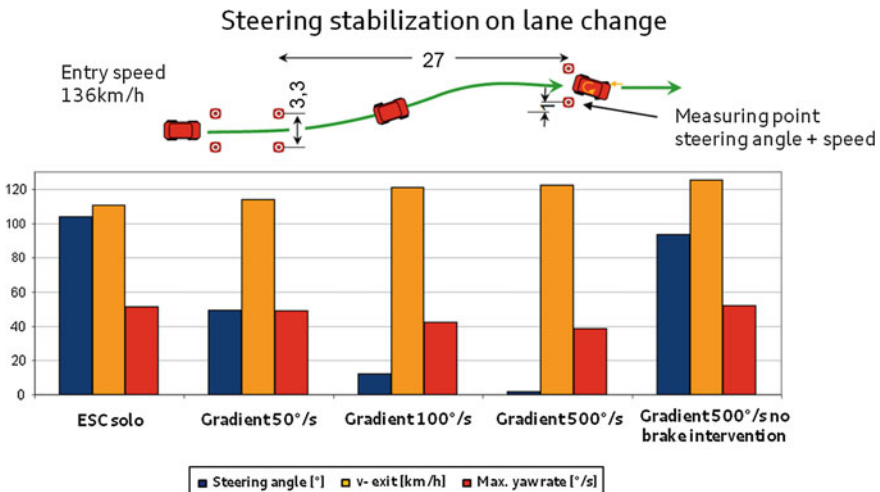


**Fig. 16.20** Steering stabilisation during a simple lane change

### 16.6.1 Steering Stabilisation at Oversteering

Specific, active countersteering of the superimposed steering system in an over-steering vehicle can quickly and precisely reduce or fully compensate the too high yaw response of the vehicle. Its low yaw inertia by which it responds to the changed tyre steer-angles enables a very fast stabilisation, especially at high speed,

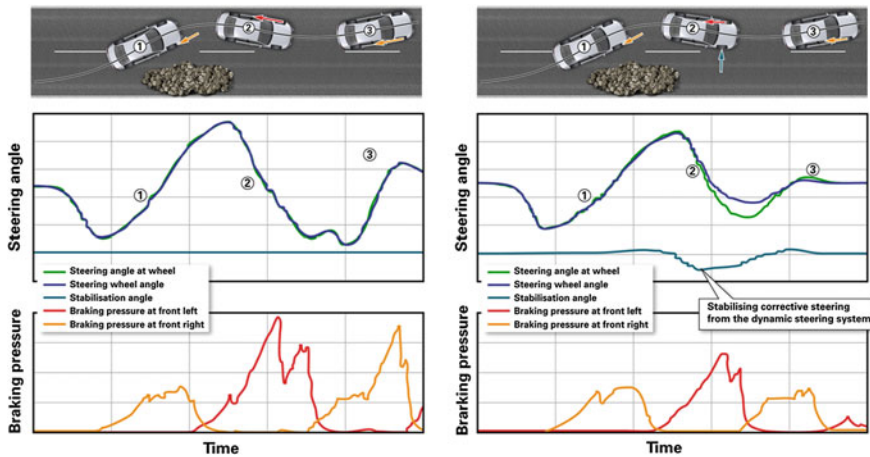


**Fig. 16.21** Steering stabilisation during a simple lane change

see Fig. 16.21. The stabilisation steer-angle that the driver requires can be significantly lowered by this engagement. A further benefit is the much lower number of brake interventions that make the overall stabilisation look very harmonious.

### 16.6.2 Steering Stabilisation at Understeering

The heterodyne engagement of a front-axle steering in an understeering vehicle is quite naturally not very effective. In this case, the strongest grip at the front axle is already passed, and a rectified additional steer-angle cannot build up any more lateral force. However, the point of highest positive engagement may be fully exploited. This requires a heterodyne engagement that opposes the driver's steer-angle, so that the typical oversteering by the driver in such a situation is limited. A partial compensation is the best solution to maintain the driver's typical steering feel without corrupting the tactile information on the grip state at the front axle. This can be achieved, for example, by a more indirect steering ratio according to the situation.

Figure 16.22 shows the functional principle of this understeering function. A vehicle without steering stabilisation passes the point of highest positive engagement at the front axle, due to a too great steer-angle. The vehicle's front wheels push out of the corner. In a car with steering stabilisation, the understeering situation can be recognised, and a specific change of the gear ratio can limit the driver's oversteering.

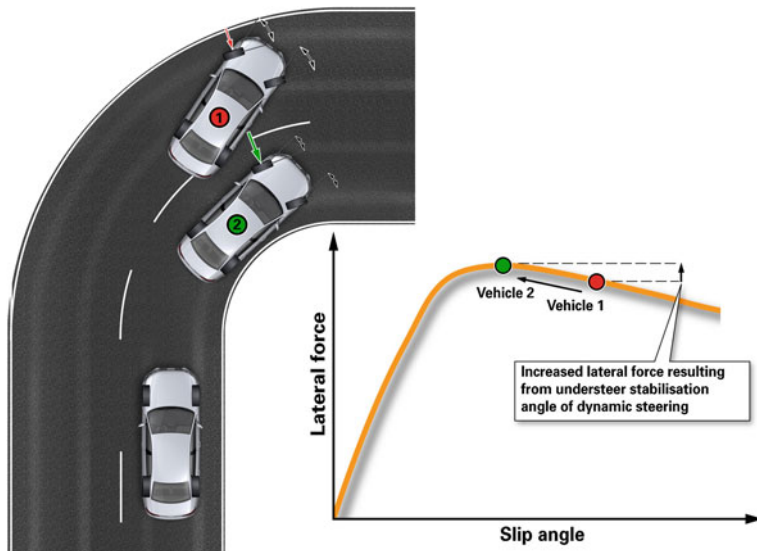


**Fig. 16.22** Understeering function of the superimposed steering system

### 16.6.3 Steering Stabilisation During Braking on Roads with Different Friction Values ( $\mu$ -split)

$\mu$ -split surfaces are marked by the fact that the road friction value is high on one side of the vehicle (e.g., asphalt) and low on the other side (e.g., ice). Braking on such a road generates a yaw torque from the higher braking powers on the side with more friction, this pulls the vehicle that way (oblique pull). To continue driving straight, the driver of a vehicle without superimposed steering system has to set a steering wheel angle that compensates the interfering yaw torque and, by consequence, the oblique pull of the vehicle.

In a vehicle with steering stabilisation, the stabilisation system can control this steer-angle autonomously, so that the driver can leave the steering wheel essentially in its straight-line position, i.e. towards the desired way. The interfering yaw response can be prevented early-on by this yaw torque compensation while a rise of the total brake pressure slightly shortens the braking distance for this manoeuvre. Figure 16.23 shows such a  $\mu$ -split manoeuvre.

## 16.7 System Safety

The ECU of the superimposed steering system does not only have to meet functional requirements, such as the superposition and control of the part of the variable steering ratio function and the externally computed stabilisation part, but

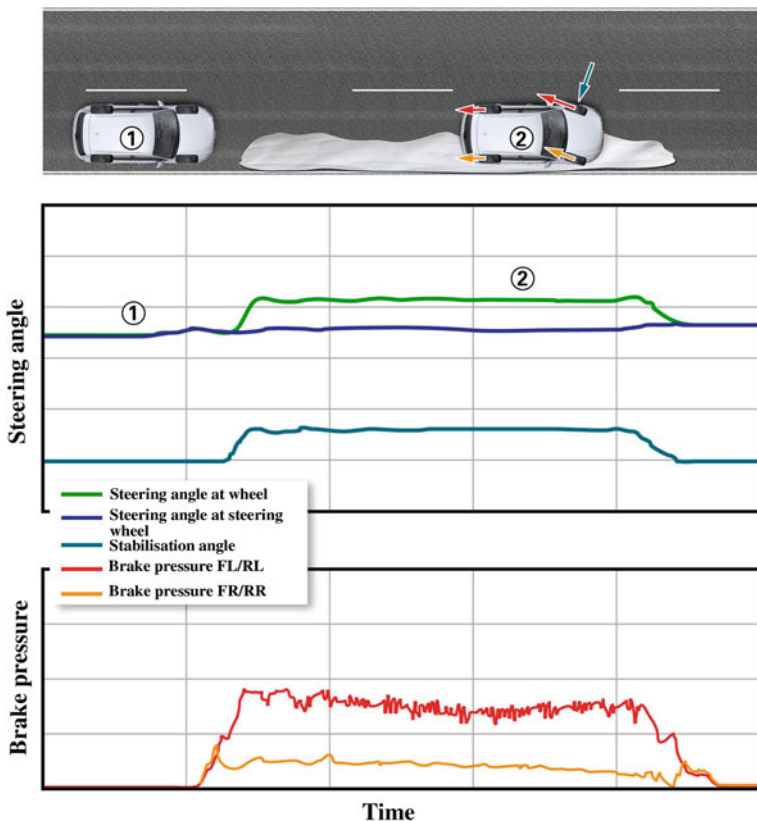


**Fig. 16.23** Stabilisation of a vehicle with network steering stabilisation during a  $\mu$ -split braking manoeuvre

it also has to electronically prevent malfunctions. The derived safety requirements for the ECU of the superimposed steering system for any malfunctions to be prevented are:

- avoid reversible and irreversible actuating errors that can be caused by the ECUs, the electric motor or the engine position sensor;
- monitor the externally computed stabilising interventions and take suitable measures, so that the highest actuating errors are not reached, see also Neukum et al. (2007).
- ensure that in the fault case, the limit for the highest permissible gear ratio jumps is not exceeded, see also Neukum et al. (2007).
- prevent a free steering situation (i.e. missing or insufficient conversion of the driver's wheel angle into the tyre steer-angles).

An assessment and requirement concept was worked out by the Association of the German Automotive Industry (VDA), dealing with individual fault patterns of

superimposed steering systems. For further information, see ‘Assessment of the Fail-Safe response of active steering systems’, see also Neukum et al. (2007).

Safely controlling these fault patterns requires a suitable safety concept and a process of development for superimposed steering systems compliant with (or at least based on) IEC 61508/ISO 26262. Basic facts of these safety standards are discussed in Sect. 15.5.

The safety concept resulting from these requirements needs a reliable monitoring and verification concept, when the system is built, to maintain the necessary fault response times and, hence, to limit the highest possible actuation errors. Figure 16.24 shows a monitoring level concept of the ECUs of Audi’s superimposed steering system.

On level 1, any software modules which are necessary from a functional point of view are integrated. This includes the signal verification and the fault strategy. All critical paths which can lead to a malfunction are diversitarily computed on level 2. This ensures that systematic fault sources (e.g., programme errors) or sporadic RAM errors cannot lead to a malfunction. Level 3 maintains, e.g., the programme run and the correct execution of the command set.

The challenge of diversitary computing is to generate on the diversitary path the same result as on the main path, using other algorithms. This shall be explained by two examples:

In a faultless state, the variable steering ratio function permits to achieve the same result by applying either the main function or the diversitary function without any relevant time delay, because this is not a regulation but a servo control. Even for a diversitary implementation, the deviation of the two paths can

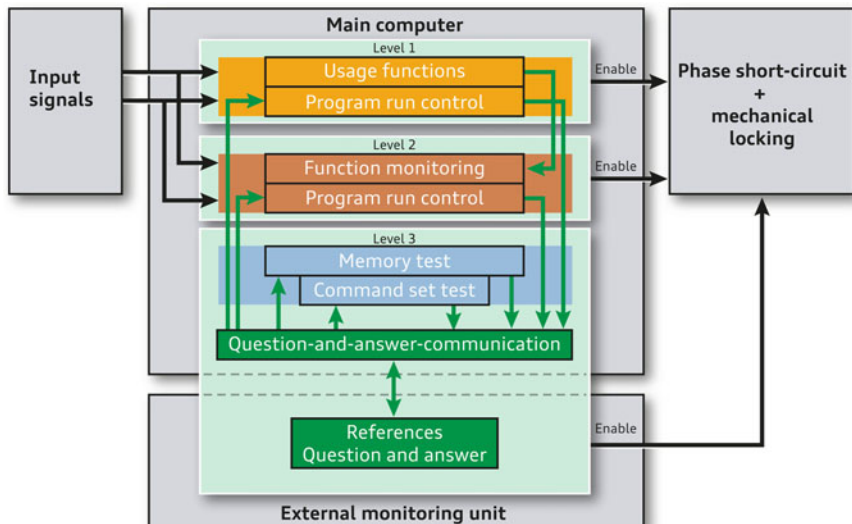


**Fig. 16.24** The 3-levels safety concept of Audi’s superimposed steering system

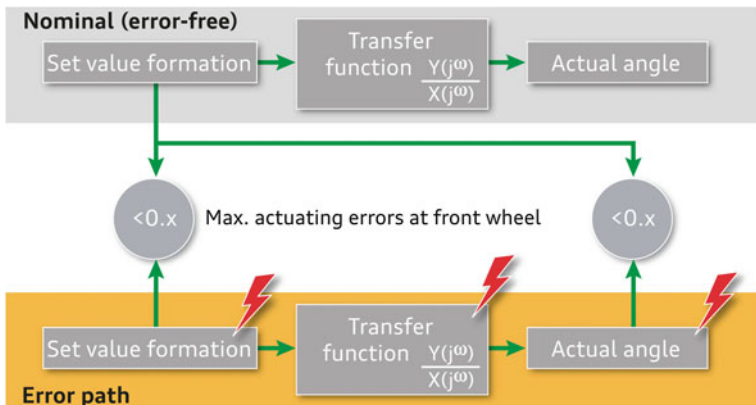


**Fig. 16.25** Examination of the position control

be kept low, because both functions can be written regardless of other interfering variables, in spite of different calculation paths.

The monitoring of the position control, including sensor analysis, shall serve as the second example. Both paths are monitored on level 2 by back-reading and controlling of the engine position signal against its nominal angle, seen in Fig. 16.25. A permissible deviation when comparing intermediate and final results of the nominal and the fault path needs to be allowed. This tolerance range is needed on account of the different algorithms and back reference variables on either path.

The system functions are gradually degraded as a function of the occurred fault. High availability is maintained as follows:

- actuate a steady steering ratio if information on driving speed is missing,
- block external stabilising interventions if low performance is predictable, e.g., by fluctuations in the on-board power system or failure of the steering power supply,
- deactivate the system in the zero passage of the steering angle if a fault is suspected, to avoid an obliquely positioned steering wheel,
- deactivate the system completely if any serious fault is present.

Other than preventing malfunctions, the ECU has to continuously supply safety-relevant signals for other vehicle systems whose ECUs rely on status and position data of the superimposed steering system (e.g., ESP and other chassis control systems).

## 16.8 The Future

Connecting the superimposed steering system with an active steering torque superposition helps to complement the advantages of both systems, so that additional functions are made accessible. Superposing a steering torque, for example, allows compensating or even partially complementing the repercussions of superimposed steering system interventions by targeted torque interventions.

These possibilities can be realised by a combination of superimposed steering system and EPS (cf. Fig. 16.26, BMW 5, model year 2010) or by combining the superimposed steering system with an additional active torque actuator (cf. Fig. 16.27, JTEKT).

**Fig. 16.26** Active front steering with electromechanical power assist in the BMW 5. *Source* BMW

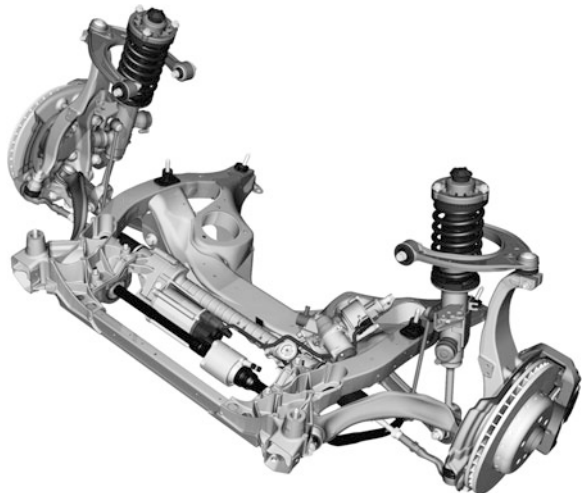
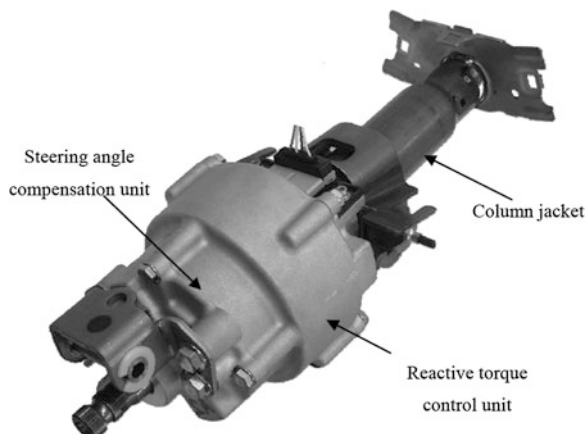


**Fig. 16.27** Active front steering with reactive torque control unit. *Source* JTEKT



Extended networking of both systems leads to an imitation of steer by wire-like functions. These systems may act like an enabler technology for completely new definitions of steering functions, due to the option of a partial decoupling of steer-angle and steering torque (cf. Sect. 18.3).

An advantage of this version is the immanent mechanical relapse level and the quick shutdown time in the fault case. However, these functions are restricted in comparison to full steer by wire with regard to performance and the decoupling of the repercussion, because of the control accuracy and resultant system repercussions. Yet electric steering and superimposed steering system represent important steps towards future steering systems. Especially the intelligent linkage of both may one day make new steering functions accessible.

## References

- Eckrich M, Bartz R (2006) Das Sicherheitskonzept der BMW-Aktivlenkung, VKU Verkehrsunfall und Fahrzeugtechnik, edition 11/2006
- Ishihara A, Kawahara S, Nakano S (2008) Development of active-front-steering systems
- Köhn P, Pauly A, Fleck R, Pischinger M, Richter T, Schnabel M, Bartz R, Wachinger M, Schott S (2003) Die Aktivlenkung—Das fahrdynamische Lenksystem des neuen 5er; Automobiltechnische Zeitschrift, speciel edition BMW 5, vol 105
- Kurz G (2010) Das Fahrwerk des neuen 5er BMW, geprägt durch moderne, Chassis Tech 2010
- Neukum A, Ufer E, Paulig J, Krüger P (2007) Bewertung des Fail-Safe-Verhaltens von Überlagerungslenkungen (VDA-Abschlussbericht)
- Reuter M (2008) Mechatronical system development of the Audi dynamic steering system. Steering Tech
- Schöpfel A, Stingl H, Schwarz R, Dick W, Biesalski A (2007) Audi drive select. ATZ und MTZ Sonderausgabe—Der neue Audi A4. Vieweg+Teubner Verlag, Wiesbaden
- Schuller J, Sagefka M, Ullmann S (2010) Funktionale Sicherheit für vernetzte mechatronische Fahrwerkregelsysteme, Aachener Kolloquium Fahrzeug- und Motorenmechanik 2010
- Shimizu Y, Kawai T, Yuzuriha J (1999) Improvement in driver-vehicle system performance by varying steering gain with vehicle speed and steering angle: VGS (Variable Gear-Ratio Steering System). In: Steering and suspension technology symposium 1999

# Chapter 17

## All-Wheel Steering

Peter Herold and Markus Wallbrecher

### 17.1 Introduction, History, Basics, Objective

Various steering systems that apply a steer-angle at the front wheels to perform their driving task were described in the preceding chapters. All-wheel steering also provides the possibility to make the back wheels steerable, in addition to the steering at the front axle.

The application of pure back-wheel steering, on the other hand, is known only from applications for forklifts, lawn mowers or similar vehicles. Here the task can be better accomplished by steering the back wheels, usually together with very big steer-angles.

Passenger cars used in standard road traffic would suffer several drawbacks from a pure back-wheel steering, though:

1. The driveability is unstable beyond a critical driving speed. This complicates the steering task and the burden of the driver. Especially at high speed, the vehicle is almost uncontrollable.
2. Legal stipulations require that the steering equipment has to actively righten the wheels into the centre position at any conceivable speed, see ECE R79. A pure back wheel steering has no righting moment, though.
3. Moving forward out of a parking space leads to bumping into the kerbs.

Hence, pure back-wheel steering is not suitable for passenger cars and trucks, the standard choice is the combination with a steering at the front axle.

The first all-wheel steering was already built in the mid-1930s. The bucket car 107 VL (W139) by Mercedes-Benz was equipped with a mechanical all-wheel

---

P. Herold (✉) · M. Wallbrecher  
BMW Group, Munich, Germany  
e-mail: peter.herold@steeringhandbook.org

M. Wallbrecher  
e-mail: markus.wallbrecher@steeringhandbook.org



**Fig. 17.1** Mercedes-Benz Model 107VL, W139 (1936) (Oswald 1987). Source [www.autoevolution.com](http://www.autoevolution.com)

steering as early as 1936. Nevertheless, this vehicle was made in small numbers, only 42 copies were delivered to the Wehrmacht (Oswald 1987) (Fig. 17.1).

All-wheel steering has been used in several kinds of automobiles during the last decades. First, Nissan developed an appreciable number of all-wheel steering systems to series production in the 1980s. All-wheel steering can be developed and designed acc. to different technical plans. A huge number of technical solutions is possible. This chapter will give an overview of the construction methods, the technically feasible plans and the active principles.

## 17.2 Construction Methods

Three basic concepts of rear-wheel steering are distinguished: mechanical, hydraulic and electromechanical.

The following table gives an overview of which manufacturers have already developed and introduced all-wheel steering to the market (Table 17.1).

### 17.2.1 Mechanical Systems

Mechanical all-wheel steering systems have a mechanical connection between front axle and rear-wheel steering, shaped like a shaft with corresponding step-up gear. This direct mechanical connection locks the steer-angles of the front and rear axle in direct dependency; a defined steer-angle at the rear axle is assigned to every steer-angle at the front axle (Fig. 17.2).

**Table 17.1** Overview of all-wheel steering systems (BMW 2005)

Manufacturer	Construction method	Configuration	Functional purposes		Steer-angle (°)	Vehicles
			WKR	FS (FDR)		
Toyota	Mechanical	Connection to the front wheel steering, gearbox	WKR	4	Celica (1990), Carina (1989)	
	Electric-hydraulic	Hydraulic pump, hydraulic valves, centring actuators	WKR	15	Mega Cruiser (1995)	
	Electric-hydraulic	Hydraulic pump, hydraulic valves, centring actuators	WKR, FS (FDR)	5	Soarer (1991), Crown (1992)	
	Electromechanical	Electric motor, gearbox, spindle drive	FS (FDR)	2	Aristo (1997), Majesta (1997)	
Nissan	Hydraulic	Hydraulic pump, hydraulic valves, centring actuators	FS (VS)	1	Skyline (1985), Silvia (1988), 180SX (1989), Fair lady Z (1989), Cefiro (1992), Laurel (1993)	
	Electromechanical	Electric motor, gearbox, spindle drive	FS (FDR)	1	Skyline (1993), Silvia (1993), Fair lady Z (1993), Laurel (1997), Cedric (1994), Stagea (1998)	
	Electromechanical	Electric motor, gearbox, spindle drive	FS (VS), FS (FDR)	Approx. 1.5 (2004)	Infinity FX50 (2008), G37 (2007), Stagea (2002), Fuga (2004)	
	Mechanical	Connection with the front wheel steering, gearbox	WKR	5	Prelude (1987), Accord (1990)	
Honda	Electromechanically	Electric motor, spindle drive	WKR, FS (VS)	8	Prelude (1991)	
	Hydraulic	Hydraulic pump, electric motor, gearbox	FS (VS)	5	626 (1988), MX-6 (1987)	
	Hydraulic	Hydraulic pump, electric motor, gearbox	FS (FDR)	7	Eunos800 (1992), RX-7 (1985)	
Mitsubishi	Electric-hydraulic	Hydraulic pump, hydraulic valves, centring actuators	FS (VS)	1.50 (1991)	Gallantly (1988), Lancer/Eterna (1988), GTO /3000GT	
	Electric-hydraulic	Hydraulic pump, hydraulic valves, centring actuators	FS (VS)	0.8 (1994)	Gallantly (1993), Emeraude (1994), Lancer/Eterna	
	Electromechanical	Electric motor, gearbox	FS (VS)	1.5 (1991)	Alcyone (1991)	

(continued)

**Table 17.1** (continued)

Manufacturer	Construction method	Configuration	Functional purposes	Steer-angle (°)	Vehicles
Daihatsu	Mechanical	Connection with the front wheel steering, gearbox	WKR	7	Mira (1992)
BMW	Electric-hydraulic	Hydraulic pump, hydraulic valves, centring actuators	FS (VS)	1.7	850i, 850csi (1992)
	Electromechanical	Electric motor, spindle drive	WKR, FS (VS), FS (FDR)	3.2.5	7 (2008), 5 GT (2009), 5 (2010)
Renault	Electromechanical	Electric motor, gearbox, spindle drive	WKR, FS (VS), FS (FDR)	3.5	Laguna GT (2008), Laguna coupe (2008)
GM	Electromechanical	Electric motor, gearbox, spindle drive	WKR, FS (VS)	12	GMC Sierra (2002), Silverado (2002)

WKR, Turning circle reduction

FS (VS), Driving stabilisation (pilot control)

FS (FDR), Driving stabilisation (electronic stability programme)

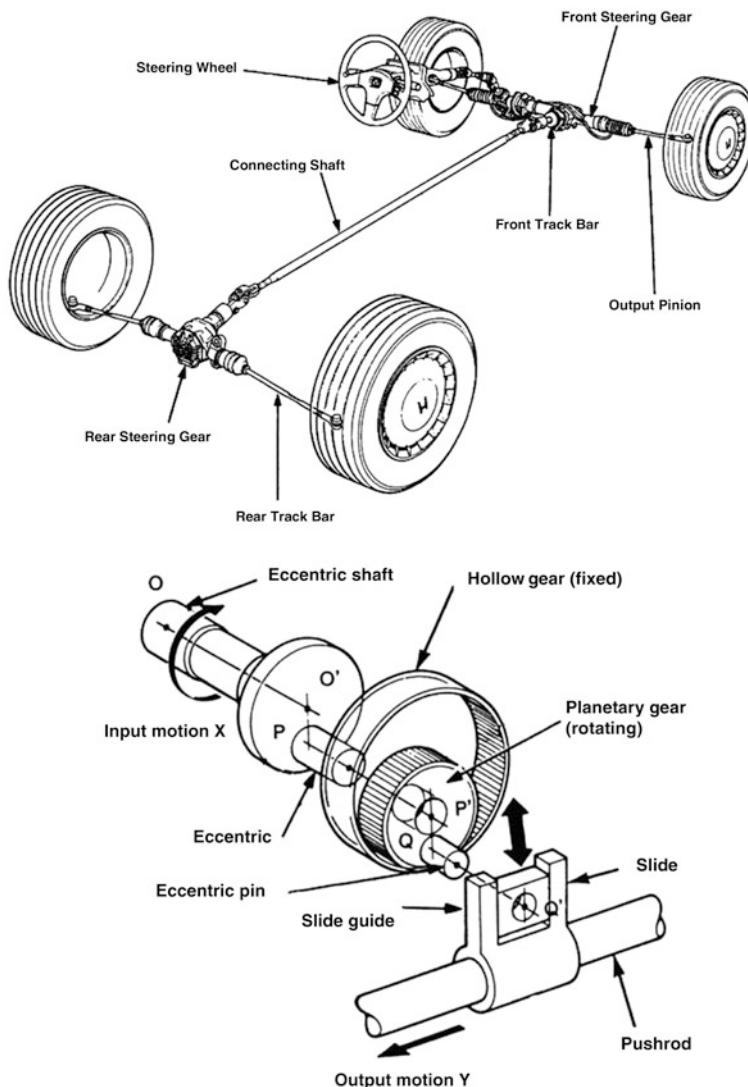


**Fig. 17.2** Mechanical all-wheel steering of Honda Prelude (Honda Accord Forum 2009)

The mechanical all-wheel steering of the Honda Prelude (1987) is designed so that for small front-axle steer-angles, the back wheels are turned in the same direction. Stability at high speed is gained that way, because the yaw impulse is smaller. With higher steer-angles (beyond a steering wheel angle of 127°), the mechanical gear ratio changes in such a way that the back wheels turn in the opposite direction of the front wheels. This improves the agility in the low speed range, e.g., when manoeuvering, see Fig. 17.3. At about 450° of steering wheel

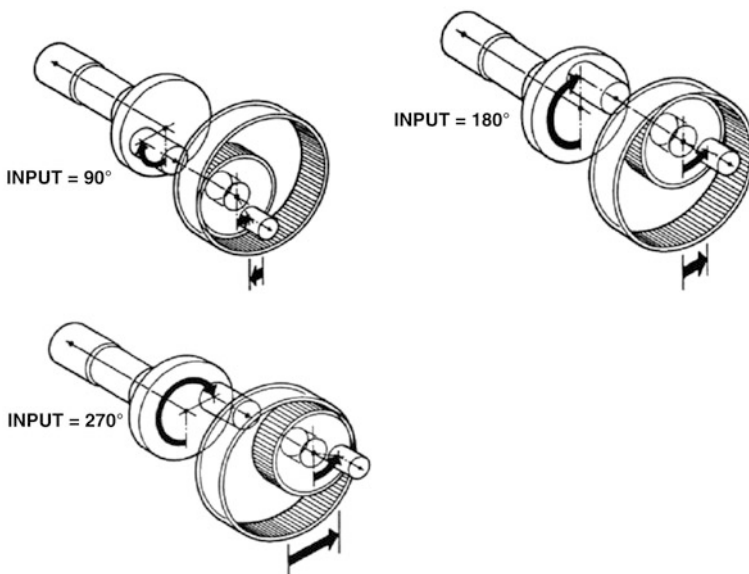


**Fig. 17.3** Active principle of the back wheel steering gear (Honda Accord Forum 2009)

angle, the back wheels have a highest steer-angle of  $5.3^\circ$  (Honda Accord Forum 2009; Zomotor and Reimpel 1991; Sano et al. 1987).

The drawback of this gearbox principle and the rigid mechanical connection with the front axle is that first, the effects of initial co-steering at small steer-angles have to be compensated (reduced agility), before countersteering takes over at higher steer-angles. If big steer-angles are required at high speed, though, this switch produces a “counteraligned” steer-angle and an oversteer response.

Honda developed an electromechanical system for the successor of the Prelude in the 1990s. It helped to remove the rigid coupling of the steer-angles at front and rear axle (see also Sect. 17.2.3).

### 17.2.2 Hydraulic Systems

The standard use of hydraulic systems, e.g., in the Nissan Skyline ‘HICAS’ (High Capacity Actively Controlled Suspension, 1985) or in the Mitsubishi Gallant (Active-Four, 1987) has been subject to different plans, see (Zomotor and Reimpel 1991). They have in common that hydraulic pressure in an actuator, consisting of cylinder and piston, builds up the necessary force at the rear-wheel steering. Very high actuating forces can be achieved by hydraulic actuators, so that even heavy vehicle classes can be steered at rest. The hydraulic cycles are very complex, though, because a system with high demands has to be developed, consisting of

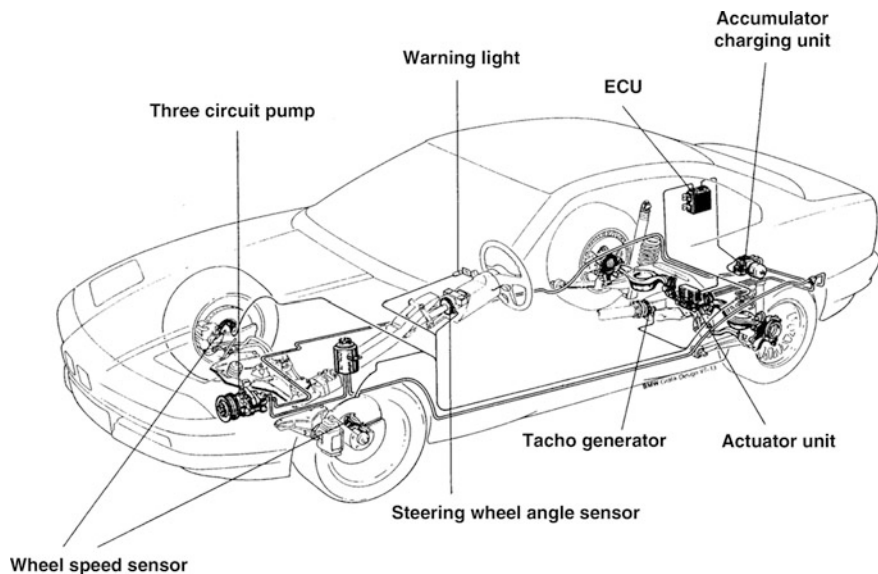


**Fig. 17.4** BMW 850i with active rear-axle kinematics (AHK) (BMW 1991/2008)

lines, pump, reservoir and actuator. Hydraulic all-wheel steering can be either purely hydraulically or electronically controlled.

An example for an electronically controlled all-wheel steering is the active rear-axle kinematics, AHK, used by BMW in the 8 models from 1992. The purpose of the development of active rear-axle kinematics was the improvement of active safe driving in the whole range of potential steering manoeuvres. For this purpose, active steering of the rear axle has to control the side forces acting on the rear axle at high lateral acceleration with regard to amplitude and phase (Wallentowitz et al. 1992) (Fig. 17.4).

The system configuration of the active rear-axle kinematics can be divided into three subsystems, shown in Fig. 17.5: hydraulic power supply and actuators, system control and monitoring, as well as the tractable construction of the integral rear axle (Wallentowitz et al. 1992). The hydraulics of the system consist of a radial piston pump that is mechanically coupled with the vane-type pump of the front-axle power steering. The third cycle of the pump, another radial piston pump, is responsible for the level control system of the vehicle. A pressure supply unit with hydraulic accumulator, accumulator valve charging and pressure sensors keeps the operational pressure for the hydraulic actuator unit in the defined operational range (Wallentowitz et al. 1992).

A control device uses the input quantities driving speed and steering wheel angle to calculate the preset steer-angle of the rear wheels. The sensors for driving speed, steering wheel angle, set position of the rear-wheel steering and the microprocessors in the control device are redundant, to meet the safety requirements.

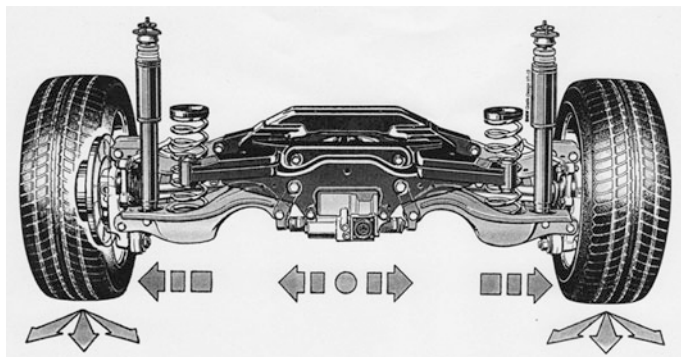


**Fig. 17.5** Active rear-axle kinematics (AHK) (BMW 1991/2008)

The arrangement of the hydraulic setting unit in the middle of the rear cross beam at the rear axle is shown in Fig. 17.5. The linear movement of the centring actuator is transferred by a double axial joint to an interlever which receives the internal bearing point of the spring drive and supports the wheel load at the rear-axle support. The interlever defines the gear ratio between actuator stroke and moving spring drive over the actuating points of double axial joint and spring drive (Wallentowitz et al. 1992).

### 17.2.3 Electromechanical Systems

Electromechanical systems asserted themselves in the course of development, because of the high complexity of the hydraulics and limited functions of the mechanical systems.

The benefits of these concepts are:

- any steer-angle can be set at the rear axle, independent of the wheel angle at the front axle
- less complicated construction
- less weight
- lower fault susceptibility.

The rear wheels of electromechanical systems are steered by an electromechanical actuator. An ECU calculates an actuator value from various input values, and an electric motor is accordingly actuated. BLDC motors are prevalent, because opposed to brush engines, they are free of wear and easier controlled by the safety system. Sensors monitor the correct positioning of the motor. The rotation of the electric motor is converted into a stroke movement by a suitable mechanical gear ratio (e.g., ball-recirculating gear with nut or spindle drive). This stroke movement

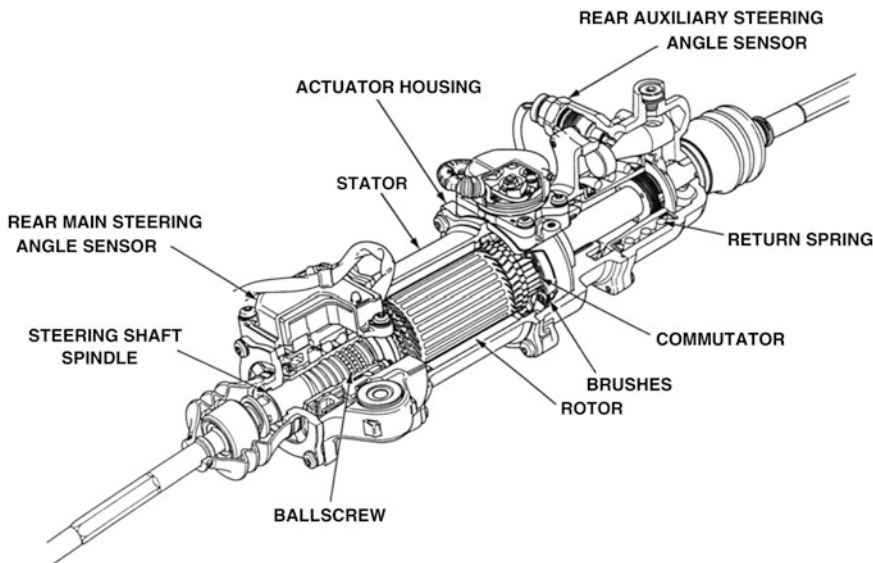


**Fig. 17.6** Actuator of the rear-wheel steering of a Honda Prelude 1991 (Honda Accord Forum 2009)

is transferred to the rear wheels by corresponding drives. Electromechanical rear-wheel steering systems provide a variety of possibilities to develop dynamic designs. Any input values can be used, e.g.: vehicle speed, steering wheel angle, yaw rate, lateral acceleration etc. They are not limited to the conversion of basic speed-sensitive steering functions, like parallel steering and countersteering, which had been common in the past, but complicated dynamic control functions can be integrated as well.

As mentioned above, Honda developed an electromechanical rear-wheel steering as early as 1991. Figure 17.6 reveals the quite complicated system configuration. An electric motor transfers its movement to a ball-recirculating gear with nut that transfers the rotation into a translation of the steering shaft spindle. The electromechanical rear-wheel steering is equipped with redundant steer-angle sensors for safety reasons. In case of a system failure, the rear wheels are rightened into their central position by the return spring.

The supplier, Kayaba Industry, developed another electromechanical rear-wheel steering which was used especially for the Japanese market in many Nissan applications, such as the Nissan Skyline. Figure 17.7 shows the interesting mechanical concept to transform the rotation of the electric servo motor into a steering movement of the rear wheels.

The electric motor transfers its rotation to a hypoidally interlocked crown wheel. A plug is eccentrically mounted on a spherical support at the crown wheel. The plug is also fastened in the tie rod shaft and can move it translationally.

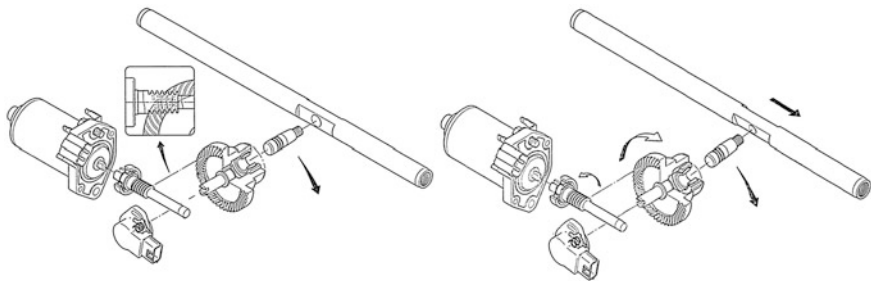
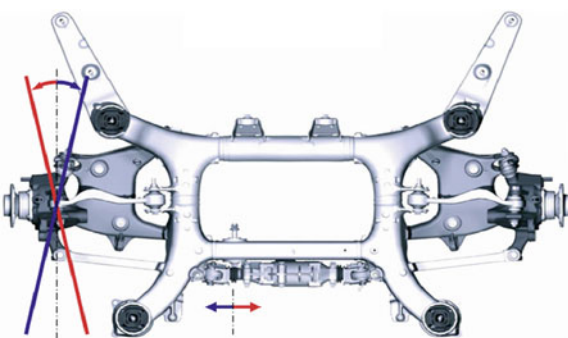


**Fig. 17.7** Active principle of the Nissan rear-wheel steering from 1993 (Kayaba 2005)

**Fig. 17.8** Arrangement of the steering actuator in the rear axle of the BMW 7 (BMW 1991/2008)



A steering movement of the rear wheels can then be executed by the tie rod and the hub carrier.

After their high tide in the 1990s, almost all the all-wheel steering systems disappeared from the market again. The reasons were the high add-on costs and functional deficits in the driving dynamics. These are described in detail in Sect. 17.3. Another reason was the availability of cheaper brake control systems, like ESP, that could realise the purpose of driving stabilisation in the upper limit range for much less costs. As mentioned above, the Japanese market and applications for light trucks are an exception.

Currently (as of March 2010), three manufacturers all over the world are using all-wheel steering in passenger cars. Electromechanical systems are found in the Renault Laguna GT (2008), the BMW 7 (2008), 5 GT (2009) and 5 (2010) as well as in the Nissan Infinity FX50 and G37 [Make it four manufacturers? What about the Audi A4/A6 Quattro, still produced in 2013?]. The depictions in Figs. 17.8 and 17.9 show the integration of the rear-wheel steering into the integral V rear axle of the BMW 7 and 5.

**Fig. 17.9** Arrangement of the steering actuator in the rear axle of the BMW 5 (BMW 1991/2008)



#### 17.2.4 Central Actuator Versus Single Wheel Actuators

In the cars of Nissan Infinity, BMW and Renault, the actuators of the rear-wheel steering are concentrically arranged at the rear axle. A central actuator is steering two wheels by a rigid connection; the same steer-angles are set at both wheels. Such a central actuator concept needs a continuous space from left to right, which is not available in some vehicle structures. For cases like that, technical designs of single wheel actuators have been supplied as an alternative to the central actuator principle, as for example the active rear-axle kinematics by ZF Lemföder (AKC (R)), Schäffler or Continental.

These are technical solutions where each rear wheel has its own mounted actuator (Fig. 17.10). Single wheel actuators also enable the adjustment of separate toe-ins for every wheel, this can be useful during assembly of the axles and when realising dynamic control functions.

The above-mentioned benefits of single-wheel actuator plans are opposed by more complexity in comparison to a central actuator concept. Not only actuators, but also sensors and actuating electronics have to be installed twice.

Additionally, mutual communication of the current steer-angles has to be maintained to keep synchronous control, and in the fault case of one actuator, the other one has to be shut down (example: private CAN concept Continental).

Single wheel actuator systems are almost twice as expensive during production, because of higher complexity and the double use of hardware. Moreover, the



**Fig. 17.10** Single wheel actuator, fair prototype by ZF Lemförder (Wiesenthal et al. 2008)

danger of potential system faults during operation in the customer vehicle is higher, and this can affect the service costs.

With regard to weight, there is not much difference between single-wheel and central actuators, the weight of the second actuator in the single wheel-concept is about as high as that of the mechanics (e.g., levers and drives) required for the central actuator.

### 17.3 Effects of an All-Wheel Steering on Vehicle Dynamics

The purpose of all the configurations of all-wheel and rear-wheel steering discussed in the preceding chapters is the improvement of the lateral dynamic driving characteristics of the respective vehicle.

While the first applications, made in the 1930s, were intended to support agility and manoeuvrability, the later realisations aimed not only for agility but essentially for an improvement of actuating response and driving stability. A mechanical all-wheel steering describes the rear wheel steer-angle  $\delta_h$  as a simple function of the front wheel steer-angle  $\delta_v$  or the steering wheel angle  $\delta_H$ :

$$\delta_h = f(\delta_v)$$

For the first electronically controlled all-wheel steering systems, the rear wheel steer-angle  $\delta_h$  is described as a function of the car's (forward) speed and the front-wheel steer-angle  $\delta_v$  or the steering wheel angle  $\delta_H$ :

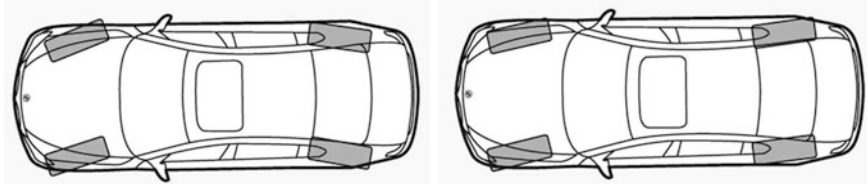


**Fig. 17.11** Opposite direction steering:  $k_p < 0$ , parallel direction steering:  $k_p > 0$

$$\delta_h = f(v_x, \delta_v)$$

In the course of development, the pure pilot control of a rear-wheel steering was lately extended by including the all-wheel steering in the Electronic Stability Programme of the vehicle. This was made possible by reasonable dynamic sensors becoming available that monitor yaw rate, longitudinal and lateral acceleration etc.

$$\delta_h = f(v_x, \delta_v, \Delta\delta_v, \delta_h, a_x, a_y, \psi, \beta \dots)$$

This chapter will discuss the dynamic effects of controlled all-wheel steering.

### 17.3.1 Kinematic Qualities of an All-Wheel steering

The transmission ratio of an all-wheel steering is described by the coefficient  $k_p$  as a quotient of the steer-angle at the back wheels and the steer-angle at the front wheels.

$$k_p = -\frac{\delta_h}{\delta_v}$$

For all-wheel steering, two active principles are generally distinguished: parallel direction and opposite direction steering (Fig. 17.11).

$k_p < 0$ : In opposite direction steering, the rear wheels are turned against the steering direction of the front wheels. The instantaneous centre of the vehicle moves forwards, this has an effect as if the wheelbase was shortened. The cornering circle shrinks, the rear axle of the vehicle moves on another trajectory, this makes the vehicle handier and more agile (Fig. 17.12 top).

$k_p > 0$ : If the rear wheels are steered in the same direction as the front wheels of a vehicle, the instantaneous centre moves to the back. The virtual extension of the wheelbase increases the stability (Fig. 17.12).

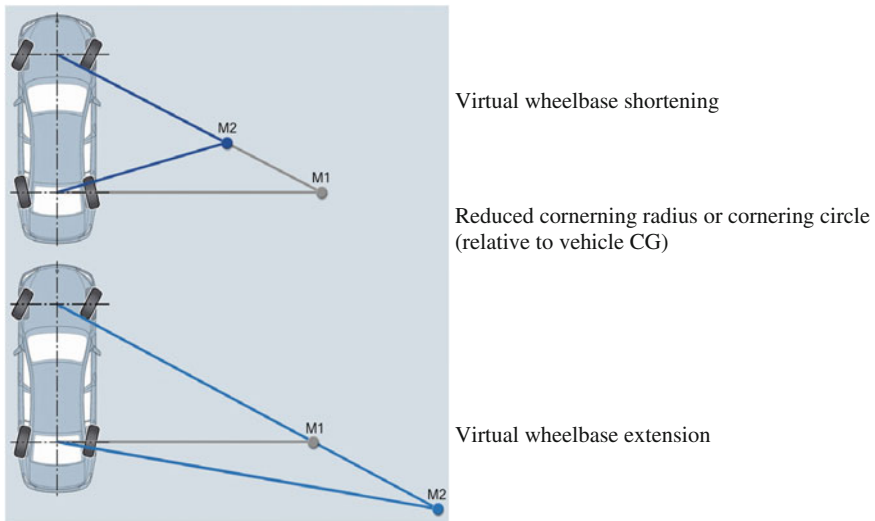


**Fig. 17.12** Change of the cornering circle and virtual change of the wheelbase (simplified kinematic representation)

### 17.3.2 Influence of an All-Wheel Steering on the Stationary Vehicle Characteristics

The effects of an all-wheel steering on the stationary vehicle characteristics shall be examined in a more thorough discussion of the steady-state circular driving. The highest accessible lateral acceleration is almost the same for vehicles with and without all-wheel steering, but the biggest difference is in the development of the car's side slip angle.

If  $k_p > 0$ , then the side slip angle in the vehicle CG decreases according to size of the steer-angle at the rear axle. In some past applications,  $k_p$  was selected in a way that theoretically the side slip angle was always compensated to zero. The reason was the view that as long as the side slip angle was zero, this would force a stable driving state.

It had been overlooked that a stable driving state is also the product of further input values, such as load change response, transitional response from the linear to the limit area etc. (Fig. 17.13).

Every now and then, the side slip angle was overcompensated by a steering intervention at the rear axle, so that negative side slip angles developed even at high speed and lateral acceleration ranges. The result was a very stable yet significantly understeering and subjectively unfamiliar driving experience.

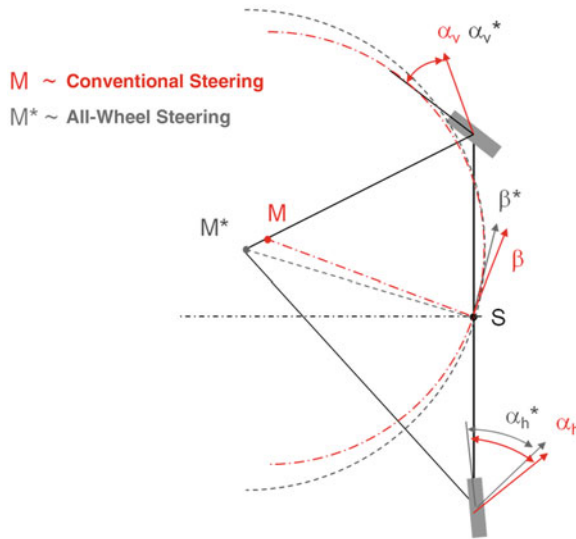


**Fig. 17.13** Changing side slip angle of a vehicle with all-wheel steering (middle to higher lateral acceleration range)

### 17.3.3 Influence of an All-Wheel Steering on the Nonstationary Vehicle Characteristics

The effects of an all-wheel steering on the nonstationary driving response will be discussed in the following by examining the response characteristics during a jump of the steer-angle and the driving response in an ISO lane change.

Figure 17.14 shows on the left side how a dynamic steering input, such as a jump of a steer-angle, quickly and steadily builds up a lateral force at the front and rear axle. This reduces the yaw response of the vehicle to a minimum, the yaw speed is building up slower while the lateral acceleration is building up faster. The transfer function of steer-angle to lateral acceleration has a lower phase shift. This produces a—for the driver—better predictable driveability at high speed.

The opposite steer-angle at the rear wheels produces an initial build-up of the lateral force at front and rear axle in the opposite direction. This produces a yaw gain, the initial lateral acceleration is lower. A more agile driveability is the result, desirable especially in the low speed range.

A driving manoeuvre like an ISO lane change demonstrates objectively how an all-wheel steering improves the driveability. The lower side slip angle is obvious (Fig. 17.15). The otherwise typical excursion of the side slip angle in the third lane of the ISO lane change is much lower. Yaw speed and lateral acceleration are much more loyal to phase (Herold et al. 2008), relative to the entered steering wheel angle.

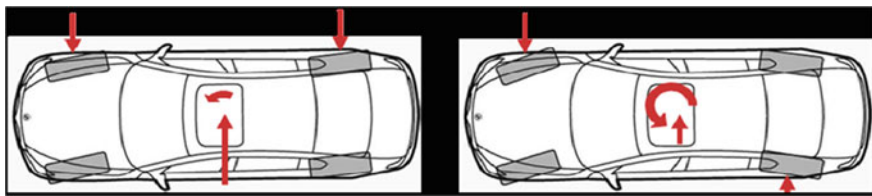


**Fig. 17.14** Vehicle response to a defined instationary steer-angle, *left side*  $k_p > 0$ , *right side*  $k_p < 0$

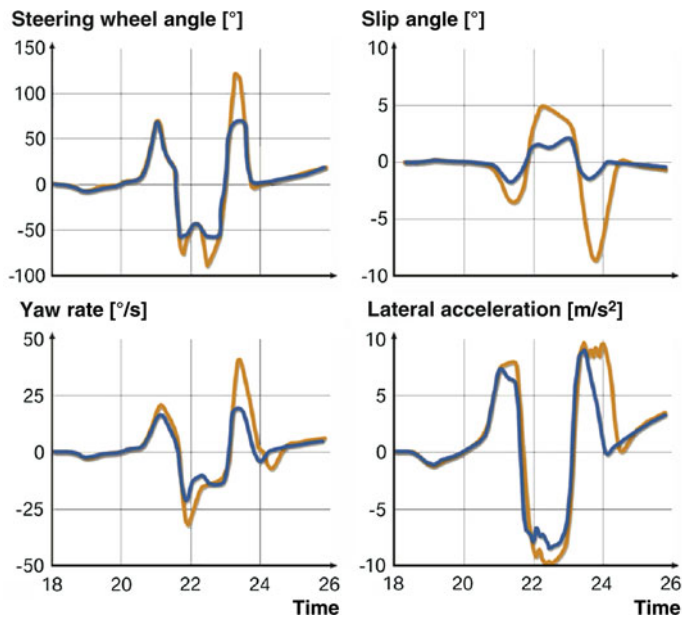


**Fig. 17.15** Simulation ISO lane change ( $k_p > 0$ ), *blue* all-wheel steering, *yellow* conventional steering (Herold et al. 2008)

#### 17.3.4 Combination of a Rear-Wheel Steering with a Superimposed Steering System at the Front Axle

Those applications of an all-wheel steering that permit a free choice of the rear wheel steer-angle make it dependent on the driving speed and on the front wheel steer-angle:

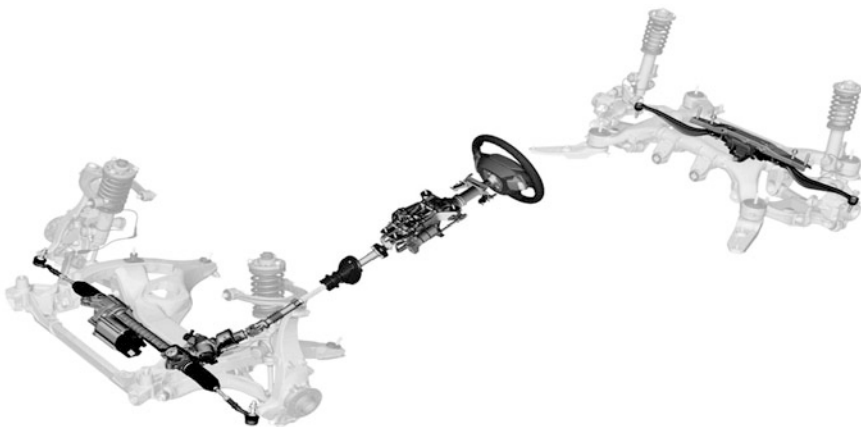


**Fig. 17.16** Integral active steering in the BMW 5 (2010)

$$\delta_h = f(v_x, \delta_v) \text{ or } k_p = f(v_x)$$

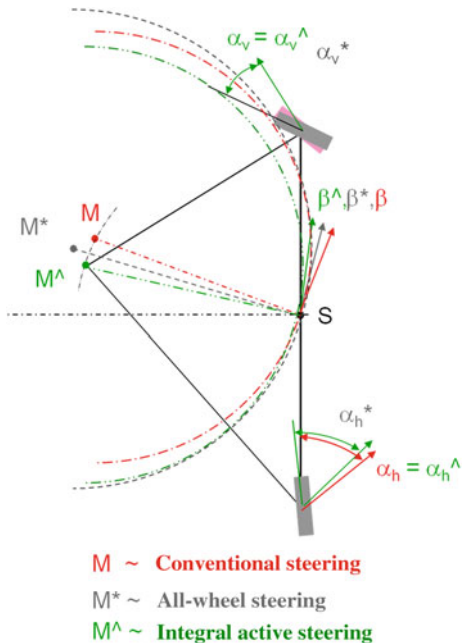
If the side slip angle is compensated by selecting  $k_p$  so that it is zero, the vehicle will understeer much more than if it did not have an all-wheel steering. Any all-wheel car that has an aligned steer-angle applied at higher speed will display this pronounced tendency to understeer. According to Zomotor and Reimpel (1991), not only the nonstationary vehicle characteristics but also the stationary ones have to be considered to perfect the driveability with the help of a rear-wheel steering. If the stationary vehicle characteristics of speed-sensitive driving characteristics should remain unchanged, the front-axle ratio has to be speed-sensitive, too (Zomotor and Reimpel 1991).

BMW was the first to introduce an all-wheel steering in 2008, the ‘integral active steering, IAS’, which can meet these requirements for a system. Figure 17.16 shows the components of the integral active steering in the BMW 5. An electromechanical power steering is combined with the already known superimposed steering system at the front axle. At the rear axle the electromechanical rear-wheel steering is applied, with the actuating points situated at the hub carriers. The ECU group in the Integrated Chassis Management is not shown.

Nissan has supplied the 4WAS system in the Infinity G37 since 2007, another combination of a rear-wheel steering with a superimposed steering system at the front axle. The 4WAS system provides for a coordinated aligned steering intervention at the front and rear axles only in the high speed range, while in the low speed range, the rear-wheel steering does not move.

The steer-angles at both axles can be selected independently from the driver’s input by combining a superimposed steering system (see Chap. 16) with a rear-wheel steering. The integral active steering achieves an almost linear rise of the yawing movement over the driver’s input when the rear wheels are turned at low speed. The better agility due to the virtual shortening of the wheelbase was

**Fig. 17.17** Stationary yaw neutrality of an integral active steering



already described in Sect. 17.3.1. The direct gear ratio of the superimposed steering system in this speed range improves convenient driving, no shuffle is needed, even in narrow corners.

Beyond 50 km/h, the rear wheels are turned in alignment with the front wheels. The stabilising steer-angle is continuously increased as a function of speed and steering wheel angle. The higher demand for a steer-angle developing then is compensated by the superimposed steering system at the front axle. The all-wheel steering is applied so that for the same speed, the cornering radius of a car with conventional steering relative to its CG is the same as the cornering radius of a car with integral active steering, see Fig. 17.17. Stationary yaw neutrality therefore results from:

$$\psi = \frac{v}{r}$$

These characteristics are also present in the driving manoeuvre ‘quasi-stationary articulation’. For  $v_x = \text{const.}$ , the steering wheel angle is slowly and consistently increased to the upper limit of the lateral acceleration. Shown in Fig. 17.18, the rear-wheel steering and the superimposed steering system at the front axle are coordinated so that the yaw rate builds up over the lateral acceleration like in the basis model.

The benefit of more driving stability, as discussed in Sect. 17.3.3, is fully preserved. With a lateral acceleration of  $8 \text{ m/s}^2$ , the side slip angle in the CG of a

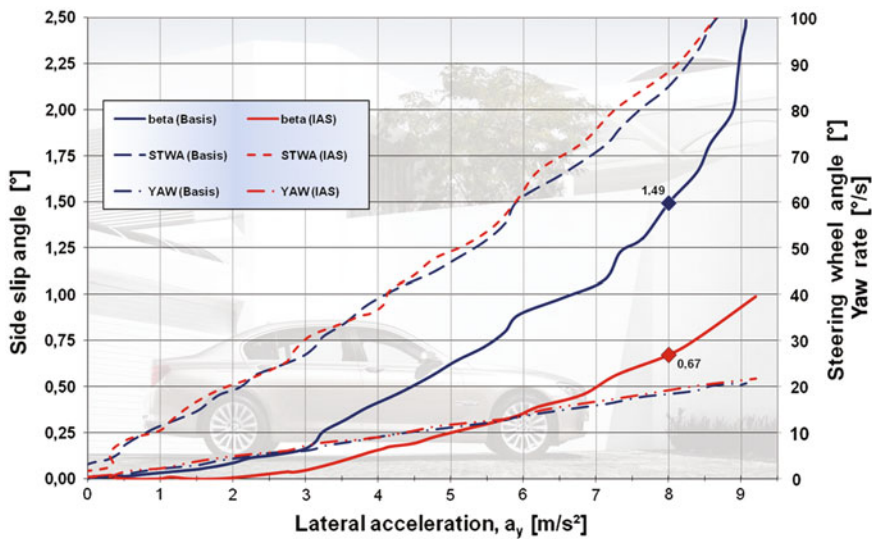


**Fig. 17.18** Integral active steering in the BMW 750I, quasi-stationary articulation at  $v_x = 100$  (km/h), (Herold et al. 2008). *Beta (basis)* Side slip angle  $\beta$  of a vehicle with conventional steering; *STWA (basis)* Steering wheel angle  $\delta_H$  of a vehicle with conventional steering; *YAW (basis)* Yaw speed  $\psi$  of a vehicle with conventional steering; *beta (IAS)* Side slip angle  $\beta$  of a vehicle with integral active steering; *STWA (IAS)* Steering wheel angle  $\delta_H$  of a vehicle with integral active steering; *YAW (IAS)* Yaw speed  $\psi$  of a vehicle with integral active steering

car with integral active steering is less than half than that of the basis vehicle, rising almost linearly, even when the lateral acceleration increases even further. The design conflict of all-wheel steering systems between driving stability and understeering, troubling driveability, described by Zomotor and Reimpel (1991), is completely resolved now.

## References

- Oswald W (1987) Mercedes-Benz Personenwagen 1886–1986. Motorbuch Verlag, Stuttgart
- BMW AG (2005) BMW internal research on providers of rear-wheel steerings
- BMW AG (1991/2008) Internal graphic documents, BMW graphics design VT-13
- Honda Accord Forum (2009) [www.accordforum.de](http://www.accordforum.de), TechArea 4WS-Four Wheel Steering Korbacher Archiv, Karl-Heinz Korbacher
- Zomotor A, Reimpel J (1991) Fachbuch Fahrwerkstechnik, Fahrverhalten. 2d edition, Vogel Buchverlag, Würzburg
- Wallentowitz H, Donges E, Wimberger J (1992) Die Aktive-Hinterachs-Kinematik (AHK) des BMW 850Ci, 850CSi. ATZ Automobiltechnische Zeitschrift 94
- Kayaba (2005) Documentation of Kayaba Industry Co. Ltd
- Wiesenthal M, Collenberg H, Krimmel H (2008) Aktive Hinterachs-Kinematik AKC—Ein Beitrag zu Fahrdynamik, Sicherheit und Komfort. 17. Aachener Kolloquium Fahrzeug- und Motoren technik

- Herold P, Thalhammer T, Gietl S (2008) Der neue BMW 7er. Die Integral Aktivlenkung—Das neue Lenksystem von BMW. ATZ Automobiltechnische Zeitschrift
- Herold P, Schuster M, Thalhammer T, Wallbrecher M (2008) The new steering system of BMW—integral active steering, synthesis of agility and sovereignty. In: FISITA world automotive congress
- Sano S, Miyoshi T, Furukawa Y (1987) Operational and design features of the steer angle dependent four wheel steering system. In: 11th international technical conference on experimental safety vehicles

# Chapter 18

## Steer by Wire

Pei-Shih Huang and Alfred Pruckner

### 18.1 Introduction

*Steer by Wire* is an automotive system that electrically transmits a steering command from an operating element (steering wheel) by an ECU to an actuator executing the steering command at the driven wheels. These systems do not have any mechanical connection between steering wheel and driven wheels. To improve handling, the driving state delivers a haptic response to the driver by an active operating element.

The hardest challenge of *Steer by Wire* systems is to meet the safety and reliability requirements with reasonable effort. A short overview of the state-of-the-art and the pros and cons of *Steer by Wire* systems will be given in the following. Then the components and especially the properties of the operating element will be more thoroughly discussed. Finally, an example of a possible functional design will be shown and aspects of safety and reliability picked out as a central theme.

#### 18.1.1 State-of-the-Art

*X-by-Wire* is now used in different technical areas. The first (analogous) Fly-by-Wire system for civilian aircraft was made for the Concorde in the 1970s. Airbus introduced the A320, a commercial aeroplane with *Fly-by-Wire* technology and without mechanical backup system, in 1987.

---

Pei-ShihHuang (✉) · A. Pruckner  
BMW Group, Munich, Germany  
e-mail: pei-shih.huang@steeringhandbook.org

A. Pruckner  
e-mail: alfred.pruckner@steeringhandbook.org

**Fig. 18.1** Concept study Fine-X by Toyota with electric single-wheel steering (Toyota 2005)



**Table 18.1** Pros and cons of *Steer by Wire*

Advantages	Disadvantages
Functions	Cost
Space	Weight
Passive safety	Complexity
Less variety	
Simpler axle geometry	
Specific feedback	
Design	
Enabler for driver assistance systems	

*Drive-by-Wire* (an electronic accelerator pedal) is a standard *X-by-Wire* system in the automotive business whose engine responds faster to accelerator pedal commands, according to the change of the pedal angle and a specific intervention into the traction control if the traction slip is too high.

*Steer by Wire* was installed so far only in special and prototype vehicles. One example is shown in Toyota's concept study Fine-X, using single-wheel steering at all four wheels (Fig. 18.1).

### 18.1.2 Pros and Cons

Table 18.1 shows an overview of the pros and cons of *Steer by Wire* systems, compared with customary systems. One essential advantage of *Steer by Wire* is the easy conversion of different additional steering functions, like driving dynamics stabilisation, VGR, variable steering feel or even autonomous driving (e.g., for autonomous parking). Another benefit is the free design of the front end. Space for the engine unit and improved correspondence of left- and right-hand driven vehicles (less variety) can be achieved, since there is no intermediate steering shaft (steering column). Because of that, requirements for passive safety (crash) can be addressed more purposefully as well.

**Fig. 18.2** Interior design with stick controls (BMW Group Research and Technology)



Separating input and response allows falling back on simpler structures for the development of front-axle systems, because desired vehicle responses can be set by the software, and interfering factors can be suppressed. Finally, new input devices, such as sticks, create the space for innovative interior design (Fig. 18.2). In addition, the Steer by Wire can be used for the application of driving assistance functionality, e.g., the so-called electronic pole in the autonomous driving. (Seewald 2008). Especially utility vehicles can save fuel and help to conserve the environment.

As for any disadvantages, note that high safety requirements and reliability to satisfy the customer are placing high demands to the redundancy of *Steer by Wire* systems, increasing costs and weight in turn. The costs are produced by the fault tolerance required in a purely electrical transmission. The driver must be able to control any possible fault that can occur in an electric system in any driving situation (Winner et al. 2004). This asks for a sophisticated safety concept (see Sect. 18.4).

In contrast to a fault-tolerant system, a fail-silent system includes a mechanical relapse level (Kilgenstein 2002). Other than electronic components, a mechanical system can be designed and sized with the help of expertise and empirical values, so that it will by all likelihood not fail within the intended lifetime, as long as the specified stress limits are observed. In this case it is sufficient if the electronic components are *fail-silent units* that switch off when a fault is registered while the steering function is maintained by the mechanical relapse level (Heitzer and Seewald 2004). One example of *Steer by Wire* with a mechanical relapse level is the heterodyne steering supplied by some vehicle manufacturers (Chap. 16). Active steering systems of this kind can assume many qualities and functions of pure *Steer By Wire* systems (Fleck 2003), but no space is saved. The steering column may either be retained as a mechanical relapse level or replaced by hydraulics (Heitzer and Seewald 2000).

The conditions for the approval of automotive steering equipment, including assembly and testing specifications, are gathered in ECE-R 79.

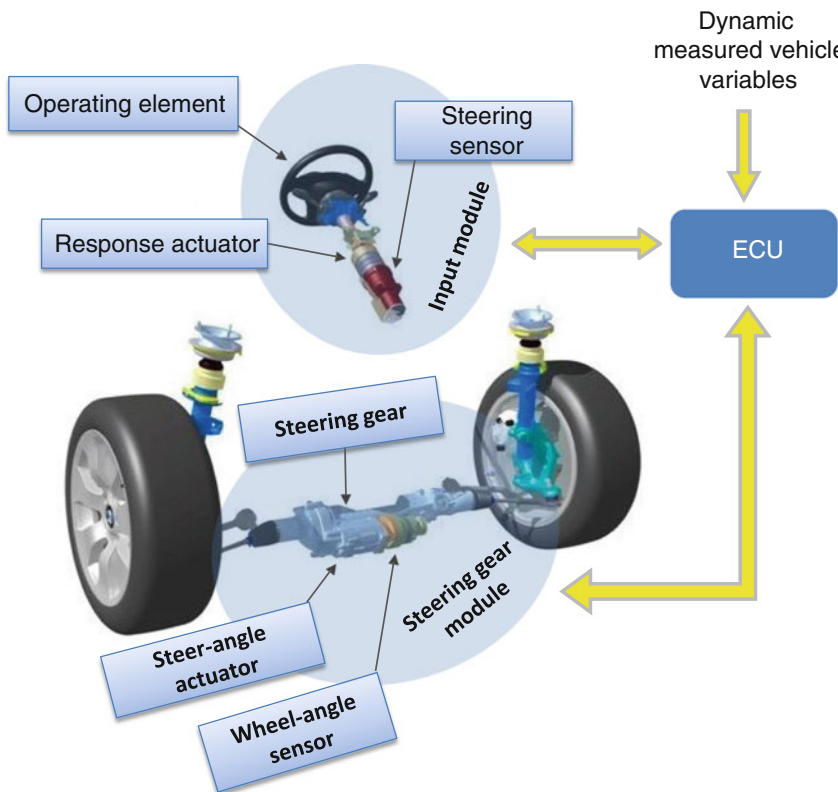


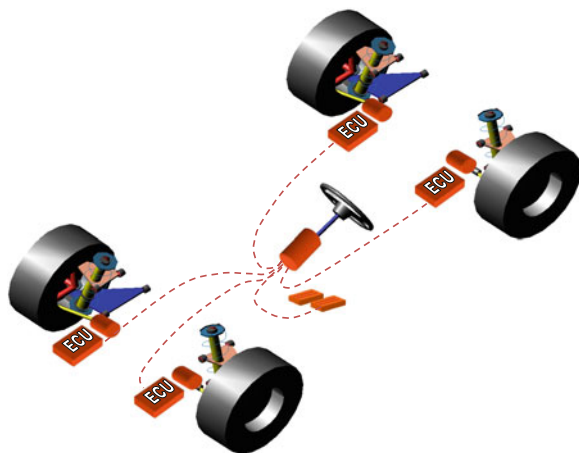
**Fig. 18.3** *Steer by Wire* concept

## 18.2 Components

Figure 18.3 shows a schematic configuration of a *Steer by Wire* system. The input module, including an operating element (e.g., steering wheel or stick), response motor and steering sensors, is responsible for the registration of the driver's input and for suggesting a steering feel. The steering gear module with steering gear, steer-angle actuator and wheel sensors implements the lateral dynamic conversion of the driver's input. Both modules are just electrically controlled by an ECU.

The response motor should be able to counteract the usual manual force of a driver, corresponding to a torque of about 10 Nm (cf. Sect. 15.4). Even an e-motor with gear ratio can hardly counteract a potential abusive torque when the driver continues to turn by force when the full steer-angle is already reached. It is useful then to integrate passive construction elements, like stop units and dampers. One condition of an ideal control is that the steering sensors measure travel and angle as well as force and torque.

**Fig. 18.4** By-Wire per wheel  
‘Corner modules’



General dynamic measured variables are available for the ECU in the Electronic Stability Program, beside *Steer by Wire* data from steering and wheel sensors, such as driving speed, yaw rate and lateral acceleration.

The steering angle actuator at the steering gear module should fulfill the power and dynamic requirements of an electric power-assisted steering system (cf. Sect. 15.4). In other words, the steering force at standby must be available in any situation, while the steering velocity of up to 500 °/s input by the driver should be translated to the wheel with the support of the steering actuator dynamically.

As an alternative to a steering gear, the connection of the two front wheels can be separated into single-wheel steering systems. This may even invoke a ‘corner module’ concept (Gombert 2007), performing the chassis functions (steering, driving, braking, vertical dynamics) at the individual wheels; the benefits are more functions, immanent redundancy and saved space (Fig. 18.4).

As for any disadvantages of the ‘corner modules’ concept, note the costs and the strong required forces at the steering actuators. They have to support the mutual, constantly acting radial forces of toe-in, camber and inclination angle at the respective wheel. An adapted axle design can at least reduce these forces in comparison to current wheel forces.

### 18.2.1 Operating Element Quality

*Steer by Wire* systems imply high versatility for designing the interaction of driver and car. Hence, the qualities of the operating element as a man-machine interface shall be discussed more precisely in the following (Huang 2004).

Passive operational controls are a very easy and cheap way to transmit the driver’s intention. Figure 18.5 compares various passive designs.

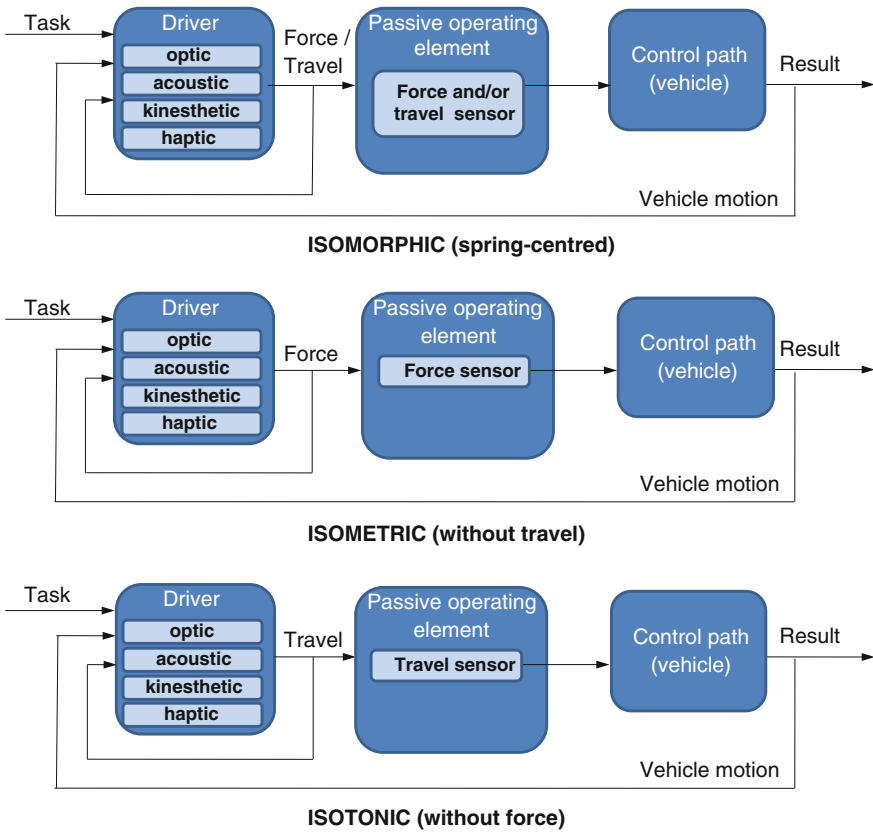


**Fig. 18.5** Comparison of different passive operating elements

The driver sees or feels the qualities of vehicle movement and the operating element and sets either force or travel at the operating element. The haptic feedback to the driver is a result of the passive quality of the operating element, which can be isomorphic (spring-centred), for example. If the spring stiffness should become very high, this is called an isometric operational control (without travel). If the spring stiffness is approaching zero, that is an isotonic operating element (without force).

A driver's input into a merely passive operating element is not suitable, on account of the non-linear vehicle qualities and the high sensitivity of automobiles to ambient influences. An essential component of safe guiding is the feedback of the current driving state to the operating element, esp. in situations when the driving dynamics are critical. Producing this feedback makes the presence of an active operating element obligatory (Huang 2004).

In contrast to passive operational controls, active controls can improve the manual control power significantly when interferences occur and the closed-loop controlled system changes. The driver may just grip the active operating element

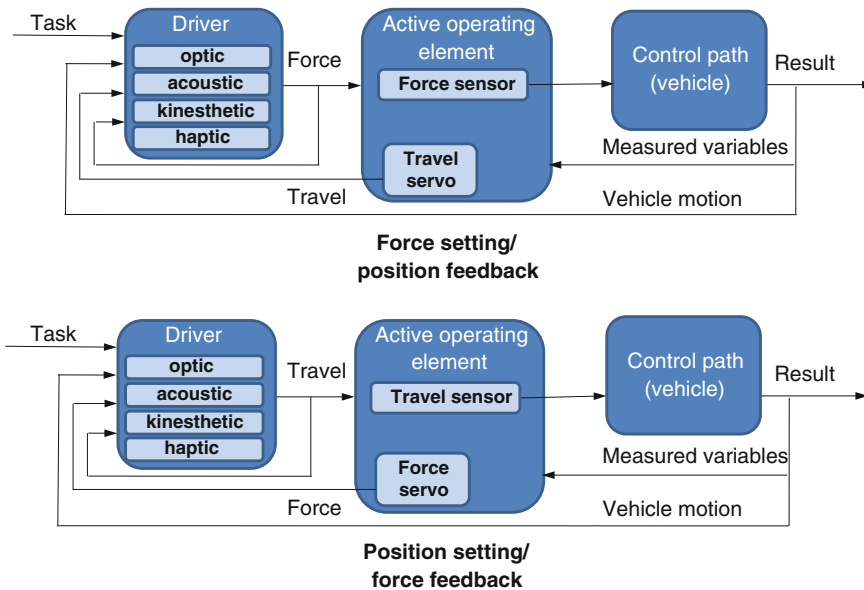


**Fig. 18.6** Active operational controls with different control concepts

tighter when an interference occurs, and thus suppress it. The network of driver, vehicle and operation is displayed in Fig. 18.6 by means of an active operating element.

In contrast to passive operational controls, the force of the **Force setting/position feedback** concept is applied to the operating element of the vehicle's closed-loop controlled system and the car response is mirrored to the driver as information on the travel. The **Position setting/force feedback** concept correspondingly has the travel of the operating element applied to the car, while the car response (cornering curvature, yaw rate or lateral acceleration) is reported to the operating element as a force. Ideally, both concepts would be equal, but in real applications, especially in the lateral dynamic limit range, there are differences which will be discussed in the following Sect. 18.3.

'Reciprocal dynamics' prevent any concept that would provide for the conversion of a force set by the driver into a position set at the actuator, reconverting its force response into a position of the operating element. As unsuitable is the reverse case: a position set at the operating element that would be converted into a force set at the actuator, which would reconvert its resulting position into a force at the operating element.

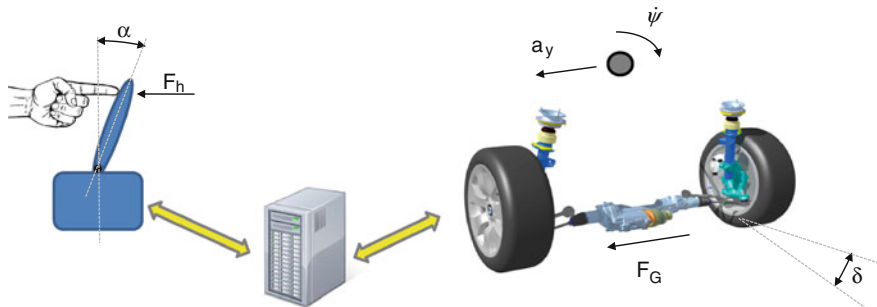


**Fig. 18.7** Processes of a *Steer by Wire* control

### 18.3 Steering Functions

The stiffness requirements of customary steering systems can be achieved by a *Steer by Wire* steering when sensor and actuator dynamics are suitably chosen. A little bit of steering clearance should be included in the functional software, so that the responding properties will not be too aggressive. The good steering feel of an electromechanical power steering may even be excelled by Steer by Wire systems, in spite of the mechanical decoupling (Koch 2009). The reason is that the friction response of the overall steering system can be almost arbitrarily tuned. The ideal way to do so is to measure the tie rod forces, but good results can also be achieved by an accurate estimate of these forces. Cybernetic attempts to design the steering feel of a *Steer by Wire* steering like that of customary, power-assisted steering are shown, e.g., in (Odenthal et al. 2003). A control that is resistant against external ambient influences means an improvement of the driving dynamics in the lateral dynamic limit area (Bunte et al. 2002). One observes that the exploitation of forces at the individual wheels allows the driver to perfectly control the lateral dynamic driving state.

The following discussion presents an approach to the interaction of driver and car by the previously discussed operating element qualities for stable driving or the lateral dynamic limit area for all speed ranges. In addition, the influence of the operating element's qualities on the compensation of interfering variables and the interaction with a combined longitudinal guide will be shown.

Figure 18.7 shows the process of a *Steer by Wire* control in a car by means of an operating element (e.g., a stick). The driver enters a force  $F_h$  or an angle  $\alpha$  into the operating element. A force  $F_G$  is generated at the gear and a steer-angle  $\delta$  at the wheel. Dynamic parameters, like lateral acceleration  $a_y$  and yaw rate  $\dot{\psi}$ , appear at the vehicle as well.

The development of the steering function of a *Steer by Wire* systems poses the question: How does a driver control a car and which parameters are involved?

At low speed the driver regulates the curvature or the curvature difference between the driving path and the predicted vehicle motion. The driver specifies the desired yaw rate and controls it with the curvature difference (feedback control).

**Table 18.2** Input and return variables for different speeds (Huang 2004)

Speed range	Input value	Feedback value
low (<25 km/h)	yaw rate $\psi'_{\text{desired}}$	Curvature $\kappa_{\text{actual}}$
medium to high (>45 km/h)	Lateral acceleration $a_y_{\text{desired}}$	yaw rate $\psi'_{\text{actual}}$

At medium to high speed, the driver reduces or controls the yaw angle error through yaw control. The driver gives a desired lateral acceleration and regulates with the yaw rate feedback, which is equivalent to a lateral acceleration feedback control loop (Table 18.2).

In the transient speed range between 25 and 45 km/h, the driver uses the curvature and the yaw angle error simultaneously as control values. Input and return in the transitional area between both speed ranges are achieved by changed weighting.

### 18.3.1 Discussion of the Normal Driving Mode

The design described above has effects on the normal driving mode that are considered for both different feedforward/feedback plans of Fig. 18.6 with the help of an accelerated circular driving on a steady radius.

The force feedforward/position feedback concept needs a constant steer-angle at low speed (the curvature is constant) while the steering torque is rising (yaw rate rises with driving speed). Medium and high speed result in a linearly rising demand for the steer-angle (yaw rate = driving speed by curvature), the steering torque is a function of the lateral acceleration. This allows constructing convenient designs that involve direct steering ratios for the low speed range and indirect steering ratios for the high speed range.

The position feedforward/force feedback concept needs a rising steer-angle and a steady steering torque for accelerated circular driving at low speed. Medium and higher speed indicate a demand for a steer-angle as a function of the accelerated circular driving, as the steering torque is linearly rising. The position feedforward/force feedback concept supplies a speed-sensitive steering ratio already at low speed. It rises significantly in the medium and high speed range. This concept is not recommended for the normal driving mode or a steering torque proportionally to the yaw rate in the middle and high speed range.

### 18.3.2 Discussion of the Lateral Dynamic Limit Range

The control concept for lateral driving in the dynamic limit range will be discussed for steady driving speed and small slip-angles or a low slip-angle rate. Assuming this, the curvature  $\kappa$  in Table 18.2 is shown as a quotient of yaw rate and speed.

**Table 18.3** Simplified input, reduced to the yaw rate—return values

Speed range	Input value	Return value
Low (<25 km/h)	yaw rate $\psi'$ desired	Curvature $\kappa$ $\text{actual} \approx \psi'_{\text{actual}}/v$
Medium to high (>45 km/h)	Lateral acceleration $a_y \text{ desired} \approx \psi'_{\text{desired}} \cdot v$	yaw rate $\psi'_{\text{actual}}$

The lateral acceleration is computed from the product of yaw rate and speed. Table 18.3 shows the influence of this conversion on feedforward and feedback values. The feedforward is proportional to the desired yaw rate in any speed range, the feedback is proportional to the actual yaw rate.

This implies for the Force feedforward/position feedback concept that the operating element will turn ‘lighter’ in the case of oversteering response (actual yaw rate is larger than desired yaw rate). That means that the force in the operating element is lowered when the position is fixed, and accordingly, the desired yaw rate is decreasing. This is equal to stabilisation. The driver does not need to react and can tell from the diminished force at the operating element that the vehicle is in the lateral dynamic limit range. Since the desired lateral acceleration is present, the driver will not readjust the steering. In case of an understeering response (actual yaw rate is smaller than the desired yaw rate), the force at the operating element rises if the position is fixed. The driver is warned by the rising force against approaching the dynamic stability limit. At the same time, this rising force prevents the driver from non-promisingly increasing the steer-angle.

In case of position feedforward and force feedback, the force at the operating element increases when the response is oversteering while the position is fixed. To counteract this critical driving situation, the driver has to reduce the input angle (according to the rising force). This requires a certain amount of practise. In case of an understeering response, the force at the operating element decreases. The driver tries intuitively to compensate the lessening force by increasing the input angle (because the desired lateral acceleration was not achieved), but in this situation, that is of no use.

Altogether, the Force feedforward/position feedback concept is again better than the Position feedforward/force feedback concept, including in the dynamic limit range. In spite of that, an overall examination has to include superior stability interventions, e.g., by individual braking interventions.

### 18.3.3 Compensating Interferences

Electronic systems can automatically compensate HF interferences. LF interferences in a range between 0.2 and 0.4 Hz that the driver can easily adjust are ideally fed back by the active operating element. The driving stability can be maintained thereby, the driver is informed by the operating element about the altered ambient conditions while the driving is getting more convenient.

For example, a vehicle that drives straight ahead may feel a rotation from interferences like crosswind or changing friction values. The position of the operating element is changed by interferences in the control concept that applies the lateral acceleration as a force feedforward and the yaw rate as a position feedback. As soon as the driver grabs the operating element tighter, a force feedforward is automatically generated which exactly counteracts the interferences. The driver thus very intuitively suppresses or compensates the interferences.

When the lateral acceleration is the position feedforward and the yaw rate is the force feedback at the operating element, interference generates again a force at the operating element. In this case, though, the driver has to ‘give way’ to this rising force and to ‘countersteer’ with the operating element, to compensate the interference. These correcting interventions are less intuitive than in the above discussed case of force feedforward/position feedback (Huang 2004).

#### 18.3.4 Combined Longitudinal—Lateral Guidance

The cutoff frequency of the driver/car control circuit is approx. 0.05 Hz to keep the distance to the vehicle ahead in the longitudinal dynamics (Donges 1982). An active operating element is not suitable for such LF controlled systems (Boller and Krüger 1978).

The interference or mutual effect (e.g., the changed lateral guidance during a powerful deceleration) at a stick-like operating element for concurrent longitudinal and lateral guidance needs to be observed. Any isometric or non-travelling, passive operating element is suitable for longitudinal guidance (Eckstein 2001). This force feedforward should ideally be combined with another force feedforward for lateral guidance. Longitudinal force feedforward combined with a lateral position feedforward is not recommendable for a combined input operating element.

### 18.4 Safety Concepts

If a customer buys a product, he or she should expect that it will work reliably. Reliability is defined as the ability of a unit to produce a demanded function under given conditions for a given time (DIN EN 50129). This means that the product has to be safe and available. Figure 18.8 shows the conflict zone of safety, availability and costs. A system which is perfectly safe will shut down at once whenever a fault occurs, and it is not available any more. A system with high availability is operated at some risk when a fault occurs, and it is therefore not safe any more. Redundancy increasing safety and availability has negative effects on the costs.

The basic condition for operating a *Steer by Wire* steering is the presence of a fault-tolerant system architecture (Heitzer and Seewald 2000). Beside the safe power supply, the ECU has to be fault-tolerant, e.g., equipped with two identical

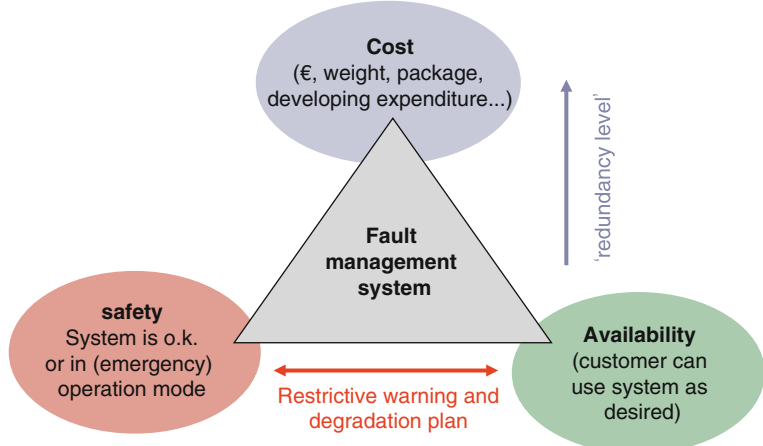


Fig. 18.8 Conflict zone safety, availability, costs

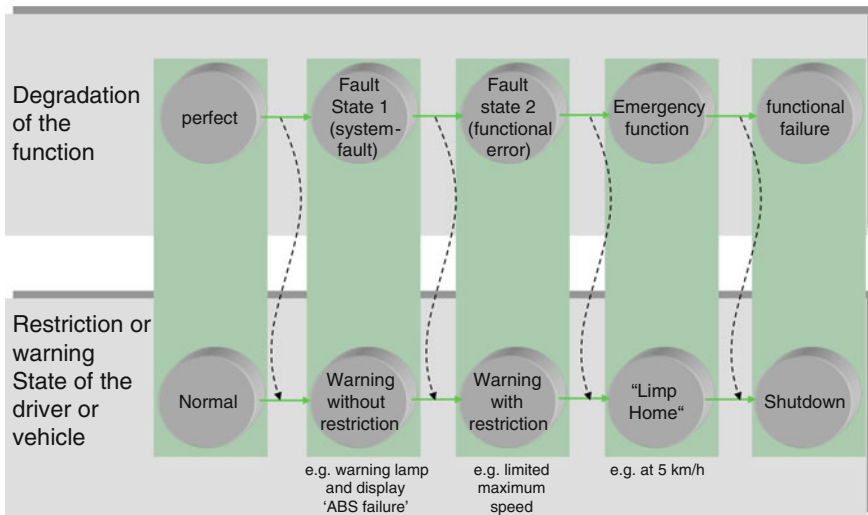


Fig. 18.9 Degradation plan with possible restrictions

*fail silent units.* If the self-monitoring of the ECU notes a fault, it has to switch off fast enough and leave the transfer of the vehicle into a safe mode to the other ECU (e.g., vehicle shutdown). Relevant sensors have to be three times redundant (two identical signals outvote a faulty third) to be able to isolate a faulty sensor signal. Actuators of a fault-tolerating configuration have to be at least twice redundant, meaning that one actuator can be set free of force when a fault is detected. The correct data transfer can be maintained by especially developed, time-triggered protocols, for example, FlexRay ([www.flexray.com](http://www.flexray.com)).

A redundancy management is defined with an operational strategy, fault management and a suitable warning and degradation plan to reduce the costs for redundancy and to keep the car ready in spite of a present fault. Figure 18.9 shows a possible degradation plan.

This way the car is still safely operatable when the wheel speed sensors fail, for example. A warning light informs the driver about the fault, and speed-sensitive steering functions are not available any more. If the active feedback motor fails, only a few steering functions can be executed by the then purely passive operating element, in this case, a reduced top speed can still sustain a safe operating mode. If only one steering actuator is available on account of another steering actuator failing, then an emergency function can be maintained at very low speed ('*limp home*'). If another actuator fails, the vehicle can still be safely brought to a halt by individual brake engagement.

## 18.5 The Future

A major part of the steering functions enabled by *Steer by Wire* is already available for a heterodyne steering (Wallbrecher et al. 2008). To exploit the additional advantages of a 'pure' Steer by Wire steering for a reasonable expenditure, all the available sensor data, actuators (steer in front, steer behind, individual brake engagement, active vertical dynamics ...) and power supply units (low voltage accumulator, high voltage accumulator, generators ...) need to be integrated into an operation and failure strategy. The commonness of electrified vehicles and more desire for steering functions, up to driver assistance systems benefiting from *Steer by Wire* technology, offer a chance to use technical synergies to reduce costs. The absence of *Steer by Wire* systems in modern standard cars shows that these synergies are not big enough yet.

## References

- Boller HE, krüger W (1978) Untersuchung eines Bedienelements mit Krafteintrag und Wegrückmeldung bei der manuellen Lenkung von Unterwasserfahrzeugen. Zeitschrift für Arbeitswissenschaften 32:254–260
- Bünte T, Odenthal D, Aksun-Güvenç B, Güvenç L (2002) Robust vehicle steering control design based on the disturbance observer. Ann Rev Control 26:139–149
- Donges E (1982) Aspekte der Aktiven Sicherheit bei der Führung von Personenfahrzeugen. Automobil-Industrie 2/82, pp 183–190
- ECE-R 79: <http://www.bmvbs.de/static/ECE/R-79-Lenkkanlagen.pdf>
- Eckstein L (2001) Entwicklung und Überprüfung eines Bedienkonzepts und von Algorithmen zum Fahren eines Kraftfahrzeugs mit aktiven Sidesticks. Fortschr.-Ber. VDI, series 12, No. 471. VDI Verlag, Düsseldorf
- Fleck R (2003) Methodische Entwicklung mechatronischer Lenksysteme mit Steer-by-Wire Funktionalität. Tagung 'fahrwerk.tech', Garching

- Gombert B (2007) X-by-Wire im Automobil: von der elektronischen Keilbremse zum e-Corner, Innovationsforum Fahrwerk Elektronik 2007, Institut für Kraftfahrwesen Aachen
- Heitzer H-D, Seewald A (2000) Technische Lösungen für Steer-by-Wire Lenksysteme. Aachener Kolloquium, Oct 2000
- Heitzer H-D, Seewald A (2004) Development of a fault tolerant, steer-by-wire steering system. SAE Nr. 2004-21-0046
- Huang P (2004) Regelkonzepte zur Fahrzeugführung unter Einbeziehung der Bedienelementeigenschaften. Dissertation, Fakultät für Maschinenwesen, TU München
- Kilgenstein P (2002) Heutige und zukünftige Lenksysteme. Tag des Fahrwerks, Institut für Kraftfahrwesen Aachen
- Koch T (2009) Bewertung des Lenkgefühls in einem Sportfahrzeug mit Steer-by-Wire Lenksystem, Aachener Kolloquium
- Odenthal D, Bünte T, Heitzer H-D, Eivker CH (2003) Übertragung des Lenkgefühls einer Servo-Lenkung auf Steer-by-Wire. Automatisierungstechnik 51
- Seewald A (2008) Auf dem Weg zur elektronischen Deichsel. AUTOMOBIL-ELEKTRONIK, December 2008
- TOYOTA: <http://www.toyota.co.jp/en/autoshows/2005/tokyo/toyota/index.html>, 2005
- Wallbrecher M, Schuster M, Herold P (2008) Das neue Lenksystem von BMW - Die Integral Aktivlenkung. Eine Synthese aus Agilität und Souveränität, Aachener Kolloquium
- Winner H, Isermann R, Hanselka H, Schürr A (2004) Wann kommt By-Wire auch für Bremse und Lenkung?, VDI report 1828, Autoreg 2004

# Chapter 19

## Overview: Driver Assistance System Functions

**Stefan Brosig and Markus Lienkamp**

### 19.1 Overview of Selected Driver Assistance System Functions Concerning Steering

The continuing increase of road traffic and rising demands to the driver have produced a huge number of assistance systems during the last years. They all support the driver's task of driving. There are systems for keeping the course which engage the brake or the driveline. It seems reasonable to include the steering into this purpose as well.

Possibilities for steering interventions do not exist only in future 'Steer by Wire' systems ([Chap. 18](#)), they are present already in the electromechanical steering (EPS —Electronic Power Steering) and the heterodyne steering ([Chap. 16](#)). In either case, the power assist is generated by an electric motor. In electromechanical steering ([Chap. 15](#)), additional steering torques can be applied to the steering wheel by a proper actuation of the electric motor. They recommend to the driver to adapt the steer-angle input to that steer-angle which suits the driving situation best. The system requires a mechanical connection between steering wheel and the front wheels, hence, the driver is able at any time 'to outvote' the steering recommendation by another steering command. Hence, the level of the additional steering wheel torques is chosen in the conflict zone between best function and highest possible safety. In a heterodyne steering (active steering), free additional angles can be set independently from the driving input.

---

S. Brosig (✉)  
Volkswagen AG, Wolfsburg, Germany  
e-mail: stefan.brosig@steeringhandbook.org

M. Lienkamp  
Technical University of Munich, Munich, Germany  
e-mail: markus.lienkamp@steeringhandbook.org

One focus of development is the interaction of the system with the driver. The steering wheel torques or angles should support the driver in controlling demanding, difficult or unfamiliar driving situations, without taking over the task of vehicle guidance. Moreover, the interactions with other driving dynamics systems and the improvement of handling and convenience are the most prominent duties of development.

Driverless steering interventions can be basically distinguished by two different areas of responsibility.

Driving stability interventions ([Sect. 19.2](#)) and assistance functions for lane-keeping, the latter being distinguished again by lane assistance ([Sect. 19.3](#)) and parking assistance ([Sect. 19.4](#)).

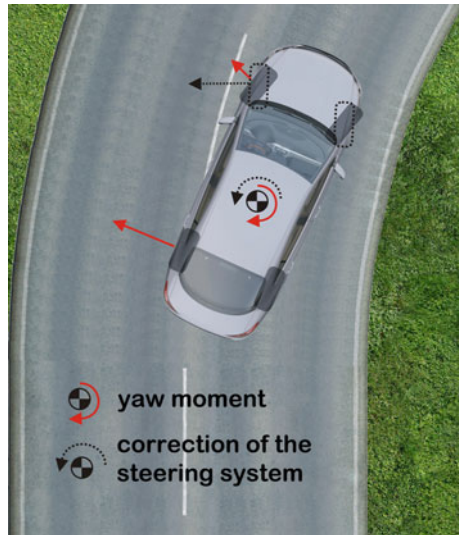
## 19.2 Driving Stability Interventions

The function described in the following determines the current driving situation on the basis of steer-angle, steering torques, lateral acceleration, yaw rate sensors and internal ESP-computed values (Brosig [2006](#); Dreyer et al. [2007](#)). The best steer-angle for the present driving situation is identified. A steering wheel torque signal is computed and superimposed to the steering wheel, meeting requirements of safety and ergonomics—in other words, the interaction between driver and support function. This should motivate the driver to adapt the self-chosen steering wheel angle to the ideal one. Driving stability interventions with superimposed wheel torque of an electromechanical steering should assist the driver in unusual situations that cannot be practised in everyday traffic, increasing the efficiency of ESP/ABS systems. Manoeuvres described in the following (yawing and  $\mu$ -split situations) can be supported in the driving response or with the help of a heterodyne steering, when an additional steer-angle is applied to the driver's input.

### 19.2.1 Function ‘Steering Recommendation’

The steering recommendation and, hence, the driverless wheel intervention should support the driver in driving—as mentioned at the beginning—both in an  $\mu$ -split situation and in the cornering response of the vehicle. The improvement of handling and braking distance, combined with high acceptance by the driver, are the most important targets of steering recommendations.

**Fig. 19.1** Oversteering of a vehicle



### 19.2.1.1 ‘Steering Recommendation’ at Yawing

‘If the car oversteers, it pushes its rear outward and turns into the corner,’ writes Laumann (2007). In this case, the driver has to compensate the yawing movement by countersteering (see Fig. 19.1).

An unskilled driver can be overwhelmed in such a situation: too long, too late or too low countersteering aggravates the situation. To safely control the vehicle, the ‘steering recommendation’ provides a superimposed steering wheel torque to the driver, pointing where to steer. The driver’s countersteering movement is optimised and ESP interventions can be avoided or reduced.

### 19.2.1.2 ‘Steering Recommendation’ in the $\mu$ -split Situation

Driving situations which support the driver in braking manoeuvres when there are asymmetrical friction values on the road are described by the generic term,  $\mu$ -split. Braking on a road that is slippery on one side turns the vehicle towards the high friction value. The driver has to steer towards the low friction value to counteract the pull towards higher friction (see Fig. 19.2). The ‘steering recommendation’ function recognises this situation, computes—based on the yaw rate of the vehicle and the brake pressure difference at the front wheels—the corrective steering wheel angle. This is applied to the steering wheel as a superimposed wheel torque, to make a recommendation. The effective correction by the negative scrub radius, in the same direction, begins later and is weaker, but it is acting in the same sense, positively. Beside improving the driveability, which the driver may positively

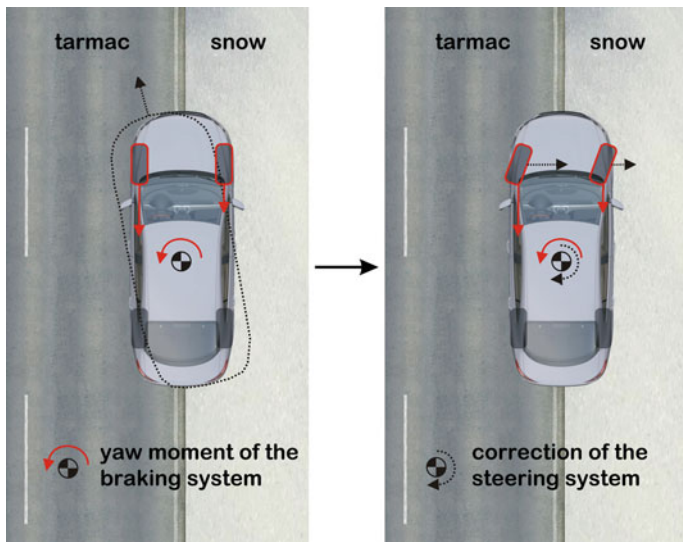


**Fig. 19.2** Vehicle in  $\mu$ -split situation

notice by less yawing, the car will also have a shorter braking distance, because the better yaw response on the part of the ABS permits stronger brake pressure differences between the left and the right side.

### 19.2.2 Ergonomics Requirements

The requirements for the ergonomics of a steering result from the qualities of the haptic senses. The driver can access response times of about 0.1 s over the haptic sensory channel (Fausten and Folke 2004). This is the fastest sensory channel of humans. A person receives this sensory information subconsciously and processes it. The only thing faster than the subconscious level are reflexes (Chap. 7).

The electromechanical steering is coupled directly to the steering wheel. The driver perceives superposed torques at the steering wheel very quickly. Hence, the level of the additional wheel torques has to be selected very carefully (Schmidt 2009; Neukum et al. 2009). The feel of steering is processed at the subconscious level and has therefore a considerable influence on:

- driveability of the vehicle
- safety perception
- acceptance of the vehicle
- vehicle brand.

Different requirements on the steering recommendation are the result:

- *Steering wheel torque interventions may never surprise the driver and have to be always understandable* in any driving situation.
  - Hence, steering wheel torque interventions have to be *always continuous*, i.e. they may not include any jumps.
- The driver has to perceive that curve and phase of the applied wheel torques agree with the feeling of proper driving or the steering movement, according to the driving situation. In other words, the characteristics of the vehicle may not be changed too much.
  - Hence, development has to create the possibility to control the steering characteristics by parameters
- furthermore, the driver has to be able at any time to outvote the *steering wheel torque* and to keep control of the vehicle in every situation.
  - This requires a limitation of the highest additional steering wheel torques. If the driver does not agree with the recommended steering wheel torques, this has to be recognised and the function deactivated, if necessary.

### 19.2.3 Safety Requirements

Safety requirements of a system intervening into the steering can be maintained by the development section with the proven and accepted methods ([Chap. 15](#)). System and signal interfaces have to be intrinsically safe, meaning that the driver should be able to control the driving situation whenever an additional steering wheel torque is applied. This assumes monitoring and limitation of the steering wheel torques and their gradients (Rohlfs et al. [2009](#)).

## 19.3 Lane Assist

[Figure 19.3](#) charts fatal accidents outside of town areas. About two thirds of all accidents in Germany develop from a collision with another object or vehicle on the road. Collisions with pedestrians account for 8 % of all accidents and departing from the lane for approx. 15 %. 21 % of all fatal accidents result from a collision with an oncoming vehicle. 34 % of all fatal accidents develop out of departing from the lane.

The lane assist registers any unintentional departure from the lane and supports the driver, for example, with a correcting steering intervention (see [Sect. 19.3.1](#)). Unintentional departure from the lane can be avoided in particular cases. The

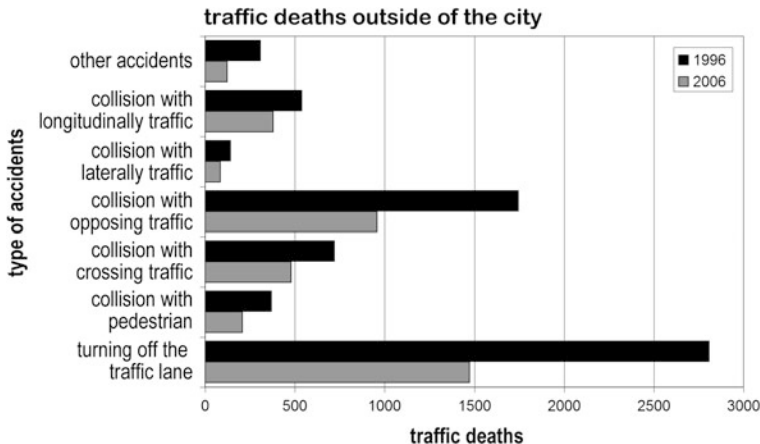


**Fig. 19.3** Fatal accidents outside of town by type of accident (*source* Federal Statistical Office of Germany)

reasons for accidents listed above, such as unintentional departure from the lane, show that the lane assist can contribute to avoid accidents.

There are different kinds of warning and support for the lane guidance of vehicles. This chapter will discuss some examples of systems that support the driver in keeping the lane, in connection with the steering (Winner et al. 2009).

Lane Departure Warning systems (LDWs) merely warn the driver by an optical, acoustic or haptic signal that the lane was left, but they do not interfere into the lane guidance. Lane Keeping Systems (LKS) support the driver in keeping the lane by intervening with a correcting wheel torque. They represent a functional extension of an LDW system.

### 19.3.1 Lane Keeping System: LKS

This chapter will discuss the function and configuration of the lane keeping system —Lane Assist—, as it is called and applied by Volkswagen. The final subsection examines comparable systems available on the market. The same safety and ergonomics requirements as discussed in Sect. 19.2.3 apply.

#### 19.3.1.1 Technical Realisation

Availability of a suitable steering system is an essential condition for the realisation of a lane keeping system. The electromechanical steering is such an actuator. This development created the precondition to superimpose additional steering wheel



**Fig. 19.4** ‘Lane assist’ system components

torques on the steering very easily. A comparison in [Chap. 11](#) shows that hydraulic steering is generally not useable for driver’s assistance.

Efficient image processing and camera technology help to construct very good lane recognition systems for a reasonable price. Figure 19.4 shows the system components of the lane keeping system.

- camera and ECU (1)
- electromechanical steering (2)
- multi function steering wheel (3)
- instrument cluster (4).

The lane keeping system can be switched on and off by a caliper at the steering shaft switch. Whether the system is switched on or off is shown by the multi function display in the menu ‘Assistant’. If the lane keeping system is switched on, a pilot light (system passive-yellow or active-green) in the instrument cluster indicates the status of the system.

A mono camera attached near the rear-view mirror traces the lane by its road markings, the signals are analysed by the interior ECU.

The electromechanical steering applies an additional wheel torque as a recommendation to the driver when the lane is unintentionally left. This steering

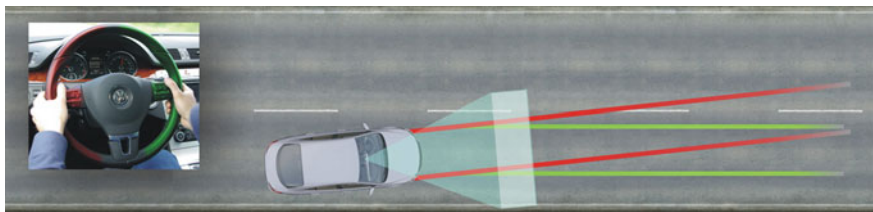


**Fig. 19.5** Function—lane keeping support

recommendation, too, can be outvoted by the driver any time (as described for the function ‘steering recommendation’ (see Sect. 19.2).

### 19.3.1.2 Functioning

The lane keeping system is designed for use on well developed country roads and highways. The system only switches to the ‘active’ state when the following criteria are met (for example: Lane Assist):

- lane recognised
- lane is wide enough
- curvature of the lane is small enough
- vehicle is in the lane
- speed is faster than 65 km/h.

A camera module in the area of the inside mirror records the road markings, and the position of the vehicle is evaluated. If the vehicle deviates from his lane, the lane assist will countersteer (see Fig. 19.5). If the highest steering wheel torque is not sufficient to keep the lane, or if the speed drops below 60 km/h, the ‘Lane Assist’ informs about the fact by a vibration of the steering wheel, indicating to the driver that the lane keeping support cannot fully support him or her and that the driver has to keep full control of the steering wheel.

### 19.3.1.3 In Practise

If the lane keeping system is activated, a yellow controlling symbol depicting a road is on. As soon as the camera has located suitable road markings, this symbol changes to green (see Fig. 19.6). Now the system is fully active. If the vehicle should leave the ideal line, the lane keeping system countersteers softly and in a continuous motion.

The system continuously analyses the driver’s steering activities to find out whether the driver still takes active part in the driving process or has yielded to being driven by the system. If the driver has yielded to the system, a note is given in the multi function display (see Fig. 19.7).



Fig. 19.6 Request to the driver

Fig. 19.7 Activity display in the estate car



If this state does not change, the system immediately switches to passive and the driver does not receive power assist any more. The system reactivates only after renewed steering activity.

### 19.3.2 *Lane Departure Warning: LDW*

The lane departure warning—discussed here for the example of the ‘Audi lane assist’—traces the road markings with an optical sensor (mono camera) and indicates upon leaving the lane by sound and a haptic signal, informing the driver by means of a vibrating steering wheel (see Fig. 19.8).

The driver can for example associate the vibration—in an Audi car generated by a vibrating engine in the steering wheel—for the rippled curb rattling. Alternatively,

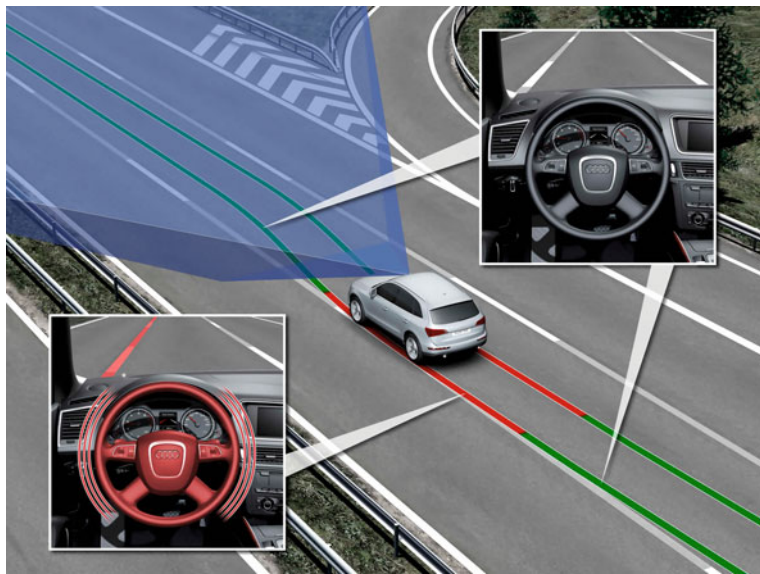


**Fig. 19.8** Function lane departure alert, example: ‘Audi Lane Assist’

the vibration can be generated by means of an electromechanical steering—provided that any is on-board. The power of the wheel’s vibration can be adapted to the driver’s needs (Vukotich et al. 2008).

Like the lane keeping system, this system should support the driver especially when driving on highways and country roads. The same speed limits apply to the activation of the system, and the same two-colour status display is found in the instrument cluster.

### 19.3.3 Selected Systems on the Market

Lane Keeping systems—**LKS**—and Lane Departure Warning systems—**LDW**—are presented with some basic data in the following (alphabetically sorted by car manufacturers). This list does not claim completeness, but shall give an overview of currently available systems on the market, in addition to those described above:

- LDW: “Audi lane assist” of Audi (A4, A5, A6, A8, Q5, Q7).
  - Camera-based (located in the foot of the inside mirror)
  - Approaching and crossing the lane → haptic warning by vibrating steering wheel (above 65 km/h)
  - Time and intensity of the vibrating wheel adjustable.

- LDW: “Lane departure warning” of BMW (5, 6, 7).
  - Camera-based (located in the foot of the inside mirror)
  - Departing from the lane → haptic signal by vibrating steering wheel (above 70 km/h).
- LKS: ‘Lane Keeping Assist System’ (LKAS) of Honda (Accord).
  - Camera-based (in the area of the inside mirror)
  - Active lane return upon approach of the edge of the lane.
- LDW: “Lane Departure Warning”/“Lane Departure Prevention” (LDP) of Infiniti (M, EX, FX—NAR).
  - Camera-based (located in the foot of the inside mirror)
  - Acoustic, optical warning shortly before leaving the lane (above approx. 70 km/h)
  - LDP active: Return to the lane upon departure by ESP intervention.
- LKS: Lane keeping system, “Driving Advisor” of Lancia (Delta).
  - Camera-based (near infrared, located above inside mirrors)
  - Active when crossing the lane → short countersteering wheel torque (in the range of 65 to 180 km/h).
- LKS: ‘Lane Keeping Assist’ of Lexus (LS460).
  - Camera-based (near infrared, located above the inside mirror)
  - Active lane return upon approach of the edge of the lane (above 70 km/h)
  - Analysis of the driver’s steering activities with potential passive switching of the system.
- LKS: ‘Lane Assist’ from Volkswagen (Passat CC, Passat).
  - Camera-based (mono camera, located above the inside mirror)
  - Active lane return upon approach of the edge of the lane (above 65 km/h)
  - Analysis of the driver’s steering activities with potential passive switching of the system when lack of activity is detected ([Sect. 19.3.1.3](#)).

### 19.3.4 The Future of Lane Keeping Support

Since electromechanical steering has become widespread, it is much easier to control the steering and, hence, driver and driving response. Automatic or autonomous driving that fully excludes the driver from the control circuit is technically feasible without major problems, but not yet qualified for the mass market, due to the complicated setting of current traffic situations and surroundings. Technical problems with detecting the environment are not yet mastered and juridical questions not yet answered. One step towards automatic driving might be the merger of assistance systems in longitudinal and lateral functions (Eigel 2010).

A combined longitudinal and lateral guiding assistance, as it was worked out in the active project (BMWi), tries to integrate longitudinal and lateral guidance into one system. An essential condition to enable the integrated longitudinal and lateral guidance to control various traffic situations is a precise detection of the environment. The traffic situation in front of the vehicle is recorded by different sensors, and their data is merged by the system into a consistent general view (Aktiv-Büro and Scholl 2008).

When a wide truck is passed on the other lane, the assistant can provide for sufficient lateral space. And, if this occurs at a road construction site, the speed can be adapted accordingly. Driving can become even more comfortable, and safer, too. A common consideration of lateral and longitudinal guiding can adapt the support to the respective traffic situation and the driver's response.

## 19.4 Parking Assist

The preceding chapters have discussed assistance systems related to steering interventions that recommend to the driver a steering wheel torque which matches the respective driving situation. The parking assist does not only recommend, it can also support the driver by independent steering into a parking spot. The condition for independent steering into a parking spot is the correct detection of the surroundings. The most common sensors to detect a parking spot are ultrasonic. In Fig. 19.9, ultrasonic sensors survey the parking spot when driving past. The sensors

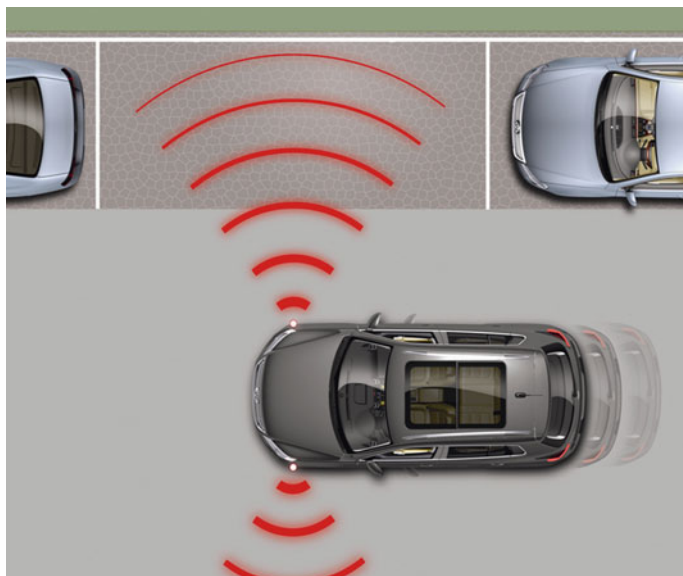


**Fig. 19.9** Parking spot detection by ultrasonic sensors

are in front, on the left and on the right, at the sides of the vehicle, to detect parking spots on both sides of the street. Surveying parking spots by cameras would be conceivable acc. to Schulz et al. (2007), for example, using an evaluating algorithm called ‘Structure from motion’ (Wook et al. 2007).

Parking by autonomous steering (semi-automatic) into a parking spot is only one version of various parking assist systems commonly in use (Winner et al. 2009).

- *informing systems*, for example, inform the driver by acoustic and/or visual indication how far away the driver still is from an object within the driving space.
- *controlled parking assist systems* suggest to the driver specific measures based on evaluated information on the surroundings. *Semiautomatic parking* is marked by the full adoption of a function—usually the lateral guidance (steering)—by the system.

In *fully automatic parking*, which is currently still in the research stage, the driver gives only an initial command to park when a parking spot has been detected and allocated, and the vehicle parks automatically in the parking spot.

#### 19.4.1 *Parking Assist System Requirements*

There are different requirements for environmental detection and, hence, for sensors and algorithms of the parking assists, according to system version and amount of support (Brandenburger 2007; Lee et al. 2004).

The following requirements for parking assist systems can be named with regard to the environmental sensors: the system has to be resistant against external influences (humidity, dirt) and detect the position of the parking spots with high resolution and accuracy. The data have to reach the ECU quickly. For a standard use it is inevitable that the system achieves low costs and low need for space. Furthermore, a comprehensible user interface has to be implemented. For systems surveying parking spots, the highest possible speed to pass by should not be too low (Blumenstock 2007).

Additional requirements have to be considered for controlled and semiautomatic parking assist systems. The parking should operate like a human driver to establish a high acceptance of the system. This means that the vehicle has to achieve a suitable final position, matching the parking situation, and the time needed for parking should be very short. The vehicle may not collide with any object, otherwise the driver has to be warned during the manual longitudinal guidance. Easy and obvious operation also contributes to the acceptance of the system.

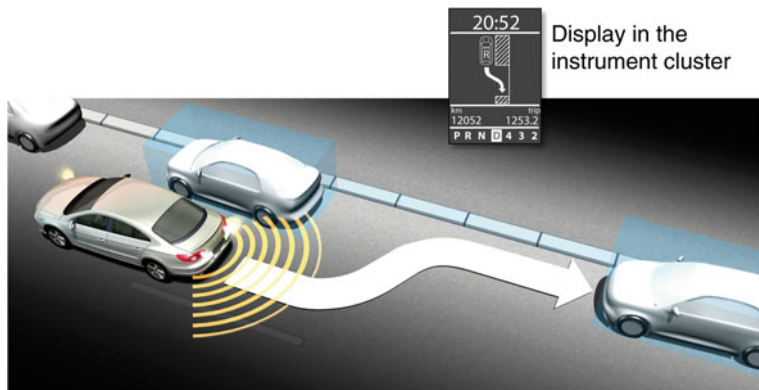


**Fig. 19.10** ‘park assist’ function

### 19.4.2 Technical Realisation

The different versions of parking assist systems were discussed in Sect. 19.4. Only semi- and fully automatic parking systems directly affect the steering. Semi-automatic parking assist systems will be the subject of this subchapter.

*Semi-automatic parking* is distinguished by the fact that the system assumes a function completely—usually the lateral guidance (steering). The parking assistant (semi-automatic—see Sect. 19.4.3) supports the driver by automatically carrying out the best steering wheel movements to park the car on the ideal line, in one backward pull, in a longitudinal parking spot on the kerb (see Fig. 19.10). The system automatically assumes the survey of the parking spot and the steering movements. The driver remains responsible for clutch, gas and brake. The system includes additional ultrasonic sensors in front and behind and gives acoustic warnings when an obstacle is drawing near. A manual intervention into the steering process or braking to standstill shuts off the power assist immediately.

ECE regulation 79 stipulates precise defaults for interventions at the steering equipment acc. to ECE regulation (2006):

In addition the driver assist steering controls shall be designed such that the driver may, at any time and by deliberate action, override the function. Whenever the Automatically Commanded Steering function becomes operational, this shall be indicated to the driver and the control action shall be automatically disabled if the vehicle speed exceeds the set limit of 10 km/h by more than 20 % or the signals to be evaluated are no longer being received. Any termination of control shall produce a short but distinctive driver warning by a visual signal and either an acoustic signal or by imposing a tactile warning signal on the steering control.

To meet the ECE regulation, status announcements about steering interventions have to be communicated to the driver. There is no demand to give the driver instructions about the nominal steer-angle, as controlled parking assist systems require. Figure 19.11 shows one way of a design that meets the ECE regulations.

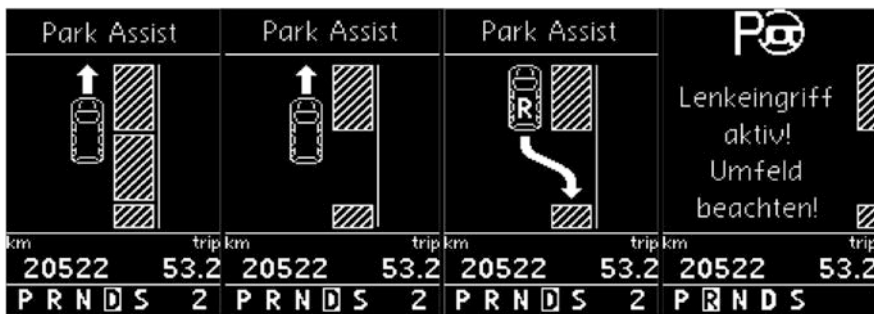


**Fig. 19.11** Example of a user interface for semiautomatic parking

Since the control of the vehicle is completely automatic, the driver can focus on the observation and supervision of the environment.

Using a semi-automatic parking assist system requires to network a huge number of components. This needs an intensive communication which is performed in most cases by a CAN Bus. The relevant components, for example, for the ‘park assist’ of Volkswagen are, acc. to Schöning et al. (2006), a parking ECU (function), calipers for activation, sensors for rev, lateral, longitudinal acceleration and steer-angle to identify the position, lateral ultrasonic sensors to survey the parking spot, front and rear ultrasonic sensors to measure the distance to other objects, a flasher to choose the side of the parking spot, an ECU for trailer detection, a warning buzzer of the parking assist, speed information of the brake ECU and of course an electromechanical steering for the lateral control.

The first semi-automatic parking assist systems are already mass-produced (Nunn 2003) (Schöning et al. 2006). Four of these systems are listed in the following chapter.

#### 19.4.3 Selected Systems on the Market

Parking steering assistants, including some basic data, are presented in the following (alphabetically sorted by car manufacturers). The listing does not claim completeness, but shall give an overview of currently available steering assist systems on the market, in addition to the one described above:

- ‘Active Parking System’ by Lancia (Delta).
  - Measuring the parking spot by ultrasonic sensors
  - Active steering by electrical intervention into the parking spot (7 km/h or less)
  - Semi-automatic (driver has to operate accelerator pedal and brake).

- ‘Active park assistant including PARKTRONIC (PDC)’ by Mercedes-Benz (A, B class).
  - Measuring the parking spot by ultrasonic sensors (up to 35 km/h)
  - Active steering by electrical intervention into the parking spot
  - Semi-automatic (driver has to operate accelerator pedal and brake).
- ‘Intelligent park assistant’ by Toyota/Lexus (LS460, LS600 h, Prius).
  - Measuring and choosing the parking spot by ultrasonic sensors and navigation display
  - Choice of lateral or longitudinal parking spot
  - Fully automatic parking invoked by loosening the brake
  - Deactivation of the parking by manual steering intervention or pressing the accelerator pedal.
- ‘Park assist’ by Volkswagen (Touran, Golf, Passat CC, Passat, Tiguan).
  - Measuring the parking spot by ultrasonic sensors
  - Active steering by electrical intervention into the parking spot
  - Semi-automatic (driver has to operate accelerator pedal and brake)
  - Deactivation of the parking by manual steering intervention.

#### **19.4.4 The Future of Parking Assists**

The technical components of modern vehicles (electronically controllable engine, brake and steering) permit an extensive control, so that, purely technically speaking, fully automatic parking would be possible. An automatically parking car was already presented in 1990 (Walzer and Grove 1990). Yet there are so far no fully automatic parking assist systems in mass-production, only research projects indicate their technical feasibility (Schanz 2005). Juridical considerations block a standard use of fully automatic parking systems. In such a case, the driver is completely released from vehicle control and the vehicle has to safely respond to any unforeseen situation. For example, the oncoming traffic has to be observed when reversely parking into a longitudinal parking spot, because the vehicle will swivel. Modern sensors can only incompletely detect traffic situations and they are much inferior to the human ability of perception (Pruckner et al. 2003). Systems which force the driver to supervise the parking actively are conceivable. A safety circuit could be imagined (e.g., in the remote control of the central locking or on-board) which requires that the driver activates the parking by the push of a button which has to be kept pushed while the parking procedure continues. The parking is cancelled as soon as the button is no longer pushed. The responsibility would remain with the driver who still has to supervise and observe the environment, inside or outside the car (dead man’s handle—Fig. 19.12).



**Fig. 19.12** Fully automatic parking with remote control

Nevertheless, semi-automatic parking assist systems offer much potential for advancements on the way to fully automatic parking. Their usability could be extended, for example, by lateral or longitudinal parking in several pulls or by assisted leaving from a parking spot. As for longitudinal guiding, automatic braking near obstacles when parking might be possible (Knoll 2005).

## References

- Aktiv-Büro, contact; WES-Office, Scholl, WE (2008) Aktive Sicherheit—AS (Project promoted by the Bundesministerium für Wirtschaft und Technologie), Juni 2008
- Blumenstock KU (2007) Platz da? Vergleich von fünf Einpark-Assistenten. Auto Motor Sport 13:2007
- Brandenburger S (2007) Semiautomatische Parkassistenten—Einparken in allen ebenslagen. In: Tagungsband zum 8. Braunschweiger symposium Automatisierungs-, Assistenz und eingebettete Systeme für Transportmittel. GZVB, Braunschweig, pp 154–159
- Brosig S (2006) Volkswagen AG; Elektromechanische Lenkung mit dynamischer Lenkempfehlung, Patent DE 102004041413 A1; Mar 2006
- Dreyer D, Schwertmann T, Brosig S (2007) Volkswagen AG; Elektromechanische Lenkung mit Lenkempfehlung; Patent DE 102006025254 A1; Dec 2007
- ECE-REGELUNG 79 Rev. 2, 20 Januar 2006, Einheitliche Bedingungen für die Genehmigung der Fahrzeuge hinsichtlich der Lenkanlage, p. 20, english translation adopted from United%20nations%20regulation%20ECER%2079 %20UNIFORM%20PROVISIONS%20CONCERNING%20THE%20APPROVAL%20OF%20VEHICLES%20WITH%20REGARD%20TO%20STEERING%20EQUIPMENT.pdf
- Eigel T (2010) Integrierte Längs und Querführung von Personenkraftwagen mittels Sliding-Mode-Regelung, AutoUni-Schriftenreihe, Band 12, Logos Verlag Berlin, herausgegeben von Volkswagen Aktiengesellschaft AutoUni

- Fausten M, Folke R (2004) Bosch Engineering GmbH, Kopplung von Bremssystemen und elektrischer Servolenkung zur Darstellung von Fahrerassistenzsystemen, Tagung 'Aktive Sicherheit durch Fahrerassistenz', Munch, Mar 2004
- Knoll P (2005) Prädiktive Fahrerassistenz—Vom Komfortsystem zur aktiven Unfallvermeidung. In: Automobiltechnische Zeitung, 107, pp 230–237
- Laumanns N (2007) Integrale Reglerstruktur zur effektiven Abstimmung von Fahrdynamiksystemen, Schriftenreihe Automobiltechnik, Institut für Kraftfahrwesen Aachen, Oct 2007
- Lee W, Uhler W, Bertram T (2004) Analyse des Parkverhaltens und Auslegung eines semiautonomen Parkassistenzsystems. In: Tagungsband zur 21. Internationale VDI/VW-Gemeinschaftstagung Integrierte Sicherheit und Fahrerassistenzsysteme, Wolfsburg 2004
- Neukum A, Paulig J, Frömmig L, Henze R (2009) Untersuchung zur Wahrnehmung von Lenkmomenten bei Pkw; Forschungsvereinigung Automobiltechnik e.V., FAT proceedings no. 222
- Nunn P (2003) Toyota Prius mit Einpark-Automatik. Auto, Motor Sport 21, 2003
- Pruckner A, Gensler F, Meitinger K-H, Gräf H, Spannheimer H, Gresser K (2003) Der Parkassistent. In: Fortschritt-Berichte VDI Reihe 12, 525. VDI Verlag: Düsseldorf 2003
- Rohlf M, Schiebe S, Müller J, Kayser T (2008) Volkswagen AG-Carmeq GmbH; 'Lane Assist'. Das neue aktive Spurhaltesystem von Volkswagen, 17. Aachener Kolloquium Fahrzeug- und Motorenmechanik 2008, Oct 2008
- Rohlf M, Brosig S, Buschhardt B, Schmidt G (2009) Volkswagen AG; Verfahren und Vorrichtung zum aktiven Halten einer Fahrspur; Patent WO2009/071210 A1, July 2009
- Schanz A (2005) Fahrerassistenz zum automatischen Einparken, Fortschritt-Berichte VDI Reihe 12, 607, VDI Verlag: Düsseldorf 2005
- Schmidt G (2009) Haptische Signale in der Lenkung: Controllability zusätzlicher Lenkmomente, Berichte aus dem DLS-Institut für Verkehrstechnik, Band 7, Deutsches Zentrum für Luft- und Raumfahrt e.V., Institut für Verkehrstechnik, Braunschweig, Oct 2009
- Schöning V, Katzwinkel R, Wuttke U, Schwitters F, Rohlf M, Schuler T (2006) Der Parklenkassistent 'Park Assist' von Volkswagen. In: Tagungsband zur 22. Internationale VDI/VW-Gemeinschaftstagung Integrierte Sicherheit und Fahrerassistenzsysteme. Wolfsburg 2006
- Schulze K, Sachse M, Wehner U (2007) Automatisierte Parkraumerkennung mit einer Rückfahrkamera. In: Tagungsband zur Elektronik im Kraftfahrzeug. Baden-Baden 2007
- Vukotich A, Popken M, Rosenow A, Lübke M (2008) Fahrerassistenzsysteme, Atz extra 'Der neue Audi Q5', June 2008
- Walzer P, Grove H-W (1990) IRVW futura—the Volkswagen research Car. SAE technical paper series, 901751
- Winner H, Hakuli S, Wolf G (2009) Handbuch Fahrerassistenzsysteme. Vieweg + Teubner Verlag: Wiesbaden
- Wook P, Pagel F, Grinberg M, Willersinn D (2007) Fraunhofer IITB; Odometry-based structure from motion. In: Proceedings of the 2007 IEEE intelligent vehicles symposium, June 2007

# **Chapter 20**

## **Outlook: The Future of Steering Systems**

**Manfred Harrer and Peter Pfeffer**

The authors firmly believe that in spite of increasing constraints, individual driving and steering of cars will still be prevalent in 2025 and beyond, and that the joy of driving will continue to be of primary importance. This means that current functions in the steering system technology will remain in focus for long term development within the dedicated development departments of vehicle and steering system developers, so that the brand specific steering feel which the driver and customer expects will be maintained in the future as well. To conclude, the authors want to assess various aspects of automotive construction connected to steering system response.

### **20.1 Autonomous Driving**

An increasing amount of vehicle sensors, electromechanical actuators and on board computing power makes it possible to provide the driver more assistance functions. This makes travelling in traffic much safer and more comfortable. Progress in the detection of what is going on around the car seems to put the vision of autonomous driving as the primary development focus. Reduced driver stress and safer and smoother traffic conditions with fewer traffic jams are generally mentioned as the advantages of autonomous driving. The assistance functions available today are still limited to support the driver in a specific situation. Indeed the current systems focus on significant deviations from rather easily detectable vehicle signals. Real time

---

M. Harrer (✉)

Dr. Ing. h.c. F. Porsche AG, Porscheplatz 1, 70435 Stuttgart, Germany  
e-mail: manfred.harrer@steeringhandbook.org

P. Pfeffer

Munich University of Applied Science, Munich, Germany  
e-mail: peter.pfeffer@steeringhandbook.org

information regarding the vehicle surroundings in order to set the immediate course of travel is more complicated to detect and interpret though. Not only the car's own motion, but also other active and passive road users, be they close or distant, need to be detected and predicted. Such an automated process needs to be even better than the human one. However, the current state-of-the-art in vehicle situation analysis and detection is still a far cry from human performance. More information and recommendations coming from a higher number of more reliable systems are to be passed to the driver in the mid-term, but they will never assume full responsibility for driving safety. Assistance systems supporting the lateral control of a vehicle by means of electromechanical steering systems as Lane Departure Warning, Lane Keeping and Closeness to the Limit Warning for the driver to move away from danger by stabilizing the vehicle will become more common and contribute to safer driving. Nevertheless, assistance systems able to fully autonomously trigger and control vehicle movement will remain science fiction within the foreseeable future.

## 20.2 Steer by Wire

Up to now, all production cars embody a steering system featuring a mechanical connection between steering wheel and tyres. This means that in any operational condition of the vehicle, the driver has direct mechanical access to the tractable wheels and can control the course by acting on the steering wheel even after the steering systems has failed.

Steering system development in the last years or decades has been based on advancements to support the required steering force and wheel angle, switching to direct mechanical transmission should the steering system fail. Particularly in case of a Fail Safe for electromechanical actuators, this connection is a good backup function because it still allows transferring driver's steering input to the wheels.

This does not apply when switching to a Steer by Wire steering system. In this case, the driver's steering effort would be electronically transferred to a steering system which is not physically connected to the steering wheel. If Steer by Wire fails, turning it off is not enough. A redundant spare system to control vehicle course needs to be installed. This means that the greatest advantage of Steer by Wire, namely more flexibility in using construction space made possible by not having steering shafts, and a standardization of left/right-hand driven systems, makes it impossible to meet the requirements for safe operational readiness of the steering system. Steer by Wire does not have any other functional advantages in comparison to mechatronic systems with a mechanical backup, which are today's standard. Indeed electro-mechanical power steering combined with wheel angle actuators offers the same capability to keep steering angle and torque under control. In short, Steer by Wire will not become standard, as it has no real advantage on current mechatronic steering systems.

## 20.3 All-Wheel Steering

Progress in basic chassis development is limited to a certain amount of improvement per generation. Bigger improvement steps in vehicle dynamic response are only possible by mechatronic system development. The use of all-wheel steering will become indispensable to get better vehicle agility and driving stability.

The advantage of all-wheel steering systems is their ability to control both the turning circle of a vehicle in the low-speed range, and the side slip angle together with the build-up of rear axle side forces as a function of speed. At present, systems with central mechatronic actuators are used by Japanese and European manufacturers for rear-wheel steering.

It may be expected that vehicle manufacturers whose brand poses high demands on dynamics will bolster the development of mechatronic actuators aimed at controlling rear axle kinematics. The already visibly increasing use of all-wheel-steering in the medium to luxury car segments will turn it to be a widespread system in the coming years.

## 20.4 Integrated Chassis Control

Many new chassis control systems have been developed and successfully been integrated in production cars during the last years. A characteristic of these new systems is their focus not only on controlling the car near the limit, but also on embedding more functions to influence drivability in everyday use.

The system architecture of most vehicles is marked by peaceful coexistence of different electronic stability control systems, regardless of how many they are: this is possible if independently developed systems feature functionalities which only partially overlap. However, if the outlook is to have a higher and higher number of control systems, peaceful coexistence becomes difficult and ultimately limited. These difficulties are due to the following circumstances: on one hand, driver input and control system intervention are defined individually for each system independent of the others. On the other hand, the fact that the vehicle is a complex system with many interacting parameters is overlooked in the design of individual controllers. This means that the potential of individual systems is not sufficiently exploited by the currently available system architecture. An improvement by peaceful cooperation of all automatic control systems is therefore not possible under the peaceful coexistence approach. Nor is an actor substitution feasible without losing performance in other areas which are relevant to customer.

The increasing number of electronic stability problems requires designing their interaction in a way that functional synergies are exploited as much as possible. This becomes possible by multiplying the interconnections between the individual systems. There is a lot of room for improvement in the area of lateral dynamics: the reason behind this is that while the steering intervention at the front or rear axle has only an effect on lateral dynamics, other types of intervention—braking on the

single tyre, or varying drive or aligning torques—initially developed for longitudinal or vertical dynamics purposes, are more and more developed with the aim of affecting lateral dynamics, too.

In the future, electromechanical steering systems will receive requests for additional steering torques from further control devices by means of signal interfaces that are already available. Haptic feedback of driving states to support driver decisions will gain in significance, for instance by reducing steering wheel torque when the friction limit of the front wheels is reached. The calculation of the additional or subtractive steering torque as a function of the driving situation could be performed by a central driving state monitor.

## 20.5 Modules and Modularization of Steering Systems

For hydraulic power steering, a strongly standardized technology has developed for decades and can be found in most production vehicles nowadays. The vane-type pumps and hydraulic steering gear are produced in such quantities that no further significant cost reductions are feasible, as their degree of maturity is very high.

The challenge that all OEMs face now is the switch to mechatronic steering systems. This switch means rising costs in comparison to established hydraulic systems, especially when it comes to high end electromechanical steering systems. The main factors for higher costs are the brushless DC motor, the ECU, the sensor set and the mandatory output reduction gear.

The most important European steering system manufacturers prefer to develop modular electromechanical steering systems. This enhances flexibility by giving the possibility to get scalable systems. Expensive components can be carried over to different product lines with little or no modifications. This relies a lot on generating standardized mechanical and electronic interfaces. It is also clear that for non brand specific steering system features, OEM-wide standards with unified goals will establish themselves. Ultimately, one-time investments for development and production will be lower, and significant cost saving will make high end steering systems accessible.

It should be noted that similar standardized development approaches appear for other parts, such as the steering column, the intermediate steering shaft and the steering wheel with its many subcomponents. System and vehicle manufacturers put a major effort into pursuing standardizing strategies to reduce one-time investments and product costs.

## 20.6 Future Markets

Future markets in the BRIC states (Brazil, Russia, India and China) will support a primarily cost efficient development of parts, components and systems. These markets will be mainly driven by small, compact and medium sized vehicles. These

segments have typically low gross margins and are highly cost sensitive. Vehicle manufacturers and system developers face the options of either optimizing established products or downgrading them, if they want to meet the continuously rising demand for effective yet inexpensive parts or components. The conventional hydraulic power assisted steering will keep a significant share in these new markets in the foreseeable future, because of its low price and the reduced quality expectations.

## 20.7 Changes in Steering Technology

Electromechanical power steering has been in use for production cars for the last twenty years. Since the beginning of its use, the focus of development was to improve steering comfort while parking. As the power to weight ratio of the first generation was very low, the use of the system was limited to compact cars. Even at the end of the last millennium the electromechanical power steering only had a 2 % share of the global market. The second generation of electromechanical steering systems could gain a significant market share at the beginning of the new millennium: thanks to higher power output, production car use was possible for the compact and medium sized segment. The global market share of electromechanical steering systems was more than 30 % in 2008. Stricter legislation aimed at reducing petrol consumption of vehicle manufacturers' fleets let the development of electromechanical power steering systems gain momentum because of their lower power consumption in comparison to hydraulic systems. Remarkable improvement rates could be achieved in Europe and Japan in the most recent years. The introduction of parallel or concentric systems made it possible to install electromechanical steering systems also on medium and luxury vehicles. In another stage of development these steering systems would eventually require currents of more than 100 A and voltage of more than 36 V to work properly. Nowadays the technology available allows any passenger car or light commercial vehicle to be steered electrically. There are more aspects which will lead to further and quicker spreading of electromechanical steering systems and a consequent decline of conventional hydraulic power steering:

- Increasing customer attention towards climate change related topics, higher petrol costs to account for the steadily rising demand and, as a consequence, towards vehicle mileage.
- Higher cost-effectiveness and safety demands from customers, requiring a more extensive use of assistance functions. Only electromechanical steering systems can be used to add lateral dynamics functions like parking assist or a given recommended steering torque.
- Electrical and hybrid vehicles are becoming more and more common, and the electromechanical power steering is the best option to be coupled with these kinds of powertrain.

All these aspects contribute to the electromechanical power steering taking the lion share of the market, making it possible through cost plummeting effects originated by rising sales to reach a global EPS market share of 50 % in 2020.

## 20.8 Steering Wheel Developments

Customers' expectations regarding vehicle quality will continue to rise with any new vehicle generation. This will be reflected in higher requirements for the car and its single components as well, the steering wheel being no exception. The target values for steering wheel natural frequency and steering wheel to steering column joint stiffness will rise further so that as little idle vibration as possible is achieved.

The tendency towards a higher degree of customisation will continue. More steering wheel colour and material options will be available to the customer. The range of steering wheel customisation will span from an inexpensive basic wheel to a very modern though reasonably priced one featuring a great number of multi-functional commands, heating and customer specific leather covers and decorations. Offering so many options to choose from obviously introduces a lot of variety, and might let product costs go out of control. To avoid that, a thorough component and subassembly strategy using standardization must be put in place.

The tendency regarding vehicle safety and airbag units is towards smaller, more compact items keeping the same airbag volume. Furthermore, the airbag systems will become adaptive, and eventually be combined with single-stage of two-stage gas generators.

Since the beginning of vehicle development, the steering wheel has been in use to control vehicle course. It has proved itself as an effective element in all operational conditions and it is familiar to the drivers today. Replacing it with alternative devices like a joystick is and will remain hardly conceivable. However, the idea to display information for the driver on the steering wheel will spread. Indeed some vehicles already indicate the vehicle configuration selected by the driver on a steering wheel display. Shifting point displays are also becoming popular among sport cars. Current studies also focus on showing important navigation information on a separate display which for instance is integrated in the steering wheel rim. In short, the steering wheel will develop into an important operating and communicating on board unit.

## 20.9 Steering Column Developments

Keeping in mind that the ongoing tendency towards more car weight should be at best stopped or even reverted, it is mandatory to have demanding weight targets for the steering column. This obviously means that the use of lightweight materials like aluminium, magnesium and composites will spread.

The number of requirements for the steering column will also be higher, covering aspects like ergonomics, adjusting range, adjusting qualities like actuating force and acoustics. Structural stiffness targets like the natural frequency are expected to become stricter both for the steering column and the intermediate steering shaft. Virtual development by means of CAE will become more important because of the need to develop cars more efficiently and with shorter time to market. When it comes to the steering column this involves more detailed models for crash response analysis, models which take longitudinal and lateral forces as well as part and production tolerances into account. The modularization of parts, already mentioned as a key point for future steering system development, will also progress further for the steering column.

## References

- Braess H-H, Seiffert U (2007) Handbuch Kraftfahrzeugtechnik. Vieweg+Teubner Verlag, Wiesbaden
- Gaedke A, Heger M, Vähning A (2010) Electric power steering in all vehicle classes—state of the art. In: 1st international Munich chassis symposium
- Heissing B, Ersoy M (2007) Fahrwerkshandbuch. Vieweg+Teubner Verlag, Wiesbaden
- Schäfer P, Harrer M, Höll M (2010) Die Synthese aus Fahrdynamik und Fahrkomfort durch den Einsatz mechatronischer Fahrwerksysteme. In: 1st international Munich chassis symposium
- Wallentowitz H, Freialdenhoven A, Olszewski I (2008) Strategien in der Automobilindustrie. Vieweg+Teubner Verlag, Wiesbaden

# Advertisements



**WITH SAFETY IN EVERY CURVE –  
AND ON ANY TERRAIN**

With its five production plants, the Willi Elbe Group is synonymous with groundbreaking steering technology. Our product range comprises complete steering columns as well as steering and drive components of modular design. Whether for passenger cars or utility vehicles, the areas of application are wide-ranging – and the topics that motivate us are equally diverse. More dynamics, better ergonomics, lower fuel consumptions, maximum resistance to temperature and corrosion... Our know-how – from design to production and assembly – is steering leading carmakers in the right direction. Find out more at [www.willielbegroup.de](http://www.willielbegroup.de)

**Steering column, electrically adjustable**  
with intermediate steering shaft



**Steering column, mechanically adjustable**  
with intermediate steering shaft (lightweight design)

**WILLI ELBE - Gelenkwellen GmbH & Co. KG**

Hofäckerstr. 10, D-71732 Tamm, Tel.: +49 (0) 71 41/ 20 50 - 0, [www.willielbegroup.de](http://www.willielbegroup.de)



©TRW Automotive 2013

# JUST THINK: ELECTRICALLY POWERED STEERING FOR EVERY CAR IN INDIA.

Cognitive Safety Systems from TRW can help protect people and the planet. A range of advanced safety technologies are helping to reduce emissions and improve fuel efficiency worldwide. TRW's Green Thinking – the safety everyone deserves.

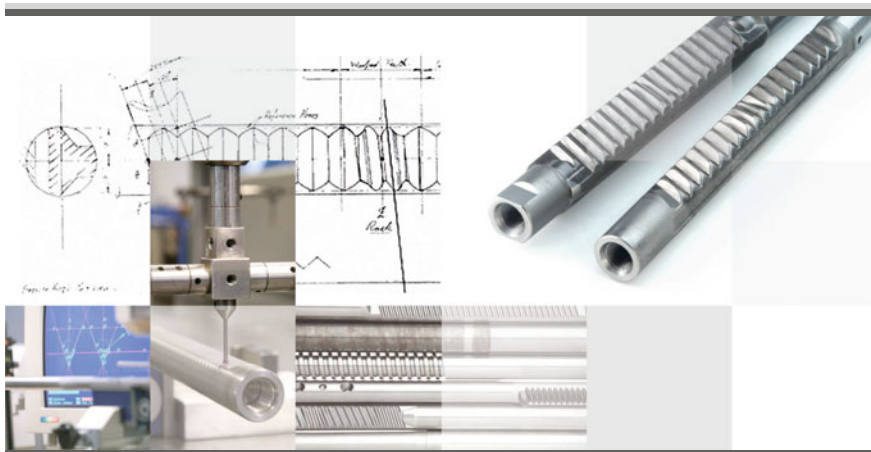
ADVANCED THINKING / SMART THINKING / GREEN THINKING

**COGNITIVE SAFETY SYSTEMS**

<http://safety.trw.com>



# STEERING SOLUTIONS ...



... FROM  
A SINGLE  
SOURCE!

MVO GmbH Metallverarbeitung Ostalb and BISHOP Steering Technology are among the world's leading companies for the development of automotive steering systems, steering racks and other components for the automotive industry. Together, they cover the entire value chain, from the development of steering gear prototypes by BISHOP Steering Technology through to the manufacturing of steering racks – particularly steering racks with variable ratio teeth – and other steering components by MVO.

More than 102 patents and patent applications in 19 countries and numerous licences granted all over the world are proof for its advanced technologies and automotive steering competence. Primary material supplies of special bright steels for steering components are provided by sister company Stahl Judenburg GmbH.

[www.mvo-g.de](http://www.mvo-g.de)  
[www.bishopsteering.com](http://www.bishopsteering.com)  
[www.bishopsteering.com.au](http://www.bishopsteering.com.au)

 **BISHOP**  
Steering Technology

 **MVO GmbH**  
Metallverarbeitung Ostalb  
BISHOP TECHNOLOGY INSIDE



## A World Leader in Electric Power Steering Systems for Quarter of a Century

We now take it for granted that vehicles are equipped with electric power steering (EPS). But it wasn't always that way: In 1988, JTEKT became the first company in the world to successfully develop and manufacture an EPS system. Today, one in four cars worldwide use JTEKT EPS systems.

Because EPS systems don't rely on the vehicle's engine for power, they help reduce fuel consumption—which also cuts vehicle CO<sub>2</sub> emissions. Indeed, EPS systems are an essential component in hybrid and electric vehicles, which are becoming increasingly popular as low-emission alternatives to conventional vehicles.

As the leading manufacturer of steering systems, JTEKT works continuously to develop new and better products that not only enhance vehicle safety and comfort, but also contribute to protecting the environment on which we all depend.



### DP-EPS :

European car makers choose JTEKT EPS systems for their outstanding safety, comfort and environmental performance.

Creating the next value

**JTEKT**

**JTEKT CORPORATION**  
[www.jtekt.co.jp](http://www.jtekt.co.jp)

JTEKT continues to steer its growth into the future

**JTEKT**

---

**Koyo**      **TOYODA**

**Steering Systems**

**Bearings**

**Driveline Components**

**Machine Tools**

**JTEKT CORPORATION**

# Index

## A

Absorbers, 229  
Accuracy, 160  
Ackermann condition, 63  
Ackermann steering, 11  
Ackermann steering wheel angle, A-angle, 85, 91  
Ackermann, Rudolf, 12  
Acoustics, 58, 121, 364  
Active steering, 463, 473  
Active-Four, 498  
Active-rear-axle kinematics (AHK), 500  
Actual, 88, 101  
Adjustable, 326  
Aerodynamics, 118  
Agility, 150  
Airbag, 192, 194, 196  
Airbag cover, 196  
All-wheel steering, 60, 494, 499  
Ampacity, 376  
Angle joint, 330, 335  
Angle sensors, magnetic, 425  
Angle superposition, 469  
Antilock Breaking system (ABS), 10  
Articulations, 159  
Artificial, 131  
ASIL, 392  
Assembly variants, 405  
Assessment criteria, 156  
Assistance characteristic curve, 46  
Assistance characteristics, 358  
Asymmetry, 220  
Asynchronous motor, 393  
At the middle of, 210  
Authentic, 149  
Autonomous driving, 514, 537  
Axial joint, 285, 286  
Axis of rotation, virtual, 63  
Axe mounting, torsional stiffness of, 98

Axle-pivot steering, 6, 12, 15

## B

Back reference variable, 490  
Ball pivot, 343  
Ball screw, 410, 413  
Ball-recirculating gear with nut, 16  
Ball-recirculating gear with nut drive, 293  
Ball-recirculating gear with nut steering, 28  
Basic, 424  
Basic structure, 193, 194  
Belt, 32  
Blank measurement, 336  
Blocked, 33  
Bode's diagram, 178  
Braking system, steering-stable, 117  
Brushless DC motor (BLDC), 421  
Buckling steering, 38  
Build up, 116  
Bump steering, 85  
Bypass, 360  
Bypass pressure, 360  
Bypass valve, 360

## C

C spring, 19  
Cam ring, 357  
Camber, 31  
Camber angle, 39  
Camber change, 70  
Camber thrust stiffness, 39  
Capacity values, 438  
Castor angle, 69  
Castor, construed, 69  
Castor offset, 69  
Catch up, 161  
Cavitation, 317  
Central actuator, 503  
Central plate principle, 446

- Centre feeling, 154, 159  
 Centre point, 167  
 Centrifuge test bench, 370  
 Centring, 223, 321  
 Centripetal acceleration, 95  
 Circular driving, steady-state, 83, 98  
 Circular driving values, 98  
 Classification, 379  
 Cleanliness classes, 350  
 Closed, 152  
 Closed loop, 28  
 Closed loop controlled system, 28  
 Column tube, 193  
 Commutator, 394  
 Compensation, 50  
 Components of the steering, 1  
 Conductivity, 436  
 Conductor material, 431  
 Conductor thickness, 431  
 Cone ring, 346  
 Container, 370, 382  
 Continuous sine, 163  
 Control, 437  
 Control plans, 464  
 Cooling coil, 375  
 Corner frequency, 179  
 Cornering, 29  
 Cornering stiffness, 94  
 Corner modules, 517  
 Correction, 462  
 Correlation analysis, characteristic-based, 155  
 Correlation and regression analysis, 165  
 Correlation coefficient, 165  
 Costs, 57  
 Course changes, 3, 152  
 Course control, 152  
 Course stability, 10  
 Crash, 199  
 Crash element, 228  
 Crosswind compensation, 50  
 Cylinder, 288  
 Cylinder pipe, 297
- D**
- Damping, 106, 289, 398, 457  
 Damping valves, 326  
 DC motor, 394  
 Decay, 369  
 Decay criterion, 369  
 Decay process, 105  
 Decorations, 192  
 Decoupling element, acoustic, 371  
 Default size, 474  
 Degassing, 365
- Degradation plan, 524  
 Degrees of freedom, 95  
 Dependent on force, 67  
 Dependent on path, 67  
 Direct current motor, 394  
 Directly Bonded Copper (DBC), 440  
 Disturbance compensation, 457  
 Drive influence, 28  
 Driveability, 215, 483  
 Drive-by-Wire, 514  
 Driver assistance, 525  
 Driver/vehicle, 28  
 Driver warning, 463  
 Driving stability, 10, 116  
 Driving stability engagements, 522  
 Drop arm, 77  
 Dummy variable technology, 166  
 Dynamic, 59, 67  
 Dynamic basic layout, 96  
 Dynamic steering, 463
- E**
- Eccentric shaft, 364  
 ECE-R, 79, 60  
 ECO, 360  
 ECU, 326, 381, 408  
 Eddy current losses, 420  
 Efficiency, 279, 283, 358, 368  
 Elastic shear modulus, 34  
 Elastocinematics, 8  
 Electrical, 383  
 Electrically powered hydraulic steering (EPHS), 383  
 Electric-hydraulic, 18  
 Electric motor, 416  
 Electric Power Steering (EPS), 403, 405  
 Electric pump unit, 22  
 Electro hydraulic power steering (EHPS), 5  
 Electromechanical, 24  
 Electronic Stability Program, integrated, 489  
 Electronically commutated motor/EC, 421  
 EMV, 205  
 Energy, 53  
 Energy consumption, 360  
 Energy management, 446  
 Energy saving pumps, 362  
 Engine order, 133  
 Environment, 58  
 Environmental requirements, 286, 407  
 EPHS, 383  
 EPS, 58, 406  
 EPSc, 406  
 EPSdp, 408  
 EPSp, 408

- EPSrc, 410  
Ergonomics, 528  
EV<sub>2</sub>, 359  
Evaluation methods of the lenkgefühl, 155  
EVLS, 10  
Excess-pressure valve (EPV), 329  
Experimental-Safety-Vehicle (ESV), 10  
Extended, 457, 461  
Extraction processes, 369
- F**  
Fast, 30  
Feedback, 152, 160  
Feedback engine, 458  
Field direction measurement, 430  
Field of work, 416  
Field weakening, 417, 421, 422  
Filling pressure, 32  
Filtration, 365  
Fixed control, 28  
Flange screw connection, 373  
Flange shaft steering, 31  
Flow control valve, 358  
Fluctuating brake forces, 154  
Force control, 28  
Fork steering, 15  
Free control, 28  
Free control stability, 116  
Frequency response test, 163, 166  
Friction moment at the steering wheel, 115  
Frictional compensation, 457, 460  
Full castor, 97  
Function noise, 124  
Functional requirements, 426
- G**  
Gas generator, 198  
Gear case, 253  
Gear noise, 408  
Gear ratio, 269, 408
- H**  
H bridge, 438  
Hall sensors, 425  
Handling qualities of a vehicle, 161  
Harmonic drive, 474  
Heterodyne steering, 418, 515, 525, 527, 528  
HICAS, 498  
High-pressure and low pressure lines, 342  
High-pressure screw connections -, 372  
Hollow shaft motor, 411  
Horn, 192  
Hydraulic power steering (HPS), 5, 58  
Hydraulic oil, 337
- Hydraulics, 18  
Hydraulic steering, 251, 267, 288
- I**  
Ideal, 153  
IEC 61508, 405  
In the broader sense, 153  
In the strict sense, 152  
Inductive, 424  
Inertia, 105, 116  
Inertia compensation, 457, 460  
Inner joint, 340, 342  
Input shaft, 281  
Instabilities, 9  
Instantaneous centre, 86, 505  
Integral active steering (IAS), 509  
Integral V rear axle, 502  
Interaction, 128  
Interfering force rocker arm, 63, 71  
Interfering information, 153  
Interfering noise, 122  
Interindividual variance, 156  
Intermediate steering shaft, 215, 217, 220  
Intraindividuelle variance, 156  
ISO 26262, 405  
ISO lane change, 507  
Isolated metal substrate (IMS), 436
- J**  
Joint gasket, 308  
Joints, 216
- K**  
KEEPS, 360  
Kerbs radius, 67  
Kickback, 276  
kinematic, 65  
kinematic effect, 31  
Kingpin axis, 79  
Kingpin inclination angle, 70  
Kingpin offset, 63  
Knuckle, 12, 63
- L**  
Lag, 181  
Lag, equivalent, 166  
Lane assist, 531  
Lane Departure Warning (LDW), 404, 463  
Lane Keeping Support (LKS), 534  
Lane Keeping System, 463  
Lankensperger, Georg, 12  
Lateral acceleration, 28, 99, 370  
Lateral acceleration gain, 114  
Lateral acceleration gradient, 115

- Lateral acceleration portion, 142  
 Lateral deformation, 37  
 Lateral dynamics, 1, 99  
 Lateral force of the tyre, 67  
 Lateral force point of application, 37  
 Lateral force potentials, 39  
 Lateral guidance, 28  
 Layout, 170  
 Layout parameter, 389  
 Leakage, internal, 297  
 Leather, 203  
 Lenkgefühl, 7, 43, 149, 153, 182  
 Lightweight construction, 348  
 Linearisation, 92  
 Locking mechanism, 474  
 Longitudinal acceleration, 370  
 Longitudinal-lateral guide, 523  
 Longitudinal movement, 34  
 Loop, 28
- M**  
 Magnetic, 393  
 Magneto-resistive sensors, 425  
 Manoeuvre, 172  
 Mark, 140  
 Markets, 548  
 Measuring equipment, 161  
 Mechanical steering, 248  
 Middle plate, 365  
 Modularisation, 212  
 Module, 481  
 Monitoring, 278  
 MOSFETs, 438  
 Motor current, 47  
 Motor topologies, 422  
 Movement equations, 80, 80, 82  
 $\mu$ -split, 528  
 $\mu$ -split brake, 50
- N**  
 Natural frequency, 116  
 Natural frequency of the steering column, 144  
 Negative, 116  
 New European driving cycle (NEFZ), 389  
 Non-linear, 37  
 Normal operating range, 79  
 NVH, 275
- O**  
 Objectification, 155  
 Objectification model based on driver, 156  
 Objective assessment of the steering behaviour, 161  
 Objective parameters, 155
- Oblique pulling, 461  
 Of external signals, 453  
 Of the axis, 83  
 Of the computer system, 454  
 Of the steering behaviour, 161  
 Of the steering feeling, 150, 152  
 Oil volume, 357  
 Oil water heat exchanger, 375  
 On centre area, 92, 167  
 On-board wiring configurations, 403  
 Open centre, 28  
 Open loop, 161  
 Operating element qualities, 520  
 Operating noises, 122  
 Operating time, 400  
 Operational stability, 193  
 Optical, 427  
 Oscillations, 48, 131  
 Outer tie rod, 81  
 Overall gear ratio, 79  
 Overload behaviour, 353  
 Oversteer, 7, 100  
 Oversteering trend, 50
- P**  
 Package, 54  
 Parameter, objective, 164  
 Park assist, 541  
 Parking, 538-543  
 Parking assistance, 528  
 Particle, 368  
 Particle sizes, 316, 368  
 Pentosin, 376  
 Perceptions, 155  
 Pinion, 249, 281  
 Pinion dovetailing, 260  
 Pinion torque, 281  
 Piston, 294  
 Pneumatic trail, 33, 37, 40, 43, 72  
 Position control, 28, 70  
 Position feedback, 519  
 Potentiometer measurement, 427  
 Power assist torque, 96  
 Power classes, 387  
 Power demand, 440  
 Power electronics/actuator, 438, 455  
 Power input, 362, 389, 445  
 Power output, 438  
 Power pump aggregate (PPA), 290, 366  
 Power requirements, 177  
 Power steering, 2, 17, 172, 403  
 Power transmission, 411  
 Power-assist, 96  
 Power-assistance, 458

Power-assisted drive, 411  
Power-assisted gear, 96, 411  
Pressure loss, 399  
Pressure pulsation, 127  
Printed circuit board (PCB), 436  
Program directives, 437  
Propulsions, 116  
Puls-width modulated control signals (PWM), 436  
Pump humming, 127  
Pump rev, 358

## Q

Quality, 57

**R**  
Rack displacement force, 282  
Rack force, 169  
Rack gaskets, 298  
Rack guide, 260  
Rack shift, 96  
Rack yoke, 261  
Rack yoke clearance, 280  
Rack-and-pinion gear, 249  
Rack-and-pinion hydrosteering, 17  
Rack-and-pinion steering, 17, 249  
Radial joint, 339, 344  
Radial piston pumps, 364  
Radius of curvature, 95, 101  
Rate limit, 172  
Rattle of the steering, 129  
Rear-wheel steering, 494, 508  
Receiver coils, 424  
Recommended torque, 521  
Reduced, 99  
Redundancy, 525  
Redundancy management, 525  
Reference point, 164  
Reference steering angle, dynamic, 101  
Relief, 382  
Required wheel angle, 173  
Requirements, legal, 60  
Residual angle after, 161  
Resolver, 424  
Resonators, 372  
Responding properties with, 248  
Response at, 179  
Response behaviour, 153  
Response time, 102  
Rev sensors, 423  
Righting factor, 72  
Righting moment, 75, 320  
Rigid, 477  
Rim, 195

Ring fitting screw connection, 371  
Risk assessment, 411  
Roll, 49  
Rolling steering, 44, 113  
Rolling steering factor, 113  
Rolling stiffness, 113  
Rolling support, 66  
Ross steering, 16  
Rotary disk valve, 183, 302  
Rotor angle, 423  
Runback filter, 368  
Runback, active, 461

## S

Safety, 448  
Safety concept, 448, 523  
Safety integrity function, 449  
Safety measures, 452  
Safety requirements, 441  
Saginaw screw connection, 373  
SAW resonators, 433  
Scrub radius, 64, 97  
Seam forms, 199  
Seat valve, 21  
Self-steering behaviour, 8, 49, 102  
Self-steering gradient, 99, 113  
Sensor joint, 354  
Sensors, 400, 423  
Separation efficiency, 368  
Sequence test, 394  
Servo oil cooler, 374  
Servo oil tank, 365  
Servo oil temperature, 377  
Servo ratio, 442  
Shimmy, 8  
Shutdown paths, 436  
Sideslip angle, 92, 109  
Sideslip angle compensation, 460  
Signal amplifier, 436  
Signal electronics, 436  
Single sine, 163  
Single sine test, 163  
Single track model, linear, 91  
Single wheel actuator, 503  
Single wheel steering, 5104  
Single-pivot steering, 6, 12  
Single-stroke, 361  
Sleeve, 304  
Slip angle, 8, 37, 39  
Slip-stiff, 29  
Slow, 29  
Sound flow curve, 123  
Sound sources, 122  
Special particles, 369

- Speed, typical, 99  
 Squirrel cage, 419  
 Squirrel, 420  
 Stabilisation, 118  
 Stability, 128  
 Stability analyses, 9  
 Stability factor, 113  
 Standard types, 4  
 Statement criterion, 177  
 Static, 60, 115  
 Steel wheel vehicles, 15  
 Steer by wire, 471, 492  
 Steering, 11–13, 16, 28, 34, 45, 46, 56, 60, 64, 68, 78, 79, 82, 103, 114, 116, 118, 122, 129, 145, 150, 153, 161  
 Steering angle, 92  
 Steering angle demand, 160  
 Steering angle jump, 154  
 Steering angle plate, 478  
 Steering arm, 76, 81  
 Steering arm angle, 96  
 Steering axis, 97  
 Steering behaviour, 131, 150, 161  
 Steering column, 193  
 Steering comfort, 323  
 Steering deviation, 309  
 Steering driveline, 194  
 Steering dynamics, 154, 161  
 Steering elasticity, 9, 113  
 Steering error, 68  
 Steering feedback, 154  
 Steering friction, 167  
 Steering functions, 426  
 Steering gain, 12, 103  
 Steering gear, 16  
 Steering kinds, 274  
 Steering layout, 450, 454  
 Steering model, 104  
 Steering on, 99  
 Steering parameter, 109  
 Steering performance, 109  
 Steering pinion, 303  
 Steering precision, 17, 154  
 Steering ratio, 42, 79, 307, 442  
 Steering rattle, 127  
 Steering recommendation, 527  
 Steering runback, 187  
 Steering shaft, 216  
 Steering stabilisation, 456  
 Steering stiffness, 98  
 Steering torque course with, 462  
 Steering torque level with, 157  
 Steering trapezoid, 82  
 Steering valve, 294  
 Steering wheel, 191  
 Steering wheel angle, 42, 96, 442  
 Steering wheel angle frequency, 151  
 Steering wheel angle jump, 154  
 Steering wheel rotary oscillations (SWRO), 132  
 Steering wheel torque, 41  
 Steering wheel torque area, 416  
 Steering wheel torque at, 153  
 Steering wheel torque calculation, 40  
 Steering wheel torque course, 42, 152  
 Steering-swivel axis, 112  
 Step input test, 162  
 Stiffness, 19, 235  
 Straight driving, 159  
 Strength requirements, 284  
 Stretch tube, 371  
 Structural stiffness, 38  
 Structure-borne sound introduction, 125  
 Structure-borne sound transmission, 133  
 Subjective assessment of the lenkgefühl, 149  
 Substrate, 433  
 Suction control, 364  
 Surface Acoustic Wave (SAW), 433  
 Swirl set, 93  
 Synchronous motor, 393  
 System layout, 386  
 System networking, 480  
 System safety, 53, 447, 487
- T**
- Tandem pump, 365  
 Tangential screw connection, 346  
 Target areas for optimum steering behaviour, 166  
 Temperature range, 442  
 Thermal, 437  
 Thick-film circuits (TFC), 437  
 Three-phase bridge, 438  
 Throttles, 374  
 Thrust angle, 39  
 Tie rod, 79, 339  
 Tie rod force parking, maximum, 442  
 Timing belt gearbox, 409, 415  
 Timing belts, 415  
 Tire components, 32  
 Tire lateral force, 33  
 Tire lateral force FYF, 43  
 Tire qualities, 32  
 Tire righting moment, 33, 34  
 Tires, lateral force, 33  
 Toe and camber change, 49  
 Toe-in and camber effect, 49  
 Toe-out on turn, 68

- Torque ripple, 157, 421  
Torque sensor, 426  
Torque vectoring, 11  
Torsion bar, 96, 304  
Torsion stiffness, 96  
Total, 98  
Total amount of dirt, 369  
Trace setting, 413  
Track diameter, 65  
Tracking, 463  
Traction potential, 38  
Trail, 78  
Trajectory, 95  
Transient behaviour, 102  
Transient response, 8, 163  
Transmission behaviour, 183  
Transmission equipment, 80  
Transmission ratio, 16, 267  
Tread galleries, 31-33  
Tuner, 372  
Tuning area, 109  
Turning circle, 496  
Turning circle diameter, 67  
Turntable steering, 11  
Types, 4
- U**  
Understeer, 8, 100  
Understeering trend, 50  
Useful informations, 154  
Utility vehicles, 2
- V**  
Vacuum filling, 366  
Valve indicator, 316  
Valve noise, 317  
Vane-type pump, 357  
Variable, 96  
Vehicle classes, 156  
Vehicle model-based, 155  
Vehicle modelling, 91  
Vehicle reference point, 164
- Vent pipe, 308  
Vibration comfort, 147  
Vibration damper, 17  
Vibration transmission, 17  
Viscosity, 376  
Volumetric efficiency, 358  
Volumetric flow, 357  
Volumetric flow characteristic curve, 358
- W**  
4WAS, 509  
Weave test, 162, 165  
Weight, 56  
Weight reset, 56, 72  
Weir and DiMarco Diagram, 166  
Weissach axis, 10  
Wheel angle range, 442  
Wheel corpus, 193, 195  
Wheel load rocker arm, 76  
Wheel loads, 49  
Wheel speed, 442  
Wheel torque, 37, 177  
Wheelbase extension, virtual, 505  
With power assist and friction effects, 106  
Working chamber, 47  
Worm gear, 407  
Worm-wheel steering, 16
- X**  
X-by-Wire, 513
- Y**  
Yaw angle, 92  
Yaw gain, 103, 166  
Yaw moment, aerodynamic, 93  
Yaw moment control, 10  
Yaw motion, 30  
Yaw neutrality, stationary, 510  
Yaw rate, 505, 510  
Yaw response, 99, 507  
Yaw steering oscillation, 116